PROCESSING TECHNIQUES FOR IMPROVED RADAR DETECTION IN SPIKY CLUTTER

by

BRIAN CLEMENT ARMSTRONG

A Thesis submitted to the University of London
for the Degree of Doctor of Philosophy
in Electronic Engineering

Department of Electronic and Electrical Engineering
University College London

July 1992

Abstract

The problem of improved radar detection of targets embedded in spiky clutter is addressed. Two main areas where improvements may be possible are investigated, namely improved clutter suppression by doppler filtering, and improved Constant False Alarm Rate (CFAR) processing. The clutter suppression performance of several doppler processors is quantified under a wide range of conditions. It is shown that in spatially homogeneous clutter ideal optimal (Hsiao) filters offer 2 to 3 dB higher improvement factor than conventional techniques. Adaptive Hsiao filters are evaluated under conditions of spatially heterogeneous clutter, and it is shown that practical losses due to filter adaptivity and spectral heterogeneity will outweigh the superior performance of ideal Hsiao filters in homogeneous clutter. It is concluded that improved doppler filtering offers little scope for improving detection performance in spiky clutter, and that more significant benefits are to be gained through improved CFAR processing. The performance of three current generation CFAR processors is evaluated in spatially uncorrelated K-distributed clutter to quantify detection losses. It is shown that losses of in excess of 10 dB can be expected in spiky clutter. Reducing the loss by exploitation of any spatial correlation of the underlying clutter power is investigated. To this end a mathematically rigorous model for spatially correlated K-distributed clutter is derived. An improved CFAR processor based on optimal weighting of reference cells is formulated and evaluated. It is shown that in highly correlated clutter CFAR loss can be reduced by 2 to 5 dB compared to Cell Averaging CFAR processors. An alternative "RDT-CFAR" processor is formulated to eliminate reliance on spatial correlation, and this is shown to reduce CFAR loss by more than 10 dB in spectrally homogeneous spiky clutter. However, an increase in false alarm rate in clutter without constant spectrum is demonstrated. The RDT-CFAR processor has been modified to eliminate dependence on surrounding range bins. The resulting "δ-CFAR" processor reduces CFAR loss by more than 10 dB in even moderately spiky clutter. It is also immune to extraneous targets and clutter edges, and its false alarm performance is insensitive to clutter spikiness.

To my Parents

Acknowledgements

I owe an immense debt of gratitude to Mr. Francois Anderson of the CSIR, South Africa, without whom this thesis would never have been started, and to Dr. Hugh Griffiths of UCL, my supervisor, without whom the thesis would never have been completed. Their support, advice, encouragement and friendship over the years has been invaluable.

I am indebted to the CSIR of South Africa for sponsoring my studies, and to GEC Marconi Research Centre (MRC) of Chelmsford and the RSRE for sponsoring portions of the research. Discussions with Dr. Andy Dean, Mr. Carlos Sarno and Mr. Rob Miller of MRC, and Dr. Chris Baker and Dr. Richard White of the RSRE were very helpful and their contributions to this thesis are acknowledged with thanks. The periodic comments of Prof. Ken Milne and Prof. Ralph Benjamin are also much appreciated.

Thanks are also due to the other members of the Antennas and Radar Group of the Electronic and Electrical Engineering Department of UCL, and in particular, Saeed Khosrowbeygi, Wolfram Titze, Declan Sheehan, and Robert Devayya, for many fruitful discussions on clutter, probability theory and "the world", and for their willing advice and assistance on my Macintosh computer.

The unending support of my wife Sharon, and her assistance in the preparation of this thesis, has been invaluable, and mere words of thanks here are wholly insufficient. Similarly, I am very grateful to Carl and Sandra Whalley for offering Sharon and I accommodation during the last six months of the thesis and for tolerating their lounge littered with computer printouts, graphs, thesis drafts, etc.. And finally, I would like to thank my daughter Kelly for knowing when to leave her father alone to work; one day she may appreciate the value of her contribution.

TABLE OF CONTENTS

LIST OF FIGURES

LIST OF TABLES

NOMENCLATURE

b : K-distribution scale parameter $\left(=\sqrt{\frac{4c}{\pi}}\right)$

b_1 : clutter spectral width deviation parameter

c : K-distribution scale parameter

f_c : clutter doppler centre frequency

f_{c_1} : centre frequency to the left of clutter edge

f_{c_2} : centre frequency to the right of clutter edge

g_i : modulation process constituent ZMG processes

h_j : OLF-CFAR weights

k : rank of test statistic in OS processor

K : number of doppler bins;
SMI sample size (Chapter 4)

$\hat{m}(i,j)$: element (i,j) of $\hat{M}$

M : binary integration threshold

M : clutter and noise covariance matrix

$\hat{\mathbf{M}}$: estimated clutter covariance matrix

M_b : binary integration detection threshold

$\mathbf{M}_1$: clutter covariance matrix to the left of clutter edge

$\mathbf{M}_2$: clutter covariance matrix to the right of clutter edge

n : number of ZMG processes (Chapter 6);
pulse index (Chapters 3,4);
burst index (Chapter 7)

N : number of bursts
order of filter (Chapters 3, 4)
number of reference cells (Chapter 5)

N_b : number of bursts

N_r : number of reference cells in CFAR window

P_c : clutter power

P_t : absolute target power

P_1 : clutter power to the left of clutter edge

P_2 : clutter power to the right of clutter edge

q : number of exceedances

r : Rayleigh speckle

r : clutter correlation vector

r_o : rank of test statistic in RDT-processor

r_1 : rank of $\hat{r}_{ij}$ in RDT-processor

r_{ij} : ratio of γ_i and γ_j

R : number of range bins in RDT-processor

$R_{uu}(k)$: ACF of u

$R_{gg}(k)$: ACF of g

$R_{vv}(k)$: ACF of v

s : exponential speckle

S : instantaneous SCNR

S : target vector

S_0 : mean SCNR

$S_{\overline{dp}}$: signal power without doppler processor for $P_d = 50\%$

S_{dp} : signal power with doppler processor for $P_d = 50\%$

T : interpulse period

u : power modulation process

v : voltage modulation process

W : doppler filter weight vector

x : compound clutter (Chapters 1-6 : voltage);
(Chapter 7 : power)

z : test statistic

α : threshold multiplier factor

α_1 : additional threshold multiplier factor for estimation of ρ in OLF processor

γ_k : Mean power in doppler bin k

$\hat{\gamma}_k$: estimate of γ_k

Δ : percentage of doppler space over which IF is averaged

ε : $\hat{\gamma}_k/\gamma_k$

ν : K-distribution shape parameter

ν_{eff} : effective shape parameter for clutter plus noise

ρ : clutter correlation coefficient
(Chapter 4 : temporal);
(Chapter 6 : spatial)

σ_n : noise power

σ_0 : clutter doppler half power bandwidth

σ_1 : clutter bandwidth to the left of clutter edge

σ_2 : clutter bandwidth to the right of clutter edge

CHAPTER 1

INTRODUCTION

1.1 MOTIVATION

Modern radars are increasingly required to detect small targets in the presence of strong clutter while simultaneously maintaining a low, and preferably constant, probability of false alarm. Two key radar subsystems for achieving this goal are the doppler filter, for suppressing clutter as far as possible, and the automatic detector, for deciding which of the filtered returns represent targets.

Much progress has been made in the field of doppler filtering over the last two decades, and Pulse Doppler (PD), Moving Target Detector (MTD) and adaptive Optimal Filter (OF) techniques have superceded simple Moving Target Indication (MTI) filters as the state of the art. The performance and theory of these techniques is well understood and documented for the case of homogeneous clutter environments. However, their performance in spatially and temporally varying clutter has not been widely addressed and little clarity or consensus exists as to which technique offers the best performance in realistically varying clutter. In addition, a number of unexplored potential shortcomings of adaptive optimal filters in realistic clutter preclude confident quantitative comparison with other filter types.

Complete elimination of clutter by doppler filtering is impossible, and additionally, detection of targets in clutter of the same ambiguous doppler velocity is often necessary. Target detection is therefore often clutter limited. Since the level of the clutter or clutter residue varies and is in general unknown, adaptive thresholding is required if an approximately constant or bounded false alarm rate is to be achieved. To this end, most radars employ Constant False Alarm Rate (CFAR) processors, which attempt to estimate the local mean clutter power and set the detection threshold accordingly. Current generation CFAR processors are optimised for operation in clutter with noise-like Rayleigh amplitude statistics. Under many conditions, however, the nature of radar backscatter from land and sea departs significantly from the Rayleigh model. In general this occurs where the number of significant scatterers within the radar resolution cell is not sufficient to ensure the validity of the central limit theorem (which leads to Rayleigh statistics of the envelope of the detected signal), and the clutter statistics depend instead on the scattering properties of the

individual scatterers constituting the clutter. This is typical of many land clutter scenarios containing sparse and randomly located large point scatterers, and of sea clutter at low grazing angles or in high resolution radar systems. The key feature of such clutter is the high probability of the clutter exhibiting values much larger than its mean power, or clutter spikes. These clutter spikes are known to cause a dramatic deterioration in the performance of conventional CFAR processors. Although the severity of the performance deterioration has not hitherto been accurately quantified, it is widely acknowledged that improved CFAR processing techniques are essential if good detection performance and satisfactory false alarm control is to be achieved in spiky clutter.

These performance and analytic limitations of current generation doppler filters and CFAR processors in spatially non-homogeneous spiky clutter therefore provide the starting point for this research, the objectives of which can be summarised as follows:

> *To quantify the performance of existing CFAR and doppler processors in spiky and spatially non-homogeneous clutter; to identify shortcomings in their performance and implementation; and to formulate and evaluate improved techniques, with particular relevance to high resolution radars.*

1.2 TECHNICAL BACKGROUND

The increased emphasis given to improved doppler filtering and detection in non-Rayleigh clutter is partly due to the trend in modern radars towards ever higher spatial resolution. This trend is motivated by the demand for more diverse, accurate and reliable information from the radar sensor. Progress in component technologies has facilitated the realisation of radars with significantly higher resolution than was previously possible.

The advantages of high radar resolution apply to both search and tracking radar functions: the higher the resolution, the smaller clutter cell and hence the lower the clutter power with which the target must compete for detection; better angular resolution provides better angular accuracy for designation in search radars and better tracking accuracy in tracking radars, particularly with regard to low elevation tracking where multipath is best countered by reductions in elevation beamwidth; and high spatial resolution affords better target discrimination between closely spaced targets and better interclutter visibility. It is also generally necessary for target recognition applications and is often seen as being beneficial in its implications for the vulnerability of the radar to countermeasures.

High spatial resolution has a number of consequences for radar processing. Two of the most important of these are that 1) the clutter no longer tends to have Rayleigh amplitude statistics, resulting in poor CFAR detection performance, and 2) there are generally fewer pulses available per dwell, which can severely compromise doppler processing performance. Additionally, high spatial resolution implies more range-angle cells to be processed, and therefore higher radar processor throughput. This may be exacerbated by the need for more sophisticated processing required to cope with non-Rayleigh clutter statistics.

1) Non-Rayleigh Clutter

When the radar spatial resolution is large, the number of scatterers in a given resolution cell tends to be sufficient to ensure the validity of the central limit theorem, thus generating Rayleigh clutter amplitude statistics. Finer radar spatial resolution, implying fewer clutter scatterers per resolution cell, will cause the failure of the central limit theorem and clutter returns will exhibit amplitude statistics which depend on the backscatter properties of the individual scattering elements or sources within the resolution cell. This generally results in clutter which is termed "spiky", and which is mathematically characterised by the third and higher order moments of the clutter envelope being higher than for Rayleigh clutter, for a common clutter power (second moment). In addition to the clutter being non-Rayleigh, the time varying nature of the clutter environment may also be exacerbated by fine radar spatial resolution.

The statistical nature of the high resolution radar environment has received a fair amount of attention in the literature over the last few years. Models now exist which are widely accepted to provide at least a phenomenological, if not mechanistic, description of high resolution radar clutter, particularly sea clutter. Although land clutter models are available they are less generally applicable due to the almost infinitely variable nature of terrains encountered. The K-distribution model in particular is now widely accepted to provide a good phenomenological description of sea clutter. Some physical justification for this model has also been proposed. The K-distribution representation of sea clutter is based on the assumption that the sea clutter in a given range bin exhibits Rayleigh voltage fluctuations (termed the "speckle"), the variance of which varies in time and space according to a gamma distribution. This compound form of the K-distribution has the particular advantage of permitting the clutter's temporal and spatial correlation properties to be properly modelled, including the effects of radar frequency agility. Provided the correct spatial ACF is used, spatially correlated K-distributed samples are not dissimilar to real clutter data. The K-distribution model is discussed in more detail in Chapter 2 and has been adopted as the primary clutter model for this thesis.

Target characteristics in high resolution radars are still widely accepted to conform to the classic Swerling models for most practical purposes, although they do break down for the extremely high resolutions typical of target recognition requirements. The most commonly adopted Swerling models, and those adopted in this thesis, are the Swerling-1 and Swerling-2 models (Sw1 and Sw2). These describe the target as having a negative exponential power PDF and fluctuations which either decorrelate very slowly relative to the radar dwell time (Sw1) or decorrelate completely between successive detection opportunities (Sw2), which can imply between pulses, bursts or scans, depending on the radar processing employed.

The performance of Constant False Alarm Rate (CFAR) detectors depends on the statistics of the noise or clutter background with which the target must compete for detection. Many CFAR processor analyses make the assumption that the background has a Rayleigh (voltage) or negative exponential (power) distribution. Should this assumption be violated an increase in false alarm probability P_{fa} and/or a reduction in target detectability can occur. It is important to know the severity of these effects should radar operation in non-Rayleigh environments be expected.

2) Reduction in dwell time

A second major implication of high radar spatial resolution is the reduction in the dwell time available per angular resolution cell if the revisit rate is to be kept constant. The number of pulses available for processing per dwell, and consequently the number of pulses per coherent processing interval, is therefore limited, thus limiting the achievable doppler resolution. This conflicts with clutter suppression and target discrimination requirements, particularly in radars intended for detecting very small targets, in which exceptionally good clutter and false target suppression is required to suppress the vast numbers of false alarms that can be expected to occur due to birds, insects, clutter motion etc..

1.3 PROJECT OBJECTIVES

We wish to improve radar detection performance in spiky clutter. Two possible areas in which this may be achieved are in improved doppler filtering, such that targets compete with less clutter residue for detection, and improved CFAR processing, to achieve more reliable discrimination between desired targets and whatever clutter residue cannot be suppressed. A third possibility is also given here for completeness, namely the use of difference channel information for detection in monopulse radars. The rationale of this technique is to avoid the usual "wastage" of the information in the difference channels

during detection processing. Specific objectives within each of these areas are given in the following subsections.

1.3.1 Improved Clutter Suppression

The adoption of the K-Distribution as the clutter model means that within a given Coherent Processing Interval (CPI) or dwell the clutter in each range bin exhibits Rayleigh amplitude fluctuations, and hence the signals being filtered in each range bin are complex Gaussian. Thus the overall non-Rayleigh nature of the clutter does not directly influence the doppler filtering, and well established linear filtering techniques can be used to provide optimal clutter suppression performance for specific optimisation criteria and subject to the validity of assumptions of clutter homogeneity. The wide range of techniques available for doppler-based clutter suppression of Rayleigh clutter are therefore directly applicable to K-distributed clutter, and special non-Gaussian filters do not need to be developed. At present, however, there is little consensus as to which technique provides the best performance under anything wider than specific clutter and target conditions. Although the relative performance of many of the techniques has been compared in the literature, no clear-cut conclusions can be drawn from the available papers: the data are often not directly comparable and sometimes contradictory, and one often gets the impression that quoted performance depends strongly on the specific clutter environment assumed. In this thesis an attempt will be made to evaluate the relative performance of many commonly proposed doppler processors under a wide range of conditions, with as few limiting assumptions as possible. The processors to be addressed include:

1. Moving Target Indication (MTI)
2. Adaptive MTI (AMTI)
3. Moving Target Detector (MTD)
4. Pulse Doppler preceded by MTI (PD&MTI)
5. Adaptive MTD (AMTD)
6. Optimal Filtering (OF)
7. Linear Prediction (LP)
8. Optimal Filtering preceded by MTI (OF&MTI)
9. Linear Prediction preceded by MTI (LP&MTI)
10. Adaptive MTI preceded by MTI (AMTI&MTI)

A wide range of clutter scenarios representative of typical land and sea clutter, possibly with weather clutter components as well, are defined. The performance of each of the doppler processors listed above is assessed in each clutter environment. Statistical analysis is then used to compare the relative performance of the various processors.

The abovementioned performance comparison uses the ideal Hsiao filter, which represents a theoretical upper bound on achievable clutter suppression, as the reference against which all other filters are compared. In practice, Hsiao filtering requires adaptive real time estimation of the clutter covariance matrix. This results in imperfect estimates of the clutter spectrum, or its covariance matrix, which after solution for the filter weight vector yields suboptimal filter performance. Practical "optimal" filters therefore suffer a loss relative to ideal optimal filters, even in spatially homogeneous clutter. Environments for which adaptive filters are specifically intended, namely temporally and spatially varying clutter, compound the problem further since the covariance matrix in the range bin being filtered will in general differ from that in the adjacent range bins used in estimating the covariance matrix.

Under conditions of spatially homogeneous clutter the magnitude of the loss due to imperfect estimation of the covariance matrix has been widely investigated. The assumption of homogeneous clutter is, however, very restrictive and will often be violated. Despite this, the losses in IF under conditions of clutter heterogeneity have not been widely quantitatively addressed in the literature. In this thesis we therefore need to quantify the effects of clutter heterogeneity on adaptive doppler filtering, and investigate the use of prefilter MTI as a means of reducing filter sensitivity to some forms of clutter heterogeneity. Three general categories of clutter heterogeneity will be investigated, namely:

1. Clutter in which the amplitude and spectral width in each range bin are randomly drawn from spatially invariant parent populations of specified characteristics.

2. Clutter edges, in which the clutter amplitude and/or spectrum exhibit a step change at some point in the range profile of the clutter.

3. Clutter which is essentially homogeneous but in which a small number of range bins are corrupted by returns with significantly different amplitude and spectral characteristics, representing point clutter sources or extraneous targets.

1.3.2 CFAR Processing in Non-Rayleigh Clutter

The scope for improvements in detection performance through improved doppler filtering is limited. In many clutter environments the detection of desired targets embedded in relatively strong clutter residue will therefore be necessary. The influence of K-distributed clutter on detection and false alarm probabilities achieved by most conventional CFAR processors has not been widely addressed in the literature. The performance of conventional CFAR processors in K-distributed clutter, and K-distributed clutter plus thermal noise, therefore

needs to be quantitatively evaluated. Three well known CFAR processors, namely the Cell Averaging (CA), Cell Averaging Greatest-Of (CAGO) and Order Statistic (OS) processors, are chosen as the basis of the analysis. Besides being of general use in the selection and evaluation of conventional CFAR processors, these results are necessary to facilitate meaningful performance assessment of improved CFAR processors introduced in later chapters of this thesis.

Severe detection losses can arise in spatially uncorrelated spiky clutter. Spatial correlation affects the performance of the CA, CAGO and OS processors, but more importantly, it offers scope for improved CFAR processors aimed specifically at exploiting spatial correlation with a view to improving detection performance in spiky clutter. It is not unreasonable to assume that the clutter modulation process will have a decorrelation distance of the same order of magnitude as the decorrelation distance of the sea surface. In some conditions this correlation distance may cover a number of range bins in the CFAR reference window. It can then be postulated that exploitation of such spatial correlation could reduce detection losses in spiky clutter: if the degree of correlation is known, then the CFAR threshold multiplier factor can be altered to better reflect the local clutter statistics in the reference window, resulting in reduced detection loss. Furthermore, weighting of reference cells to improve the estimate of the clutter power in the test cell is an intuitively obvious extension to further enhance detection performance. Three specific research objectives for this phase of the project can therefore be defined as:

1) Extend current models for K-distributed clutter to enable spatially correlated clutter to be simulated and rigorously mathematically represented.

2) Quantify the potential benefits of exploiting spatial correlation, by defining and analysing "Ideal CFAR Detection" in spatially correlated clutter.

3) Formulate and evaluate a CFAR processor aimed at reducing detection losses in spatially correlated spiky clutter.

An alternative means of improving CFAR performance in spiky clutter is to reduce the reliance on surrounding range bins as the sole source of information for estimating the background in the test cell in order to establish the threshold. Exploitation of the two other domains in which potential reference data are available, namely the doppler and time domains, should therefore be investigated. Current techniques such as post-detection binary integration and range-doppler CFAR processing offer modest benefits at best. Additionally, false alarm control downstream by Track-While-Scan processing is not an

ideal solution as it can cause saturation of the plot extractor and missed or corrupted true tracks. A research objective of this thesis was therefore stated as formulating a means of exploiting information from other time and/or doppler bins in the vicinity of the test cell to ascertain the background level in the test cell, in radars employing doppler filter banks and multiple bursts per dwell. The resulting Range-Doppler-Time CFAR processor must be evaluated and detection benefits assessed.

The objectives of the CFAR processing research in this thesis can therefore be summarised as follows:

1. To analyse the performance of several existing single pulse CFAR processor implementations in K-Distributed clutter, with specific emphasis on the effects of clutter spikiness and spatial correlation.

2) Quantify the potential benefits of exploiting spatial correlation, and formulate and evaluate a CFAR processor aimed at reducing detection losses in spatially correlated spiky clutter.

3) Formulate and evaluate range-doppler-time CFAR processing techniques which reduce reliance on surrounding range bins in deriving the estimate of the clutter power in the test cell.

1.3.3 The Use of the Difference Channel information for Detection

For completeness, another possibility for achieving improved detection performance will be mentioned here: it is reasonable to argue that detection performance could be improved by the exploitation of *all* available information within the radar, and indeed possibly from other external sources. Many radars are dual- or multi-function systems, being required to perform both search and tracking functions. With the exception of radars with fully adaptive active array antennas, such radars would therefore usually incorporate Azimuth and Elevation Monopulse Difference channels, the outputs of which are not normally used during detection modes. It was reasoned that this implies the wastage of some potentially useful information and techniques were conceived to include such information in the detection procedure. These ideas were developed and analysed and the results are presented in the paper "The use of Difference Channel Information for Detection in Monopulse Radars", appended as Appendix 1.1. Some proposals for developing the techniques further are presented in the paper, and possible connections with detection in K-distributed clutter are also mentioned. This work is not central to this thesis, and a more detailed discussion

has therefore not been included in the body of this thesis.

1.3.4 Scope and Limitations

Some limitations on the scope of this thesis need to be noted. Firstly, the "processing" to which the title refers is limited primarily to processing related to automatic detection. It is therefore taken to include doppler filtering for clutter suppression and CFAR processing; track processing, specifically Track-While-Scan (TWS) processing, pulse compression techniques, and Synthetic Aperture Radar (SAR) processing are not covered.

Since spiky clutter is particularly problematic in high resolution radar systems, the focus of this thesis is on high resolution radars and processing techniques are developed in that context[1]. It was therefore assumed that the total number of pulses available will, in general, be limited due to the relatively short dwell time spent in each angular resolution cell, and so CFAR techniques which rely on the post detection integration of a large number of independent pulses or "first detections" are not considered. This is motivated by reasoning that in a modern radar the available pulses would be coherently filtered for optimal clutter suppression, with only as many CPIs being used as are necessary for blind velocity elimination and doppler ambiguity resolution. The output of the doppler filter in each range cell for each CPI then represents the independent "pulse" entering the CFAR processor. The number of independent "pulses" is thus the number of CPIs per dwell, which for low PRF radars would seldom be much more than three or four. Deviations from this assumption and the effect of increasing the number of bursts per dwell are addressed in Chapter 7.

The CFAR processing phase of the study analyses the CFAR detection performance in homogeneous K-distributed clutter and homogeneous K-clutter and Noise. This limitation of homogeneity is not considered to be severely restrictive since the K-distribution model is in any case a modulated Gaussian model, which can inherently account for some spatial fluctuations in mean clutter power. The assumed homogeneity of the clutter implies that the results of this study would be most applicable to sea clutter, and possibly extended weather clutter. However, broadening the definition slightly to include locally homogeneous clutter would additionally include many land clutter scenarios in the definition, provided some

[1]Note that the term "high resolution" as used in this thesis refers to conventional radar systems with fine spatial resolution, with range resolution typically of the order of ten metres and angular resolution of the order of a degree. Although finer range resolution radars are possible, they are not considered to represent the "typical" radar relevant to this project. The results presented in this thesis could nevertheless be applied to the performance analysis of such radars provided the target models used are modified accordingly. Again, synthetic aperture radars are not considered in this thesis.

form of segmentation between clutter regions is performed. Explicitly excluded from the CFAR processor analyses is a quantification of the effects of clutter discretes (strong, largely fixed, clutter "point" sources), extraneous targets in the region of interest, birds and insects, and anomalous effects such as angels. Results are presented for the common cases of Swerling 1 and 2 fluctuating targets (Rayleigh voltage distribution), which for single pulse analyses are identical. Results are often calculated numerically owing to the analytic intractability of the analysis for the K-distribution. Empirical relationships are established to facilitate application of this work to cases not explicitly covered herein.

1.4 PROJECT OUTLINE

Chapter 2 provides a historical review of models for sea clutter, introduces the K-distribution model, and presents a summary of some clutter amplitude and spectral characteristics. Adaptive optimal filters are discussed and various adaptation algorithms are compared. CFAR processing techniques, including non-parametric techniques, are reviewed.

The clutter suppression performance of doppler processors is evaluated and compared in Chapter 3. The relative performance of several well known doppler processors is examined under a wide range of clutter conditions, with particular attention being paid to the performance of AMTD processors. A large number of clutter scenarios are considered in an attempt to give results which are not too dependent on specific conditions. The clutter parameters are chosen to reflect land and sea clutter environments, including possible weather clutter components. Suitable performance measures are discussed, with particular attention being paid to filter-bank processing and M/N detection. The improvement factor of each type of processor is evaluated in each clutter scenario, and the loss relative to the optimal filter is determined. Statistical data analysis is used to reduce the data to manageable proportions and allow key conclusions to be drawn.

The performance of adaptive Hsiao-optimal filters in non-homogeneous backgrounds is investigated in Chapter 4. The case of practical adaptive estimation of the covariance matrix, and limiting cases where the estimate of the covariance matrix tends to the mean clutter covariance matrix, are considered. Three classes of non-homogeneous backgrounds are studied, namely 1) clutter in which the amplitude and spectral width in each range bin are randomly drawn from spatially invariant independent gamma distributed parent populations, 2) clutter edges, in which the range profiles of the clutter amplitude and/or spectrum exhibit a step change, and 3) homogeneous clutter in which some range bins are corrupted by returns with significantly different amplitude and spectral characteristics,

representing point clutter sources or extraneous targets. The use of pre-filter MTI is investigated as a means of reducing filter sensitivity to some classes of clutter non-homogeneity.

The problem of single pulse CFAR detection of Rayleigh fluctuating targets in spatially uncorrelated K-distributed clutter is addressed in Chapter 5. The performance of three types of well known CFAR processors, namely the CA, CAGO, and OS CFAR processors, is examined for several cases of desired false alarm probability and the number of reference cells used in the CFAR processor. Curves for the detectability loss due to the "spikiness" of the clutter are presented and values for the additional loss due to CFAR thresholding are tabulated. The effects of incorrectly estimating the clutter shape parameter ν are investigated. Empirical expressions are derived for ideal- and CFAR- detection losses in spiky clutter

The problem of CFAR detection in clutter with spatially correlated underlying variance, or modulation process, is addressed in Chapter 6. The case of complete correlation of the modulation process is addressed first and it is shown that the potential exists for a reduction in detection loss of in excess of 10 dB in highly correlated clutter. The K-distribution model is extended to facilitate the incorporation of spatial correlation properties. The key advantages of this model over previous models are that the spatial correlation is introduced to Gaussian processes, thus enabling well established linear filtering techniques to be used, the resulting clutter process is strictly K-distributed, and it leads to usable expressions for the multivariate modulation and clutter processes. The CFAR problem is then viewed as one of optimal filtering in multiplicative noise. The optimal filter and the corresponding CFAR processor are derived. Methods of estimating the local spatial correlation in real time and their effects on detection loss are discussed. An analytic formulation of performance prediction is presented with sample results for representative processor and system parameters.

The exploitation of the doppler and time domains is investigated in Chapter 7. The rationale behind the range-doppler-time CFAR processor, and a modification thereof, is discussed. The ideal case, assuming an infinite number of range reference cells and spectrally homogeneous clutter, is then considered to establish an upper bound on the performance of the RDT processor, and confirm that it is a promising area for further investigation. Thereafter more practical cases are examined: the statistics of the errors in the so-called "power normalisation terms" are determined and their effect on false alarm rate and detection performance is evaluated. Results are presented for a number of cases and the performance is compared to that of conventional processors. Deterioration in false alarm performance in spectrally non-homogeneous clutter is investigated. As a solution to this

problem the modified processor using only the test doppler in setting the threshold, termed the δ-CFAR, is presented. An example is presented to illustrate the superiority of the δ–CFAR processor proposed here over conventional processors, when using realistic radar system parameters.

Finally, the key results presented in this thesis are summarised in Chapter 8. Areas for further work are discussed and some conclusions regarding improved detection in spiky clutter are presented.

CHAPTER 2

LITERATURE REVIEW AND BACKGROUND THEORY

2.1 A REVIEW OF SOME CLUTTER CHARACTERISTICS

2.1.1 General Definitions

The term "clutter" refers to unwanted backscatter from the radar environment (land, sea, clouds, birds, etc.) which interferes with the primary function the radar is performing, be it detection or tracking. The clutter signal is comprised of the vector sum of all unwanted contributing sources or scatterers within the radar resolution cell. The relative movement of these sources with respect to each other, or changes in the phase between sources (caused by frequency agility), causes the clutter signal to fluctuate in time.

Four main factors are of importance in determining the effect of clutter returns on radar performance, namely 1) The mean amplitude of the clutter returns, related to the average backscatter reflectivity, 2) The spectral characteristics of the clutter signal, 3) The amplitude statistics of the backscattered signal, and 4) The spatial characteristics of the clutter. The first of these aspects has received a great deal of attention over the years and widely applicable theoretical and empirical models now exist for predicting clutter reflectivity as a function of important parameters such as frequency, polarisation, type of clutter, grazing angle and so on. Although the spectral characteristics of clutter cannot always be mechanistically explained, sufficient experimental data have been published to allow reasonably accurate estimates of clutter spectral characteristics to be obtained in many situations. These will be addressed in section 2.1.4. The amplitude statistics have also received a great deal of attention but only recently have models been proposed which accurately describe the non-Gaussian nature of clutter under some conditions. The impact of these models on radar performance has not yet been fully analysed. Finally, the spatial characteristics of the clutter returns have not yet received much attention; in the case of land clutter this is probably due to the extreme variability of data for different environments; in the case of sea clutter and weather clutter, some data illustrating spatial characteristics have been reported but generally applicable models for spatial properties have not been proposed.

The mean clutter reflectivity is not addressed here since for homogeneous clutter this affects only the mean Signal to Clutter Ratio (SCR), the implications of which are straightforward

and well understood. In this review of clutter characteristics and suitable clutter models, we will therefore concentrate on aspects relating to the amplitude and spatial characteristics of the clutter, and provide a brief review of spectral characteristics. The assumed homogeneity of the clutter in subsequent CFAR processor analyses implies that the results of this research would be most applicable to sea clutter, and possibly extended weather clutter. For this reason the emphasis in this chapter lies strongly on sea clutter characteristics and models. The characteristics of clutter discretes, birds and insects, and anomalous effects such as angels are not covered.

2.1.2. Sea Clutter: Basic Principles

The signal received by the radar due to sea backscatter is the vector sum of the fields caused at the radar by each of the individual scattering sources (waves, ripples, spray, interactions between simple sources, etc.) within the spatial resolution cell in question. The largely random movement of the scattering sources relative to each other causes the vector sum to fluctuate randomly, causing in turn a random fluctuation in the received backscatter energy. This fluctuation in the received signal causes the clutter return to exhibit characteristics which are somewhat similar to radar thermal noise, the amplitude statistics of which are described by the Rayleigh probability density function (PDF). It is now well known, however, that under many operating conditions, particularly at low grazing angles and in radars with high spatial resolution, the clutter appears "spiky" and the amplitude statistics deviate from being noise-like, with a wider range of clutter amplitudes being likely. The clutter amplitude PDF therefore differs from that of thermal noise (Rayleigh PDF) most notably in having longer "tails", ie. the PDF does not roll off as steeply for high values of clutter amplitude. This is statistically described by the third and higher moments of the sea clutter PDF being higher than for Rayleigh noise, for equal powers (second moments) in the clutter and noise signals. Several alternative PDF's have been proposed which better describe the amplitude distribution of spiky sea clutter, and these are discussed later.

The rate at which the scatterers move relative to one another determines the rate of the fluctuations in clutter amplitude in a given radar spatial resolution cell. The observed clutter amplitude may therefore be correlated from one observation to the next. It has been found that clutter fluctuation rates can be roughly divided into two main regimes: 1) Fast fluctuations (short correlation times, of the order of milliseconds), such that the clutter is largely decorrelated from pulse to pulse. These fluctuations arise as a result of the relative movement of scatterers in the resolution cell. 2.) Slow fluctuations (long correlation time, of the order of hundreds of milliseconds or seconds), such that the clutter is essentially correlated over the period of the radar dwell time, but decorrelated from one observation to the next. Several mechanisms have been attributed to this phenomenon, relating to the

number of scatterers within a resolution cell, or the mean strength of each scatterer in the resolution cell. Additionally, very slow fluctuations (very long term correlation, of the order of minutes or hours) are sometimes also considered, such that the overall clutter characteristics are essentially correlated over several radar observations, but vary over all possible radar operating conditions. These fluctuations are caused by factors such as the sea state and wind conditions. Recently an additional very fast fluctuating component has also been reported (Helmken, 1990), with mean velocity equal to the wind velocity, which has been attributed to turbulence induced clear air refractive scattering.

An alternative way of viewing slow fluctuations in sea clutter is in terms of spatial correlation. That is, the swell structure of the sea may cause the mean clutter amplitude in one spatial resolution cell to be related to that in adjacent cells, by some as yet unspecified mechanism. Different physical regions of operation, and regions of sea with different sea state and wind conditions, would also yield sea clutter with different statistics, relating to very long term correlation. Fast fluctuations, or short term temporal correlation, are not easily represented in terms of spatial correlation, since the mechanisms involved generally cover a far smaller area than the radar spatial resolution cell, implying independence of these mechanisms from cell to cell. Fast fluctuations are usually handled in the frequency domain through their Doppler characteristics, which are discussed in section 2.1.4.

The clutter amplitude statistics, defined usually by the PDF, and the spatial and temporal correlation properties, defined either by the Autocorrelation Function (ACF), and/or the Doppler spectrum, jointly completely describe the statistical properties of the sea clutter, on which radar performance calculations must be based. This study is concerned with both aspects; the amplitude statistics are obviously of importance since the detection procedures used are based on the amplitude of the received signal relative to the estimated background noise or clutter level. The correlation properties of sea clutter, including the spatial correlation properties, are also of interest since we are concerned with doppler processors operating over several pulses, and CFAR processors operating over a range window of several range cells in length and possibly over several bursts as well.

2.1.3 Historical Review of Models for Sea Clutter Amplitude Statistics

The non-Rayleigh nature of sea clutter statistics under certain operating conditions has been known for some time. One of the earlier attempts to model this statistically was by Norton et al. (1955), who used a Ricean distribution (ie. the envelope of a complex Gaussian signal plus a constant) to model the return from a given sea patch over a time which was short compared to the slow fluctuation rate of the sea. Although this is effective in

modelling certain types of land clutter where there is an essentially fixed clutter source present, it is inadequate in modelling the slowly fluctuating component in sea clutter. Most of the work prior to the mid 1960s was, however, aimed at modelling clutter surfaces with a view to determining the mean clutter reflectivity, and to a lesser extent, the short time doppler spectrum. To this end, Katzin (1957) presented some theory for scattering from a smooth surface with facets of dimension of the order of a wavelength. Although he noted the existence of clutter spikes which were attributed to interference effects at low grazing angles, no detailed statistical modelling was attempted. Three years later Spetner and Katz (1960) published "Two Statistical Models for Radar Terrain Returns", which - despite the title - was useful for modelling sea clutter as well. The two models presented, namely of specularly reflecting facets on a continuous surface, and a large number of independent elementary scatterers, form the basis of many models still in use. These models, however, resulted in discrepancies with experimental data with regard to the wavelength dependence of the clutter reflectivity and some polarisation effects, and Long (1965) proposed the "two mechanism model". In this model the sea is taken as consisting of a wind dependent fine structure (which Long attributed to ripples) of elementary scatterers, modelled as randomly oriented dipoles, superimposed upon a larger structure of smooth facets, related to the swell structure. Guinard and Daley (1970) also presented a composite surface model, consisting of a slightly rough surface superimposed on a swell structure which gives an average "tilt" to the surface. These two-mechanism models provide reasonable estimates for clutter reflectivity as a function of frequency, grazing angle and polarisation under most conditions, and are of interest in later models which address the clutter amplitude statistics.

Later in the 1960s, the importance of statistical models for clutter distributions in time, space, and amplitude, as well as doppler frequency, was recognised. George (1968) proposed the Log-Normal distribution as suitable for modelling spiky sea clutter, but it has been demonstrated by several authors than in general the Log-Normal distribution has tails which are too high: the true situation seems to lie between the Rayleigh and the Log-Normal distributions. Trunk (1969) and Trunk and George (1970) suggested that the so-called "contaminated" normal distribution, based on the I and Q components of the complex signal having a PDF described by the sum of two Gaussian distributions of different variances, was a better description of sea clutter amplitude statistics. This equates physically to the sea clutter consisting of a mixture of Normally distributed quantities. However, this model never found wide acceptance, possibly due to the lack of mechanistic justification for the model and its relative mathematical inconvenience. More recently several authors have proposed that the Weibull distribution yields a good fit with experimentally measured data, facilitated in part simply by it being a two parameter distribution.

While the experimental data matches are certainly quite good, there again appears to be little justification for this model based on physical mechanisms, and it does not enable the various correlation domains to be adequately handled. It does also not provide a physically justified means of generating simulated data of arbitrary correlation properties.

Long (1983) summarised the state of the art at the beginning of the 1980s as follows: "Neither the Rayleigh, the Log-Normal, nor the Contaminated normal actually describe all observed distributions. The echo, it would seem, consists of rapid fluctuations (dopplers) that are Rayleigh distributed plus a component that is fluctuating slowly, and for which distributions have not yet been reported." This modulated Rayleigh representation of sea clutter was in fact introduced as early as 1972 by Trunk (1972), who stated that "the non-Rayleigh distribution of sea clutter ... is caused by the spatial variation of the returned power σ_0". To support this assertion he presented a "Time Varying Rayleigh" model, whereby the return from a patch of sea exhibits Rayleigh statistics, the power of which varies over some time period which is long relative to the fast (Rayleigh) fluctuations. Trunk did not, however, propose a PDF for the spatial or slow temporal fluctuations. In addition, he used statistical tests for significance to demonstrate that the short term PDF is not in fact exactly Rayleigh but rather approximated by the Chi- or Ricean distributions, with only the Ricean having any physical significance. He further proposed that such spatially modulated models would be useful for representing land clutter in some situations.

Experimental observations made by workers at RSRE in the late seventies and early to mid eighties also indicated that irrespective of radar resolution cell size (within reasonable limits) and sea conditions, the clutter in a given range cell is approximately Rayleigh distributed over a short period (relative to the slow fluctuations). The mean value of the clutter amplitude, or the clutter power, however, was found to vary slowly in time and from range cell to range cell. This again suggested that a modulated Gaussian model should provide a good representation of sea clutter, and the K-distribution was proposed as such a model which yielded a good fit with experimental data and which was relatively mathematically tractable. An advantage with modulated Gaussian models is their inherent ability to represent short, medium and long term correlation of arbitrary ACF. Some physical justification for the K-distribution has also been presented (eg. Ward et. al (1990), Jakeman and Pusey (1983), Oliver (1984), and Lewinski (1976)). The properties and physical interpretation of the K-distribution will be dealt with in more detail in the next section of this chapter. The K-distribution was first proposed for sea clutter by Jakeman and Pusey in 1976, around which time its application to describing the scattering of coherent laser light was also being investigated (eg. Parry and Pusey (1979), Parry et. al. (1978), Parry (1981)). Since then several papers have appeared in the literature describing

properties of the K-distribution, presenting empirical relationships for relating distribution parameters to wind conditions and radar polarisation (eg. Ward and Watts, 1982, 1985), and assessing aspects of radar performance in K-distributed clutter (eg. Watts, 1985, 1987, Watts et. al., 1990). Chan (1990) presents quite extensive data showing the superiority of the K-distribution over the Rayleigh, Weibull and Log-Normal distributions under a wide range of conditions.

2.1.4 Sea Clutter Doppler Spectrum

The doppler spectrum of sea clutter has received widespread attention. A vast amount of data is available in the literature and a comprehensive review of sea clutter spectra is beyond the scope of this thesis. However, some selected papers are listed below as an entry point into the field of modelling sea clutter spectra. Long (1983) provides a good summary of research into sea clutter spectra up to about the mid-1970s. More recently Helmken (1990) has presented some results of studies into L- and S-band sea clutter data. Chan (1990), reports on an analysis of sea clutter data at X-, S- and L- band, UHF and VHF, and shows that clutter spectra are strongly dependent on the radar frequency. Atanassov et. al (1990) separate sea clutter data into "bursts" and "pauses", and characterise the spectra of the two classes at X- and Q- band. Ward et. al (1990) have also reported some characteristics of coherent sea clutter data, noting particularly the higher order spectral characteristics. Maurer et. al. (1990) report on the spectrum of some anomalous returns due to ducting, which have been observed with high regularity. Sittrop (1985) presents empirical equations for the spectral width as a function of radar and environmental parameters and presents some plots of spectral width as a function of the angle between the wind direction and the radar boresight, with sea state and wind speed as parameters.

From all these data the key features of sea clutter relevant to this study can be summarised as:

1) Sea clutter generally has a bimodal spectrum. The strength of the high doppler frequency component reduces with increasing radar frequency. For X-band or higher radar frequencies this component becomes negligible, such that the clutter appears unimodal.

2) The dominant component has a mean velocity of typically 0.15 to 0.25 of the wind velocity and a standard deviation of the order of 0.5 to 1 m/s, and is held to correspond to capillary wave structure (Helmken, 1990). The weaker component with mean velocity of the same order as the wind velocity and spread equal to or wider than the spread of the dominant component is variously attributed to wind

blown spray and droplets (Long, 1983; Atanossov, 1990), clear air scattering (Helmken, 1990), and high orbital velocity at breaking waves (Atanossov, 1990).

3) The mean doppler shift of both the dominant and minor spectral components is dependent on the wind speed and the angle between the wind direction and the radar boresight. This implies that clutter suppression of non-zero mean doppler clutter is essential if sea clutter is to be effectively suppressed.

4) In situations of homogeneous sea clutter it is often assumed that the doppler characteristics are constant over range. However, in many cases the spectrum varies considerably between range bins. This can be compounded by spatial variations in the underlying clutter variance, and some evidence exists to suggest that the doppler characteristics can be related to the mean clutter amplitude in each cell (Atanassov, 1990). No models have been proposed for describing either the spatial spectral variations or the correlation between the local amplitude and spectrum. This is addressed further in Chapter 4.

2.2 THE K-DISTRIBUTION MODEL FOR CLUTTER

The K-distribution was introduced to the field of radar clutter with a view to the specific application of statistically modelling non-Rayleigh sea clutter, and most literature has concentrated in this area. Recently, however, some papers have also appeared which discuss the applicability of the K-distribution to land clutter under certain conditions (eg. Oliver, 1988).

As already mentioned, the K-distribution is a form of modulated Gaussian distribution: a complex Gaussian process is modulated by a function whose PDF is chi-distributed. This equates to modulating the *power* of the Rayleigh envelope of the Gaussian signal with a gamma distributed variable. When applied to radar sea clutter this represents the case where the clutter voltage in a given resolution cell exhibits rapid[1] Rayleigh fluctuations, the mean power of which varies in time with a "slow"[2] fluctuation rate, and from one resolution cell to the next, according to a gamma distribution. The degree of correlation of the modulation between resolution cells depends on the spatial correlation properties of the

[1]The term "rapid" is taken here to imply that the Rayleigh fluctuations are essentially completely decorrelated from one detection opportunity to the next, presumably through the use of frequency agility over a sufficient bandwidth and/or the the use of a high radar frequency.
[2]The term "slow" is taken here to indicate that the clutter modulation process remains entirely correlated over the radar Coherent Processing Interval (CPI).

sea surface. In this study, since we are concerned with single dwell detection, the temporal and azimuthal fluctuations of the modulation are not of significance and instead we represent all fluctuations as occurring over *range*. Hence only correlation of the modulation process in range will be considered. The rapid Rayleigh fluctuations, usually termed the *speckle*, are entirely decorrelated from one range bin to the next.

Before defining the K-distribution in mathematical terms and discussing some of its properties, the basis of the assumed gamma distributed spatial power variations and the locally Rayleigh fluctuating speckle will be briefly discussed. Dealing with the speckle first, it is assumed to have Rayleigh amplitude fluctuations for the following reasons:

1. The Two Parameter models which form the basis of modulated Gaussian distributions postulate that the fine structure, which gives rise to the speckle, consists of small scatterers such as ripples and spray. It is reasonable to expect that a large number of these will be present in each resolution cell of a practical radar, thus causing conditions in which the central limit theorem, and hence Rayleigh envelope statistics, is valid.

2. Experimental evidence published in the literature indicates that the speckle is close to Rayleigh, and is often statistically indistinguishable from being Rayleigh (eg. Ward et. al., 1990).

3. As will become apparent in the body of this thesis, the assumed complex Gaussian nature of the speckle has fortuitous analytical benefits. The most important of these is that the since the clutter in a given range cell exhibits Rayleigh amplitude fluctuations, the ideal clutter suppression filter is a linear filter. The analysis of such a filter operating on complex Gaussian signals is much simpler than for a non-linear filter acting on non-Gaussian signals.

The case for the adoption of the gamma distribution for the spatial or slow temporal fluctuations in clutter power is not so straightforward. As yet no conclusive mechanistic argument has appeared to justify the gamma distribution, and at present the main reasons for the rather widespread acceptance of the gamma distribution of power (giving the K-distribution) seem to be the good fit it provides with experimental data (Chan, 1990) and the relative tractability of the associated mathematics. In addition, several plausible mechanistic explanations have been offered, which although maybe not being conclusive individually, do collectively provide a somewhat persuasive argument, especially since neither the Weibull nor the Log-Normal Distributions are based on *any* mechanistic

explanation. These include:

1. The gamma distribution is a single sided two-parameter distribution. It therefore has the correct basic properties and the flexibility required to enable it to adequately model the power fluctuations.

2. As the shape parameter of the gamma distribution tends to ∞, the gamma PDF tends to a delta function. This implies that the resulting K-distribution tends to the Rayleigh distribution. Thus the requirement is met that the resulting distribution should encompass the Rayleigh distribution as a special case.

3. The gamma distribution has been obtained as the first term of the Laguerre expansion of an arbitrary one sided PDF (Lewinski, 1976). The gamma distribution is therefore an approximation to any PDF that may exactly represent the power fluctuations.

4. The gamma distribution has been shown to be the general approximate solution for the intensity distribution of the sum of a number of random vectors. Terrain scatterers and complex cultural targets have been represented by the random vector model (Lewinski, 1976).

5. It is intuitively reasonable to expect that if the power fluctuations obey a given distribution at one radar resolution, then they should obey the same distributions at other resolutions. This is experimentally and theoretically true for the gamma distribution, with changes in radar resolution requiring only changes in the gamma distribution shape parameter.

6. The gamma distribution has been shown to represent the bunching of scatterers arising from a birth-death-migration process, which is a plausible representation of the fine structure of the sea surface (Jakeman and Pusey, 1983).

We now proceed with a more mathematical description of the K-distribution. We define the exponential speckle s, the Rayleigh speckle $r = \sqrt{s}$, the gamma distributed power modulation process u, the voltage envelope modulation process $v = \sqrt{u}$, and the overall clutter voltage x, such that $x = vr = \sqrt{su}$. If the PDF of the speckle is given by :

$$p_r(r|v) = \frac{\pi r}{2v^2} \exp\left[\frac{-\pi r^2}{4v^2}\right] \qquad \ldots (2.1a)$$

and the PDF of the voltage envelope modulation process v is given by

$$p_v(v) = \frac{2\nu^{2\nu}}{\Gamma(\nu)} v^{2\nu-1} e^{-b^2\nu^2} \qquad \ldots (2.1b)$$

then the PDF of the clutter voltage x is found to be given by:

$$p_x(x) = \int_0^\infty p_r(r|v)\, p_v(v)\, dv = \frac{4c}{\Gamma(\nu)} (cx)^\nu K_{\nu-1}(2cx) \quad (0 \le x < \infty) \qquad \ldots (2.1c)$$

where $K_\nu(x)$ is a modified Bessel function, ν is a shape parameter dependent on the "spikiness" of the clutter, and c is a power parameter, such that the mean clutter power $P_c = \nu/c^2$. The value of ν can vary between 0.1 for very spiky clutter to ∞ for Rayleigh clutter. The Complementary Cumulative Distribution Function (CCDF) of the K-distribution, ie. Prob ($X \ge x$), is given by:

$$P(X \ge x) = \frac{2}{\Gamma(\nu)} (cx)^\nu K_\nu(2cx) \qquad (0 \le x < \infty) \qquad \ldots (2.2)$$

The sum of N identical K-distributed variables cannot in general be obtained in closed form. However, for values of $\nu = m + 1/2$, m = 0, 1, 2, ..., closed form expressions have been derived, and these are given in Appendix 2.1. In particular, it can be noted that for $\nu = 0.5$, the K-distribution reduces to the exponential distribution, the sum of N of which yields a gamma distribution of shape parameter $\nu' = N$. For $\nu = 1.5$, the K-distribution reduces to a gamma distribution of shape parameter $\nu' = 2$, the sum of N of which yields a gamma distribution of shape parameter $\nu' = 2N$. For $\nu = m + 5/2$, the K-distribution can be expressed as a mixture of gamma distributions, which although interesting does not seem to have any physical significance or analytic advantages.

The moments of the K-distribution are given by

$$\overline{x^n} = \frac{1}{c^n} \frac{\Gamma(\nu + n/2)}{\Gamma(\nu)} \Gamma(1 + n/2) \qquad \ldots (2.3)$$

from which the variance is found to be $\overline{X^2} = \nu/c^2$ and the mean value $\overline{X} = ((\sqrt{\pi})/2c)\Gamma(\nu+1/2)/\Gamma(\nu)$. In general it has been shown that the moments of the K-distribution always lie between those of the Rayleigh and Log-Normal Distributions, for matched first and second moments, which agrees well with experimental data.

When the K-distributed clutter is simultaneously present with radar thermal noise or other

Rayleigh distributed interference, the overall distribution is no longer K-distributed and cannot be expressed in closed form. However, closed form expressions can be found for the even moments of the overall distribution and Watts (1987) has derived an expression which enables the Clutter-to-Noise Ratio (CNR), the scale parameter c and the shape parameter ν to be uniquely determined through knowledge of the first three even moments of the overall signal. If the presence of thermal noise is neglected then c and ν can be determined from the first two even moments, in which case an "effective" shape parameter ν_{eff} is determined which is related to the true value of ν and the CNR by

$$\nu_{eff} = \nu \left(1 + \frac{1}{CNR}\right)^2 \qquad \ldots (2.4)$$

This expression, which will henceforth be referred to as Watts' approximation, is often used as a simple means of representing K-clutter plus noise. An evaluation of the effect of errors introduced by Watts' approximation is given in Chapter 5. Other methods of dealing with K-clutter plus noise based on Pade Approximations have also been proposed (Ritcey, 1989), but these will not be covered here since they are also approximations and seem to offer little over Watts' simple approximation other than significantly more difficult mathematics.

An important property of K-distributed clutter is its response to doppler filtering. The clutter in each range bin is modelled as exhibiting Rayleigh fluctuations, with the variance of these fluctuations remaining constant within the CPI (if not the entire dwell period). The quadrature components of the signal in each range bin therefore exhibit locally short term stationary Gaussian amplitude statistics. Filtering of these quadrature Gaussian components will yield a complex Gaussian signal of power multiplied by the power gain of the filter. For a given range bin, the envelopes of the signals in each doppler bin of a filter bank are therefore all Rayleigh distributed, with power given by the power gain of the corresponding filter. The power of these Rayleigh processes still varies from range bin to range bin according to the gamma distribution, exactly as if no filtering had been performed. The output in each doppler bin is therefore K-distributed with the same shape parameter as the input clutter signal, and with the power modified by the filter's power gain. As mentioned in Chapter 1, this enables the doppler filtering and CFAR processing to be analytically separated, providing linearity of the filter is assured.

Although the K-distribution has been applied primarily to sea clutter, recent papers have also indicated its applicability to other types of clutter. Miller (1989) proposes the K-distribution for modelling weather clutter. The justification for Rayleigh fluctuations within

a range bin is obvious, and Miller shows that the power variation in range is well described by the gamma distribution, resulting in the overall weather clutter PDF being K-distributed. Oliver (1988) shows that the K-distribution model is capable of representing land clutter textures in regions of homogeneous clutter provided the spatial Autocorrelation Function (ACF) used is correct. Oliver's work concentrated on 2-dimensional SAR imagery, but it would not appear to preclude 1-dimensional (range) clutter images in conventional high resolution radars in certain clutter environments. Finally, another interesting feature of the K-distribution is that it arises from the perfect Moving Target Indicator (MTI) filtering of a modulated Ricean distribution in which the fixed component varies with arbitrary PDF and the noise component varies with gamma PDF. Such a model, though not proposed in the literature, can be expected to be representative of many land clutter scenarios due to the large number of independently variable parameters and the fact that it allows both fixed and fluctuating clutter sources to be modelled. The K-distribution would therefore be suitable for representing land clutter in radars employing practical MTI filtering or MTD processing, provided that the clutter suppression at zero doppler effectively suppresses the fixed clutter components.

For completeness, and to give the reader unacquainted with the K-distribution a feel for the PDF and CDF of the K-distribution, plots of the PDF and CCDF are illustrated in Figs. 2.1 and 2.2 respectively for different values of ν. It can be noted that for $\nu < 0.5$ an integrable singularity exists at $x = 0$ in the PDF. This complicates analysis significantly and care must be taken to ensure that numerical techniques can adequately handle this singularity.

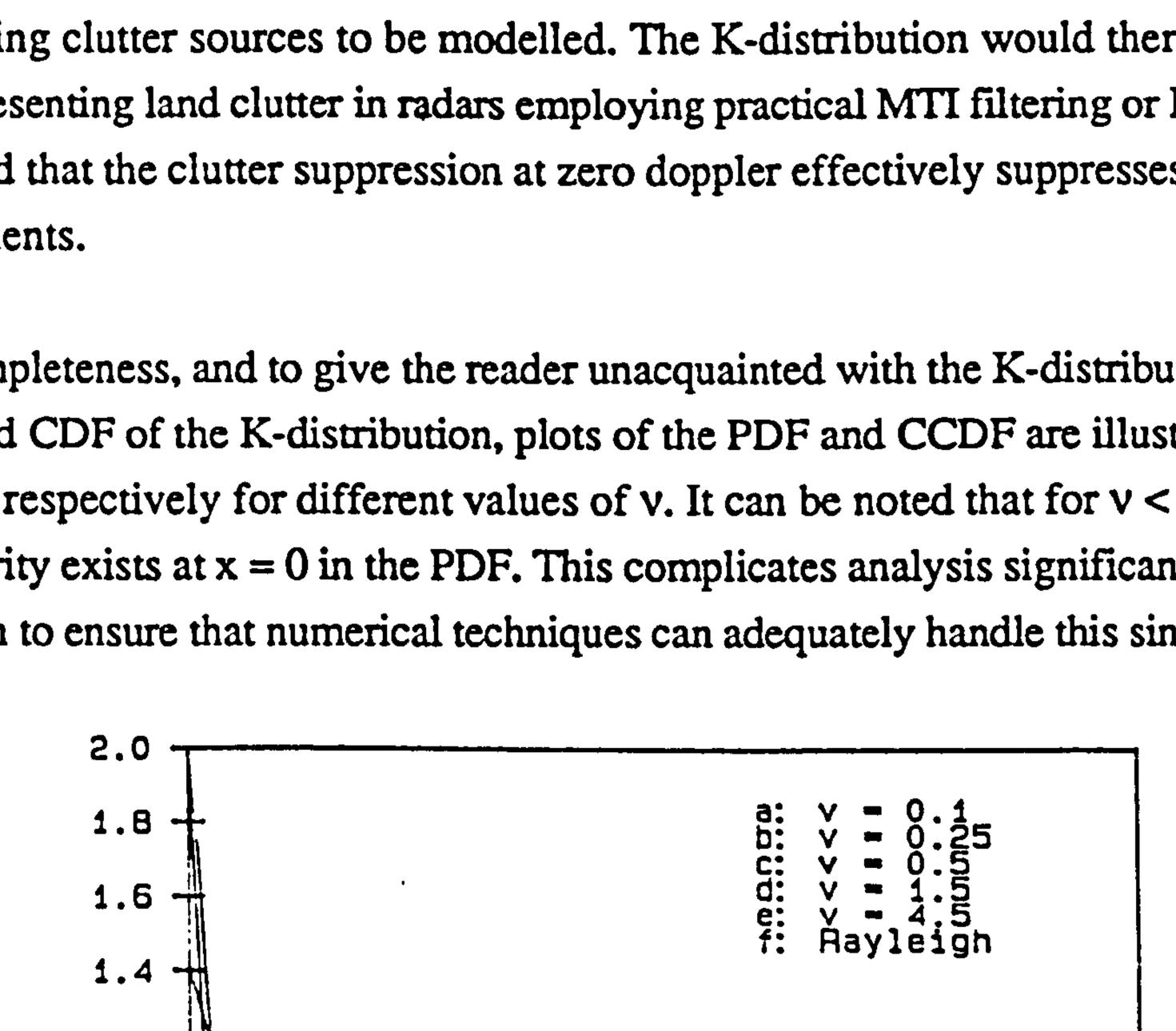

Fig. 2.1 *K-distribution PDF for various values of ν, for normalised power*

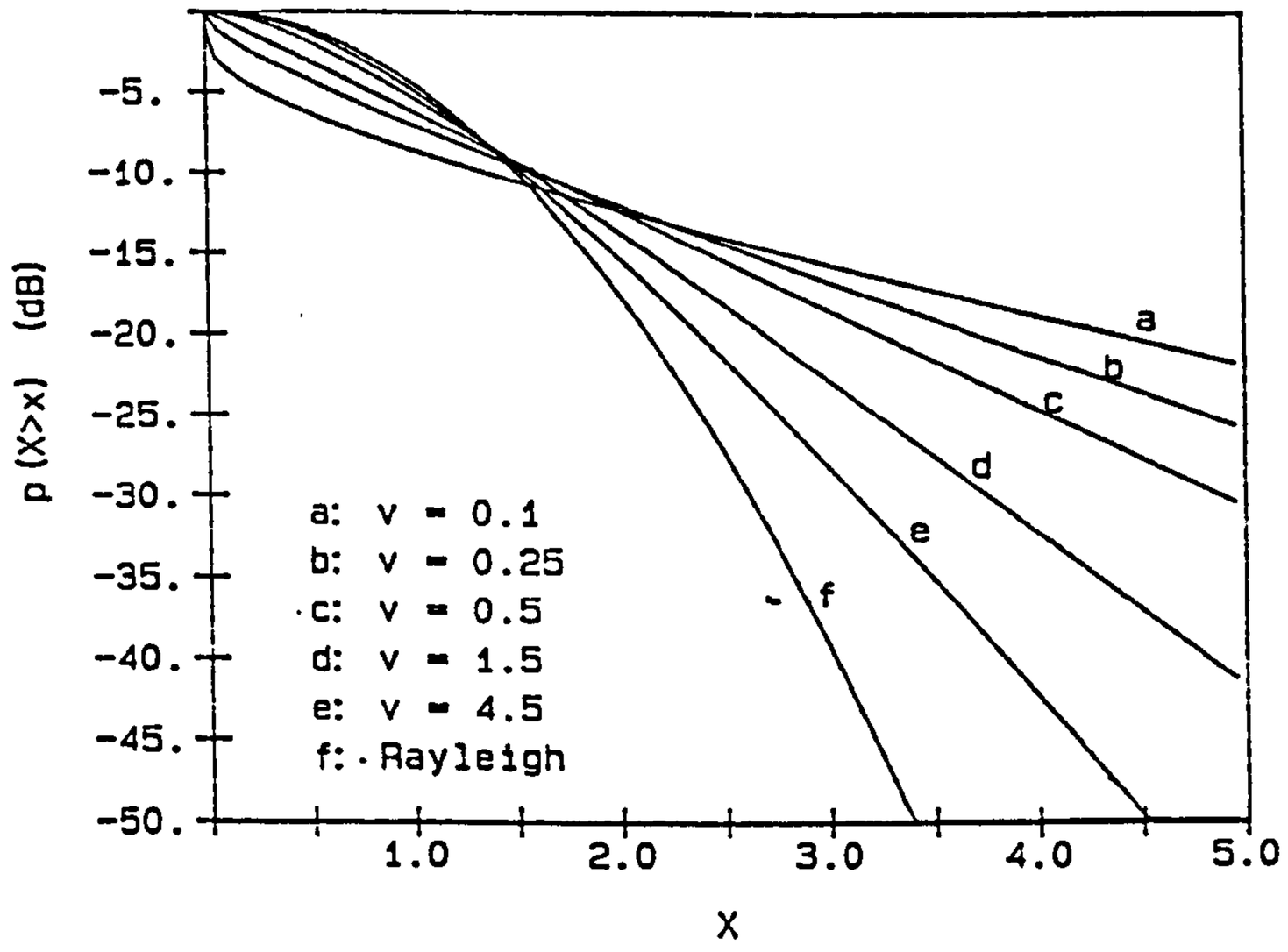

Fig. 2.2 *K-distribution CCDF for various values of* ν*, for normalised power*

2.2 A REVIEW OF ADAPTIVE DOPPLER PROCESSING TECHNIQUES

In this brief review a summary of the performance considerations and possible limitations of several techniques for adaptive cancellation of clutter are discussed. A brief description of each technique is also provided.

Clutter suppression filters are generally based on an autoregressive model for the time samples of the clutter returns, resulting in a linear Finite Impulse Response (FIR) filter for cancellation. Fully adaptive clutter cancellation techniques differ in the optimisation criteria chosen, and in the manner in which new input data is used in updating the weights of the cancellation filters. Two alternative optimisation criteria are usually used, namely 1) the maximisation of the improvement factor (Hsiao, 1974), and 2) the minimisation of the clutter residue (eg. Farina, 1984). Under conditions of negligible thermal noise and a uniform PDF for target doppler over the radar's doppler space, the two criteria are equivalent.

If the optimality criterion chosen is the maximisation of the Signal to Clutter-plus-Noise Ratio (SCNR) at the filter output (which generally equates to the maximisation of detection probability) then the optimum filter weight vector $\mathbf{w} = \{w_1, \ldots w_N\}$ is given by the solution of the matrix equation $\mathbf{w} = \mathbf{M}^{-1}\mathbf{s}$, where $\mathbf{M}$ is the clutter covariance matrix and $\mathbf{s}$ is the vector of returns from the desired target, usually chosen as a unit magnitude complex

vector rotating at the desired target doppler (Hsiao 1974). The resulting filter is often referred to as a Hsiao filter. Since the target doppler is in general unknown in practical situations, a bank of filters, each tuned to a particular target doppler, is required. Hsiao filters provide the best possible performance for non-fluctuating or slowly fluctuating targets provided the covariance matrix **M** is accurately known.

If the filter is optimised to minimise the clutter residue (as opposed to optimising the output SCNR for a desired target doppler as for the Hsiao approach) a "Linear Predictor" (LP) filter results (Farina, 1984). In this case the filter coefficients are obtained from the solution of $\mathbf{w} = \mathbf{M}^{-1}\mathbf{r}$, where **r** is the correlation vector between the i^{th} and the $i+j^{th}$ received clutter samples, with j = 1...N. Linear predictors are not "tuned" to a given target doppler and hence a single filter is sufficient, as opposed to the bank of filters in the Hsiao approach. However, this implies that Linear Predictor filters do not exploit the possibility of coherent integration and hence their performance is generally inferior to that of Hsiao filters. Absolute performance again depends on the accuracy with which **M** can be estimated.

The key aspect to achieving effective adaptivity is the accurate explicit or implicit estimation of the clutter covariance matrix **M** (some methods yield the weights directly without actually determining **M**). In practice **M** has to be estimated on-line from a number of range cells in the vicinity of that being filtered. This causes errors in **M** and hence sub-optimal performance. The effects of resulting errors are addressed in Chapters 3 and 4 of this thesis, along with other limitations of adaptive optimal filters.

Various techniques for estimating **M** have been proposed, including:

1. Least Mean Square or Minimum Square Error adaptation (LMS)
2. Normalised LMS (NLMS)
3. Sample Matrix Inversion (SMI)
4. Direct Matrix Inversion (DMI)
5. Gram Schmidt Orthogonalisation (GS)
6. Parametric estimation (PE)

A brief description of each of these techniques is provided in Appendix 2.2. In view of the fact that the SMI technique is a maximum likelihood estimator of **M**, is numerically equivalent to the Gram-Schmidt algorithm, shows good convergence properties, is computationally feasible, and is intuitively easy to understand, it has been adopted as the method of estimating **M** in subsequent analyses in this thesis.

2.2.1 Performance Considerations

The relative performance of various of the abovementioned techniques has been compared in several papers. However, no clear-cut conclusions can be drawn from these papers as to the most effective technique; the data are often not directly comparable and sometimes contradictory, and one often gets the impression that quoted performance depends strongly on the specific clutter environment assumed. Nevertheless, in this section an attempt will be made to draw together consistent trends in the available data.

In general the adaptation of the filter to the local environment is performed by estimating the clutter spectrum, or equivalently its covariance matrix, by averaging over several range cells in the region of interest. The size of the range window needed for averaging equates to the transient response of the processor. It is clearly desirable to reduce this as far as possible. The difference between the steady state improvement factor achieved by an optimal filter in which the clutter covariance matrix is known *a priori*, and one in which it is adaptively estimated, is the steady state loss. These two performance factors - the transient response and the steady state loss - are the most commonly used criteria for comparing the performance of various adaptive techniques, along with implementation issues such as the computational throughput (usually measured in terms of the number of complex multiplications required per unit time), numeric precision, and storage requirements. In addition, the suitability of the techniques for staggered PRI or burst-to-burst frequency agile waveforms may be important. Although not widely addressed in the literature, the response of the processors to non-homogeneous environments, multiple or extraneous targets, pulsed interference, and fluctuating targets may be important.

With regard to the choice of optimisation criteria, several authors have shown that the maximisation of the improvement factor (yielding the "Hsiao filter") invariably yields better results in terms of final detection probabilities than the minimisation of the clutter residue (yielding the "linear predictor") (Farina, 1988; D'Addio, 1984; Barbarossa, 1987; Hansen, 1980). This is probably attributable to the fact that in the former situation some of the degrees of freedom of the filter are employed to give coherent integration of the target signal, rather than giving diminishing returns on clutter cancellation. However, this implies a bank of filters to cover all possible target dopplers, and the associated collapsing losses do not seem to have been included in the comparisons. The magnitude of the superior performance of Hsiao filters to linear predictors depends strongly on the assumed clutter spectra, clutter to noise ratio, and target parameters; values quoted generally lie in the range 0-2 dB, but in some (possibly unrepresentative) situations the difference can be more than 10 dB (Barbarossa, 1987).

Generally speaking, it would appear from most of the literature on the topic that steady state losses of the order of 2 - 8 dB can be achieved for "realistic" parameters (Reed, 1974; Farina, 1983, 1984a; 1984b; Gibson, 1985). The transient response of the various techniques differs widely; the LMS algorithm sometimes does not converge to the optimum for almost infinite numbers of range bins (Reed, 1974; Nitzberg, 1986), whereas the DMI or SMI techniques approach steady state performance using about 20 range bins (Reed, 1974; Farina, 1983). More stringent constraints on the transient response increase the steady state loss considerably: a linear predictor averaging over 6 range bins has been shown to exhibit a steady state loss in improvement factor of 6 - 9 dB, depending on the order of the filter and the clutter environment (Farina, 1988). Similar or worse behaviour can be expected from the adaptive techniques used to give the weights of Hsiao filters.

The question then arising is whether or not adaptive techniques with stringent transient response constraints give any benefit compared to conventional MTI, adaptive MTI, or pulse doppler FFT techniques. There is little doubt that in homogeneous Gaussian clutter the steady state performance of optimal techniques surpasses that of conventional processors if the number of reference cells is large. The magnitude of the increase in improvement factor depends on several factors, including the assumed clutter spectral properties, the CNR, and the number of pulses processed. Some theoretical studies have indicated that, for the same total number of pulses used, Hsiao filters provide 5 - 20 dB better improvement factor than a conventional binomially weighted MTI followed by a coherent integrator (Hsiao, 1974; D'Addio, 1984; Barbarossa, 1987; Schleher, 1982). These figures, however, are based on the clutter covariance matrix being known *a priori*, not adaptively estimated, and are derived from only a few specific clutter scenarios which may be particularly severe for MTI-based filters. The greatest benefits also occur under fairly specific conditions of high CNR (~60 dB) and broad clutter spectra. Some results have been published for the performance of lattice linear predictor filters in real radar systems (Gibson, 1985); the improvement factor has been compared to "normal" MTI filters under a large number of adverse conditions. The linear prediction filter was shown to consistently outperform the MTI by of the order of 5 - 10 dB for rain and snow clutter, despite a dynamic range limitation of 36 dB in the radar used. It is not clear from these results, however, whether the adversity of the conditions was more significant for the linear predictor or MTI filters. For ground clutter the conventional MTI seemed to offer slightly better performance than the linear predictor, due no doubt to a breakdown of the assumption of clutter homogeneity. In general these measured results are therefore not inconsistent with the abovementioned theoretical results if the effects of adaptivity are borne in mind.

The limitations of adaptive techniques, discussed in the next section, have led to the development of the MTD processor (Anderson, 1980), and recently to the Adaptive MTD (AMTD) processor (D'Addio, 1985; Galati, 1985). The MTD processor assumes the most likely clutter suppression requirement for each possible target velocity and the optimal filter is accordingly implemented. This eliminates the need for real time estimation of the clutter spectrum and solution for the filter weights, at the expense of sub-optimal filter implementations in some clutter. The advantages claimed for MTD processing as opposed to MTI-FFT techniques include 1) the burst length is arbitrary, 2) there is greater freedom in the positioning of zeroes in the frequency response, and the shaping of the associated rejection notches, and 3) each filter can have a different frequency response, thereby approaching optimal performance for that target doppler under many clutter conditions. This is particularly beneficial in doppler regions near zero where the minimisation of tangential fading motivates the narrowest possible rejection notch. Published results indicate that MTD processors approach optimal performance under a wide range of conditions (2 - 10 dB loss, depending on the clutter spectrum), and consistently outperform conventional techniques by several dBs (Hansen, 1980; Anderson, 1980; D'Addio, 1985). No direct comparison has been found in the literature comparing the performance of AMTD and adaptive optimal techniques.

Further developments of the MTD processor have yielded the Adaptive MTD: the selection of the bank of filters is made from a library of several possible choices, the choice being dependent on the local clutter environment. Current techniques limit the adaptation to the presence or absence of significant stationary ground clutter, implemented by a clutter map. This clearly has limited applicability to systems in which either the platform or the clutter is moving, or in which an essentially infinite number of elevation positions are available, such as in a mechanically scanned pencil beam radar. Nevertheless, within these limitations, performance close to the optimum has been demonstrated (D'Addio, 1985).

2.2.2. Limitations of Adaptive Techniques.

In this section some of the acknowledged and potential limitations of adaptive processors are mentioned with a view to indicating possible areas in which they can either be made more practicable or should be discounted as possible solutions.

1. *Clutter heterogeneity*

   A major limitation is the assumption of clutter homogeneity, both in terms of amplitude and spectral statistics. The impact of amplitude non-homogeneity has been addressed

and found to be relatively minor under some conditions (Nitzberg, 1990). However, that analysis assumed a constant clutter spectrum.

2. *The effect of clutter edges*

Although existing adaptive optimal techniques may yield better performance than conventional techniques in homogeneous clutter, they can be expected to perform poorly in the presence of step transitions between regions of significantly different clutter spectra, since the weights will not be properly adapted to either type of clutter. This region of poor performance can be expected to extend over a large portion of the reference window, thus preventing detection over a significant range window in the region of the edge (10 to 20 range bins could extend several hundred metres, or even a kilometre or two). This is particularly unattractive since it is often these regions in which target unmasking is likely to occur and where rapid detection therefore has the highest priority.

3. *Extraneous targets and pulsed interference*

Strong extraneous point returns and pulsed interference will corrupt the estimate of the covariance matrix, resulting in incorrect filter weights being derived. The magnitude of the resulting reduction in the steady state improvement factor has not been analysed in the literature, but it is reasonable to believe that this could be significant in many realistic situations. In view of the great lengths to which designers go to eliminate the effects of extraneous targets in subsequent detection stages of the radar, this would seem somewhat unsatisfactory and techniques should be developed to improve the robustness of the estimation to extraneous targets.

4. *Cancellation of point clutter*

Adaptive techniques will provide little or no cancellation of isolated point clutter such as clutter discretes (towers, fences etc.) or residual chaff puffs. It is particularly important that these clutter sources are suppressed since they *will* cause false alarms if they pass through the doppler processor: the CFAR detector will detect them due to their point nature. MTI and FFT processors will at least provide substantial, even though not optimal, suppression of fixed clutter discretes.

5. *Multiple targets*

Multiple targets (ie. point returns with the same spectrum as the target) may reduce target detectability by capturing, or at least biasing, the adaptive algorithms into placing a null at target doppler. Again, no analyses have been found in the literature on this topic.

6. *Clutter limiting*

Optimal techniques provide the most dramatic performance enhancement for high CNRs (50 - 60 dB). In many situations, especially in sea clutter, this seldom be a realistic assumption, and performance of optimal techniques will be less impressive. In conditions where the CNR *is* say 60 dB, then the clutter, due to its spiky nature, will regularly exceed the dynamic range of the radar. Range cells in which limiting has occurred will either be tagged and excluded from subsequent processing, thus reducing the data available to the adaptation algorithms and possibly causing problems due to "holes" in the data stream, or will not provide valid data to the adaptation algorithms and corrupt the estimate of the clutter spectrum. The effects of limiting on adaptive algorithms have not yet been addressed in the literature.

7. *Non-Gaussian clutter spectra*

The theoretical performance analyses of optimal techniques is based on the assumption that the clutter consists of spectral components with Gaussian shape. Should the clutter deviate from this assumption, the performance benefits may vanish for those techniques which assume the form of the spectrum *a priori*, such as parametric techniques. The superior performance of adaptive techniques quoted for uni- or bi-modal Gaussian clutter will also be diminished in environments in which the clutter spectrum is better matched to the fixed shape of the MTI/FFT notches.

8. *PRI stagger limitations*

It is claimed that certain adaptation techniques allow the use of a staggered PRI. This is based on the reasoning that the effects of the stagger on the covariance matrix and hence the filter coefficients are known and can therefore be compensated for in the solution for thé filter weights. However, in Hsaio filters part of the improvement factor is achieved by coherent integration; in doppler ambiguous radars the unknown target doppler will fold down to a different "processor" doppler for each PRI used, thus precluding the possibility of integration gain and the use of filter banks each "tuned" to a different doppler frequency. Thus only linear predictors, which do not divide the doppler space into bins, permit the use of pulse-to-pulse PRI agility. The usual (relatively minor) reduction in clutter suppression can be countered, albeit at considerable effort, by changing the filter weights each PRI.

The first four of these limitations are considered to be the most serious, and are addressed in Chapter 4 of this thesis.

2.2.3 Summary

Adaptive optimal techniques provide a theoretically attractive method of achieving the best possible clutter suppression in a given clutter environment, giving better performance than conventional techniques in theoretical studies. They provide the most dramatic improvements in performance in situations of multi-modal clutter, clutter with broad spectra, and where the number of pulses is limited. According to the available literature there appears to be little to choose between the Hsiao and the linear prediction approaches: the marginally better performance of the Hsiao approach is balanced by other advantages of the linear prediction approach: only a single filter is needed, not a filter bank; no collapsing losses will therefore be introduced in subsequent detection processors; and linear predictors are compatible with staggered PRI waveforms.

However, adaptive optimal techniques suffer from several limitations in practical situations which have thus far limited their progress from theoretical concepts to real radar processors. In particular, the limitations imposed on their performance by non-homogeneous clutter, extraneous and multiple targets, clutter edges, point clutter, and possibly clutter limiting, are of concern. In some such situations, the complete adaptivity available may actually yield a reduction in performance.

The MTD processor has been proposed as an effective and efficient implementation of the Hsiao filter optimised for some pre-defined clutter environment. No on-line adaptivity is incorporated, thereby greatly reducing computational requirements and overcoming some of the limitations of fully adaptive techniques. Performance has been shown to consistently outperform MTI-FFT processors. The Adaptive MTD processor has been proposed as a means of enhancing the performance and flexibility of MTD processors, offering a practical means of achieving near optimal improvement factors under a wide range of conditions. Thus far, however, the degree of adaptivity reported is limited to countering fixed ground clutter by means of a clutter map.

2.3 CONSTANT FALSE ALARM RATE PROCESSING

2.3.1 Basic Theory

Radar automatic detection requires that the detection processor performs a test to ascertain whether a target is present in each radar resolution cell where detection is attempted. Analytically this is formulated as a hypothesis test between two hypotheses representing the conditions of target absent (H0) and target present (H1). The absence of *a priori* information regarding the probability of a target being present, and the use of the

commonly chosen optimisation criteria of maximising the probability of detection for a fixed probability of false alarm, implies that the optimum statistical test for detection is the Neyman-Pearson test. This corresponds to setting a threshold in the signal amplitude domain and declaring that any sample which exceeds the threshold corresponds to the H1 hypothesis, ie. target present. If the amplitude statistics of the radar thermal noise, external interference and/or clutter (henceforth collectively termed either the *noise* or *background*) with which the target must compete for detection are well known, that is if the shape *and* the variance of the noise pdf are known, then a threshold can easily be determined which will yield the desired probability of false alarm, P_{fa}. Such a situation is referred to as *ideal detection*. Unfortunately, the variance of the clutter and interference will, in practice, vary from one region of radar coverage to another, and even the variance of the radar thermal noise will vary with time. This, together with the fact that the clutter could quite commonly deviate from a Rayleigh amplitude PDF, necessitates the use of an adaptive threshold if a constant false alarm rate is to be maintained. In order to set the threshold correctly the CFAR processor therefore attempts to estimate the variance, and in some cases the shape of the PDF, of the background noise at each instant and at each position that a detection is attempted. This corresponds practically to estimating the variance (and possibly PDF) in each instrumented range bin of the radar, after each CPI (or pulse if non-coherent processing is used), and in some cases in several doppler bins.

CFAR processors which assume that the background conforms to a certain PDF and estimate only the parameters of the distribution (typically the variance, and possibly a shape or correlation parameter), are termed parametric CFAR processors. The assumed noise PDF defines the relationship between the noise variance (and any additional parameters) and the required threshold. Parametric CFAR processors therefore inherently assume that the class of noise PDF is known, and generally only achieve their design performance if that assumption is valid. Most well known existing CFAR processors, such as the three analysed in Chapter 5, are parametric CFAR processors. CFAR processors which either attempt to estimate the PDF themselves, or which intrinsically yield a constant P_{fa} irrespective of the noise PDF, are termed non-parametric CFAR processors. These are generally based on non-parametric statistical techniques such as rank tests or sign tests.

Parametric CFAR processors are considered first. In general these attempt to estimate the background noise power by forming a so-called test statistic derived from a number of range bins (the reference cells) surrounding the cell under test (the test cell), as illustrated in Fig. 2.3. The test statistic is multiplied by a threshold multiplier factor α, which determines the false alarm probability, and the signal in the test cell is then compared with the resulting

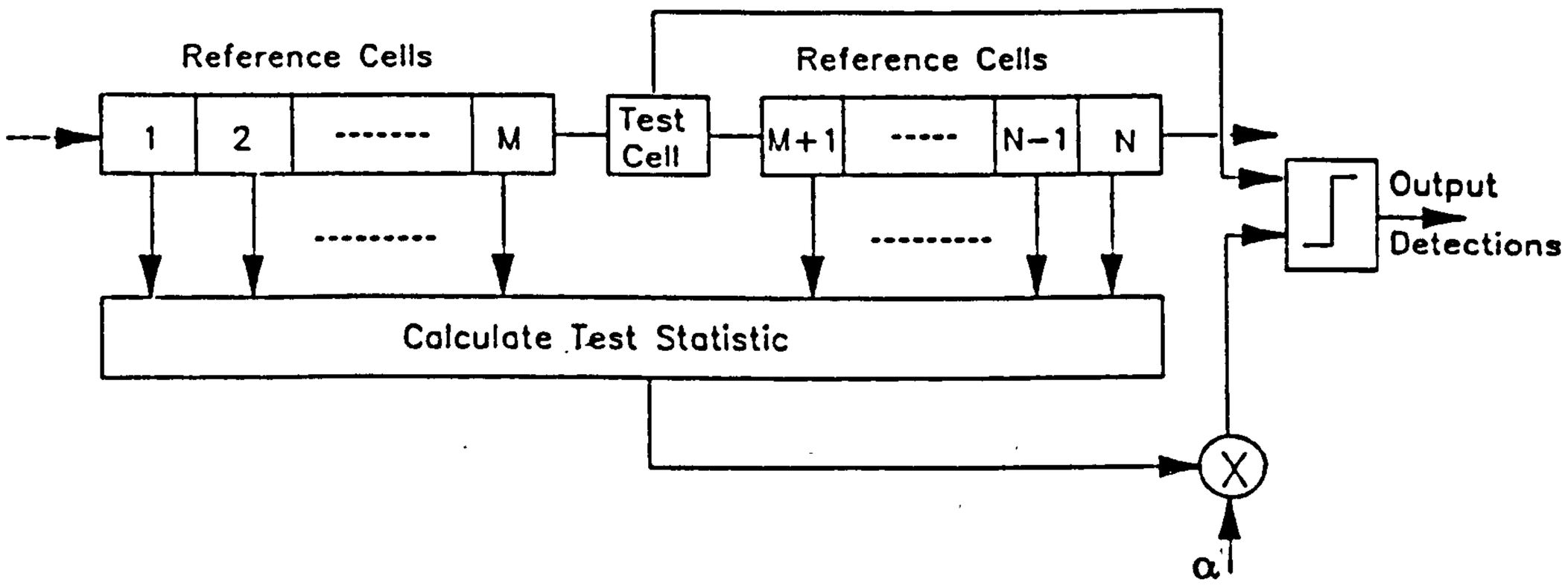

Fig 2.3. *Generalised CFAR Processor Architecture*

threshold T. A detection is declared if the signal in the test cell exceeds the threshold. The region covered by the reference cells is termed here the CFAR window. Since the CFAR processor estimates the noise variance from only a limited number of surrounding range bins, the estimate of the noise variance will be inexact and some margin for error must be incorporated. This implies a threshold higher than would be necessary if the noise variance were known exactly, resulting in a loss in detectability relative to ideal detection, termed the CFAR loss. Furthermore, it is clear that if the noise power changes from one level to another within the CFAR window (corresponding to a clutter edge), or if some of the noise samples within the CFAR window contain samples which are not representative of the overall noise, such as large point sources (usually referred to as extraneous targets), then the estimate of the variance will be incorrect and CFAR performance will suffer. Two negative effects can occur: firstly, if the variance is estimated too high, the threshold will be higher than it should be and target masking will occur. Secondly, at a clutter edge, the threshold may be biased lower than it should be by the region of lower clutter power and higher false alarm rates can occur. Finally, if the noise distribution deviates from that which was assumed to be valid, then the relationship between the variance and the appropriate threshold will vary, resulting again in either an increase in the false alarm rate or a loss of detectability. The response of a given type of CFAR processor to these problems is often used as the basis for comparing CFAR processor performance and selecting the best processor for a given application. In brief, four commonly used performance measures are:

1. The CFAR loss under nominal conditions of homogeneous noise of known PDF.
2. The response of the processor to extraneous targets.
3. The response of the processor to clutter edges.
4. The response of the processor, either in terms of increased false alarm rate or increased CFAR loss, to the noise PDF deviating from the nominal PDF.

In some cases, instead of declaring a detection immediately, the first threshold is followed by a binary integrator, the output of which is fed to a second threshold which declares a detection if at least M out of the N pulses integrated were first threshold detections. This binary integration is far easier to implement than pre-detection non-coherent integration and gives only slightly less integration gain if the second threshold M is chosen correctly. In radars with coherent filter bank doppler processors the most common detection scheme employs single-doppler CFAR processors, with OR selection logic between doppler bins, followed by M/N binary integration over N bursts. The M/N binary integration does not provide significant benefits in terms of false alarm control, and is incorporated primarily to enable detection of targets in clutter occupying a large portion of the radar's doppler space.

Post-detection binary integration following conventional CFAR detection will not be considered in much detail for the following reasons:

1. Rayleigh fluctuating targets which are decorrelated from one CPI or burst to the next by frequency agility or inherent fluctuations will exhibit identical amplitude characteristics to those of clutter spikes. Thus any post detection integration intended to eliminate clutter spikes will also suppress target detections.

2. Post-detection binary integration operates on the output of conventional single pulse CFAR detectors. Therefore improvements in the performance of the single pulse detector will improve overall system performance even in systems employing post-detection integration.

3. In many situations the analysis is, in any case, straightforward: if the target and noise returns are decorrelated from pulse to pulse, the effect of binary integration is evaluated simply through a process of statistical cumulation. That is, if P_d and P_{fa} are independent from pulse-to-pulse, the post integrator values of detection probability $\overline{P}_d$ and false alarm probability $\overline{P}_{fa}$ are obtained from the binomial distribution. Again, the required decorrelation between successive pulses may occur naturally in some cases (Swerling 2 targets in white noise), and would also arise as a result of frequency agility.

4. As mentioned in Chapter 1 the number of pulses in each dwell time will invariably be limited in high resolution radars. Clutter suppression requirements will often necessitate that as many of these pulses as possible are used in each CPI, the number being limited only by blind speed elimination, ambiguity resolution and

counter-countermeasures requirements for PRF and frequency agility on either a burst to burst or pulse to pulse basis. The number of independent "pulses" entering the CFAR processor, and hence available for binary integration, will therefore be small, limiting the potential benefit that can be obtained from binary integration.

5. The performance benefits associated with binary integration of detections in K-distributed clutter has been analysed in some detail in a number of papers (eg. Watts 1985, Ward, 1985). These results are valid irrespective of the form of the initial single pulse detector used. Therefore even in situations where binary integration is usefully employed, further performance improvements will require improvements in the performance of the initial single pulse detector.

2.3.2 Types of parametric CFAR processors and their properties

From a conceptual point of view the different types of parametric CFAR processors differ primarily in the way they form the test statistic and in its resulting characteristics, notwithstanding the possible use of subsequent binary integration. Three types of CFAR processors are analysed in this thesis, namely the Cell Averaging (CA), Cell Averaging Greatest Of (CAGO) and Order Statistic (OS) CFAR processors. They have been selected since they are widely encountered, and most other parametric processors are derivatives of these three. The CA processor is the simplest of the three processors discussed here, merely calculating the average of the signals in the reference cells as the test statistic z, i.e.

$$z = \frac{1}{N_r} \sum_{N_r} x_i \qquad \ldots (2.5)$$

where x_i is the signal in reference cell i, $-N_r/2 \leq i \leq N_r/2$, $i \neq 0$, and N_r is the number of reference cells used. For a given number of reference cells the CA processor provides minimum loss under conditions of homogeneous Rayleigh noise backgrounds. If the noise in the reference cells is corrupted by the presence of additional targets or large discrete clutter sources (extraneous targets); or if the CFAR window covers transitions from one clutter power to another; or if the clutter deviates from the Rayleigh assumption, then an increase in the probability of false alarm P_{fa} and a reduction in the detection probability P_d can result. Quantitative analyses of CA processor performance in the first two of the above situations have been widely reported, with Ghandi (1988) providing a good summary.

The CAGO processor was introduced (Hansen, 1973) to counter the problem of clutter edges. This is attempted by selecting only the greater of the two values of the averages of the reference cells on either side of the test cell, i.e.

$$z = \max\left[\sum_{i=-1}^{-M_r} x_i \; ; \sum_{i=1}^{M_r} x_i\right] \qquad \ldots (2.6)$$

where $M_r = N_r/2$ and the test cell is assumed to lie at i=0. This gives better performance in non-homogeneous clutter at the expense of slightly increased loss (~0.1 dB) under ideal conditions. The CAGO processor is, however, extremely sensitive to extraneous targets due to fewer cells being used in forming the averages of the leading and lagging window halves. It is also about as sensitive as the CA processor to non-Rayleigh clutter.

The OS processor was proposed by Rohling (1983) as a means of overcoming the problem of extraneous targets. This is attempted through ordering the signals in the N reference cells into ascending order and selecting the k^{th} sample of the ordered sequence as the test statistic. The N-k strongest signals in the reference cells do therefore not unduly bias the estimate of noise power, giving improved performance in the presence of extraneous targets. Under ideal conditions performance is generally optimised if k is set to about 7N/8. However, in practice a value of k ~ 3N/4 provides better resilience to several extraneous targets while maintaining acceptable loss under ideal conditions and giving a measure of immunity to clutter edges (Rohling, 1983). Ritcey (1990) argues that in fact it may be better to use k as low as N/2, and tolerate the slightly higher loss, in order to maintain good detectability if target bunching or numerous extraneous targets are expected. The response to clutter edges differs depending on the chosen value of k: for small values of k in the region of N/2 to 2N/3, the OS processor performs well in detecting targets that are close to the clutter edge, but suffers a marked increase in false alarm rate in the region of the clutter edge. For large values of k, the desired false alarm rate is maintained well in the region of the clutter edge, at the expense of a larger masked region around the edge, where targets will not be detected .

Several derivatives of these CFAR processors have been proposed. These include the Censored Mean Level Detector (CMLD), the Excision Mean Level Detector (EMLD) and the Cell Averaging Smallest Of (CASO) CFAR processor. The CMLD (Ritcey, 1986) attempts to overcome the problems of both clutter edges and extraneous targets, while maintaining low nominal loss, by excluding the a smallest samples and the b largest samples from the calculation of the sample mean. This corresponds to ordering the samples in ascending order as for the OS processor, but then taking the sample mean of the the $(a+1)^{st}$ to $(b-1)^{st}$ samples, ie.

$$z = \sum_{i=a+1}^{b-1} r_{i:N_r} \qquad \ldots(2.7)$$

where the $r_{i:N_r}$ are the ordered samples of the samples x_i in the reference cells. Since more samples are used in the determination of the test statistic than in the OS processor, the nominal CFAR loss is lower[3], while under conditions of extraneous targets and clutter edges the performance is roughly similar to that of the OS processor. These advantages are achieved at the expense of processor complexity, since both the ordering (as for the OS) and the averaging (as for the CA) need to be performed. The EMLD, introduced by Goldman and Bar-David (1988) and analysed further by Conte et. al. (1989), attempts to overcome the effects of several extraneous targets by censoring from the averaging operation all returns above some value β. However, the performance is sensitive to the chosen value of β and the false alarm rate varies depending on how many samples exceed this excision value. The EMLD does not seem to offer any significant benefits over the aforementioned techniques, but is at least not much more difficult to implement than the CA processor. The EMLD could possibly be useful in pulse jamming scenarios where very large numbers of extraneous targets exist, provided that subsequent binary integration is performed to prevent jamming pulses from being declared detections. The CASO processor was introduced by Trunk (1978) in an attempt to alleviate the problem of target masking caused by two closely spaced targets. It is the reverse of the CAGO processor in that it selects as the test statistic the *smaller* of the partial sums of the signals in the leading and lagging halves of the reference window. As would be expected the CASO processor suffers slightly higher loss than the CA processor in homogeneous clutter, but it has been shown (Trunk, 1978) that it does indeed perform well in resolving two closely spaced targets. Gandhi (1988) shows, however, that if an extraneous target is present on each side of the test cell, performance degrades rapidly due to at least one of these being included in the test statistic and hence raising the threshold. He also shows that the CASO processor exhibits very poor false alarm performance in the region of clutter edges. Several variations of the aforementioned processors also exist which are too numerous to address here.

All of the abovementioned CFAR processors are sensitive to deviations from the assumptions of Rayleigh noise and in this thesis the degree of sensitivity to such deviations is analysed. To date little has been published on the performance of the CFAR processors described above in non-Rayleigh clutter or noise, and particularly K-distributed clutter. Similarly, little literature exists covering CFAR techniques designed specifically for operation in non-Rayleigh environments. Most of the papers that do exist in this field

[3]It has been shown (Ritcey, 1986) that for a=0 and under conditions of exponentially distributed noise, the CMLD gives an unbiased minimum variance estimate of the noise power and therefore has the same loss as a CA processor using b reference cells

address CFAR performance in Weibull and Log-Normal clutter (eg. Goldstein, 1973; Weber, 1985; Schleher 1975; Levanon, 1992), which as stated in Chapter 2 do not seem to be the best models available for non-Rayleigh sea clutter, or indeed non-Rayleigh land clutter. Nevertheless, these papers are useful for comparisons with the analyses performed in this project. This is particularly true for the Weibull results since special cases of both the Weibull and K-distributions reduce to the exponential distribution. Some empirical models for detection performance prediction in K-distributed clutter have been presented (Watts, 1990b), but these do not address CFAR techniques. Another paper by Watts et. al. (1990a) describes a specific form of multi-pulse CFAR processor, based on the CA processor, for operation in K-distributed clutter. The material in that paper is only relevant if a large number of pulses are available per dwell.

3.3.3 Non-parametric CFAR processors

A non-parametric CFAR processor is one which assumes no *a priori* knowledge of the clutter amplitude statistics. The term "non-parametric" derives from formal non-parametric statistics where it refers to the idea that the possible clutter PDFs comprise such a large set that they cannot be indexed by a finite number of parameters. Thus "non-parametric" techniques are required. In radar detection processing, the two fundamental techniques used for non-parametric detection are the Sign Test and the Wilcoxon test. In their basic form, these tests require that the signal phase is known *a priori*, an unrealisable condition for radar detection. Modifications of these techniques are therefore used to enable them to operate on signals of unknown phase, and the corresponding practical implementations for radar detection are the Generalised Sign Test (GST) processor (Hansen, 1975) and the Mann-Whittney Detector (MWD) (Hansen, 1972). A detailed definition of these processors will not be included here since, as will be shown later, they are not suitable for systems where a strictly limited number of pulses or bursts is available. In addition, some other conditions for the attainment of non-parametric CFAR are not met in K-distributed clutter.

The GST processor essentially compares the signal in each range bin to that in the N_r surrounding range bins on a given pulse, and counts the number of times the test cell exceeds the reference cells. This count is integrated over a number of pulses M_i and the result is compared to a threshold. The MWD compares the test cell to the $N_r x M_i$ reference cells over the dwell of M_i pulses and counts the number of times that the test cell exceeds the reference cells. This count is integrated over the M_i pulses and the result is compared to a threshold. Since ranking as opposed to pure sign testing is performed in the MWD, it is more efficient than the GST processor. For non-parametric CFAR performance to be

achieved, both techniques require that the $N_r x M_i$ samples are statistically independent. This is not true in general for clutter backgrounds with narrow spectra. In particular it is not true for K-distributed clutter, even if its doppler spectrum is white, since the clutter power modulation is assumed to be approximately constant over the dwell period and this introduces correlation between pulses for the samples in each range bin.

The other major restriction on the usefulness of processors based on these two techniques is that both require the number of pulses M_i to be quite large if acceptable detection loss is to be maintained. Hansen (1975) shows that for $M_i > 16$ and $N_r > 8$, and for $P_{fa} = 10^{-6}$, the loss is less than 2 dB for non-fluctuating targets. For the more common case of fluctuating targets the loss is much higher. The loss also increases rapidly as M_i falls below 16.

Several variations of these two basic methods have been proposed. The most widespread technique, as presented by Trunk (1974) and Dillard (1970), is the ranking of the test cell with respect to the reference cells, followed by weighted rank integration over a number of pulses. Performance of these techniques falls off rapidly as the number of pulses M_i falls below about 20, for N_r in the region 16 to 32. They also require the independence of all of the $N_r x M_i$ pulses, which is, as discussed above, often not true.

It is concluded that these non-parametric CFAR techniques are not appropriate for CFAR detection under the conditions applicable to this thesis. They will not therefore be considered any further.

2.3.4 Illustrative example

To conclude this section, a brief illustrative example of the four CFAR processor performance measures mentioned earlier is presented. Fig. 2.4 shows the threshold set by CA, CAGO and OS processors operating on K-distributed clutter with v=0.5, with the number of reference cells N=32. The threshold multiplier factor α is set to achieve $P_{fa} = 10^{-4}$. For the OS processor k is chosen as 20. A 14.77 dB clutter edge is located at range bin no. 240. A number of closely spaced targets of 16 dB SCR are located between range bins 70 and 95, with isolated targets at range bins 150 and 230.

Considering the resulting threshold values several points can be noted. For the CA detector it is apparent that the closely spaced targets raise the threshold between range bins 60 and 110 so much that none of the targets are detected. The isolated target at range bin 150 is detected, but the presence of the clutter edge raises the threshold in the region of range bin 240, thereby masking the target at range bin 230. Close examination of the figure also

indicates that a false alarm will occur in range bin 246, due to the threshold being biased down by the low region of clutter power still within the CFAR window. It is evident that for the CAGO processor the closely spaced targets are even more comprehensively masked by each other. Again the isolated target at range bin 150 is detected and the target at range bin 230 is masked by the clutter edge. The clutter spike at sample 246 does not, however, cause a false alarm in the CAGO processor.

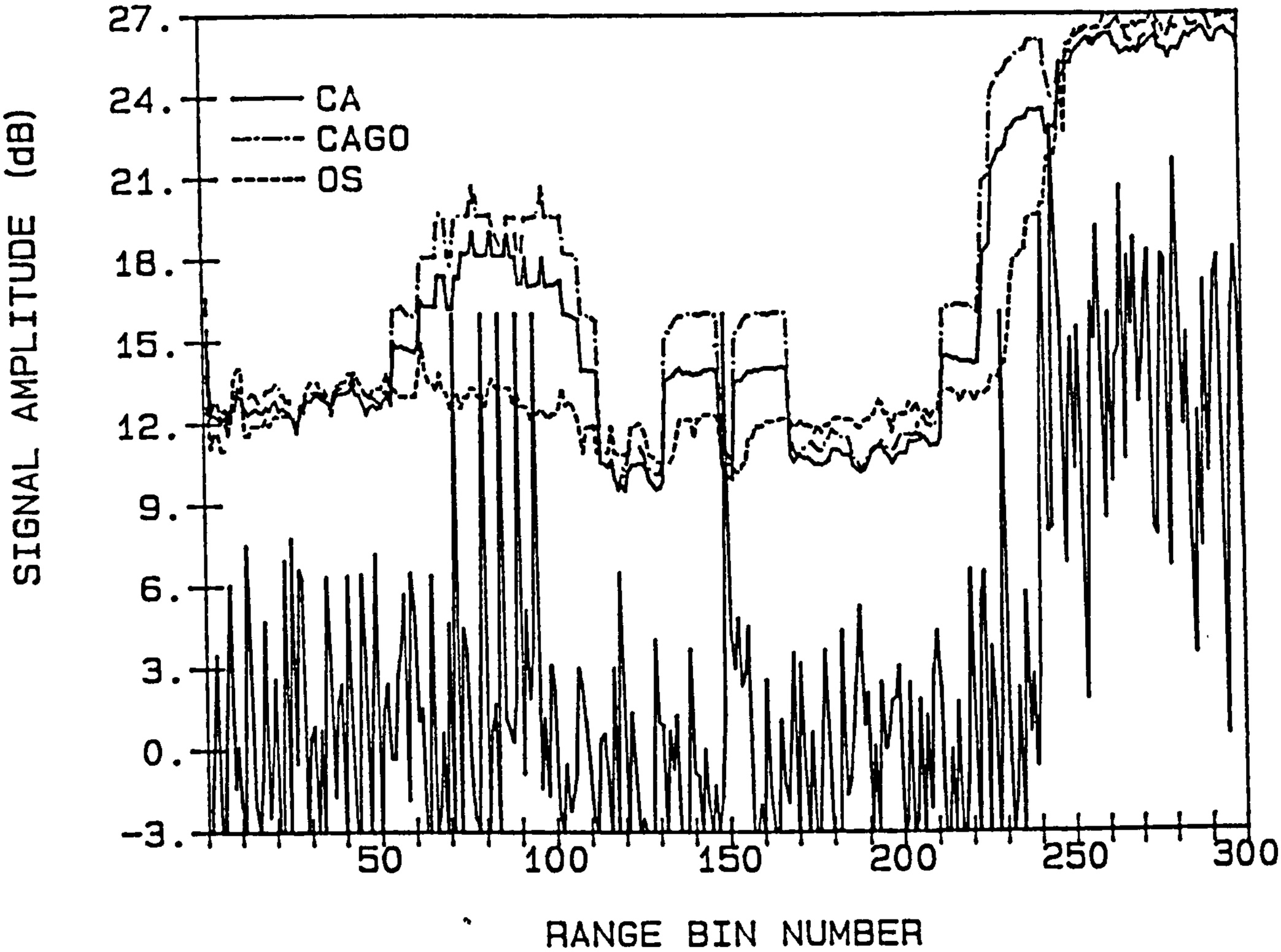

Fig. 2.4. *Example of Thresholds Calculated by CA, CAGO and OS Processors*

The OS processor can be seen to resolve the closely spaced targets and exhibits no discernable increase in the threshold in that region. The isolated target at range bin 150 is, of course, detected, and the target at range bin 230 is now detected and is not masked by the clutter edge. This is achieved at the expense of a false alarm at range bin 246 caused by the clutter edge, and almost another false alarm at sample 243. The choice of a higher value of k, of around 27 or 28, would eliminate the false alarms at the clutter edge, but would extend the region of target masking caused by the clutter edge to the left, causing masking of the target at range bin 230. It is also apparent that in regions of homogeneous clutter the threshold is lowest for the CA processor and highest for the OS processor, reflecting the nominal loss for these respective processors.

CHAPTER 3

A COMPARISON OF DOPPLER PROCESSING TECHNIQUES FOR CLUTTER SUPPRESSION

3.1 INTRODUCTION

A wide range of techniques for doppler-based clutter suppression are now practicable due to advances in signal processing hardware and the theory of optimal filtering. At present, however, there is little consensus as to which technique provides the best performance under anything wider than specific clutter and target conditions. Although the relative performance of many of the techniques has been compared in the literature, no clear-cut conclusions can be drawn from the available papers: the data are often not directly comparable and sometimes contradictory, and one often gets the impression that quoted performance depends strongly on the specific clutter environment assumed. In this Chapter an attempt has been made to evaluate the relative performance of many commonly proposed doppler processors under a wide range of conditions, with as few limiting assumptions as possible.

The processors addressed here, a brief description of which is provided in the next section, are:

1. Moving Target Indication (MTI)
2. Adaptive MTI (AMTI)
3. Moving Target Detector (MTD)
4. Pulse Doppler preceded by MTI (PD&MTI)
5. Adaptive MTD (AMTD)
6. Optimal Filtering (OF)
7. Linear Prediction (LP)
8. Optimal Filtering preceded by MTI (OF&MTI)
9. Linear Prediction preceded by MTI (LP&MTI)
10. Adaptive MTI preceded by MTI (AMTI&MTI)

A wide range of clutter scenarios representative of typical land and sea clutter, possibly with weather clutter components as well, are defined. The performance of each of the doppler processors listed above is assessed in each clutter environment. Statistical analysis is then used to compare the relative performance of the various processors.

3.2 DESCRIPTION OF DOPPLER PROCESSORS

3.2.1 Optimal Filtering (OF)

Optimal filtering has been discussed in section 2.2. Note that in this Chapter ideal estimation of the clutter covariance matrix is assumed. This implies that the clutter must be homogeneous and the number of reference cells used to estimate **M** tends to ∞. In practice the covariance matrix has to be estimated on-line from a number of range cells in the vicinity of that being filtered. This, along with possible clutter heterogeneity, causes errors in $\widehat{\mathbf{M}}$ and hence sub-optimal performance. The consequent losses are addressed in Chapter 4 of this thesis. Techniques for estimating **M** and some other limitations of adaptive optimal filters have been addressed in section 2.2.

3.2.2 Linear Prediction (LP)

Linear predictor filters have been introduced in section 2.2. In this Chapter ideal estimation of the clutter covariance matrix is assumed. This implies that the clutter must be homogeneous and the number of reference cells used to estimate **M** must tend to ∞. In practice the covariance matrix has to be estimated on-line from a number of range cells in the vicinity of that being filtered. This, along with possible clutter heterogeneity, causes errors in $\widehat{\mathbf{M}}$ and hence sub-optimal performance. Note that linear predictors are not "tuned" to a given target doppler and hence a single filter is sufficient, as opposed to the bank of filters required by the Hsiao approach. This implies that collapsing losses associated with detection over a bank of several parallel filter outputs are not present in LP filters, and account of this must be taken in performance comparisons with Hsiao optimal filters.

3.2.3 Moving Target Detection (MTD)

In a Moving Target Detector a bank of FIR filters is implemented, each of which is "tuned" to a different desired target doppler. The sidelobe response of each filter depends on the design criteria and the assumed clutter environment. The MTD can be viewed as an approximation to a bank of optimal Hsaio filters provided the assumed clutter environment accurately reflects the true situation. However, absence of accurate knowledge of the true clutter spectrum generally results in a more arbitrary approach to MTD filter bank design, in which a number of filter transfer function parameters are specified and filters are designed accordingly, usually by interactive techniques owing to the absence of rigorous top-down design methods for FIR filters. The filter transfer function parameters most usually of interest include the main lobe width, the depth and width of the notch at zero doppler, and the first and average sidelobe levels. In this Chapter six MTD filter banks have been designed to compare the relative importance of these parameters and investigate the influence of the choice of parameters on overall Improvement Factor performance. The first three MTDs correspond to situations in which land clutter suppression is considered

particularly important, while the latter three place no additional emphasis on suppression of zero-doppler clutter and are hence more representative of sea- or weather clutter suppression filters. The design criteria and definitions of the six MTD filter banks are given in Appendix 3.1.

With regard to the MTD filter designs outlined in the appendix, some additional points should also be noted. In some cases the number of filters could be reduced with little increase in collapsing loss; however, this has not been done here to simplify direct performance comparison. Similarly, filter 0 could be omitted from MTDs 1 to 3; it has again been included to facilitate direct comparison. In both cases the additional collapsing loss associated with the extra filters is negligible. In all cases a sidelobe level of less than about -60 dB relative to the noise level was not considered particularly advantageous due to dynamic range limitations in the radar.

3.2.4 Pulse Doppler with MTI (PD&MTI)

Pulse Doppler refers to processors in which a filter bank is implemented by means of a FFT. The FFT processor is usually preceded by a conventional 2- or 3-pulse MTI canceller. This is done primarily to achieve sufficient suppression of strong zero-doppler clutter while maintaining reasonable freedom over the selection of the window function and the corresponding frequency response. (In the past the preceding MTI canceller was also required to ease dynamic range requirements due to numerical precision constraints; this is no longer so significant due to advances in processing component technology.)

In this study a 3-pulse canceller followed by an 8-pulse FFT is used to facilitate direct comparison with a 10-pulse optimal or MTD processor. Four different window functions have been examined, namely the Hanning, Hamming, Blackman and Kaiser-Bessel windows, the latter with a range of values of the variable parameter b, where for even N (N ≡ order of the filter) and n = 0...N-1 (n is the index of the n^{th} received pulse), the window functions are given by:

Hanning: $$w(n) = 0.5\left\{1 + \cos\left[\frac{2\pi}{N}\left(n + \frac{1}{2} - \frac{N}{2}\right)\right]\right\}$$

Hamming: $$w(n) = 0.54 + 0.46\cos\left[\frac{2\pi}{N}\left(n + \frac{1}{2} - \frac{N}{2}\right)\right]$$

Blackman: $$w(n) = 0.42 + 0.5\cos\left[\frac{2\pi}{N}\left(n + \frac{1}{2} - \frac{N}{2}\right)\right] + 0.08\cos\left[\frac{4\pi}{N}\left(n + \frac{1}{2} - \frac{N}{2}\right)\right]$$

Kaiser: $$w(n) = [I_0(b)]^{-1}.I_0\left[b\sqrt{1 - \left(\frac{2}{N-1}\left(n - \frac{N}{2} + \frac{1}{2}\right)\right)^2}\right]$$

The normalised overall frequency response of filters 1, 2, 3 and 4 obtained using a Hamming window are shown in Fig 2.1. Filters 5, 6 and 7 are mirror images about the PRF of filters 3, 2 and 1 respectively. The passband of the FFT and the notch of the MTI coincide in filter 0, which is therefore not useful and the frequency response is unimportant.

Note that subsequent analyses assume unity noise gain normalisation on the MTI canceller and the FFT processor. This does not yield unity noise gain in each of the 8 filters; the filters near to 0.5 of the PRF have more than unity noise gain while others have less than unity noise gain.

3.2.5 Optimal Filter with MTI and Linear Predictor with MTI (OF&MTI and LP&MTI)

In many situations strong isolated point sources of clutter are present in a background of more homogeneous clutter of different spectral characteristics. These point clutter sources have two effects on adaptive filtering techniques, namely:

1) When the point clutter is in the cell to be filtered, the covariance matrix used in calculating the filter coefficients is based on the homogeneous clutter background. The filter is therefore optimised for a different clutter spectrum and does not cancel the point clutter optimally.

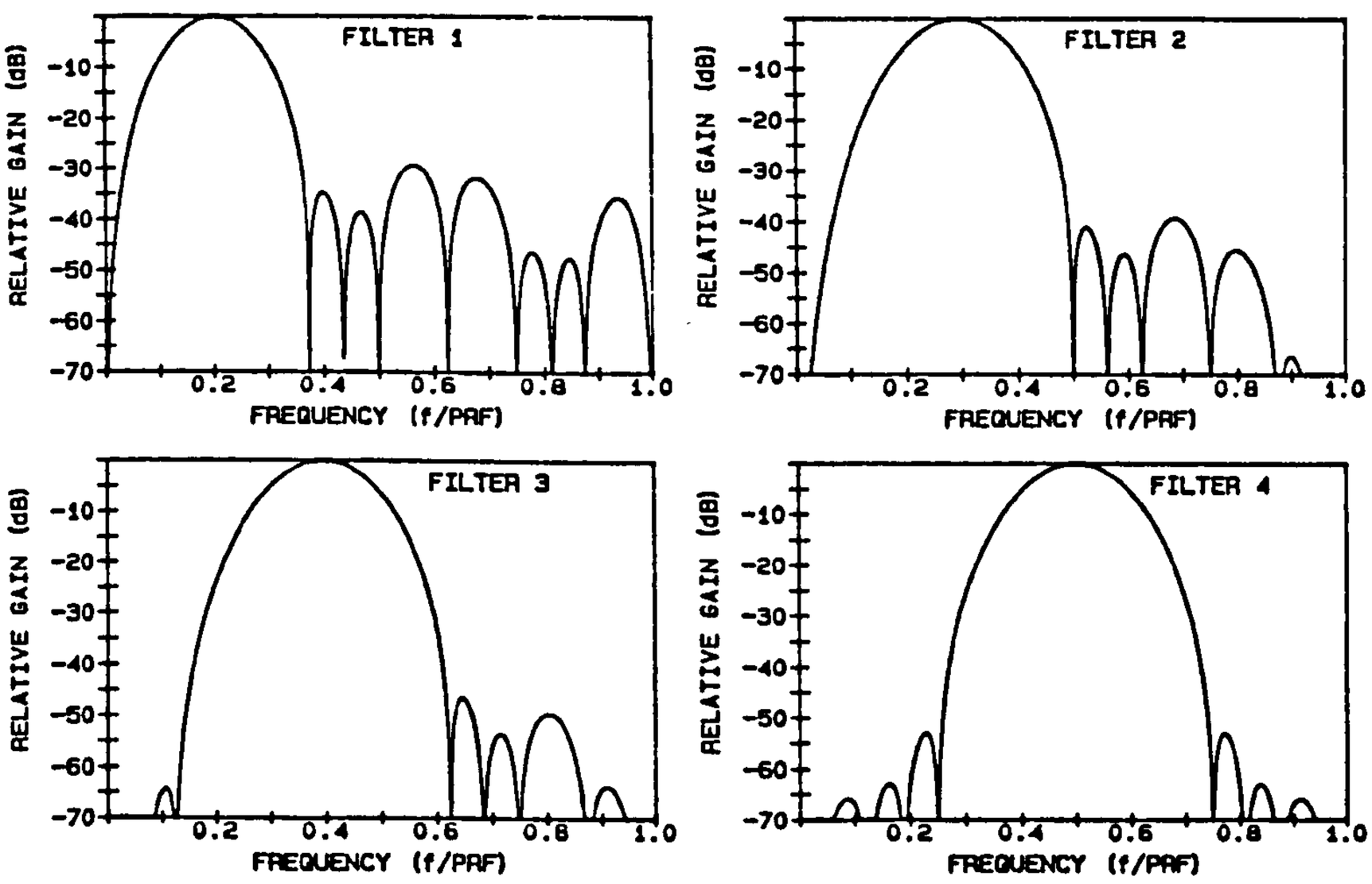

Fig. 3.1: *Normalised Frequency Response of PD&MTI Processor*
(Hamming window, 3-pulse MTI, 8-pulse FFT)

2) When the point clutter is in the reference cells it may dominate the estimate of the covariance matrix by virtue of the strength of its return. This results in a poor estimate of the covariance matrix since 1) the spectrum of the discrete is different to the background, and 2) essentially one dominant sample is used in estimating **M**, thereby degrading estimation accuracy. The filter therefore exhibits sub-optimal performance in a region around the point clutter of the extent of the reference window.

One means of partially overcoming these problems is to insert an MTI canceller before the optimal filter to largely cancel the discrete clutter, thus minimising corruption of the estimate of **M** and providing some minimum cancellation of the point clutter. In this thesis binomial 3-pulse cancellers followed by 8-pulse optimal and linear predictor filters have been examined and compared with 10-point optimal or linear predictor filters without MTI. The 8-pulse filters are designed in exactly the same way as previously discussed, except that the matrix equation used to determine the weights must reflect the clutter covariance matrix after MTI filtering. Assuming a constant PRI waveform this is calculated by 1) defining the pre-MTI clutter spectrum; 2) applying the suitably normalised MTI transfer function; 3) Determining the post-MTI clutter correlation vector from the magnitude of the inverse Fourier transform of the power spectrum; and 4) constructing the covariance matrix from the correlation vector **r** with elements $m(i,j) = r(|i - j|)$ if $i \geq j$, and $m(i,j) = (r(|i - j|))^*$ if $i < j$, where * denotes complex conjugation.

Note that in this Chapter ideal estimation of the clutter covariance matrix is assumed. This implies that the clutter must be homogeneous and the number of reference cells used to estimate **M** must tend to ∞. The performance data presented in this Chapter therefore indicate the loss introduced by the insertion of an MTI filter when the clutter is homogeneous and point clutter sources are *not* present. In Chapter 4 the performance of the composite MTI-optimal adaptive filter is addressed when point clutter sources *are* present, either in the test cell or the reference cells, and for a finite number of reference cells used in estimating the covariance matrix.

3.2.6 Adaptive MTI (AMTI) and AMTI with MTI (AMTI&MTI)

AMTI is a well known technique of improving MTI clutter suppression in clutter with non-zero mean doppler by adaptively moving the null of the MTI frequency response to coincide with the dominant clutter spectral components (Lewis, 1986). For clutter with a symmetrical spectrum about its mean the optimum location for the null is at the clutter mean frequency (Ekstrom, 1974). In general AMTI is applied to binomial cancellers by varying only the phase of the canceller coefficients. If cancellation of bimodal clutter is required, AMTI cancellers may be cascaded with MTI or further AMTI cancellers.

In this analysis a 3-pulse AMTI is considered. In addition, we consider a 3-pulse AMTI preceded by a conventional 3-pulse MTI for the cancellation of zero-doppler clutter, the idea being that the AMTI will then "clean up" the residue and any non-zero doppler components. In both cases the null of the AMTI response is assumed to be set to the mean value of the clutter or residue; no errors in the positioning of the null are accounted for and hence the results can be expected to be slightly optimistic.

3.2.7 Adaptive MTD (AMTD)

In order to improve filter performance in spatially heterogeneous clutter the concept of Adaptive MTD has been proposed (D'Addio, 1985; Gibson, 1985), in which a MTD filter bank is selected from a library of several possible choices, the choice being dependent on the locally applicable clutter environment. Current techniques generally limit the adaptation to the presence or absence of significant stationary land clutter, implemented by a clutter map. This appears to have limited applicability to systems in which the platform-clutter relative movement is fast compared to the radar scan rate or frame time, or in which an essentially infinite number of elevation positions are available, such as in a mechanically scanned pencil beam radar. Nevertheless, within these limitations, performance close to the optimum has been claimed (D'Addio, 1985).

The performance of an AMTD system is limited by the number of filters from which the selection will be made, the accuracy of selection, and the performance of the chosen filter bank in the local clutter. In this study the filter library is assumed to consist of a subset of the six MTD filter banks defined above as well as PD&MTI processors with Hamming or Kaiser (b=6) windows. Filter selection logic is not addressed here: ideal selection of the appropriate filter is assumed for all clutter in all resolution cells. The results thus give an upper bound on AMTD performance. A lower bound could be obtained by assuming that the worst filter is chosen in each case.

After a preliminary investigation the following AMTD filter libraries were selected for detailed analysis:

Table 3.1
AMTD Filter Library Definition

AMTD No.	Filters in Library	
1.	MTD2	MTD3
2.	MTD2	MTD4
3.	MTD2	MTD6
4.	MTD2	PD&MTI[1]

Table 3.1 (cont.)

AMTD No.	Filters in Library			
5.	MTD3	MTD4		
6.	MTD3	MTD6		
7.	MTD3	PD&MTI[1]		
8.	MTD4	MTD6		
9.	MTD4	PD&MTI[1]		
10.	MTD2	MTD4	PD&MTI[1]	
11.	MTD2	MTD3	MTD4	
12.	MTD3	MTD4	MTD6	
13.	MTD3	MTD4	PD&MTI[1]	
14.	MTD4	MTD6	PD&MTI[1]	
15.	MTD2	MTD3	MTD4	MTD6
16.	MTD3	MTD4	MTD6	PD&MTI

[1] In all cases a hamming window was used for the PD&MTI processor.

3.3 CLUTTER SCENARIOS

Bimodal clutter spectra were assumed in this Chapter for land and sea clutter scenarios. This includes unimodal clutter as a special case where the strength of one of the clutter components is negligible. In all cases Gaussian spectral components were assumed. Although this assumption may often be violated in practice the actual shape of the spectrum, particularly the far out spectral tails, is not expected to have much impact on the *relative* performance of the various filters. The spatial and amplitude statistics do not affect most of the analyses in this study; in cases where they are important, as in Section 3.4 following, spectrally homogeneous clutter with a Rayleigh amplitude distribution is assumed unless otherwise stated.

All clutter scenarios considered here have been taken as being equally probable and important, with no weighting being applied in subsequent statistical analyses.

3.3.1 Land Clutter

For land clutter the parameters used to define the clutter environments were:

1. CNR_1, the CNR of the zero-doppler component.
2. The spectral width of the zero-doppler component, measured in terms of the standard deviation σ_1 of the Gaussian spectrum.
3. CNR_2, the CNR of the second clutter component.
4. The standard deviation σ_2 of the second clutter component.
5. The centre frequency f_{c_2} of the second clutter component.

It was assumed that the zero-doppler clutter component corresponds to a dominant return from the land, with a consequent narrow spectrum, while the second clutter component corresponds to weaker but spectrally broader rain, chaff or clouds (or possibly wind agitation of vegetation). The values of the above parameters considered appropriate for this study were therefore as follows:

Table 3.2

Definition of Land Clutter Scenarios

Parameter	Values considered					Units
CNR_1:	20	40	60			(dB relative to thermal noise)
σ_1:	0.003	0.01	0.03			(relative to PRF)
CNR_2:	-50	10	20	30		(dB relative to thermal noise)
σ_2:	0.01	0.03	0.1			(relative to PRF)
f_{c_2}:	0.0	0.125	0.25	0.375	0.5	(relative to PRF)

These values comprise a set of 540 clutter scenarios, of which 414 are distinct since σ_2 and f_{c_2} are irrelevant for $CNR_2 = -50$ dB. Note that $f_{c_2} \leq 0.5$; it is not necessary to set $f_{c_2} > 0.5$ since setting $f_{c_2} = 0.625$, 0.75, 0.875 and 1.0 would give identical results to $f_{c_2} = 0.375$, 0.25, 0.125 and 0.0 respectively, due to a uniform target doppler PDF and the reverse symmetry of the corresponding filters in each filter bank. 450 of these scenarios, including all the distinct ones, are assigned an index 1 - 450 as defined in Appendix 2.2. Limited repetition of $CNR_2 = -50$ dB has been maintained to ensure that later statistical data analyses do not swamp this case.

3.2 Sea Clutter

Sea clutter often exhibits bimodal spectral characteristics. The dominant component with a mean velocity of typically 0.15 to 0.25 of the wind velocity and a standard deviation of the order of 0.5 to 1 m/s, while the weaker component has mean velocity of the same order as the wind velocity and spread equal to or wider than that of the spread of the dominant component. In addition to the bimodal sea clutter, rain and chaff may be present; however, this will have mean velocity similar to the wind velocity and spread similar to that of the secondary sea clutter component. The clutter spectrum is therefore still likely to be essentially bimodal and so limiting this study to bimodal clutter in sea scenarios does not necessarily preclude the possibility of simultaneous rain or chaff. [In cases where the radar vertical beamwidth is wide enough to illuminate the sea surface and of sufficient height to incorporate wind shears, a third clutter component would sometimes be necessary for

accurate modelling.]

Bimodal sea clutter is characterised in the same terms as given above for land clutter, with the additional parameter f_{c_1}, the centre frequency of the dominant clutter component.The values of the characterising parameters considered appropriate for sea clutter for this study were as given in Table 3.3 below.

Table 3.3
Definition of Sea Clutter Scenarios

Parameter	Values considered					Units
CNR_1:	20	40				(dB relative to thermal noise)
σ_1:	0.01	0.1				(relative to PRF)
f_{c_1}:	0.0	0.25	0.5			(relative to PRF)
CNR_2:	-20	10	30			(dB relative to thermal noise)
σ_2:	1.0	2.0				(relative to σ_1)
f_{c_2}:	0.0	0.2	0.4	0.6	0.8	(relative to PRF)

These values comprise a set of 360 clutter scenarios, of which several are not distinct since σ_2 and f_{c_2} are irrelevant for CNR_2 = -20 dB. 300 of these scenarios, including the 252 distinct ones, are assigned an index 1 - 300 as defined in Appendix 3.3. Limited repetition of CNR_2 = -20 dB has been maintained to ensure that later statistical data analyses do not swamp this case.

3.4. A NOTE ON PERFORMANCE MEASURES

We wish to quantify the relative performance of various doppler processors. The quantity of interest is the reduction in signal power which can be achieved, compared to the unfiltered case, while still maintaining the required detection probabilities. We term this the "true Improvement Factor", defined as $IF_{true} = S_{\overline{dp}}/S_{dp}$, where S_{dp} and $S_{\overline{dp}}$ are the signal powers required for detection with and without doppler processing respectively. The standard definition of IF which is commonly used to compare the performance of doppler processors is:

$$IF = \frac{SCNR|_{out}}{SCNR|_{in}} \qquad \ldots (3.1)$$

which for single filter systems with unstaggered PRI gives $IF = IF_{true}$. However, in multi-filter or staggered PRI systems modifications are necessary to achieve accurate values of the true improvement factor. Firstly, each filter in a filter bank will exhibit a different IF.

Simple averaging of the IFs is inappropriate since the radar does not average the outputs, but attempts independent detection on each filter output. This is approximately the same as selecting the filter in which the SCNR is highest, which corresponds to that with the highest IF. The IF of the best filter in a filter bank will therefore be taken as the IF of the filter bank as a whole for a given target doppler and clutter scenario. Note that the collapsing loss associated with detection on N independent filter outputs must be accounted for in comparing the performance of filter bank processors to single filter processors such as linear predictors or AMTI cancellers[1].

This value of the IF of the filter bank as a whole is still, however, dependent on the assumed target doppler, which is in general unknown. The average improvement factor IF_{av} is thus often taken as the doppler dependent IF averaged over all target dopplers between 0 and the PRF, assuming uniform target doppler probability. This tends to give pessimistic results since it assumes that targets compete directly with the dominant clutter in some situations, whereas in reality PRF stagger is almost always employed to eliminate blind speeds and ensure that the target will not be obscured by narrow band clutter at least part of the time. In burst processing radars, M_b/N_b detection logic will generally be applied. Simplistically, in such cases the IF in only the best M_b out of N_b of the bursts is thus relevant, which is broadly equivalent to saying the IF is only relevant in the best M filters in the bank of N filters. (Although M_b/N_b may often be similar to M/N, this will not necessarily be true). It is therefore proposed that a more appropriate doppler independent measure of IF is IF_Δ, defined as the average of the doppler dependent IF over only the best Δ % of the doppler space.

To validate this proposed performance measure the radar processing system illustrated in Fig. 3.2 has been considered. The true improvement factor has been investigated by determining the signal power S_{dp} required with doppler processing to achieve 50% detection probability with a false alarm probability of 10^{-6}, and the signal power $S_{\overline{dp}}$ required without doppler processing. The losses and appropriate thresholding considering the collapsing of the filter banks and the M_b/N_b detection logic are addressed in Appendix 3.4. Assumptions regarding clutter and target statistics and a brief overview of the method of analysis are also given in the appendix.

---

[1] There is also a small collapsing detection gain due to finite detection probabilities in more than one filter in the filter bank. This is generally smaller than the collapsing loss and will not be considered in this study.

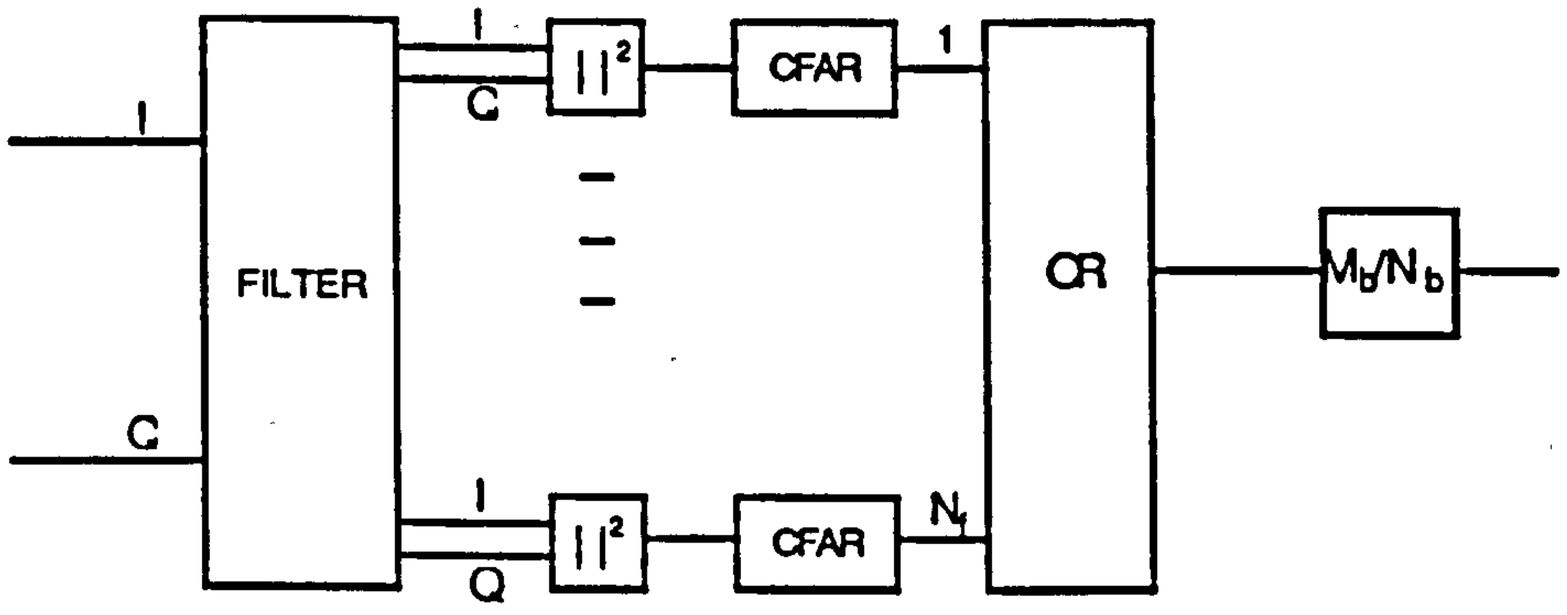

Fig. 3.2: *Outline of Doppler and Detection Processing*

Results were calculated for several bimodal clutter scenarios defined by combinations of the following clutter parameters:

CNR_1:	40					(dB relative to thermal noise)
σ_1:	0.01	0.1				(relative to PRF)
f_{c_1}:	0.0	0.5				(relative to PRF)
CNR_2:	-20	30				(dB relative to thermal noise)
σ_2:	1.0	2.0				(relative to σ_1)
f_{c_2}:	0.0	0.2	0.4	0.6	0.8	(relative to PRF)

The true IF was determined by calculating P_d as a function of S_{dp} and S_0, and finding those values which gave $P_d = 50\%$. The approximation IF_Δ was determined as described above for various values of Δ. Results are illustrated in Fig. 3.3a for $\Delta = 30\%$ and Fig. 3.3b for $\Delta = 100\%$, where each dot plotted represents the IF achieved by a given type of filter in a given clutter scenario..It is clear that $\Delta = 30\%$ gives good accuracy whereas averaging over the whole doppler space gives results which are consistently pessimistic by 3 to 5 dB.

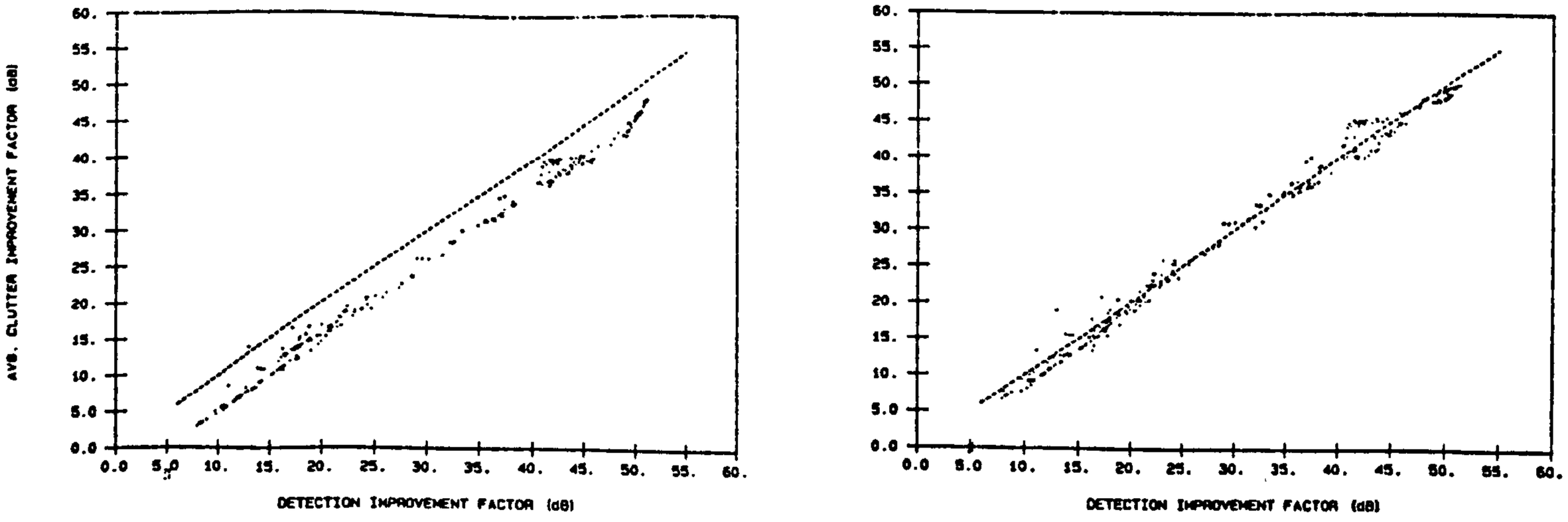

Fig. 3.3: *Approximate IF vs. True detection Improvement Factor*
a) $\Delta = 100$ %, b) $\Delta = 30$ %
($M_b/N_b = 1/3$; $P_d = 50\%$; $N_f = 10$; $P_{fa} = 10^{-6}$)

3.5 PERFORMANCE COMPARISON

The approximate improvement factor IF_Δ has been calculated for values of Δ = 5%, 30%, 70% and 100% (ie. where the doppler dependent IF has been averaged over the best 5%, 30%, 70% and 100% of the doppler space respectively) for each of the filter types described in Section 3.2, for each of the land and sea clutter scenarios given in Section 3.3.

Full results of IF_Δ for each type of filter, clutter scenario and the value of Δ are provided in Appendix 3.5. A more sensitive measure for comparing performance is the reduction in IF obtained by a given filter compared to the maximum possible IF, which is constrained by the clutter spectrum and the number of pulses processed, and is given by the IF obtained by the optimal filter assuming exact knowledge of M. This difference in IF represents a loss L_{if} compared to the optimum processor. The value of L_{if} has been calculated and sample results for several filter types are illustrated in Fig 3.4 for land clutter and Fig. 3.5 for sea

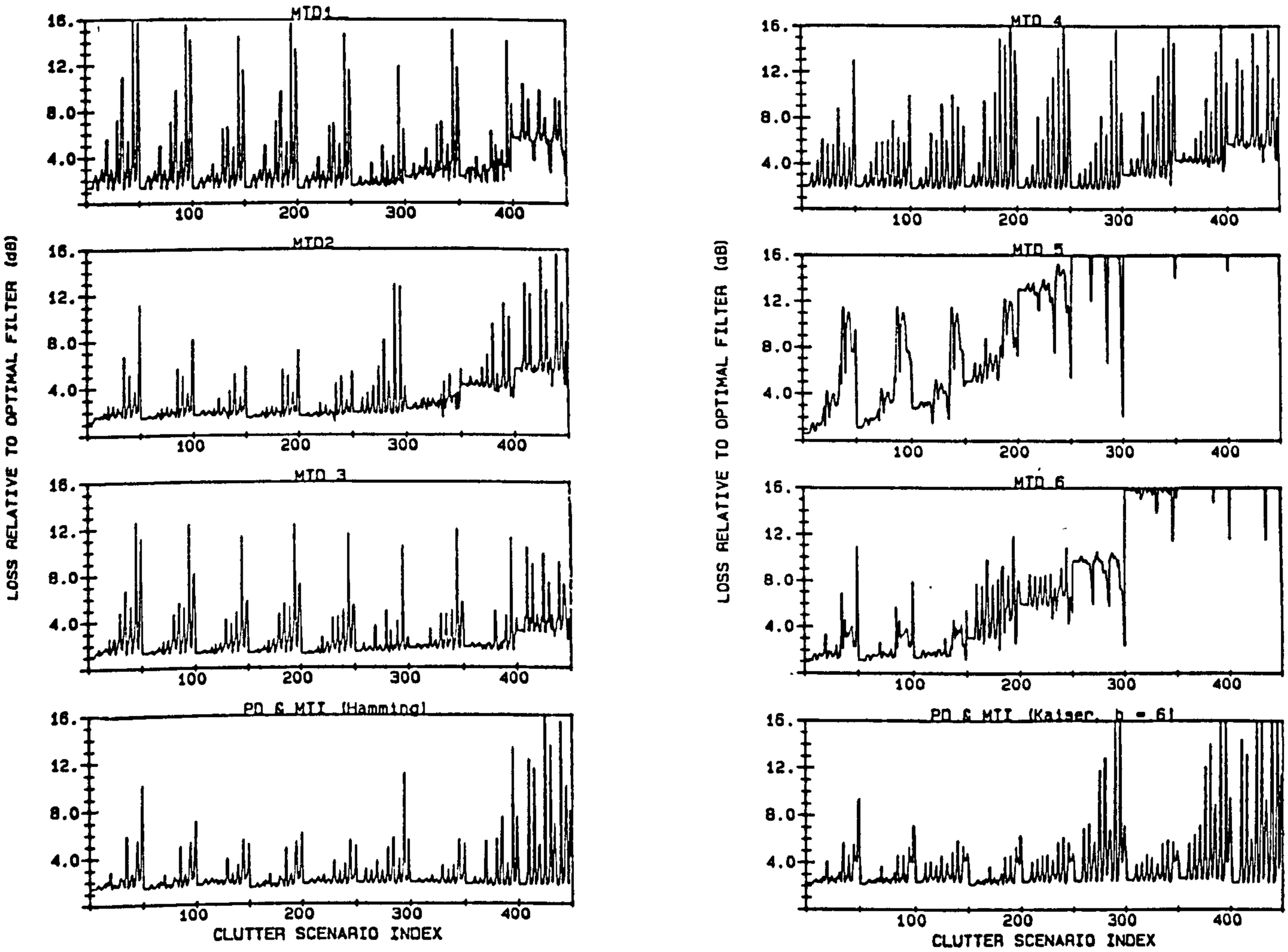

Fig. 3.4: *Loss Relative to Optimal Filter for Land Clutter Scenarios*

(Δ = 30 %; N_f = 10)

clutter, which give the loss for each clutter scenario, indexed on the horizontal axis as defined in Appendix 3.2 and 3.3. The value of L_{if} is summarised in Fig. 3.6 in terms of a histogram of the loss suffered by each filter over the 750 land and sea clutter scenarios, for $\Delta = 30\%$. (Note the different horizontal axis scale for the AMTI&MTI filter). Results for simple MTI and AMTI filters, which give substantially poorer performance, are not shown in Fig. 3.6.

The single filter implementations (ie. LP, LP&MTI and AMTI&MTI) can be seen to suffer higher loss than the filter bank implementations. These results, however, exclude the collapsing losses inherent in multi-filter processors. The collapsing loss is tabulated in Table 3.4 for various values of P_{fa}, N and the number of reference cells N_r used in the CFAR processor.

Table 3.4
Collapsing Loss in Multi-filter Processors

	$P_{fa} = 10^{-4}$			$P_{fa} = 10^{-6}$		
	N = 5	N= 8	N = 10	N = 5	N = 8	N = 10
$N_r = 8$	4.17	4.52	4.68	5.48	5.78	5.92
$N_r = 16$	2.39	2.66	2.78	2.84	3.05	3.15
$N_r = 32$	1.55	1.78	1.89	1.64	1.81	1.89
$N_r = 64$	1.15	1.36	1.46	1.06	1.21	1.28
Ideal	.75	.95	1.04	.50	.64	.70

These figures assume $P_d = 50\%$, CA CFAR processing, and Rayleigh clutter amplitude statistics. They would increase noticeably should strongly spiky clutter amplitude statistics be assumed.

The results have been further reduced to obtain simple mean values of loss for each type of filter. Two means have been calculated, namely the mean of the linear IF, subsequently expressed in dBs, and the mean of the dB value of the IF. The former is the more rigorous mathematically and is widely used in the literature, but is very sensitive to "rogue" clutter scenarios indicated by high spikes in Figs. 3.4 and 3.5, which may not warrant such influence on the results. The latter appears to correspond better to the mean increase in signal power required to achieve detection, probably due to the approximate linearity of detection probability with the log of signal power in the region of $P_d = 50\%$. Both measures, averaged over all 750 land and sea clutter scenarios, are given in Table 3.5 for various values of Δ.

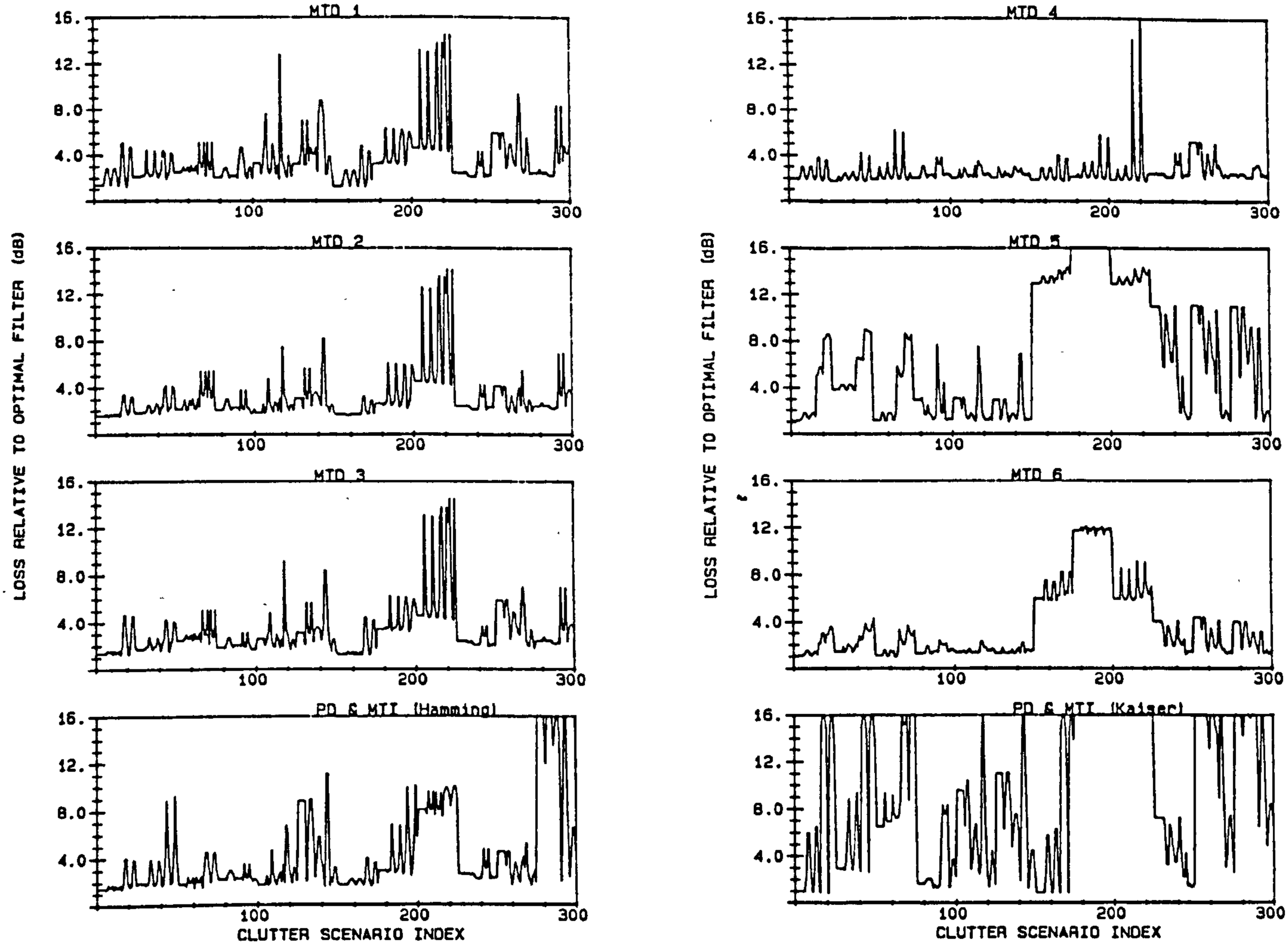

Fig. 3.5: *Loss Relative to Optimal Filter for Sea Clutter Scenarios*

($\Delta = 30\ \%$; N=10)

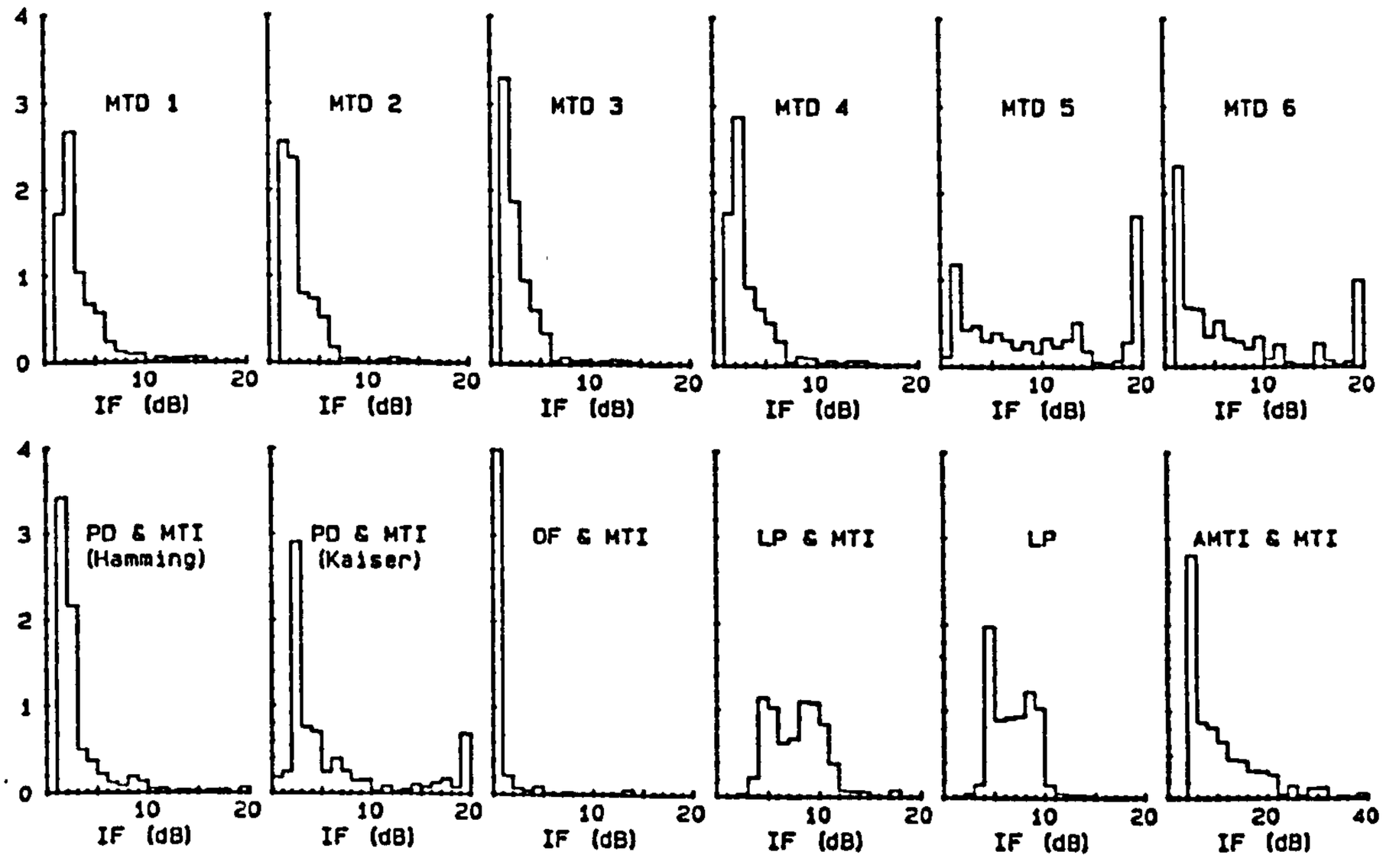

Fig. 3.6: *Histogram of Loss Relative to Optimal Filter for Land and Sea Clutter Scenarios ($\Delta = 30\ \%$; $N = 10$).*

The performance of the AMTD processors defined in Section 3.3.6 has been evaluated in the same terms as above. The loss compared to the optimal filter has been calculated assuming ideal filter bank selection. The value of L_{if} achieved by some of the better AMTD filter bank combinations is illustrated in Fig 3.7a for land clutter and Fig. 3.7b for sea clutter, which again give the loss for each clutter scenario, indexed on the horizontal axis, as defined in Appendix 3.2 and 3.3. The mean values of L_{if} are tabulated for each of the 16 AMTD filter bank combinations in Table 3.6

Table 3.5
Average L_{if} for Different Doppler Processors,
Averaged over all Land and Sea Clutter

Filter Type	Mean(L_{if})$_{dB}$				[Mean(L_{if})]$_{dB}$			
	Δ=5%	Δ=30%	Δ=70%	Δ=100%	Δ=5%	Δ=30%	Δ=70%	Δ=100%
MTD 1	2.677	3.556	4.267	4.300	4.224	4.907	5.550	5.558
MTD 2	2.572	3.135	3.702	3.736	3.520	4.050	4.617	4.647
MTD 3	2.192	2.878	3.470	3.506	3.046	3.737	4.396	4.426
MTD 4	3.006	3.568	4.210	4.282	4.894	5.258	5.711	5.746
MTD 6	6.910	7.664	8.151	8.202	17.097	17.479	17.365	17.349
PD&MTI[1]	2.584	3.262	3.760	3.795	5.202	5.593	5.477	5.484
OF	.000	.000	.000	.000	.000	.000	.000	.000
PD&MTI[2]	5.744	6.643	7.267	7.297	12.168	14.096	15.134	15.096
OF&MTI	.572	.652	.845	.876	1.921	1.699	1.779	1.795
LP&MTI	6.371	7.860	8.742	8.763	8.144	8.862	9.487	9.494
LP	5.319	6.842	7.708	7.721	6.518	7.373	8.043	8.049
AMTI&MTI	10.330	10.853	11.977	12.095	21.438	21.574	22.104	22.120
AMTI	18.154	18.070	18.439	18.530	27.422	27.491	27.622	27.618
MTD 5	11.698	12.168	12.265	12.261	26.229	26.337	25.449	25.266

Notes: [1] Hamming window [2] Kaiser window, b = 6

Table 3.6
Average L_{if} for AMTD Processors

AMTD No.	Mean(L_{if})$_{dB}$				[Mean(L_{if})]$_{dB}$			
	α=5%	α=30%	α=70%	α=100%	α=5%	α=30%	α=70%	α=100%
1	2.012	2.611	3.197	3.234	2.640	3.259	3.932	3.969
2	2.392	2.848	3.353	3.388	3.173	3.551	3.978	4.006
3	2.160	2.759	3.293	3.328	2.925	3.452	3.952	3.983
4	1.924	2.579	3.124	3.159	2.600	3.150	3.694	3.728
5	1.955	2.481	2.995	3.034	2.477	2.950	3.455	3.489
6	1.767	2.421	2.955	2.994	2.242	2.870	3.434	3.471
7	1.809	2.465	3.002	3.039	2.241	2.851	3.443	3.481
8	2.408	3.013	3.610	3.680	3.799	4.242	4.703	4.752
9	1.870	2.437	2.928	2.968	2.542	2.961	3.372	3.406
10	1.808	2.350	2.836	2.872	2.419	2.831	3.249	3.280
11	1.839	2.329	2.851	2.891	2.219	2.659	3.180	3.218
12	1.694	2.247	2.738	2.778	2.147	2.641	3.090	3.125
13	1.682	2.218	2.690	2.728	2.033	2.483	2.927	2.963
14	1.681	2.236	2.721	2.766	2.359	2.779	3.184	3.221
15	1.619	2.154	2.650	2.691	1.953	2.440	2.912	2.950
16	1.522	2.060	2.523	2.562	1.861	2.325	2.761	2.798

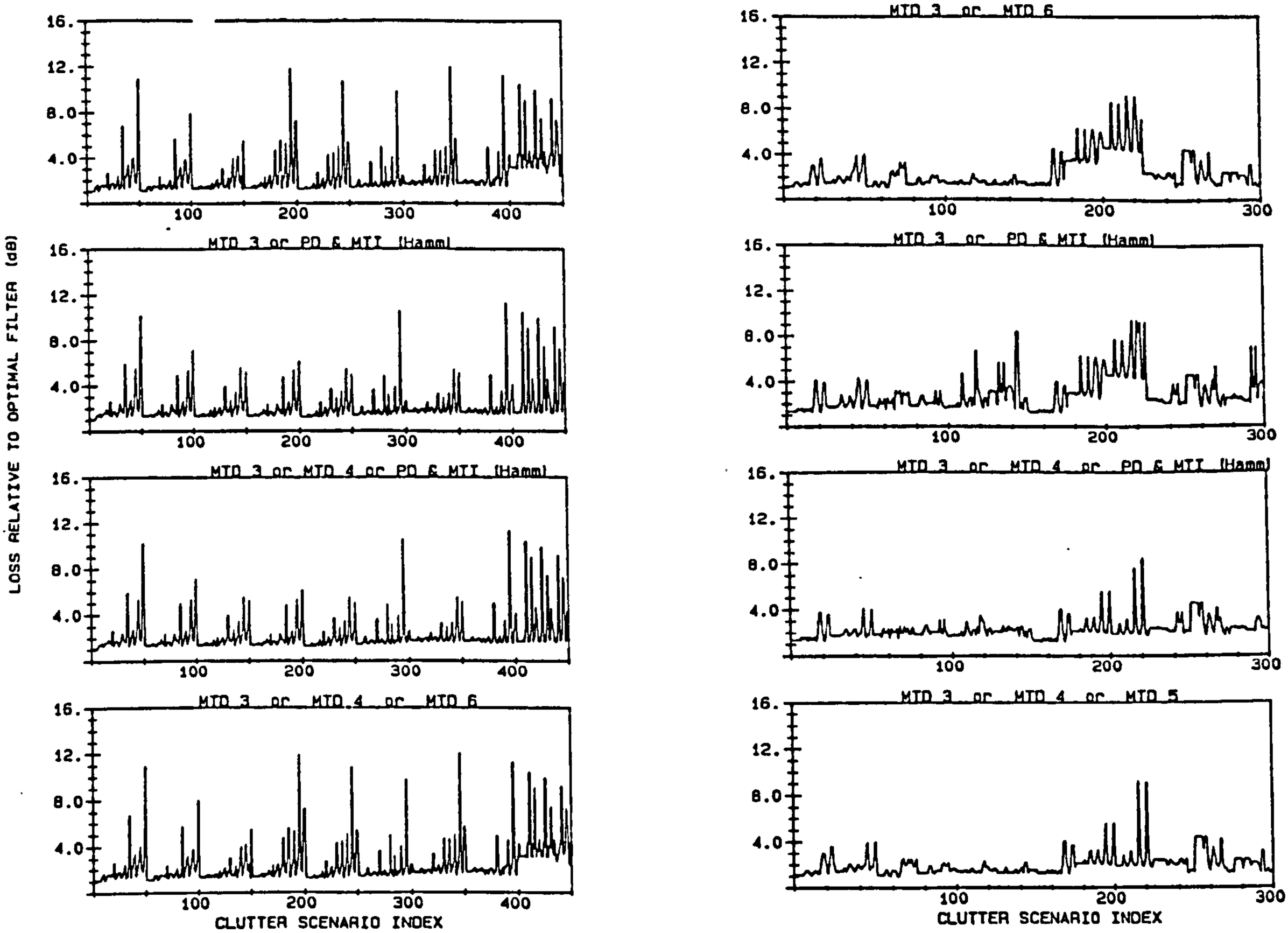

Fig. 3.7: *Loss Relative to Optimal Filter a) Land Clutter b) Sea Clutter*

Data corresponding to Tables 3.5 and 3.6 for individual averages of land and sea clutter are given in Appendix 3.5. We conclude that for land clutter:

* PD&MTI processing with a Hamming window provides the best performance (L_{if30} = 2.49 dB), followed by the MTD 3 processor (L_{if30} = 2.62 dB).

* Of the AMTD processors, Combination 6 is best if the library contains two filter banks, reducing L_{if30} by ~ 0.3 dB/0.7 dB depending on whether dBs are taken before or after averaging.

* AMTD Combination 13 is the best if the library contains three filter banks, reducing L_{if30} by ~ 0.35 dB/0.75 dB depending on whether dBs are taken before or after averaging.

* AMTD Combination 16 is best if the library contains four filter banks, reducing L_{if30} by ~ 0.4 dB/0.8 dB depending on whether dBs are taken before or after averaging.

For sea clutter:

* The MTD 4 processor provides the best performance (L_{if30} = 2.61 dB), followed by MTD 2 (L_{if30} = 3.12 dB).

* Of the AMTD processors, Combination 8 is best if the library contains two filter banks, reducing L_{if30} by ~ 0.6 dB/0.95 dB depending on whether dBs are taken before or after averaging.

* AMTD Combination 12 is the best if the library contains three filter banks, reducing L_{if30} by ~ 0.7 dB/1.05 dB depending on whether dBs are taken before or after averaging.

* AMTD Combination 16 is best if the library contains four filter banks, reducing L_{if30} by ~ 0.75 dB/1.1 dB depending on whether dBs are taken before or after averaging.

For an average of land and sea clutter:

* The MTD 3 processor provides the best performance (L_{if30} = 2.88 dB), followed by MTD 2 (L_{if30} = 3.13 dB).

* Of the AMTD processors, Combination 6 is best if the library contains two filter banks, reducing L_{if30} by ~ 0.5 dB/0.9 dB depending on whether dBs are taken before or after averaging.

* AMTD Combination 13 is the best if the library contains three filter banks, reducing L_{if30} by ~ 0.7 dB/1.4 dB depending on whether dBs are taken before or after averaging.

* AMTD Combination 16 is best if the library contains four filter banks, reducing L_{if30} by ~ 0.85 dB/1.6 dB depending on whether dBs are taken before or after averaging.

3.6 DISCUSSION

Examination of the available data indicates that an IF of typically 2 to 3 dB less than the optimum can be expected from MTD or PD&MTI processors. The design of such processors depends to some extent on the spectrum of the clutter in which the radar is expected to operate; however, the use of M/N detection logic combined with PRF stagger has the effect of emphasising the performance in those filters which are clearest of clutter. This motivates for reduced far out sidelobes at the expense of a broader main lobe and lower coherent integration gain in noise. Only if clutter occupying a high proportion of the doppler space and without strong narrowband components is expected does it seem desirable to allow the sidelobes to rise as a consequence of pursuing a narrower mainlobe.

The choice of window function applied to PD&MTI processing can be seen to affect the loss quite dramatically. For both land and sea clutter a Hamming window gives the best performance out of the window functions considered in this study. No consistent superiority of MTD processors over PD&MTI processors can be identified; indeed, in terms of the overall mean IF of the land clutter scenarios the Hamming windowed PD&MTI provides the best performance. This is despite specific shaping of the MTD processors to cancel zero-doppler clutter and without considering the (marginally) lower collapsing loss of the 8-filter PD&MTI processor. MTD processing cannot therefore be justified in terms of clutter suppression alone. It does however have advantages in allowing an arbitrary number of parallel filters to be implemented; ten were assumed in this study but fewer could be used, allowing considerable hardware savings with minimal increase in straddling loss.

The loss in IF_Δ has been defined in relation to the IF_Δ achieved by an optimal filter. Practical optimal filters (both Hsiao type and linear predictor filters) also suffer some loss relative to the ideal optimum due to their need to adapt to the local environment. The magnitude of this loss is the subject of Chapter 4, but, as will be shown, for Hsiao type filters it is typically of the order of 2 to 4 dB in spatially homogeneous clutter environments. In terms of the mean loss suffered by adaptive optimal filters and MTD or PD&MTI filters, the results in this Chapter therefore give no justification for the considerable additional complexity associated with adaptive optimal filtering. Only if the loss "spikes" in Figs. 3.4 and 3.5 (ie. rare clutter scenarios where the loss in IF is quite large) can absolutely not be tolerated is there a case for employing such filters. Even then spatial heterogeneity of the amplitude and/or spectral statistics of the clutter, particularly the existence of point clutter sources, causes additional losses which may exceed the gains hoped for by using the adaptive optimal filter. The use of MTI cancellers to reduce the

problem of point clutter sources can be seen to introduce a mean loss of only 0.2 to 1.2 dB in homogeneous clutter, and would therefore appear to be a viable option.

The results presented in Section 3.5 indicate that linear predictor type filters, optimal in terms of clutter residue minimisation, provide inferior performance to a bank of Hsiao optimal filters, even after accounting for collapsing losses. This is because the coherent integration gain of "tuned" Hsaio filters exceeds the collapsing loss, yielding substantial net gain compared "untuned" linear predictor filters. Some results to the contrary have appeared in the literature (D'Addio, 1984; Barbarossa, 1987; Farina, 1988). However, these have generally not considered the use of PRF stagger which empasises the performance of filters in the more clutter free regions of doppler space. Judicious selection of clutter spectra also occasionally yields LP performance almost as good as OF performance before subtracting collapsing losses, and hence better overall performance, but only in very few of the clutter scenarios considered in this study was that the case. The superior performance of Hsiao optimal filters under the conditions assumed in this study can therefore be stated with some confidence. However, if the target is assumed to be fast fluctuating with effectively white doppler spectrum, then coherent integration is not feasible and LP filtering would be more appropriate. Also, if the clutter is very spiky, collapsing losses may increase substantially depending on the type of CFAR processor employed, and LP filtering may again be more efficient.

The use of AMTD does not appear to provide dramatic benefits compared to conventional MTD: where two filter banks are available to choose from the loss can be reduced by about 0.5 dB; a choice of three filter banks reduces the loss by 0.7 dB; and selection from four filter banks reduces the loss by about 0.85 dB. Comparison of Figs. 3.4 with 3.7a and Figs. 3.5 with 3.7b also indicates that little reduction of loss "spikes" associated with "rogue" clutter scenarios is achieved. In addition, non-ideal filter bank selection will reduce the benefits of AMTD from their already meagre levels. Justification of AMTD processing on the grounds of clutter suppression therefore seems very dubious.

The above discussions are based solely on clutter suppression considerations. They must be qualified with regard to true velocity estimation: narrow and uniformly shaped mainlobes ease the problem of resolving doppler ambiguities and generally yield more accurate estimates of true target velocity. Should high emphasis be placed on these functions, filter design will be accordingly affected. In processors where true velocity information is utilised for false alarm rejection, thereby permitting lower thresholds to be used, a balance will be needed between clutter suppression and mainlobe width. Exact optimisation of filter design will be strongly dependent on specific algorithms and assumed clutter spectra, and is a topic which is not widely addressed in the literature. It may well be

that this is the only real justification for AMTD processing, but this has not yet been convincingly demonstrated.

In this study N, the number of pulses coherently processed, has been chosen as 10. Higher values would further enhance the performance of the filter bank processors compared to the single filter processors, but is unlikely to noticeably affect the performance of the filter bank processors relative to each other. Smaller values of N (say N = 5, allowing 2-pulse MTI with a 4-pulse FFT in the case of PD&MTI processing) would reduce the difference between the filter bank and single filter processors. In either case the reduction in IF relative to the optimum does not change very dramatically.

3.7 CONCLUSIONS

The conclusions of this Chapter are summarised as follows:

1. The IF averaged over all doppler is not an appropriate measure for expressing filter performance in cases where a filter bank is used, where PRF stagger is used, and where targets are assumed to fluctuate much slower than the PRF. A more appropriate measure is IF_{Δ}, the doppler dependent IF averaged over the best Δ % of the doppler space.

2. The MTD filter designated MTD3 gives the best performance averaged over all the clutter scenarios considered in this study.

3. PD&MTI processors achieved the best performance using a Hamming window, in which case the mean loss was only about 0.4 dB greater than that for MTD3, averaged over all the clutter scenarios considered.

4. Adaptive optimal techniques do not seem justifiable, since the loss associated with adaptive estimation of the clutter covariance matrix can be expected to be as large as or greater than the loss suffered by MTD or PD&MTI techniques.

5. Notwithstanding point 4 above, consistently superior performance of adaptive Hsiao type optimal filters over linear predictor filters has been demonstrated.

6. Adaptive MTD processing only seems to reduce the mean loss in IF by less than 1 dB with minimal improvement of "rogue" cases. It does not seem to be justifiable in terms of clutter suppression alone.

7. The role of true velocity estimation in false alarm elimination (possibly as a consequence of track initiation) needs to be examined further, and may provide the only real justification for AMTD processing.

8. With the exception of work related to point 7 above, improved doppler processing techniques would not appear to be a fruitful area of research aimed at improving detection performance in high resolution radars.

CHAPTER 4

PERFORMANCE OF ADAPTIVE OPTIMAL DOPPLER PROCESSORS IN HETEROGENEOUS CLUTTER

4.1 INTRODUCTION

4.1.1 Background

In the previous Chapter it has been shown that ideal optimal (Hsiao) filtering techniques offer superior improvement factor (IF) performance compared to conventional MTD and Pulse Doppler filtering techniques. The mean magnitude of this improvement in IF, averaged over a wide range of clutter conditions, is in the region of 2 to 3 dB. In practice, however, "ideal" optimal filtering is not possible due to the absence of accurate *a priori* knowledge of the local clutter spectral characteristics, which therefore have to be estimated on-line. This results in imperfect estimates of the clutter spectrum, or its covariance matrix M, which after solution for the filter weight vector yields sub-optimal filter performance. Practical "optimal" filters therefore suffer a loss relative to ideal optimal filters, even in spatially homogeneous clutter. Environments for which adaptive filters are specifically intended, namely temporally and spatially varying clutter, compound the problem further since the covariance matrix in the range bin being filtered will in general differ from that in the adjacent range bins used in estimating the covariance matrix.

Under conditions of spatially homogeneous clutter the magnitude of the loss due to imperfect estimation of the covariance matrix has been widely investigated. It has been shown (Reed et al, 1974) that the relative reduction in IF depends only on the number of reference cells K used in estimating M (provided $K \geq N$, the order of the filter), and closed form expressions for losses in IF have been published for this case. The assumption of homogeneous clutter is, however, very restrictive and will often be violated. Despite this, the losses in IF under conditions of clutter heterogeneity have not been widely quantitatively addressed in the literature. In this Chapter we therefore address the effects of clutter heterogeneity on adaptive doppler filtering, and investigate the use of pre-filter MTI as a means of reducing filter sensitivity to some forms of clutter heterogeneity.

Three general categories of clutter heterogeneity are investigated, namely:

1. Clutter in which the amplitude and spectral width in each range bin are randomly drawn from spatially invariant parent populations of specified characteristics. This could represent, for example, high resolution sea clutter, sea clutter plus weather clutter, or land clutter due to windblown fields or trees. For this chapter we limit our attention to unimodal clutter.

2. Clutter edges, in which the clutter amplitude and/or spectrum exhibit a step change at some point in the range profile of the clutter. This typically represents cases of transition between land and sea clutter, shadowed and illuminated surface clutter, or dominant sea and weather clutter etc.

3. Clutter which is essentially homogeneous but in which a small number of range bins are corrupted by returns with significantly different amplitude and spectral characteristics, representing point clutter sources or extraneous targets. The strength, spectral characteristics and the number of extraneous targets will be varied.

In this Chapter we restrict the order of the filter to the range $5 \leq N \leq 20$. It was felt that this represents the most fruitful region for the application of adaptive optimal filters. Practical implementation of higher order filters poses computational difficulties, primarily due to the required matrix inversion of NxN matrices, but also estimation of the covariance matrix. Lower order filters have too few degrees of freedom to yield significant benefits from full adaptivity.

Only non-concurrent processing has been addressed, ie. the test cell is not considered to be included as one of the reference cells. This yields marginally inferior performance against targets with known spectrum, but, unlike concurrent processing, is not susceptible to self-masking by targets with spectra different to that assumed in solving the filter weight equation. It is also a necessary assumption for many analytic results in the literature which assume independence between the estimate of the covariance matrix and the test cell covariance matrix.

4.1.2 Review of Relevant Literature

Reed at. al (1974) investigated the convergence rate in adaptive arrays under conditions of homogeneous Gaussian backgrounds, for Sample Matrix Inversion (SMI) estimation

of the filter weights. They derive a simple analytic expression for the loss suffered by adaptive filters when the number of range bins K used in estimating the covariance matrix is finite but larger than the filter order N. They also show that the ratio between the improvement factor achieved with adaptive estimation of the covariance matrix, and that achieved with *a priori* knowledge of the covariance matrix, is beta distributed. Unfortunately, they do not present expressions for the PDF of the clutter residue power, which would provide useful insight into the effect on detection performance of adaptive weight estimation.

Farina and Protopapa (1988) give some results for the detection loss introduced by adaptive estimation of the covariance matrix in Linear Predictor adaptive filters, including some results for cases of K<N. The loss is shown to be in the region of 5 to 10 dB for their cases analysed. These results are, however, restricted to very specific clutter and filter parameters and are therefore not of wide general usefulness.

Nitzberg (1990) has addressed the reduction in IF suffered by SMI algorithms when the clutter amplitude is heterogeneous, specifically gamma-modulated Gaussian speckle (ie. K-distributed clutter) with homogeneous spectrum. He shows that in most cases the loss is relatively small, but does not explicitly consider cases of very spiky clutter ($\nu<0.5$). He also neglects possible second order effects of increased variance (and spikiness) of the clutter residue due to amplitude heterogeneity.

Gerlach and Kretschmer (1990, 1991) investigate convergence properties of Gram-Schmidt and SMI adaptive algorithms. They show that the two algorithms are equivalent for infinite numerical accuracy. Concurrent and non-concurrent processors are addressed and expressions for the loss in IF due to adaptive estimation of the covariance matrix are presented for Gaussian and non-Gaussian inputs. Nevertheless, amplitude and spectral spatial homogeneity are assumed and no non-homogeneous effects are considered.

The lack of research into non-homogeneous effects in adaptive filters appears to be mainly due to analytic difficulties associated with the joint PDF of the estimated covariance matrix. Under conditions of homogeneous and stationary inputs this is described by the complex Wishart distribution (Goodman, 1963); no equivalent expression has been found in the literature for non-homogeneous inputs. Furthermore, the complex Wishart distribution (and indeed the real Wishart distribution) are only non-singular for $K \geq N$, and theorems regarding addition of Wishart matrices are only valid for all matrices having equal covariance matrices. This precludes the possibility of constructing non-homogeneous Wishart matrices as the sum of dissimilar homogeneous

covariance matrices. These analytic difficulties have necessitated the use of simulations as a means of evaluating performance in non-homogeneous clutter.

4.1.3 Some Theory and Definitions

In view of the superior performance of Hsiao optimal filters compared to Linear predictor filter, we concentrate on the former in this Chapter. The filter weights are determined by solving the matrix equation

$$\mathbf{W} = \mu \mathbf{M}^{-1}\mathbf{S} \qquad \ldots (4.1)$$

where $\mathbf{W}$ is the desired filter weight vector

$\mathbf{M}^{-1}$ is the matrix inverse of the covariance matrix of the clutter on which the filter operates

$\mathbf{S}$ is the vector of target returns, which is generally taken as a constant power complex vector rotating at the appropriate target doppler frequency[1]

μ is an arbitrary constant.

The improvement factor (IF) is then calculated as:

$$IF = \frac{S/C_{out}}{S/C_{in}} = \frac{\mathbf{W}^H\mathbf{S}\mathbf{S}^T\mathbf{W}}{\mathbf{W}^H\mathbf{M}\mathbf{W}} \qquad \ldots (4.2)$$

where ^{T} represents transpose and ^{H} conjugate transpose. This corresponds to the ideal adaptive optimal filter since the filter weights are based on exact knowledge of $\mathbf{M}$. Adaptive filters generally obtain an estimate $\widehat{\mathbf{M}}$ of the local clutter covariance matrix by estimating its elements $\widehat{m}(i,j)$ according to the expression:

$$\widehat{m}(i,j) = \frac{1}{K}\sum_{k=1}^{K} x_{ik}x_{jk}^{*} \qquad \ldots (4.3)$$

where x_{ik} is the i^{th} received sample in the k^{th} range bin, * represents complex conjugation, and K is the number of reference range bins used in the region of the bin being filtered. The spatial resolution cell to which the filter is applied is termed the *test cell*, the resolution cells used in estimating the covariance matrix are termed the *reference cells*,

[1] If targets with broader spectra are envisaged, S must be replaced by the target correlation vector. Absolute Hsiao filter performance will deteriorate if the target spectrum occupies a significant portion of the doppler space; relative performance is not expected to be dramatically affected.

and the region covered by the reference cells is called the *reference window.*

Eqn. (4.3) represents a maximum likelihood estimator of **M** for K>N (Reed, 1974). Since for K<∞, $\widehat{\mathbf{M}} \neq \mathbf{M}$, and $\widehat{\mathbf{W}} = \mu\widehat{\mathbf{M}}^{-1}\mathbf{S}$, we have that $\widehat{\mathbf{W}} \neq \mathbf{W}$, with the estimated weights yielding a lower improvement factor than the ideal weights. This represents a loss which will be termed here the *IF loss*, L_{if}, and is defined as the ratio between the IF achieved by the adaptive filter being analysed under test conditions and the IF achieved by the reference filter under the reference conditions, ie.:

$$L_{if} = \frac{IF_{test}}{IF_{ref}} = \frac{\dfrac{\widehat{\mathbf{W}}^H \mathbf{S}\mathbf{S}^T \widehat{\mathbf{W}}}{\widehat{\mathbf{W}}^H \mathbf{M}_t \widehat{\mathbf{W}}}}{\dfrac{\mathbf{W}_{ref}^H \mathbf{S}\mathbf{S}^T \mathbf{W}_{ref}}{\mathbf{W}_{ref}^H \mathbf{M}_{ref} \mathbf{W}_{ref}}} \qquad \ldots (4.4)$$

where $\widehat{\mathbf{W}}$ are the weights derived from the estimated covariance matrix

$\mathbf{M}_t$ is the true local covariance matrix of the clutter in the test cell

$\mathbf{M}_{ref}$ is the true covariance matrix of the reference clutter

$\mathbf{W}_{ref}$ are the weights derived from $\mathbf{M}_{ref}$

Note that in clutter with spatially varying amplitude and/or spectrum, $\mathbf{M}_t \neq \mathbf{M}_{ref}$. In this study $\mathbf{M}_{ref}$ is taken as the covariance matrix of clutter with spectral width equal to the mean of the spatially varying spectral width and power equal to the mean of the spatially varying power. In spatially invariant clutter, $\mathbf{M}_t = \mathbf{M}_{ref}$, and Reed et. al. (1974) have obtained the following closed form expression for the IF loss for $K \geq N$:

$$L_{if} = \frac{K - N + 2}{K + 1} \qquad \ldots (4.5)$$

This is independent of the covariance matrix and the desired target vector. For K < N, the joint PDF of $\widehat{\mathbf{M}}$ is singular and a closed form expression is not available. The loss also becomes strongly dependent on the clutter covariance matrix and the target vector.

An alternative definition of loss, which is arguably more relevant to radar performance studies, particularly if the filter introduces random modulation to the clutter residue power, is to define the loss as the mean increase in signal power required to achieve a specified expected detection probability when using the test filter, under test conditions, compared to the signal power required when using the reference filter under reference conditions. This definition of loss will be termed the *detection loss*, L_{pd}. Due to the non-linearity of the expression for detection probability, L_{if} and L_{pd} will differ, and as will be

seen later, the difference can be considerable. The precise magnitude of L_{pd} will depend on the detection processing employed. For comparative purposes, in the absence of more specific information and in an attempt to ensure that results here are as general as possible, ideal adaptive threshold detection has been assumed for this study, ie. the threshold in each range-doppler bin is set to achieve the specified false alarm probability in that bin. This implies that the detector can somehow precisely determine the mean clutter residue power in each range doppler bin. For adaptive filtering in non-homogeneous clutter, the instantaneous signal-to-residue ration in each range doppler bin is a random variable, denoted here S/R. Then on the assumption of ideal adaptive threshold detection the expected detection probability is:

$$\overline{P}_d = E\left[\exp\left[\frac{-\ln(P_{fa})}{1 + S/R}\right]\right] \qquad \ldots (4.6)$$

which cannot usually be calculated analytically since the PDF of S/R is not known, and for this study has been obtained by arithmetic averaging of simulation data. Denoting by $S_{50}|_{ideal}$ the signal power required to achieve $\overline{P}_d = 50\%$ when using ideal weights, under reference clutter conditions, and by $S_{50}|_{test}$ the signal power required to achieve $\overline{P}_d = 50\%$ when using adaptive weights in the required non-homogeneous clutter conditions, the detection loss is defined as

$$L_{Pd} = \frac{S_{50}|_{ideal}}{S_{50}|_{test}} \qquad \ldots (4.7)$$

In calculating improvement factors it was shown in the previous Chapter that it is necessary to consider the portion of the radar's doppler space over which the IF is calculated and averaged. Most studies in the literature (eg. Nitzberg) deal only with the case of a single filter tuned to a specific desired doppler. As was shown in Chapter 3 this is not a suitable performance measure in a radar systems context and the IF needs instead to be averaged over a finite portion of the doppler space. The percentage of the doppler space over which averaging must be performed depends on radar waveform and processing parameters and is typically in the region 30% to 70%. In this Chapter IF and loss figures have been calculated for different percentages of the doppler space over which the IF has been averaged, and results are quoted with respect to these percentages. As will be shown later, the loss can vary considerably depending on the doppler space percentages averaged.

In all cases here the clutter is assumed to have Gaussian spectrum. This is the most

common assumption for clutter suppression studies and is a good first approximation to many clutter conditions. The spectral width parameter adopted for this study is therefore the standard deviation σ_0 of the Gaussian clutter spectrum, so that the spectrum is defined by:

$$H(f) = \frac{1}{\sqrt{2\pi\sigma_0^2}} \exp[-(f-f_c)^2/2\sigma_0^2] \quad \ldots (4.8)$$

Multi-modal and more complicated clutter spectral shapes can be constructed by the linear superposition of a number of Gaussian clutter sources.The element m(i,j) of the clutter covariance matrix **M** of a single clutter source with Gaussian spectrum defined by eqn. (4.8) is given by:

$$m(i,j) = P_c \, \rho^{(i-j)^2} \exp[-j2\pi(i-j)f_cT] \quad \ldots (4.9)$$

where $\rho = e^{-2(\pi\sigma T)^2}$ is the clutter correlation coefficient
f_c is the centre frequency of the clutter
T is the inter-pulse period
P_c is the mean clutter power
σ_0 is the standard deviation of the clutter spectrum.

The covariance matrix of multimodal clutter is obtained merely through the addition of the contributions of each of the spectral components.

4.2 EFFECT OF CLUTTER HETEROGENEITY ON FILTER PERFORMANCE

4.2.1 Introduction

As previously mentioned, adaptive filter performance is generally analysed by assuming that the clutter has the same amplitude and spectrum over the extent of the reference window. This assumption is, of course, an idealisation of reality, as both the amplitude and spectrum can in fact vary considerably in space. A great deal has been published regarding the nature of the amplitude fluctuations, and a number of models exist for various types of non-Rayleigh clutter. In this Chapter the K-distribution model has been adopted to describe the amplitude fluctuations for the following reasons:

1. It is widely regarded as the best model for high resolution and/or low grazing angle sea clutter. Although not primarily intended for land clutter scenarios, the

K-distribution seems to be adequate for many such situations, where other models do not seem to offer any advantages in terms of statistical accuracy or physical justifiability.

2. The compound form of the K-clutter model makes it particularly suitable for modelling clutter with arbitrary and fluctuating doppler spectrum, since the spectral characteristics do not affect the amplitude statistics.

In accordance with the K-distribution model, we therefore assume in this thesis that the local clutter power in each range bin is independently drawn from a Gamma distribution of expected value equal to the mean clutter power P_c and shape parameter ν. Negligible spatial correlation is assumed here due to the absence of spatial correlation data or models. It is shown in Chapter 6 that high degrees of spatial correlation are required to significantly affect CFAR processor detection performance; since SMI covariance matrix estimation is analogous to CA-CFAR processing, it is likely that high spatial correlation would be required to appreciably influence the results presented here.

The choice of model for spectral fluctuations is more arbitrary: very little has appeared in the literature on this topic. Although some authors have reported certain features of spectral fluctuations of sea clutter (eg. Chan 1990, Attanasov 1990, Helmken 1990, Nohara 1991), no model seems to have been proposed, let alone accepted, for these fluctuations. In the absence of any more concrete data on which to base a model for the spectral fluctuations, it is therefore proposed that, as a first approximation, the local spectral width of the clutter is drawn from a gamma distribution with width parameter b_1 defined as

$$b_1 = \frac{\text{std. deviation of spectral width}}{\text{mean spectral width}} \qquad \ldots (4.10)$$

Thus the higher b_1, the greater the variation in spectral width; $b_1 = 0$ yields a Kronecker delta at the mean spectral width; $b_1 = 1$ yields an exponential distribution with mean value equal to the mean spectral width. For this study values of b_1 in the range $0 \leq b_1 \leq 0.8$ have been considered. Wider variation seems improbable and for computational reasons is more difficult to analyse. The gamma distribution has been adopted since 1) it yields an analytically tractable model which is also easy to simulate, 2) it satisfies the requirement of being a two parameter single-sided distribution, 3) it has been obtained as the first term in a Laguerre series expansion of any one-sided distribution and therefore represents an approximation to whatever the true distribution may be, and 4) it contains as a special

case the necessary limiting form where the standard deviation of the spectral fluctuations tends to zero (the gamma shape parameter tends to ∞).

The spectral width is assumed to be independent of the local clutter amplitude. Although some evidence exists to suggest there may be some correlation between the two parameters, it is insufficient to define the nature of such correlation. The local spectral width in each range bin is assumed to be independently drawn from the parent distribution.

Four clutter scenarios have been used in the performance analyses which follow. These are defined as:

Case 1	$P_c = 30$ dB	$\sigma_0 = 0.02$
Case 2	$P_c = 60$ dB	$\sigma_0 = 0.02$
Case 3	$P_c = 30$ dB	$\sigma_0 = 0.05$
Case 4	$P_c = 60$ dB	$\sigma_0 = 0.05$

In all cases the clutter power is expressed relative to radar thermal noise and the spectral width relative to the PRF. The clutter centre frequency f_c is taken as zero in all cases. This is not restrictive since the target doppler is assumed to vary over the remainder of the doppler space.

4.2.2 Limiting Cases

In homogeneous clutter, as $K \to \infty$, $\widehat{M}$ tends to an exact description of covariance matrix of the clutter in test cell and so $\widehat{W} \to W$; however, in heterogeneous clutter, as $K \to \infty$, $\widehat{M}$ tends to the expected value of the clutter covariance matrix which would in general differ from that in the test cell. Thus $\widehat{W} \neq W$ and this introduces a reduction in the improvement factor achieved in each cell, and hence in the mean IF and target detectability.

In this section limiting cases are examined to illustrate the effect of clutter heterogeneity only on the loss in improvement factor and target detectability, excluding additional losses caused by $K<\infty$. These results thus indicate an upper bound on performance in heterogeneous clutter. A particular advantage of examining limiting cases is that they yield semi-analytic expressions which require only simple numerical integration to produce quantitative results; for finite K, performance evaluation in non-homogeneous clutter requires extensive and time-consuming Monte-Carlo simulation.

4.2.2.1 Amplitudé Heterogeneity

In this section it is assumed that the power of the clutter in each range bin is independently drawn from a Gamma distribution of mean value P_c (ie, the mean clutter power) and shape parameter ν. Within each range bin the clutter is assumed to exhibit Rayleigh speckle with pulse-to-pulse correlation defined by the covariance matrix M, which is assumed to remain constant over all range bins notwithstanding the varying amplitude scaling factor. The clutter thus conforms to the K-distribution model.

As $K \to \infty$, for each element m(i,j) of the estimated covariance matrix we have:

$$\hat{m}(i,j) \rightarrow E[m_k(i,j)] = \int_0^{\infty} u\, \rho^{(i-j)^2} \exp[-j(2\pi T f_c)^2]\, p_u(u)\, du = P_c m(i,j) \quad \ldots (4.11)$$

from which the filter weights are derived using (4.1).

The IF loss and detection loss have been calculated for this limiting case for various values of N, ν, and the four clutter scenarios defined in the previous section. Figs. 4.1a to 4.1d illustrate the IF loss and Detection loss as a function of ν for clutter cases 1 to 4 respectively, for N = 10 and Δ = 10% and Δ =90%. More complete data for N = 5, 10, 20 and Δ =10%, 30%, 50%, 70% and 90% are tabulated in Appendix 4.1. The following main points can be noted with reference to the data presented:

1. The Detection loss is negative and therefore represents a detection *gain*. This is, in fact, not surprising since an ideal detector has been assumed in calculating detection probabilities. In spatially modulated clutter, the ideal detector assumption is known to yield reductions in the SNR required for detection, as discussed in some detail in Chapters 6 and 7. A more realistic CFAR detector assumption would undoubtedly reverse these apparent gains.

2. The percentage of the doppler space Δ over which the IF or detection probability is averaged can be seen to have significant impact on the loss. 90% averaging yields losses which are in general about double the single tuned filter case (10% averaging), and in some instances the difference is considerably higher.

3. The magnitude of the loss is significant but cannot be considered dramatic: even for moderately spiky clutter (ν = 0.5), the loss is generally only of the order of a few tenths of a dB. These figures are notably lower than those presented by Nitzberg for the non-limiting case. This is addressed further in subsection 4.2.4.

4. The magnitude of the loss depends only slightly on the clutter parameters: 90% averaging can be seen to exhibit slight variation in loss between clutter scenarios (in general, the more severe the clutter, ie. the stronger the clutter and the wider its spectrum, the higher the loss will be), whereas for 10% averaging the difference in loss in different clutter scenarios is negligible.

5. Examination of the tabulated data in Appendix 4.1 indicates that the order of the filter has only a minor impact on the magnitude of the loss (although the absolute IF varies considerably), and that the preceding general points are also valid for N = 5 and N = 20. The loss is about 30% worse for N = 5 than for N = 10, which is in turn about 20% worse than for N = 20.

A discussion of these observations, and some conclusions that can be drawn from them, is deferred until the discussion of all results in Section 4.5.

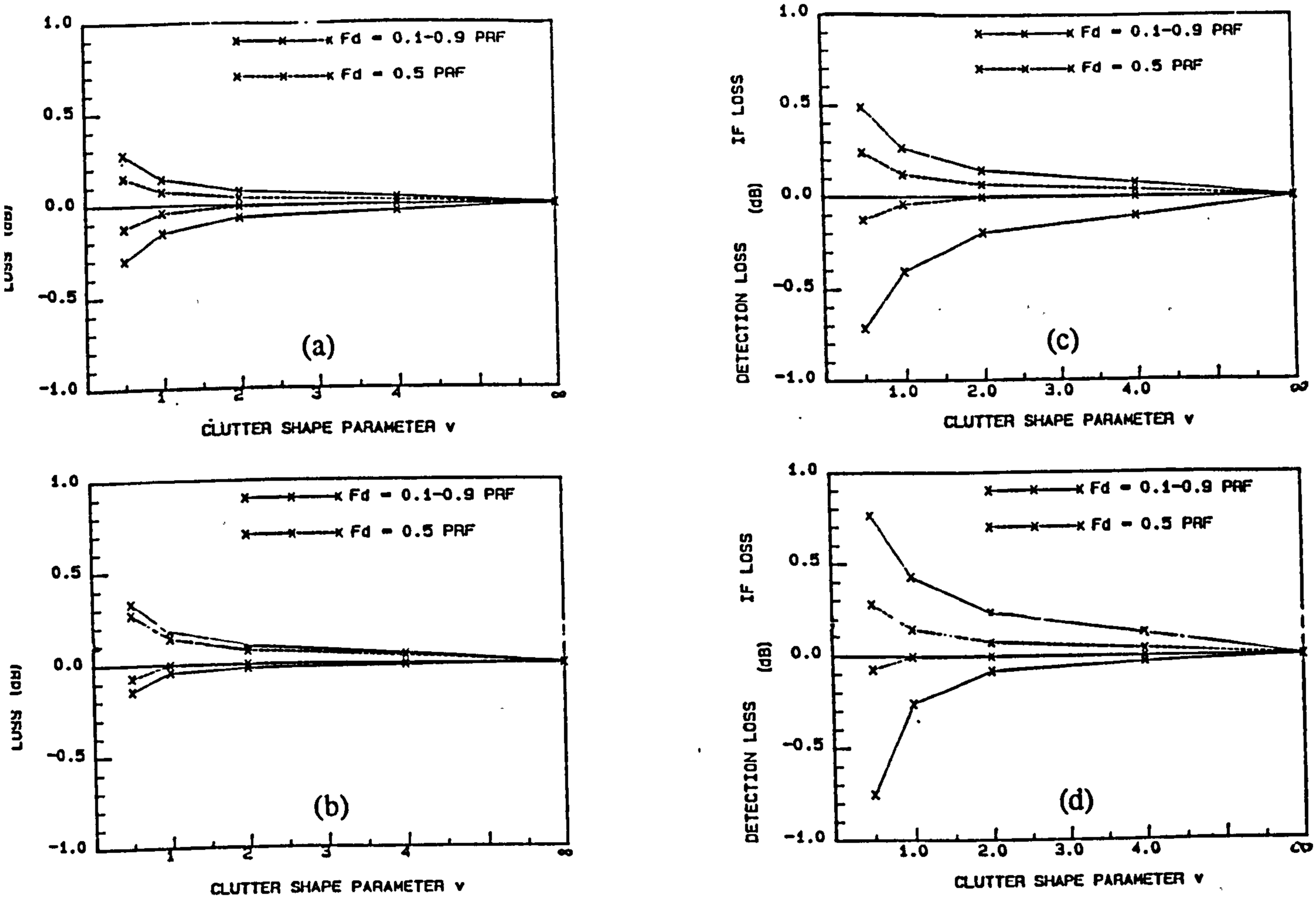

Fig. 4.1: *IF Loss and Detection Loss for Amplitude Heterogeneous Clutter (N=10)*

a) $P_c = 30$ dB; $\sigma_0 = 0.02$ b) $P_c = 60$ dB; $\sigma_0 = 0.02$

c) $P_c = 30$ dB; $\sigma_0 = 0.05$ d) $P_c = 60$ dB; $\sigma_0 = 0.05$

4.2.2.2 Spectral Heterogeneity

It is assumed here that the clutter amplitude is non-fluctuating whereas the spectrum in each range bin is independently drawn from a gamma distribution of mean equal to the mean standard deviation of the clutter spectrum. Under these conditions, as $K \to \infty$, the elements of the estimated covariance matrix are given by:

$$\hat{m}(i,j) \rightarrow E[m(i,j)] = \int_0^{\infty} P_c \left[e^{-2(\pi\sigma T)^2}\right]^{(i-j)^2} \exp[-j(2\pi T f_c)^2]\, p_\sigma(\sigma)\, d\sigma$$

$$= \frac{P_c\, e^{-j(2\pi T f_c)^2}}{\phi^{\kappa}\Gamma(\kappa)} \int_0^{\infty} \sigma^{\kappa-1} \exp\left[-\frac{\sigma}{\phi} - 2\{(i-j)\pi\sigma T\}^2\right] d\sigma \quad \ldots (4.12)$$

where $\phi = b_1\sigma_0^2$ and $\kappa = b_1^{-2}$. This yields a covariance matrix which is not only different to the instantaneous covariance matrix of the clutter in any range bin, but is also different to that of spectrally Gaussian clutter with width σ_0 and power P_c. Thus M_{ref} and M_t in eqn. (4.4) are not equal, and the loss introduced therefore has two components, namely 1) a loss arising from the fact that $\widehat{M} \neq M_{ref}$, ie. the expected estimated covariance matrix differs from the covariance matrix of spectrally homogeneous clutter with the same mean width and power, and 2) a loss arising since $M_{ref} \neq M_t$, ie. the spectrally varying clutter in the test cell has a different instantaneous covariance matrix to that in the reference cells.

The IF, IF loss and detection loss have been calculated for the four clutter cases defined in section 4.2.1 for values of b_1 in the range $0 \leq b_1 \leq 0.8$, for N = 5; 10; 20, and for differing degrees of averaging over the doppler space. Figs. 4.2a to 4.2d illustrate the IF loss and Detection loss as a function of b_1 for clutter cases 1 to 4 respectively, for N = 10 and Δ=10% and Δ=90%. More complete data for N = 5, 10, 20 and Δ= 10%, 30%, 50%, 70% and 90% are tabulated in Appendix 4.2.

The following main points can be noted with reference to the data presented:

1. In this case the magnitude of the loss depends strongly on the clutter parameters. In general, the more severe the clutter, the higher the loss will be.

2. The percentage of the doppler space over which the IF or detection probability is averaged can be seen to have significant impact on the loss. With the exception of the worst clutter case (case 4), 90% averaging yields losses which are in general about 2 to 5 times the single tuned filter case (10% averaging). The loss in the worst case clutter scenario does not exhibit the same strong dependence on the

extent of doppler averaging since even the central filters are stressed by the severity of the clutter and suffer rapid deterioration in performance with the introduction of spectral fluctuations.

4. The loss is very large in very severe clutter (case 4), even for low values of b_1. For less severe clutter, the loss only becomes dramatic for $b_1 > 0.2$ to 0.5, which may be higher than practical spectral fluctuations often encountered.

5. Examination of the tabulated data in Appendix 4.2 indicates that the order of the filter does not have dramatic impact on the magnitude of the loss.

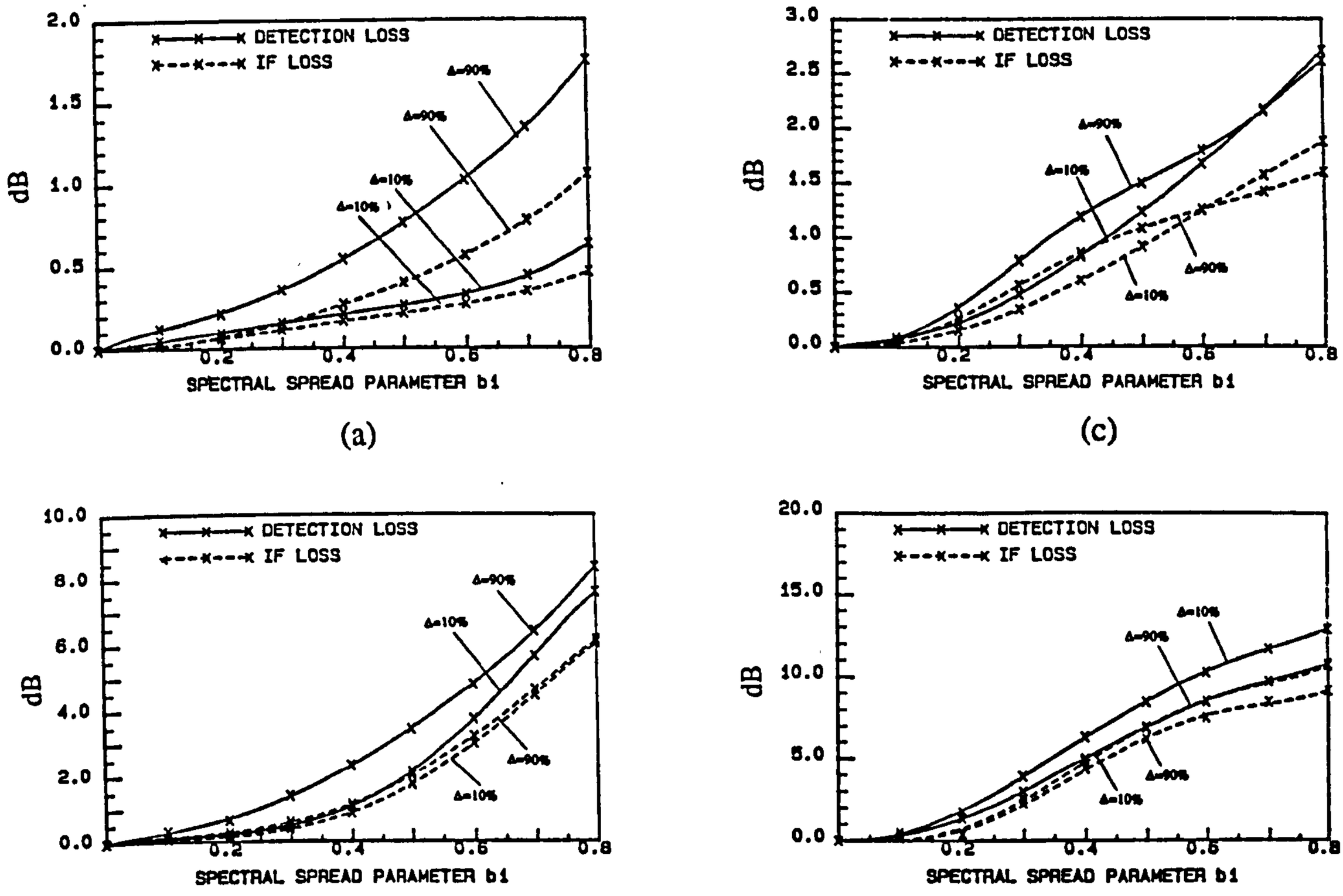

Fig. 4.2: *IF Loss and Detection Loss for Spectrally Heterogeneous Clutter (N=10)*

a) $P_c = 30$ dB; $\sigma_0 = 0.02$ b) $P_c = 60$ dB; $\sigma_0 = 0.02$

c) $P_c = 30$ dB; $\sigma_0 = 0.05$ d) $P_c = 60$ dB; $\sigma_0 = 0.05$

4.2.2.3 Amplitude and Spectral Heterogeneity

In this case the amplitude and spectral width fluctuations defined in the previous two subsections are considered to occur simultaneously and independently. Expressions for the elements of the estimated covariance matrix follow immediately from eqns. (4.11) and (4.12). Results have been computed for the four clutter cases defined in section 4.2.1, for $\nu = 0.5; 1.0; 2.0; 4.0; \infty$; for $0 \leq b1 \leq 0.8$; and for differing degrees of doppler space averaging. They are illustrated for N = 10 in Figs. 4.3 and 4.4: Figs. 4.3a to 4.3d show the IF loss as a function of b_1, with ν as a parameter, for clutter cases 1 to 4 respectively; Figs. 4.4a to 4d show the detection loss as a function of b_1, with ν as a parameter, for clutter cases 1 to 4 respectively. It can be seen that the detection and IF losses follow the same trends as those noted in the previous two subsections for either amplitude or spectral fluctuations. The key point to note here is that the losses due to amplitude and spectral fluctuations are, in general separable. This has obvious benefits with regard to analysis of adaptive filters in heterogeneous clutter.

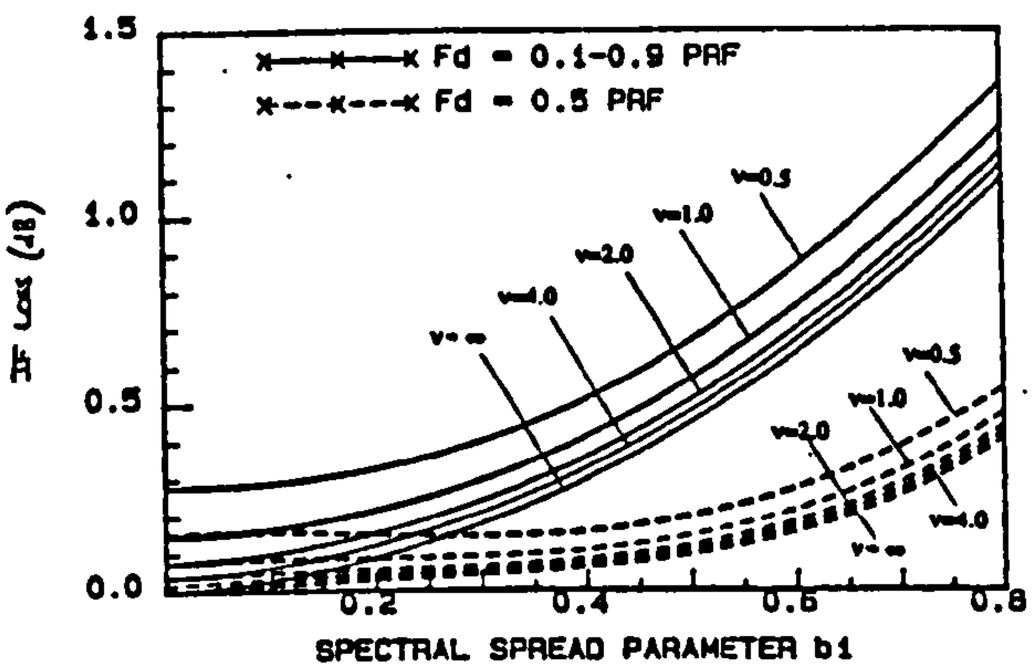

(a)

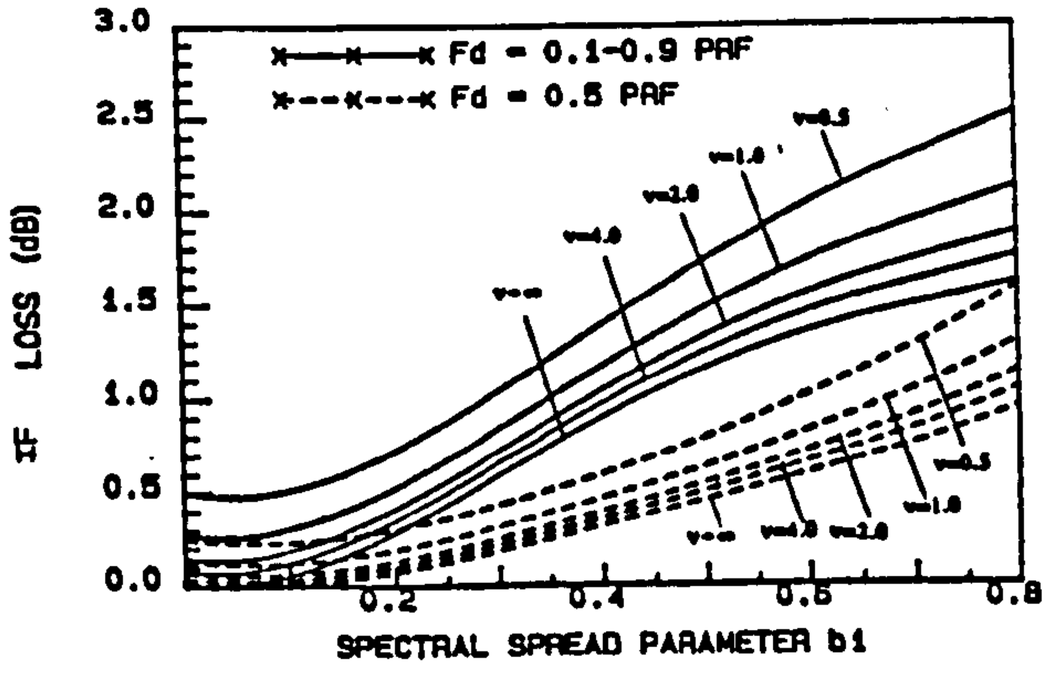

(c)

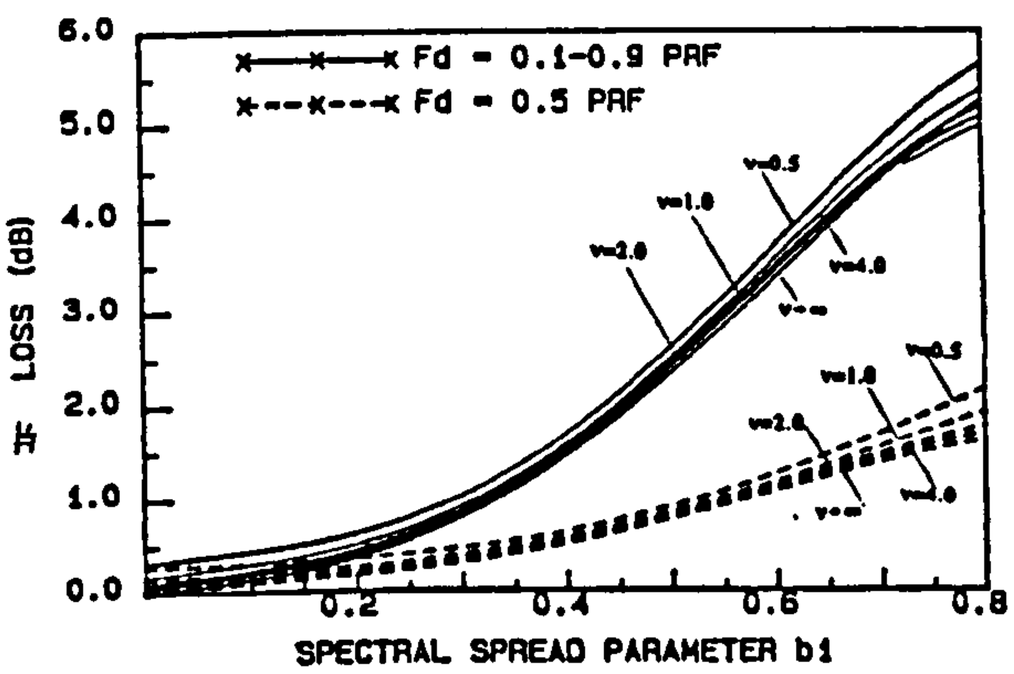

(b)

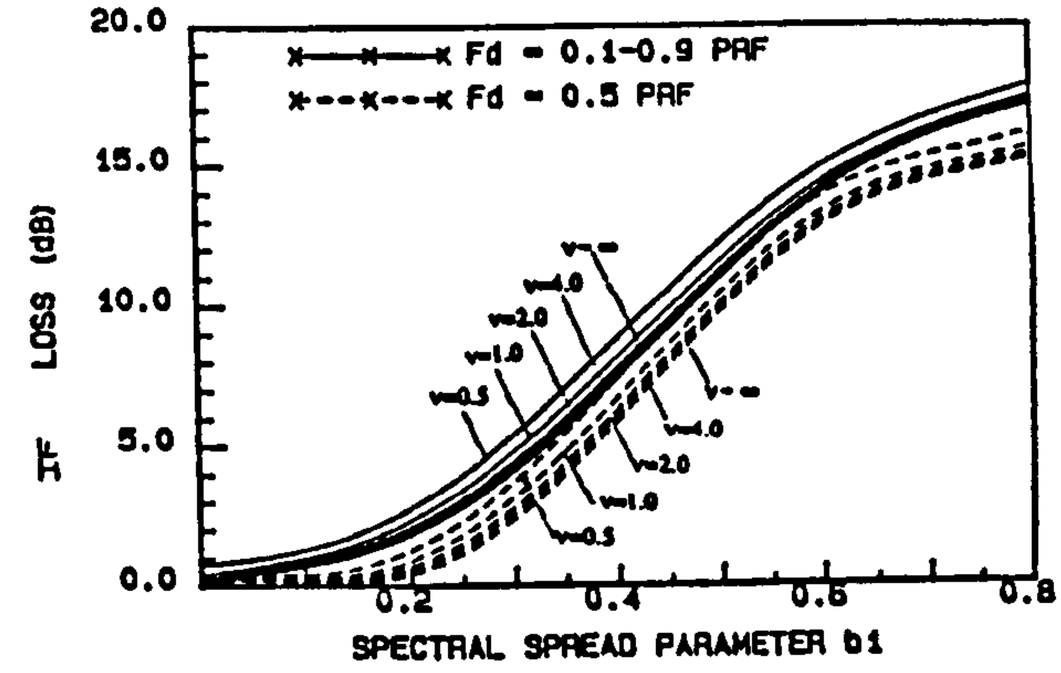

(d)

Fig. 4.3: *IF Loss for Amplitude and Spectrally Heterogeneous Clutter (N=10)*

a) $P_c = 30$ dB; $\sigma_0 = 0.02$ b) $P_c = 60$ dB; $\sigma_0 = 0.02$

c) $P_c = 30$ dB; $\sigma_0 = 0.05$ d) $P_c = 60$ dB; $\sigma_0 = 0.05$

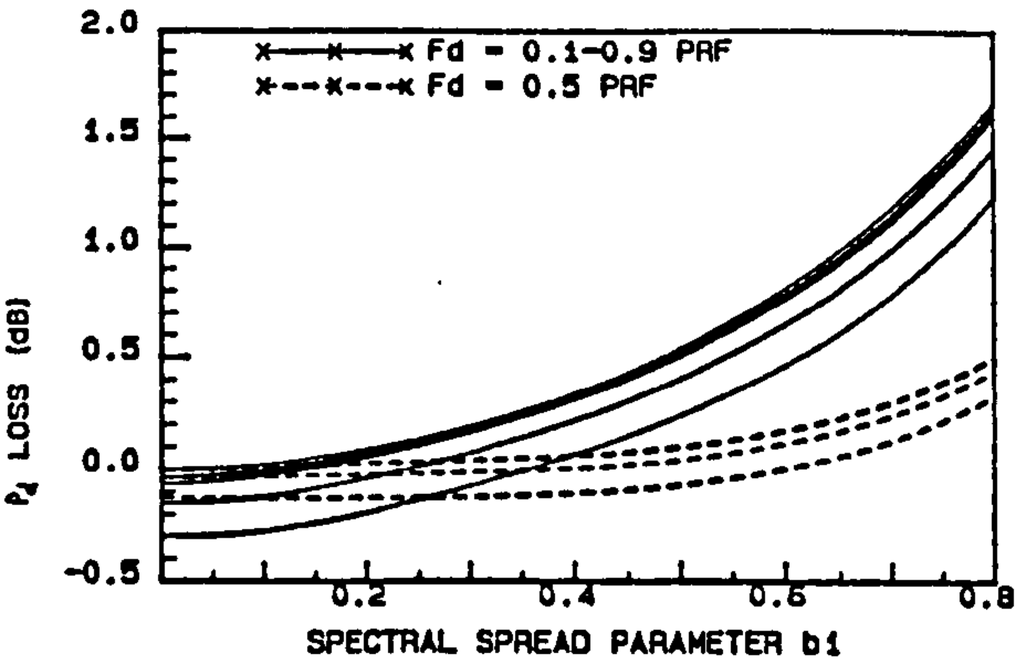

(a)

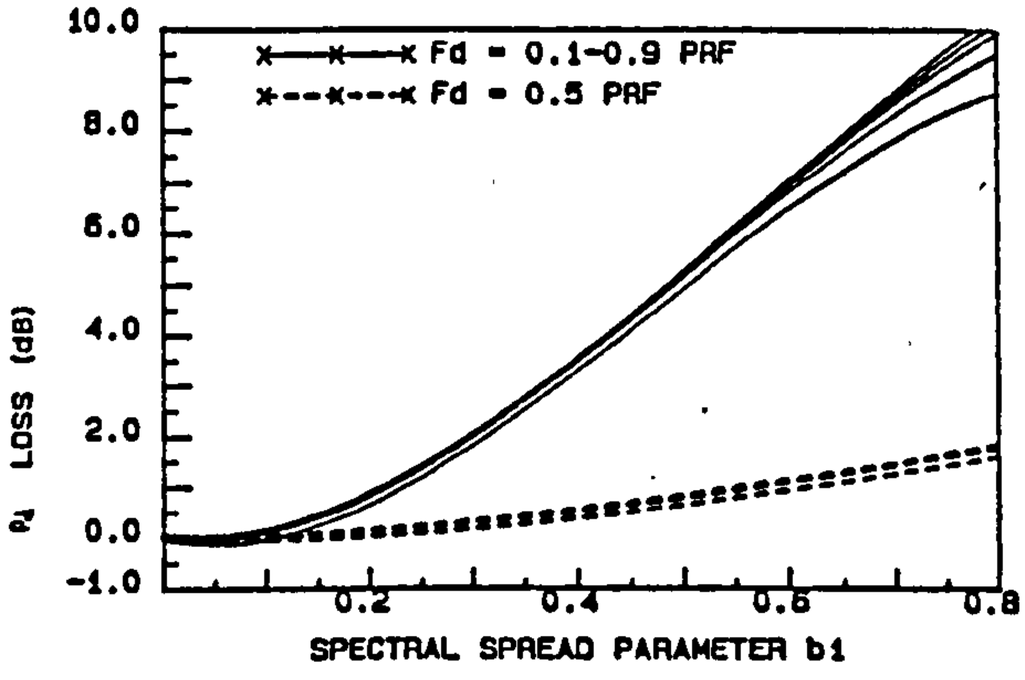

(b)

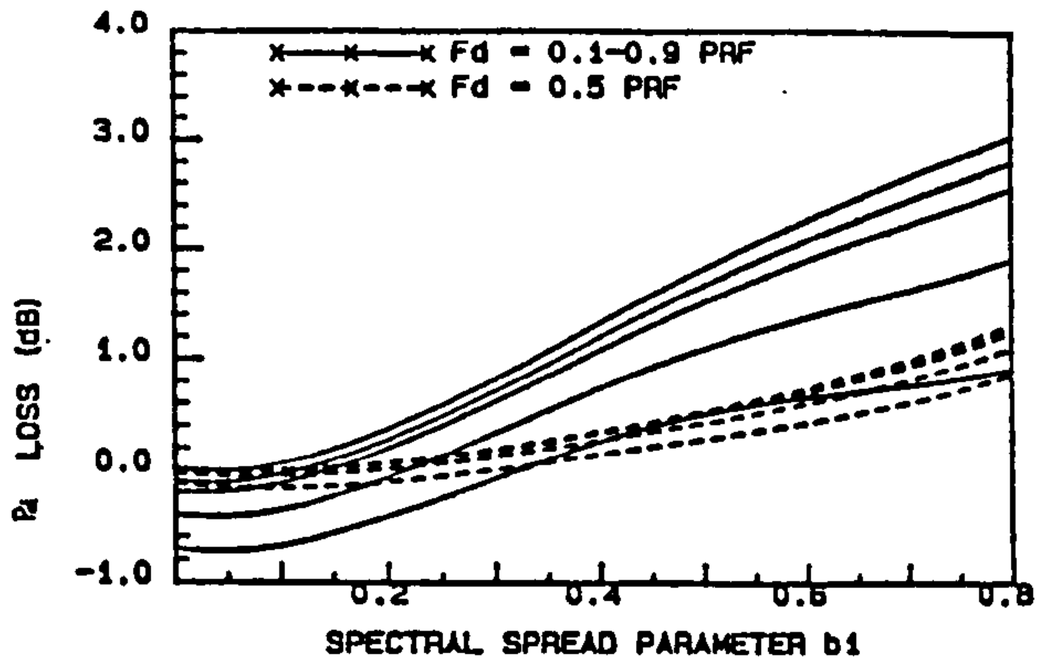

(c)

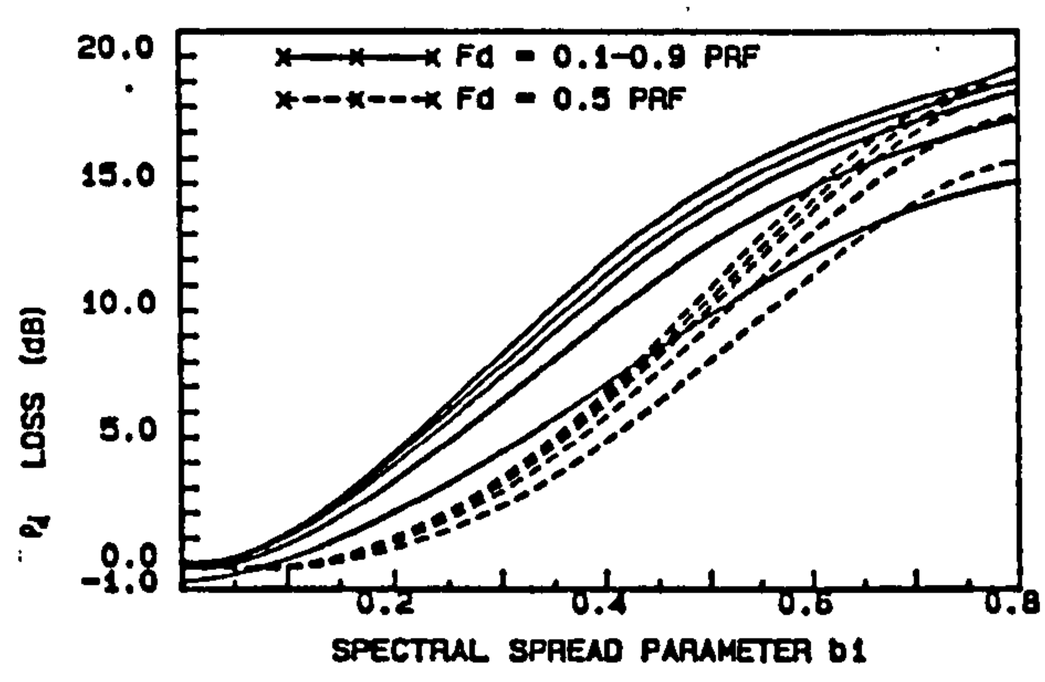

(d)

Fig. 4.4: *Detection Loss for Amplitude and Spectrally Heterogeneous Clutter (N=10)*

a) $P_c = 30$ dB; $\sigma_0 = 0.02$ b) $P_c = 60$ dB; $\sigma_0 = 0.02$

c) $P_c = 30$ dB; $\sigma_0 = 0.05$ d) $P_c = 60$ dB; $\sigma_0 = 0.05$

4.2.3 Amplitude and Spectral Heterogeneity with Finite K

Despite the utility of limiting cases for giving insight into the losses introduced by non-homogeneous clutter, it is important to examine whether those results are representative of the more realistic case where $K<\infty$. In this section we therefore present simulation results for finite K.

The simulation technique is fairly straightforward, if computationally demanding, and will not be discussed here. Due to the time taken to run the programs, simulations have only been performed for N = 10. It is felt, however, that the key conclusions listed later will remain valid for other values of N. Results are presented for clutter cases 2, 3 and 4 defined in section 4.2.1, for $\nu = 0.5$ and $\nu = \infty$, for the spectral spread parameter b_1 in

range $0 \leq 0.6$, for K = 10, 20, 40, 80, ∞. Figs. 4.5a and 4.5b show the IF loss for ν = 0.5 and $\nu = \infty$ respectively, for clutter case 4, and 10% doppler averaging. Fig. 4.6 shows similar data for clutter case 3. Full data for clutter cases 2, 3, and 4, and for Δ = 10%, 30%, 50%, 70%, and 90%, are tabulated in Appendix 4.3.

Upon examination of Figs. 4.5 and 4.6 and the data in Appendix 4.3 it can be noted that:

1) The simulated results tend to the limiting case results of the previous subsections as $K \rightarrow \infty$.

2) For $b_1 = 0$ and $\nu \rightarrow \infty$, the simulated data give very good agreement (to within about 0.1 dB) with Reed's closed form expression for homogeneous environments. This and point (1) above testify to the integrity of the simulation.

3) In agreement with Nitzberg's results, these simulations show that reducing K increases the IF loss due to amplitude heterogeneity, which can become considerable. The difference between the IF loss for $\nu \rightarrow \infty$ and ν =0.5 is about 0.2 dB for $K \rightarrow \infty$, 2 dB for K=40, 3 dB for K = 20 and 3.5 dB for K = 10. This can be explained by the fact that amplitude heterogeneity reduces the effective number of samples from which the estimate of the covariance matrix is derived.

4) Reducing K can be seen (somewhat surprisingly) to *reduce* the losses due to spectral heterogeneity. This is a consequence of the arithmetic averaging of IF, where the greater variation in $\widehat{M}$ occasionally yields negligible error with M_t, thereby yielding high improvement factors which bias the arithmetic average upwards. The significance of this observation is discussed further in Section 4.5.

5) In less severe clutter (cases 1, 2 and 3) the IF loss caused by finite K is far larger than that caused by spectral heterogeneity.

6) The IF loss due to amplitude fluctuations is roughly separable from the IF loss due to spectral heterogeneity.

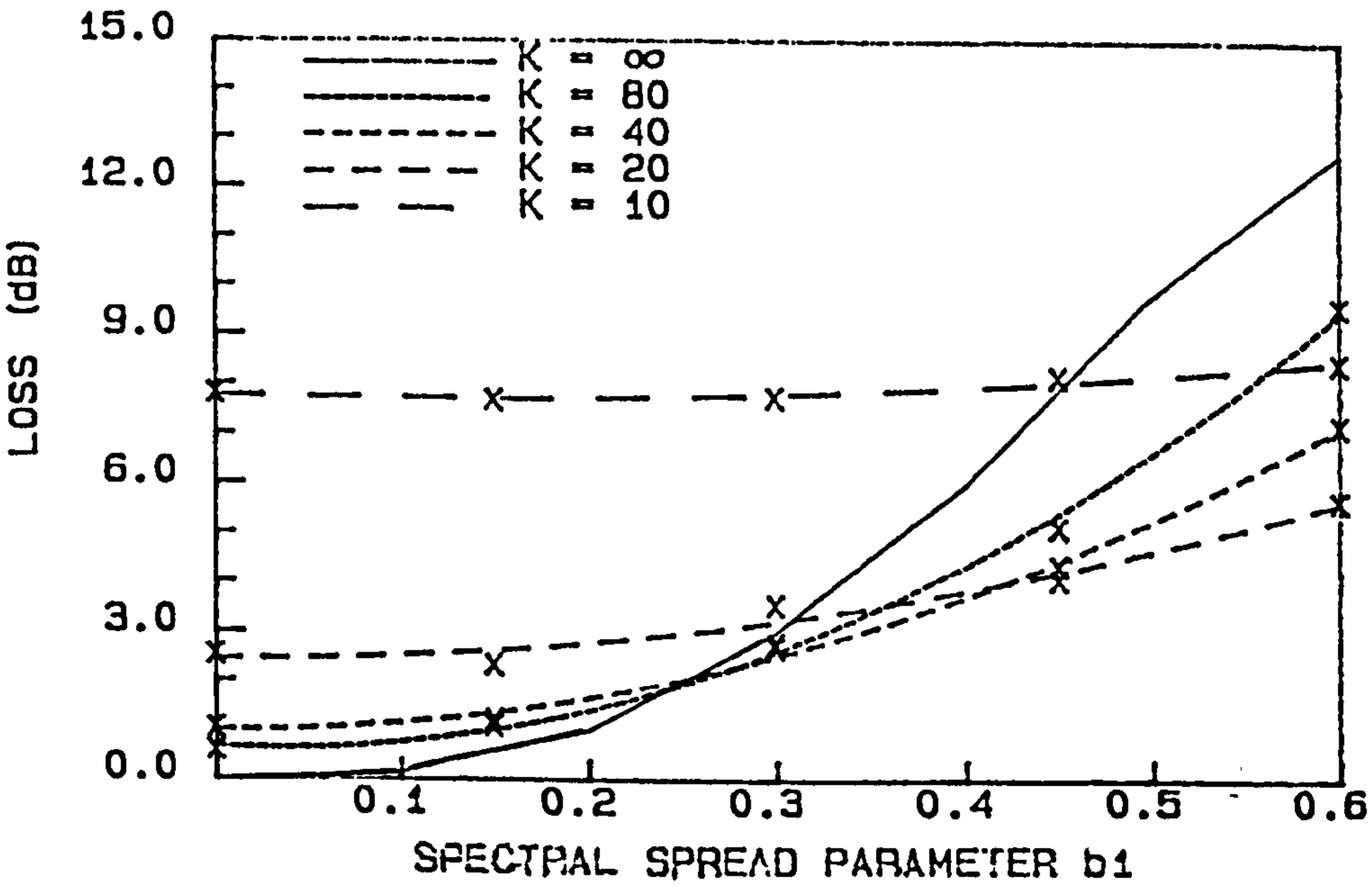

(a)

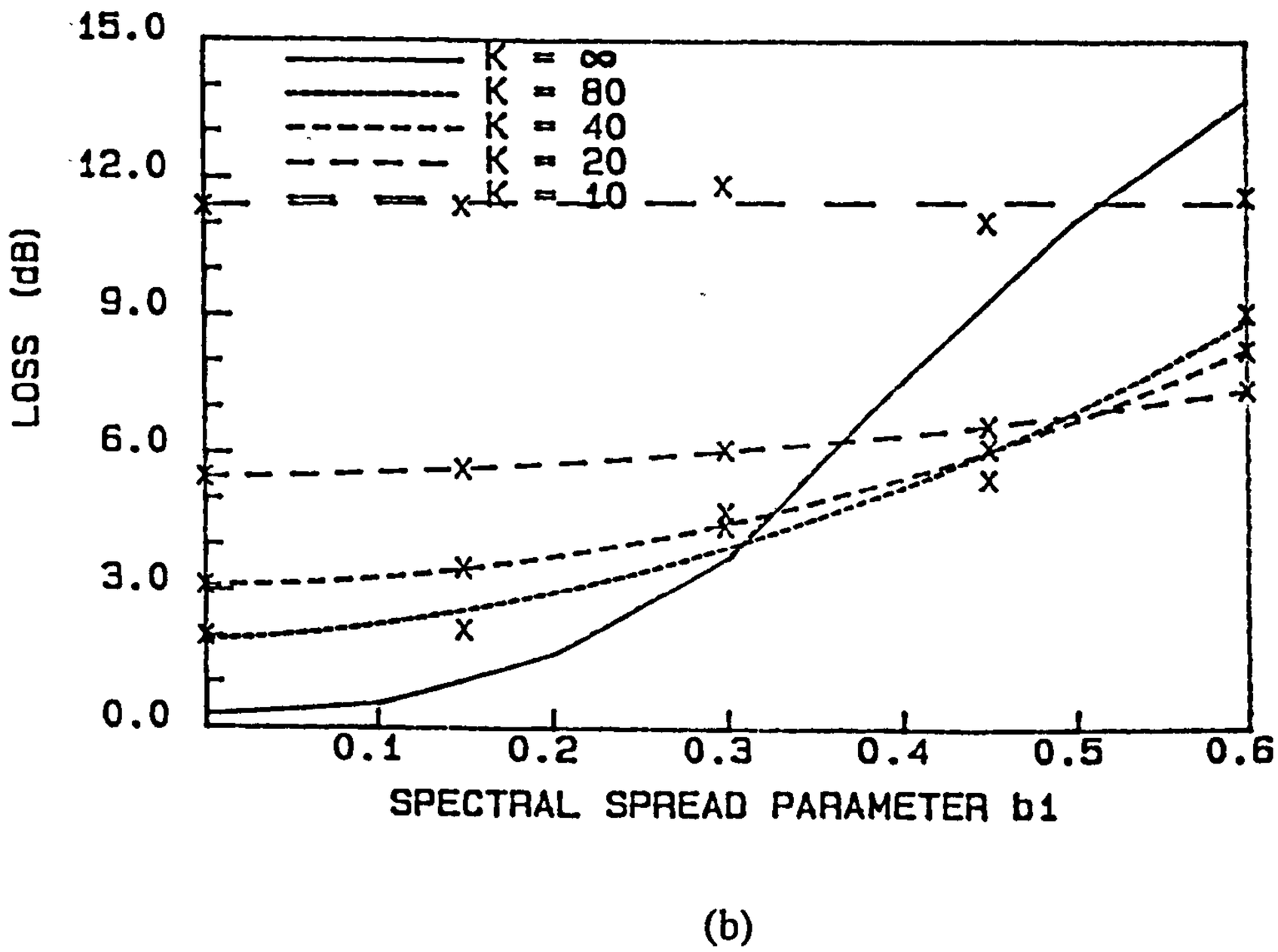

(b)

Fig. 4.5: *IF Loss for Amplitude and Spectrally Heterogeneous Clutter ; K<∞*

a) $\nu \to \infty$ b) $\nu = 0.5$

$N = 10$; $P_c = 60$ dB; $\sigma_0 = 0.05$

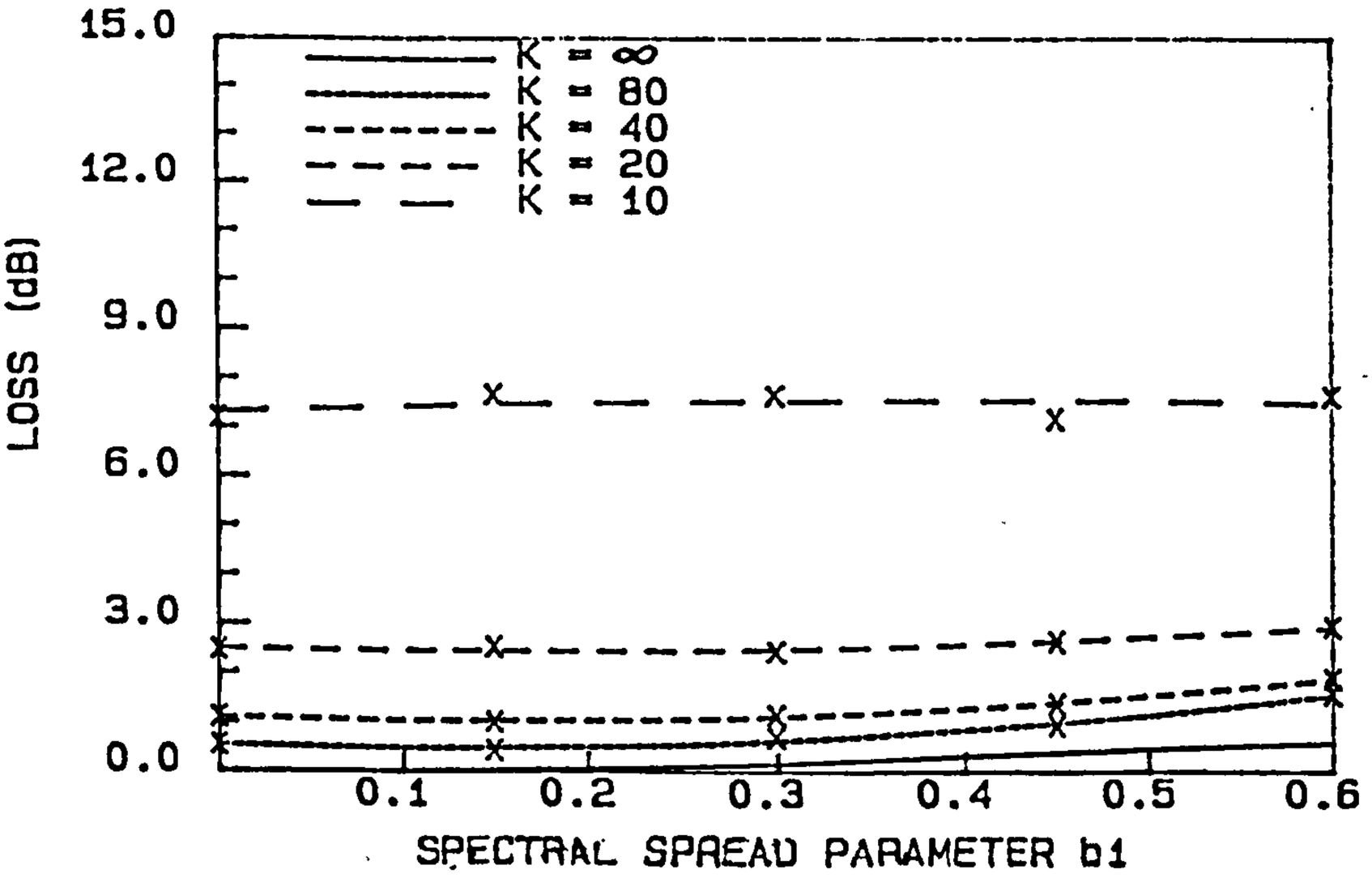

(a)

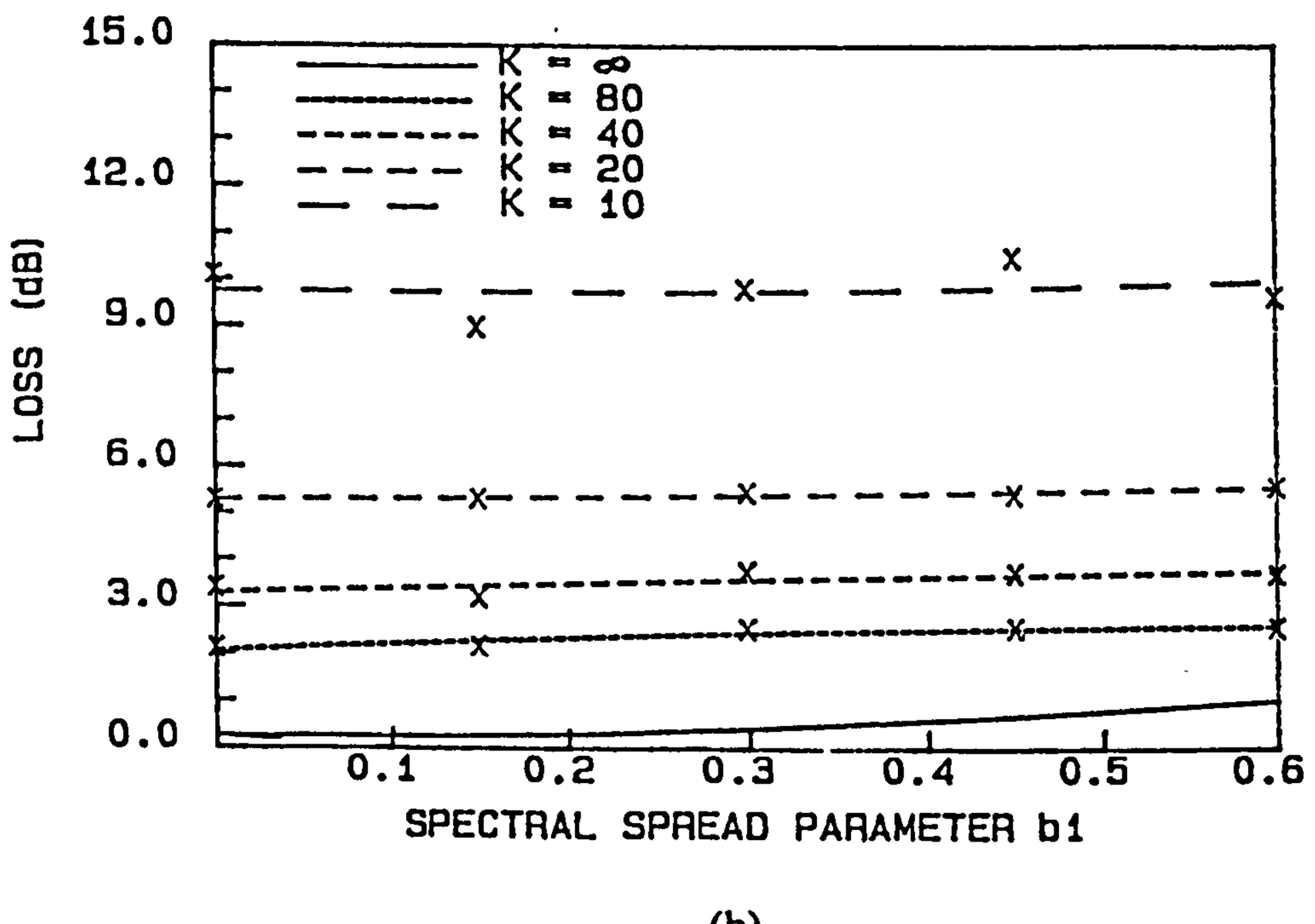

(b)

Fig. 4.6: *IF Loss for Amplitude and Spectrally Heterogeneous Clutter ; K<∞*

a) $\nu \to \infty$ b) $\nu = 0.5$

$N = 10$; $P_c = 30$ dB; $\sigma_0 = 0.05$

4.3 EDGE EFFECTS

In this section we examine the performance of adaptive optimal filters in the region of clutter edges. The edges considered consist of amplitude and/or spectral step changes in range. Sliding window processing, as opposed to block processing, has been assumed for the estimation of the clutter covariance matrix. (Sliding window processing does, of course, include block processing as a special case where the block is centred at the instantaneous centre of the sliding window).

The clutter on either side of the edge is assumed to be homogeneous with unimodal Gaussian spectrum. The edge scenario is therefore completely defined by the parameters P_1, σ_1 and f_{c1} of the clutter comprising one side of the edge; and P_2, σ_2 and f_{c2} of the clutter comprising the other side of the edge. In order to keep the study within manageable limits, eight different edge scenarios have been defined. These are defined in Table 4.1, in which the power P is expressed in dB relative to thermal noise, and the spectral spread σ and clutter centre frequency f_c are expressed relative to the PRF.

Table 4.1
Edge Scenario Definition

Edge Scenario	P_1	σ_1	f_{c1}	P_2	σ_2	f_{c2}
1	50	0.02	0	30	0.1	0.2
2	50	0.02	0	30	0.1	0.0
3	50	0.02	0	30	0.1	0.5
4	30	0.02	0	40	0.1	0.2
5	30	0.02	0	40	0.1	0.0
6	30	0.02	0	40	0.1	0.5
7	60	0.02	0	30	0.1	0.0
8	50	0.02	0	30	0.05	0.0

The IF loss averaged over the entire doppler space has been evaluated by simulation for these edge scenarios for N=10. Results are plotted in Figs. 4.7a to 4.7h. The horizontal axis represents range, with the edge being located at range = 0. The number of reference bins used is K=10 (ie. 10 x 20m range bins for this illustration), K=20 (ie. 20 x 10m range bins), and $K \rightarrow \infty$ (ie. an essentially infinite number of infinitesimal range bins). The latter case corresponds to the limiting cases of the previous section, and is useful in that it enables analytic expressions for the estimated covariance matrix and hence IF loss to be used. The estimated covariance matrix $\widehat{M}$ is obtained as:

$$\widehat{M} = \frac{n}{n_2} M_1 + (1 - \frac{n}{n_2}) M_2 \qquad \ldots (4.13)$$

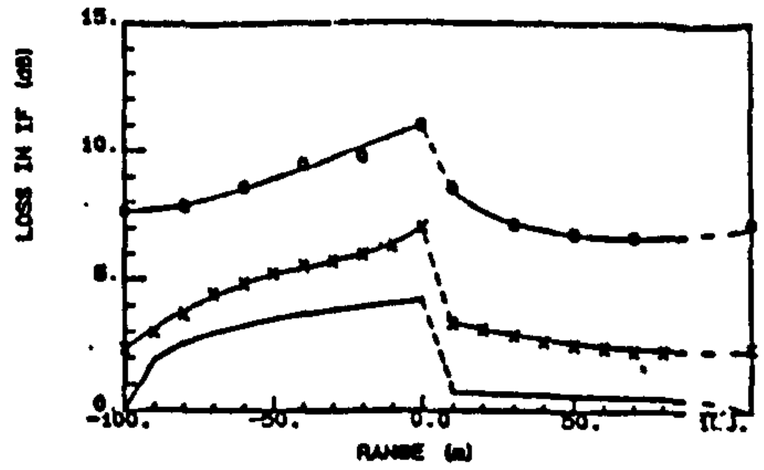

(a)

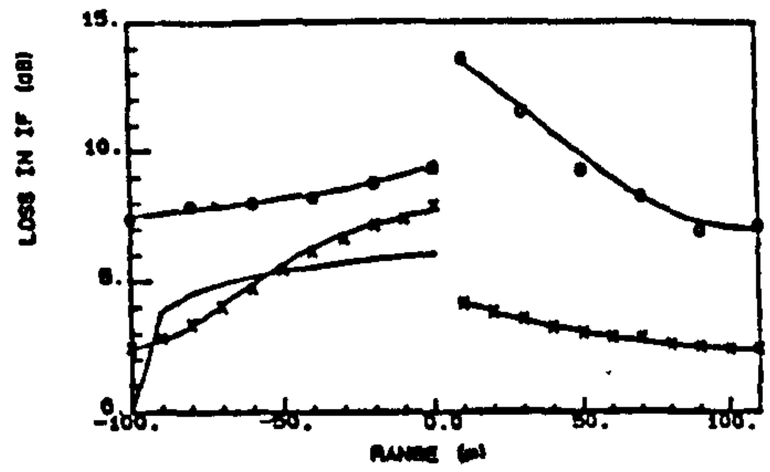

(d)

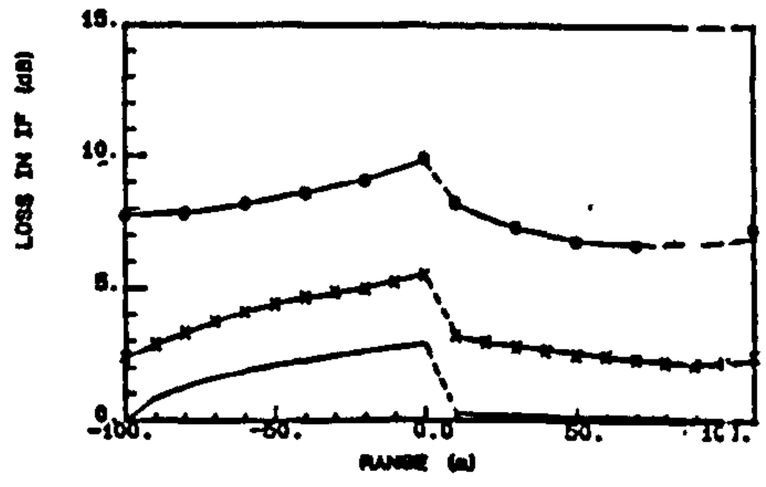

(b)

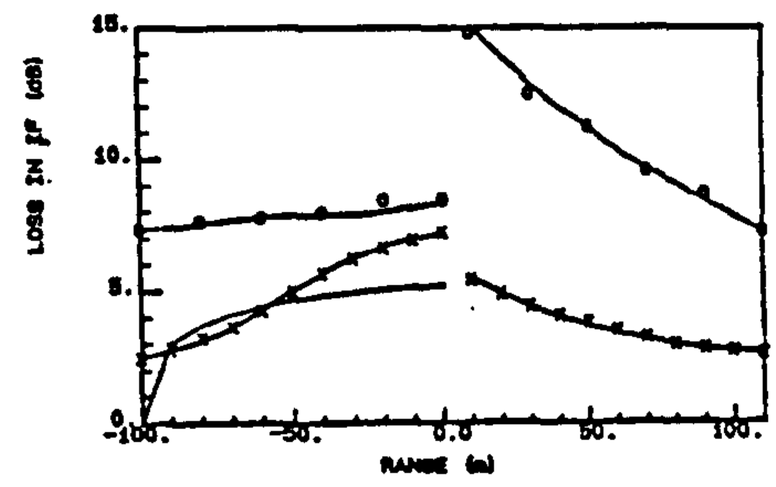

(e)

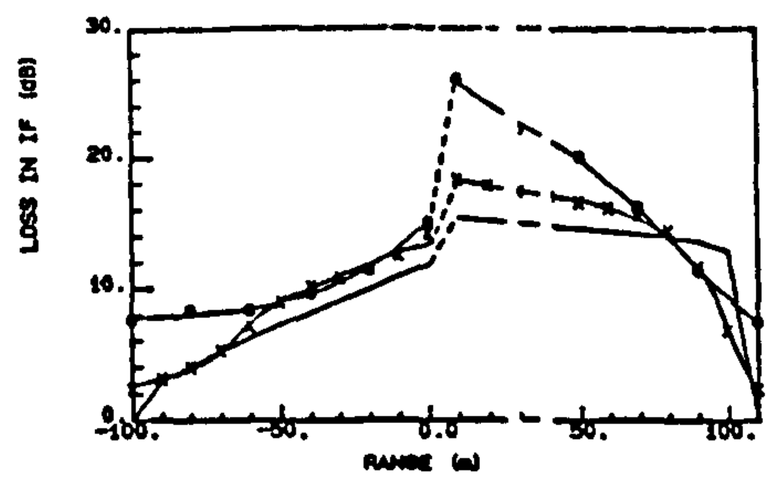

(c)

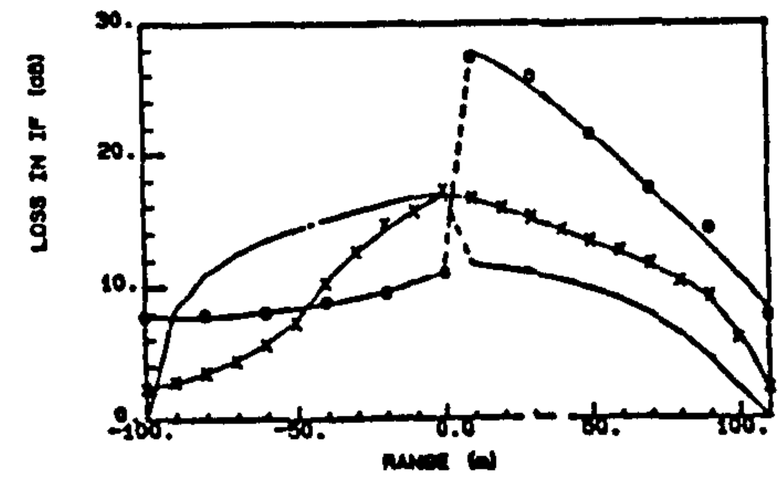

(f)

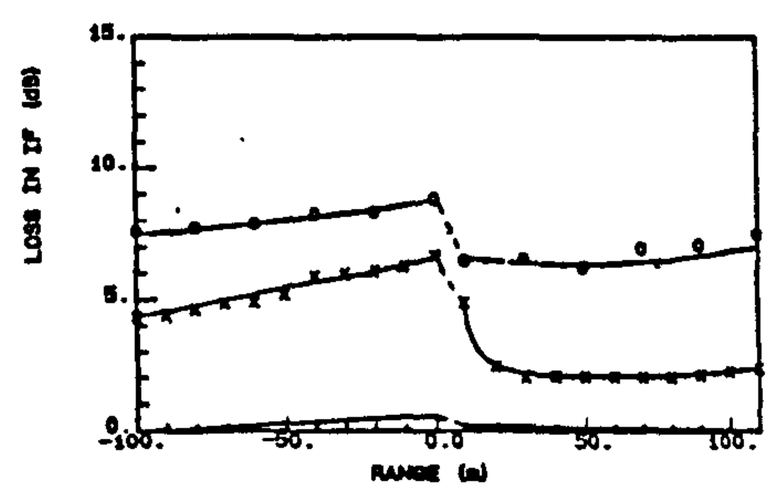

(g)

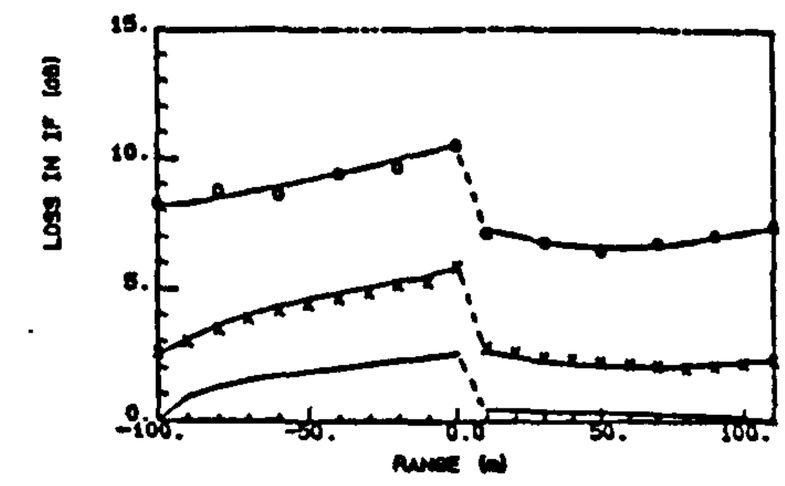

(h)

Fig. 4.7: *IF Loss around Clutter Edges (N=10)*

a) Edge Scenario 1 b) Edge Scenario 2 c) Edge Scenario 3 d) Edge Scenario 4

e) Edge Scenario 5 f) Edge Scenario 6 g) Edge Scenario 7 h) Edge Scenario 8

x---x---x K=20 o--o--o K=10 ------- K→∞

where M_1 and M_2 are the covariance matrices of the clutter on either side of the edge, and r_1 and r_2 are the proportions of "clutter 1" and "clutter 2" covered by the reference window respectively. Note that in Fig. 4.7 the the IF loss to the left of range = 0 assumes the the test cell contains clutter 1; to the right of range = 0 the test cell contains clutter 2.

The following observations are worth noting:

1) There can be a fairly severe loss in IF (often 5 dB and occasionally more than 10 dB) in the region of clutter edges, over and above the loss due to finite-size reference windows. This loss is worst at the clutter edge and in general, for finite K, tapers off smoothly as the test cell moves away from the edge. A step increase in loss as the reference window encompasses the edge is not evident for finite K.

2) The limiting case can give a useful indication of the order of magnitude of the loss that can be expected at a clutter edge, notwithstanding the additional loss due to finite K. The limiting case tends to give a more immediate increase in loss as the reference window starts encompassing the clutter edge (from ±100m to ± 90m in Fig. 4.7).

3) The IF loss due to clutter edges depends primarily on the difference in centre frequencies of the clutter on either side of the edge; the results presented here do not show consistent trends in the loss as a function of the difference in spectral width or power of the clutter on either side of the edge.

4.4. THE USE OF PRE-FILTER MTI TO REDUCE IF LOSS

Often clutter edges or point sources will contain one clutter component that is stationary. In such situations one possibility for reducing the increased IF loss in the region of clutter edges or point clutter sources is the insertion of an MTI filter before the adaptive filter. This is intended to 1) remove zero doppler components from the test cell irrespective of whether or not these are present in the reference windows, with the adaptive filter only suppressing any remaining clutter residue, and 2) remove zero doppler components which may dominate the reference cells but which are not present in the test cell.

For a fair comparison of filter performance it is necessary to keep the total number of pulses used by the composite MTI-adaptive filter equal to the number of pulses used by

normal adaptive filter alone. For this analysis the total number of pulses has been set as N=10, for reasons discussed earlier. Thus since a 3-pulse binomially weighed MTI filter is assumed, the cascaded optimal filter must be an eight pulse filter. The estimated covariance matrix for the adaptive filter is obtained through the usual SMI method, but operating on data that have already been filtered by the MTI. The N-3 adaptive weights are then calculated from eqn. (4.1), and the composite filter weights are obtained from the convolution of the MTI weights and the adaptive filter weights. Normalisation to ensure unity noise gain is analytically desirable.

The effectiveness of pre-filter MTI against point clutter sources and clutter edges is evaluated in the following subsections.

4.4.1 Effectiveness of Pre-filter MTI against point clutter sources

The reduction in IF caused by point clutter sources or extraneous targets has two facets, namely:

1. The reduction in IF on the clutter background when one or more point clutter sources are present in the reference window. Term this loss L_{bg}.
2. The reduction in improvement factor on the point clutter itself, when the reference window contains mainly the clutter background, but also possibly a limited number of other point clutter sources. Term this loss L_{pc}.

These two losses have been evaluated by simulation for a range of clutter parameters. The point clutter is assumed to be strong, spectrally narrow, and stationary; its parameters have accordingly been set as $f_{c_{pc}} = 0$, $\sigma_{pc} = 0.02$ relative to the PRF, and $P_{pc} = 30$, 45, or 60 dB relative to thermal noise. The parameters of the background clutter, which (excluding the point clutter sources) is considered to be homogeneous, have been varied more widely, with 12 distinct parameters sets defined by the combinations of:

$f_{c_{bg}}$	= 0.;	0.25;	0.5	relavite to the PRF
σ_{bg}	= 0.05;	0.1		relative to the PRF
P_{bg}	= 30;	50		dB relative to thermal noise

Thus 36 different background/point-clutter scenarios have been investigated. In each case either 0, 1, 2 or 4 point clutter sources were taken as being present in the 20 range bin reference window. The IF losses L_{bg} and L_{pc} have been estimated for these 144

parameter combinations using 500-trial simulations. An overview of the results is given in Fig. 4.8, which plots the IF achieved with MTI against that achieved without MTI, for both background and point clutter in the test cell. Points plotted above the y=x line thus indicate superior IF of the MTI-adaptive composite filter.

It is apparent from Fig. 4.8 (data points in circle (1)) that the use of pre-filter MTI provides a certain minimum IF (~20 dB) against stationary point clutter sources, which under some background conditions are not suppressed at all. However, if the background clutter has a mean doppler frequency of about half the PRF (data points in circle (2)), the incorporation of a pre-filter MTI can cause a very low IF against the background, as would be expected. In general, however, it can be seen from the majority of the data points in Fig. 4.8 that the use of pre-filter MTI improves the IF more against the point clutter sources than it reduces the IF against the background.

A more quantitative comparison of performance is given in Fig. 4.9: the difference between the IF achieved with pre-filter MTI and that achieved without MTI is plotted as a function of the clutter scenario, with the number N_i of interfering point clutter sources in the reference window as a parameter (N_i = 0, 1, 2, 4). The clutter scenario index is defined in Appendix 4.4.

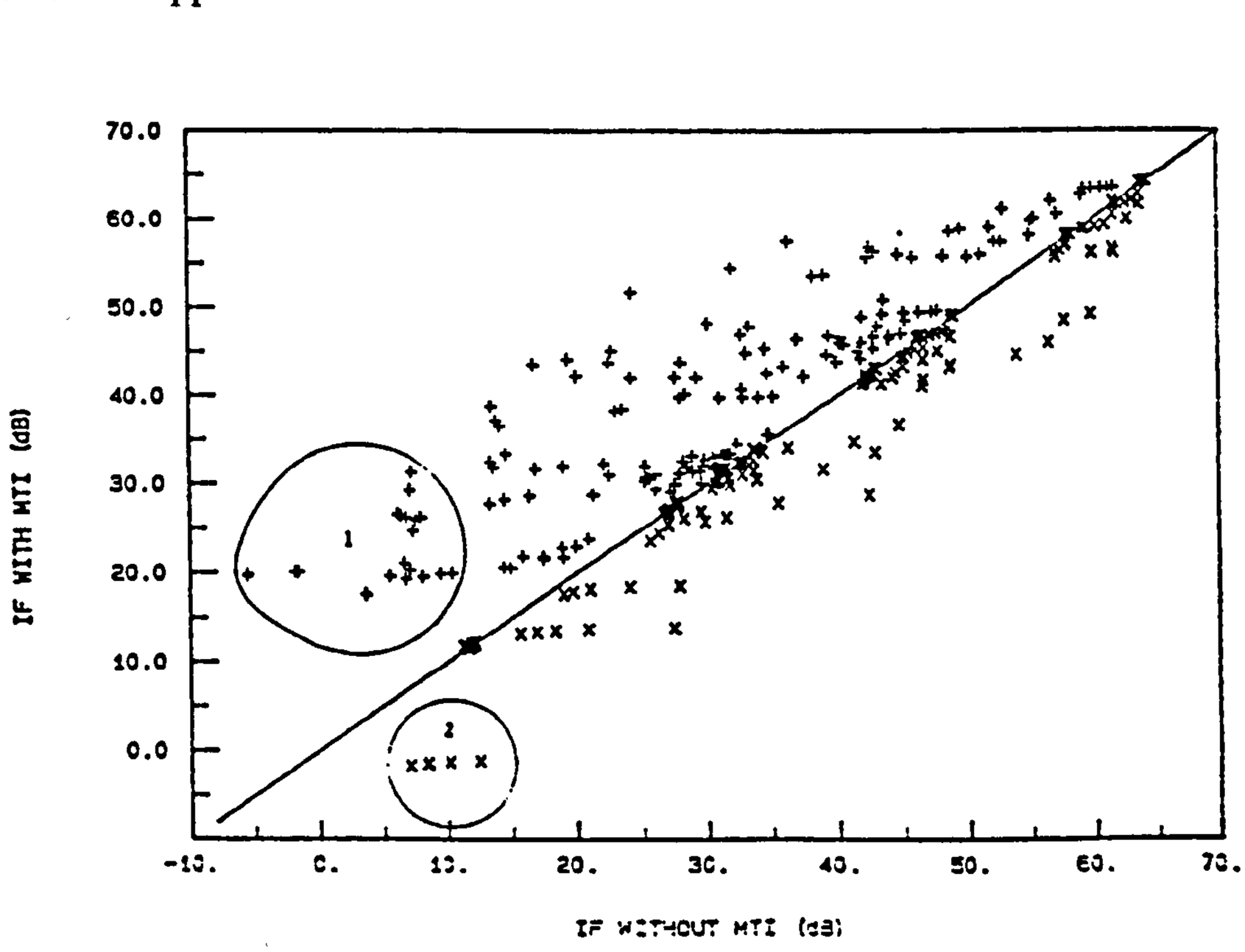

Fig. 4.8: *Effect of pre-filter MTI on IF Loss in the presence of Point clutter sources*
x: IF against background clutter +: IF against point clutter sources

The following points can be noted with regard to Fig. 4.9:

1) It is interesting to note that the use of pre-filter MTI actually gives a slightly better IF against the background clutter than the filter without MTI, which is supposedly optimised for the background clutter. This seemingly impossible result can be explained by noting that when MTI is employed an eight pulse adaptive filter is employed. From eqn. (4.5) this will suffer lower loss in IF due to $K < \infty$ than will a 10 pulse adaptive filter. Setting K= 20 gives a difference in loss of .67 dB between N= 10 and N' = 8, which agrees well with Fig. 4.9.

2) Only when $f_{cbg} = 0.5$ does the pre-filter MTI cause noticeable reductions in IF against the background. This is as expected since under these conditions the MTI filter would suppress targets in the clutter free regions of the doppler space (ie. around zero doppler). Even if $f_{cbg}=0.5$, the IF reduction to be can quite minor ($\leq$3 dB) if more than one point clutter source is present in the reference cells or if the background clutter is relatively weak and narrow ($\sigma_{bg} = 0.05$; $P_{bg} = 30$ dB).

3) The use of pre-filter MTI gives large improvements in IF against the stationary point clutter, particularly if no point clutters fall in the reference window. This confirms intuitive predictions. The improvement in IF is of the order of 10 dB for the "average" clutter scenario. The only case where no significant improvement in IF against the point clutter is achieved is when the point clutter is weak (30 dB) and the background is also stationary.

4.4.2 Effectiveness of Pre-filter MTI against clutter edges

The performance of a 10-pulse composite filter (3-pulse MTI cascaded with an 8-point adaptive filter) has been evaluated for the same eight clutter edge scenarios defined in section 3. Results are illustrated in Fig. 4.10a to 4.10h, for scenarios 1 to 8 respectively.

The IF loss due to finite K is smaller when using pre-filter MTI than for the adaptive filter without MTI, as mentioned in the previous subsection. This lower IF loss is maintained, and sometimes increased, in the composite filter as the test cell approaches the clutter edge, giving a 0.5 to 2 dB reduction in IF loss. This is true for all edge scenarios for clutter to the left of the clutter edge, ie. when the clutter has zero centre frequency, irrespective of the parameters of the clutter to the right of the edge. It is also true for the clutter to the right of the edge for all cases except where the clutter centre frequency is 0.5, in which case pre-filter MTI introduces quite a large loss (~10 dB) which converges with the loss of the adaptive filter without MTI as the test cell approaches the clutter edge.

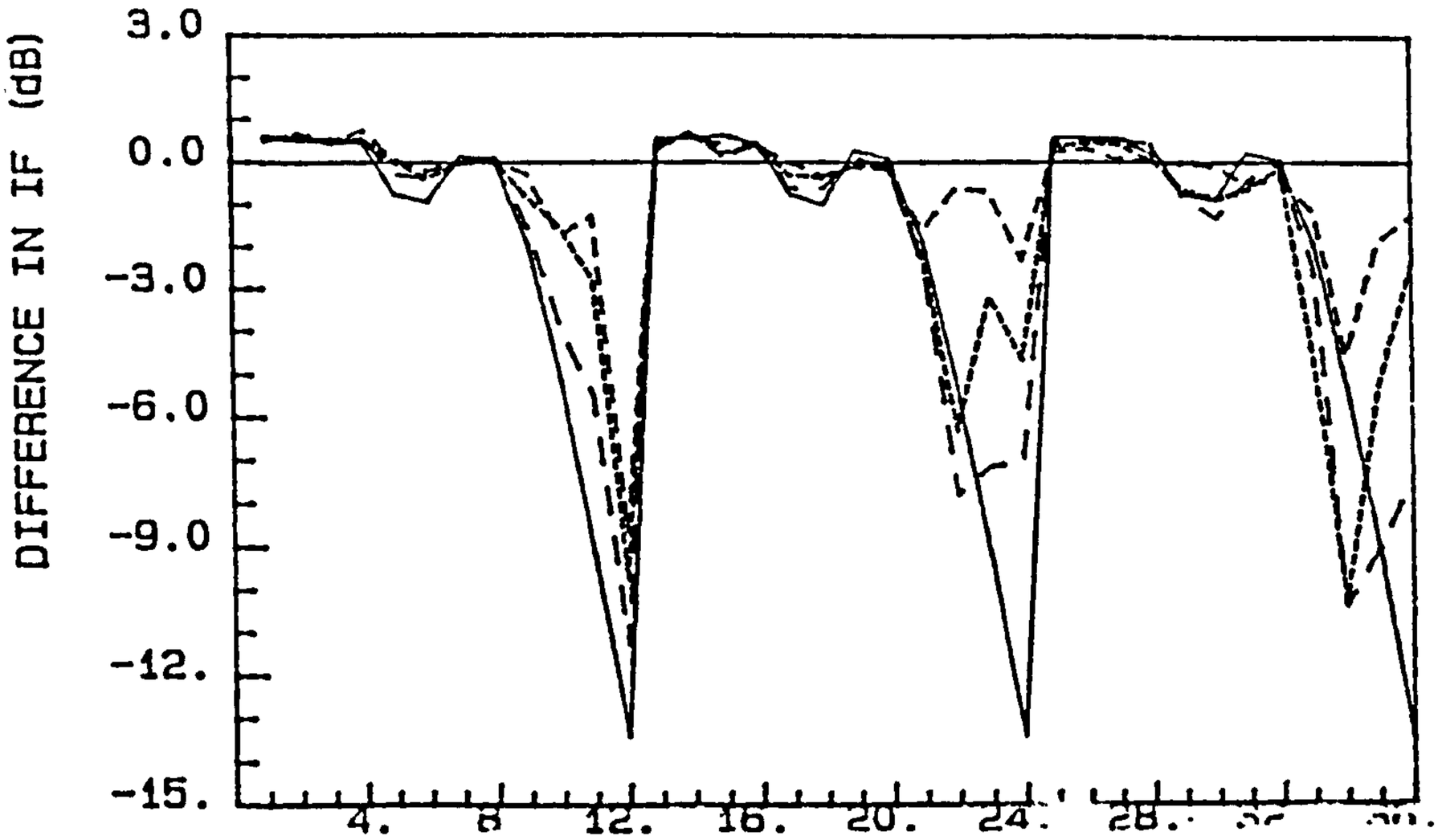

(a)

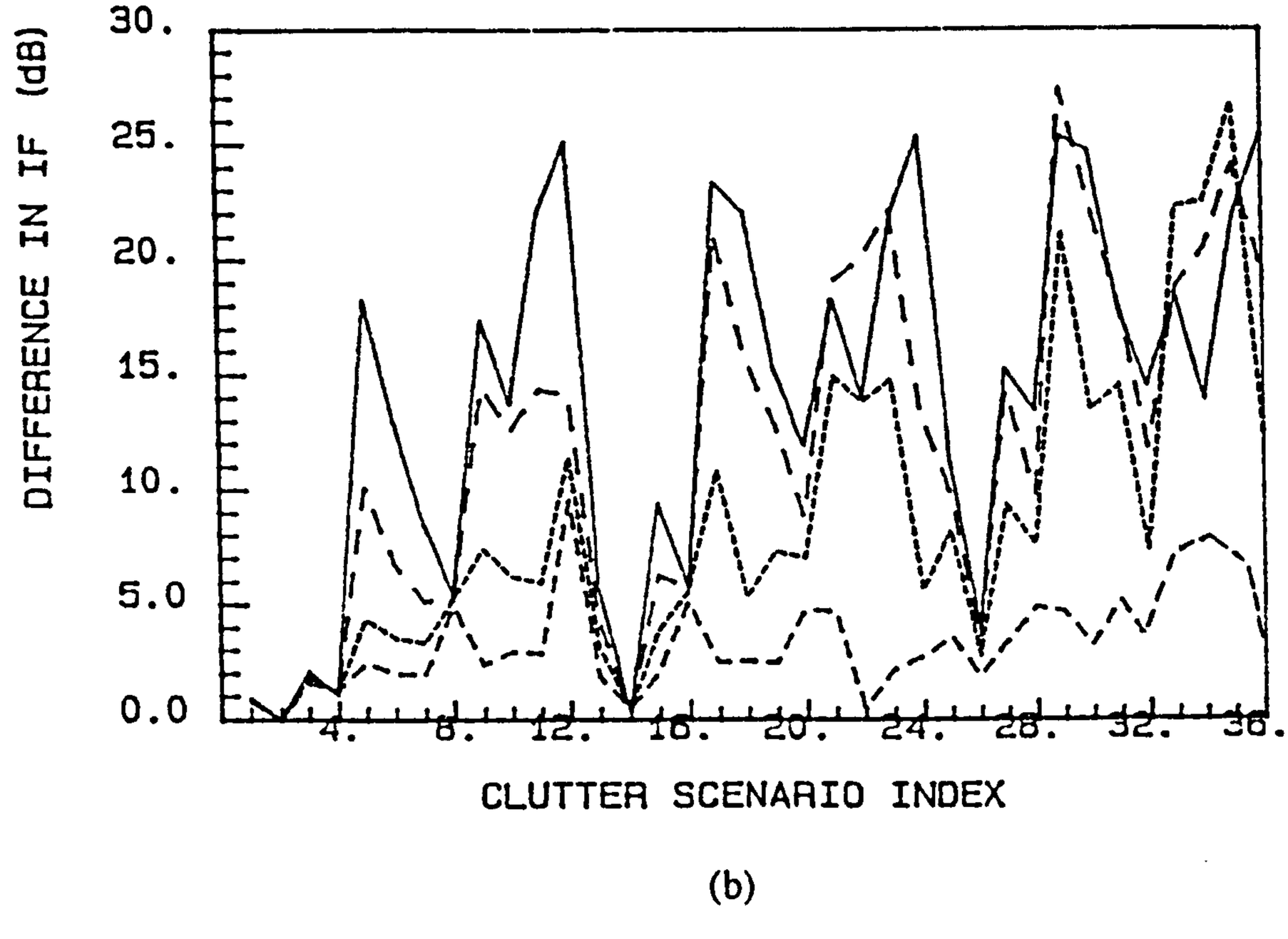

(b)

Fig. 4.9: *Effect of pre-filter MTI on IF Loss in the presence of Point clutter sources, (N=10)*

a) IF against background clutter b) IF against point clutter sources

——————— No point clutter sources in reference cells

— — — — 1 point clutter source in reference cells

---------- 2 point clutter sources in reference cells

— — — 4 point clutter sources in reference cells

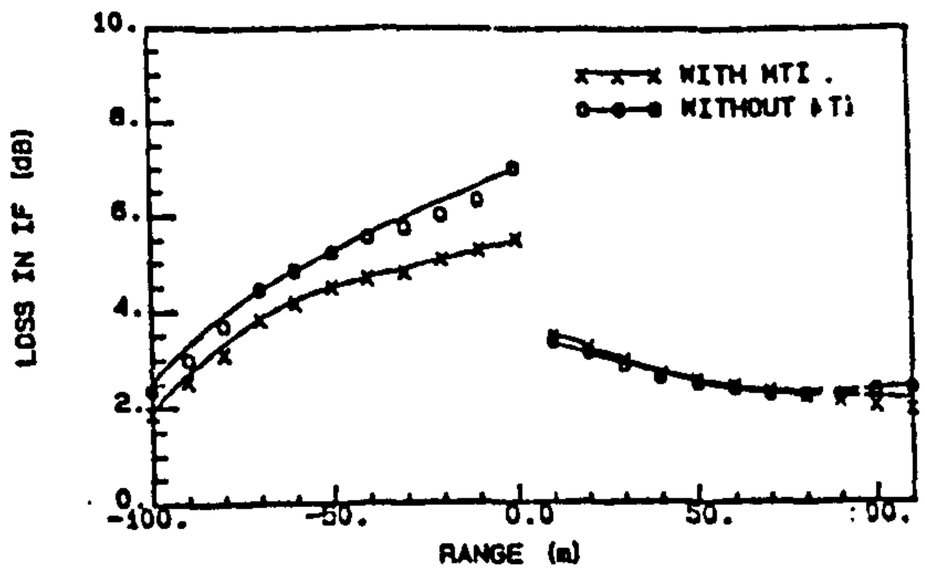

(a)

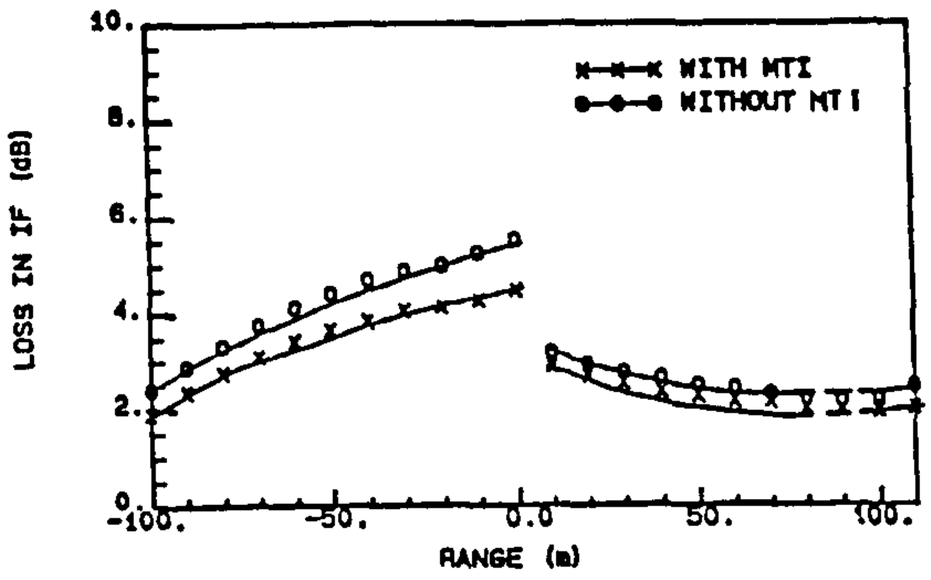

(b)

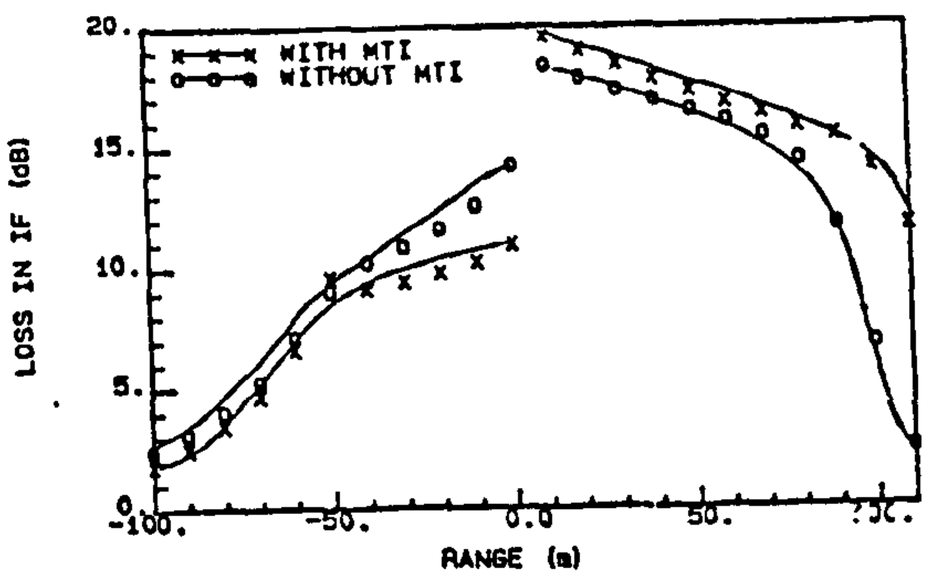

(c)

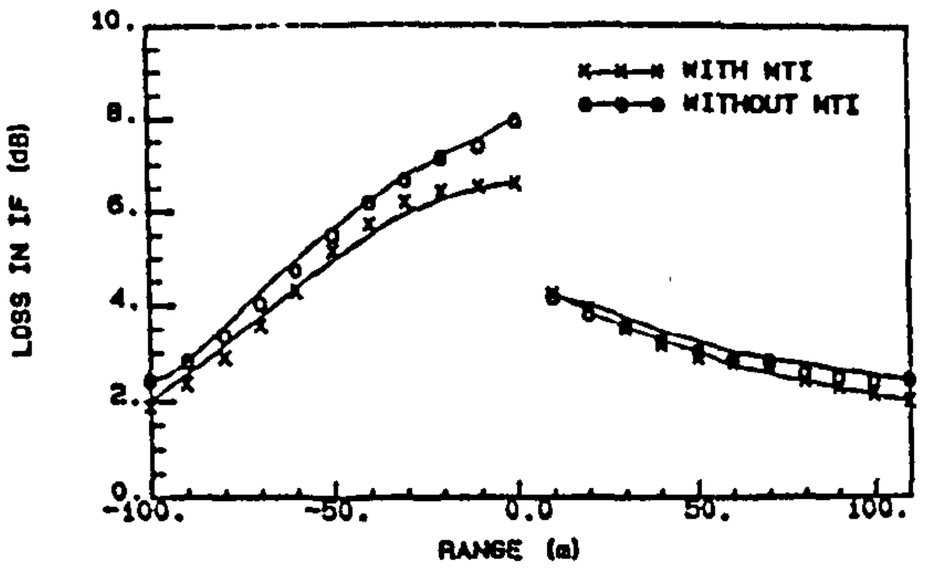

(d)

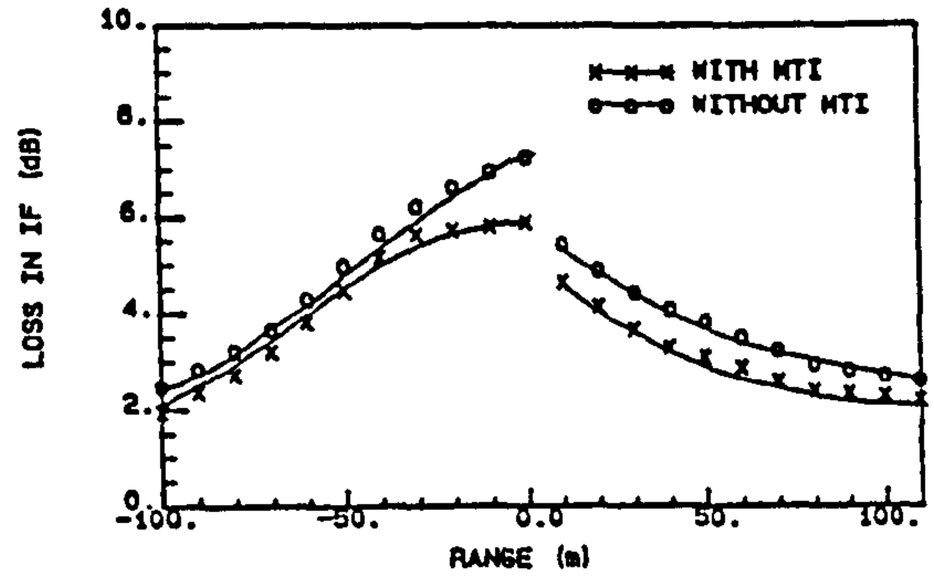

(e)

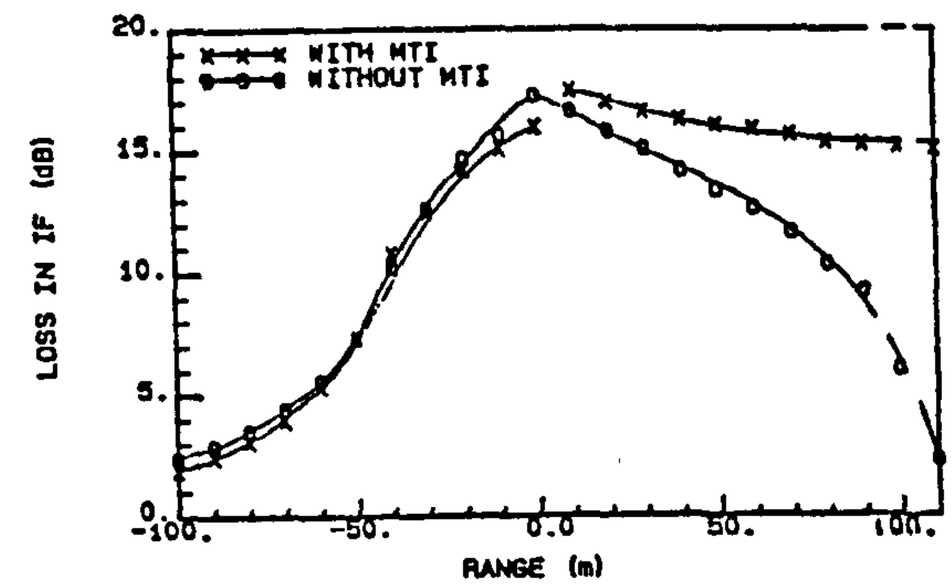

(f)

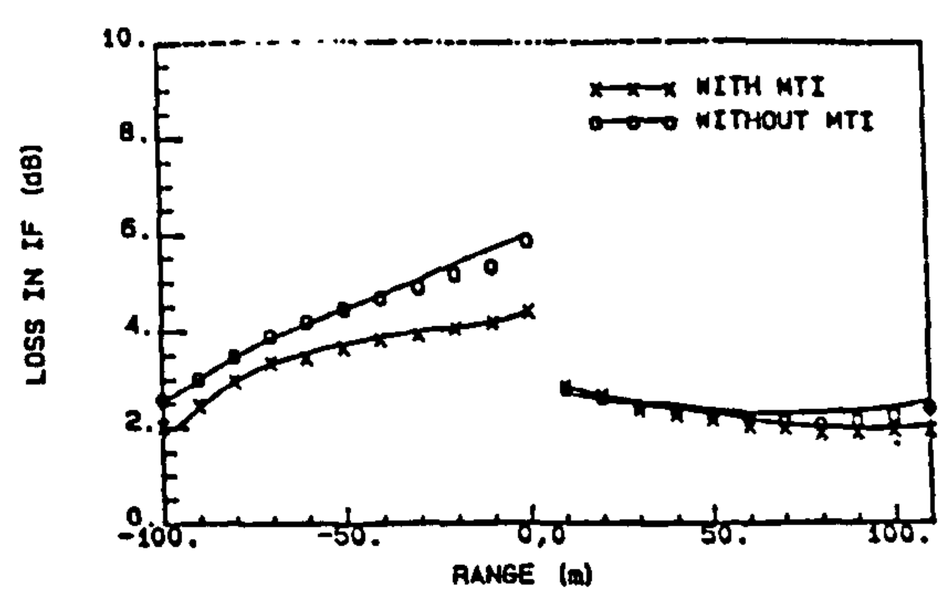

(g)

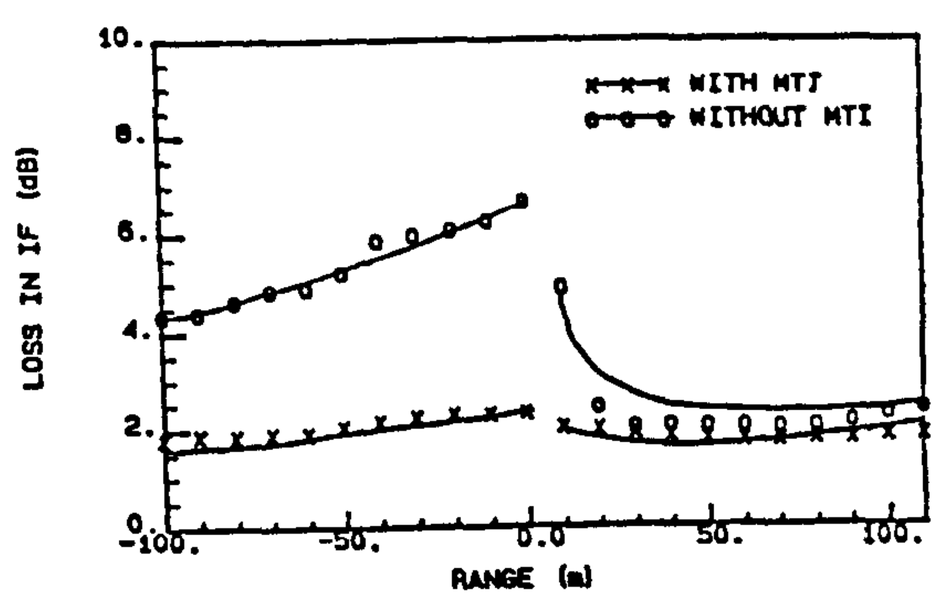

(h)

Fig. 4.10: *Effect of Pre-filter MTI on IF Loss around Clutter Edges (N=10)*

a) Edge Scenario 1 b) Edge Scenario 2 c) Edge Scenario 3 d) Edge Scenario 4

e) Edge Scenario 5 f) Edge Scenario 6 g) Edge Scenario 7 h) Edge Scenario 8

x---x---x with MTI o---o---o without MTI

4.5. DISCUSSION

In section 4.1.3 the detection loss was proposed as a more representative measure of filter performance in terms of the filter's effect on overall radar performance. Provided the detection processing assumed in calculating the detection loss reflects that employed in the radar being analysed, this should indeed be the case. Unfortunately, the assumption of ideal detection used here yields results which are often very optimistic compared to practical CFAR processors. This is exemplified by the apparent detection *gain* given by adaptive filters in clutter with amplitude heterogeneity, when the IF is reduced and the detection loss by practical CFAR processors is known to increase severely. This questions the credibility of the detection loss based on the assumption of ideal detection, which has therefore not been calculated for non-limiting cases.

This does not alter the fact that the IF is not an ideal measure of adaptive filter performance in the context of the radar system as a whole. For example, the reduced IF loss in spectrally heterogeneous clutter for $K<\infty$ compared to the limiting case is misleading: this IF loss represents the arithmetic mean of the IF obtained on the n trials; very low values of IF on some trials do not pull the mean IF down noticeably, whereas the clutter residue spikes corresponding to those low IF trials would have dramatic impact on detection performance. In general, the smaller K and the more widely fluctuating (in amplitude and spectrum) the clutter, the higher the variance in the IF, and hence the IF loss, and the worse the detection performance achieved by practical detectors. This indicates that higher order moments of the IF than simply the mean need to be known if the effect of filter performance on detection performance is to be assessed with any confidence. Unfortunately accurate estimation of higher order moments requires far more simulation trials than estimation of the mean; this is likely to limit the scope of evaluations of filter performance to specific filter and clutter parameters.

Despite the lack of quantitative descriptions of the higher order moments, it can be noted that the mean IF represents an upper bound on filter performance. Any increases in the variance or higher order moments of the IF can only cause a deterioration in detection performance. This allows some conclusions to be drawn from the data presented in previous sections of this Chapter. Amplitude heterogeneity introduces significant IF losses, in the region of 1 to 5 dB for most conditions of interest; spectral heterogeneity introduces significant IF losses, in the region of 1 to 15 dB for most conditions of interest; and the loss introduced by adaptive estimation of the covariance matrix with finite K is also notable, generally in the region of 2 to 8 dB. It is therefore evident that

practical adaptive optimal filters will suffer losses of several dB relative to ideal optimal filters in many clutter environments. Comparison to other doppler processors analysed in the previous Chapter then shows that adaptive filters will, in general, offer poorer performance than conventional MTD and PD processors, even excluding further losses which can be expected due to increased higher order moments, which do not apply to MTD and PD processors.

The loss introduced by adaptive estimation of the covariance matrix with finite K is the only of the losses mentioned above over which the radar designer has any control. There is, however, little scope for its reduction since K cannot be increased arbitrarily due to processing constraints and, more importantly, the larger the reference window, the higher the probability of it encompassing clutter edges and/or point clutter sources, and the further the effects of edges and extraneous targets will be extended. These effects include increased clutter residue and increased IF loss in the region of clutter edges or in the presence of point clutter sources or extraneous targets. For many edge scenarios the magnitude of the increase in IF loss is often about 5 dB and occasionally more than 10dB, over and above the loss due to finite-size reference windows. This loss is worst at the clutter edge and in general, for finite K, tapers off smoothly as the test cell moves away from the edge.

The incorporation of a standard MTI filter before the adaptive filter has been shown to offer significant performance benefits in situations where a few stationary point clutter sources are present in a homogeneous clutter background with a different spectrum. It also provides some benefits on both sides of clutter edges in which clutter on one side of the edge has a dominant stationary component. Even in homogeneous clutter the use of pre-filter MTI reduces the loss due to adaptive estimation of the covariance matrix with finite K, by of the order of 1 dB. From Chapter 3 it can be seen that this is approximately equivalent to the mean loss suffered by MTI-optimal composite filters relative to ideal adaptive processors over a wide range of clutter scenarios. It can therefore be concluded that pre-filter MTI will significantly enhance filter performance in many non-homogeneous clutter scenarios, with negligible loss on average in homogeneous clutter.

The use of pre-filter MTI only introduces significant losses when the clutter background, or the clutter on one side of a clutter edge, has a wide spectrum centred at about half the PRF. This could be countered by employing more than one MTI, with the notch of each at a different doppler. This idea can be expanded to a more general composite filter, comprising say a 5-pulse MTD filter bank, each of which is cascaded with a 6-pulse adaptive optimal filter. The rationale is that the adaptive filter would improve the

performance against the "rogue" clutter scenarios mentioned in Chapter 3, which are the main shortcoming of MTD filters, while the MTD filter would maintain good performance (or at least an acceptable minimum) in non-homogeneous clutter. The steady state loss due to adaptive estimation of the covariance matrix would also be significantly reduced for K held constant.

Limiting cases (ie. for $K \rightarrow \infty$) have been analysed in this Chapter in an attempt to obtain analytic solutions to the IF loss in non-homogeneous environments, thereby eliminating the need for tedious simulations. It is evident that the limiting cases do not, in general, reflect the loss for practical values of K with great accuracy. Nevertheless, they can give an indication of the order of magnitude of losses due to non-homogeneous clutter. The error is expected to be not incomparable to the error in detection loss due to neglecting the higher order moments of the IF and clutter residue, and limiting cases may therefore be useful for giving first order estimates of filter performance in heterogeneous clutter.

4.6 CONCLUSIONS

The performance of adaptive Hsiao-optimal filters in non-homogeneous backgrounds has been examined, for practical adaptive estimation of the covariance matrix, and for limiting cases where the estimate of the covariance matrix tends to the mean clutter covariance matrix. Three classes of non-homogeneous backgrounds have been studied, namely:

1. Clutter in which the amplitude and spectral width in each range bin are randomly drawn from spatially invariant independent gamma distributed parent populations.

2. Clutter edges, in which the clutter amplitude and/or spectrum exhibit a step change at some point in the range profile of the clutter.

3. Clutter which is essentially homogeneous but in which a small number of range bins are corrupted by returns with significantly different amplitude and spectral characteristics, representing point clutter sources or extraneous targets.

The use of pre-filter MTI has been investigated as a means of reducing filter sensitivity to some classes of clutter non-homogeneity.

The following conclusions can be drawn from this study:

1) Adaptive filters suffer significant reductions in IF in non-homogeneous clutter environments.

2) These losses are generally greater than the benefit afforded by ideal adaptive processors over other conventional (MTD, PD) doppler processors. Practical adaptive optimal filters are therefore not as effective as MTD or PD processors in suppressing clutter, and particularly non-homogeneous clutter.

3) Careful consideration needs to be given to the choice of performance measures for assessing filter performance. The mean IF loss is an optimistic performance measure in adaptive doppler processors. The true impact on radar detection performance will be increased by higher order moments of the IF loss and clutter residue. More accurate analysis requires higher order moments to be quantified, with strong implications on the number of simulation trails necessary for acceptable error.

4) More accurate performance analysis will, however, only be meaningful if the models of clutter heterogeneity used in this study, particularly for spectral heterogeneity, are validated. Further research into the characterisation of heterogeneous clutter is essential before models can be used with any confidence to assess radar performance in heterogeneous clutter environments.

5) The most promising means of achieving improved clutter suppression in heterogeneous clutter while maintaining near-optimal performance in homogeneous clutter appears to be the use of MTD-adaptive filter hybrid processors. Research to quantify the benefits of such techniques is necessary.

6) It is the author's opinion that adaptive optimal filtering alone does not provide a means of significantly improving radar detection performance in non-homogeneous clutter. It is felt that more significant gains in detection performance are most likely to be achieved by improved post-filter detection techniques.

CHAPTER 5

CONVENTIONAL CFAR DETECTION IN SPATIALLY UNCORRELATED K-DISTRIBUTED CLUTTER

It has been shown in the previous Chapters that scope for improvements in clutter suppression through doppler filtering is limited. In many clutter environments the detection of desired targets embedded in relatively strong clutter residue will therefore be necessary. If the unfiltered clutter returns are spiky, then so too will be the residue, the spikiness of which may in fact be compounded if adaptive doppler processors are used. Discrimination of targets from the spiky clutter residue based on amplitude thresholding alone can result in severe detection losses and increases in false alarm rate.

The influence of K-distributed clutter on detection and false alarm probabilities achieved by most conventional CFAR processors has not been widely addressed in the literature. In this Chapter the performance of the CA, CAGO and OS processors is therefore quantitatively evaluated for K-distributed clutter backgrounds, and K-distributed clutter plus thermal noise. Empirical expressions for the CFAR loss are derived. Besides being of general use in the selection and evaluation of conventional CFAR processors, the results derived in this Chapter are necessary to facilitate meaningful performance assessment of improved CFAR processors introduced in later Chapters of this thesis.

The analysis presented here is limited to single "pulse" detection of Rayleigh (voltage) fluctuating targets, where the term "pulse" in fact relates here to a single detection opportunity. This may arise from a true single pulse or from a batch processed burst of pulses. The effects of post detection integration of several pulses have been addressed in some detail by Watts (1985) and Ward (1985), and their results can be used in conjunction with the single pulse results presented in this Chapter to assess the performance of CFAR processors employing post detection integration.

The entire analysis can be performed on power signals if it is assumed that the processor operates on the output of a square law detector. This allows Rayleigh voltage distributions to be transformed into exponential power distributions, greatly simplifying the analysis. This mathematical expediency, to which we resort in later Chapters of this thesis, is widely adopted in CFAR analyses presented in the literature and is generally justified by the assertion that square law envelope detection is slightly more optimal than linear envelope

detection, and the results do not differ greatly in any case. In spiky clutter, however, dynamic range considerations would generally argue for linear detection to be used. Indeed, the K-distribution as defined in eqn. (2.1) in Chapter 2 of this thesis is explicitly a voltage distribution when applied to radar sea clutter. It was therefore decided to perform all analyses in this Chapter based on linear envelope detection.

5.1 DETECTION IN UNCORRELATED K-CLUTTER ONLY

This section addresses the detection performance of various types of CFAR detectors in homogeneous K-distributed clutter only, i.e. the noise level is assumed to be sufficiently low in comparison to the clutter signal as to be negligible. This is true for CNRs of greater than 15 to 20 dB, depending on the shape parameter ν. It is also assumed in this section that the clutter modulation process is completely decorrelated from one range bin to the next. Detection performance is evaluated in terms of the SCR required for achieving a specified probability of detection, for a specified false alarm probability P_{fa}. A detectability loss, that is the additional SCR required to achieve P_d with given P_{fa}, over and above that for ideal detection in Rayleigh noise or clutter, is then calculated. Strictly speaking the detectability loss is a function of the required P_d, but for most CFAR implementations and P_d's of interest the loss varies negligibly with P_d in the range $30\% \le P_d \le 90\%$[1]. For this Chapter all losses are based on P_d=50%. It is also initially assumed that the threshold multiplier factor used to yield the required false alarm probability is based on correct knowledge of the clutter shape parameter ν. Deviations from this assumption are analysed in section 5.1.5.

In general the analysis is performed as follows: the pdf $p_z(z)$ of the test statistic is found as described in subsequent paragraphs of this section. Having obtained $p_z(z)$, the false alarm rate is obtained from:

$$P_{fa} = \int_0^\infty \left\{ \frac{2c^\nu}{\Gamma(\nu)} (\alpha z)^\nu K_\nu(2c\alpha z) \right\} p_z(z)\, dz \qquad \ldots (5.1)$$

where the term in the brackets { } is merely the complementary CDF at αz of the K-distributed clutter. Inversion of the solution of this expression yields the threshold multiplier factor α required for a specified false alarm rate. In general this must be numerically calculated, with $\nu = 0.5$ giving a simple analytic expression which can be used

[1] The effect of the required detection probability on the detection loss is discussed in more detail in section 4.1.6.

for verification of numerical accuracy. Examples of the required value of α are given as a function of P_{fa} and ν in Fig. 5.4 later in section 5.2.5.

The probability of detecting a target of signal-to-clutter ratio S_0 is given by:

$$P_d(S_0) = \int_0^\infty P_t(x>\alpha z)\, p_z(z)\, dz \qquad \ldots (5.2)$$

where $P_t(X>\alpha z)$ is the complementary CDF at αz of the target plus clutter voltage, given by:

$$P(x>\alpha z) = \int_0^\infty \frac{2b^{2\nu}}{\Gamma(\nu)} u^{2\nu-1} \exp\left[\frac{-(\alpha z)^2}{P_t + 4u^2/\pi} - (bu)^2\right] du \qquad \ldots (5.3)$$

where $b=\sqrt{(4/\pi)}.c$ and P_t is the absolute target power, given by $S_0\nu/c^2$. Unfortunately no closed form expression has been found for eqn. (5.3). However, for moderate to large signal-to-noise ratios (>10 dB), as are of interest here since we assume that detection probabilities of better than about 50% are required, we can simplify this expression to that of the complementary CDF of a Rayleigh target, of signal strength equal to the combined clutter plus target power. This is possible since the tails of the distribution are not of great significance for the evaluation of detection probability once the threshold multiplier factor α has been set, since they effect the resulting detection probability only very slightly. Only the "bell shaped" central region of the target plus clutter PDF is of significance, and the presence of a small clutter component (-10 dB relative to the target signal) affects only the far out tails of the power-normalised target plus clutter PDF to any noticeable extent. The magnitude of the error introduced by this approximation is discussed in section 5.1.6. The approximate complementary CDF of the target plus clutter is then:

$$P_t(x>\alpha z) \approx \exp\left[\frac{-(\alpha z)^2}{(1+S_0)\nu/c^2}\right] \qquad \ldots (5.4)$$

5.1.1 Cell Averaging CFAR Processor

On the assumption of completely uncorrelated homogeneous clutter in each of the reference cells, the PDF of the test statistic of the CA CFAR detector is obtained from the N-fold convolution of the clutter PDF with itself, where N is the number of reference cells used in estimating the background clutter or noise level. In the case of the clutter being K-distributed, this result cannot in general be represented in closed form. For the special case

of the clutter shape parameter $\nu = m + {}^1/2$, m = 0, 1, 2..., closed form expressions are indeed possible, and these are given in Appendix 2.1 (eqn. 2.1.13). The very simple form for $\nu = 0.5$ (eqn. 2.1.4) is particularly useful as a check for numerical techniques. Instead of calculating the N-fold convolution a numerical alternative is to take the FFT of the PDF of the K-Distributed reference noise, raise the resulting complex characteristic function to the power of N, take the inverse FFT, and take the real part of the resulting complex PDF as the PDF of the sum of N K-distributed variables. This is computationally more efficient than N-fold convolution but care must be taken to ensure that the numerical precision of the FFT is sufficient, as well as that the array size is sufficiently long to prevent aliasing of the characteristic function or the final PDF, since the mean of the output PDF is N times that of the input PDF.

It should be noted that for $\nu < 0.5$ the clutter PDF tends to infinity as x tends to 0. This complicates the numerical evaluation of the test statistic of the CA processor since both numerical convolution and Fourier transformation of data containing singularities is unreliable. This has been handled in this study by introducing quantisation to the clutter PDF, making it a discrete PDF, which is finite for all x. Provided the quantisation spacing is sufficiently fine (~1/200 of the clutter variance) accuracy is not significantly degraded. (In studies into the effects of quantisation, deviations from the continuous case only became significant for quantisation of 1/16 to 1/32 of the clutter variance).

The detection performance of CA CFAR detectors has been analysed for sample values of ν (0.1, 0.25 , 0.5 , 1.5 , 2.5 , 4.5 , 9.5 , ∞), for various false alarm rates and numbers of reference cells N. Results are shown in Fig. 5.1, which plots the CFAR loss relative to ideal detection in Rayleigh noise as a function of the shape parameter ν. It is evident that the detection loss is strongly dependent on ν, and is also fairly strongly dependent on the number of reference cells used and the desired false alarm rate. For spiky clutter ($\nu \sim 0.5$) a detection loss of about 20 dB is possible. The smaller the number of reference cells, and the higher the desired value of P_{fa}, the more sensitive the processor becomes to increasing clutter spikiness, i.e. lower values of ν.

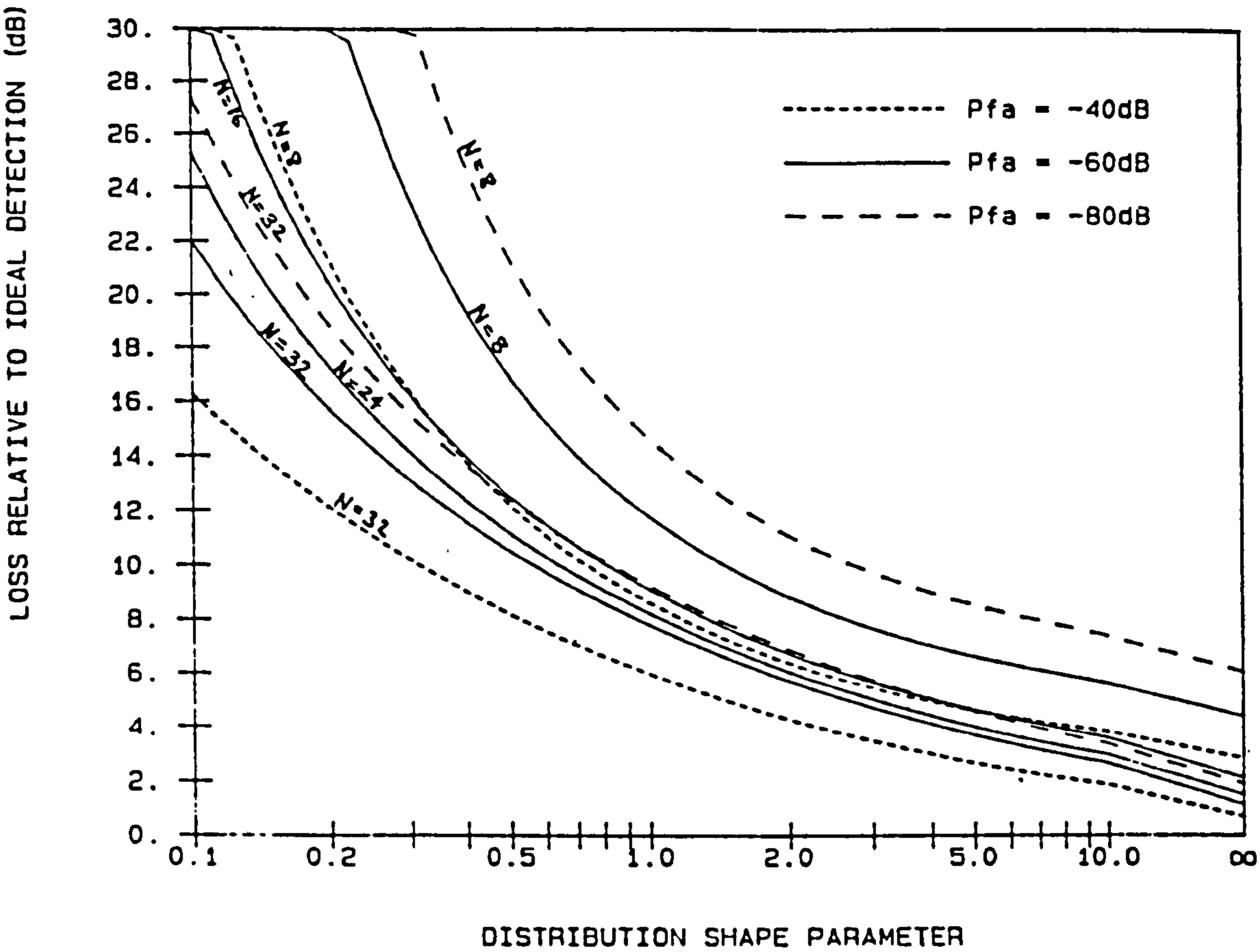

Fig. 5.1. *Detection loss vs v for the CA detector.*

5.1.2 Cell Averaging Greatest Of CFAR Processor

In the case of the CAGO detector the test statistic is obtained from the selection of the greatest value of the sums of the reference cells on either side of the test cell, as described in Chapter 2. The PDF of these sums is obtained as before by the N/2-fold convolution of the clutter PDF with itself, as for the CA processor, merely replacing the term N with N/2. The PDF of the greatest of two such signals, each with PDF f(z), is then given by:

$$p_z(Z) = 2\, f(z)\, F(z) \qquad \ldots (5.5)$$

where F(z) is the CDF of f(z). This then represents the PDF of the test statistic to be substituted into eqns. (5.1) and (5.2), with the detection performance subsequently being calculated in the identical manner to that for the CA CFAR processor.

Detection performance has been numerically evaluated for the same sample values of ν used for the CA CFAR processor, for various false alarm rates and numbers of reference cells. Results are shown in Fig. 5.2, which plots the CFAR loss relative to ideal detection in Rayleigh noise as a function of the shape parameter ν. Again it is evident that the detection loss is strongly dependent on ν, and is also fairly strongly dependent on the number of reference cells used and the desired false alarm rate. For spiky clutter ($\nu \sim 0.5$) a detection loss of about 20 dB is again possible. The smaller the number of reference cells, and the higher the desired value of P_{fa}, the more sensitive the processor becomes to increasing clutter spikiness. Comparison of Figs. 5.1 and 5.2 indicates that the CAGO processor suffers slightly higher loss than the CA processor. This is to be expected since the clutter conditions, although non-Rayleigh, are nevertheless assumed to be homogeneous, and the superior performance of the CA processor in homogeneous backgrounds is well known. The CAGO processor can also be seen to be slightly more sensitive to reductions in N than the CA processor.

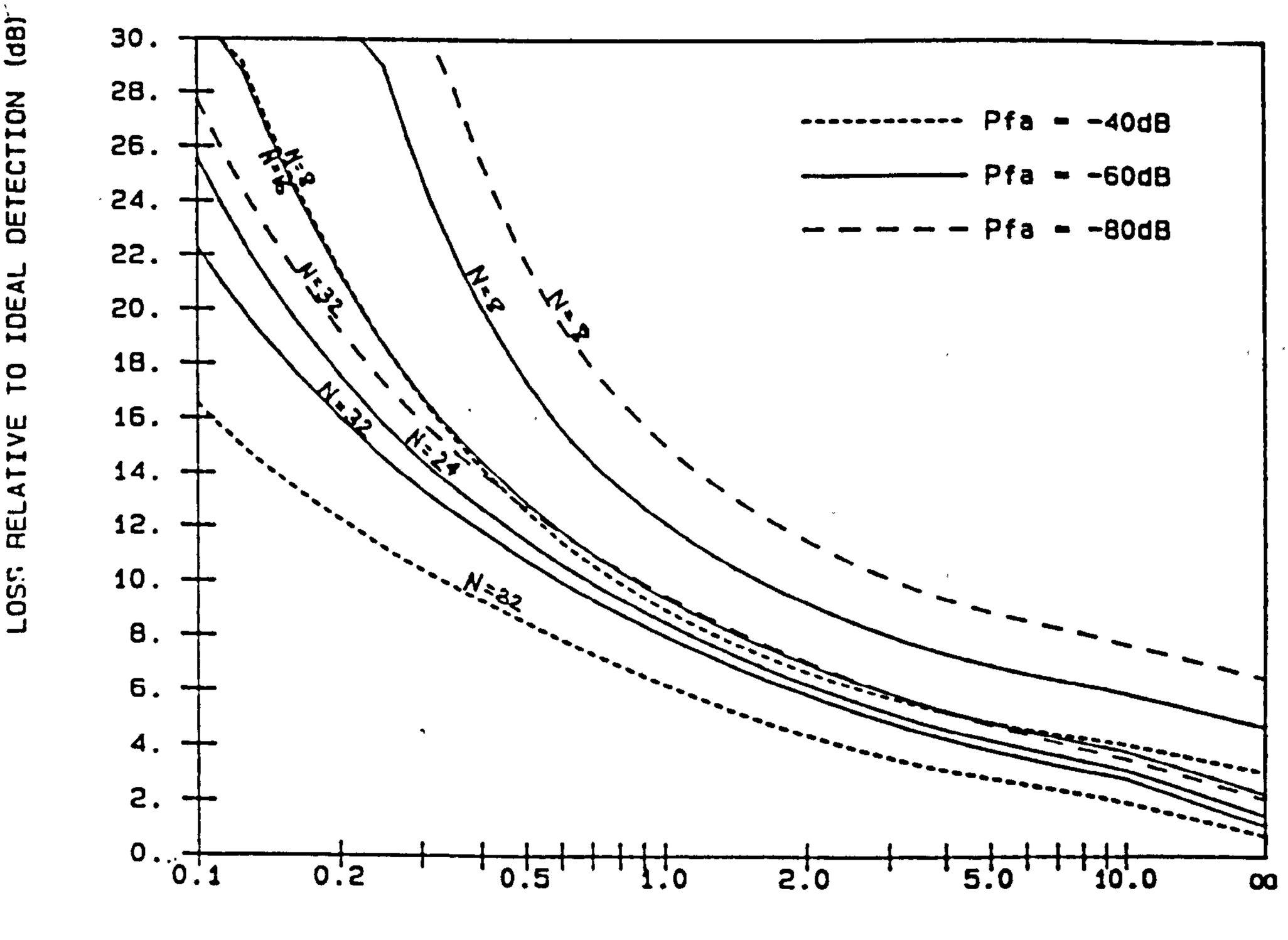

Fig. 5.2. *Detection loss vs ν for the CAGO detector.*

5.1.3 Order Statistic CFAR Processor

In the OS-CFAR processor the test statistic is taken as the k^{th} cell of the N ordered reference cells, as described in Chapter 2. If the PDF of the clutter in each reference cell is a continuous function p(X), with CDF P(x), the PDF of the test statistic is (Rohling, 1983):

$$p(z) = k\binom{N}{k} p(x)\, P(x)^{k-1} [1-P(x)]^{N-k} \qquad \ldots (5.6)$$

Substituting the PDF and CDF for K-distributed clutter, the PDF of the test statistic is given by:

$$p_z(z) = 2ck\binom{N}{k}\left[\frac{2(cz)^{\nu}}{\Gamma(\nu)}\right]^{N-k+1} K_{\nu-1}(2cz)\, [K_{\nu}(2cz)]^{N-k}\left[1 - \frac{2(cz)^{\nu}}{\Gamma(\nu)} K_{\nu}(2cz)\right]^{k-1} \qquad \ldots (5.7)$$

which can be simplified for $\nu = m + 1/2$, $m = 0, 1, 2, \ldots$. For example for $\nu = 0.5$ and $\nu = 1.5$, the PDF's of the test statistic can be simplified to:

$$\nu = 0.5: \quad p_z(z) = 2ck\binom{N}{k} e^{-2c(N-k+1)z}\left[1 - e^{-2sz}\right]^{k-1}$$

$$\nu = 1.5: \quad p_z(z) = 4c^2k\binom{N}{k} z\,(1+2cz)^{N-k} e^{-2c(N-k+1)z}\left[1 - (1 + 2xz)e^{-2sz}\right]^{k-1} \qquad \ldots (5.8)$$

These expressions are substituted into eqns. (5.1) and (5.2), following which detection performance is calculated in the same manner as in section 5.1.

Detection performance has been numerically evaluated for the same sample values of ν used for the CA and CAGO CFAR detectors, for various false alarm rates and numbers of reference cells N. The rank k of the sample to be used in the formation of the test statistic is taken as 3N/4, a compromise between optimal performance and good resilience to interfering targets and clutter edges (Rohling, 1983). Since the clutter is assumed to be homogeneous the choice of k in the region $N/2 \leq k \leq 7N/8$ is not expected to make much difference to the performance of the OS processor. Results are shown in Fig. 5.3, which plots the CFAR loss relative to ideal detection in Rayleigh noise as a function of the shape parameter ν. Again it is evident that the detection loss is strongly dependent on ν, and is also fairly strongly dependent on the number of reference cells used and the desired false alarm rate. For spiky clutter ($\nu \sim 0.5$) a detection loss of about 20 dB is again possible. The smaller the number of reference cells, and the higher the desired value of P_{fa}, the more sensitive the processor becomes to increasing clutter spikiness. Comparison of Fig. 5.3 with Figs. 5.1 and 5.2 indicates that the OS processor suffers notably higher loss than the CA and CAGO processors, particularly for small values of ν. The OS processor can also be seen to be more sensitive to reductions in N than the CA processor.

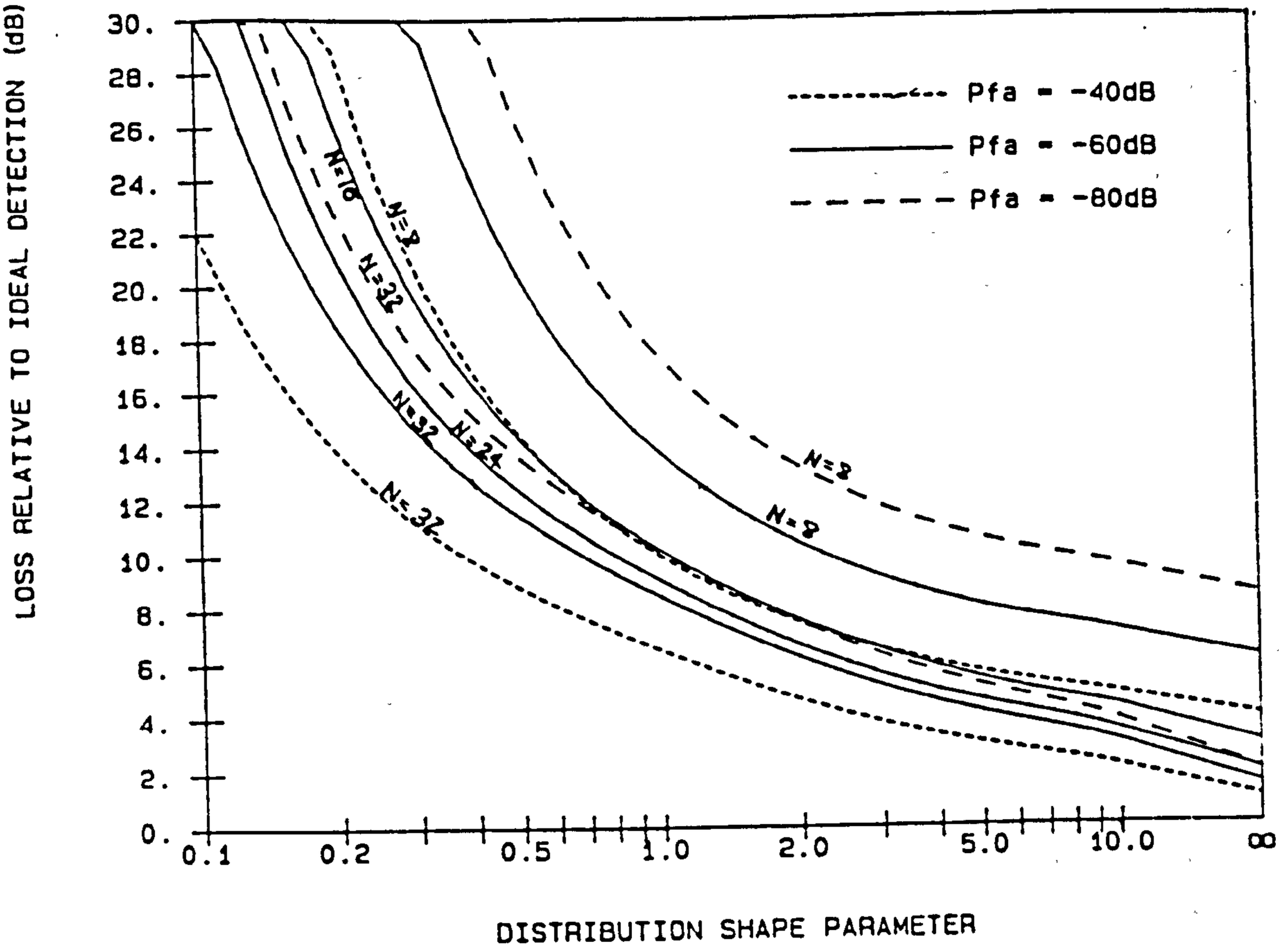

Fig. 5.3. *Detection loss vs ν for the OS detector.*

5.1.4 Loss Associated with CFAR Thresholding

The loss curves presented in the preceding three subsections have shown the overall detection loss including the dominant effect of the loss associated with the fact that the background against which the target must compete for detection is spiky K-Distributed clutter instead of Rayleigh clutter or noise. In order to determine the detection loss associated purely with the use of CFAR thresholding, specifically excluding the direct effects of clutter spikiness, it is necessary to determine the loss that an ideal linear detector would suffer in the same spiky clutter environment and subtract this from the overall loss. This ideal detector loss can be obtained by using the method given by Watts (1985) for ideal fixed threshold detection in uncorrelated K-distributed clutter. In this ideal situation it is assumed that the threshold is set using explicit knowledge of both the clutter power and the shape parameter, ie. knowledge of both ν and c, instead of just ν as has been previously assumed in the preceding three subsections.

Having calculated the ideal detection loss $L_i(\nu,P_{fa})$, the loss associated purely with CFAR thresholding, referred to as the CFAR loss L_c, is obtained from:

$$L_c(\nu,P_{fa},N) = L_t(\nu,P_{fa},N) - L_i(\nu,P_{fa}) \quad \ldots (5.9)$$

where $L_t(\nu,P_{fa},N)$ is the total loss as illustrated in Figs. 5.1 to 5.3. The CFAR loss will differ according to the type of CFAR processor used. It can be noted again that strictly speaking the required detection probability affects all three factors in eqn. (5.9) above. However, the influence of varying P_d in the range $30\% \leq P_d \leq 90\%$ is practically negligible and has been omitted from this analysis.

The CFAR loss for each of the CFAR processors under consideration here has been calculated for the same sample values of ν, N and P_{fa} used in the preceding three subsections . Full results are tabulated in Table A5.1.1 in Appendix 5.1. Table 5.1 below provides a sample of these data, giving the CFAR loss for the three CFAR processors discussed for N = 16 and N = 32, at sample values of ν, for a false alarm probability of 10^{-6}. The first column labelled $L_i(\nu,10^{-6})$ gives the loss associated with ideal fixed threshold detection in spiky clutter of clutter of shape parameter ν for $P_{fa} = 10^{-6}$ and $P_d = 50\%$. It can be seen from the table that a CFAR loss of greater than 2 dB can commonly be expected in spiky clutter, with much greater losses of up to tens of dBs being possible in extreme cases of very spiky clutter and small N. The superior performance of the CA processor is again evident. The advantages of using a large number of reference cells can also be seen to be more pronounced for low values of ν, where the use of only 16 as opposed to 32 reference cells can introduce an additional loss of 2 dB to 5 dB under most reasonable conditions, and more in extreme cases.

Table 5.1

CFAR Loss for Sample Values of ν (dB)

	$L_i(\nu,10^{-6})$	CA		CAGO		OS	
		N = 16	N = 32	N = 16	N = 32	N = 16	N = 32
$\nu = 0.10$	13.95	19.49	8.20	19.73	10.00	34.78	17.33
$\nu = 0.25$	10.83	7.43	3.52	7.73	3.87	11.68	5.48
$\nu = 0.50$	8.59	4.24	2.07	4.67	2.38	6.10	3.02
$\nu = 1.5$	5.42	2.50	1.24	2.80	1.45	3.50	1.77
$\nu = 9.5$	1.83	2.13	1.05	2.37	1.22	2.95	1.45
$\nu = \infty$	0	2.12	1.04	2.35	1.20	2.93	1.44

5.1.5 Effect of Incorrect Estimation of the Shape Parameter ν

The preceding discussions have assumed that the value of the shape parameter ν is explicitly known, presumably through real time analysis of clutter data. Assumed

knowledge of the shape parameter enters the analysis through the PDF of the test statistic and the CDF of the clutter in the test cell under conditions of no target being present, both of which depend on the clutter PDF, and hence ν. The main effect of changing the value of ν is to change the threshold multiplier factor α needed to achieve a specified false alarm probability. Errors in estimating ν will thus result in an incorrect value of α being used, causing a degradation in detector performance. If the threshold is set too high (ν is estimated too low), the consequence will be increased detection loss; if the threshold is set too low (ν is estimated too high), the consequence will be increased false alarm probability. The approximate magnitude of the loss associated with the former error, that is ν being estimated too low and hence the threshold being set too high, is obtained simply from the detection loss curves of the previous sections: the difference between the detection loss at the estimated value of ν and at the true value of ν is the approximate[2] additional loss due to incorrect estimation of ν. Under most operating conditions the performance degradation due to ν being estimated too high and the threshold being set too low, will, however, be of more interest in that it may cause a notable increase in P_{fa}. To examine the severity of this increase in P_{fa}, as a function of the size of the error in the estimate of ν, the false alarm probability is now evaluated as a function of ν and α.

For a given value of ν, the false alarm probability is calculated as a function of α from eqn (5.1). This takes account of the CFAR detector implementation and the number of reference cells N in the form of the PDF of the test statistic $p_z(z)$. Eqn (5.1) has been evaluated as a function of α for several sample values of ν, for the CA, CAGO and OS CFAR processors, for various numbers of reference cells N. Manipulation of the resulting data yields plots of the form shown in Figs. 5.4a, 5.4b and 5.4c for the CA, CAGO and OS processors respectively, for processors using 32 reference cells. These graphs represent contours of constant false alarm rate over the ν-α plane, i.e. the threshold required for a given false alarm rate as a function of ν. To determine the increase in P_{fa} due to errors in estimating ν, simply note the difference between P_{fa} at the estimated and true values of ν, based on a threshold appropriate for the desired false alarm rate at the *estimated* value of ν. The horizontal spacing between contours in Fig. 5.4 gives a measure of the sensitivity of the false alarm probability to errors in the estimated value of ν.

---

[2] Although this is not exactly accurate, due to the incorrect pdf of the test statistic under this scenario being used in analysing the loss at the estimated value of ν, the results given by this simplification differ negligibly from the true situation.

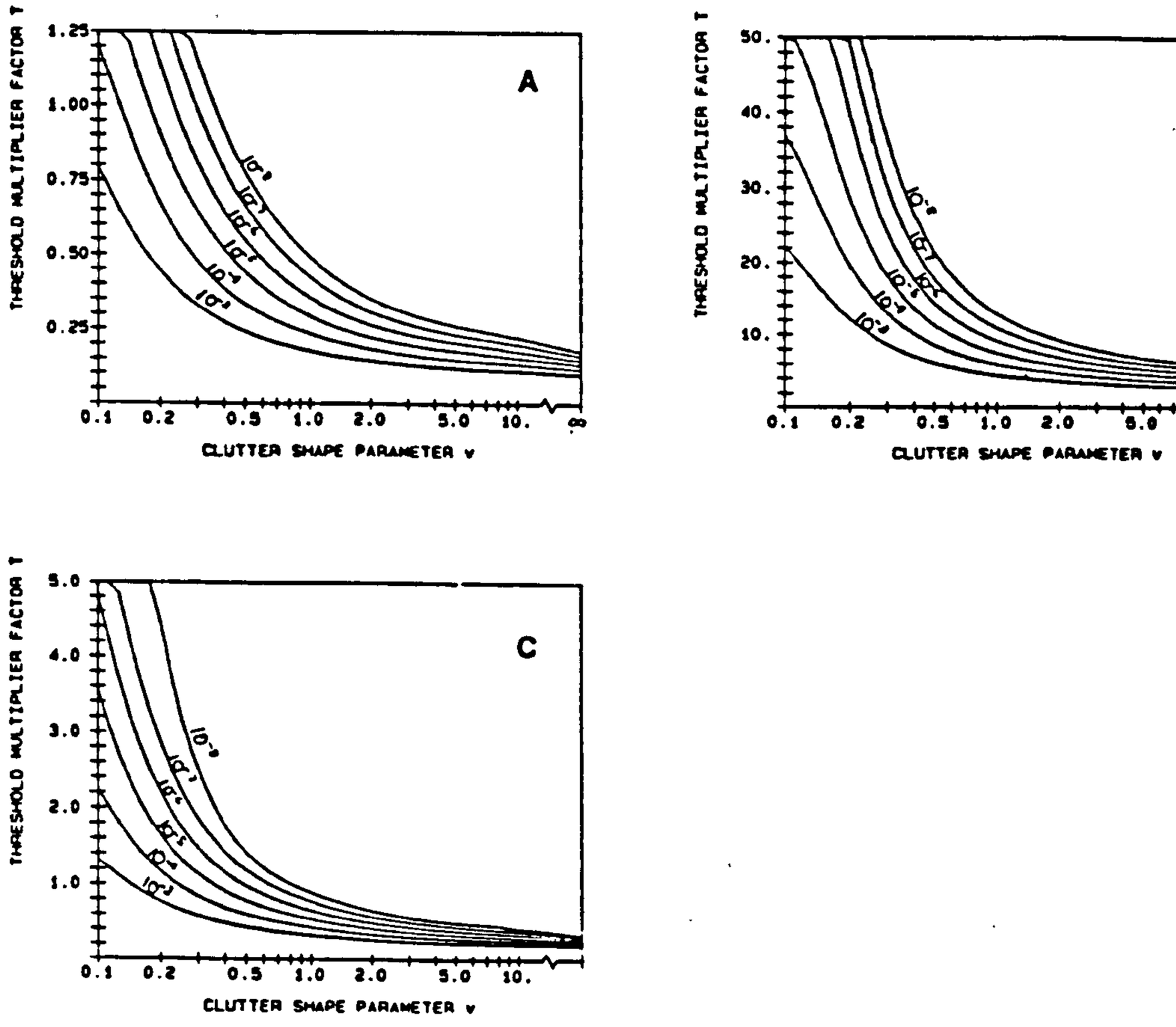

Fig. 5.4. *Contours of constant P_{fa} in the ν–T plane*
a) CA b) OS c) CAGO (N=32).

Similar plots to those illustrated in Fig. 5.4 have been generated for other values of N for the CA, CAGO and OS CFAR processors. The results have not been included here for reasons of brevity and are instead given in Appendix 5.2. Some general trends are evident from examination of all this data, namely :

1) All three types of processor are approximately equally sensitive to errors in the estimated value of ν. This is to be expected since ν has a direct effect on the PDF of the test cell, whereas it has a substantially less noticeable effect the PDF of the test statistic. Therefore, since the use of the test cell and the PDF of the signal in the test cell is identical for all three types of CFAR processor, the effect of changing ν is similar for all three CFAR processors.

2) The number of reference cells used in forming the test statistic does not significantly influence the sensitivity of the CFAR processors to errors in the estimated value of ν. This is again to be expected, with the same reasoning as for point (1) above.

3) All three CFAR processors are somewhat (±50%) more sensitive to errors in the estimated value of ν for low false alarm rates (~10^{-8}) than for higher false alarm rates (~10^{-4}), as evidenced by the closer horizontal spacing between contours in Fig. 5.4 for the higher false alarm probabilities.

4) The three types of CFAR processors are all notably more sensitive to errors in the estimated value of ν for small values of the clutter shape parameter than for large values. The effect of increasing clutter spikiness is therefore again to compound any problems which may exist in the detection processing.

Table 5.2 gives approximate values for the increased false alarm probability as a function of the true and estimated values of ν, for a nominal false alarm probability of 10^{-6} for a CA processor using 32 reference cells. For other types of processors using different N the results are not notably different. In the extreme case of a detector being designed for operation in a Rayleigh environment with the threshold determined on that basis, but having to operate in a spiky K-distributed clutter environment, the false alarm probability will vary as a function of ν. Examination of Fig. 5.4 indicates that under these circumstances, for a design P_{fa} of 10^{-6} under Rayleigh noise conditions, a false alarm probability of worse than 10^{-2} is possible in even moderately spiky ($\nu \leq 2$) clutter. This example illustrates the importance of accounting for the true clutter amplitude statistics in the design of the CFAR processor.

Table 5.2

Increased P_{fa} due to Errors in ν

(Nominal $P_{fa} = 10^{-6}$; N = 32; CA processor)

ν_{est}	ν_{true}		
	0.75 ν_{est}	0.50 ν_{est}	0.25 ν_{est}
10	$10^{-5.5}$	$10^{-5.0}$	$10^{-4.2}$
2	$10^{-5.2}$	$10^{-4.5}$	$10^{-3.3}$
0.5	$10^{-5.0}$	$10^{-4.0}$	$10^{-2.5}$

5.1.6 Errors due to Numerical Approximations

In this section the magnitude of errors introduced by two approximations mentioned in the preceding subsections of this Chapter are analysed: the simplification of the expression for the CDF of the Signal plus Clutter (eqns. (5.3) and (5.4)) is discussed first, with the influence of the required value of P_d on the loss being addressed later.

As mentioned at the beginning of section 5.1 no closed form expression has been found for the complementary CDF of the target-plus-clutter voltage given by eqn. (5.3), which has therefore been simplified to that of the complementary CDF of a Rayleigh target, of power equal to the combined target-plus-clutter power, given by eqn. (5.4). This approximation will cause an error in the value of P_d obtained for a given SCR, resulting in an error in the estimated detection loss. This error in the detection loss is the quantity that will be used here for quantifying the approximation error.

Clearly the accuracy of the approximation will improve for increasing SCR's. Therefore the approximation will be least accurate for those situations requiring the lowest SCR to achieve the desired value of P_d, for a given value of ν. From the preceding sections it is evident that this corresponds to low P_{fa} and P_d and high N, and for the range of parameters considered in this Chapter the worst approximation accuracy will therefore occur for P_d = 50%, N = 32 and $P_{fa} = 10^{-4}$. The approximation error has been calculated for these parameters over a range of values of ν. The results are as follows:

Table 5.3
Error due to Approximation for $P_t(X>tx)$

ν	Approximation error (dB)
0.5	0.00084
1.5	0.00124
2.5	0.00122
4.5	0.00107

For larger ν, the CCDF's of the clutter and target become increasingly similar causing the approximation to become increasingly accurate. For smaller ν, the increase in SCR required to achieve the specified P_d easily negates the increasing difference between the clutter and target CCDF's. It is therefore concluded that this approximation for the form of the target plus clutter CCDF introduces a worst case error of only ~0.001 dB, which can be ignored.

The effect of the required value of P_d on the detection loss has been investigated by calculating the results presented in sections 5.1.1 to 5.1.3 for $P_d = 50\%$ and $P_d = 90\%$, and calculating the difference between the two sets of results. Full results are tabulated in Appendix 5.3. Suffice to note here that in general the difference in the detection loss is substantially less than 0.1 dB and is often only 0.01 dB. Note that this is true for the detection *loss*, not the absolute SCR or SNR required to achieve a specified value of P_d, which is indeed a function of P_d.

5.2. DETECTION IN UNCORRELATED CLUTTER PLUS NOISE.

5.2.1 Numerical Analysis

In practical situations the clutter signal is added to radar thermal noise. The preceding sections have assumed that the CNR is sufficiently high to allow the presence of the noise to be neglected. However, when the CNR lies in the region -10 dB < CNR < 20 dB, the noise will reduce the effects of more spiky clutter, and the detection performance cannot be predicted with confidence merely through knowledge of the detection performance in K-clutter or thermal noise alone. As mentioned in Chapter 2 of this report, Watts (1987) gives an approximation for representing a clutter plus noise signal as a K-distribution of higher order. [specifically, $\nu_{eff} = \nu\,[(1 + 1/CNR)^2]$. In this section we perform an exact numerical analysis of detection in the clutter plus noise signal and determine the effect of additive noise on detection performance. The results are compared to Watts' approximation.

Unfortunately the PDF of K-distributed clutter plus Rayleigh noise cannot be expressed in closed form, and is instead given by:

$$p(x) = \frac{2b^{2\nu}x}{\Gamma(\nu)} \int_0^{\infty} \frac{y^{2\nu-1}}{\sigma_n^2 + 4y^2/\pi} \exp\left[\frac{-x^2}{2\sigma_n^2 + 4y^2/\pi} - (by)^2\right] dy \qquad \ldots (5.10)$$

where b is as defined for eqn. (5.3) and $2\sigma_n^2$ is the noise power. The CCDF of the K-distributed clutter plus noise is as given by eqn. (5.3), but replacing the term P_t with $2\sigma_n^2$. For $\nu < 0.5$ these becomes an improper integrals. A better form for numerical evaluation is obtained by the simple substitution $w = y^{2\nu}$, giving the PDF as:

$$p_x(x) = \frac{b^{2\nu}x}{\nu\Gamma(\nu)} \int_0^{\infty} \frac{1}{\sigma_n^2 + 4w^{1/\nu}/\pi} \exp\left[\frac{-x^2}{2\sigma_n^2 + 4w^{1/\nu}/\pi} - b^2\, w^{1/\nu}\right] dw \qquad \ldots (5.11)$$

Once the PDF of the signal in the CFAR detector reference cells has been obtained from (5.11) above, the analysis of CFAR detector performance is identical to that for K-clutter only as described in sections 5.1.1 to 5.1.3. Note that since we assume a Rayleigh fluctuating target, i.e. Swerling 1 or 2, the exact expression for the complementary CDF of the target plus clutter plus noise signal is identical to that given in eqn. (5.3), provided that the quantity P_t is modified to reflect the target to clutter-plus-noise power. The approximation described in sections 5.1 and 5.1.6 is still valid, however, and is in fact more accurate due to the clutter plus noise signal being closer to Rayleigh than the clutter alone.

Detection performance of the CA and OS CFAR detectors has been calculated for various values of P_{fa}, P_d and N, for the same sample values of ν used in the previous section, and for a range of values of CNR. Presentation of these results is difficult due to the large number of parameters which affect the results: ν, CNR, N, P_{fa}, and the type of CFAR processor all influence the absolute detection loss. One way of presenting these data is in terms of the percentage variation in detectability loss as a function of clutter-to-noise ratio, relative to the loss for noise only and clutter only of specified shape parameter ν, i.e. for noise only the relative loss is 0%, for clutter only the relative loss is 100%. Sample results are illustrated in Figs. 5.5a and 5.5b for CA processor for 32 and 16 reference cells respectively. The precise results depend on the parameters mentioned above, and the form of the curves of the type given in Fig. 5.5 thus differ for each set of parameters. However, examination of these figures and other data not reproduced here allows some general trends to be noted. The value of P_{fa} affects the percentage loss relative to clutter only by only about 10% to 15% over the range of P_{fa} from 10^{-4} to 10^{-8}, with the higher value applying at $P_{fa} = 10^{-8}$. The number of reference cells used does not significantly affect the percentage loss for the CA and CAGO detectors, whereas for the OS processor the number of reference cells does affect the percentage loss: fewer reference cells reduce the percentage loss, with a variation of 10% to 20% (depending on the CNR) between N = 32 and N = 8. This is explained by the greater sensitivity of the OS processor to the form of the lower regions of the PDF of the background signal. As would be expected, the presence of noise affects the detection performance over a wider range of CNR's for low values of ν than for high values. For $\nu = 0.1$, a CNR of -10 dB still yields a relative loss of 15% to 25% (depending on N and P_{fa}) of the clutter only loss, whereas for $\nu > 1.5$ this figure is less than 5%. Similarly, for a CNR of 20 dB, $\nu = 0.1$ suffers only 70% to 85% of the clutter only loss, whereas for $\nu > 1.5$ this figure is greater than 95%.

5.2.2 Error Analysis of Watts' Approximation

It is clear that the preceding results only enable accurate prediction of performance in clutter-plus-noise for the specific cases that are numerically evaluated; too much variation in results is evident to allow for reasonably accurate interpolation of results between parameters affecting the analysis. The method that has been proposed by Watts (1987) facilitates simpler analysis by approximating the K-clutter plus noise simply as K-distributed clutter of higher order, with $\nu_{eff} = \nu\,[(1 + 1/CNR)^2]$, where ν_{eff} is the shape parameter of the approximating K-distributed clutter. This approximation is based on determining ν from the second and fourth moments of the clutter-plus-noise voltage, but assuming that no noise is present. It gives a reasonable fit to the tails of the distribution, notwithstanding a slight lowering of the far out tails, but gives a poor fit in the region of the

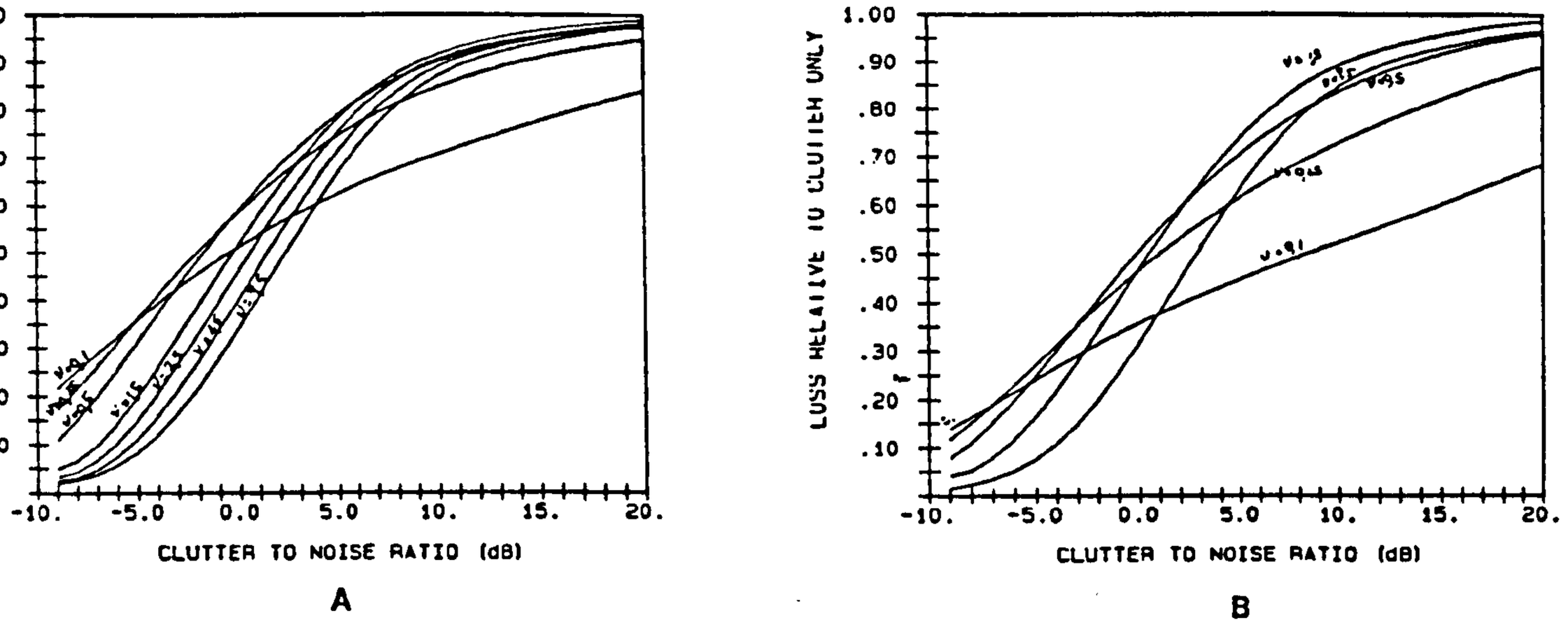

Fig. 5.5. *Relative loss vs CNR for a CA processor: a) N = 32 b) N = 16.*

peak of the PDF, ie. for low amplitudes. Both of these regions affect CFAR detection performance and hence the errors in the detection loss arising as a result of the use of this approximation have been examined.

The main quantity of interest is the signal to clutter-plus-noise ratio required to achieve a desired P_d for a specified P_{fa}. The true values have been calculated numerically using the method outlined earlier in this section. The approximate values based on Watts' approximation have been evaluated by calculating ν_{eff} as described and then determining the corresponding loss from the data represented in Figs. 5.1 to 5.3 of section 5.1. The error arising as a result of the approximation is then obtained from the difference between the two sets of results. This has been calculated for N = 8, 16, 24, 32; for $P_{fa} = 10^{-4}$, 10^{-6}, 10^{-8}; for P_d = 25%, 50%, 70%, 90%; and for the CA and OS processors. The results are tabulated in Appendix 5.4. The mean error over all of these parameters has been calculated and the results are shown in Table 5.4 for $0.25 \leq \nu < 10$ and for -6 dB $\leq$ CNR $\leq$ 21 dB. It is evident that in general the approximation is most accurate for moderate to high values of CNR (> ~3 dB), with resulting errors being of the order of only 0.1 to 1 dB, depending on the value of ν (or about 0.5 % to 5 % of the detection loss). For lower values of CNR larger errors are apparent, due primarily to the incorrect approximation of the distribution tails which determine the required threshold multiplier factor α. Nevertheless errors are still

quite small (~20 %) compared to the magnitude of the detection loss. It is therefore felt that Watts' approximation is an adequately accurate, simple means of addressing the issue of additive thermal noise when analysing detection performance in K-distributed clutter.

Table 5.4

Mean Error in Required SNR due to Watts' Approximation (dB)

CNR (dB)	ν					
	0.25	**0.5**	**1.5**	**2.5**	**4.5**	**9.5**
-6	1.59	****	****	****	****	****
-3	1.52	1.13	****	****	****	****
0	0.86	0.83	0.49	0.25	****	****
3	0.15	0.40	0.34	0.23	0.10	****
6	0.72	0.07	0.18	0.16	0.08	****
9	1.08	0.17	0.08	0.04	0.40	****
12	1.12	0.23	0.02	0.02	0.01	0.04
15	1.01	0.20	0.01	0.05	0.02	0.04
18	0.82	0.16	0.01	0.06	0.02	0.03
21	0.62	0.11	0.01	0.07	0.03	0.03

Note: **** denotes ν_{eff} out of range of analysis ($.25 \leq \nu_{eff} \leq 10$)

5.3 EMPIRICAL FORMULAE FOR ESTIMATING DETECTION LOSS

The results presented in the previous sections of this Chapter only give the detection loss for specific parameter values, and tractable analytic expressions are not available which give the detection loss as a function of the relevant variable parameters (i.e. ν, P_{fa}, P_d, CNR, N, the type of CFAR processor). In this section empirical relationships of the form

$$L = f(x_1; x_2; \ldots x_n) \qquad \ldots (5.12)$$

where L is the Loss, and x_1; x_2; $\ldots x_n$ are detector and clutter parameters, are therefore derived to facilitate simple and reasonably accurate prediction of detection loss without resorting to a full numerical analysis. Expressions are derived for the ideal fixed threshold loss L_i and the CFAR loss L_c as defined in section 5.1.4, from which the total detection loss L_t can be immediately determined. The CFAR loss is different for each of the three CFAR processors analysed and hence a separate expression has been derived for L_c each CFAR processor. Although both L_i and L_c are, strictly speaking, functions of P_d, variation of P_d in the region $30\% < P_d < 90\%$ has insignificant effect on the loss and consequently P_d

is not included as a variable parameter in the empirical expressions. Furthermore, the CNR has not been included as a parameter since it has been shown in Section 5.2.2 that this can be handled by Watts' approximation, providing that the resulting value of ν_{eff} is used in the expressions derived here instead of ν. The ideal fixed threshold loss L_i is therefore a function of P_{fa} and ν, while the CFAR loss L_c for each type of CFAR processor is a function of P_{fa}, ν and N. The accuracy of the empirical relationships is analysed to illustrate their applicability.

5.3.1 Approximation for L_i

The following expression has been found to approximate the ideal fixed threshold detection loss L_i:

$$\ln(L_i) = a_1\omega^3 + a_2\omega^2 + a_3\omega + a_4 \qquad ...(5.13)$$

where $\omega = \ln(\nu)$

$$a_4 = 1.5047\,[-\log(P_{fa}) - 2.39]^{0.1711}$$

$$a_3 = 0.0874\,\ln\,[-\log(P_{fa}) - 0.33] - 0.5850$$

$$a_2 = 0.0169\,\ln\,[-\log(P_{fa}) + 1.0\,] - 0.0850$$

$$a_1 = 0.0018\,\ln\,[-\log(P_{fa}) + 3.0\,] - 0.0010$$

This expression is valid for $0.1 \le \nu \le 10$ and $10^{-4} \le P_{fa} \le 10^{-8}$. The error arising due to the use of this approximation has been evaluated for sample values of ν and P_{fa} and the results are given in Table 5.5 below. Since the expression was derived as a least squares fit to the natural log of the loss, the error is roughly proportional to the magnitude of the loss, thereby maintaining approximately constant relative error over all ν.

Table 5.5
Approximation Error for L_i
(Absolute error in dB)

	$\nu = 0.1$	$\nu = 0.25$	$\nu = 0.5$	$\nu = 1.5$	$\nu = 2.5$	$\nu = 4.5$	$\nu = 9.5$
$P_{fa} = 10^{-4}$	0.745	0.115	0.010	0.003	-0.012	-0.038	-0.072
$P_{fa} = 10^{-6}$	0.998	0.164	0.015	0.002	-0.020	-0.059	-0.122
$P_{fa} = 10^{-8}$	1.149	0.200	0.024	-0.015	-0.020	-0.078	-0.173

A higher order polynomial in ln(ν) would reduce the error further at the expense greater complexity. This was not considered necessary since in most practical situations errors in the assumed value of ν will introduce larger errors than those due to the approximation.

5.3.2 Approximation for L_c

The following expression has been found to approximate the CFAR detection loss L_c:

$$\ln(L_c) = -(p + 0.5)\,[b_1\omega^4 + b_2\omega^3 + b_3\omega^2 + b_4\omega + b_5]\,\exp[c_1.\ln(N) - c_2] \qquad ...(5.14)$$

where $\omega = \ln(\nu)$

$p = \log(P_{fa})$

and the coefficients b_1, b_2, b_3, b_4, b_5, c_1 and c_2 are given for the three CFAR processors in Table 5.6 below.

Table 5.6
Coefficients for Expression for L_c

	b_1	b_2	b_3	b_4	b_5	c_1	c_2
CA	0.006763	-0.005184	0.172136	-0.419457	0.353335	-1.03831	1.9005
CAGO	-0.001957	-0.010293	0.126950	-0.403245	0.519645	-0.99116	1.7380
OS	0.001526	-0.020672	0.176920	-0.429784	0.715318	-1.03080	1.8697

This expression and the coefficients given above are valid for $0.1 \le \nu \le 10$; $8 \le N \le 32$; and $10^{-4} \le P_{fa} \le 10^{-8}$. The error arising due to the use of this approximation has been evaluated for sample values of N, ν and P_{fa} and the full results are given in Appendix 5.5. The full results have been averaged over P_{fa} and N (for $N \ge 16$) for each of the three CFAR processors and these summarised results are shown in Table 5.7 below. Since the expression was derived as a least squares fit to the natural log of the loss, the error is roughly proportional to the magnitude of the loss, thereby maintaining approximately constant relative error over all ν.

Table 5.7

Approximation Error for L_c

(Absolute error in dB)

	$\nu = 0.1$	$\nu = 0.25$	$\nu = 0.5$	$\nu = 1.5$	$\nu = 2.5$	$\nu = 4.5$	$\nu = 9.5$
CA	1.553	0.179	0.021	0.026	0.037	0.044	0.030
CAGO	1.238	0.099	0.078	0.074	0.060	0.049	0.059
OS	1.559	0.324	0.025	0.053	0.057	0.056	0.030

It can be seen that in general the error is less than 0.1 dB, except for very small ν where the error relative to the CFAR loss is still small, ~ 5%. Higher order polynomials in $\ln(\nu)$ and $\ln(N)$ would reduce the error further at the expense greater complexity. This was again not considered necessary since in most practical situations errors in the assumed value of ν will introduce far larger errors than those due to the approximation above.

5.4 DISCUSSION OF RESULTS

The performance of the CA, CAGO and OS CFAR processors has been analysed under conditions of no correlation of the underlying clutter modulation between adjacent range bins. It has been shown that a rather large (~10 dB) detectability loss occurs in spiky clutter. The magnitude of this loss is dependent on ν (the lower the value of ν, the higher the loss), the number of reference cells used by the CFAR processor, and the desired false alarm probability. Detection probability does not have a noticeable effect on the loss.

The loss associated with CFAR thresholding has been evaluated. It has been shown that the CFAR loss increases with increasing clutter spikiness, and can be in excess of 10 dB for very spiky clutter. It is also evident that the OS processor suffers the worst increase in CFAR loss due to spiky clutter, which can be several dBs higher than for the CA processor. For all CFAR processors considered in this report it is apparent that reducing the number of reference cells compounds the increase in loss caused by spiky clutter. Empirical formulae have been derived which give the loss for ideal fixed threshold detection and the loss associated with CFAR thresholding in K-distributed clutter environments. These formulae have ν, N and P_{fa} as parameters. It has been shown that in general the error associated with these empirical relationships is better than 0.1 dB.

The variation in false alarm probability due to errors in estimating ν has been analysed. It has been shown that all three CFAR processors are roughly equally sensitive to errors in

the estimated value of ν, and that the number of reference cells does not have a strong influence on the sensitivity to errors in ν. The lower the required false alarm probability and the lower the value of ν, the more sensitive the CFAR processors become to errors in ν. Operation in K-Distributed clutter with $\nu \sim 0.5$ but with the CFAR threshold set for a Rayleigh environment can result in a 1000 to 10000 fold increase in false alarm probability.

The effects of additive thermal noise on detection performance have been investigated and errors introduced by Watts' approximation have been determined. It is concluded that this approximation provides an adequately accurate, simple means of including the effects of thermal noise in detection performance analyses.

With regard to the selection of the most suitable type of CFAR processor it has been shown that the OS processor is the most susceptible of the three processors analysed here to the effects of spiky clutter: the loss increases more rapidly with increasing clutter spikiness (decreasing ν) and decreasing N. It is realised, however, that the ultimate choice of the type of CFAR processor to be used will depend on other factors as well, such as the susceptibility to clutter edges and extraneous targets, for which the superior performance of the OS processor is well known (Rohling, 1983; Ghandi, 1987).

One possible solution to the contradictory requirements of minimising CFAR loss in spiky clutter while maintaining tolerance to interfering targets and clutter edges could be offered by the CMLD processor mentioned in Chapter 2: this processor has been shown (Ritcey, 1986) to provide the same performance in exponential clutter (ie. $\nu = 0.5$) as a CA processor using the same number of reference cells as are summed in the CMLD processor. For other $\nu \neq 0.5$ analytic or numerical analysis has not been attempted since the mathematical manipulations used by Ritcey are not valid and the ordering of the reference cells prior to summation in the CMLD processor means that the cells being summed are no longer statistically independent, thereby precluding the determination of the PDF of the test statistic by the usual means. However, it is not unreasonable to argue that if the performance is the same for the fairly spiky case of $\nu = 0.5$ then it will not be significantly different for other values of ν. The CFAR loss and quantisation loss in general spiky clutter can then be assumed to be about the same as that for a CA processor using the same number of reference cells as are summed in the CMLD processor. This would minimise CFAR loss while maintaining resilience to extraneous targets and clutter edges.

It is clear from the work presented in this Chapter that two main problem areas exist with regard to detection in non-Rayleigh clutter, and specifically K-Distributed clutter. These are 1) how to maintain a constant false alarm probability, and 2) how to minimise the detection

loss due to spiky clutter. The former of these problems has hitherto been addressed by non-parametric techniques as discussed in Chapter 2 (if a reasonably large number of pulses is available), or by the use of CFAR processors which effectively estimate the shape and scale parameters of the clutter, such as Ravid and Levanon's Maximum Likelihood OS processor (Ravid, 1992). Both of these options are susceptible not only to the severe ideal detection losses quoted earlier in this chapter, but also to significantly increased CFAR loss, of the order of 5 - 10 dB. This implies an overall loss relative to ideal detection in Rayleigh clutter of in excess of 20 dB in spiky clutter. The minimisation of detection loss in spiky clutter has been addressed to some extent by using post detection binary integration, which only gives significant benefits if the modulation process can be decorrelated from pulse to pulse. This is generally improbable .

If we aim to maintain the desired P_{fa} in spiky clutter and simultaneously keep the detection loss to approximately the level suffered in thermal noise, then additional information must be used in the detection procedure. The only sources of additional information are the various correlation domains of the clutter and target signals. The correlation properties of relevance here are the range correlation and short- and medium-term temporal correlation properties. Other temporal and spatial correlation properties are not useful since we preclude the possibilities of scan-scan averaging and clutter mapping, as mentioned in Chapter 1. The exploitation of these correlation domains in order to improve detection performance is the subject of the following chapters of this thesis.

CHAPTER 6

CFAR DETECTION IN SPATIALLY CORRELATED K-DISTRIBUTED CLUTTER

6.1 INTRODUCTION

It has been shown in the previous chapter that severe detection losses can arise in spatially uncorrelated spiky clutter. This loss consists of two components, namely 1) the "ideal detection loss", defined as the detection loss in non-Rayleigh clutter relative to detection in Rayleigh clutter, assuming exact knowledge of the mean clutter power, and 2) the CFAR loss, defined as the additional loss due to CFAR thresholding. The scope for reducing the overall detection loss with range-acting amplitude-thresholding CFAR processors is, of course, limited by the ideal detection loss: improved processing cannot hope to improve on ideal detection. This lower bound on detection loss is only valid, however, if the clutter is spatially uncorrelated. Spatial correlation will affect the performance of the CA, CAGO and OS processors, but more importantly, it offers scope for improved CFAR processors aimed specifically at exploiting spatial correlation with a view to improving detection performance in spiky clutter.

Recall that the K-distribution arises from the assumption that the clutter consists of Rayleigh speckle, the variance of which is modulated by a gamma distributed modulation process. In analysing the detection performance of range-acting CFAR processors, the variation of the clutter signal over range, instead of over time, is of importance. Hence the gamma distributed modulation process is considered as fluctuating with range, and in some practical situations the underlying clutter modulation will not be completely uncorrelated from one range bin to the next as has been assumed in the preceding chapter. (The speckle is always completely decorrelated from range bin to range bin). The clutter modulation process can be related to the surface profile of the sea and has been mechanistically explained in terms of bunching of contributing scatterers and local tilting of the mean surface slope (see Chapter 2). If there is indeed close correlation between the sea surface profile and the modulation process - and experimental evidence suggests there is (eg. Long, 1981) - then it is reasonable to assume that the clutter modulation process will have a decorrelation distance of the same order of magnitude as the decorrelation distance of the sea. In well developed swell conditions a periodic component of period equal to the swell length projected along the radar boresight should be present in the range autocorrelation

function, and experimental evidence in the literature tends to support this supposition. Under extreme conditions of a long decorrelation distance of the modulation process and a short reference window of the CFAR detector (in terms of physical distance), the clutter modulation process may be essentially completely correlated over the reference cells covered by the CFAR processor. In more realistic conditions, the modulation process will exhibit partial correlation between range bins in the reference window.

Both of these situations will affect the detection performance of the CFAR processors. If the degree of correlation is known, then the threshold multiplier factor can be altered to better reflect the local clutter statistics in the reference window, resulting in reduced detection loss. The simple if unrealistic situation of the clutter modulation process being completely correlated over the CFAR reference window is addressed first, in section 6.2. The more general situation of a partially correlated modulation process is addressed next. This requires extension of the K-distribution model to cover partially correlated modulation processes, and this is addressed in section 6.3. An "Ideal CFAR detector" for partially correlated clutter is defined and evaluated in section 6.4 to establish an upper bound on detection performance in spatially correlated K-distributed clutter. The development and evaluation of a practical CFAR processor designed to exploit spatial correlation is presented in section 6.4. The analyses for both complete and partial spatial correlation assume that there is negligible thermal noise and that the clutter shape parameter ν is correctly known.

6.2 COMPLETELY CORRELATED CLUTTER MODULATION

If the clutter modulation process is assumed to be completely correlated over the range extent of the CFAR reference window, then the clutter within the CFAR reference window at a given position is Rayleigh distributed. The clutter is still assumed to be K-distributed, however, through the mean power of the locally Rayleigh clutter being modulated by a gamma distributed variable over an extended area. Since the clutter in the reference window is now Rayleigh distributed, the CFAR detectors will perform as expected for Rayleigh noise, except that an additional source of fluctuation in the signal-to-clutter ratio is introduced by the modulation of the clutter power.

Mathematically we represent this as follows: for a given CFAR detector and specified false alarm rate the detection probability in clutter with a Rayleigh voltage PDF is denoted by $P_d(S|C)$, a function of the instantaneous signal-to-clutter power ratio S conditioned on the clutter power C. The probability $p_c(C)$ of the clutter power taking on a value C is gamma distributed with shape parameter ν, ie.

$$p(C) = \frac{1}{\lambda\Gamma(\nu)} C^{\nu-1} \exp(-C/\lambda) \qquad \ldots (6.1)$$

where λ is a power parameter. The overall probability of detection is given by:

$$\overline{P}_d = \int_0^{\infty} P_d(S|C)\, p_c(C)\, dC \qquad \ldots (6.2)$$

The average detection probability $\overline{P_d}$ is therefore dependent on the form of $P_d(S|C)$, which is in theory dependent on the type of CFAR detector and the number of reference cells used. In practice, however, for conditions of Rayleigh noise the form of $P_d(S|C)$ is so similar for all situations considered here that the resulting curves are indistinguishable from each other, notwithstanding a shift between curves dependent on the different CFAR loss for different processors, numbers of reference cells and false alarm probabilities. It turns out in fact that the form of $P_d(S|C)$ is well approximated by the expression for ideal detection of Sw2 targets in Rayleigh noise, i.e.

$$P_d(S|C) = \exp\left[\frac{-\ln(P_{fa})}{1+(S|C)}\right] \qquad \ldots (6.3)$$

provided the appropriate CFAR loss is included in the value of S. It can then be shown that substitution of this expression into eqn. (6.2) with a little manipulation yields the following expression for P_d:

$$\overline{P}_d = \frac{(b^2 S_0)^{\nu}}{\Gamma(\nu)} \int_0^{\infty} \frac{1}{x^{\nu+1}} \exp\left[\frac{-b^2 S_0}{x} - \frac{\ln(P_{fa})}{1+x}\right] dx \qquad \ldots (6.4)$$

where S_0 is the mean signal-to-clutter ratio. This expression has been evaluated over a range of values of ν and the results are illustrated in Fig. 6.1. These curves represent the difference in SCR required for a given probability of detection between range correlated K-clutter of shape parameter ν and Rayleigh noise, under the assumed conditions of complete correlation of the clutter modulation function. The absolute SCR required is obtained by adding this loss (gain) to the CFAR loss of the detector in question for Rayleigh noise (obtained from Figs. 5.1 to 5.3 of Chapter 5), which is added to the value of SNR required for ideal detection, given by (6.2) above. It is evident from Fig. 6.1 that under conditions of complete correlation of the modulation process, for a given CFAR processor implementation and parameters, a significant detection gain can result from spiky clutter, relative to detection in Rayleigh clutter. This is particularly notable for moderate to low values of P_d. It must be stressed, however, that the assumption of complete correlation of the modulation process over the CFAR processor's reference window is somewhat unrealistic.

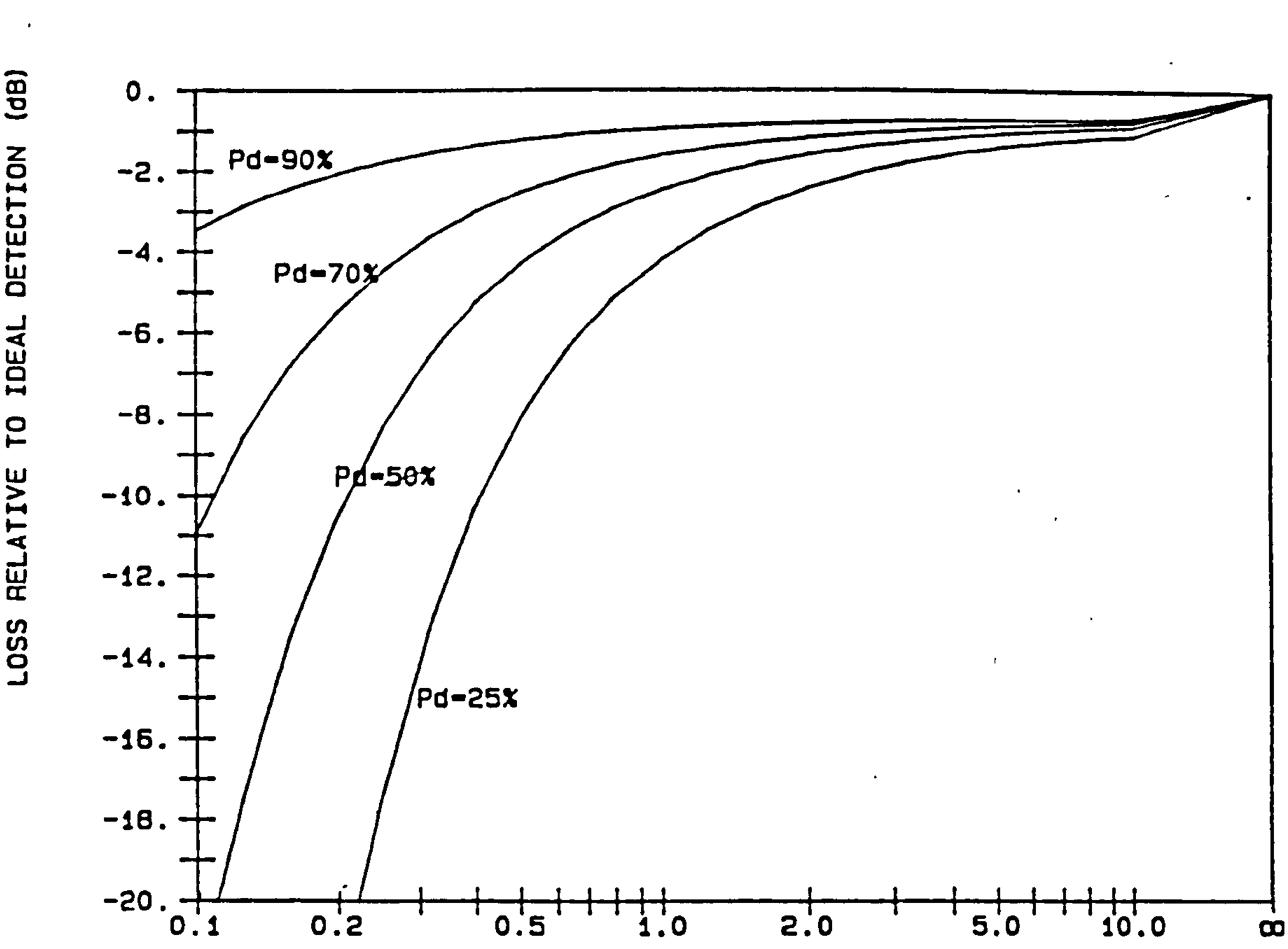

Fig 6.1: *Detection Loss for Completely Correlated Clutter*

6.3 A MODEL FOR SPATIALLY CORRELATED K-DISTRIBUTED CLUTTER

Before the performance of existing and improved CFAR processors can be evaluated in spatially correlated clutter, it is necessary to derive a mathematical representation of the partially correlated modulation process. Oliver and Tough (1984) have described a method of generating spatially correlated clutter based on linear filtering of an uncorrelated gamma process. This yields the correct modulation process ACF, but the resulting clutter is not exactly K-distributed and consequently has incorrect higher order moments, which may be of particular significance for false alarm rate analyses for low values of Pfa. Convenient mathematical representations of the correlated modulation and clutter processes are also not available using this technique. In this section a procedure is presented which yields precisely K-distributed samples of arbitrary spatial ACF, and which provides in addition the analytic description of the multivariate PDFs of the modulation process and potentially the K-clutter.

In this section we concentrate on a description of the correlated modulation process, which provides the basis for detection performance analyses and from which spatially correlated clutter can be generated. The correlation properties of the speckle are not considered here since a) the speckle is invariably modelled as being independent in adjacent range bins, and b) the rapid temporal (Doppler) fluctuations of the speckle are easily modelled owing to its complex Gaussian nature. It is also usually assumed that the modulation process exhibits negligible temporal fluctuations within the radar coherent processing interval or dwell. We therefore limit development of the theory to the 1-dimensional (range) modulation process; extension to the 2-dimensional case is straightforward using identical techniques provided a 2-D filter is used on the constituent Gaussian processes.

Recall that we define the K-distributed clutter x, the voltage modulation process v, the power modulation process u, and the Rayleigh speckle r, such that $x = rv = r\sqrt{u}$. Since u is gamma distributed, for $\nu = (m+1)/2$; $m = 0, 1, 2...$, it reduces to the chi-square distribution. This can be generated as the sum of the squares of $n = 2\nu$ independent zero mean Gaussian (ZMG) processes g_i. Correlation of the modulation process can then be introduced on the constituent Gaussian processes by well established linear filtering techniques. A non-linear transformation, defined later in this section, is used to transform a modulation process of order parameter $\nu' = m + 1/2$ into one of arbitrary $\nu > 0$. This technique for modelling correlated K-clutter is illustrated in Fig. 6.2.

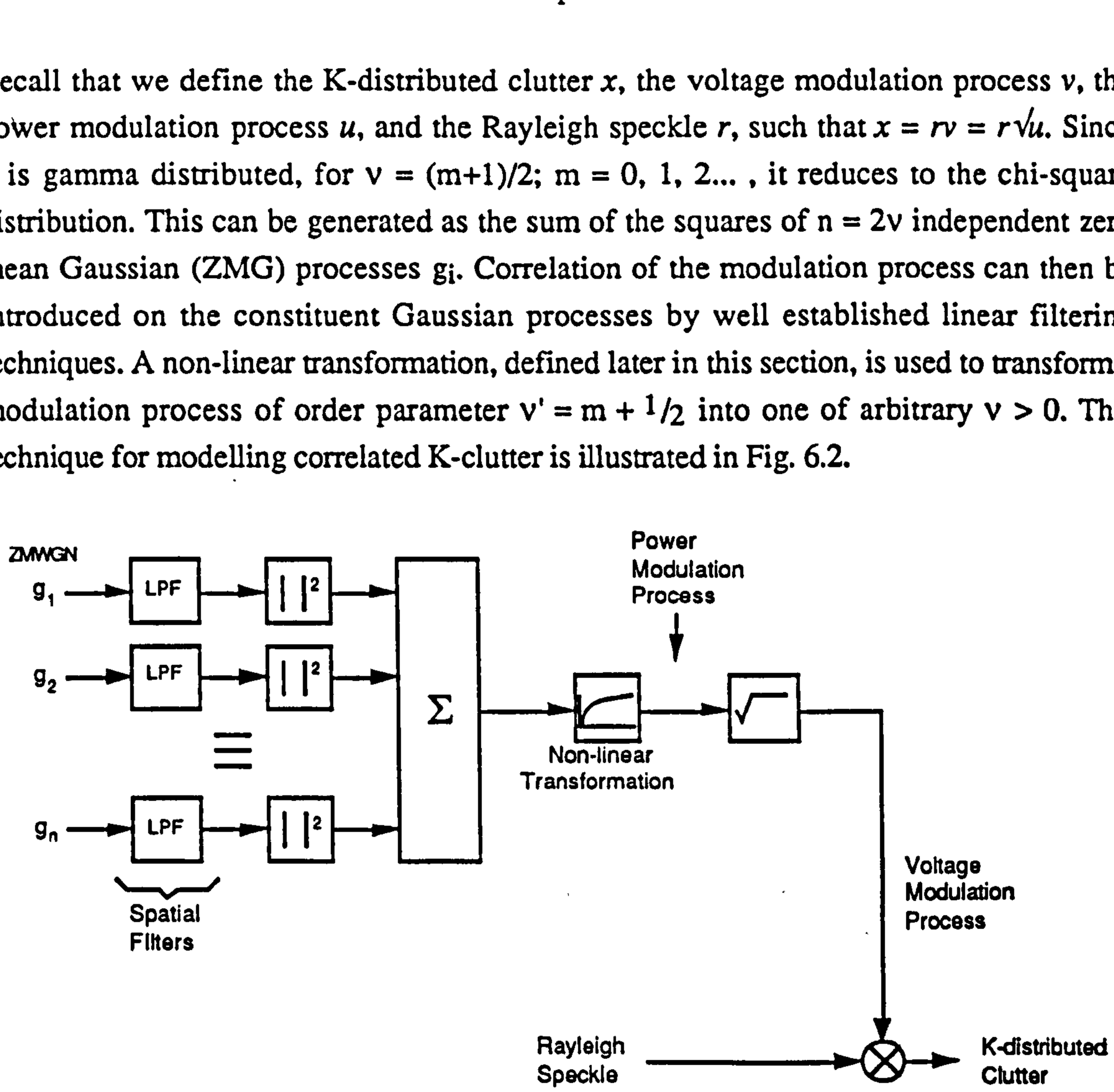

Fig. 6.2: *Method of simulating spatially correlated clutter*

6.3.1 Bivariate pdf of the modulation process

Consider a sample of n independent unit variance ZMG vectors $G_i = \{g_{i1}, g_{i2}\}$ with $E(g_{i1}.g_{i2}) = \rho^2$. Then define the random variables:

$$u_j = \sum_{i=1}^{n} g_{ij}^2 \qquad (j = 1, 2) \qquad \ldots (6.5)$$

each of which is $\chi^2(n)$, ie. chi-squared with n degrees of freedom. Then, given all the g_{i2}, the g_{i1} can be represented as $g_{i1} = \rho g_{i1}^2 + z_i.\sqrt{(1-\rho^2)}$, where the z_i are iid. N(0,1) random variables. Substituting this into eqn. (6.5) we find that the conditional PDF of u_1, given u_2, has a non-central chi-square distribution with variance parameter $\sigma^2 = (1-\rho^2)$ and non-central parameter

$$\lambda = \sum_{i=1}^{n} \rho^2 g_{i2}^2 = \rho^2 u_2 \qquad \ldots (6.6)$$

which gives $p(u_1|u_2)$ as:

$$p(u_1|u_2) = \frac{1}{2(1-\rho^2)} \left(\frac{u_1}{\rho^2 u_2}\right)^{\frac{n-2}{4}} \exp\left[-\left(\frac{u_1+\rho^2 u_2}{2(1-\rho^2)}\right)\right] . I_{\frac{n}{2}-1}\left(\frac{\rho\sqrt{u_1 u_2}}{1-\rho^2}\right) \qquad \ldots (6.7)$$

The bivariate gamma PDF of the modulation process is then obtained as:

$$p_{u_1 u_2}(u_1;u_2) = p_{u_1|u_2}(u_1|u_2) p_{u_2}(u_2)$$

$$= \frac{1}{2^{\nu+1}\rho^{\nu-1}(1-\rho^2)\Gamma(\nu)} (u_1 u_2)^{\frac{\nu-1}{2}} \exp\left[-\left(\frac{u_1+u_2}{2(1-\rho^2)}\right)\right] . I_{\nu-1}\left(\frac{\rho\sqrt{u_1 u_2}}{1-\rho^2}\right) \qquad \ldots (6.8)$$

where $p_{u2}(u_2)$ is $\chi^2(n)$ distributed, and $\nu = n/2$ is the usual K-distribution shape parameter. It is not difficult to verify that the marginal PDFs of u_1 and u_2 are in fact the correct univariate gamma distributions, ie. gamma distributions with shape parameter ν and scale parameter 2. The expected value is therefore 2ν, and generation of clutter with mean power P_c therefore requires multiplication of either the unit-mean exponential speckle, the modulation process , or the compound clutter, by a factor $P_c/2\nu$.

The bivariate chi- distribution of the voltage modulation process is obtained by setting $v_1 = +\sqrt{u_1}$ and $v_2 = +\sqrt{u_2}$, from which:

$$p_{v_1;v_2}(v_1,v_2) = \frac{1}{2^{\nu-1}\rho^{\nu-1}(1-\rho^2)\Gamma(\nu)}(v_1v_2)^{\nu}\exp[-(\frac{v_1^2+v_2^2}{2(1-\rho^2)})].I_{\nu-1}(\frac{\rho v_1 v_2}{1-\rho^2}) \quad \ldots (6.9)$$

It is worth noting that the effects of pre-detection integration are easily incorporated into the above model merely through modifying the square law speckle PDF to be gamma distributed with shape parameter $\kappa = N_i$, the number of pulses non-coherently integrated. This is possible due to the assumption that the modulation process remains constant in each range-angle bin during the radar dwell period.

6.3.2 ACF of the modulation process

The correlation between u_1 and u_2 and between v_1 and v_2 is obtained from $E(u_1.u_2)$ and $E(v_1.v_2) = E[\sqrt{(u_1.u_2)}]$ respectively, where E(.) denotes expectation, such that:

$$E[(u_1u_2)^m] = \int_0^{\infty}\int_0^{\infty}(u_1u_2)^m p_{u_1;u_2}(u_1,u_2)\,du_1du_2 \quad \ldots (6.10)$$

where $m = 1/2$ for the voltage modulation process and $m = 1$ for the power modulation process. Substituting eqn. (6.8) into eqn. (6.10), with some manipulation gives:

$$E[(u_1u_2)^m] = \frac{2^{2m}(1-\rho^2)^{\nu+2m}}{\Gamma(\nu)}\sum_{i=0}^{\infty}\rho^{2i}\frac{[\Gamma(\nu+i+m)]^2}{\Gamma(i+1)\Gamma(\nu+i)} \quad ; \quad 0<\rho<1 \quad \ldots (6.11)$$

This gives the correlation coefficient between two samples of the modulation process in terms of the correlation coefficient ρ between corresponding samples of the constituent Gaussian process. The extreme values of $\rho = 0;1$ are easily calculated from the marginal PDFs of the modulation process; for $\rho = 0$ we have $E(u_1.u_2) = [E(u)]^2 = 4\nu^2$ and $E(v_1.v_2) = [E(v)]^2 = 2[\Gamma(\nu + 1/2)/T(\nu)]^2$; for $\rho = 1$ we have $E(u_1.u_2) = [E(u^2)] = 4\nu(\nu + 1)$ and $E(v_1.v_2) = [E(u)] = 2\nu$.

If we vary ρ as a function of of the lag $k = |i - j|$ between the samples g_{i1} and g_{i2} (and hence between u_1 and u_2), then eqn. (6.11) can be used to describe the ACF of u in terms of that of the g_i. The reverse operation requires inversion of eqn. (6.11) which in general does not appear to be analytically possible but can be numerically performed if necessary. Setting $m = 1$, eqn. (6.11) can be manipulated to give a simplified (and easily invertable) expression for the ACF of the power modulation process u as:

$$R_{uu}(k) = 4\nu[(R_{gg}(k))^2 + \nu] \quad \ldots (6.12)$$

where $R_{gg}(k)$ is the ACF of the g_i. For $m = 1/2$ (ie. for the ACF of the voltage modulation process v) a simplification $R_{vv}(k)$ is only possible for $\nu = 1/2$, for which:

$$R_{vv}(k) = (2/\pi)[\cos\phi + \phi\sin\phi] \qquad \ldots (6.13)$$

where $\phi = \arcsin[R_{gg}(k)]$.

6.3.3 Transformation for arbitrary ν

Just as the univariate gamma distribution is a generalisation of the chi-squared distribution, so too can the preceding derivations be generalised by letting ν take on arbitrary positive values $\nu \neq (m+1)/2$. It has been shown (Griffiths, 1970) that eqn. (6.8) is infinitely divisible, and is therefore valid for arbitrary real $\nu>0$. Practically, however, simulation of the modulation process requires further consideration since it is impossible to have a non-integer number of constituent Gaussian processes, which for the reasoning outlined in section 6.3.1 would be necessary for $\nu \neq (m+1)/2$. Therefore a memoryless non-linear transformation is required to transform a $\chi^2(n)$ process u into a gamma distributed process u" of shape parameter ν, ie. u" is $\Gamma(\theta,\nu)$, where θ is any desired scale parameter. This is achieved as follows: it is known from probability theory that if $u' = f_1(u)$, where $f_1(.)$ is given by the CDF of u, then u' is uniformly distributed over the interval (0,1), ie. UNIF(0,1); Similarly, $u' = f_2(u'')$ is UNIF(0,1) if $f_2(.)$ is the CDF of u". We therefore have $f_2(u'') = f_1(u)$, ie.:

$$\frac{1}{\Gamma(\nu)}\gamma(\nu;\frac{u''}{\theta}) = \frac{1}{\Gamma(\frac{n}{2})}\gamma(\frac{n}{2};\frac{u}{2}) \qquad \ldots (6.14)$$

where $\gamma(.;.)$ is the incomplete gamma function (as defined by Gradshteyn, 1980) and θ is the scale parameter of the transformed gamma distribution, which can be selected to give the required mean value of the modulation process. Eqn. (6.14) must be solved for u" in terms of u to give the required transformation $u'' = f_2^{-1}[f_1(u)]$, for which no analytic solution has been found. Choosing n = 2 for convenience, so that the CDF $P_u(u) = 1 - e^{-u/2} = f_1(u)$, we obtain

$$u = -2\ln[\,1 - \frac{1}{\Gamma(\nu)}\gamma(\nu;\frac{u''}{\theta})] \qquad \ldots (6.15)$$

which is easily numerically inverted to give the required transformation, yielding a correlated gamma process of arbitrary positive real ν. Although analytic proof will not be provided, it has been found using numerical techniques that eqns. (6.8) and (6.11) are still valid for this generalisation. A similar transformation can be derived for the voltage modulation process.

6.3.4 Some properties of the correlated K-clutter model

Although most of the following properties will not be used in this thesis, they are included here for completeness:

a) Characteristic function of the power modulation process:

From Griffiths (1970), the characteristic function of the power modulation process u is:

$$\Phi_u(t_1,t_2,\ldots,t_p) = |\, \mathbf{I} - i\mathbf{PT} \,|^{-n/2} \qquad \ldots (6.16)$$

where p is the order of the multivariate process, **I** is the identity matrix, **P** is the correlation matrix of the constituent Gaussian processes, and **T** is a diagonal matrix with elements $(t_1,t_2,\ldots,t_m)$.

b) Trivariate PDF of the modulation process

Some manipulation of a result by Jensen (1970) gives the trivariate PDF of a process with characteristic function defined by eqn. (6.16) as:

$$p_u(u_1,u_2,u_3) = \Psi(u_1,\nu)\,\Psi(u_2,\nu)\,\Psi(u_2,\nu) \sum_{k=0}^{\infty} b_k \sum_{[k]} B(k)\; L_{h_1}(u_1,\nu)\, L_{h_2}(u_2,\nu)\, L_{h_3}(u_3,\nu) \qquad \ldots (6.17)$$

where $\Psi(u,\nu) = \dfrac{1}{\Gamma(\nu)}\, u^{\nu-1}\, e^{-u}$ are the marginal gamma PDFs

$$B(k) = \frac{[\Gamma(\nu)]^3\, h_1!\, h_2!\, h_3!}{\Gamma(\nu+h_1)\,\Gamma(\nu+h_2)\,\Gamma(\nu+h_3)} \frac{k!}{k_1!\, k_2!\, k_3!\, k_4!}\, 2^{k_4}\, \rho_{12}^{2k_1+k_4}\, \rho_{13}^{2k_2+k_4}\, \rho_{23}^{2k_3+k_4}$$

$$b_k = \frac{\Gamma(\nu+k)}{k!\,\Gamma(\nu)}$$

$L_h(u,\nu) = (-1)^h\; L_h^{\nu-1}(u)$; where $L_h^{\nu-1}(u)$ is the usual Laguerre polynomial

$h_1 = k - k_3$; $\quad h_2 = k - k_2$; $\quad h_3 = k - k_1$

$\rho_{12} \equiv E(g_{i1}\, g_{i2})$ $\quad \rho_{13} \equiv E(g_{i1}\, g_{i3})$ $\quad \rho_{23} \equiv E(g_{i2}\, g_{i3})$

and the summation over [k] indicates the summation over all combinations of k_1, k_2, k_3 and k_4, such that $k_1+k_2+k_3+k_4 = k$. Note that in the above the u_i have been defined as:

$$u_i = \frac{1}{2} \sum_{j=1}^{N} g_{ij}^2$$

which conforms to the model for the correlated gamma modulation process provided the scale factor 1/2 is taken into account.

c) Markov property

It has been shown (Griffiths, 1970) that if the constituent Gaussian processes g_i are Markov processes , then so too is the gamma modulation a Markov process of the same order. This property enables relatively simple expressions for the p^{th} order multivariate PDFs to be obtained for modulation processes with exponential ACFs (first order Markov process), ie. $p(u_1 \ldots u_n) = p(u_1|u_2)p(u_2|u_3)\ldots p(u_{n-1}|u_n)p(u_n)$.

d) Bivariate K-distribution

Compounding the bivariate voltage modulation process (with pdf given by eqn. 6.9) with the Rayleigh speckle gives the bivariate K-distribution, which can be shown to be:

$$p(x_1,x_2) = \frac{(x_1x_2)^{(2-\nu)/2}}{2^{\nu-3/2}\,\mu^{\nu+3/2}\sqrt{1-\rho^2}\,\Gamma(\nu)} \sum_{i=0}^{\infty} \left(\frac{\rho^2}{2(1-\rho^2)\mu\, x_1x_2}\right)^i$$

$$\times \frac{1}{i!\,\Gamma(\nu+i)} K_{i+\nu-1/2}\left(\frac{2x_1}{\sqrt{2\mu(1-\rho^2)}}\right) K_{i+\nu-1/2}\left(\frac{2x_2}{\sqrt{2\mu(1-\rho^2)}}\right) \quad \ldots (6.18)$$

where μ is the scale parameter of the compounded speckle such that the overall clutter power is $P_c = 2\nu\mu$.

e) ACF of compound K-distributed clutter

We seek $E[(y_iy_j)^m]$, where y is the square law detected compound clutter and m=1 for the ACF of the power process (which will be termed K^2-distributed) and $m=\frac{1}{2}$ for the K-distributed voltage process. Since y=us, and u and s are independent and s_i and s_j are independent, we have $E[(y_iy_j)^m] = E[(u_is_iu_js_j)^m] = E[(u_iu_j)^m]\,E[(s_is_j)^m]$. Therefore:

$$E[(y_iy_j)^m] = E[(s)^m]^2\,E[(u_iu_j)^m] \qquad \text{for } i \neq j \qquad \ldots (6.19)$$

where $E[(s)^m]$ is merely the the mean value of the speckle[1] and $E[(u_iu_j)^m]$ is the correlation between samples of the modulation process given by eqn (6.10). [Note that for i=j in the above $E[(y_iy_i)^m]$ merely becomes the $2m^{th}$ moment about 0 of the compound clutter. For m=1, $E[(y)^{2m}] = 4\mu^2\nu(\nu+1)$; for $m=\frac{1}{2}$, $E[(y)^{2m}] = E[y] = 2\mu\nu$.]

6.4 IDEAL CFAR DETECTION IN SPATIALLY CORRELATED CLUTTER

In order to establish the potential benefits to be gained by exploiting spatial correlation properties of the clutter, we first determine the limitations imposed by the clutter model itself, excluding detection losses caused by processor implementation and real time

[1] Specifically $E(s) = \mu$ and $E[(s)^{1/2}] = \sqrt{(2\mu)}$

adaptation requirements. Ideal detection performance in K-clutter has hitherto been addressed (Watts, 1985) for the extreme cases where the modulation process is completely decorrelated between adjacent range bins ($\rho = 0$), and where it is constant over the region covered by the detector (ie. $\rho \rightarrow 1$, such that $p(u_n|u_{n-1})$ tends to a δ function at u_{n-1}). We now evaluate the ideal detection performance for intermediate values of ρ.

In range-acting detection processing the test cell itself cannot be used to establish the threshold. We therefore define "ideal" detection to imply that the value of the modulation process is exactly known in the two range bins adjacent the test cell (one on either side). [This assumes that the modulation process is first order Markov and that the speckle is iid. in adjacent range bins. If these assumptions are violated knowledge of the modulation process in additional range bins is needed for detection to be ideal.] In addition the values of ν, μ and ρ are assumed to be explicitly known. Then, given ν, μ and ρ, the ideal detector sets the detection threshold based only on the known values of u_1 and u_3 (where range bin 2 is the test cell). No improvement is possible through knowledge of the values of the speckle process or any other samples of the modulation process. We can then write the threshold as $T(u_1;u_3)$, with the expected value of the false alarm probability being:

$$\overline{P_{fa}}\,(u_1,u_3) = \int_0^\infty \exp\left[\frac{-T(u_1,u_3)}{\mu u_2}\right] p(u_2|u_1,u_3)\, du_2 \qquad \ldots(6.20)$$

where $p(u_2|u_1,u_3) = p(u_1,u_2,u_3)/p(u_1,u_3)$, where $p(u_1,u_2,u_3)$ and $p(u_1,u_3)$ are given by eqns. (6.18) and (6.8) respectively. Inversion of the solution to (6.20) gives the function $T(u_1;u_3)$. The detection probability on a target with power P_t and signal to clutter ratio (SCR) $S_0 = P_t/2\mu\nu$ is obtained from:

$$\overline{P_d} = \int_0^\infty \int_0^\infty \int_0^\infty \exp\left[\frac{-T(u_1,u_3)}{\mu u_2 + P_t}\right] p(u_2|u_1,u_3)p(u_1,u_3)\, du_2\, du_1\, du_3$$

$$\approx \int_0^\infty \int_0^\infty \exp\left[\frac{-T(u_1,u_3)}{2\nu\mu(1+S_0)}\right] p(u_1,u_3)\, du_1\, du_3 \qquad \ldots(6.21)$$

where $p(u_1,u_3) = p(u_1|u_3)p(u_3)$; $p(u_1|u_3)$ is obtained from eqn. (6.7); $p(u_3)$ is gamma distributed with shape parameter ν and scale parameter θ=2, and $\rho_{13} = \rho_{12}^2$.

Eqns. (6.20) and (6.21) have been evaluated for sample values of ν and P_{fa} and results are illustrated in Fig. 6.3 for $P_d = 50$ % and $P_{fa} = 10^{-6}$ and $P_{fa} = 10^{-4}$. It is evident that several dBs of gain relative to the case for an uncorrelated modulation process are achievable for

moderate to high values of ρ.

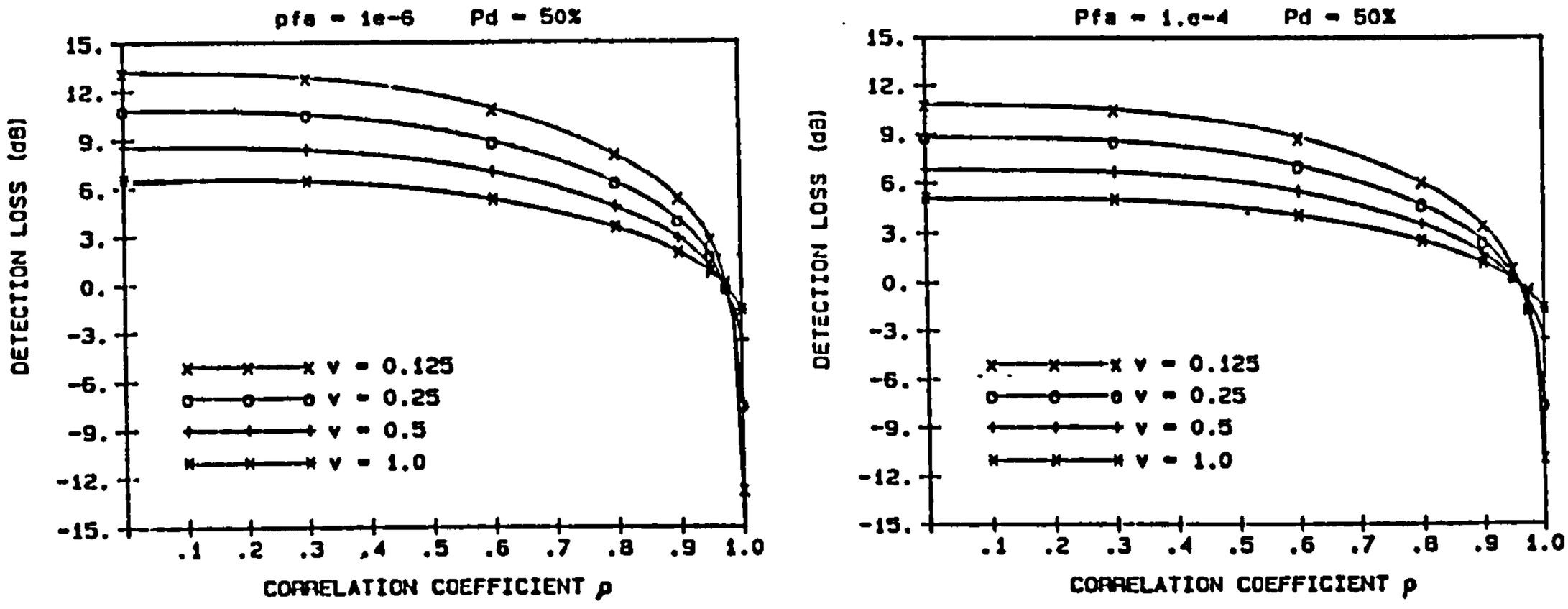

Fig. 6.3: *Ideal detection loss in spatially correlated clutter*
a) $P_{fa} = 10^{-6}$ b) $P_{fa} = 10^{-4}$ ($P_d = 50\%$; $\nu = 0.5$)

6.5 CFAR DETECTION IN SPATIALLY CORRELATED CLUTTER

For ideal detection it was assumed that the values of the modulation process in the cells on either side of the test cell (ie. u_1 and u_3), the overall scale parameter μ, and the values of ρ and ν are precisely known. In a CFAR processor, some or all of these quantities have to be adaptively estimated from a limited number of samples. This is optimally achieved through deriving implementations of classic estimation techniques such as Minimum Mean Square Error (MMSE) or Maximum Likelihood (ML) estimators to estimate the values of the modulation process in the cells adjacent to the test cell. One analytically tractable solution is to impose a linear constraint on the structure of an MMSE estimator. This yields an optimal filter for a correlated stochastic process in multiplicative Rayleigh or exponential noise. The coefficients of the resulting filter depend on the value of ρ; in this thesis we first assume that ρ is explicitly known, and thereafter assume that it is estimated from a finite number of

samples, with the effects of the consequent error being discussed. The estimation of ν is not considered here; it is assumed to be provided from an external source. The effects of errors in the assumed value of ν have been addressed in the previous chapter.

6.5.1 Derivation of the Weights for the Linear MMSE Filter for Multiplicative Noise.

Adaptive CFAR processors attempt to estimate the mean value of the Rayleigh (or exponentially) distributed signal in the test cell, which is multiplied by a threshold factor α to give the desired P_{fa}. This is a simple matter if the signals in the reference cells have the same mean as in the test cell, or if a few reference cells are corrupted by non-representative samples, as assumed in the previous chapter. If, however, the mean value of the background signal is a random variable with arbitrary ACF, these methods suffer performance degradation. In situations where the spatially correlated K-clutter model applies, the mean value of the clutter is a correlated stochastic process, ie. the modulation process, corrupted by multiplicative speckle. We therefore need to derive an "optimal" filter for estimating a random quantity when the observations are corrupted by multiplicative exponential or Rayleigh noise.

We derive, from classic Wiener filter theory, the linear MMSE filter for the clutter power process, since this yields a simpler detection performance analysis than the voltage case. Identical principles would, however, apply if filtering of the clutter voltage process was required. For a clutter power return $y = us$, we wish to obtain an estimate $\hat{u}$ of u through a weighted linear combination of N adjacent samples y_i of y, ie.:

$$\hat{u}_i = \sum_{j=-N/2}^{N/2} h_j\, y_{i-j} \qquad h_0 = 0$$

$$= \sum_{j=-N/2}^{-1} h_j\, y_{i+j} + \sum_{j=1}^{N/2} h_j\, y_{i+j} \qquad \ldots (6.22)$$

Since $h_{-j} = h_j$ we only need find the required weights h_j for j = 1 to N/2. These are determined through through differentiating the expected value of the mean square error with respect to h_i, equating the result to 0, and solving for the h_i in terms of the ACFs of u and s ie. if $\varepsilon = u - \hat{u}$ is the estimation error, then we solve $E(\varepsilon . y_{i-k}) = 0$, ie.:

$$\frac{\partial[E(\varepsilon^2)]}{\partial h_k} = E\left[\frac{\partial(\varepsilon^2)}{\partial h_k}\right] = 2E\left[\varepsilon \frac{\partial \varepsilon}{\partial h_k}\right] = 2E[\varepsilon y_{i-k}] = 2E\left[\left(\sum_{j=1}^{N/2} h_j y_{i-j} - u_i\right) y_{i-j}\right] = 0$$

$$\therefore \quad E\left[h_j \sum_{j=1}^{N/2} y_{i-j}\, y_{i-k}\, u_i \right] = E[u_{i-j}\, u_{i-k}\, s_{i-k}]$$

and since y=us, exploiting the independence between u and s gives N/2 equations of the form:

$$\sum_{j=1}^{N/2} h_j R_{ss}(j-k) \,.\, R_{uu}(j-k) = \mu R_{uu}(k) \qquad k = 1...N/2 \qquad \ldots (6.23)$$

This can be written in matrix form as:

$$\mathbf{h}\, R_{ss} \otimes R_{uu} = \mu \mathbf{g} \qquad \ldots (6.24a)$$

which is solved using the usual matrix methods, where $\otimes$ represents an element-by-element product and

$$\mathbf{h} = [h_1, h_2, \ldots . h_{N/2}]^T$$

$$\mathbf{g} = [R_{uu}(1), R_{uu}(2), \ldots . R_{uu}(N/2)]^T$$

$$\mathbf{R_{ss}} = \begin{bmatrix} 2\mu^2 & \mu^2 & \cdots & \mu^2 \\ \mu^2 & 2\mu^2 & & \vdots \\ \vdots & & \ddots & \mu^2 \\ \mu^2 & \cdots & \mu^2 & 2\mu^2 \end{bmatrix}$$

$$\mathbf{R_{uu}} = \begin{bmatrix} R_{uu}(0) & R_{uu}(1) & \cdots & R_{uu}(N/2-1) \\ R_{uu}(1) & R_{uu}(0) & & \vdots \\ \vdots & & \ddots & R_{uu}(1) \\ R_{uu}(N/2-1) & \cdots & R_{uu}(1) & R_{uu}(N/2-1) \end{bmatrix} \qquad \ldots (6.24b)$$

The resulting CFAR processor for detection in spatially correlated K-distributed clutter has the structure illustrated in Fig. 6.4. For want of a better name it is termed the Optimal Linear Filter (OLF) CFAR processor. The block labelled "estimate ρ" is described later in section 6.5.3. Note that for r=0 and r=1 eqn. (6.24a) gives all the weights as equal, as would be expected, and the processor is equivalent to the CA processor.

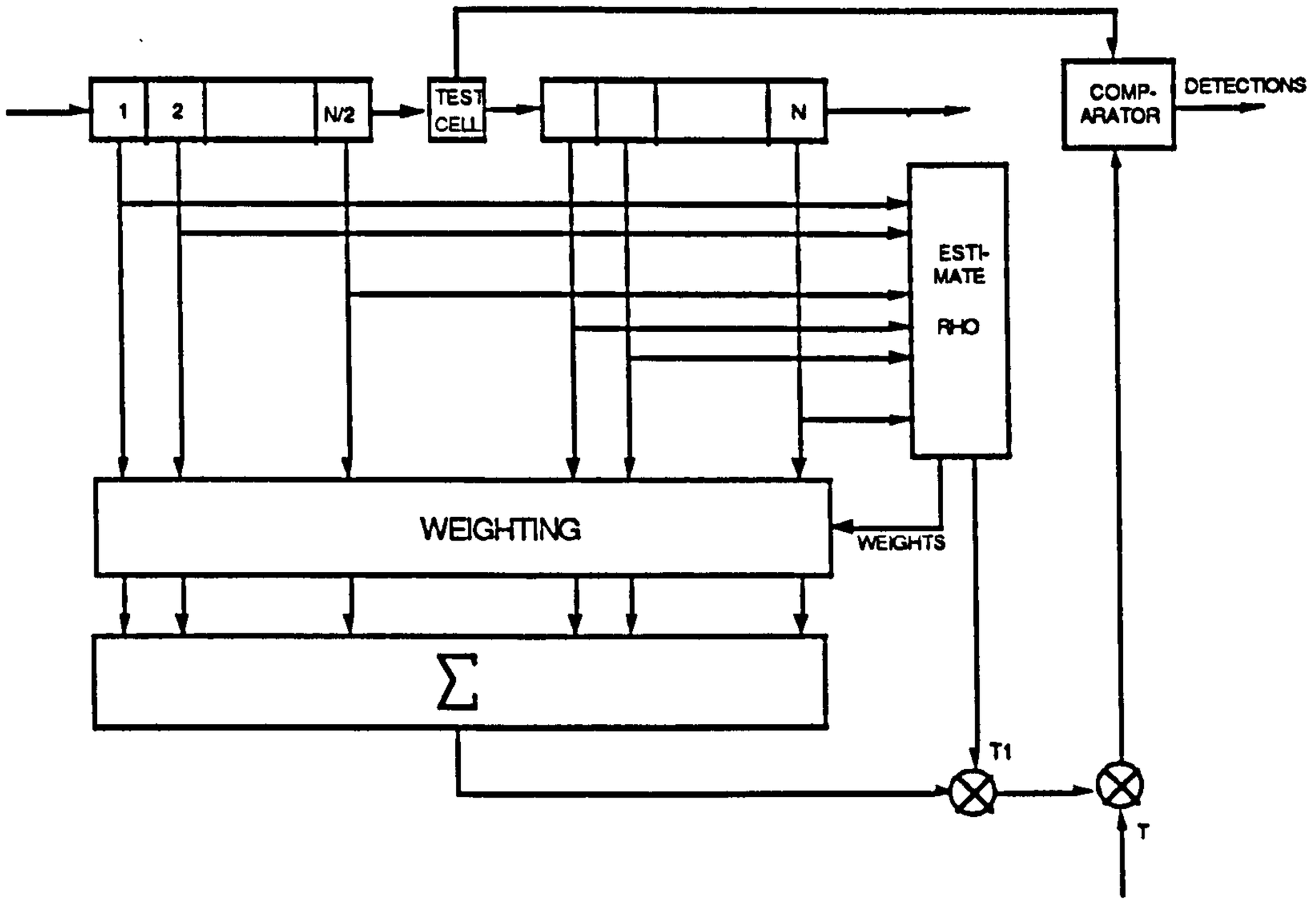

Fig. 6.4: *OLF-CFAR Processor Block Diagram*

6.5.2 Determination of Threshold Settings.

We wish to determine the value of the threshold multiplier α required to achieve the desired mean P_{fa}. Given u_0, the value of the modulation process in the test cell, and $\hat{u}$, as defined by eqn. (6.22), then:

$$P_{fa}(u_0,\hat{u}) = \exp[-(\alpha\hat{u})/(\mu u_0)] \qquad \ldots (6.25)$$

Since $\hat{u}/\mu$ is a random variable, we have:

$$= P_{fa}(u_0,\alpha) = \int_0^{\infty} \exp[-\frac{\alpha\hat{u}}{\mu u_0}].p_{\hat{u}/\mu}(\hat{u}).d\hat{u} \quad = M_{\hat{u}/\mu}(\frac{-\alpha}{u_0}) \qquad \ldots (6.26)$$

where $M_{\hat{u}/\mu}(\frac{-\alpha}{u_0})$ is the MGF of $\hat{u}/\mu$ at $-\alpha/u_0$. Noting that the exponential speckle s_i can be written as $s_i = \mu s'_i$, where s' is a unit mean negative exponential variate, $\hat{u}/\mu$ can be written as:

$$\frac{\hat{u}}{\mu} = \frac{1}{\mu}\sum_{i=-N/2}^{N/2} h_i\,\mu s'_i\,u_i = \sum_{i=-N/2}^{N/2} h_i\,s'_i\,u_i \qquad \ldots (6.27)$$

where $h_0 = 0$. So $\hat{u}/\mu$ is the sum of N independent weighted exponential variables, with weights h_iu_i, which can be shown to have MGF given by

$$M(t) = \prod_{i=-N/2}^{N/2} \left[\frac{1}{1 - h_i u_i t}\right] \qquad \ldots (6.28)$$

from which

$$M_{\underline{u}}\hat{}_{\mu}\left(\frac{-\alpha}{u_0}\right) = \prod_{i=-N/2}^{N/2} \left[\frac{1}{1 - h_i u_i \frac{-\alpha}{u_0}}\right] \qquad \ldots (6.29)$$

Then, exploiting the Markov property of u, recalling that the marginal PDFs of u are gamma distributed with shape parameter ν and scale parameter θ=2, and using eqn. (6.7), the expected value of P_{fa} over all u_i and u_0 is:

$$P_{fa} = \int_0^{\infty} \int_{u} M\hat{u}_{\mu}\left(\frac{-\alpha}{u_0}\right) p_{u\,|u_0}(u\,|u_0)\, p_{u_0}(u_0)\, du\; du_0$$

$$= \int_0^{\infty} \left[\frac{1}{(1-\rho^2)\rho^{\nu-1}}\right]^N \frac{[\Theta(u_0;\alpha)]^2}{2^{\nu+N}\Gamma(\nu)} \exp\left[\frac{-u_0(1+\rho^2)}{1-\rho^2}\right] du_0 \qquad \ldots (6.30)$$

where u represents the vector $\{u_1, u_2 \ldots u_{N/2}\}$, du represents $du_1 du_2 \ldots du_{N/2}$, and

$$\Theta(u_0,\alpha) = \int_{u} \exp\left[\frac{-1}{2(1-\rho^2)}\{u_{N/2} + (1+\rho^2)(u_1+\ldots+u_{N/2})\}\right]$$

$$\times \prod_{i=1}^{N/2} \left[\frac{I_{\nu-1}\left(\frac{\rho\sqrt{u_i u_{i-1}}}{1-\rho^2}\right)}{1 - A_i u_i}\right] du \qquad \ldots (6.31)$$

where $A_i = h_i\alpha/u_0$. $\Theta(u_0,\alpha)$ can be solved numerically by decomposing it into N/2 nested single integrals rather than a single multiple integral, as follows:

$$\Theta(u_0,\alpha) = \int_0^{\infty} \frac{I_{\nu-1}(c\sqrt{u_0 u_1})}{1+A_1 u_1} \exp\left[\frac{(1+\rho^2)\, u_1}{2(1-\rho^2)}\right] \int_0^{\infty} \frac{I_{\nu-1}(c\sqrt{u_1 u_2})}{1+A_2 u_2} \exp\left[\frac{(1+\rho^2)\, u_2}{2(1-\rho^2)}\right] \int_0^{\infty} \ldots$$

$$\ldots \int_0^{\infty} \frac{I_{\nu-1}(c\sqrt{u_{m-2} u_{m-1}})}{1+A_{m-1} u_{m-1}} \exp\left[\frac{(1+\rho^2)\, u_{m-1}}{2(1-\rho^2)}\right]$$

$$\times \int_0^{\infty} \frac{I_{\nu-1}(c\sqrt{u_{m-1} u_m})}{1+A_m u_m} u_m^{(\nu-1)/2} \exp\left[\frac{u_{m-1}}{2(1-\rho^2)}\right] du_m du_{m-1} \ldots du_2 du_1$$

$$\ldots (6.32)$$

where $c = \rho(1-\rho^2)^{-1}$ and m =N/2.

Thus eqn. (6.30) gives P_{fa} as a function of α, from which the required value of α can be

determined as a function of the correlation of the modulation process. Having determined the required value of α, detection probabilities are calculated as follows: for a target of power P_t and mean SCNR $S_0 = P_t/2\mu\nu$, given u_0 and $\hat{u}$, the detection probability is

$$P_d(u_0;\hat{u}) = \exp\left[\frac{-\alpha\hat{u}}{\mu u_0 + P_t}\right] = \exp\left[\frac{-\alpha}{u_0 + 2\nu S_0}\left(\frac{\hat{u}}{\mu}\right)\right] \quad \ldots (6.33)$$

Taking expected values over u_0 and $\hat{u}$, the overall detection probability is obtained in exactly the same manner as P_{fa} above, except that A_i in eqn. (6.31) is instead given by :

$$A_i = \frac{\alpha h_i}{u_0 + 2\nu S_0} \quad \ldots (6.34)$$

6.5.3 Estimation of the Correlation Coefficient.

The value of ρ affects the required value of α and the consequent false alarm and detection probabilities. Absence of *a priori* knowledge of ρ and spatial variations in ρ therefore necessitate real time estimation of the its local value. If the estimate $\hat{\rho}$ is distributed according to a pdf $p_{\hat{\rho}}(\hat{\rho})$, then the overall value of P_{fa} is given by:

$$P_{fa} = \int_0^1 P_{fa}[\alpha_1.\alpha(\hat{\rho})].p_{\hat{\rho}}(\hat{\rho})\, d\hat{\rho} \quad \ldots (6.35)$$

where $P_{fa}[\alpha_1.\alpha(\hat{\rho})]$ is the false alarm probability given α (which is in turn a function of the estimated value of $\hat{\rho}$), and α_1, an additional multiplier factor used to maintain the desired P_{fa}. The lower the variance of $\hat{\rho}$, the lower α_1 and the additional loss will be. Since $E(x_i.x_{i+1})$ and $E(y_i.y_{i+1})$ are monotonically increasing functions of ρ, we can instead estimate either of these quantities and then deterministically relate that estimate to ρ. Mathematically rigorous minimum variance or maximum likelihood estimators of ρ have not been successfully formulated. Several intuitively derived estimators of ρ have been investigated, in which ρ in range bin i and on pulse j is derived from estimates of either $\hat{E}(x_ix_{i+1})$ or $\hat{E}(y_iy_{i+1})$, ie.:

$$\hat{\rho}_{i,j} = f_x\left(\hat{E}(x_ix_{i+1})\right)$$

or

$$\hat{\rho}_{i,j} = f_y\left(\hat{E}(y_iy_{i+1})\right) \quad \ldots (6.36)$$

where $f_x(.)$ is the inverse of eqn (6.19) with m=1/2 (for which a numerical solution is required), and $f_y(.)$ is the inverse of eqn (6.19) with m=1, which is analytically simple. It has been found by simulation that the estimator which yields the lowest value of α_1 and hence the lowest eventual detection loss is:

$$\hat{E}(xx) = \sum_{k=0}^{N_i-1} L\left[\frac{\sum_{m=-N_r}^{N_r} x_{i+m,j-k} \cdot x_{i+m+1,j-k}}{\sum_{m=-N_r}^{N_r} x_{i+m,j-k}^2}\right] \quad \ldots (6.37)$$

where $L[z] = z \qquad z_{min} \le z \le z_{max}$

$= z_{min} \qquad z < z_{min}$

$= z_{max} \qquad z > z_{max} \quad \ldots(6.38)$

where z_{max} and z_{min} are the maximum and minimum values of z for $N_r \to \infty$, given by:

$$z_{max} = \frac{E(x_i x_j)|_{\rho=1}}{E(x^2)} = \frac{E(u^2)E(s)^2}{E(x^2)} = \frac{E(s)^2}{E(s^2)} = \frac{\pi}{4}$$

$$z_{min} = \frac{E(x_i x_j)|_{\rho=0}}{E(x^2)} = \frac{E(x)^2}{E(x^2)} = \frac{\pi[\Gamma(\nu+1/2)]^2}{4\nu[\Gamma(\nu)]^2} \quad \ldots (6.39)$$

and $x_{i,j}$ is the sample in the i^{th} range bin on the j^{th} pulse

N_r is the number of reference cells used for estimating ρ (which need not be the same as N, the number of reference cells used for estimating u)

N_i is the number of pulses available for estimating ρ

A functional block diagram of a practical implementation of the estimator of ρ defined above is illustrated in Fig. 6.5.

A closed form expression for the PDF of $\hat{\rho}$ has not been found. It has therefore been obtained by simulation for selected values of ρ, N_r and N_i. The number of trials necessary was determined by running the simulation 5 times for each set of parameters, with sufficient trials per simulation to ensure that the loss results did not differ by more than 0.1 dB. The average of the 5 simulations was then used for the calculation of final results illustrated in the next section.

Detection performance was calculated by substituting the simulated PDF of $\hat{\rho}$ into eqn. (6.35) for a range of values of α_1, determining the value of α_1 required to maintain the desired value of P_{fa}, and substituting the compound threshold multiplier $\alpha\alpha_1$ for α in eqns. (6.33) and (6.34) for detection performance analysis. The additional fluctuation introduced to the test statistic by estimation of ρ has negligible effect on detection performance and has therefore been neglected. Results are presented in the next section.

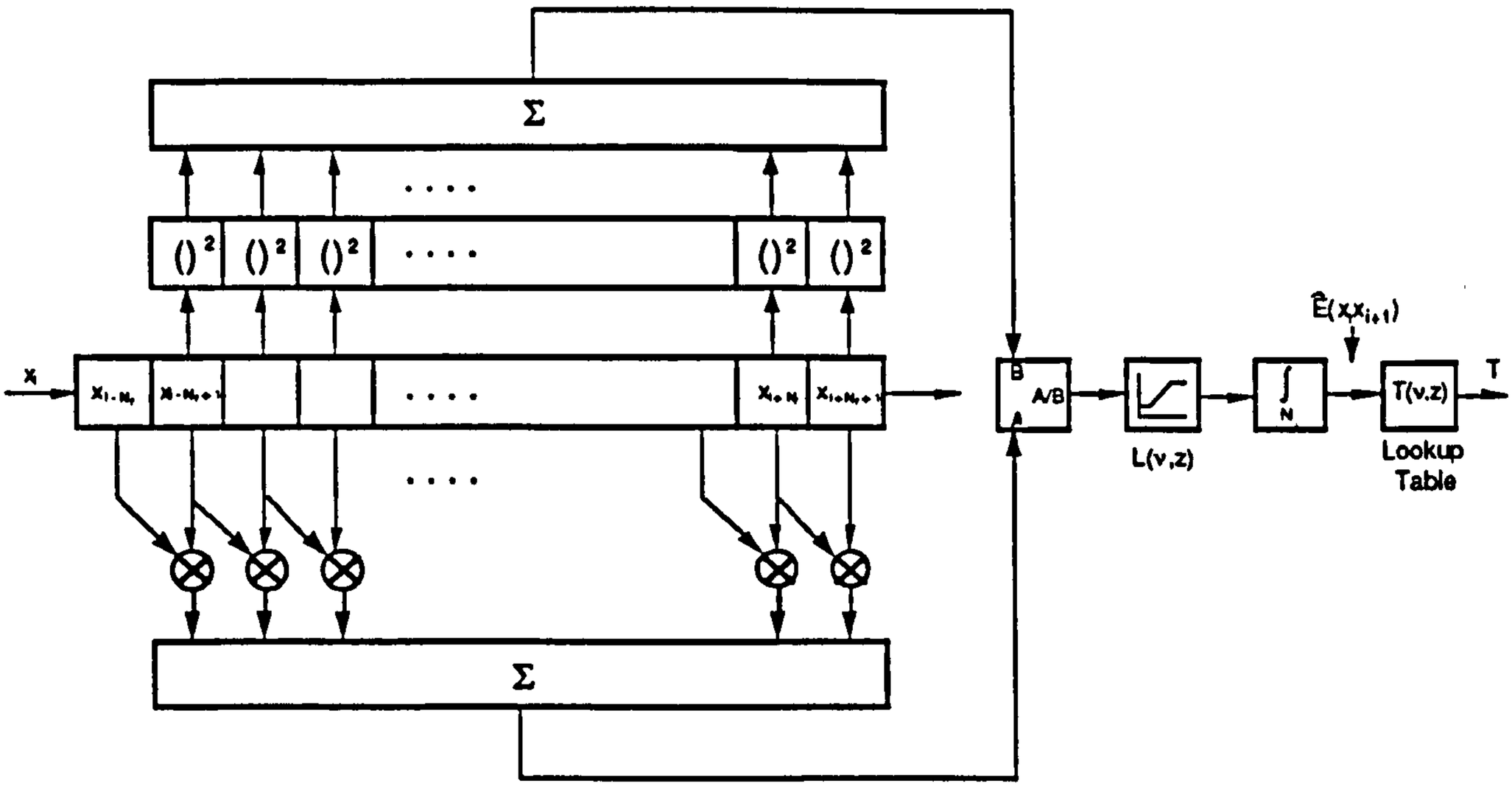

Fig. 6.5: *Block diagram of Estimator of Spatial Correlation*

6.5.4 Detection Performance Results

We define CFAR loss as the difference between the SCR required for a given probability of detection using the CFAR detector, including the effects of estimating ρ, and the SCR required for ideal detection (discussed in section 6.3) in clutter with the same spatial correlation and shape parameter, as given in Fig. 6.3. Sample results are illustrated in Fig. 6.6 for ν =0.5, N=16, and P_d = 50%, for various values of N_i and N_r. The curve representing the CA detector represents the case where the threshold is not adapted according to the local value of ρ.

It can be seen from Fig. 6.6 that CFAR loss can be reduced by about 2 to 4 dB for moderate to high spatial correlation. It is evident that on-line estimation of ρ does not dramatically increase the CFAR loss even for N_i=1 and N_r=50. Also note that despite the fact that CFAR loss increases with increasing ρ, the SCR required for detection decreases: the loss illustrated above is relative to the ideal detector which has SCR decrease faster than the loss increases for increasing ρ. The reduction in the SCR required for P_d=50% and $P_{fa}=10^{-6}$ achieved by the OLF-CFAR processor relative to CA-CFAR detection in uncorrelated clutter is tabulated in Table 6.1.

Table 6.1

OLF-CFAR Processor Gain Relative to CA Processor

in uncorrelated clutter

(N=16, $P_d = 50\%$; $P_{fa} = 10^{-6}$, $\nu = 0.5$)

	$N_i=1;\ N_r=50$	$N_i=4;\ N_r=50$	$N_i=8;\ N_r=100$	**ρ known**
ρ=0.3	0	0	0	0
ρ=0.6	0.9	1.0	1.2	1.3
ρ=0.8	2.0	2.2	2.5	2.7
ρ=0.9	3.1	3.4	3.6	3.8
ρ=0.95	3.6	4.2	4.8	5.0

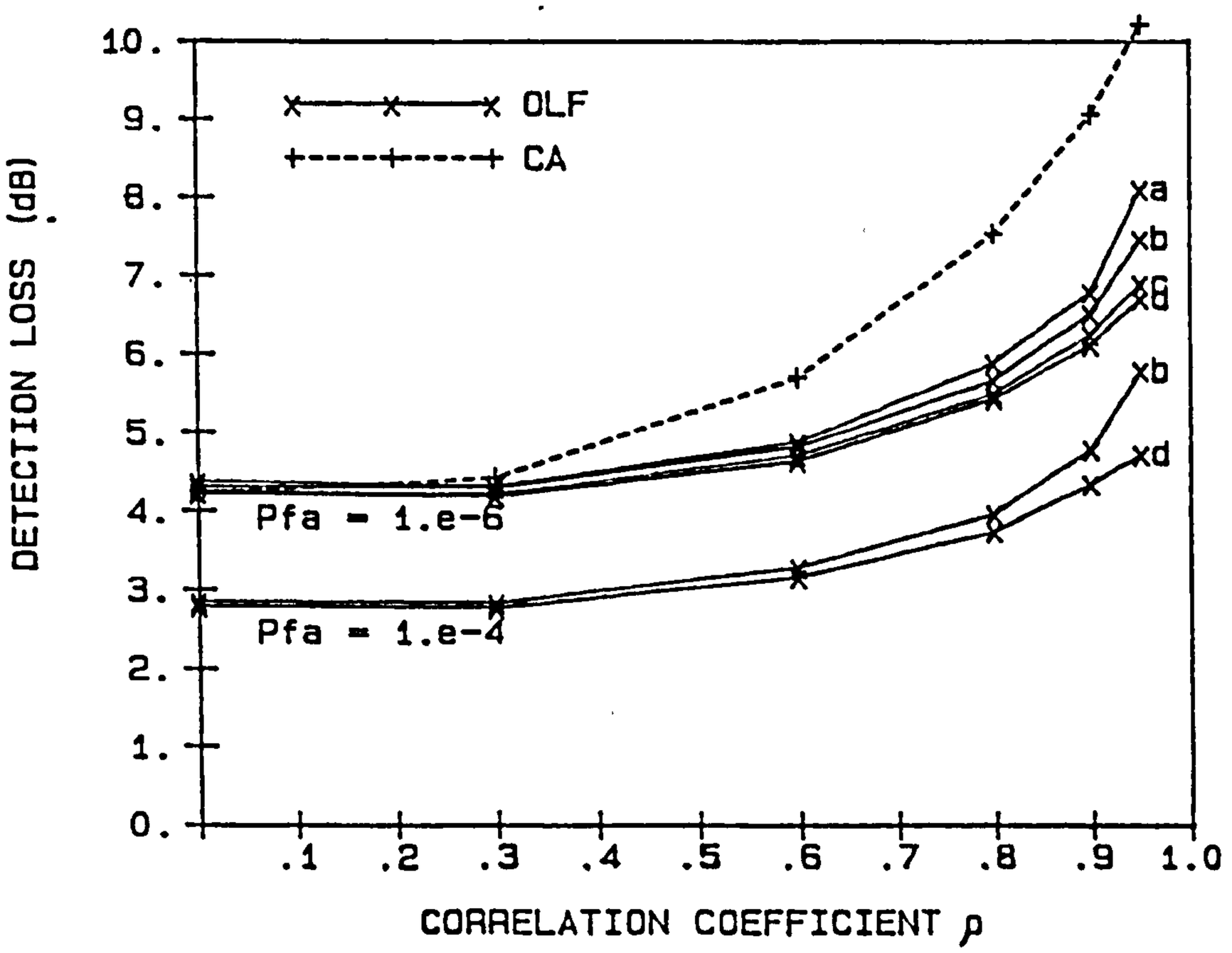

Fig. 6.6: *CFAR Loss as a function of ρ for CA and OLF processors*
(N=16, $P_d = 50\%$; $P_{fa} = 10^{-6}$, $\nu = 0.5$)
a) $N_i=1; N_r=50$ b) $N_i=4; N_r=50$ c) $N_i=8; N_r=100$ d) **ρ known exactly**

6.5.5 Discussion

It is evident that moderate gains can be achieved by the OLF processor if the clutter exhibits significant spatial correlation. These results are based on the assumption of an exponential spatial ACF of the clutter; this represents a fairly pessimistic case (possibly representative of choppy seas) and other ACFs, such as Gaussian, are expected to enhance the relative performance of the OLF Processor. Unfortunately analytic or numerical evaluation of

performance in clutter with spatial ACFs other than exponential is not possible since they cannot be represented by first order Markov models, and the multiple integral $\Theta(u_0,\alpha)$ in eqns. (6.30) and (6.31) cannot be decomposed into N/2 nested integrals. Exploitation of other ACFs would also require estimation of more correlation terms than simply $\rho_{i,i+1}$. Formulation and analysis of appropriate estimators is difficult. In practice either multiple lookup tables or real-time filter weight calculation would be required.

It is evident from fig. 6.6 that there is relatively high CFAR loss for high values of ρ, indicating the potential for a further saving of several dBs for high ρ. The high CFAR loss is probably a consequence of the linear constraint on the estimator of the modulation process. Non-linear techniques based on Bayesian estimation of the modulation process, given the clutter samples and the modulation and speckle conditional pdfs, appear to offer a promising means of reducing the CFAR loss.

It is worth noting that the main contribution to the improved performance of the OLF-processor is due to estimating ρ and adapting the threshold accordingly; this accounts for about 75% of the dB value of the improvement. The use of an optimally weighted rather than an unweighted estimate only accounts for about 25% of the reduction in CFAR loss. Again, other ACFs than exponential are likely to increase the effect of optimal weighting.

Methods of reducing the sensitivity of the processor to extraneous targets need to be addressed. This applies to both the estimator of ρ and the optimally weighted estimator of the modulation process in the test cell. If censoring of the largest samples, as in the CMLD processor, is used in the optimally weighted estimator of u_0, a different set of weights would, theoretically, be required for each permutation of censored samples. Simplifications are not immediately obvious and it is unclear how optimally weighted estimators will behave if some samples are censored and the weights are not correctly modified. It can be noted that increases in P_{fa} due to non-stationary clutter are expected to be somewhat counteracted by the fact that clutter edges will effectively reduce the estimate of the local spatial correlation, thereby increasing the threshold in the region of the clutter edge.

6.6 CONCLUSIONS

The performance of conventional CFAR processors has been examined in completely spatially correlated clutter. It has been shown that under these conditions a reduction in detection loss of more than 10 dB is possible relative to the spatially uncorrelated case, in even moderately spiky clutter. This indicates that spatial correlation may offer the basis for

reducing CFAR loss in more realistic conditions of partial spatial correlation.

A model for spatially correlated K-distributed clutter of arbitrary spatial ACF has been presented. The modulation process is generated as the sum of the squares of a number of independent ZMG processes, followed by a non-linear transformation to obtain a gamma distributed process of arbitrary ν. A key advantage of this intuitively simple model over previous models is that the spatial correlation is introduced to Gaussian processes, thus enabling any required ACF to be obtained by well established linear filtering techniques, while simultaneously maintaining a gamma distribution for the resulting process. The strictly K-distributed clutter is obtained by multiplying the spatially correlated modulation with the speckle, onto which the desired doppler spectrum has been imposed. The model has particular analytic benefits in that leads to usable expressions for the multivariate PDFs and ACFs of the modulation and clutter processes.

Based on this model ideal detection performance in spatially correlated clutter has been analysed to ascertain an upper bound on CFAR detection performance in spatially correlated clutter. It is apparent that a potential benefit of several dBs is possible if the CFAR processor is designed to exploit the spatial correlation and if improved estimates of the modulation process can be obtained.

A CFAR processor has been formulated and analysed in which spatial correlation is exploited through real time estimation of the local value of the spatial correlation coefficient ρ with corresponding adaptation of the threshold multiplier factor α. In order to improve the estimate of the modulation process in the test cell a linear MMSE estimator of the modulation process has been derived, with weights dependent on the clutter's spatial ACF. It has been shown that under conditions of moderate to high spatial correlation with exponential ACF, a reduction of 1 to 5 dB is possible in the SCR required for a specified P_d and P_{fa}. More dramatic reductions are predicted for clutter with a Gaussian spatial ACF.

It is concluded that the OLF-CFAR processor represents a promising technique for improving detection performance in spiky sea clutter, subject to the requirements that the spatial extent of targets of interest is less than the correlation distance of the clutter, and that the radar has sufficiently fine range resolution to exploit whatever spatial correlation may be present. Should these conditions not be met, improved detection performance in spiky clutter will require other processing techniques in which the modulation process in the range-reference window does not form the sole basis of the detection hypothesis test.

CHAPTER 7

MULTI-BURST RANGE-DOPPLER CFAR PROCESSING IN SPATIALLY UNCORRELATED K-DISTRIBUTED CLUTTER

7.1 RATIONALE

The CFAR processors examined thus far in this thesis have all relied on the assumption that the mean background level in the test range bin can to some extent be determined from that in a number of surrounding range bins. The collapse of this assumption in spiky clutter results in the severe losses noted in previous Chapters, even if the spikiness is homogeneous. Non-homogeneous clutter, such as partially shadowed land clutter or urban clutter, could cause even more catastrophic deteriorations in performance. The key weakness in conventional CFAR processors can therefore be identified as the reliance on surrounding range bins as the sole source of information for estimating the background in the test cell in order to establish the threshold. Exploitation of the two other domains in which potential reference data is available, namely the doppler and time domains, is therefore investigated in this Chapter.

Consider first the time domain: post-detection binary integration of conventionally detected signals in K-clutter has been shown to offer modest benefits at best (eg. Watts, 1985). Clutter maps (eg. Lops, 1989), updated every scan of the radar, offer a form of range-referenceless CFAR processing, and are indeed probably the best option in many static radars in slowly changing environments. However, the inherently low update rate of threshold data largely precludes their use in mobile systems, in environments where the local clutter amplitude fluctuates at a rate faster than the radar scan rate or frame time (such as with sea clutter for typical search and acquisition radars), or in many types of radar which cannot afford long clutter map settling times after activation, such as tracking radars during auto-acquisition phases. More optimal utilisation of multiple bursts by pre-detection non-coherent integration is also not an attractive solution since 1) this precludes the possibility of subsequent velocity ambiguity resolution, and 2) targets, which fall in a different doppler bin on each burst, will not be integrated. False alarm control downstream by Track While Scan processing is not an ideal solution as it can cause saturation of the plot extractor and missed or corrupted true tracks.

The doppler domain only appears to have been exploited to date in simple range-doppler CFAR processors, essentially 2-dimensional versions of the standard CA processor. It is immediately evident that such processors are only effective in environments in which the spectrum of the background is essentially flat over the doppler space or partitions thereof, otherwise strong doppler components cause masking of smaller targets in adjacent dopplers in which the targets would normally be visible. This limitation precludes simple range-doppler CA techniques from being used in most practical radar systems.

The objective of this Chapter was therefore to formulate a means of exploiting information from other time and/or doppler bins in the vicinity of the test cell to ascertain the background level in the test cell, in radars employing doppler filter banks and multiple bursts per dwell. Current radars often comprise single-doppler CFAR processors, followed by OR selection logic between dopplers on each burst, followed by M/N binary integration over the N bursts. In this Chapter a variation of this architecture is presented. We take as a point of departure that:

1) In order to reduce susceptibility of the processor to spiky clutter, the test statistic must be derived primarily from samples in the same range cell as the test sample.
2) Several doppler bins are available in each range cell, and on each burst. The type of filter implemented is unimportant provided several essentially non-overlapping doppler bins are created. The CFAR processor presented in this Chapter is therefore not applicable to systems employing MTI or AMTI doppler processors.
3) Each detection opportunity (ie. the radar dwell) consists of more than one burst, typically three to eight. It is assumed that the target and clutter speckle are decorrelated between bursts by frequency agility.
4) The underlying clutter modulation is assumed to remain constant over all bursts within a dwell. This requires that 1) the radar is range-unambiguous or employs a constant PRF waveform if range-ambiguous clutter is present, and 2) the decorrelation time of the clutter modulation process is longer than the radar dwell. This latter assumption is reasonable for most radars and clutter environments.

Two main observations can then be made in formulating a Range-Doppler-Time CFAR processor. Firstly, the reference samples are now drawn from other burst and doppler bins in the same range bin as the test cell (and in fact including the test cell, as will be shown later). If a target is present it will cause returns in one doppler on each burst, and a simple average of the reference samples over doppler and bursts would include some target returns, which would increase the threshold and prevent a detection of the target return in the test cell. Measures therefore need to be taken to prevent target self-masking. This is attempted here by the use of order statistics in setting the threshold, the rationale

being that the relative immunity of order statistic filters to outliers will provide the required threshold robustness against the relatively small number of target returns.

Secondly, to overcome the problem of doppler bins containing strong clutter from masking weaker targets in other doppler bins, the samples in each doppler bin need to be normalised such that all reference samples used to generate the threshold have the same power, irrespective of the actual clutter power in each doppler. The appropriate power normalisation terms need to be adaptively estimated; they could either be estimated from surrounding range bins, or from scan-scan estimation as in a clutter map. Ideally the errors involved in adaptive power normalisation should not depend on clutter spikiness. In this Chapter an implementation of the former range-acting approach is proposed and evaluated. Scan-scan derived estimation has not been investigated further here since it could be achieved by translation of the range-acting algorithm, with minor modification, into the scan-scan domain. Furthermore, from a performance point of view, only the statistics of the errors in the power normalisation terms are of interest, not the source of the estimate.

The functional block diagram of a CFAR processor conforming to the abovementioned requirements is outlined in Fig. 7.1. This processor will be termed a Range-Doppler-Time (RDT) CFAR processor. It can be seen that the range-acting aspect of the processor affects the threshold only in a secondary manner, via the estimated power normalisation terms. In addition, the estimation accuracy of the power normalisation terms is shown later in this Chapter to be independent of the clutter modulation process. These two features provide the RDT processor with a large measure of immunity to clutter spikiness. However, as with any range-acting estimator, the power normalisation section of the processor relies on spatial stationarity of the parameter being estimated - in this case the clutter spectrum - and would suffer a deterioration in performance in spectrally fluctuating clutter. A variant of this range-doppler-time processor is therefore presented in section 7.4; this processor derives the threshold from samples only in the same doppler bin as the test cell, thereby obviating assumptions of spectral stationarity, at the expense of increased loss in thermal noise and subject to not unreasonable lower limits on the number of bursts employed.

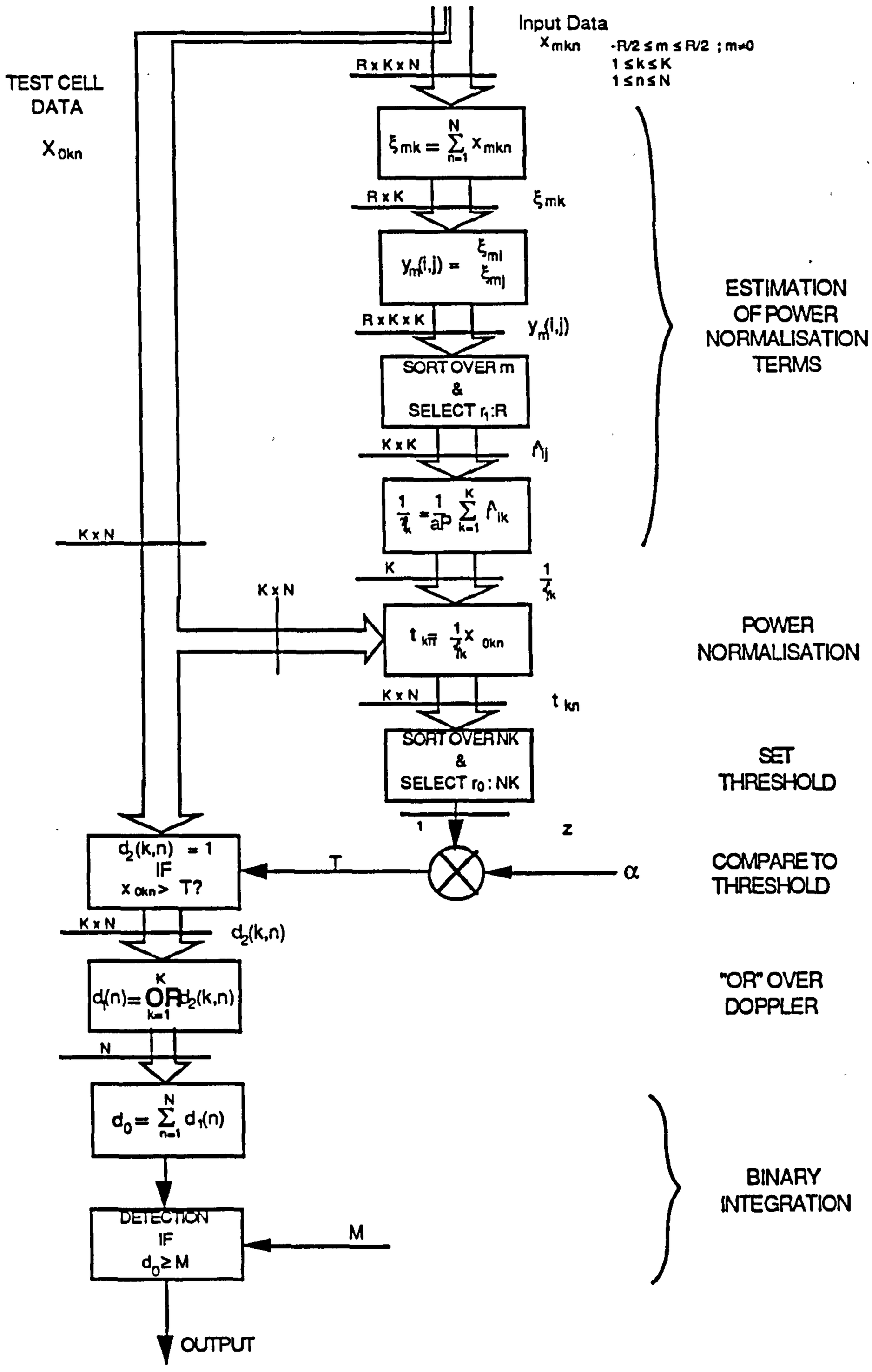

Fig. 7.1: *Functional Block Diagram of the RDT CFAR processor*

The rest of this Chapter is organised as follows: The ideal case assuming perfect power normalisation is considered next in section 7.2 to establish an upper bound on the performance of the RDT processor, and confirm that it is a promising area for further investigation. Thereafter the more practical case of adaptive power normalisation is examined in section 7.3: the statistics of the errors in the power normalisation terms are determined and their effect on false alarm rate and detection performance is evaluated. Results are presented for a number of cases and the performance is compared to that of conventional processors. Deterioration in false alarm performance in spectrally non-homogeneous clutter is investigated. As a solution to this problem the modified processor using only the test doppler in setting the threshold, termed the δ-CFAR, is presented in the following section, ie. section 7.4. An example is presented to illustrate the superiority of the δ–CFAR processor proposed here over conventional processors, when using realistic radar system parameters. A Summary and some conclusions are presented in section 7.5.

7.2 IDEAL CASE: PERFECT POWER NORMALISATION

In this section we assume perfect power normalisation of each doppler in order to determine an upper limit on the performance achievable by a RDT-CFAR processor. That is, we assume that there is no error between the outputs of the power normalisation estimator of Fig 7.1 and the true background power in each doppler. This represents the situation where the number of range reference cells covered by the RDT processor tends to infinity and the uncorrupted background is spectrally homogeneous.

The assumption that all dopplers have been perfectly gain normalised implies that the background in each of the doppler bins on each burst is iid. unit mean exponential noise. We take as the estimator of the background power the r_0^{th} largest of the NK burst-doppler samples in the test range cell. This sample will be termed the *test statistic*, and the detection threshold is set at a constant α times the test statistic. Under the target absent hypothesis a false alarm will occur if at least one of the doppler bins in a burst exceeds the threshold, on at least M out of the N bursts. That is, we perform a logical OR operation over doppler followed by conventional M/N detection over the bursts.

The performance analysis comprises four main parts, namely:

1) Determining the probability that some of the burst-doppler samples in the test range cell will exceed the threshold and cause or contribute to a false alarm.
2) Given a certain number of exceedances, calculating the probability of a false alarm following ORing over doppler and M/N binary integration over N bursts.

3) Combination of parts (1) and (2) above to yield the expected P_{fa} alarm given the threshold multiplier factor α, and inversion of the resulting relationship to give the value of α required for the desired P_{fa}.
4) Calculating the detection probability as a function of SCNR using the the value of α obtained above. Solution of the inverse function for $P_d = 50\%$ can then yield the detection loss relative to the ideal detector.

These four components of the analysis are described in the following subsections.

7.2.1 Probability of an exceedance

The overall probability of false alarm depends on the probability of a number q of the NK reference samples exceeding the threshold. The probability of having q samples which exceed the threshold, or *exceedances*, is derived from the joint order statistic $x_{r_0};x_s$ ($r_0 < s$) of the ordered reference samples. If $x_s \geq \alpha x_{r_0}$, then at least NK-s+1 of the reference samples exceed the threshold, ie. given s, we have prob[$q \geq$ NK-s+1] = prob[$x_s \geq \alpha x_{r_0}$]. For samples independently drawn from a parent population with common PDF p(x) and CDF P(x), the joint PDF of the order statistics x_{r_0} and x_s is given by (David, 1981):

$$p(x_r;x_s) = \frac{NK}{(r-1)!(s-r-1)!(NK-s)!} [P(x_r)]^{r-1} p(x_r) [P(x_s) - P(x_r)]^{s-r-1} p(x_s) [1 - P(x_s)]^{NK-s} \quad \ldots (7.1)$$

Then setting $p(x) = e^{-x}$, $P(x) = 1 - e^{-x}$, eqn. (7.1) becomes:

$$p(x_r;x_s) = k_1 (1 - e^{-x_r})^{r-1} [e^{-x_s} - e^{-x_r}]^{s-r-1} e^{-x_r - x_s(1 + NK - s)} \quad \ldots (7.2)$$

where $k_1 = \frac{NK}{(r-1)!(s-r-1)!(NK-s)!}$

Setting $z = x_r/x_S$ gives $p_z(z) = k_1 \int_0^\infty x_r \, p_{r,s}(x_r;zx_r) \, dx_r$, and so:

$$\text{prob}(z > \alpha) = \int_\alpha^\infty p_z(z) \, dz$$

$$= k_1 \int_\alpha^\infty \int_0^\infty x e^{-x(s-r) - xz(1+NK-s)} [1-e^{-x}]^{r-1} [1-e^{-zx+x}]^{s-r-1} \, dx \, dz \quad \ldots (7.3)$$

Changing the order of integration and substituting $w = e^{-z}$, after some manipulation we get:

$$p(z>\alpha) = k_1 \int_0^{\infty} \sum_{i=0}^{s-r-1} (-1)^i \binom{s-r-1}{i} \frac{1}{1+NK-s+i} \exp[-x(s-r-i+\alpha(1+NK-s+i))]\,[1 - e^{-x}]^{r-1}\,dx \quad \ldots (7.4)$$

Making the substitution $y = e^{-x}$, and manipulating into a form suitable for using Gradshteyn identity 3.191.3 (Gradshteyn, 1980) finally gives:

$$p(z>\alpha) = k_1 \sum_{i=0}^{s-r-1} (-1)^i \binom{s-r-1}{i} \frac{1}{1+NK-s+i} \frac{\Gamma(s-r-i+\alpha(1+NK-s+i))\,\Gamma(r)}{\Gamma(s-i+\alpha(1+NK-s+i))} \quad \ldots (7.5)$$

The probability of 0 exceedances is then

$$p(q=0) = 1 - p(z\geq\alpha)|_{s=NK} \quad \ldots (7.6a)$$

and

$$\begin{aligned} p(z\geq\alpha)|_{s=NK} &= p(q\geq 1) \\ &= \text{probability of at least one exceedance} \\ &= p(q=1) \text{ or } p(q=2) \text{ or } p(q=3) \ldots \\ &= p(q=1) + p(q=2) + p(q=3) + \ldots \end{aligned}$$

$$\begin{aligned} p(z\geq\alpha)|_{s=NK-1} &= p(q\geq 2) \\ &= p(q=2) + p(q=3) + p(q=4) + \ldots \end{aligned}$$

and so on. Solving for p(q=1), p(q=2) etc. then gives:

$$\begin{aligned} p(q=1) &= p(z\geq\alpha)|_{s=NK} - p(z\geq\alpha)|_{s=NK-1} \\ p(q=2) &= p(z\geq\alpha)|_{s=NK-1} - p(z\geq\alpha)|_{s=NK-2} \\ &\text{-} \\ &\text{-} \\ p(q=NK-r) &= p(z\geq\alpha)|_{s=r+1} \end{aligned} \quad \ldots (7.6b)$$

The desired PDF $p_q(q)$ for the number of exceedances is therefore obtained from eqns. (7.6a) and (7.6b), which are in turn obtained from (7.5). Due to the processor architecture it is apparent that the location of each exceedance is independent and uniformly random over N and K.

7.2.2 Probability of a false alarm, given q exceedances

Given $p_q(q)$ it is now necessary to derive P_{fa} over the K doppler bins and N bursts. The key question now is how many bursts have at least one exceedance among the K

dopplers? To solve this problem we resort to occupancy theory, in whose terms the problem is one of drawing "balls" (the exceedances) from a population in an urn containing K balls of each of the N colours (the NK doppler- burst reference cells). If q balls are randomly drawn from the urn we wish to know how many balls of each colour have been drawn (ie. how many exceedances in each burst). Note that this represents sampling without replacement since each burst-doppler cell can contain only one exceedance.

From discrete probability theory it is known that if $n_1, n_2, n_3 .. n_N$ are the numbers of balls of each colour drawn from the urn, then the distribution of $n_1, n_2, n_3 .. n_N$ is a multivariate hypergeometric distribution (Johnson, 1969).

We are interested in the number of bursts containing at least one exceedance, ie. the number of colours of balls of which at least one is drawn from the urn. Equivalently we can seek the number of colours of balls of which no samples are drawn from the urn. This can be obtained from the multivariate hypergeometric class size distribution (Patil, 1968), described by:

$$p(n_0;n_1;n_2;\ldots;n_q) = \frac{N!}{n_0!\, n_1! \ldots n_q!} \frac{\binom{K}{0}^{n_0}\binom{K}{1}^{n_1}\cdots\binom{K}{q}^{n_q}}{\binom{NK}{q}} \qquad \ldots (7.7)$$

where $n_0 \equiv$ the number of colours of which no balls were drawn
ie.the number of bursts without exceedances
$n_1 \equiv$ the number of colours of which one ball was drawn
ie.the number of bursts with one exceedance
etc.

and

$$i = 0, 1, \ldots \le \min(q;K)$$
$$n_i = 0, 1, \ldots \le \min(q/i; N)$$
$$\sum_i n_i = N$$
$$\sum_i i n_i = q$$

Then the PDF of the number of bursts with no exceedances is given by the marginal distribution of n_0, i.e.

$$p(n_0) = \sum_{n_1,n_2 \ldots n_q} p(n_0;n_1;n_2;\ldots;n_q) \qquad \ldots (7.8)$$

where the summation is over all permutations of $n_1, n_2, .. n_q$ such that $n_1+n_2+ ..+n_q = N-n_0$ and $n_1+2n_2+ .. qn_q = q$. Finally for M/N detection, the probability of false alarm given q is obtained as:

$$\begin{aligned} P_{fa}(q) &= \text{probability that M or more of the N bursts contain an exceedance} \\ &= \text{probability that N - M or less bursts do not contain an exceedance} \\ &= \sum_{j=0}^{N-M} p(n_0 = j) \end{aligned} \quad \ldots (7.9)$$

7.2.3 Expected probability of false alarm

Eqns. (7.8) and (7.9) are functions of q, the total number of exceedances, which is a random variable with PDF $p_q(q)$ defined by eqn. (7.5) earlier. Therefore, the expectation of false alarm probability is obtained from:

$$p(n_0 = j) = \sum_{q=0}^{NK-r} p(n_0 = j|q)\, p_q(q) \quad \ldots (7.10)$$

and, noting that $p_q(q)$ is in fact a function of the threshold multiplier α, we finally get:

$$P_{fa}(\alpha) = \sum_{j=0}^{N-M} \sum_{q=0}^{NK-r} p(n_0 = j|q)\, p_q(q|\alpha) \quad \ldots (7.11)$$

where $p(n_0=j|q)$ is given by eqn. (7.8) and $p_q(q|\alpha)$ is given by eqns. (7.6) and (7.8).

7.2.4 Probability of Detection

Under the target-present hypothesis, namely H_1, assume that 1) only a single target is present in the test range bin, 2) the target spans only one cell in doppler, and 3) the target doppler varies randomly between bursts. Then the target return falls in exactly N of the NK burst-doppler bins, so that N bins contain exponential noise with PDF:

$$p_x(x) = \frac{1}{1+S} e^{-x/1+s} \quad \ldots (7.12a)$$

where S is the instantaneous SCNR, and N(K-1) bins contain background with PDF:

$$p_x(x) = e^{-x} \quad \ldots (7.12b)$$

Under these conditions the CDF of the r^{th} order statistic is (Ghandi, 1988):

$$P_{x_r}(x_r)=\sum_{i=r}^{NK}\sum_{L=\max(0;i-N)}^{\min(i;NK-N)}\binom{NK-N}{L}\binom{N}{i-L}e^{-(NK-N-L)x_r-(N-i+L)x_n/1+s}\,(1-e^{-x_r})^{L}(1-e^{-x_n/1+s})^{i-L} \quad \ldots (7.13)$$

Ideally we should now derive the bivariate PDF x_s/x_r. Unfortunately the analysis becomes intractable due to the form of $p(x_r;x_s)$ under the two-class model, and more importantly the non-random selection of the burst doppler bin in which the target falls, since there is one target return in every burst. Therefore make the simplifying approximation that the value of x_r is independent of the actual target samples received. Provided NK >> N this will not introduce serious errors. We then note that the probability of an exceedance in any burst is given by the probability that the largest of the K doppler bins' samples in the burst will exceed the threshold. The PDF of the maximum sample of K samples, each with different PDF $p_k(x)$ and CDF $P_k(x)$, is given by (David, 1981) as:

$$p_{K:K}(x) = \left[\prod_{k=1}^{K} P_k(x)\right]\sum_{k=1}^{K}\frac{p_k(x)}{P_k(x)}$$

$$= (1-e^{-x})^{K-2}\left[(K+1)(1-e^{-x/1+S})e^{-x} + (1-e^{-x})\frac{e^{-x/1+S}}{1+S}\right] \quad \ldots (7.14)$$

Evaluation of the above indicates that for S ≥ 10 dB, there is negligible difference between (7.14) and the target PDF (7.12a) in the regions of interest. This allows the detection performance, given the threshold $z = \alpha x_r$, to be approximated as:

$$P_d(z) = \int_z^{\infty}\frac{1}{1+S}e^{-x/1+S}\,dx \quad \ldots (7.15)$$

Substituting $\alpha x_r = z$, taking expectation with respect to x_r, and changing the order of integration, then yields:

$$\overline{P}_d = \int_0^{\infty} P_{x_r}(x_r)\frac{\alpha}{1+S}e^{-\alpha x_n/1+S}\,dx_r \quad \ldots (7.16)$$

Substituting eqn. (7.13) for $P_{xr}(x_r)$ and setting $e^{-xr} = u$ gives:

$$\overline{Pd} = \sum_{i=r}^{NK}\sum_{L}\binom{N-r}{L}\binom{r}{i-L}\frac{\alpha}{1+S}\int_0^1 u^{N-r-L-1+\frac{r-i+L+\alpha}{1+S}}(1-u)^{L}(1-u^{1/1+S})^{i-L}\,du \quad \ldots (7.17)$$

which is a function of S. Expanding the second binomial and using Gradshteyn relation 3.191.3 then gives:

$$\overline{P}_d(S) = \sum_{i=r}^{NK} \sum_{L} \binom{N-r}{L} \binom{r}{i-L} \frac{\alpha}{1+S} \sum_{j=0}^{i-L} (-1)^j \binom{i-L}{j} \frac{\Gamma(L+1)\Gamma(N-r-L+\frac{r-i+L+\alpha+j}{1+S}}{\Gamma(N-r+1+\frac{r-i+L+\alpha+j}{1+S})} \quad \ldots (7.18)$$

where the limits for L are as in eqn. (7.13). This is much simpler than the expression given by Ghandi (1988) which is a 4-fold summation, the inner two summations of which have more terms than the innermost summation in (7.18).

Of major interest here is performance in spiky clutter. Note that eqn. (7.18) is a function of S, the instantaneous signal to clutter-plus-noise ratio. Since the clutter power is randomly modulated by a gamma distributed modulation process, S is also a random variable, defined by $S = S_0/u_0$, where S_0 is the target power and u_0 is the instantaneous value of the modulation process in the test range bin. If, without loss of generality, we let $E(u_0) = 1$, then S_0 represents the mean SCNR. The final result, namely the expected value of P_d as a function of S_0, is then obtained by substituting $S_0/u_0 = S$ into (7.18) and integrating over the PDF of u_0, ie:

$$\overline{\overline{P_d}}(S_0) = \int_0^\infty \overline{P_d}\left(\frac{S_0}{u_0}\right) p_{u_0}(u_0)\, du_0 \quad \ldots (7.19)$$

where $p_{u_0}(u_0)$ is GAM(1/ν; ν) for negligible thermal noise.

To summarise the performance analysis of the ideal case of perfect power normalisation:

1) P_{fa} is obtained as a function of the threshold multiplier α, and the parameters M, N, K and r_0, from eqn. (7.11), which is in turn obtained from eqns. (7.5) and (7.6)
2) Inversion of the result prescribes the value of α required for the specified P_{fa}.
3) The detection probability as a function of the instantaneous SCNR is obtained from eqn. (7.18). The expected detection probability in spiky clutter is obtained as a function of mean SCNR S_0 from eqn. (7.19).
4) The detection performance relative to an ideal detector is best examined by comparing the value of S_0 required to achieve Pd = 50%. This is obtained by numerically inverting eqn (7.19).

Sample results have been calculated for $P_{fa} = 10^{-4}$ and the following system parameters:

1) M = 1 N = 3 K= 16 r_0 = 32
2) M = 2 N = 5 K= 16 r_0 = 53
3) M = 3 N = 8 K= 16 r_0 = 86

4) M = 1 N = 3 K= 8 $r_0 = 16$
5) M = 2 N = 5 K= 8 $r_0 = 27$
6) M = 3 N = 8 K= 8 $r_0 = 43$

They have been included in Fig. 7.2 along with results for non-ideal cases, and will be discussed in Section 7.3.5.

7.3 ESTIMATION OF THE POWER NORMALISATION TERMS

In this section the estimator of the power normalisation terms is described and the influence on detection performance of adaptive power normalisation is assessed.

The normalisation processor is based on the assumption that the relative powers between the dopplers remains constant over the processor's range reference window. We therefore seek an estimator of the power in each doppler with which to normalise the samples in the dopplers in the test range cell. Two alternatives have been examined, namely:

1) A standard Order Statistic mean level estimator acting independently on each doppler.
2) An estimator based only the power ratios between dopplers

The false alarm probability performance of the former approach was found to be sensitive to the degree of clutter spikiness (ie. the shape parameter ν), albeit less dramatically than conventional CFAR processors. For this reason detection performance was not evaluated in any detail and the analysis of the former approach will not be included in this thesis.

Some notation and the structure of the estimator of the power normalisation terms is defined in the next subsection. Thereafter the performance analysis follows similar principles to the ideal case, except that additional approximations are required. The performance analysis can be outlined as follows:

1) Determining the PDF of the power normalisation terms.
2) Determining the PDF of the power normalised samples in the test range bin.
3) Determining the PDF of the test statistic
4) Determining the PDF of the maximum sample in a burst under the target absent hypothesis
5) Determining the probability that the maximum sample within a burst will exceed the threshold and cause or contribute to a false alarm, as a function of the

threshold multiplier α.

6) Calculating the probability of a false alarm following M/N detection over N bursts as a function of α, and inversion of the result to give the necessary value of α for the prescribed P_{fa}.
7) Determining the PDF of the maximum sample in a burst under the target present hypothesis
8) Calculating the detection probability on each burst, and after M/N detection, as a function of instantaneous SCNR, using the the value of α obtained above.
9) Calculating the expected detection probability as a function of the expected SCNR. Solution of the inverse function for $P_d = 50\%$ can then yield the detection loss relative to the ideal detector.

7.3.1. Some notation and a description of the power normalisation processor

The square-law detector output of the received sample in range bin m ($1 \le m \le R$), in doppler bin k ($1 \le k \le K$), and on burst n ($1 \le n \le N$) is denoted x_{mkn}, which can be written as:

$$x_{mkn} = u_m \gamma_k s_{mkn} \quad \ldots (7.20)$$

where

s_{mkn} is the speckle in range-doppler-burst bin (m,k,n), and is iid. unit mean exponential noise for all m,k,n on the assumption of essentially non-overlapping doppler filters.

γ_k is the mean power in the k^{th} doppler bin, which is assumed invariant with range, and depends on the clutter spectrum and the filter response.

u_m is the modulation process (ie. the local clutter RCS) in the m^{th} range bin. It is invariant with doppler (a property of K-clutter) and time (on the assumption that the correlation time of the modulation process is much longer than the radar dwell time), and is gamma distributed with mean value 1 and shape parameter ν.

Define the power ratio between doppler bins i and j as r_{ij}, ie.

$$r_{ij} = \frac{\gamma_i}{\gamma_j} \quad \ldots (7.21)$$

and define $y_m(i,j)$ as:

$$y_m(i,j) = \frac{\sum_{n=1}^{N} x_{min}}{\sum_{n=1}^{N} x_{mjn}} = \frac{\gamma_i \sum_{n=1}^{N} s_{min}}{\gamma_j \sum_{n=1}^{N} s_{mjn}} \qquad \ldots (7.22)$$

Thus $y_m(i,j)$ can be seen to be an estimator of r_{ij} and is independent of u_m. The statistics of the modulation process, and hence the clutter spikiness, would therefore not affect an estimator of the power normalisation terms based on the $y_m(i,j)$. We therefore seek an estimator of the power normalisation term $1/\gamma_k$ for each doppler k, based only on the $y_m(i,j)$.

In order to determine the structure of the estimator, assume initially that the power ratios r_{ij} are known. Then define:

$$P = \gamma_1 + \gamma_2 + \ .... + \gamma_K = \sum_{k=1}^{K} \gamma_k \qquad \ldots (7.23)$$

[P as defined above represents the total power; however, its actual value does not in fact need to be determined since it appears in the result only as a scaling factor operating equally on all dopplers. Its value is therefore arbitrary and can be chosen to suit processing requirements and limitations.] Dividing eqn. (7.23) by $P\gamma_j$ and substituting eqn. (7.21) gives:

$$\frac{1}{\gamma_k} = \frac{1}{P} \sum_{i=1}^{K} r_{ik} \qquad \ldots (7.24)$$

where, by definition, $r_{ij}=1$.

It is now necessary to investigate the form of an estimator of the r_{ij}. We seek an estimator which has the following properties:-

1) It should use all the available reference cell samples x_{mkn}.
2) It must be unbiased (ie. $E(\hat{r}_{ij}) = r_{ij}$)
3) It should be robust against contamination by non-representative samples in the reference window.
4) It should have "minimum" variance.

Rigorous Maximum Likelihood or Minimum Variance estimators are intractable for this problem and also are highly unlikely to provide any measure of immunity against non-representative samples in the reference window. Drawing on OS-CFAR knowledge of

previous Chapters, it is therefore proposed to use an estimator of the form:

$$\hat{r}_{ij} = \frac{1}{a} y_{r_1:R}(i,j) \qquad \ldots (7.25)$$

That is, the estimate $\hat{r}_{ij}$ is taken as the r_1^{th} largest sample of the R ordered values of $y_m(i,j)$. Such an estimator meets the requirements above, subject to the following notes:

1) The choice of r_1 affects the variance of the estimate: higher values of r_1 tend to yield smaller estimation variance at the expense of reduced immunity to extraneous targets. In general r_1 is chosen in the range $R/2 \leq r_1 \leq 3R/4$.
2) The constant term a in (7.25) is defined by $a = E[y_{r_1:R}(i,j)|_{\gamma_i=\gamma_j=1}]$ and ensures that the estimator is unbiased. It depends only on r_1, R and N, and is therefore *a priori* known.
3) $y_m(i,j)$ is defined as above in (7.22) in order to achieve minimum variance. It is easy to verify that the variance of the $\hat{r}_{ij}$ based on $y_m(i,j)$ as defined above in (7.22) is lower than would be achieved if averaging over the N bursts was performed *after* division between dopplers.

Finally, substituting the estimator $\hat{r}_{ij}$ for r_{ij} in (7.24) gives the estimator for the power normalisation terms $1/\gamma_k$ as:

$$\frac{1}{\hat{\gamma}_k} = \frac{1}{Pa}\sum_{i=1}^{K} \hat{r}_{ik} = \frac{1}{Pa}\sum_{i=1}^{K} y_{r_1:R}(i,k) \qquad \ldots (7.26)$$

A functional block diagram of the RDT processor illustrating the power normalisation estimator defined above is illustrated in Fig. 7.1. The notation and dimension of data at various points in the processor is included in the diagram.

7.3.2. Statistics of the power normalisation terms

The PDF of the power normalisation terms $1/\widehat{\gamma_k}$ obtained from eqn. (7.26) is now derived. The PDF of x_{mkn} is negative exponential with mean $u_m\gamma_k$. The PDF of $\xi_{mk} = \sum_n x_{mkn}$ is therefore gamma distributed with shape parameter N and scale parameter $u_m\gamma_k$. It therefore follows that $y_m(i,j)$ is F-distributed (Johnson, 1969), ie.:

$$p_{y_m(i,j)}(y) = \frac{\Gamma(2N)}{\Gamma(N)^2}\left(\frac{\gamma_j}{\gamma_i}\right)^2 \frac{y^{N-1}}{[1+\frac{\gamma_j}{\gamma_i}y]^{2N}} \qquad \ldots (7.27)$$

To get the PDF of the order statistic $y_{r1:m}(i;j)$ we first need the CDF of $y_m(i;j)$, simple expressions for which have not been found in the literature. By definition:

$$P(Y_m \leq y) = I_\omega(N;N) \qquad \ldots (7.28)$$

where

$$\omega = \frac{y\gamma_i/\gamma_i}{1+y\gamma_i/\gamma_i}$$

and $I_\omega(N;N)$ is an incomplete Beta function. But from David (1981) p. 8:

$$I_{P(y)}(r;n-r+1) = \sum_{i=r}^{n} \binom{n}{i} [P(y)]^i [1-P(y)]^{n-i} \qquad \ldots (7.29)$$

and setting $P(y) = y/1+y$; $r = N$; and $n = N+N-1 = 2N-1$, we then get:

$$P(Y_m<y) = \sum_{i=N}^{2N-1} \binom{2N-1}{i} \left[\frac{\left(\frac{\gamma_i}{\gamma_i}\right)y}{1+\frac{\gamma_i}{\gamma_i}y}\right]\left[1 - \frac{\frac{\gamma_i}{\gamma_i}y}{1+\frac{\gamma_i}{\gamma_i}y}\right]^{2N-1-i}$$

$$= \frac{1}{\left(1+\frac{\gamma_i}{\gamma_i}y\right)} \sum_{i=N}^{2N-1} \binom{2N-1}{i} \left(\frac{\gamma_i}{\gamma_i}y\right)^i \left[\frac{\frac{\gamma_i}{\gamma_i}y}{1+\frac{\gamma_i}{\gamma_i}y}\right]\left[1\frac{\frac{\gamma_i}{\gamma_i}y}{1+\frac{\gamma_i}{\gamma_i}y}\right]^{2N-1-i} \qquad \ldots (7.30)$$

From eqn. (7.25) $\hat{ar}_{ij}$ is defined as the r_1^{th} out of R order statistic of the $y_m(i;j)$. Its PDF can be obtained as :-

$$p_{\hat{ar}_{ij}}(\hat{r}) = r\binom{R}{r}[1-P_{y_{ij}}(\hat{r})]^{R-r}\,[P_{y_{ij}}(\hat{r})]^{r-1}\,p_{y_{ij}}(\hat{r})$$

$$= r\binom{R}{r}\frac{\Gamma(2N)}{\Gamma(N)^2}\left(\frac{\gamma_j}{\gamma_i}\right)^N \hat{r}^{N-1}\,[1+\frac{\gamma_i}{\gamma_i}\hat{r}]^{1-R(2N-1)}$$

$$\times\left[\sum_{p=0}^{N-1}\binom{2N-1}{p}\left(\frac{\gamma_j}{\gamma_i}\hat{r}\right)^p\right]^{R-r}\left[\sum_{p=n}^{2N-1}\binom{2N-1}{p}\left(\frac{\gamma_j}{\gamma_i}\hat{r}\right)^p\right]^{r-1} \qquad \ldots (7.31)$$

This describes the marginal PDFs of each of the $y_{r1:R}(i;j)$ terms in eqn. (7.26). Strictly speaking these terms are not independent, due to the same data series being used in the denominator in calculating the $y_m(i;j)$ m= 1..R. The multivariate PDF is, unfortunately, not tractable. However, the resulting dependence is weak and can generally be ignored in analyses (David, 1981), even when averaging of the $y_m(i;j)$ is used as opposed to using order statistics. The use of order statistics to estimate $E(y_m(i;j))$ will further reduce dependence between the $y_{r1:R}(i;j)$ (i;j= 1...k) since the r^{th} order statistic may correspond to a different range bin for each i and j. We therefore approximate the $y_{r:R}(i;j)$ as being independent with PDF as defined by eqn. (7.31).

To obtain the PDF of the power normalisation terms $1/\hat{\gamma}_k$ recall from eqn. (7.26) that they are obtained as the summation over i of the $y_{r1:R}(i;k)$. Hence the PDF of $aP/\hat{\gamma}_k$ is obtained through convolution of the PDFs of $y_{r1:R}(i;k)$ i=1 to K, given by eqn. (7.31); or through multiplication of their K characteristic functions followed by inverse fourier transformation. Neither approach is feasible analytically. For reasons of computational efficiency the FFT approach has been used here.

It can now be noted that the PDF of $1/\hat{\gamma}_k$, will vary according to the values of the γ_k's (ie. the clutter spectrum), since large $\hat{r}_{ij}$ in (7.26) will dominate the the summation and hence the estimate $1/\hat{\gamma}_k$. It is evident that the PDFs of the $1/\hat{\gamma}_k$ are bounded by two extreme cases, namely where 1) all the γ_k's are equal, yielding the lowest estimation variance, and 2) where one of the γ_k's is much greater than all the others and thus dominates the others in the summation of (7.26). This yields one $1/\hat{\gamma}_k$ (corresponding to the the large γ_k) with low variance, while the other $1/\widehat{\gamma_k}$'s have higher variance. These two cases are considered separately below.

a) all the γ_k's are equal

As usual the characteristic function of $y_{r1:R}(i;j)$ is defined as

$$\Phi_{y_{r1:R}(i,k)}(t) = \int_{-\infty}^{\infty} p_{y_{r1:R}(i,k)}(y)\, e^{jty}\, dy \qquad \ldots(7.32)$$

Then by eqn. (7.26) and the properties of characteristic functions, the characteristic function of $aP/\hat{\gamma}_k$ is:

$$\Phi_{aP/\gamma_k}(t) = \prod_{i=1}^{K} \Phi_{y_{r1:R}(i,k)}(t) \qquad \ldots(7.33)$$

and the PDF of $1/\widehat{\gamma_k}$ is therefore:

$$p_{1/\hat{\gamma}_k}(x) = \frac{1}{2\pi aP}\int_{-\infty}^{\infty} \Phi_{aP/\hat{\gamma}_k}(t)\, e^{-jtx/aP}\, dt \qquad \ldots(7.34)$$

This is analytically intractable but has been implemented using fourier transforms. For practical reasons the characteristic function of the partial sum of eqn. (7.26) excluding $\hat{r}_{kk}$ was computed and inverse fourier transformed, whereafter the PDF of $\hat{r}_{kk}$ (a delta function at aP) was included by convolution.

b) A single dominant γ_k.

Arbitrarily choose doppler bin 1 as the dominant doppler, ie. $\gamma_1 >> \gamma_k$, k = 2,3,...K.

Then, from eqn. (7.26):

$$\frac{1}{\hat{\gamma}_1} = \frac{1}{Pa}\sum_{i=1}^{K} \hat{r}_{i1} \qquad \ldots (7.35a)$$

and

$$\frac{1}{\hat{\gamma}_k} = \frac{1}{P}\sum_{i=1}^{K} \hat{r}_{ik} \approx \frac{y_{r_1:R}(1,k)}{Pa} \qquad 2 \le k \le K \qquad \ldots (7.35b)$$

The PDF of $1/\hat{\gamma}_1$ is therefore calculated in exactly the same manner as when all the γ_k are equal. The PDF of $1/\hat{\gamma}_k$ ($k \neq 1$) is merely the PDF of $y_{r_1:R}(1,k)$ scaled by 1/Pa, given by eqn. (7.31).

7.3.3. PDF of the test statistic and maxima within a burst

We have thus far derived expressions for the PDF of the power normalisation terms. It is now necessary to determine the PDF of the threshold, and the probability of the power-normalised samples exceeding the threshold, thereby causing or contributing to a false alarm.

The rigorous analysis used for calculating false alarm probability in the ideal case of perfect power normalisation relies on two assumptions, namely that:

1) the samples in the NK burst-doppler bins in the test range cell are iid.
2) they are exponentially distributed (this is enables the derivation of the closed form expression of eqn. (7.5)).

For non-ideal cases the first assumption is violated since 1) the same $1/\hat{\gamma}_k$ is used to normalise over all N bursts in each doppler, and 2) the PDFs of the $1/\hat{\gamma}_k$ will not be identical if the γ_k are not equal. In such cases the bivariate PDF of two joint order statistics of the samples in the test range cell can only be expressed in terms of permanents (Vaughan, 1972; Minc, 1978); these are neither numerically nor analytically tractable for anything other than the two-class situation addressed by Ritcey (1986), which is of no use for the K-class situation of interest here. Furthermore, the exponential background in each cell is multiplied by a random variable with finite variance (in violation of the second assumption above for the ideal case), and so the expectation of the permanent expression with respect to the power normalisation terms would need to be calculated. This does not appear to be possible.

In view of the intractability of the bivariate order statistic PDF of a K-class population, in

which the mean of each class is a (non-identically distributed) random variable, simplifying approximations are necessary. Two options have been investigated, namely:

1) Assume that the $1/\hat{\gamma}_k$ are iid. (which is true if all γ_k are equal) and that the value of $1/\hat{\gamma}_k$ within doppler k is independently drawn for each burst n = 1 ... N. Then all the samples in the test range bin *are* iid and the ideal analysis can be used. Although this approximation has minimal effect on the threshold statistics, the exceedance probabilities are noticeably affected since the tails of the distribution are modified by the approximation.

2) A reasonable approximation allowing the derivation of the bivariate PDF to be bypassed is to assume that the threshold estimator (the r_0^{th} out of the NK ordered samples) is independent of the few largest samples, or exceedances, which cause a false alarm. Provided r_0 is not too large (say in the region $NK/2 \leq r_0 \leq 2NK/3$) this approximation should not introduce significant inaccuracies due to the relative immunity of median processors and OS processors to outliers. The analysis of the threshold statistics and the exceedance statistics can now be separated, with more acceptable approximations being used: the PDF of the test statistic is based on approximation (1) given above, which is sufficiently accurate here since the tails of the distribution do not have strong influence on the test statistic PDF. The PDF of the exceedances in any burst can be calculated exactly with no further simplifications necessary, thus preserving the tails of the exceedance PDF.

In view of the exact representation of the exceedance PDF the latter option was adopted for this analysis. The effects of the approximations are expected to be as follows:

1) Approximation of independence of the test statistic and the exceedances:
The effect is expected to be minor in view of the robustness of median filters in the presence of outliers. Nevertheless, there is a slight positive correlation between the exceedances and the threshold. Thus in cases where a few very large samples - potential exceedances - are present, the threshold will also be raised, thereby reducing the probability of false alarm, and allowing a lower threshold multiplier factor to be used. The true P_{fa} would therefore be lower than predicted using this approximation, and the approximation can be considered to introduce a pessimistic bias to the analysis.

2) Approximation of independence of the $1/\hat{\gamma}_k$ on each burst within a doppler:
This assumption is made only in the calculation of the test statistic PDF. In effect

it reduces the variance of the test statistic since the effective number of independent samples from which the test statistic is derived is increased. The magnitude of errors introduced by this approximation are difficult to predict, but since the variance of the power normalisation terms is much less than that of the iid. exponential noise within a doppler with which it is multiplied, errors should not be very large. The approximation will, however, introduce an optimistic bias to the analysis since the assumed independence reduces the threshold variance, thus allowing a lower threshold multiplier to be used or yielding a lower P_{fa} than would actually be the case.

3) Approximation that all the $1/\hat{\gamma}_k$ are iid.:
This assumption is also made only in the calculation of the test statistic PDF. Under conditions of all γ_k equal, the $1/\hat{\gamma}_k$ are iid. and no approximation is required. When $\gamma_1 >> \gamma_k$, $1/\hat{\gamma}_1$ has lower variance than the other $1/\hat{\gamma}_k$, (k = 2...K). Therefore we approximate $1/\hat{\gamma}_1$ as having the same PDF of the other $1/\hat{\gamma}_k$, (k = 2...K). This will introduce a slight pessimistic bias to the analysis when $\gamma_1 >> \gamma_k$, since the variance of the test statistic will in fact be lower than predicted using this approximation. The error is expected to be small since only one of the K PDFs is modified by the approximation, and in the true situation the K-1 estimates $1/\hat{\gamma}_k$ with broader PDF (the ones unmodified by the approximation) would dominate the PDF of the test statistic.

Therefore the expected major approximation error will to some extent be counteracted by the other two approximation errors. Based on these approximations, the PDF of the test statistic and the exceedances can now be calculated.

a) PDF of the test statistic.
The received samples in the test range bin on each burst are normalised with the power normalisation terms $1/\hat{\gamma}_k$ corresponding to the doppler bin in question. The samples in the test range bin t_{kn} (k indexes doppler, n indexes burst number) are therefore obtained as:

$$t_{kn} = \frac{x_{0kn}}{\hat{\gamma}_k} = u_0 \frac{\gamma_k}{\hat{\gamma}_k} s_{0kn} \qquad \ldots (7.36)$$

The modulation process term u_0 can henceforth be neglected for the false alarm rate analysis since it applies to all samples in the test range bin. Now define $\varepsilon_k = \hat{\gamma}_k/\gamma_k$; for all γ_k equal, all the ε_k are iid. with $E(\varepsilon_k) = 1$ and PDF defined by eqn. (7.34) scaled by γ_k. For $\gamma_1 >> \gamma_k$, the PDF of ε_1 is approximated by that of the other ε_k, following which all

ε_k are iid. with $E(\varepsilon_k) = 1$ and PDF defined by (7.35), scaled by γ_k. Using the approximation that ε_k is independent for each burst n within a doppler, and dropping the k subscript on ε, since all ε_k are now assumed iid., the PDF of the samples in the test range cell is:

$$p_t(t) = \int_0^\infty \varepsilon e^{-t\varepsilon} p_\varepsilon(\varepsilon)\, d\varepsilon \qquad \ldots (7.37)$$

which is easily solved numerically. If $P_t(t)$ denotes the CDF of t, then the test statistic, taken as the r_0^{th} order statistic of the NK samples in the test range cell, has PDF given by:

$$p_z(z) = r_0 \binom{NK}{r_0} p_t(z)\, [P_t(z)]^{r_0-1}\, [1 - P_t(z)]^{NK-r_0} \qquad \ldots (7.38)$$

b) PDF of the Maxima in any burst.

The probability of having at least one exceedance in any burst is equivalent to the probability that the largest of the K dopplers' samples within that burst exceeds the threshold. The PDF of the maximum sample t_{max} of K samples t_k, each with different PDF $p_k(t)$ and CDF $P_k(t)$, is given by (David, 1981):

$$p_{t_{max}}(t) = \left[\prod_{k=1}^{K} P_k(t)\right] \sum_{k=1}^{K} \frac{p_k(t)}{P_k(t)} \qquad \ldots (7.39)$$

Noting that $t_{kn} = \varepsilon_k u_0 s_{0kn}$, and dropping the n subscript (since we are now working within a single burst) and the modulation process term u_0 (which applies to all samples in the test range cell), the PDFs $p_k(t)$ and CDFs $P_k(t)$ are given by:

$$p_k(t) = \varepsilon_k e^{-\varepsilon_k t}$$
$$P_k(t) = 1 - e^{-\varepsilon_k t} \qquad \ldots (7.40)$$

Therefore

$$p_{t_{max}}(t) = \int_0^\infty \int_0^\infty \cdots \int_0^\infty p_{t_{max}}(t|\varepsilon_1, \varepsilon_2, \ldots \varepsilon_k) p_{\varepsilon_1}(\varepsilon_1) p_{\varepsilon_2}(\varepsilon_2) \cdots p_{\varepsilon_k}(\varepsilon_k)\, d\varepsilon_1 d\varepsilon_2 \ldots d\varepsilon_k \qquad \ldots (7.41)$$

Substituting eqn. (7.40) into (7.39), and (7.34) or (7.35) and (7.39) into (7.40), changing the order of summation and integration, and some manipulation yields:

$$p_{t_{max}}(t) = \sum_{k=1}^{K} \left[\int_0^\infty \varepsilon_k e^{-\varepsilon_k t}\, p_{\varepsilon_k}(\varepsilon_k) d\varepsilon_k\right] \prod_{\substack{j=1 \\ j \neq k}}^{K} \int_0^\infty (1 - e^{-\varepsilon_j t})\, p_{\varepsilon_j}(\varepsilon_j) d\varepsilon_j \qquad \ldots (7.42)$$

and since all the ε_k are iid. we get:

$$p_{t_{max}}(t) = K\left[\int_0^\infty \varepsilon e^{-\varepsilon t}\, p_\varepsilon(\varepsilon) d\varepsilon\right]\left[\int_0^\infty (1-e^{-\varepsilon t})\, p_\varepsilon(\varepsilon)\, d\varepsilon\right]^{K-1} \quad \ldots (7.43)$$

which is easily solved by numerical techniques.

7.3.4. Probability of false alarm

Having obtained the PDF of the test statistic $p_z(z)$ from eqn. (7.38) and the PDF of the maxima within a burst $pt_{max}(t)$ from eqn. (7.43), the probability of false alarm on any one burst is calculated as a function of the threshold multiplier factor α as:

$$P_{fa_1}(\alpha) = \text{Prob}\,[t_{max} > \alpha z] = \text{prob}\left[\frac{t_{max}}{\alpha} > z\right] = \int_0^\infty p_z(z) \int_z^\infty \alpha\, p_{max}(\alpha t)\, dt\, dz \ldots (7.44)$$

Performing M/N detection over N bursts, the final output P_{fa_0} is:

$$P_{fa_0}(\alpha) = \sum_{n=M}^{N} \binom{N}{n} [P_{fa_1}(\alpha)]^n\, [1 - P_{fa_1}(\alpha)]^{N-n} \quad \ldots (7.45)$$

The required threshold α is obtained through (numerical) inversion of eqn. (7.45).

7.3.5. Detection probability

Under the target present hypothesis it is again impossible to find the bivariate PDF of the ordered sample since, as in the false alarm analysis, the ε_k are still not iid. Furthermore, target returns are also now present which introduce another N classes to the reference samples, since each target return may be multiplied by a different ε_k. The assumption of independence between the burst maxima and the test statistic made in the false alarm analysis is not suitable here since for strong target signals N of the burst doppler samples will contain large returns, which will bias the test statistic upwards. In order to avoid this assumption we therefore determine the PDF of test statistic z for two limiting cases:

1) when the target signal is very weak, in which case the target presence does not influence E(z) and $p_z(z)$ is as for the target absent case.

2) when the target signal is very strong, in which case target returns occupy the N largest of the NK ordered samples. The test statistic can then be considered as the r_0:NK-N order statistic when the NK-N reference samples contain only clutter and/or noise. The test statistic PDF is then given by eqn. (7.38), except replacing

NK with (NK-N).

The PDF of the maximum of the samples in the K dopplers within a burst n is again given by eqn. (7.39). Under conditions of a target being present (in say doppler 1), the PDF and CDF of the single sample in the burst containing the target return is given by:

$$p_1(t) = \frac{\varepsilon_1}{(1+S)} e^{-\varepsilon_1 t/(1+S)}$$

$$P_1(t) = 1 - e^{-\varepsilon_1 t/(1+S)} \qquad \ldots (7.46)$$

where S is the instantaneous SCNR and ε_1 is as defined in section 7.3.3. The PDF and CDF of the other K-1 samples in the burst which do not contain target returns are given by eqn. (7.40). Substituting eqns. (7.46) and (7.40) into eqn. (7.39), and rearranging terms, gives:

$$p_{t_{max}}(t) = \frac{\varepsilon_1}{1+S} e^{-\varepsilon_1 t/1+S} \prod_{j=2}^{K} \{1-e^{-\varepsilon_j t}\} + (1-e^{-\varepsilon_1 t/1+S}) \sum_{j=2}^{K} \varepsilon_j e^{-\varepsilon_j t} \prod_{\substack{p=2 \\ p \neq j}}^{K} (1-e^{-\varepsilon_p t/1+S}) \qquad \ldots (7.47)$$

term 1 terms 2, 3, ...K

which as indicated is a summation of K terms. Since the ε_k are iid. random variables with PDF $p_{\varepsilon k}(\varepsilon_k)$ equation (7.41) must be used again here to give the the PDF of the maxima in each burst. Substituting eqn. (7.47) into (7.41), noting that $p_{\varepsilon i}(\varepsilon_i) = p_{\varepsilon j}(\varepsilon_j)$ for all i,j ≥ 2, and some rearranging gives:

$$\text{Term 1} = \int_0^\infty \frac{\varepsilon}{1+S} e^{-\varepsilon t/1+S} p_\varepsilon(\varepsilon) d\varepsilon \left[\int_0^\infty \{1-e^{-\varepsilon_j t}\} p_\varepsilon(\varepsilon) d\varepsilon\right]^{K-1} \qquad \ldots (7.48a)$$

$$\text{Terms 2,3...K} = (K-1)\left[\int_0^\infty (1-e^{-\varepsilon t/1+S}) p_\varepsilon(\varepsilon)\, d\varepsilon\right]\left[\int_0^\infty \varepsilon e^{-\varepsilon t} p_\varepsilon(\varepsilon)\, d\varepsilon\right]\left[\int_0^\infty (1-e^{-\varepsilon t}) p_\varepsilon(\varepsilon)\, d\varepsilon\right]^{K-2} \qquad \ldots (7.48b)$$

Then defining

$$I_1 = \int_0^\infty \frac{\varepsilon}{1+S} e^{-\varepsilon t/1+S} p_\varepsilon(\varepsilon)\, d\varepsilon$$

$$I_2 = \int_0^\infty (1-e^{-\varepsilon t}) p_\varepsilon(\varepsilon)\, d\varepsilon$$

$$I_3 = \int_0^\infty (1-e^{-\varepsilon t/1+S}) p_\varepsilon(\varepsilon)\, d\varepsilon$$

$$I_4 = \int_0^{\infty} \varepsilon e^{-\varepsilon t}\, p_\varepsilon(\varepsilon)\, d\varepsilon \qquad \ldots (7.49)$$

each of which can be evaluated numerically, gives a final expression for the PDF of the maximum sample in each burst as:

$$p_{t_{max}}(t) = I_2^{K-2}\,[I_1\, I_2 + I_3\, I_4] \qquad \ldots (7.50)$$

The probability that the maximum sample on each burst will exceed the threshold is given as a function of the threshold multiplier factor α and the instantaneous SCNR by:

$$P_{d_1}(\alpha;S) = \text{Prob}[t_{max}(S)|_{H_1} > \alpha z] = \text{Prob}\left(\frac{t_{max}}{\alpha} > z\right)$$

$$= \int_0^{\infty} p_z(z) \int_z^{\infty} \alpha\, p_{t_{max}}(\alpha t|S)\, dt\, dz \qquad \ldots (7.51)$$

where α is obtained as described in Section 7.3.3; $p_{t_{max}}(\alpha t|S)$ is defined in eqns. (7.49) and (7.50), and $p_z(z)$ is defined by eqn. (7.38), with either NK or (NK-1) as the number of reference samples, depending on which of the limiting cases defined at the beginning of this subsection is adopted. Then, for M/N detection:

$$\overline{P}_{d_0}(\alpha;S) = \sum_{n=M}^{N} \binom{N}{n} [P_{d_1}(\alpha;S)]^n\, [1-P_{d_1}(\alpha;S)]^{N-n} \qquad \ldots (7.52)$$

Since u_0 is a GAM(1/ν;ν) random variable, the expected detection probability is obtained by substituting eqn. (7.52) above into eqn (7.19).

Notes:

1) Using $v=\sqrt{u}$ and $p_v(v)$ in eqn. (7.19) yields an integral which does not tend to ∞ as $\nu \to 0$ (for $\nu \geq 1/2$) and is hence easier to integrate numerically.
2) The implicitly assumed independence between P_{d1} on different bursts in eqn. (7.52) is true for the limiting cases considered here, since the test statistic is unaffected by the target returns under the limiting assumptions.
3) The limiting cases using either NK or NK-N as the number of reference samples in eqn. (7.38) indicates bounds on detection probability. The true value of P_d lies between these extremes. As an approximation to the true value, noting that for small SCNRs $N_{ref} \to$NK whereas for high SCNRs $N_{ref} \to$NK-N, the detection probability for non-limiting cases can be averaged as:

$$\tilde{P}d_0 = P_{d_o}|_{NK} - P_{d_o}|_{NK\text{-}N}[P_{d_o}|_{NK} - P_{d_o}|_{NK\text{-}N}] \qquad \ldots (7.53)$$

7.3.6. Sample Results

The preceding analysis has been carried out for $P_{fa} = 10^{-4}$ and the following system parameters:

a)	M = 1	N = 3	K= 16	$r_0 = 32$
b)	M = 2	N = 5	K= 16	$r_0 = 53$
c)	M = 3	N = 8	K= 16	$r_0 = 86$
d)	M = 1	N = 3	K= 8	$r_0 = 16$
e)	M = 2	N = 5	K= 8	$r_0 = 27$
f)	M = 3	N = 8	K= 8	$r_0 = 43$

In all cases R = 32 (the number of range reference bins used in calculating the power normalisation terms) and $r_1 = 25$, a compromise between minimising the variance of the $1/\hat{\gamma}_k$ and immunity to extraneous targets. Results are illustrated in Fig. 7.2, where the graphs (a) to (f) correspond to the parameter combinations (a) to (f) given above. Each graph shows the post-filter single pulse SCNR required to achieve $P_d = 50\%$, as a function of the clutter spikiness. Note that the horizontal axis represents $1/\nu$, where ν is the usual K-distribution shape parameter, as this yields curves which are easier to interpolate and have better resolution in the regions of ν of interest.

Each graph illustrates the post-filter single pulse SCNR required for $P_d = 50\%$ for the following detectors and assumptions:

1) The "ideal" detector, in which the background power in each burst-doppler bin is assumed explicitly known, and the threshold set accordingly. No CFAR losses are present and this detector represents an absolute upper bound on achievable detection performance.

2) The "Ideal RDT" CFAR processor discussed in section 7.2, in which perfect power normalisation between dopplers was assumed. This processor gives an upper bound on the performance that can be achieved by RDT processors with adaptive power normalisation.

3) The adaptively normalised RDT CFAR processor discussed in the previous subsection, with the assumptions of a) all γ_k equal, and b) $\gamma_1 >> \gamma_k$. In both cases the weighted average (defined by eqn. (7.53)) of detection probability between the two limiting cases mentioned in section 7.3.5 has been used.

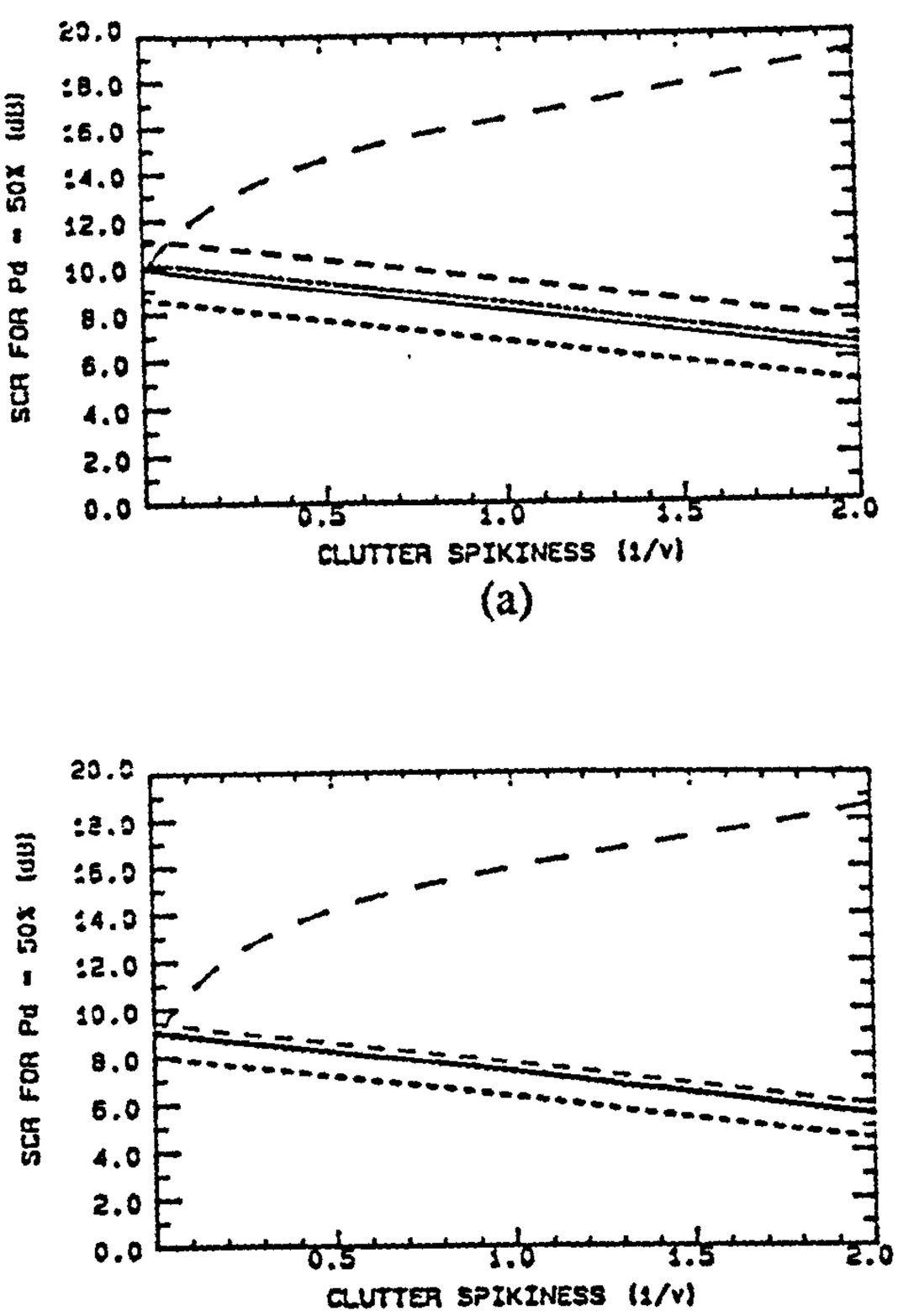

(a)

(b)

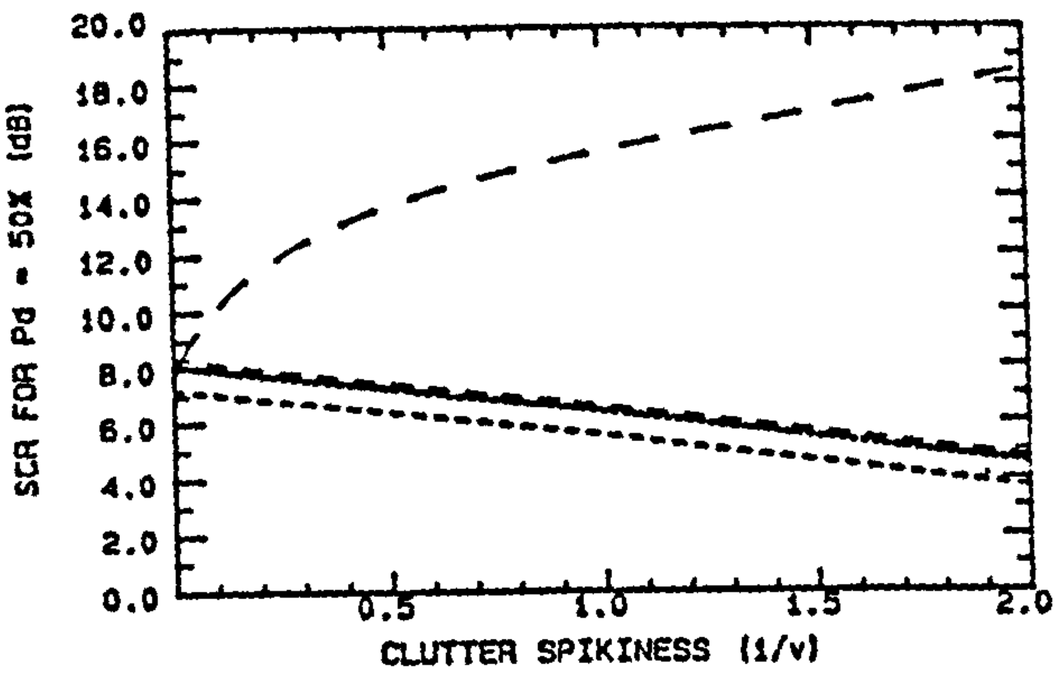

(c)

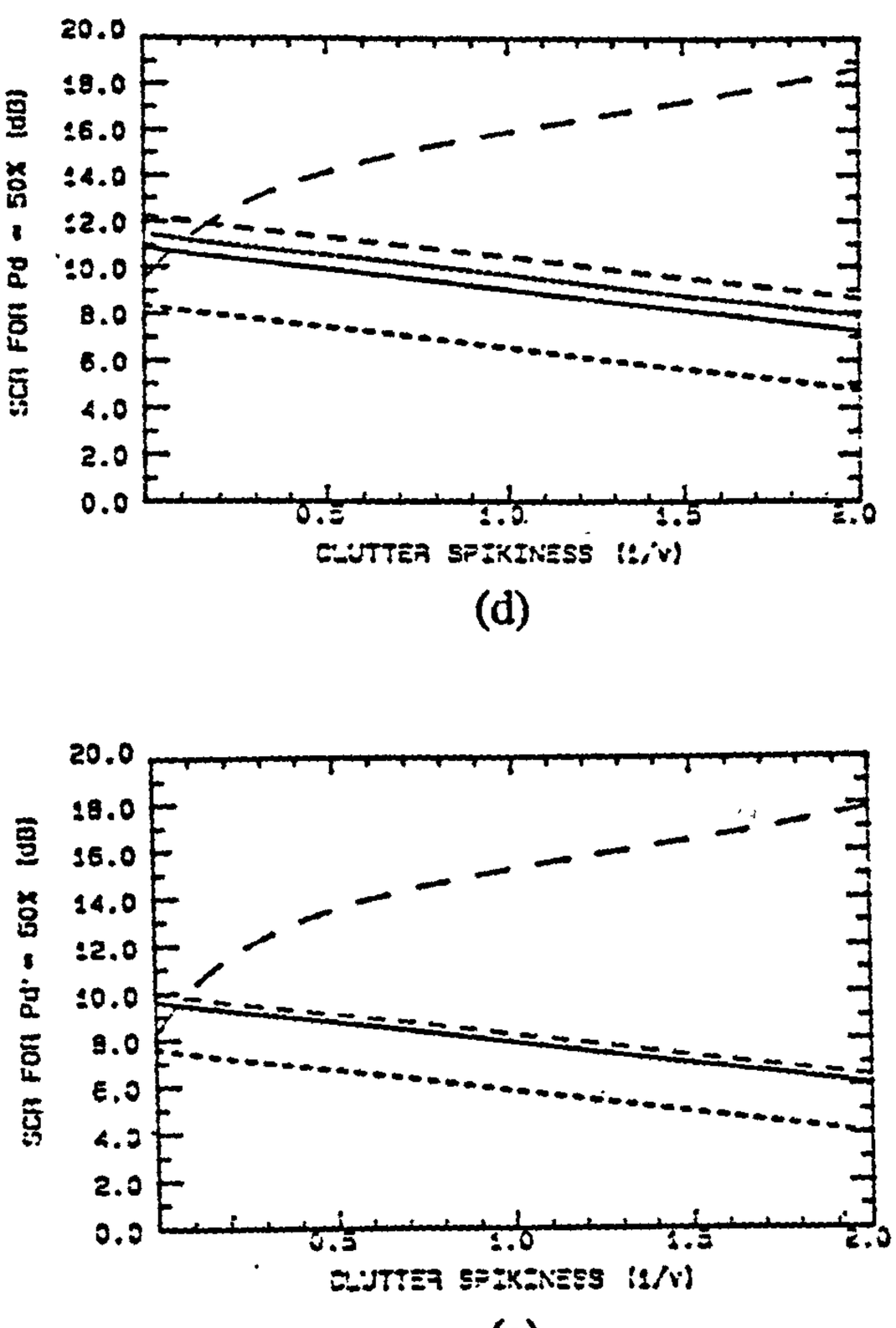

(d)

(e)

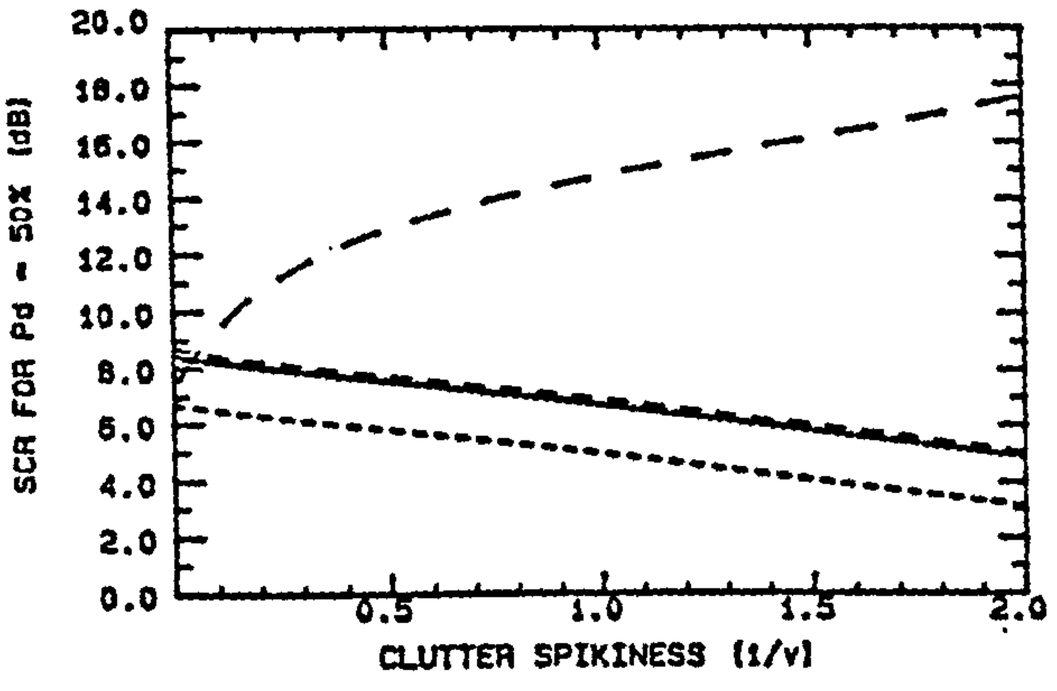

(f)

Fig. 7.2: *Performance of Ideal, RDT and conventional OS CFAR processors*
$P_d = 50\%, P_{fa} = 10^{-4}$

- - - - - - - ideal processor
——————— RDT processor with perfect power normalisation
. . . . . RDT processor with adaptive power normalisation, all γ_k equal
— — — — RDT processor with adaptive power normalisation, $\gamma_1 >> \gamma_k$
— — — conventional OS-CFAR processor.

4) A conventional OS CFAR processor with N=32, K=25, assuming ν is explicitly known. Adaptive estimation of ν, as would be necessary in practice, would introduce further losses of the order of 5 - 10 dB.

The following observations can be made with respect to Fig. 7.2:

1) The CFAR loss of the RDT processor, that is the difference between the curves for the ideal detector and the various RDT -processors, is independent of the clutter spikiness parameter ν. The *detection* loss, however, that is the difference between the SCNR required for Pd = 50% by an ideal detector in Rayleigh backgrounds (ie. exponential square law outputs) and the RDT processor in spiky backgrounds, can actually be negative. This therefore represents a gain which arises due to the non-linear nature of the detection characteristic since in spiky clutter, for the same mean clutter power, more range cells have underlying modulation below the mean value (which is biased high by the few spikes), in which a high detection probability is achieved.

2) The magnitude of the CFAR loss is in the region of 1 to 2 dB, depending on the parameters K and N. The larger K and N the lower the loss, with the dependence on K being stronger than the dependence on N.

3) The RDT-processor gives in excess of 10 dB improvement in detectability over the conventional OS-CFAR processor in even moderately spiky clutter ($\nu \sim 0.7$). In Rayleigh clutter the RDT-processor suffers a loss relative to the OS-CFAR processor of only about 1 dB for N = 8, and about 0 dB for N = 16. Note, however, that the OS processor performance illustrated is based on the assumption of *a-priori* knowledge of the clutter shape parameter ν. In practice ν will have to be estimated on line. This will introduce further loss to the OS processor of the order of 5 - 10 dB (Ravid, 1992).

4) For adaptive power normalisation under the assumption of all the γ_k equal, and for N = 5 and N = 8, the weighted average (between the limiting cases using NK and NK-N reference samples in eqn. (7.38)) yields a value of S_{50} which is about 0.1 dB lower than that for perfect power normalisation. This is clearly impossible and can be explained by 1) the assumption of independence of the $1/\hat{\gamma}_k$ within a doppler in calculating the PDF of the test statistic introduces an optimistic bias to the analysis, as discussed in section 7.3.3, and 2) the weighting applied in eqn.

(7.53) may not give sufficient weight to the NK-N limiting case of detection probability. Nevertheless the NK and NK-N limiting cases differ by only about 0.6 dB for K=16 and 1.2 dB for K=8, implying an error of less than 0.3 dB and 0.6 dB respectively.

5) As would be expected from the analysis, the RDT processor suffers a slight loss if all the γ_k are not equal. This situation is bounded by the case where one doppler dominates (ie. $\gamma_1 >> \gamma_k$; k = 2...K), where a loss of only 1.3, 0.3 and 0.2 dB respectively for N = 3, N = 5 and N = 8 is evident. The loss is largely independent of K and arises as a result of less averaging between the $\hat{r}_{ik}$ of eqn. (7.26).

The RDT-CFAR processor requires that the underlying clutter power remains constant over all N bursts. This implies that a constant PRF be used if range-ambiguous clutter is present, in which case blind speed elimination would still be achieved by burst-burst frequency agility. Alternatively, interleaving the pulses for each transmit frequency, instead of using successive contiguous bursts could extend the unambiguous range to N times the instrumented range, thereby all but eliminating the effect of range-ambiguous clutter.

7.3.7. Performance deterioration in spectrally heterogeneous backgrounds

The preceding analysis has assumed that the clutter spectrum is constant over range and is independent of clutter amplitude. This is the same idealisation that is made in most adaptive doppler filtering analyses, and will similarly break down under some conditions. Even if the spectrum of the clutter is constant, amplitude-fluctuating clutter in the presence of background thermal noise will cause a composite spectrum which is not constant owing to the fluctuating level of the noise floor. This causes sub-optimal performance in the RDT-CFAR processor since the level of the noise relative to the clutter in the test range bin may differ from the mean. Thus the power normalisation terms, approximately equal to the inverse of the mean spectrum, may not reflect the instantaneous spectrum in the test cell. Therefore after power normalisation some dopplers may have mean level significantly higher than the overall reference sample mean, and samples in those dopplers have higher probability of exceeding the threshold and causing a false alarm.

This situation has been examined by simulation since, as previously mentioned, analytic expressions for the test statistic are not available in multi-class reference sample

populations. The false alarm probability has been simulated for K = 16; M/N = 1/3 and K = 8; M/N = 3/8. In each case r_0 was set at the nearest integer to 2NK/3; NK-2N; and NK-N. (The rationale for the use of higher r_0 is that the test statistic will be drawn from dopplers with high mean level, thereby reducing the possibility of samples in the poorly normalised dopplers exceeding the threshold.) In addition, the use of increased threshold multiplier factors α' was investigated by setting $\alpha' = \alpha$; 1.5α; 2α; and 4α. The clutter spectrum was assumed to be Gaussian with one-sided half-power bandwidth of 0.03 PRF, 0.1 PRF and 0.25 PRF and mean CNR = 0, 10, 20, 30, 40, 50, 60 dB. The clutter power was assumed to be gamma distributed with $\nu = 0.5$. For each of combination of these parameters, the probability of false alarm was estimated by performing 10000 trials. Each trial consisted of generating the NK burst-doppler samples, performing power normalisation by the mean spectrum, ordering the samples and selecting the test statistic, comparing each sample to the threshold, logically ORing over doppler, and performing M/N detection over the bursts. The number of non-zero outcomes were counted and averaged to give an estimate of P_{fa}. The use of only 10000 trials was necessitated by computing limitations and gives poor accuracy for $P_{fa} \sim 10^{-4}$; however, it is sufficient to quantify significant increases in P_{fa} above this level.

Results for a clutter spectral width of 0.1 of the PRF are illustrated in Fig. 7.3 for K=16 and M/N=1/3; and in Fig. 7.4 for K=8 and M/N=3/8. The following points can be noted:

1) There is a significant increase in P_{fa} for many values of CNR of practical interest.
2) The increase in P_{fa} is less severe for high values of r_0.
3) The increase in P_{fa} can be greatly reduced by moderate increases in the threshold multiplier factor, particularly for high values of r_0.
4) There is not a notable difference in the increase in P_{fa} between K=16; M/N=1/3 and K=8; M/N=3/8.

Similar results for clutter spectral widths of 0.03 and 0.25 of the PRF are tabulated in Appendix 7.1. Although these results are a little erratic due to the low false alarm counts, they show that for these spectral widths the increase in P_{fa} is not as severe as that illustrated in Figs. 7.3 and 7.4. Analysis of the value of u_0 used during trials giving a false alarm indicated that false alarms are generally associated with very low values of u_0, where the power normalisation terms underestimate the level of the noise relative to the clutter, so that dopplers in which the noise dominates the clutter are in fact amplified by power normalisation. For very wide and very narrow clutter spectra this affects several dopplers, thereby enabling the threshold to "track" incorrectly normalised dopplers more closely. For intermediate spectral widths, however, only a few doppler bins furthest

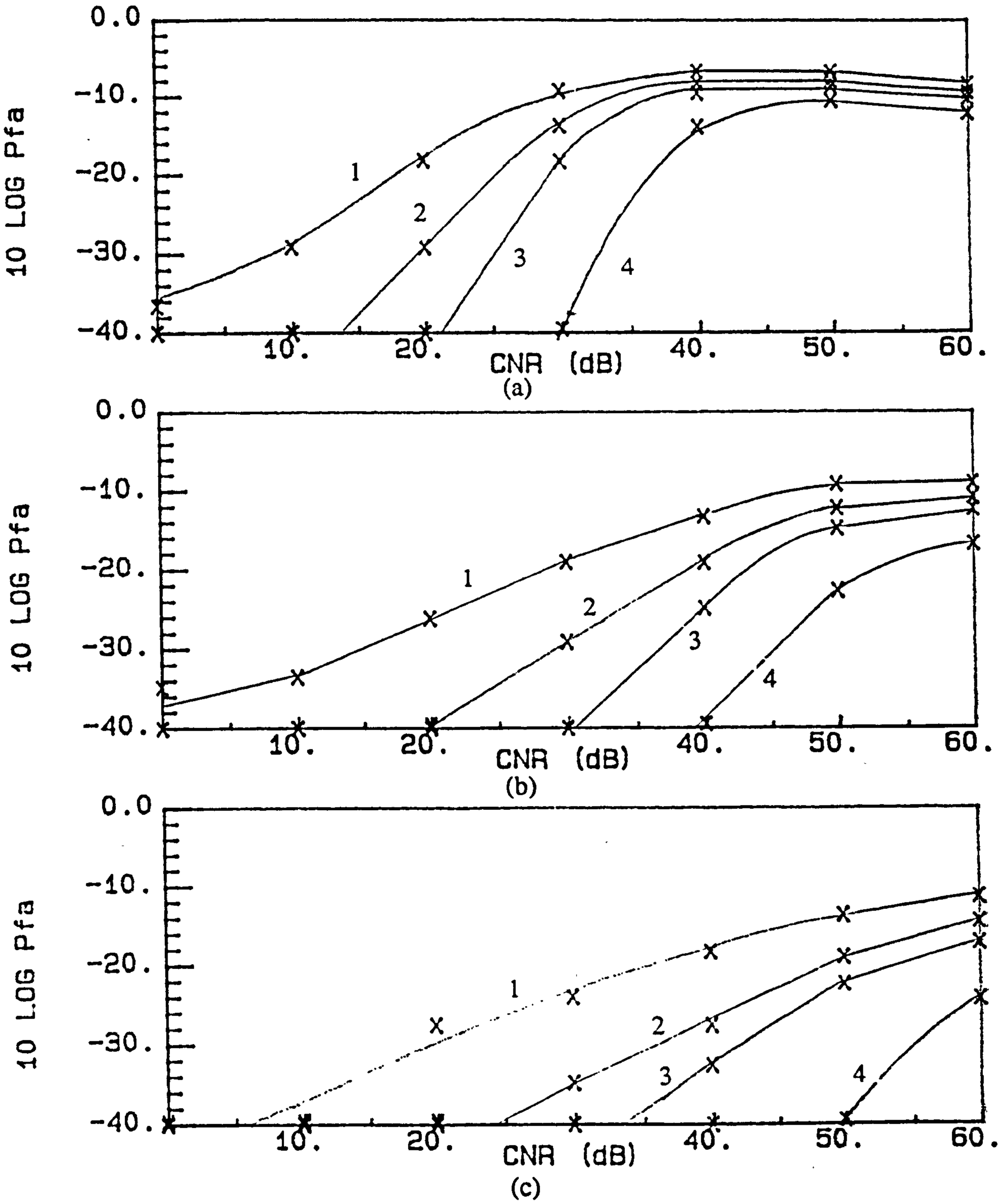

Fig. 7.3: *False Alarm Probability in Clutter with Finite CNR. K = 16; MIN= 113*

Clutter spectral width = 0.1 PRF, $\nu = 0.5$ a) $r_0 = 2NK/3$; b) $r_0 = NK-2N$; c) $r_0 = NK-N$

(1) $\alpha' = \alpha$ (2) $\alpha' = 1.5\alpha$ (3) $\alpha' = 2\alpha$ (4) $\alpha' = 4\alpha$.

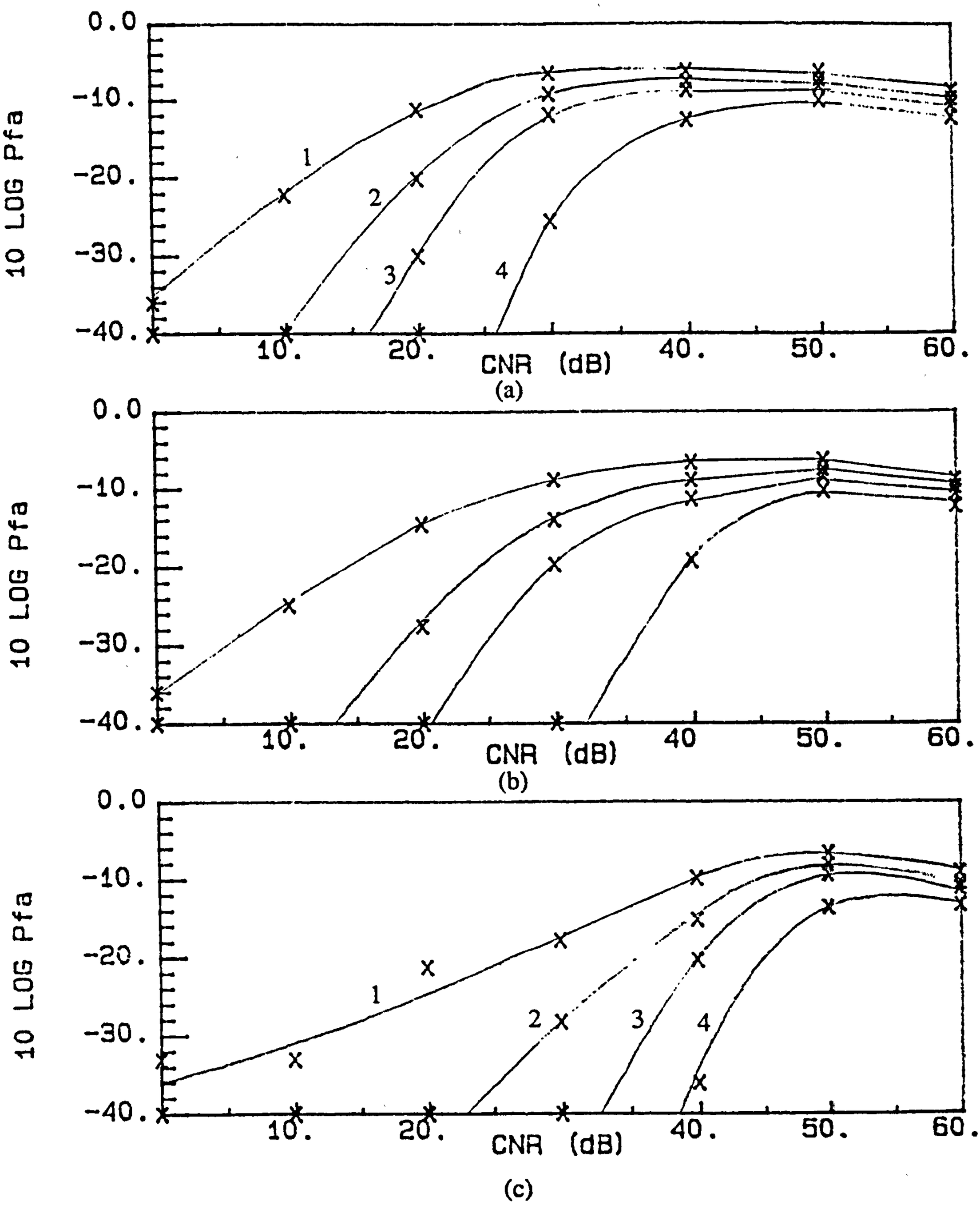

(a)

(b)

(c)

Fig. 7.4: *False Alarm Probability in Clutter with Finite CNR. K = 8; MN= 318*

Clutter spectral width = 0.1 PRF, v = 0.5 a) $r_0 = 2NK/3$; b) $r_0 = NK-2N$; c) $r_0 = NK-N$

(1) $\alpha' = \alpha$ (2) $\alpha' = 1.5\alpha$ (3) $\alpha' = 2\alpha$ (4) $\alpha' = 4\alpha$.

away from the peak of the clutter spectrum are "amplified" by incorrect power normalisation. These few doppler bins thus regularly exceed the threshold, causing the observed increase in P_{fa}.

Despite the fact that the results presented in Figs. 7.3 and 7.4 are worst case results, it is evident that under certain practical conditions the RDT processor suffers an increase in P_{fa} which can only be partially counteracted by the use of a higher value of r_0 and/or an increased threshold multiplier factor (at the expense of increased loss). The false alarm probability is also not constant under conditions of spectrally varying clutter or finite CNRs. These problems, although shared by conventional CFAR processors and in fact less severe than for the OS processor, may limit the practical applications of the RDT-CFAR processor.

7.4 MULTI-BURST CFAR PROCESSOR WITHOUT RANGE REFERENCING

7.4.1 Rationale and Processor Description

The deterioration in performance suffered by the RDT processor in spectrally heterogeneous backgrounds arises due to the fact that the power normalisation terms, derived from surrounding range bins, are not necessarily representative of the spectrum in the test range bin. It is reasonable to argue, therefore, that a solution to this problem lies in formulating a processor which does not require power normalisation, and thereby avoids any use of data from range bins other than the test range bin. Such a processor is presented in this section.

Functionally the processor can be described as follows:

* For each doppler, sort the returns from the N bursts into ascending order.
* Select the r_0^{th} ordered sample in each doppler as the test statistic for that doppler.
* Multiply the K test statistics by the threshold multiplier factor α, to obtain the threshold for each doppler.
* Compare each of the N received samples in each doppler to the corresponding threshold.
* Logically OR the NK threshold decisions over doppler, and perform M/N detection over the N bursts.

It is evident that the threshold in each doppler is derived only from samples in the test

range bin in that same doppler. No power normalisation terms are required, and therefore no other range bins are used either for estimation of the power normalisation terms or for conventional background power estimation in each doppler. The impulse response of the processor in range is thus a δ-function, and accordingly the processor outlined above will henceforth be termed the δ-CFAR processor.

7.4.2 False Alarm Probability

The probability of false alarm can be examined by the following argument: in each doppler the samples exceeding the threshold can be viewed as balls drawn from an urn containing N balls of N colours. The number of balls drawn from the urn is a random number ψ with probability function $p(\psi)$. This trial is independently repeated in each doppler, ie. K times. A false alarm occurs if at least M of the N balls are represented at least once in the K trials. This argument implies that the joint probability of the n^{th} burst being represented i times among the K trials is described by the multivariate binomial distribution (Krishnamoorthy, 1951; Johnson, 1969), conditioned on ψ. This has a relatively simple probability generating function but an analytically awkward probability function, apparently only expressible as K-fold nested loops of Krawtchouk polynomials (Krishnamoorthy, 1951). Obtaining the distribution compounded over all possible values of ψ is difficult. Furthermore, the occupancy distribution of the resulting compound distribution is ultimately required, and this has defied analytic and numerical analysis. Analysis of P_{fa} based on existing discrete distribution theory does therefore not appear to be feasible.

An alternative approach is now presented. Assume initially that at most two exceedances can occur in each doppler, ie. $p(\psi) = 0$ for $\psi>2$. Let the number of dopplers containing two exceedances (henceforth termed *doubles*) be κ_2, the number of dopplers containing one exceedance (termed *singles*) be κ_1, and the number of dopplers containing no exceedances (termed *zeroes*) be κ_0. Clearly $\kappa_0+ \kappa_1+\kappa_2 = K$. The probability of having a zero, single or double in any one doppler is denoted p_0, p_1 and p_2 respectively. These values are obtained from:

$$p_0 = 1 - p(Z>\alpha)|_{s=N}$$
$$p_1 = p(Z>\alpha)|_{s=N}$$
$$p_2 = p(Z>\alpha)|_{s=N-1} \qquad \ldots (7.54)$$

where $p(Z>\alpha)$ is obtained from eqn. (7.5), substituting N for NK. Then the probability of having κ_2 doubles amongst the K dopplers is given by the binomial distribution, $BIN(K; \kappa_2; p_2)$, ie.

$$p(\kappa_2) = \binom{K}{\kappa_2} p_2^{\kappa_2} (1 - p_2)^{K-\kappa_2} \qquad \ldots (7.55)$$

For a given value of κ_2, the doubles will occupy n_2 bursts, with n_2 being a random variable. No general formula for the distribution of n_2 has been found in the literature or obtained by the author. However, noting that the exceedances from any one double cannot occupy the same burst, but that exceedances from different doubles can occupy the same burst, tedious but moderately simple combinatoric analysis has yielded the following expressions for the probability function of n_2:

for $\kappa_2 = 0$: $p(n_2 = 0) = 1$
$p(n_2 \neq 0) = 0$

for $\kappa_2 = 1$: $p(n_2 = 2) = 1$
$p(n_2 \neq 2) = 0$

for $\kappa_2 = 2$: $p(n_2 \leq 1) = 0$
$p(n_2 = 2) = 1/N$
$p(n_2 = 3) = 2/N$
$p(n_2 = 4) = (N-3)/N$
$p(n_2 > 4) = 0$

for $\kappa_2 = 3$: $p(n_2 \leq 1) = 0$
$p(n_2 = 2) = 1/N^2$
$p(n_2 = 3) = 8/N^2$
$p(n_2 = 4) = (3N-5)/N^2$
$p(n_2 = 5) = 6(N-4)/N^2$
$p(n_2 = 6) = (N-4)(N-5)/N^2$
$p(n_2 > 6) = 0$ $\qquad \ldots (7.56)$

Fortunately, for values of α, N, M, K and r_0 applicable to this analysis, $p(\kappa_2) \rightarrow 0$ for $\kappa_2 \geq 4$, thus sparing us from deriving $p(n_2)$ for $\kappa_2 \geq 4$. Given κ_2, then the number of singles κ_1 in the $K-\kappa_2$ dopplers not containing doubles is $BIN(K-\kappa_2; \kappa_1; p_1)$. A number η of these singles will fall in the same bursts as those occupied by the doubles. It is easy to show that η is a $BIN(K-\kappa_2; \eta; n_2/N)$ random integer. The remaining $\kappa_1-\eta$ singles will be multinomially distributed (Johnson, 1969) amongst the $N-n_2$ bursts not occupied by doubles. The number of bursts occupied by the singles not falling in a burst occupied by a double is therefore given by the occupancy distribution (Johnson, 1969), ie.:

$$p(j) = \binom{N-n_2}{j} \sum_{i=0}^{j} (-1)^j \binom{j}{i} \left[\frac{j-i}{N-n_2}\right]^{\kappa_1-\eta} \quad \ldots (7.57)$$

The probability of false alarm, given n_2, κ_1 and η, is then the probability that at least $M-n_2$ of the the $N-n_2$ bursts unoccupied by doubles will be occupied by singles, ie.

$$\begin{aligned} P_{fa}(\eta,n_2) &= \text{probability that at least } M-n_2 \text{ of the } N-n_2 \text{ bursts are occupied} \\ &= \text{prob}(\, j \geq M-n_2) \\ &= \sum_{j=M-n_2}^{N-n_2} p(j) \end{aligned}$$

Summing over all possible values of η, changing the order of summation, noting that the innermost summation over η then represents a binomial expansion, and some re-arranging, gives:

$$P_{fa}|n_2;\kappa_1 = \frac{1}{N^{\kappa_1}} \sum_{j=M-n_2}^{N-n_2} \binom{N-n_2}{j} \sum_{i=0}^{j} (-1)^j \binom{j}{i} [n_2 + j - i]^{\kappa_1} \quad \ldots (7.58)$$

Then, since n_2 and κ_1 are random variables, and n_2 depends in turn on the random variable κ_2, the overall probability of false alarm is given by:

$$P_{fa} = \sum_{\kappa_2=0}^{3} p(\kappa_2) \sum_{n_2=0}^{2\kappa_2} p(n_2|\kappa_2) \sum_{\kappa_1=0}^{K-\kappa_2} p(\kappa_1)\, P_{fa}|n_2;\kappa_1 \quad \ldots (7.59)$$

For $M \leq 2$ and/or $r_0 \geq N-2$ this represents the exact final answer. For $M \geq 3$ and $r_0 < N-2$ it is necessary to consider the probability of triple exceedances; for $M \geq 4$ and $r_0 < N-3$ it is necessary to consider the probability of quadruple and triple exceedances, etc. The probability of having a triple, quadruple quintuple etc. exceedance in any one doppler is p_3, p_4, p_5 etc. respectively, and is obtained in the same way as in eqn. (7.54) with s = N-2; N-3; N-4; ...etc. The probability of having κ_3 triple exceedances amongst the K dopplers is then BIN(K; κ_3; p_3), the probability of having κ_4 quadruple exceedances amongst the K dopplers is BIN(K; κ_4; p_4), etc. Fortunately the probability of more than one triple, quadruple etc. occurring amongst the K dopplers is negligible and so combinatoric analysis as for doubles and singles is avoided. We can then note that :

For $M \leq 2$ or $r_0 \leq N-2$

P_{fa} = Probability of false alarm due to singles and doubles in the K dopplers.

$= P_{fa}(2\text{'s};\ 1\text{'s})$ $\quad \ldots (7.60a)$

For $M = 3$ and $r_0 \leq N-3$

P_{fa} = Probability of a triple in any doppler

or

Probability of false alarm due to singles and doubles in the K dopplers.

$$= p_3 + P_{fa}(2's;\ 1's) \qquad \ldots (7.60b)$$

For $M = 4$ and $r_0 \leq N-4$

P_{fa} = Probability of a quadruple

or

Prob. of a triple in any doppler *and* P_{fa} due to singles and doubles in the other K-1 dopplers

or

Probability of false alarm due to singles and doubles in the K dopplers

$$= p_4 + p_3\ P'_{fa}(2's;\ 1's) + P_{fa}(2's;\ 1's)$$
$$= p_4 + P_{fa}(3's;\ 2's;\ 1's) + P_{fa}(2's;\ 1's) \qquad \ldots (7.60c)$$

For $M = 5$ and $r_0 \leq N-5$

P_{fa} = Probability of a quintuple

or

Probability of a quadruple in any doppler *and* P_{fa} due to singles, doubles and triples in the other K-1 dopplers and N-4 bursts

or

Probability of a triple in any doppler *and* P_{fa} due to singles and doubles in the other K-1 dopplers and N-3 bursts

or

Probability of false alarm due to singles and doubles in the K dopplers

$$= p_5 + p_4\ P'_{fa}(3's,\ 2's;\ 1's) + p_3\ P'_{fa}(2's;\ 1's) + P_{fa}(2's;\ 1's) \ldots (7.60d)$$

etc.

where:

$P_{fa}(2's;\ 1's)$ is obtained from eqn. (7.59)

$P'_{fa}(2's;\ 1's)$ is obtained from eqn. (7.59) except setting N'=N-3; K'=K-1; and noting that $p(\kappa_2)$ is now defined by an occupancy distribution since some of the doubles may fall in bursts occupied by the triple

$P'_{fa}(3's,\ 2's;\ 1's) = p'_3$ $P'_{fa}(2's;\ 1's)$ is obtained from $P'_{fa}(2's;\ 1's)$ except setting N"=N-4 and K"=K-1 and noting that p'_3 reflects the probability that the triple may fall partially in bursts occupied by the quadruple.

This reasoning can be extended to cover cases of $M \geq 6$ and $r_0 \leq N-6$. It becomes increasingly complex and will seldom be necessary, since, as shown later, a value of r_0 of approximately 3N/4 tends to give optimal performance. Eqn. (7.60), and eqn. (7.59) can then be used to calculate P_{fa} as a function of α, following which numerical inversion of the result yields the value of α required for the desired value of P_{fa}. This has been performed for several sample parameters. A discussion of the results is deferred until the comparison between the performance of conventional and δ-CFAR processors presented in section 7.4.4.

7.4.3 Detection probability

An analytic evaluation of detection probability of the δ-CFAR processor has not been successfully completed. This is due to the lack of convenient expressions for the bivariate PDF of the joint order statistic $x_{r0}; x_s$ under the two-class sample model, when the number of samples n_k of one of the classes (the target returns) is a random number.

Detection probability has therefore been evaluated as a function of S, the instantaneous SCNR, by Monte-Carlo simulation. For each set of parameters N, K, r_0, M, and P_{fa} of interest, and for S = -2, -1,....23 dB, 2000 detection trials were performed to provide Pd(S) data equivalent to that obtained for the ideal RDT-processor from eqn. (7.18). Since in spiky clutter S is itself a random variable, the expected detection probability is obtained by numerical substitution of the simulated data for Pd(S) into eqn. (7.19)

A discussion of the results is deferred until the comparison between the performance of conventional and δ-CFAR processors presented in section 7.4.4.

7.4.4 A Comparative example between conventional and δ-CFAR processors.

Clearly the more pulses available per dwell the better the detection performance that will be achieved, irrespective of the processing employed. It is also intuitively obvious, and confirmed by results presented later in this subsection, that the loss suffered by the δ-CFAR processor will reduce with increasing number of bursts N available per dwell. However, the number of bursts is a direct function of the number of pulses available per dwell, N_d, and the number of pulses per burst required by the doppler filter, N_f, ie. $N = N_d/N_f$, and so N is constrained by other systems requirements and cannot be increased arbitrarily. A meaningful comparison of detection performance is therefore only achieved

if N_d is kept constant for all processors examined. For a given number of pulses per dwell, increasing N to reduce δ-CFAR loss would also imply lower N_f, and hence lower coherent integration gain and often worse clutter leak-through into nominally clutter-free doppler bins.

For this comparison the total number of pulses available per dwell has therefore been fixed for all processors considered. The comparison is made subject to the following assumptions:

* 100 pulses are available per dwell, and these can be divided into an arbitrary number of CPIs.
* No pulses are used for clutter stabilisation.
* The number of filters in the bank is the same as the number of pulses per CPI. ie. K = N_f. Therefore $NK \leq 100$.
* The design false alarm probability per range bin per dwell is taken as 10^{-4}.

The conventional processor used as the basis of the comparison operates on 3 bursts, each of 32 pulses, using 1/3 detection for elimination of blind speeds. The rationale of this selection is that 1) the CFAR processor does not operate over multiple bursts and so there is no processing benefit to be gained from arbitrary increases in the number of bursts N, 2) coherent integration gain and clutter suppression should be maximised by maximising the number of pulses per burst, equivalent to K, and 3) N = 3 is taken as the minimum number of bursts with which satisfactory doppler response will be achieved, in which case M = 1 is necessary for satisfactory doppler visibility. This dictates that the number of pulses per burst must be ≈ 100/3, from which we set K = 32. These 32 filters are taken as the output of a 32-point Hamming weighted FFT. The CFAR processor is taken as either a 32 or 16 range-bin OS processor, with the reference sample (denoted k in Chapter 5) set as $r_1 = 12$ or $r_1 = 24$ respectively. *A-priori* knowledge of the clutter shape parameter ν is assumed. In practice ν will have to be estimated on line. This will introduce an additional loss of the order of 5-10 dB (Ravid, 1992) to the detectability results presented below.The false alarm probability per range bin per dwell of 10^{-4} requires $P_{fa} = 10^{-5.98} \approx 10^{-6}$ for each burst-doppler bin; thus P_d vs. SCNR curves for each burst can be obtained using threshold data used in section 5.2.3 of this thesis for OS processors with $P_{fa} = 10^{-6}$. The overall probability of detection after 1/3 binary integration is then $\overline{P}_d = 1 - (1-P_d)^3$.

The δ-CFAR processor has been examined for three sets of parameters utilising about 100 pulses per dwell, namely:

1) N = 8; K = 12; M = 3

2) N = 10; K = 10; M = 4
3) N = 12; K = 8; M = 5

In each case a number of values of r_0 have been used to investigate its effect on performance. The K filters are taken as being implemented by a K-point Hamming weighted FFT.

The values of α required for $P_{fa} = 10^{-4}$ using a δ-CFAR processor have been calculated for each of the three sets of parameters listed above, for various values of r_0. Results are tabulated in Table 7.1.

Table 7.1
Threshold Multiplier Factor α for δ-CFAR processor, $P_{fa} = 10^{-4}$

M/N=3/8; K=12	M/N=4/10; K=10	M/N=5/12; K=8
$r_0 = 4$: $\alpha = 32.44$	$r_0 = 5$: $\alpha = 18.75$	$r_0 = 7$: $\alpha = 9.28$
$r_0 = 5$: $\alpha = 16.84$	$r_0 = 6$: $\alpha = 11.89$	$r_0 = 8$: $\alpha = 6.84$
$r_0 = 6$: $\alpha = 9.60$	$r_0 = 7$: $\alpha = 7.96$	$r_0 = 9$: $\alpha = 5.07$
$r_0 = 7$: $\alpha = 5.15$	$r_0 = 8$: $\alpha = 5.37$	$r_0 = 10$: $\alpha = 3.67$

The detection probability has been calculated as a function of the mean SCNR using the simulated data discussed in the previous subsection and taking expectation with respect to the modulation process u_0 as in sections 7.2.4 and 7.3.5, for the clutter shape parameter ν = 0.25, 0.333, 0.5, 1.0, 2.0, 4.0, 8.0, and ∞. The δ-CFAR loss (relative to ideal threshold setting for corresponding values of P_{fa}, M, N and K) has been calculated for each value of r_0 and its corresponding threshold, tabulated above. The results for CFAR loss are tabulated in Table 7.2 below.

Table 7.2
CFAR Loss (in dB) for δ-CFAR Processor, $P_{fa} = 10^{-4}$

M/N=3/8; K=12	M/N=4/10; K=10	M/N=5/12; K=8
$r_0 = 4$: $L_c = 6.32$	$r_0 = 5$: $L_c = 4.55$	$r_0 = 7$: $L_c = 3.53$
$r_0 = 5$: $L_c = 5.20$	$r_0 = 6$: $L_c = 4.06$	$r_0 = 8$: $L_c = 3.43$
$r_0 = 6$: $L_c = 4.77$	$r_0 = 7$: $L_c = 3.78$	$r_0 = 9$: $L_c = 3.50$
$r_0 = 7$: $L_c = 5.90$	$r_0 = 8$: $L_c = 4.01$	$r_0 = 10$: $L_c = 4.52$

As expected, the loss increases with decreasing N, and is minimum for $r_0 \approx 3N/4$. For higher values of r_0 target self masking becomes significant since the r_0^{th} order statistic will more often contain a target return. This implies that the target must compete with itself for detection, yielding effectively $P_d = 0$ in bursts containing about $N-r_0+1$ or more target returns. Clearly, the higher r_0, the more often this will occur. For values of r_0 lower than 3N/4 the probability of triple, quadruple etc. exceedances rises sharply, which must be counteracted by steep increases in the threshold multiplier α, at the expense of increased loss, to maintain the desired P_{fa}.

Since the number of pulses per burst, and hence the achievable integration gain, differs for each of the δ-CFAR implementations and the conventional OS processor, comparison between processors is best achieved based on the pre-filter SCNR required to achieve the desired P_d and P_{fa}. This requires calculation of the coherent integration gain G_i achieved by the doppler filter in each implementation, which for Hamming weighting has been found to be:

$K = N_f = 32$: $G_i = 13.7$ dB
$K = N_f = 12$: $G_i = 9.45$ dB
$K = N_f = 10$: $G_i = 8.66$ dB
$K = N_f = 8$: $G_i = 7.69$ dB

The pre-filter SCNR required by each processor implementation for $P_d = 50\%$ and a flat clutter-plus-noise spectrum has been calculated. This is illustrated in Fig. 7.5. It is immediately evident that the δ-CFAR processors offer dramatically superior performance to conventional OS processors is spiky clutter. The δ-CFAR curves illustrated correspond to the value of r_0 which gives minimum loss, as indicated in Table 7.2.

The following points can be emphasised:

1) The δ-CFAR processor does not use reference range bins and is therefore entirely immune to clutter edges, interfering targets etc. This also implies that the false alarm performance is completely independent of the PDF of the modulation process. Furthermore, the δ-function range impulse response of δ-CFAR processors will greatly enhance interclutter visibility, thereby yielding additional detection benefits to those indicated by Fig. 7.5.

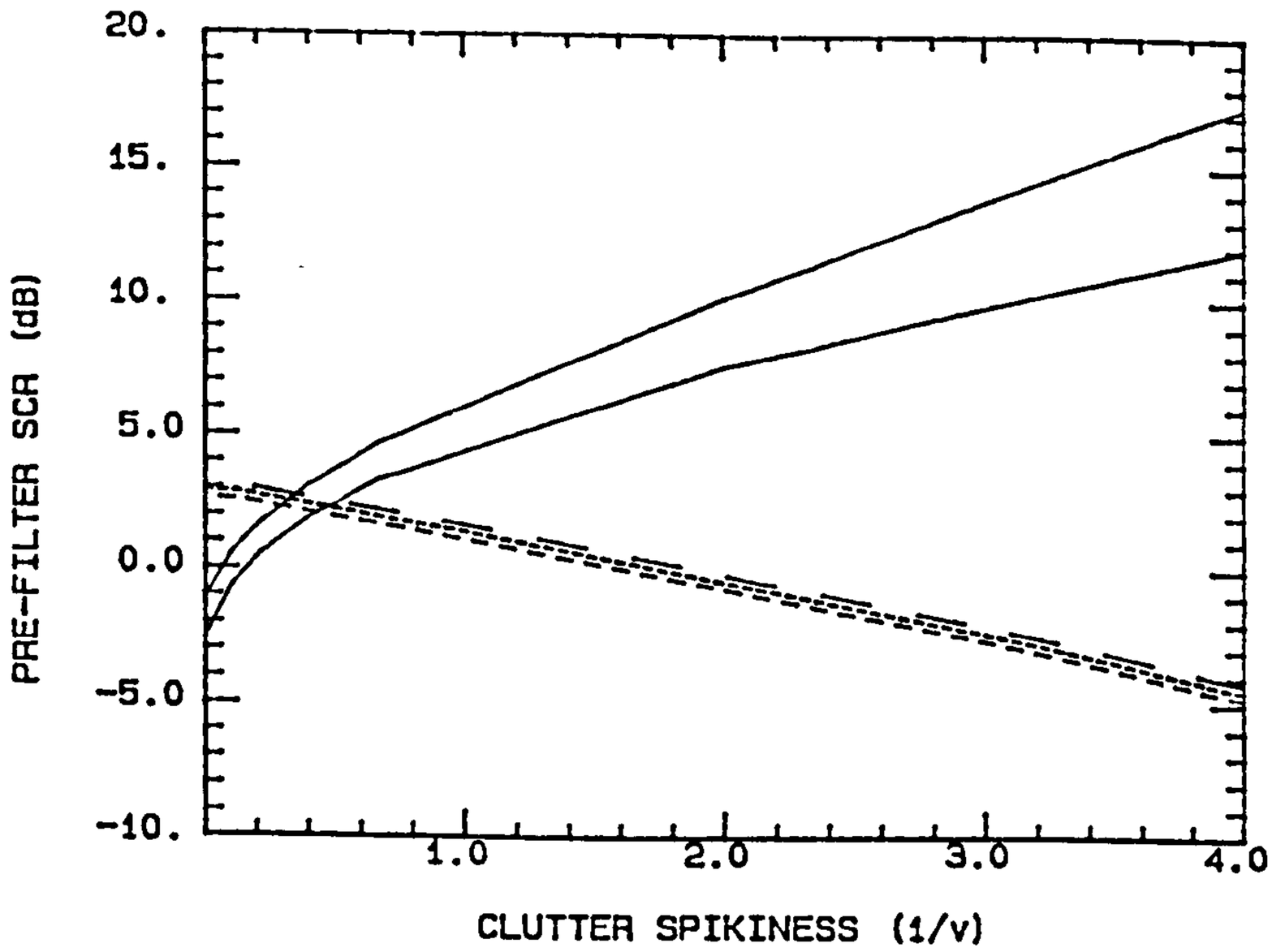

Fig 7.5: *Pre-filter SCNR for P_d=50% for δ-CFAR and conventional OS processors ($P_{fa}=10^{-4}$; $NK \approx 100$)*

———— OS processor; N_{ref}=16 (top curve) and N_{ref}=32 (lower curve)
- - - - - - - - δ-CFAR processor; N=12; K=8 ; M=5
— — — · δ-CFAR processor; N=10; K=10; M=4
— — – δ-CFAR processor; N=8 ; K=12; M=3

2) The performance of none of the processors illustrated depends on the clutter spectrum per se, and hence the relative performance of the various processors is not expected to differ in non-white clutter spectra, notwithstanding different achievable clutter residue, and hence different target detectability, in the K doppler bins.

3) Note that for the OS-CFAR processors the on-line estimation of the clutter shape parameter ν will introduce further losses of the order of 5 - 10 dB.

4) For lower values of P_d the superiority of the δ-CFAR processors is even more marked; for higher values it is slightly diminished. This is because the gamma distributed modulation process introduces fluctuation into the instantaneous SCNR, yielding higher P_d at low mean SCNRs and lower P_d at very high SCNRs than in unmodulated clutter. Thus for P_d < 50% the δ-CFAR curves in

would fall off more steeply with increasing 1/v; for $P_d > 50\%$ they would fall off more slowly.

5) K = 10 yields the best δ-CFAR performance in flat spectra. However, larger K (ie. lower N) may be beneficial in some clutter environments, where the increased δ-CFAR loss is counteracted by reduced clutter residue in some dopplers.

6) Another feature of the δ-CFAR processor is that if all target returns fall in the same doppler, target self-masking is certain, yielding $P_d = 0$. This situation will only arise, however, for targets in the first doppler ambiguity. In high frequency radars with low to moderate PRFs often targets of interest will fall in higher doppler ambiguities, whereas unwanted "targets", such as birds or clutter breakthrough, will be doppler unambiguous. This inherent rejection of velocity-unambiguous targets may often be desirable.

The δ-CFAR processor requires that the underlying clutter power remains constant over all N bursts. As with the RDT-CFAR processor, this implies that a constant PRF be used if range-ambiguous clutter is present, in which case blind speed elimination would still be achieved by the burst-burst frequency agility necessary for decorrelation of clutter speckle and target returns.

It is worth briefly considering some processing implications. The OS processor requires N_{ref} (usually > 16) reference cells to be sorted into ascending order, for each range bin tested in each doppler on each burst; ie. for each range bin, N_{ref} samples need to be sorted NK times. For the δ-CFAR processor, each range bin requires N samples to be sorted K times. Thus only 1/K as many sorting operations, each of which is N/N_{ref} as long, need to be performed by the δ-CFAR processor. This represents a dramatic reduction in computing requirements.

As a final comment it can be noted that the CFAR loss could be reduced, with only slight increase in complexity, by using a censored mean level estimator for the test statistic, as described in section 2.3, instead of a single order statistic. Analysis of such a processor would, however, be significantly more difficult.

7.5 SUMMARY

Current CFAR processors have been shown to perform poorly in non-homogeneous or spiky clutter. Two alternative CFAR processors applicable to radars employing multiple bursts per dwell and filter bank doppler processors have been presented. These have been termed the RDT (Range-Doppler-Time) CFAR processor and the δ-CFAR processor.

One of the key features of the RDT-CFAR processor is the use of power normalisation between dopplers. Exact analytic expressions for the false alarm probability and detection probability have been derived for the case of ideal estimation of the power normalisation terms. For adaptive estimation of the power normalisation terms approximate expressions for the false alarm probability and detection probability, requiring simple numerical integration, have been derived. It has been shown that for flat clutter-plus-noise spectra, or very large CNR, the RDT processor offers greatly enhanced performance in spiky clutter relative to conventional processors. In addition, performance is independent of the clutter spikiness. Order statistics have been used in the range-based estimation of the power normalisation terms to maximise immunity to extraneous targets and clutter edges.

However, it has been shown that the RDT-CFAR processor suffers a fairly severe increase in P_{fa} in clutter with a spatially varying spectrum, which includes moderately narrowband clutter with finite CNR and a randomly varying modulation process. This cannot be completely countered by using a higher choice of r_0 or threshold multiplier factor. This may limit the practical applicability of the RDT-CFAR processor.

The δ-CFAR processor has been proposed as a means of overcoming the shortcomings of the RDT and conventional CFAR processors. A analytic expression for false alarm probability has been derived and detection probability has been evaluated by Monte-Carlo simulation. Comparison to conventional OS processors has shown that dramatic performance improvements (~10 to 20 dB) can be achieved in spiky clutter, with minimal loss (~3dB) in thermal noise. This loss (relative to the OS processor) in thermal noise would be eliminated if real time estimation of the clutter shape parameter is required in the OS processor. In addition to greatly reduced CFAR loss, the main features of the δ-CFAR processor are:

1) It is completely immune to extraneous targets and clutter edges, and will thus offer enhanced multiple target discrimination and interclutter visibility.

2) Its false alarm performance is entirely independent of the clutter amplitude statistics (provided the speckle is exponential).

3) It provides inherent rejection of doppler-unambiguous (ie. slow moving) targets.

4) It is computationally far less demanding than the RDT or conventional CFAR processors.

CHAPTER 8

CONCLUSIONS

8.1 SUMMARY

This thesis has investigated ways of improving radar detection performance in spiky clutter. Following a literature review to ascertain appropriate clutter models and establish the state of the art, two main areas were examined, namely:

1) Quantitatively evaluating the clutter suppression of several types of doppler filters in homogeneous and non-homogeneous clutter environments, and investigating the use of adaptive and hybrid filters to achieve improved target detection.

2) Investigating current and improved CFAR processing techniques to minimise detection losses in spiky clutter or spiky clutter residue.

8.1.1 Improved clutter suppression by Doppler filtering

The relative performance of several well known doppler processors has been examined under a wide range of clutter conditions, with particular attention being paid to the performance of AMTD processors. A large number of clutter scenarios were considered in an attempt to give results which are not too dependent on specific conditions. The clutter parameters were chosen to reflect land and sea clutter environments, including possible weather clutter components. Suitable performance measures were discussed, with particular attention being paid to filter-bank processing and M/N detection. The improvement factor of each type of processor was evaluated in each clutter scenario, and the loss relative to the optimal filter (with *a priori* knowledge of the covariance matrix) was determined. The insertion of MTI cancellers before Linear Predictor or Hsaio optimal filters for dealing with point clutter was investigated. Statistical data analysis was used to reduce the data to manageable proportions and allow key conclusions to be drawn. It was shown that AMTD offers only a slightly higher improvement factor than conventional MTD or Pulse Doppler processing, of which MTD processing has the marginally better performance. Linear Predictor processors were shown to be inferior to Hsiao optimal filters, and pre-filter MTI cancellers inserted before Hsiao filters or Linear Predictors

were shown to introduce an average loss of the order of 1 dB in homogeneous clutter. Conventional AMTI and MTI filters are shown to provide dramatically inferior performance under many clutter environments.

This doppler filter performance comparison indicated that techniques such as PD, MTD and AMTD suffer a loss of about 2 to 3 dB relative to Hsiao filtering in which exact knowledge of the covariance matrix of the (homogeneous) clutter was assumed. Realistic assessment of the merits of optimal filtering, however, necessitated the evaluation of adaptive optimal filter performance under more realistic conditions. The performance of adaptive Hsiao-optimal filters operating in spatially and time-varying clutter backgrounds was therefore investigated. The case of practical adaptive estimation of the covariance matrix, and limiting cases where the estimate of the covariance matrix tends to the mean clutter covariance matrix, were considered. Three classes of non-homogeneous backgrounds were studied, namely 1) clutter in which the amplitude and spectral width in each range bin are randomly drawn from spatially invariant independent gamma distributed parent populations, 2) clutter edges, in which the range profiles of the clutter amplitude and/or spectrum exhibit a step change, and 3) homogeneous clutter in which some range bins are corrupted by returns with significantly different amplitude and spectral characteristics, representing point clutter sources or extraneous targets. The use of pre-filter MTI was investigated as a means of reducing IF losses in some classes of clutter non-homogeneity. It was shown that adaptive filters suffer significant reductions in IF in non-homogeneous clutter environments. These losses are generally greater than the benefit afforded by ideal adaptive processors over other conventional doppler processors. It has been noted that the mean IF loss is an optimistic performance measure in adaptive doppler processors. The true impact on radar detection performance will be increased by higher order moments of the IF loss and clutter residue. Better characterisation of heterogeneous clutter is necessary before radar performance in heterogeneous clutter environments can be assessed with confidence. It was concluded that adaptive optimal filtering alone does not provide a means of significantly improving radar detection performance over MTD or AMTD processors, and hybrid MTD-adaptive filters were proposed as the most promising doppler filtering technique for heterogeneous clutter. It was felt that more significant gains in detection performance are most likely to be achieved by improved post-filter CFAR processing.

8.1.2 Improved CFAR processing

The following papers relevant to the work summarised in this subsection have been published:

* Armstrong, B.C., and Griffiths, H.D., "CFAR detection of fluctuating targets in spatially correlated K-distributed clutter, *IEE Proceedings, Part F*, Volume 138, Number 2, April 1991, pp. 139-152.

* Armstrong, B.C., and Griffiths, H.D., "Modelling spatially correlated K-distributed clutter", *IEE Electronics Letters*, Volume 27, Number 15, 18th July 1991, pp. 1355 - 1356.

* Armstrong, B.C., and Griffiths, H.D., "Improved CFAR detection in spatially correlated K-distributed clutter", *Proceedings of the CIE Radar Conference*, 1991, pp. 415-418.

* Armstrong, B.C., and Griffiths, H.D., "False alarm control in spiky clutter by multi-burst range-doppler processing", *Proceedings of the IEE 1992 Radar Conference.*

Single pulse CFAR detection of Rayleigh fluctuating targets in spatially uncorrelated K-distributed clutter was investigated to establish a baseline from which to formulate and assess improved CFAR processors. The performance of three types of well known CFAR processors, namely the CA, CAGO, and OS CFAR processors, was examined, and curves for the detectability loss due to clutter spikiness were presented along with values for the additional loss due to CFAR thresholding. The effects of incorrectly estimating the clutter shape parameter ν were investigated. Empirical expressions were derived for the ideal- and CFAR- detection losses in spiky clutter

The possibility of exploiting spatial correlation in the clutter in order to reduce detection losses was investigated. The extreme case where the modulation process is essentially completely correlated within the CFAR reference window was addressed first and it was shown that the potential exists for a reduction in detection loss of in excess of 10 dB in highly correlated clutter. The K-distribution model was then extended to facilitate the incorporation of spatial correlation properties. Based on this model "ideal" CFAR detection performance in spatially correlated clutter has been analysed. It is apparent that a potential benefit of several dBs is possible if the CFAR processor is designed to exploit the spatial correlation and if improved estimates of the modulation process can be

obtained. The former is achieved through real time estimation of the local value of the spatial correlation; the latter is achieved in this thesis through obtaining a linear MMSE estimate of the modulation process instead of the usual unweighted average: the CFAR problem was viewed as one of optimal filtering in multiplicative noise, and the optimal filter and the corresponding OLF-CFAR processor were derived. Methods of estimating the local spatial correlation in real time and their effects on detection loss were investigated. A semi-analytic formulation of performance prediction was presented with sample results for representative processor and system parameters. It was shown that the OLF-CFAR processor, with estimation of the local value of the clutter correlation coefficient, can yield a gain of 1 to 3 dB relative to a CA processor. Further benefits can be expected in clutter with other than exponential spatial ACFs. It was concluded that the OLF-CFAR processor represents a promising technique for improving detection performance in spiky sea clutter, subject to the requirements that the spatial extent of targets of interest is less than the correlation distance of the clutter, and that the radar has sufficiently fine range resolution to exploit whatever spatial correlation may be present. Should these conditions not be met, improved detection performance in spiky clutter will require other processing techniques in which the modulation process in the range-reference window does not form the sole basis of the detection hypothesis test.

CFAR techniques aimed at reducing the reliance on surrounding range bins for estimating the background in the test cell in order to establish the threshold were therefore investigated. This was achieved by exploiting the two other domains in which potential reference data is available, namely the doppler and time domains. Two alternative CFAR processors applicable to radars employing multiple bursts per dwell and filter bank doppler processors were formulated, and these have been termed the RDT (Range-Doppler-Time) CFAR processor and the δ-CFAR processor.

It has been shown that for flat clutter-plus-noise spectra or large CNR the RDT processor offers greatly enhanced performance in spiky clutter relative to conventional processors. In addition, performance is independent of the clutter spikiness. Order statistics have been used in the range-based estimation of the power normalisation terms to maximise immunity to extraneous targets and clutter edges. However, it has been shown that RDT-CFAR processors suffer a severe increase in P_{fa} in clutter with a spatially varying spectrum, which cannot be completely countered by using a higher reference sample rank or multiplier factor. This may limit the practical applicability of the RDT-CFAR processor.

The δ-CFAR processor was proposed as a means of overcoming the shortcomings of the RDT and conventional CFAR processors. A analytic expression for false alarm

probability has been derived and detection probability has been evaluated by Monte-Carlo simulation. Comparison with conventional OS processors has shown that dramatic performance improvements (~10 to 20 dB) can be achieved in spiky clutter, with minimal loss (~3dB) in thermal noise. This loss (relative to the OS processor) in thermal noise would be eliminated if real time estimation of the clutter shape parameter is required in the OS processor. In addition to greatly reduced CFAR loss, the δ-CFAR processor offers complete immunity to extraneous targets and clutter edges, has false alarm performance which is independent of the clutter amplitude statistics, provides inherent rejection of doppler-unambiguous targets, and is computationally far less demanding than the RDT or conventional CFAR processors.

8.1.3 The use of the difference channels for detection in monopulse radar

For completeness the key conclusions regarding the use of monopulse difference channel information for detection are now summarised. Further discussion of these results can be found in the paper on this topic[1] which is reproduced in Appendix 1.1 of this thesis. It has been shown that certain linear combinations of the Sum channel with the Difference channels can give a detection gain relative detection using the Sum channel only. The magnitude of this gain varies between 2 dB and 6 dB, depending on the radar scenario assumed and the required detection parameters.The results illustrated in the paper have concentrated on single pulse detection of Sw0 and Sw1 targets. In general the gain associated with the use of the combination patterns for detection is about 0.5 dB higher for Sw0 targets than for Sw1 targets. The difference in performance between the combination patterns and the use of the Sum beam only for other Swerling models can be expected to be between that for the Sw0 and Sw1 targets, although the absolute detection probabilities for a given SNR may differ.

The angle detector operating on only one angular dimension has been analysed for sample parameters and has been shown to be capable of providing CFAR performance in uncorrelated Rayleigh noise environments with moderate loss in detection performance, compared to ideal detection of coherently integrated pulses. An upper bound on detection performance has been found for an angle detector operating on both angular dimensions, and this has been shown to reduce the detection loss in uncorrelated Rayleigh noise to about 0.5 dB. The angle detector has only been evaluated for Sw0 point targets on boresight of the Sum beam at reasonably high SNRs and has neglected straddling losses and radar imperfections such as imbalances between channels.

[1] Armstrong, B.C., and Griffiths, H.D., "The use of difference channel information for detection in monopulse radars", *IEE proc. Pt. F*, vol. 138, No. 3, June 1991, pp. 199-210.

The angle detector technique discussed is at this stage only a rough outline of a detector which could be based on this technique. Further refinements are possible in the choice of the size and shape of bins, the use of matched bins and non-binary integration, and optimal combination of information derived from both angular dimensions and the range dimension in a detector based on correlation in the indicated 3-D position of the received signal. The incorporation of some pre-processing on the complex indicated angle could also be used to improve the robustness of the angle detector, giving better CFAR performance under a wider range of conditions of external interference, noise and clutter. The angle detector could also potentially provide some information regarding the nature of the object being illuminated, for instance whether it is a point or distributed scatterer, and on the physical position of the scatterer. This latter information could possibly be used as the basis for reducing the effect of large clutter discretes through recognising that they are on the surface. (The accuracy of the estimated position of such clutter discretes would invariably be high owing to their large RCS). The angle detector could also be used in conjunction with conventional detection techniques to provide additional independent decision opportunities per observation.

To conclude, it has been shown that the use of information in the Difference channels can be used to provide a significant improvement in the detection capability of monopulse radars. This can be realised either through the formation of so-called composite beams or the use of the Complex Indicated Angle for detection. The former realisation essentially achieves this improvement through recovery of the information normally discarded at the outputs of the monopulse comparator and through creating multiple independent decision opportunities per observation. The benefits which can be obtained, of the order of 3 to 5 dB detection gain, are achieved at the expense of hardware complexity: full range processing is required on the Difference channels to be used, and combination techniques require four full parallel detectors and some combinational logic. The angle detector has been shown to provide CFAR performance under noise conditions with moderate CFAR loss even with very few pulses per observation. This CFAR performance is also achieved without reference to adjacent range cells, a potentially useful characteristic. The processing implications of the angle detector are not yet clear but the lack of the need for comparisons with adjacent range cells and the small number of bins required should make it relatively efficient compared to some conventional CFAR techniques.

8.2 KEY CONCLUSIONS

A few general conclusions can be drawn from the specific conclusions given at the end of each Chapter.

The scope for improving detection performance by improved doppler filtering techniques is limited (if doppler space and burst length constraints are held constant): Adaptive MTD processors offer less than 1 dB better performance on average than current generation doppler processors such as MTD and Pulse Doppler, even if ideal filter bank selection is assumed. AMTD filtering cannot therefore be justified by clutter suppression considerations alone. Hsiao optimal filtering - a theoretical upper bound on achievable improvement factor - offers on average only 2 to 3 dB better IF than MTD and Pulse Doppler processors. Incorporation of adaptivity into the optimal filter (in this thesis by means of the SMI algorithm) eliminates this apparent superiority of optimal filters, even in homogeneous clutter, if a realistic sample size is assumed in the estimation of the covariance matrix. Performance deteriorates further in non-homogeneous clutter where the estimated covariance matrix does not tend to that in the test cell, yielding significantly sub-optimal performance. The deleterious effects of non-homogeneous clutter can to some extent be countered by the insertion of a conventional MTI canceller before the optimal filter; this reduces loss in non-homogeneous clutter with negligible increase in loss in homogeneous clutter. Extending this concept of hybrid processors, MTD/ adaptive-optimal hybrid filters appear to offer the best prospect of achieving filter performance significantly better than current generation doppler processors. However, since ideal Hsiao filtering represents an upper bound on the achievable improvement factor, at most 2 to 3 dB benefit can be obtained.

It is more profitable to pursue improved CFAR processor performance as a means of attaining the desired improvement in overall radar detection performance. Current generation CFAR processors, even those like Ravid's Maximum Likelihood ML-OS processor which estimate the local clutter spikiness to maintain constant P_{fa}, have been shown to suffer severe losses (often in excess of 10 or even 20 dB) in spiky clutter because they take signal amplitude as the only defining characteristic of a target: targets are only detected by virtue of the fact that they are larger than the threshold, which is set larger than the clutter to prevent false alarms. This is also true of the OLF-CFAR processor for spatially correlated clutter presented in Chapter 6. CFAR detection losses in spiky clutter can only be reduced if detections are based on features other than amplitude which unambiguously characterise targets as opposed to clutter. The RDT-CFAR

processor presented in Chapter 7 essentially uses the target spectrum, as well as amplitude, to discriminate between targets and clutter: any deviation in the spectrum in the test range cell, compared to that in reference range cells, causes incorrect power normalisation between dopplers and consequent detection of the target. This gives dramatic benefits (in excess of 10 dB gain relative to conventional processors) provided the clutter spectrum does not itself deviate from the mean in the test range bin, thereby appearing target-like and causing the noted increases in P_{fa}. The δ-CFAR processor uses as the defining characteristic of targets that they are velocity (ie. doppler) ambiguous, whereas clutter is velocity unambiguous. Subject to this condition being met, robust performance only a few dBs worse than the ideal is achieved.

The defining target characteristics on which detection can be based will differ for different radars and applications: a high frequency (X-band or higher) radar intended for detecting fast closing targets in spiky sea clutter would meet the condition of target velocity ambiguity, whereas say an S-band radar for detecting small boats in spiky sea clutter would not. In the latter case, if target amplitude cannot provide the required detection performance, spectral width, polarisation etc. could be possibly be exploited and appropriate CFAR processors defined. It is concluded that the form of CFAR processor to be used depends strongly on radar, clutter and target parameters; the reliance on amplitude discrimination alone yields wholly unsatisfactory performance in spiky clutter and other defining characteristics need to be identified and exploited if detection performance is to be improved.

The main contributions of this thesis are considered to be:

1) Evaluation of adaptive optimal filter performance in non-homogeneous clutter, and proposing and evaluating the use of pre-filter MTI to reduce IF losses.

2) The formulation of the model for spatially correlated K-distributed clutter.

3) The formulation and analysis of the "ideal-" and OLF-CFAR processors for spatially correlated K-distributed clutter.

4) The formulation and analysis of the RDT-CFAR processor and δ-CFAR processor.

In addition, the doppler filter performance comparison of Chapter 3 is far more extensive than anything previously found in the literature, allowing some general conclusions to be

drawn regarding filter selection. In particular, quantitative evaluations of AMTD performance have not previously appeared. Similarly, the evaluation in Chapter 5 of CFAR processor performance in K-distributed clutter has not appeared elsewhere in the relevant mainstream literature. The use of difference channel information is a novel technique for improving detection performance in monopulse radars, and it is felt that the research described in the appended paper lays the foundation for more thorough investigations in this field.

8.3 FURTHER WORK

It is felt that the following areas require further research:

1) Hybrid MTD/adaptive-optimal filters need to be evaluated in both homogeneous and non-homogeneous clutter. The optimal division of pulses between the MTD and adaptive-optimal filter stages, and the number of parallel optimal filters attached to each MTD filter, need to be investigated.

2) The precise impact of deteriorations in adaptive optimal filter performance in homogeneous clutter on radar detection performance needs further consideration; the simple arithmetic mean of the IF gives optimistic results which are in reality degraded by increased higher order moments of the IF loss and clutter residue. Ideally the PDF of the IF and clutter residue needs to be determined to enable realistic assessment of detection performance, in conjunction with the actual detection processing employed by the radar.

3) The performance of the "ideal" and OLF-CFAR processors in spatially correlated clutter with other than exponential spatial ACF needs to be quantified. Although the solution for the optimal weights is valid for non-exponential ACFs, estimation of multiple correlation coefficients and the subsequent selection of threshold multiplier factors needs to be addressed.

4) The detection performance of systems employing δ-CFAR processors needs to be evaluated as a function of absolute target velocity, for representative clutter spectra and PRF stagger patterns, and for various radar frequencies and PRFs. This is necessary in order to establish practical limitations to δ-CFAR applicability.

5) The techniques of exploiting the difference channel information in monopulse radars have thus far only been evaluated in detail for the case of radar thermal noise. External noise (uncorrelated) and clutter (correlated) may cause deviations from the predicted performance, particularly for correlated clutter in the angle detector. The evaluation of the performance of these techniques taking account of the abovementioned factors is the first priority should further work on this topic be performed.

REFERENCES

Anderson, J.R. and Karp, D., (1980), "Evaluation of the MTD in a high-clutter environment", *Proc. IEEE Int'l Radar Conf.*, 1980, pp. 219-224.

Attanasov, V.B., et. al., (1990), "Experimental study on nonstationary X- and Q-band radar backscattering from the sea surface", *IEE Proc.*, Vol. 137, Pt. F, No. 2, April 1990, pp. 118-124.

Barbarossa, S., D'Addio E. and Galati, G., (1987), "Comparison of optimum and linear prediction techniques for clutter cancellation", *IEE Proc.*, Pt. F, Vol. 134, No. 3, June 1987, pp. 277-282.

Blake, S., (1988), "OS-CFAR theory for multiple targets and nonuniform clutter", *IEEE Trans. Aerosp. and Electronic Systems*, Vol. AES-24, No. 6, Nov. 1988, pp. 785-790.

Chan, H.C., (1990), "Radar sea-clutter at low grazing angles", *IEE Proc.*, Vol. 137, Pt. F, No. 2, April 1990, pp. 102-122.

Conte, E., Longo, M. and Lops, M., (1989), "Analysis of the excision CFAR detector in Multiple Target Situations", *Proc. of the 1989 International Symposium on Noise and Clutter Rejection in Radars and Imaging Sensors*, Kyoto, 1989, pp. 566-571.

D'Addio, E., Farina, A. and Studer, F.A., (1984), "Performance comparison of optimum and convetional MTI and doppler processors", *IEEE Trans. Aerosp. and Electronic Systems*, Vol. AES-20, No. 6, Nov. 1984, pp. 707-715.

D'Addio, E. and Galati, G., (1985), "Adaptivity and design criteria of a latest generation MTD processor", *IEE Proc.*, Vol. 132, Pt. F, No. 1, Febr. 1985, pp. 58-64.

David, H.A., (1981), "Order Statistics, 2nd Ed", John Wiley and Sons, 1981.

Dillard, G.M. and Antoniak, C.E., (1970, "A practical distribution-free detection procedure for multiple range-bin radars", *IEEE Trans. Aerosp. and Electronic Systems*, Vol. AES-6, No. 5, Sept. 1970, pp. 629-635.

Ekstrom, J.L., (1974), "MTI clutter locking for arbitrary clutter spectral shapes", *IEEE Trans. Aerospace and Elect. Systems*, Nov. 1974, pp. 872-874.

Farina, A., Studer, F.A. and Turco, E., (1983), "Adaptive methods to implement the optimum radar signal processor", *Proc. of the Int'l Radar Symposium*, India, 1983, pp. 42-47.

Farina, A. and Studer, F.A., (1984a), "Adaptive implementation of the optimum radar signal processor", *Proc. of the Int'l Radar Symposium*, Paris, 1983, pp. 93-102.

Farina, A. and Studer, F.A., (1984b), "Application of the Gram-Schmidt algorithm to optimum radar signal processing", *IEE Proc.*, Pt. F, Vol. 131, No. 2, April 1984, pp. 739-745.

Farina, A. and Protopapa, A., (1988), "New results on linear prediction for clutter cancellation", *IEEE Trans.*, Vol. AES-24, No. 3, May 1988, pp. 275-286.

Galati, G., et. al., (1985), "On the cancellation of bimodal clutter in doppler-ambigous radar", *Proc. IEEE Int'l Radar Conf*, 1985, pp. 204-209.

George, S.F., (1968), "The detection of nonfluctuating targets in log-normal clutter", *NRL Report 6796*.

Gerlach, K. and Kretschmer, F.F., (1990), "Convergence properties of Gram-Schmidt and SMI adaptive algorithms", *IEEE Trans. Aerosp. and Electronic Systems*, Vol. AES-26, No. 1, Jan. 1990, pp. 44-55.

Gerlach, K. and Krestchmer, F.F., (1990), "Convergence properties of Gram-Schmidt and SMI Adaptive Algorithms: Pt. II, *IEEE Trans. Aersp. and Electronic Systems*, Vol. AES-27, No. 1, Jan. 1991, pp. 83-90.

Ghandi, P.P. and Kassan, S.A., (1988), "Analysis of CFAR processors in nonhomogeneous background", *IEEE Trans. Aerosp. and Electronic Systems*, Vol. AES-24, No. 4, July 1988, pp. 427-445.

Gibson, C. and Haykin, S., (1985), "Radar performance studies of adaptive lattice clutter-suppression filters", Reproduced in "Advances in radar techniques", Edited by J. Clarke, Peter Peregrinus, London, 1985.

Goldman, H. and Bar-David, I., (1988), "Analysis and application of the excision CFAR detector", *IEE Proc.*, Vol. 135, Pt. F, No. 6, Dec. 1988, pp. 563-575.

Goldstein, G.B., (1973), "False alarm regulation in log-normal and Weibull clutter", *IEEE Trans. Aersp. and Electronic Systems*, Vol. AES-9, Jan 1973, pp. 84-92.

Goodman, N.R., (1963), "Statistical analysis based on a certain multivariate complex Gaussian distribution (an introduction)", *Annals of Math. Stat.*, Vol. 34, March 1963, pp. 152-177.

Gradshteyn, I.S. and Ryzhik, I.M., (1980), "Tables of integrals, series and products", Academic Press, 1980.

Griffiths, R.C., (1970), "Infinitely divisible multivariate gamma distributions", Sankhya series A, 32, 1970, pp. 393-404.

Guinard, N.W. and Daley, J.C., (1970), "An experimental study of a sea clutter model", *Proc. of the IEEE*, Vol. 58, No. 4, April 1970, pp. 543-550.

Hansen, V.G., (1972), "Detection performance of the narrow-band Wilcoxom detector against Gaussian noise", *IEEE Trans. on Info. Techn.*, Vol. IT-18, No. 5, Sept. 1972.

Hansen, V.G., (1973), "Constant false alarm rate processing in search radars", *Proc. of the IEE 1973 Int'l Radar Conf.*, London 1973, pp. 325-332.

Hansen, V.G. and Olsen, B.A., (1975), "Nonparametric radar extraction using a generalised sign test", *IEEE Trans. Aerosp. and Electronic Systems*, Vol. AES-7, No. 5, Sept. 1975, pp. 942-950.

Hansen, V.G. and Michelson, D., (1980), "A comparison of the performance against clutter of optimum, pulse doppler and MTI processors", *Proc. IEEE Int'l Radar Conf.*, 1980, pp. 211-218.

Helmken, H.F., (1990), "Low-grazing-angle radar backscatter from the ocean surface", *IEE Proc.*, Vol. 137, Pt. F, No. 2, April 1990, pp. 113-117.

Hsaio, J.K., (1974), "On the optimisation of MTI clutter rejection", *IEEE Trans.*, Vol. AES-10, No. 5, September 1974, pp. 622-629.

Jakeman, E. and Pusey, P.N., (1983), "A model for non-Rayleigh sea echo", *IEEE Trans. Ant. and Propag.*, Vol. AP-24, No. 6, May 1983, pp. 806-814.

Jensen, D.R., (1970), "A generalisation of the multivariate Rayleigh distribution", Sankhya series A, 32, 1970, pp. 193-206.

Johnson, N.L. and Kotz, S., (1969a), "Distributions in statistics: Continuous univariate distributions 1", John Wiley and Sons, 1969.

Johnson, N.L. and Kotz, S., (1969b), "Discrete distributions", John Wiley and Sons, 1969.

Katzin, M., (1957), "On the mechanisms of radar sea clutter", *Proc. of the IRE*, Vol. 45, No. 1, Jan. 1957, pp. 44-54.

Krishnamoorthy, A.S., (1951a), "Multivariate binomial and Poisson distributions", Sankhya, 11, 1951, pp. 117-124.

Krishnamoorthy, A.S. and Parthasarathy, M., (1951b), "A multivariate gamma-type distribution", *Annals of Mathematical Statistics*, 22, 1951, pp. 549-557.

Lewinski, D.J., (1976), "Nonstationary probabilistic target and clutter scattering models", *IEEE Trans. Ant. and Propag.*, Vol. AP-31, No. 3, Nov. 1976, pp. 490-498.

Lewis, B.L., Kretschmer, F.F. and Shelton, W.W., (1986), "Aspects of radar signal processing", Artech House, 1986, pp. 237-243.

Long, M.W. (1965), "On the polarisation and wavelength dependence of sea echo", *IEEE Trans. on Ant. and Propag.*, Vol. AP-13, No. 5, Sept. 1965, pp. 749-754.

Long, M.W., (1983), "Radar reflectivity of land and sea", Artech House, 1983.

Lops, M. and Orsini, M., (1989), "Scan-by-scan averaging CFAR", *IEE Proc.*, Vol. 136, Pt. F, No. 6, Dec. 1989, pp. 249-254.

Miller, R.J., (1989), "A coherent model of radar weather clutter", not yet published.

Minc, H., (1978), "Encyclopedia of mathematics and it applications, Vol. 6: Permanents", Addison-Wesley Publishing, 1978.

Nitzberg, R., (1986), "Normalised LMS algorithm degradation due to estimation noise", *IEEE Trans.*, Vol. AES-22, No. 6, Nov. 1986, pp. 740-449.

Nitzberg, R., (1990), "An effect of range-heterogeneous clutter on adaptive doppler filters", *IEEE Trans.*, Vol. AES-26, No. 3, May 1990, pp. 475-480.

Nohara, T.J. and Haykin, S., (1991), "Canadian East Coast Radar Trials and the K-distribution", *IEE Proc.*, Vol. 137, Pt. F, No. 2, April 1991, pp. 80-88.

Norton, K.A., Vogler, L.E., Mansfield, W.E. and Short, P.J., (1955), "The probability distribution of the amplitude of a constant vector plus a Rayleigh distributed vector", *Proc. of the IRE*, Vol. 43, Oct. 1955, pp. 1354-1361.

Oliver, C.J., (1984), "A model for non-Rayleigh scattering statistics", *Optica Acta 1984*, Vol. 31, No. 6, pp. 701-722.

Oliver, C.J., (1988), "The representation of correlated clutter textures in coherent images", *Inverse Problems 4*, 1988, pp. 843-866.

Oliver, C.J.and Tough, R.J.A., (1986), "On the simulation of correlated K-distributed random clutter", *Optica Acta*, 1986, 33, pp. 223843-866.

Parry, G., Pusey, P.N., Jakeman, E. and McWhirter, J.G., (1978), "The statistical and correlation properties of light scattered by a random phase screen", *Coherence and Quantum Optics IV*, Plenum Publishing, New York, 1978.

Parry, G. and Pusey, P.N., (1979), "K distributions in atmospheric attenuation of laser light", *J. Optical. Soc. of America*, Vol. 69, No. 5, May 1979, pp. 796-798.

Parry, G., (1981), "Measurement of atmospheric turbulence induced intensity fluctuations in a laser beam", *Optica Acta*, 1981, Vol. 28, No. 5, pp. 715-728.

Patil, G.P., Joshi, S.W. and Rao, C.R., (1968), "A dictionary and Bibliography of discrete distributions", Oliver and Body, 1968.

Ravid, R. and Levanon, N., (1992), "Maximum likelihood CFAR for Weibull Background", *IEE Proc.*, Vol. 39, Pt. F, No. 3, 1992.

Reed, I.S., Mallett, J.D. and Brennan, L.e., (1974), "Rapid convergence rate in adaptive arrays", *IEEE Trans.*, Vol. AES-10, No. 6, Nov. 1974, pp. 853-863.

Ritcey, J.A., (1986), "Performance analysis of the censored mean-level detector", *IEEE Trans. Aerosp. and Electronic Systems*, Vol. AES-22, No. 4, July 1986, pp. 443-454.

Ritcey, J.A. and Hwang, J., (1990), "Detection performance and systolic architectures for OS-CFAR detectors", *Proc. of the IEEE 1990 Int'l Radar Conf.*, Arlington, 1990, pp. 112-116.

Ritcey, J.A., (1990), "Approximate solutions to the PDF of K-distributed clutter plus noise", Journal unknown.

Rohling, H., (1983), "Radar CFAR thresholding in clutter and multiple target situations", *IEEE Trans. Aerosp. and Electronic Systems*, Vol. AES-19, No. 4, July 1983, pp. 608-621.

Schleher, D.C., (1975), "Radar detection in log-normal clutter", *Proc. of the IEEE 1975 Radar Conf.*, Washington DC, April 1975, pp. 262-267.

Schleher, D.C., (1982), "Performance comparison of MTI and coherent doppler processors", *Proc. of IEE Radar-82*, pp. 154-158.

Spetner, L.M. and Katz, I., (1960), "Two statistical models for terrain return", *IRE Trans. on Ant. and Propag.*, Vol. AP-8, No. 3, May 1960, pp. 242-246.

Trunk, G.V., (1969), "Detection of targets in non-Rayleigh sea clutter", *IEEE EASCON Record*, 1969, pp. 239-245.

Trunk, G.V. and George, S.F., (1970), "Detection of targets in non-Gaussian sea clutter", *IEEE Trans. Aerosp. and Electronic Systems*, Vol. AES-6, Sept. 1970, pp. 620-638.

Trunk, G.V., (1972), "Radar properties of non-Rayleigh sea clutter", *IEEE Trans. Aerosp. and Electronic Systems*, Vol. AES-8, No. 1, March 1972, pp. 196-204.

Trunk, G.V., Cantrell, B.H. and Queen, F.D., (1974), "Modified generalized sign test processor for 2-D radar", *IEEE Trans. Aerosp. and Electronic Systems*, Vol. AES-10, No. 5, Sept. 1974, pp. 574-582.

Trunk, G.V., (1978), "Range resolution of targets using automatic detectors", *IEEE Trans. Aerosp. and Electronic Systems*, Vol. AES-14, No. 4, Sept. 1978, pp. 750-755.

Vaughan, R.J. and Venables, W.N., (1972), "Permanent expressions for order statistic densities", *Journal of the Royal Statist. Soc. B, 34*, 1972, pp. 302-310.

Ward, K.D. and Watts, S., (1982), "A radar sea clutter model and its application to performance assessment", *IEE Conf. Publ. 216*, (Radar '82), 1982, pp. 203-207.

Ward, K.D. and Watts, S., (1985), "Radar sea clutter", *Microwave Journal*, June 1985, pp. 109-118.

Ward, K.D., Baker, C.J. and Watts, S., (1990), "Maritime surveillance radar, Part 1: Radar scattering from the ocean surface", *IEE Proc.*, Vol. 137, Pt. F, No. 2, April 1990, pp. 51-62.

Watts, S., (1985), "Radar detection prediction in sea clutter using the compound K-distribution model", *IEE Proc.*, Vol. 132, Pt. F, No. 7, Dec. 1985, pp. 613-620.

Watts, S., (1987), "Radar detection prediction in K-distributed sea clutter and thermal noise", *IEEE Trans. Aerosp. and Electronic Systems*, Vol. AES-23, No. 1, Jan. 1987, pp. 40-45.

Watts, S., Baker, C.J. and Ward, K.D., (1990a), "Maritime surveillance radar, Part 2: Detection performance in sea clutter", *IEE Proc.*, Vol. 137, Pt. F, No. 2, April 1990, pp. 63-72.

Watts, S. and Wicks, D.C., (1990b), "Empirical models for detection prediction in K-distributed radar sea clutter", *Proc. of the IEEE 1990 Int'l Radar Conf.*, Arlington, 1990, pp. 189-194.

Weber, P. and Haykin, S., (1985), "Order statistic CFAR processors for two-parameter distributions with variable skewness", *IEEE Trans. Aerosp. and Electronic Systems*, Vol. AES-21, Nov. 1985, pp. 819-831.

APPENDIX 1.1

THE USE OF DIFFERENCE CHANNEL INFORMATION FOR DETECTION IN MONOPULSE RADARS

Reproduced from
IEE Proc. Pt. F, vol. 138, No. 3, June 1991, pp. 199-210.

PAGE/PAGES EXCLUDED UNDER INSTRUCTION FROM UNIVERSITY

APPENDIX 2.1

CLOSED FORM EXPRESSIONS FOR THE SUM OF N K-DISTRIBUTED VARIABLES

The K-distribution is:

$$p(x) = \frac{4c}{\Gamma(\nu)} (cx)^{\nu} K_{\nu-1}(2cx) \qquad \ldots (A2.1.1)$$

For $\nu = m+1/2$; $m = 0, 1, 2, \ldots$, we can write $K_{\nu-1}(2cx)$ as:

$$K_{m+1/2}(2cx) = \sqrt{\frac{\pi}{2}} \frac{e^{-2cx}}{\sqrt{2cx}} \sum_{i=0}^{m} \frac{(m+i)!\ (2cx)^{-i}}{i!\ (m-i)!\ 2^{i}} \qquad \ldots (A2.1.2)$$

For $\nu = 1/2$, substituting eqn (A2.1.2) into (A2.1.1) yields an exponential distribution such that:

$$p(x) = 2ce^{-2cx} \qquad \ldots (A2.1.3)$$

from which the sum of N such variables is easily shown to have a PDF given by:

$$p_N(x) = \frac{2c}{\Gamma(N)} (2cx)^{N-1} e^{-2cx} \qquad \ldots (A2.1.4)$$

For $\nu = 3/2$, eqn.(A2.1.1) reduces to:

$$p(x) = 4c^2 x\, e^{-2cx} \qquad \ldots (A2.1.5)$$

from which the PDF of the sum of N such variables is easily shown to be:

$$p_N(x) = \frac{(2c)^{2N}}{\Gamma(2N)} x^{2N-1} e^{-2cx} \qquad \ldots (A2.1.6)$$

For $\nu > m + 3/2$, the PDF of the sum of N variables is calculated as follows. For notational simplicity let $y = 2cx$; $\gamma = c\sqrt{\pi} / ((2^m\Gamma(\nu))$ and $a_i = (m+i)! / (2^i\, i!\, (m-i)!)$. Thus (A2.1.1) can be rewritten as:

$$p(y/2c) = \gamma e^{-y} \sum_{i=0}^{m} \alpha_i y^{m+1-i} \qquad \ldots (A2.1.7)$$

The moment generating function of this PDF is thus:

$$M(\theta) = \int_0^{\infty} p(y)\, e^{-\theta y}\, dy$$

$$= \gamma \sum_{i=0}^{M} \alpha_i \frac{(M+1-i)\,!}{(1+\theta)^{m+2-i}} \qquad \ldots (A2.1.8)$$

Addition of N independent variables with the characteristic function (A2.1.8) implies that the characteristic function of the sum, denoted $M_N(\theta)$, is given by:

$$M_N(\theta) = [M(\theta)]^N \qquad \ldots (A2.1.9)$$

Letting $1/(1+\theta) = \phi$, and $a_i\,(m+1-i)! = b_i = [(m+i)!\,(m+1-i)] / (2^i\, i!)$, eqn (A2.1.9) can be expanded using eqn (A2.1.8) as follows:

$$M_N(\theta) = \gamma^N \phi^{2N} \left[\sum_{i=0}^{m} \beta_i \phi^{m-i} \right]^N \qquad \ldots (A2.1.10)$$

Separating the m^{th} term of the summation and performing a binomial expansion allows (A2.1.10) to be rewritten as:

$$M_N(\theta) = \gamma^N \phi^{2N} \beta_m^N \sum_{j_0=0}^{N} \binom{N}{j_0} \beta_m^{-j_0} \left[\sum_{i=0}^{m-1} \beta_i \phi^{m-i} \right]^{j_0} \qquad \ldots (A2.1.11)$$

Repeating this step (m-1) times and re-ordering terms gives:

$$M_N(\theta) = \gamma^N \sum_{j_0=0}^{N} \sum_{j_1=0}^{j_0} \sum_{j_2=0}^{j_1} \cdots\cdots \sum_{j_{m-1}=0}^{j_{m-2}} \binom{N}{j_0} \binom{j_0}{j_1} \binom{j_1}{j_2} \cdots \binom{j_{m-2}}{j_{m-1}} \cdot\cdot$$

$$\cdots \beta_m^{N-j_0} \beta_{m-1}^{j_0-j_1} \beta_{m-2}^{j_1-j_2} \cdots\cdots \beta_1^{j_{m-2}-j_{m-1}} \beta_0^{j_{m-1}} \phi^{2N+j_0+j_1+j_2+\cdots\cdots+j_{m-1}} \quad \cdots (A2.1.12)$$

The inverse Laplace Transform of (A2.1.12) then gives the PDF of the sum of N variables, i.e.

$$p_N(y) = \gamma^N e^{-y} \sum_{j_0=0}^{N} \sum_{j_1=0}^{j_0} \sum_{j_2=0}^{j_1} \cdots \sum_{j_{m-1}=0}^{j_{m-1}} \binom{N}{j_0} \binom{j_0}{j_1} \cdots \binom{j_{m-2}}{j_{m-1}} \frac{\beta_m^{N-j_0} \beta_{m-1}^{j_0-j_1} \cdots \beta_0^{j_{m-1}}}{\Gamma(2N + j_0 + j_1 + \cdots + j_{m-1})}$$

$$\cdot y^{2N-1+j_0+j_1+\cdots+j_{m-1}} \quad \cdots (A2.1.13)$$

APPENDIX 2.2

SUMMARY OF DIFFERENT ADAPTATION TECHNIQUES FOR ADAPTIVE DOPPLER FILTERING

1. Least Mean Square (LMS) / Minimum Square Error (MSE)

These two equivalent formulations yield a simple recursive estimator of the covariance matrix of the N samples. It is characterised by a long (sometimes infinite) convergence time which is strongly dependent on the clutter environment. About N x the number of loops (which can be large) complex multiplications are required to arrive at the filter weights. It has the advantages of requiring only low numerical precision in the multipliers and it suffers insignificant weight noise in thermal noise environments, rising to a few dBs of weight noise in some clutter environments.

2. Normalised LMS (NLMS)

A modification of the LMS routine to provide rapid convergence. Initial analyses indicated that it generally yields a 3 to 10 fold reduction in transient response and sometimes more, and is less affected by the form of clutter spectrum than the LMS. The increase in steady state loss was thought to be negligible. However, later analyses which included the effects of weight noise showed that the weight noise is quite large (~4 dB) even in thermal noise environments, and rising quite rapidly in clutter environments. In addition, weight noise effectively increases the convergence time to about that of the LMS algorithm. The NLMS would therefore seem not to provide any real benefits over the LMS algorithm.

3. Sample Matrix Inversion (SMI)

A Maximum Likelihood estimate of the clutter covariance matrix M is obtained simply as the arithmetic average of the corresponding elements of the covariance matrix in each of the range bins over which the covariance matrix is estimated. This is followed by matrix inversion and solution for the filter weights. The convergence time is reduced by an order of magnitude compared to the LMS algorithm, and is insensitive to the clutter parameters, with the number of cells averaged $K \sim 2N$ for steady state loss ≤ 3 dB (where N is the order of the canceller). The technique is applicable to any clutter spectrum since no assumptions are made regarding *a priori* knowledge of the spectrum. $(7/6)N^3$ complex multiplications are required to arrive at the filter weights; however, these only need to be calculated at most every N pulses, and often less frequently, thereby reducing the computation rate. High numerical accuracy ($\geq$ 10 bits) is required to avoid excessive weight noise.

4. Direct Matrix Inversion (DMI)

In this technique the inverse M^{-1} of the clutter covariance matrix is recursively estimated directly from the clutter samples. The identity matrix is usually taken as the initialisation condition; the N range bins in the region of the bin being filtered are then used to successively refine the estimate of M^{-1}. The rate of convergence is controlled by a "smoothing parameter" α, the value of which determines the balance between transient response and steady state error. It appears as though suitable selection of α gives $k \approx 10$ to 20 for a steady state error of 2 - 3 dB (this is quoted for N = 4; more comprehensive performance analyses including the effects of other values of N have not been reported). Again, no *a priori* assumptions are made as to the form of M^{-1} so the technique is insensitive to specific clutter parameters. Computationally $3N^2 + N$ complex multiplications are involved in deriving the filter weights; high numerical accuracy ($\geq$ 10 bits) is required to maintain a steady state loss in the region of 2 dB. The technique appears to have no simple parallel processing implementation, but in some applications the recursive structure (operating over range) may have some advantages over the block averaging structure of other techniques. It may have particular benefits in reducing masking on one side of clutter edges, at the expense of worse masking on the other side.

5. Gram Schmidt Orthogonalisation (GS)

The GS technique derives directly from optimal processing theory; it involves the successive decorrelation of one sample with the next until all samples in a processing interval are uncorrelated with each other to achieve whitening of the clutter returns, followed by a filter matched to the expected target doppler. No *a priori* assumptions are made regarding the clutter spectrum and hence performance is independent of the clutter actually present (within the limitations of N). Low steady state loss is achieved with moderately rapid convergence rates: for $N \leq 6$, we need $K \approx 10N$ for steady state loss of 0.5 dB in thermal noise, ~1dB with a single clutter source present, and ~ 2dB with 2 spectrally different clutter sources present. The technique has the advantages of a parallel and modular implementation, the clutter signal is whitened, preventing re-integration downstream, and no feedback is involved in the estimation of the coefficients and hence the filter is always stable. About $3N^2 - 2N$ complex multiplications are required with high numerical accuracy.

6. Parametric Estimation (PE)

In this technique the form of the overall clutter spectrum (eg. two Gaussian components of different widths, mean frequencies and amplitudes, in white noise) is assumed *a-priori*, with the parameters of the model then being estimated in real time. The corresponding optimal filter coefficients are calculated off-line and selected according to the estimated spectral parameters. This can yield significant computational savings and allows lower

numerical accuracy to be used. It has also been shown that provided the model chosen is correct and the parameter estimation is accurate, performance is essentially not degraded by the discretisation of parameters relative to the optimal filter for a specified N. However, the performance of the technique depends strongly on the validity of the clutter model, with good performance only being achieved under the assumed conditions. Furthermore, the steady state loss, transient response and efficiency will be directly limited by the algorithms used to estimate the clutter parameters. Although some results indicate that K ≈ 10 gives good estimates of parameters for a single Gaussian component clutter spectrum, the estimation of parameters in other clutter environments is not well documented and questions remain as to the form, efficiency, accuracy and transient response of parameter estimation algorithms.

7. Kalman Filtering

Although Kalman filter techniques have been described for clutter cancellation (Farina, 1984), they achieve adaptivity by updating the state vectors over successive pulses, thereby precluding their use in systems where a limited number of pulses is available per dwell or where even relatively low rate frequency and PRI agility is required. They will therefore not be covered any further in this thesis.

APPENDIX 3.1

DESCRIPTION OF MTD FILTER BANKS

The design goals for the MTD filter banks were as follows:

MTD 1: Intended for particularly severe land clutter. Therefore:

* Maximise the width and depth of the zero doppler notch in all filters.
* Sidelobe levels and main lobe width not too important.

The normalised frequency response of filters 1, 2, 3, and 5 are illustrtaed in Fig. A3.1.1. Filters 9, 8, and 7 are mirror images of filters 1, 2 and 3 respectively. Filters 4 and 6 are frequency translated versions of filter 5 to centre frequencies of 0.4 and 0.6 respectively. Filter 0 is arbitrarily chosen as a frequency shifted (to a centre frequency of 0) version of filter 5.

MTD 2: Gives some emphasis to land clutter suppresion, but assumes that cancellation of rain/chaff is also important. Therefore:

* Minimise the sidelobe level while maintaining a zero doppler notch.
* Accept reductions in the width and depth of the zero doppler notch.

The normalised frequency response of filters 1, 2, and 5 are illustrated in Fig. A3.1.2. Filters 9 and 8 are mirror images of filters 1 and 2 respectively. Filters 3, 4, 6 and 7 are frequency shifted versions of filter 5 to centre frequencies of 0.3, 0.4, 0.6 and 0.7 respectively. Filter 0 is arbitrarily chosen as a frequency shifted (to a centre frequency of 0) version of filter 5.

MTD 3: A compromise between MTD 1 and MTD 2, ie. some moving clutter suppresion is required, while maintaining strong emphasis on land clutter suppression. The normalised frequency response of filters 1, 2, 3, and 4 are illustrtaed in Fig. A3.1.3. Filters 9, 8, 7 and 6 are mirror images of filters 1, 2, 3 and 4 respectively. Filter 5 is identical to that in MTD 1. Filter 0 is arbitrarily chosen as a frequency shifted (to a centre frequency of 0) version of filter 5.

MTD 4: No particular emphasis is given to zero doppler clutter suppression. However, very good out-of-band rejection is required. Therefore:

* Minimise sidelobe level.
* Accept increase in main lobe width.

The normalised frequency reponse of filter 5 of MTD 4 is shown in Fig. A3.1.4a. Other filters are frequency shifted versions of this response to frequencies of 0, 0.1, ...0.9.

MTD 5: No emphasis is given to zero doppler clutter suppression, and no very strong clutter is expected; this would be applicable if the primary concern is the accurate estimation of true target doppler. Therefore:

* Minimise the main lobe width for a specified RMS sidelobe level, in this case -30 dB relative to the peak of the passband.

The frequency reponse of filter 5 of MTD 5 is shown in Fig. A3.1.4b. Other filters are frequency shifted versions of this response to frequencies of 0, 0.1, ...0.9.

MTD 6: A compromise between MTD 4 and MTD 6, in which the specified RMS sidelobe level is -40 dB.The normalised frequency reponse of filter 5 of MTD 6 is shown in Fig. A3.1.4c. Other filters are frequency shifted versions of this response to frequencies of 0, 0.1, ...0.9.

In all analyses in this study the gain of all filters has been normalised to give unity gain for white noise inputs (note that in Figs A1 to A4 different normalisation relative to the peak gain has been used). In noise limited detection scenarios the peak filter gain has a direct effect on detection performance; the peak gains of each of the filters in the six MTD banks is therefore given in Table A1.1 for completeness

Table A1.1
Peak Gain of Filters in MTD Filter Banks
(dB relative to thermal noise)

	Filter 0	Filter 1	Filter 2	Filter 3	Filter 4	Filter 5	Filter 6	Filter 7	Filter 8	Filter 9
MTD 1	8.11	8.10	9.28	8.45	8.11	8.11	8.11	8.45	9.28	8.10
MTD 2	8.11	9.65	8.78	8.11	8.11	8.11	8.11	8.11	8.78	9.65
MTD 3	8.11	9.65	9.09	8.45	8.33	8.11	8.33	8.45	9.09	9.65
MTD 4	8.11	8.11	8.11	8.11	8.11	8.11	8.11	8.11	8.11	8.11
MTD 5	9.44	9.44	9.44	9.44	9.44	9.44	9.44	9.44	9.44	9.44
MTD 6	8.93	8.93	8.93	8.93	8.93	8.93	8.93	8.93	8.93	8.93

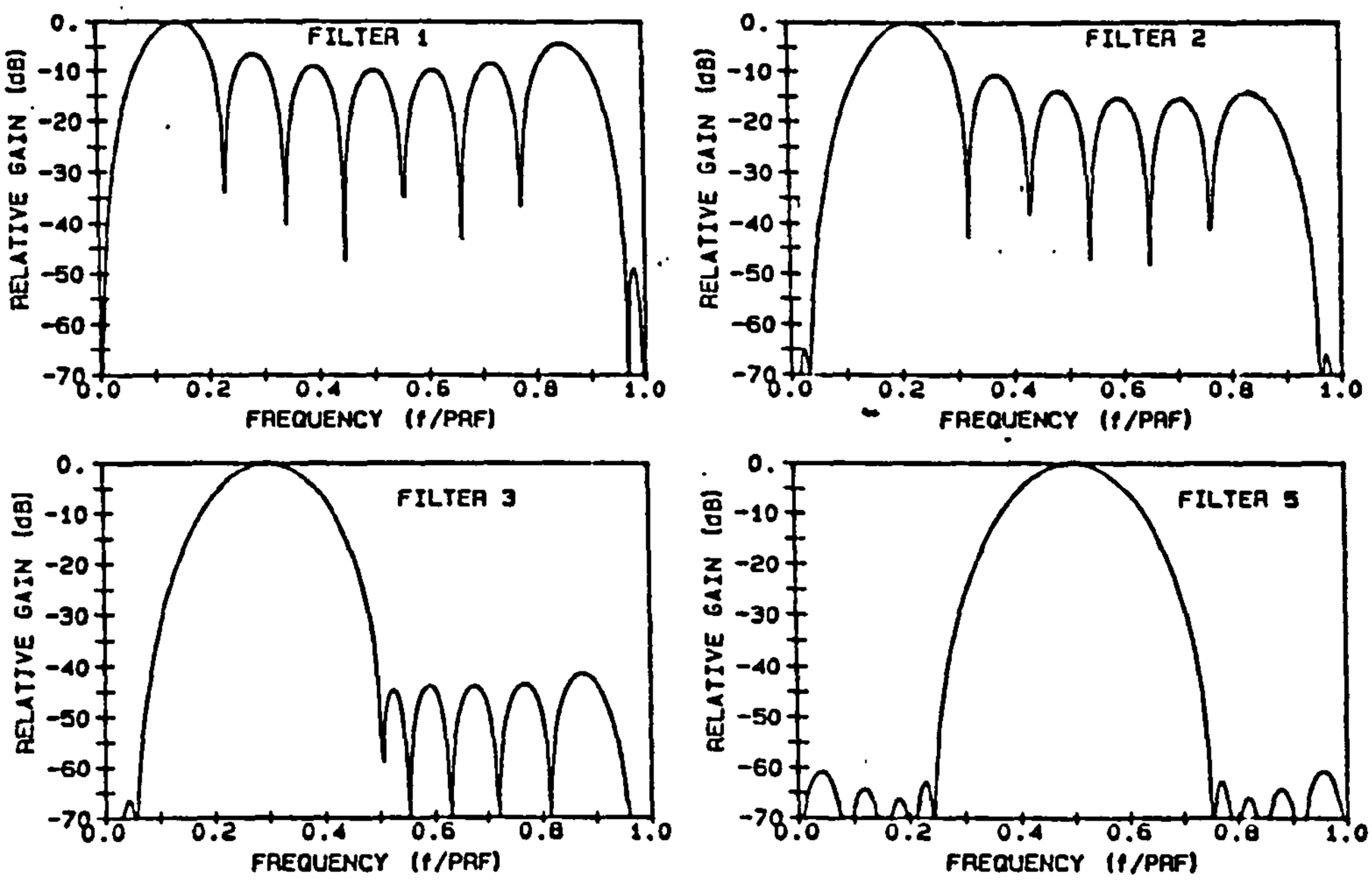

Fig. A3.1.1: *Normalised Frequency Response of Filters in MTD 1*

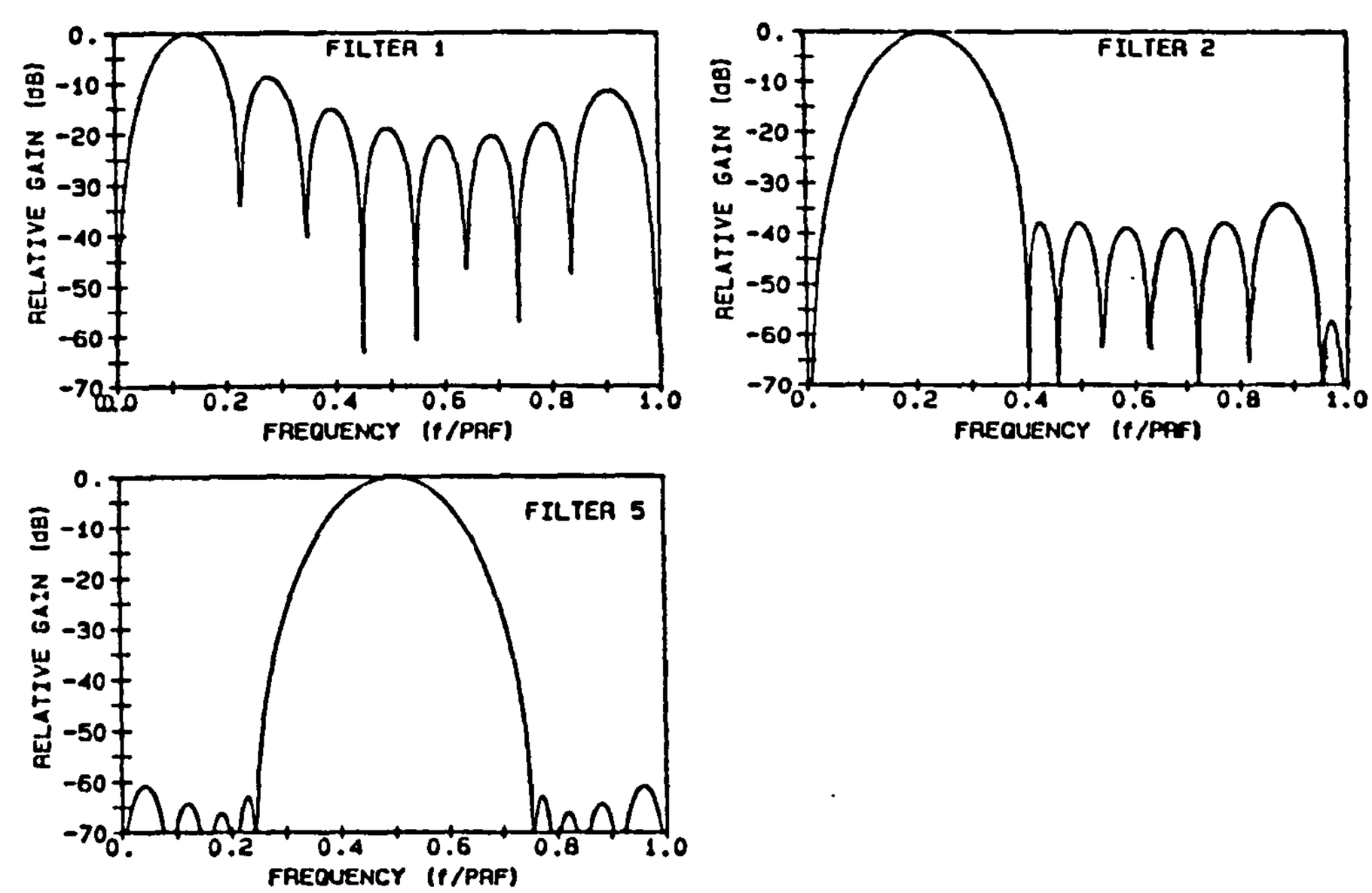

Fig. A3.1.2: *Normalised Frequency Response of Filters in MTD 2*

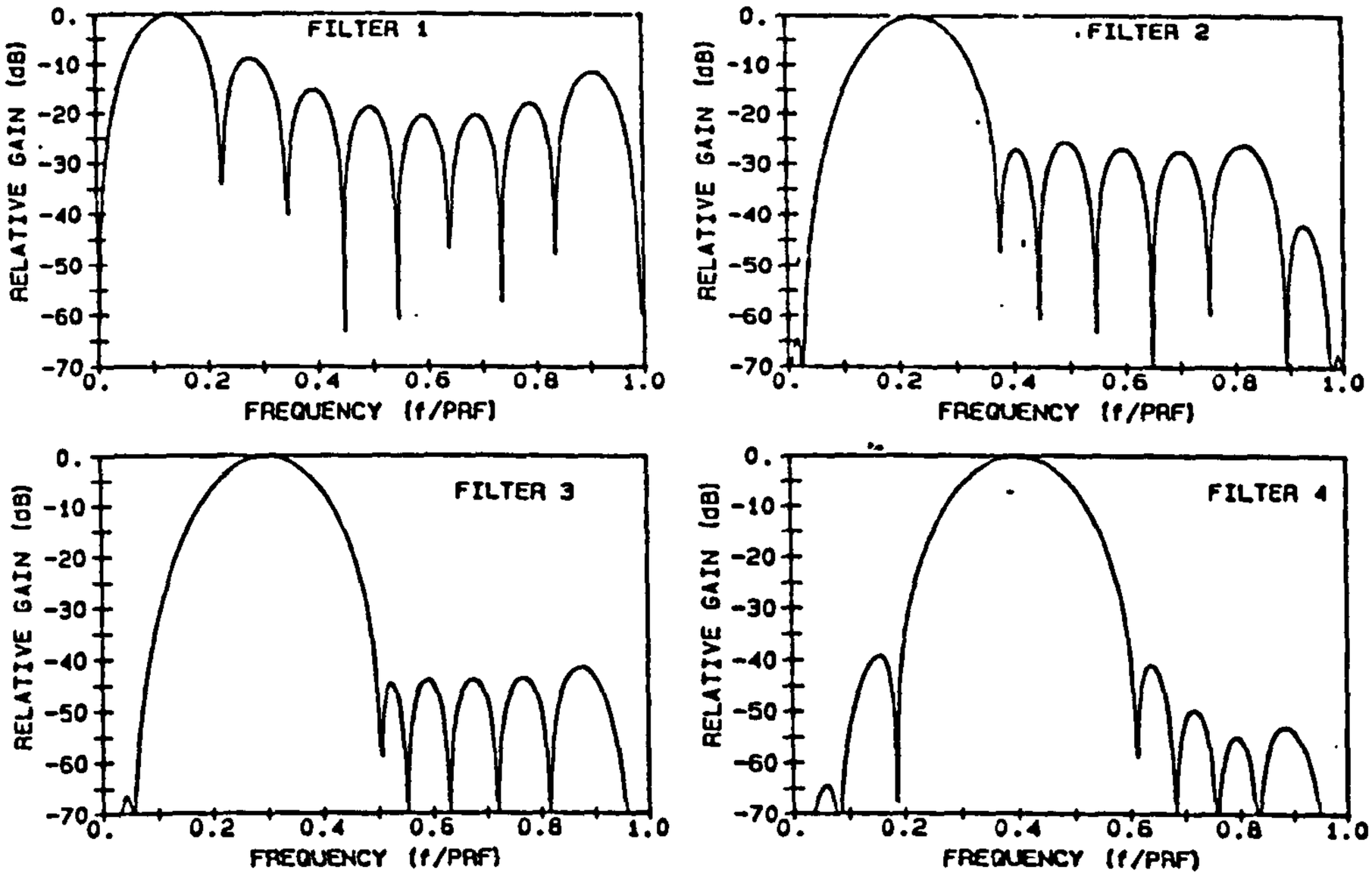

Fig. A3.1.3: *Normalised Frequency Response of Filters in MTD 3*

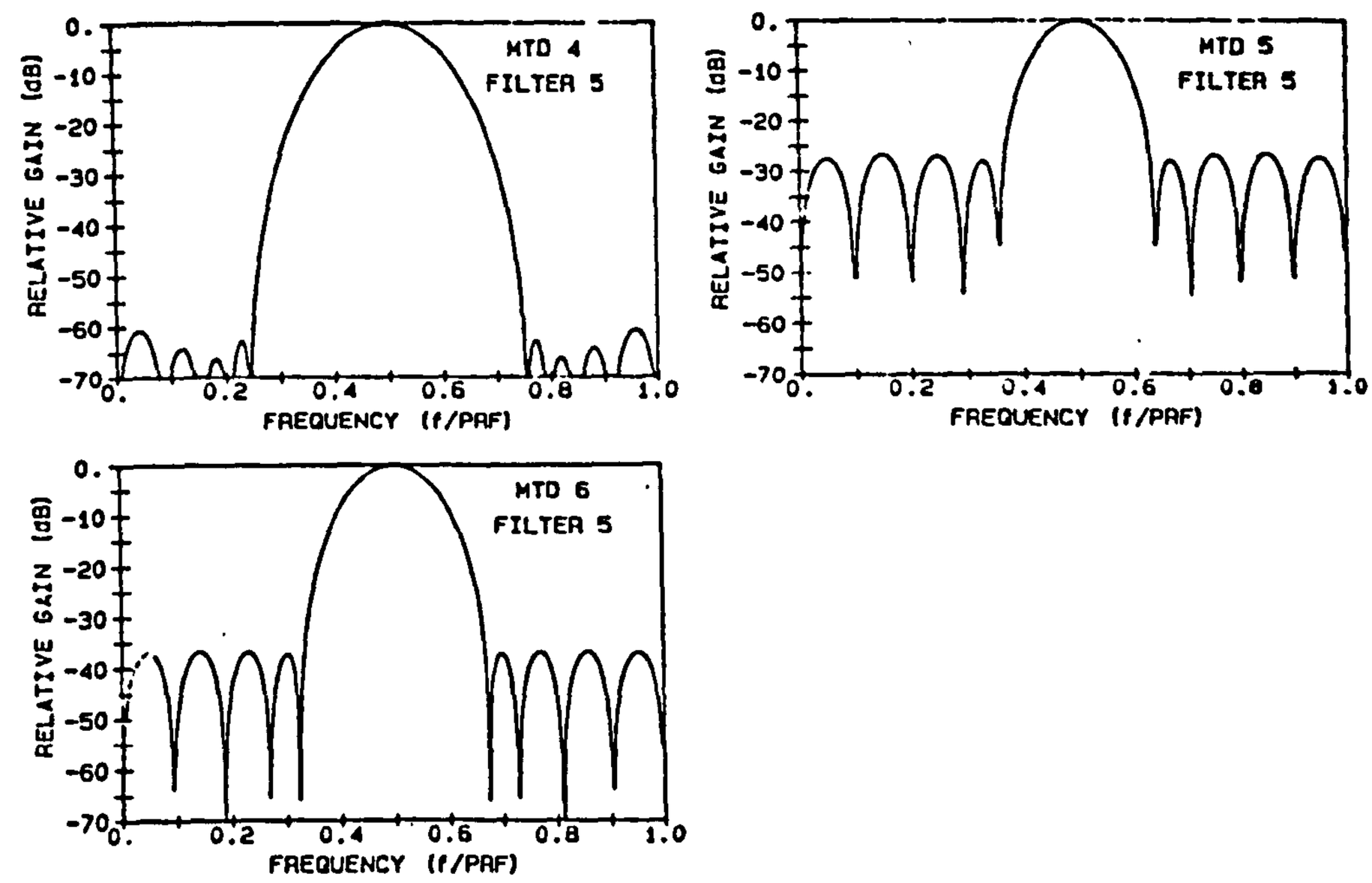

Fig. A3.1.4: *Normalised Frequency Response of Filters*
a) MTD 4; b) MTD 5; c) MTD 6

APPENDIX 3.2

DEFINITION OF LAND CLUTTER SCENARIOS

Index	CNR_1	σ_1	CNR_2	σ_2	fc_2
1	20.000	.003	-50.000	.010	.000
2	20.000	.003	-50.000	.010	.125
3	20.000	.003	-50.000	.010	.250
4	20.000	.003	-50.000	.010	.375
5	20.000	.003	-50.000	.010	.500
6	20.000	.003	10.000	.010	.000
7	20.000	.003	10.000	.010	.125
8	20.000	.003	10.000	.010	.250
9	20.000	.003	10.000	.010	.375
10	20.000	.003	10.000	.010	.500
11	20.000	.003	10.000	.030	.000
12	20.000	.003	10.000	.030	.125
13	20.000	.003	10.000	.030	.250
14	20.000	.003	10.000	.030	.375
15	20.000	.003	10.000	.030	.500
16	20.000	.003	10.000	.100	.000
17	20.000	.003	10.000	.100	.125
18	20.000	.003	10.000	.100	.250
19	20.000	.003	10.000	.100	.375
20	20.000	.003	10.000	.100	.500
21	20.000	.003	20.000	.010	.000
22	20.000	.003	20.000	.010	.125
23	20.000	.003	20.000	.010	.250
24	20.000	.003	20.000	.010	.375
25	20.000	.003	20.000	.010	.500
26	20.000	.003	20.000	.030	.000
27	20.000	.003	20.000	.030	.125
28	20.000	.003	20.000	.030	.250
29	20.000	.003	20.000	.030	.375
30	20.000	.003	20.000	.030	.500
31	20.000	.003	20.000	.100	.000
32	20.000	.003	20.000	.100	.125
33	20.000	.003	20.000	.100	.250
34	20.000	.003	20.000	.100	.375
35	20.000	.003	20.000	.100	.500
36	20.000	.003	30.000	.010	.000
37	20.000	.003	30.000	.010	.125
38	20.000	.003	30.000	.010	.250
39	20.000	.003	30.000	.010	.375
40	20.000	.003	30.000	.010	.500
41	20.000	.003	30.000	.030	.000
42	20.000	.003	30.000	.030	.125
43	20.000	.003	30.000	.030	.250
44	20.000	.003	30.000	.030	.375
45	20.000	.003	30.000	.030	.500
46	20.000	.003	30.000	.100	.000
47	20.000	.003	30.000	.100	.125
48	20.000	.003	30.000	.100	.250
49	20.000	.003	30.000	.100	.375
50	20.000	.003	30.000	.100	.500

Index	CNR_1	σ_1	CNR_2	σ_2	fc_2
51	20.000	.010	-50.000	.010	.000
52	20.000	.010	-50.000	.010	.125
53	20.000	.010	-50.000	.010	.250
54	20.000	.010	-50.000	.010	.375
55	20.000	.010	-50.000	.010	.500
56	20.000	.010	10.000	.010	.000
57	20.000	.010	10.000	.010	.125
58	20.000	.010	10.000	.010	.250
59	20.000	.010	10.000	.010	.375
60	20.000	.010	10.000	.010	.500
61	20.000	.010	10.000	.030	.000
62	20.000	.010	10.000	.030	.125
63	20.000	.010	10.000	.030	.250
64	20.000	.010	10.000	.030	.375
65	20.000	.010	10.000	.030	.500
66	20.000	.010	10.000	.100	.000
67	20.000	.010	10.000	.100	.125
68	20.000	.010	10.000	.100	.250
69	20.000	.010	10.000	.100	.375
70	20.000	.010	10.000	.100	.500
71	20.000	.010	20.000	.010	.000
72	20.000	.010	20.000	.010	.125
73	20.000	.010	20.000	.010	.250
74	20.000	.010	20.000	.010	.375
75	20.000	.010	20.000	.010	.500
76	20.000	.010	20.000	.030	.000
77	20.000	.010	20.000	.030	.125
78	20.000	.010	20.000	.030	.250
79	20.000	.010	20.000	.030	.375
80	20.000	.010	20.000	.030	.500
81	20.000	.010	20.000	.100	.000
82	20.000	.010	20.000	.100	.125
83	20.000	.010	20.000	.100	.250
84	20.000	.010	20.000	.100	.375
85	20.000	.010	20.000	.100	.500
86	20.000	.010	30.000	.010	.000
87	20.000	.010	30.000	.010	.125
88	20.000	.010	30.000	.010	.250
89	20.000	.010	30.000	.010	.375
90	20.000	.010	30.000	.010	.500
91	20.000	.010	30.000	.030	.000
92	20.000	.010	30.000	.030	.125
93	20.000	.010	30.000	.030	.250
94	20.000	.010	30.000	.030	.375
95	20.000	.010	30.000	.030	.500
96	20.000	.010	30.000	.100	.000
97	20.000	.010	30.000	.100	.125
98	20.000	.010	30.000	.100	.250
99	20.000	.010	30.000	.100	.375
100	20.000	.010	30.000	.100	.500

Index	CNR_1	σ_1	CNR_2	σ_2	fc_2
101	20.000	.030	-50.000	.010	.000
102	20.000	.030	-50.000	.010	.125
103	20.000	.030	-50.000	.010	.250
104	20.000	.030	-50.000	.010	.375
105	20.000	.030	-50.000	.010	.500
106	20.000	.030	10.000	.010	.000
107	20.000	.030	10.000	.010	.125
108	20.000	.030	10.000	.010	.250
109	20.000	.030	10.000	.010	.375
110	20.000	.030	10.000	.010	.500
111	20.000	.030	10.000	.030	.000
112	20.000	.030	10.000	.030	.125
113	20.000	.030	10.000	.030	.250
114	20.000	.030	10.000	.030	.375
115	20.000	.030	10.000	.030	.500
116	20.000	.030	10.000	.100	.000
117	20.000	.030	10.000	.100	.125
118	20.000	.030	10.000	.100	.250
119	20.000	.030	10.000	.100	.375
120	20.000	.030	10.000	.100	.500
121	20.000	.030	20.000	.010	.000
122	20.000	.030	20.000	.010	.125
123	20.000	.030	20.000	.010	.250
124	20.000	.030	20.000	.010	.375
125	20.000	.030	20.000	.010	.500
126	20.000	.030	20.000	.030	.000
127	20.000	.030	20.000	.030	.125
128	20.000	.030	20.000	.030	.250
129	20.000	.030	20.000	.030	.375
130	20.000	.030	20.000	.030	.500
131	20.000	.030	20.000	.100	.000
132	20.000	.030	20.000	.100	.125
133	20.000	.030	20.000	.100	.250
134	20.000	.030	20.000	.100	.375
135	20.000	.030	20.000	.100	.500
136	20.000	.030	30.000	.010	.000
137	20.000	.030	30.000	.010	.125
138	20.000	.030	30.000	.010	.250
139	20.000	.030	30.000	.010	.375
140	20.000	.030	30.000	.010	.500
141	20.000	.030	30.000	.030	.000
142	20.000	.030	30.000	.030	.125
143	20.000	.030	30.000	.030	.250
144	20.000	.030	30.000	.030	.375
145	20.000	.030	30.000	.030	.500
146	20.000	.030	30.000	.100	.000
147	20.000	.030	30.000	.100	.125
148	20.000	.030	30.000	.100	.250
149	20.000	.030	30.000	.100	.375
150	20.000	.030	30.000	.100	.500

Index	CNR_1	σ_1	CNR_2	σ_2	fc_2
151	40.000	.003	-50.000	.010	.000
152	40.000	.003	-50.000	.010	.125
153	40.000	.003	-50.000	.010	.250
154	40.000	.003	-50.000	.010	.375
155	40.000	.003	-50.000	.010	.500
156	40.000	.003	10.000	.010	.000
157	40.000	.003	10.000	.010	.125
158	40.000	.003	10.000	.010	.250
159	40.000	.003	10.000	.010	.375
160	40.000	.003	10.000	.010	.500
161	40.000	.003	10.000	.030	.000
162	40.000	.003	10.000	.030	.125
163	40.000	.003	10.000	.030	.250
164	40.000	.003	10.000	.030	.375
165	40.000	.003	10.000	.030	.500
166	40.000	.003	10.000	.100	.000
167	40.000	.003	10.000	.100	.125
168	40.000	.003	10.000	.100	.250
169	40.000	.003	10.000	.100	.375
170	40.000	.003	10.000	.100	.500
171	40.000	.003	20.000	.010	.000
172	40.000	.003	20.000	.010	.125
173	40.000	.003	20.000	.010	.250
174	40.000	.003	20.000	.010	.375
175	40.000	.003	20.000	.010	.500
176	40.000	.003	20.000	.030	.000
177	40.000	.003	20.000	.030	.125
178	40.000	.003	20.000	.030	.250
179	40.000	.003	20.000	.030	.375
180	40.000	.003	20.000	.030	.500
181	40.000	.003	20.000	.100	.000
182	40.000	.003	20.000	.100	.125
183	40.000	.003	20.000	.100	.250
184	40.000	.003	20.000	.100	.375
185	40.000	.003	20.000	.100	.500
186	40.000	.003	30.000	.010	.000
187	40.000	.003	30.000	.010	.125
188	40.000	.003	30.000	.010	.250
189	40.000	.003	30.000	.010	.375
190	40.000	.003	30.000	.010	.500
191	40.000	.003	30.000	.030	.000
192	40.000	.003	30.000	.030	.125
193	40.000	.003	30.000	.030	.250
194	40.000	.003	30.000	.030	.375
195	40.000	.003	30.000	.030	.500
196	40.000	.003	30.000	.100	.000
197	40.000	.003	30.000	.100	.125
198	40.000	.003	30.000	.100	.250
199	40.000	.003	30.000	.100	.375
200	40.000	.003	30.000	.100	.500

Index	CNR_1	σ_1	CNR_2	σ_2	fc_2
Z01	40.000	.010	-50.000	.010	.000
Z02	40.000	.010	-50.000	.010	.125
Z03	40.000	.010	-50.000	.010	.250
Z04	40.000	.010	-50.000	.010	.375
Z05	40.000	.010	-50.000	.010	.500
Z06	40.000	.010	10.000	.010	.000
Z07	40.000	.010	10.000	.010	.125
Z08	40.000	.010	10.000	.010	.250
Z09	40.000	.010	10.000	.010	.375
Z10	40.000	.010	10.000	.010	.500
Z11	40.000	.010	10.000	.030	.000
Z12	40.000	.010	10.000	.030	.125
Z13	40.000	.010	10.000	.030	.250
Z14	40.000	.010	10.000	.030	.375
Z15	40.000	.010	10.000	.030	.500
Z16	40.000	.010	10.000	.100	.000
Z17	40.000	.010	10.000	.100	.125
Z18	40.000	.010	10.000	.100	.250
Z19	40.000	.010	10.000	.100	.375
Z20	40.000	.010	10.000	.100	.500
Z21	40.000	.010	20.000	.010	.000
Z22	40.000	.010	20.000	.010	.125
Z23	40.000	.010	20.000	.010	.250
Z24	40.000	.010	20.000	.010	.375
Z25	40.000	.010	20.000	.010	.500
Z26	40.000	.010	20.000	.030	.000
Z27	40.000	.010	20.000	.030	.125
Z28	40.000	.010	20.000	.030	.250
Z29	40.000	.010	20.000	.030	.375
Z30	40.000	.010	20.000	.030	.500
Z31	40.000	.010	20.000	.100	.000
Z32	40.000	.010	20.000	.100	.125
Z33	40.000	.010	20.000	.100	.250
Z34	40.000	.010	20.000	.100	.375
Z35	40.000	.010	20.000	.100	.500
Z36	40.000	.010	30.000	.010	.000
Z37	40.000	.010	30.000	.010	.125
Z38	40.000	.010	30.000	.010	.250
Z39	40.000	.010	30.000	.010	.375
Z40	40.000	.010	30.000	.010	.500
Z41	40.000	.010	30.000	.030	.000
Z42	40.000	.010	30.000	.030	.125
Z43	40.000	.010	30.000	.030	.250
Z44	40.000	.010	30.000	.030	.375
Z45	40.000	.010	30.000	.030	.500
Z46	40.000	.010	30.000	.100	.000
Z47	40.000	.010	30.000	.100	.125
Z48	40.000	.010	30.000	.100	.250
Z49	40.000	.010	30.000	.100	.375
Z50	40.000	.010	30.000	.100	.500

Index	CNR_1	σ_1	CNR_2	σ_2	fc_2
Z51	40.000	.030	-50.000	.010	.000
Z52	40.000	.030	-50.000	.010	.125
Z53	40.000	.030	-50.000	.010	.250
Z54	40.000	.030	-50.000	.010	.375
Z55	40.000	.030	-50.000	.010	.500
Z56	40.000	.030	10.000	.010	.000
Z57	40.000	.030	10.000	.010	.125
Z58	40.000	.030	10.000	.010	.250
Z59	40.000	.030	10.000	.010	.375
Z60	40.000	.030	10.000	.010	.500
Z61	40.000	.030	10.000	.030	.000
Z62	40.000	.030	10.000	.030	.125
Z63	40.000	.030	10.000	.030	.250
Z64	40.000	.030	10.000	.030	.375
Z65	40.000	.030	10.000	.030	.500
Z66	40.000	.030	10.000	.100	.000
Z67	40.000	.030	10.000	.100	.125
Z68	40.000	.030	10.000	.100	.250
Z69	40.000	.030	10.000	.100	.375
Z70	40.000	.030	10.000	.100	.500
Z71	40.000	.030	20.000	.010	.000
Z72	40.000	.030	20.000	.010	.125
Z73	40.000	.030	20.000	.010	.250
Z74	40.000	.030	20.000	.010	.375
Z75	40.000	.030	20.000	.010	.500
Z76	40.000	.030	20.000	.030	.000
Z77	40.000	.030	20.000	.030	.125
Z78	40.000	.030	20.000	.030	.250
Z79	40.000	.030	20.000	.030	.375
Z80	40.000	.030	20.000	.030	.500
Z81	40.000	.030	20.000	.100	.000
Z82	40.000	.030	20.000	.100	.125
Z83	40.000	.030	20.000	.100	.250
Z84	40.000	.030	20.000	.100	.375
Z85	40.000	.030	20.000	.100	.500
Z86	40.000	.030	30.000	.010	.000
Z87	40.000	.030	30.000	.010	.125
Z88	40.000	.030	30.000	.010	.250
Z89	40.000	.030	30.000	.010	.375
Z90	40.000	.030	30.000	.010	.500
Z91	40.000	.030	30.000	.030	.000
Z92	40.000	.030	30.000	.030	.125
Z93	40.000	.030	30.000	.030	.250
Z94	40.000	.030	30.000	.030	.375
Z95	40.000	.030	30.000	.030	.500
Z96	40.000	.030	30.000	.100	.000
Z97	40.000	.030	30.000	.100	.125
Z98	40.000	.030	30.000	.100	.250
Z99	40.000	.030	30.000	.100	.375
300	40.000	.030	30.000	.100	.500

Index	CNR_1	σ_1	CNR_2	σ_2	fc_2
301	60.000	.003	-50.000	.010	.000
302	60.000	.003	-50.000	.010	.125
303	60.000	.003	-50.000	.010	.250
304	60.000	.003	-50.000	.010	.375
305	60.000	.003	-50.000	.010	.500
306	60.000	.003	10.000	.010	.000
307	60.000	.003	10.000	.010	.125
308	60.000	.003	10.000	.010	.250
309	60.000	.003	10.000	.010	.375
310	60.000	.003	10.000	.010	.500
311	60.000	.003	10.000	.030	.000
312	60.000	.003	10.000	.030	.125
313	60.000	.003	10.000	.030	.250
314	60.000	.003	10.000	.030	.375
315	60.000	.003	10.000	.030	.500
316	60.000	.003	10.000	.100	.000
317	60.000	.003	10.000	.100	.125
318	60.000	.003	10.000	.100	.250
319	60.000	.003	10.000	.100	.375
320	60.000	.003	10.000	.100	.500
321	60.000	.003	20.000	.010	.000
322	60.000	.003	20.000	.010	.125
323	60.000	.003	20.000	.010	.250
324	60.000	.003	20.000	.010	.375
325	60.000	.003	20.000	.010	.500
326	60.000	.003	20.000	.030	.000
327	60.000	.003	20.000	.030	.125
328	60.000	.003	20.000	.030	.250
329	60.000	.003	20.000	.030	.375
330	60.000	.003	20.000	.030	.500
331	60.000	.003	20.000	.100	.000
332	60.000	.003	20.000	.100	.125
333	60.000	.003	20.000	.100	.250
334	60.000	.003	20.000	.100	.375
335	60.000	.003	20.000	.100	.500
336	60.000	.003	30.000	.010	.000
337	60.000	.003	30.000	.010	.125
338	60.000	.003	30.000	.010	.250
339	60.000	.003	30.000	.010	.375
340	60.000	.003	30.000	.010	.500
341	60.000	.003	30.000	.030	.000
342	60.000	.003	30.000	.030	.125
343	60.000	.003	30.000	.030	.250
344	60.000	.003	30.000	.030	.375
345	60.000	.003	30.000	.030	.500
346	60.000	.003	30.000	.100	.000
347	60.000	.003	30.000	.100	.125
348	60.000	.003	30.000	.100	.250
349	60.000	.003	30.000	.100	.375
350	60.000	.003	30.000	.100	.500

Index	CNR_1	σ_1	CNR_2	σ_2	fc_2
351	60.000	.010	-50.000	.010	.000
352	60.000	.010	-50.000	.010	.125
353	60.000	.010	-50.000	.010	.250
354	60.000	.010	-50.000	.010	.375
355	60.000	.010	-50.000	.010	.500
356	60.000	.010	10.000	.010	.000
357	60.000	.010	10.000	.010	.125
358	60.000	.010	10.000	.010	.250
359	60.000	.010	10.000	.010	.375
360	60.000	.010	10.000	.010	.500
361	60.000	.010	10.000	.030	.000
362	60.000	.010	10.000	.030	.125
363	60.000	.010	10.000	.030	.250
364	60.000	.010	10.000	.030	.375
365	60.000	.010	10.000	.030	.500
366	60.000	.010	10.000	.100	.000
367	60.000	.010	10.000	.100	.125
368	60.000	.010	10.000	.100	.250
369	60.000	.010	10.000	.100	.375
370	60.000	.010	10.000	.100	.500
371	60.000	.010	20.000	.010	.000
372	60.000	.010	20.000	.010	.125
373	60.000	.010	20.000	.010	.250
374	60.000	.010	20.000	.010	.375
375	60.000	.010	20.000	.010	.500
376	60.000	.010	20.000	.030	.000
377	60.000	.010	20.000	.030	.125
378	60.000	.010	20.000	.030	.250
379	60.000	.010	20.000	.030	.375
380	60.000	.010	20.000	.030	.500
381	60.000	.010	20.000	.100	.000
382	60.000	.010	20.000	.100	.125
383	60.000	.010	20.000	.100	.250
384	60.000	.010	20.000	.100	.375
385	60.000	.010	20.000	.100	.500
386	60.000	.010	30.000	.010	.000
387	60.000	.010	30.000	.010	.125
388	60.000	.010	30.000	.010	.250
389	60.000	.010	30.000	.010	.375
390	60.000	.010	30.000	.010	.500
391	60.000	.010	30.000	.030	.000
392	60.000	.010	30.000	.030	.125
393	60.000	.010	30.000	.030	.250
394	60.000	.010	30.000	.030	.375
395	60.000	.010	30.000	.030	.500
396	60.000	.010	30.000	.100	.000
397	60.000	.010	30.000	.100	.125
398	60.000	.010	30.000	.100	.250
399	60.000	.010	30.000	.100	.375
400	60.000	.010	30.000	.100	.500

Index	CNR_1	σ_1	CNR_2	σ_2	fc_2
401	60.000	.030	-50.000	.010	.000
402	60.000	.030	-50.000	.010	.125
403	60.000	.030	-50.000	.010	.250
404	60.000	.030	-50.000	.010	.375
405	60.000	.030	-50.000	.010	.500
406	60.000	.030	10.000	.010	.000
407	60.000	.030	10.000	.010	.125
408	60.000	.030	10.000	.010	.250
409	60.000	.030	10.000	.010	.375
410	60.000	.030	10.000	.010	.500
411	60.000	.030	10.000	.030	.000
412	60.000	.030	10.000	.030	.125
413	60.000	.030	10.000	.030	.250
414	60.000	.030	10.000	.030	.375
415	60.000	.030	10.000	.030	.500
416	60.000	.030	10.000	.100	.000
417	60.000	.030	10.000	.100	.125
418	60.000	.030	10.000	.100	.250
419	60.000	.030	10.000	.100	.375
420	60.000	.030	10.000	.100	.500
421	60.000	.030	20.000	.010	.000
422	60.000	.030	20.000	.010	.125
423	60.000	.030	20.000	.010	.250
424	60.000	.030	20.000	.010	.375
425	60.000	.030	20.000	.010	.500
426	60.000	.030	20.000	.030	.000
427	60.000	.030	20.000	.030	.125
428	60.000	.030	20.000	.030	.250
429	60.000	.030	20.000	.030	.375
430	60.000	.030	20.000	.030	.500
431	60.000	.030	20.000	.100	.000
432	60.000	.030	20.000	.100	.125
433	60.000	.030	20.000	.100	.250
434	60.000	.030	20.000	.100	.375
435	60.000	.030	20.000	.100	.500
436	60.000	.030	30.000	.010	.000
437	60.000	.030	30.000	.010	.125
438	60.000	.030	30.000	.010	.250
439	60.000	.030	30.000	.010	.375
440	60.000	.030	30.000	.010	.500
441	60.000	.030	30.000	.030	.000
442	60.000	.030	30.000	.030	.125
443	60.000	.030	30.000	.030	.250
444	60.000	.030	30.000	.030	.375
445	60.000	.030	30.000	.030	.500
446	60.000	.030	30.000	.100	.000
447	60.000	.030	30.000	.100	.125
448	60.000	.030	30.000	.100	.250
449	60.000	.030	30.000	.100	.375
450	60.000	.030	30.000	.100	.500

APPENDIX 3.3

DEFINITION OF SEA CLUTTER SCENARIOS

Index	CNR_1	σ_1	fc_1	CNR_2	σ_2	fc_2
1	20.000	.010	.000	-20.000	.010	.000
2	20.000	.010	.000	-20.000	.010	.200
3	20.000	.010	.000	-20.000	.010	.400
4	20.000	.010	.000	-20.000	.010	.600
5	20.000	.010	.000	-20.000	.010	.800
6	20.000	.010	.000	10.000	.010	.000
7	20.000	.010	.000	10.000	.010	.200
8	20.000	.010	.000	10.000	.010	.400
9	20.000	.010	.000	10.000	.010	.600
10	20.000	.010	.000	10.000	.010	.800
11	20.000	.010	.000	10.000	.020	.000
12	20.000	.010	.000	10.000	.020	.200
13	20.000	.010	.000	10.000	.020	.400
14	20.000	.010	.000	10.000	.020	.600
15	20.000	.010	.000	10.000	.020	.800
16	20.000	.010	.000	30.000	.010	.000
17	20.000	.010	.000	30.000	.010	.200
18	20.000	.010	.000	30.000	.010	.400
19	20.000	.010	.000	30.000	.010	.600
20	20.000	.010	.000	30.000	.010	.800
21	20.000	.010	.000	30.000	.020	.000
22	20.000	.010	.000	30.000	.020	.200
23	20.000	.010	.000	30.000	.020	.400
24	20.000	.010	.000	30.000	.020	.600
25	20.000	.010	.000	30.000	.020	.800
26	20.000	.010	.250	-20.000	.010	.000
27	20.000	.010	.250	-20.000	.010	.200
28	20.000	.010	.250	-20.000	.010	.400
29	20.000	.010	.250	-20.000	.010	.600
30	20.000	.010	.250	-20.000	.010	.800
31	20.000	.010	.250	10.000	.010	.000
32	20.000	.010	.250	10.000	.010	.200
33	20.000	.010	.250	10.000	.010	.400
34	20.000	.010	.250	10.000	.010	.600
35	20.000	.010	.250	10.000	.010	.800
36	20.000	.010	.250	10.000	.020	.000
37	20.000	.010	.250	10.000	.020	.200
38	20.000	.010	.250	10.000	.020	.400
39	20.000	.010	.250	10.000	.020	.600
40	20.000	.010	.250	10.000	.020	.800
41	20.000	.010	.250	30.000	.010	.000
42	20.000	.010	.250	30.000	.010	.200
43	20.000	.010	.250	30.000	.010	.400
44	20.000	.010	.250	30.000	.010	.600
45	20.000	.010	.250	30.000	.010	.800
46	20.000	.010	.250	30.000	.020	.000
47	20.000	.010	.250	30.000	.020	.200
48	20.000	.010	.250	30.000	.020	.400
49	20.000	.010	.250	30.000	.020	.600
50	20.000	.010	.250	30.000	.020	.800

Index	CNR_1	σ_1	fc_1	CNR_2	σ_2	fc_2
51	20.000	.010	.500	-20.000	.010	.000
52	20.000	.010	.500	-20.000	.010	.200
53	20.000	.010	.500	-20.000	.010	.400
54	20.000	.010	.500	-20.000	.010	.600
55	20.000	.010	.500	-20.000	.010	.800
56	20.000	.010	.500	10.000	.010	.000
57	20.000	.010	.500	10.000	.010	.200
58	20.000	.010	.500	10.000	.010	.400
59	20.000	.010	.500	10.000	.010	.600
60	20.000	.010	.500	10.000	.010	.800
61	20.000	.010	.500	10.000	.020	.000
62	20.000	.010	.500	10.000	.020	.200
63	20.000	.010	.500	10.000	.020	.400
64	20.000	.010	.500	10.000	.020	.600
65	20.000	.010	.500	10.000	.020	.800
66	20.000	.010	.500	30.000	.010	.000
67	20.000	.010	.500	30.000	.010	.200
68	20.000	.010	.500	30.000	.010	.400
69	20.000	.010	.500	30.000	.010	.600
70	20.000	.010	.500	30.000	.010	.800
71	20.000	.010	.500	30.000	.020	.000
72	20.000	.010	.500	30.000	.020	.200
73	20.000	.010	.500	30.000	.020	.400
74	20.000	.010	.500	30.000	.020	.600
75	20.000	.010	.500	30.000	.020	.800
76	20.000	.100	.000	-20.000	.100	.000
77	20.000	.100	.000	-20.000	.100	.200
78	20.000	.100	.000	-20.000	.100	.400
79	20.000	.100	.000	-20.000	.100	.600
80	20.000	.100	.000	-20.000	.100	.800
81	20.000	.100	.000	10.000	.100	.000
82	20.000	.100	.000	10.000	.100	.200
83	20.000	.100	.000	10.000	.100	.400
84	20.000	.100	.000	10.000	.100	.600
85	20.000	.100	.000	10.000	.100	.800
86	20.000	.100	.000	10.000	.200	.000
87	20.000	.100	.000	10.000	.200	.200
88	20.000	.100	.000	10.000	.200	.400
89	20.000	.100	.000	10.000	.200	.600
90	20.000	.100	.000	10.000	.200	.800
91	20.000	.100	.000	30.000	.100	.000
92	20.000	.100	.000	30.000	.100	.200
93	20.000	.100	.000	30.000	.100	.400
94	20.000	.100	.000	30.000	.100	.600
95	20.000	.100	.000	30.000	.100	.800
96	20.000	.100	.000	30.000	.200	.000
97	20.000	.100	.000	30.000	.200	.200
98	20.000	.100	.000	30.000	.200	.400
99	20.000	.100	.000	30.000	.200	.600
100	20.000	.100	.000	30.000	.200	.800

Index	CNR_1	σ_1	fc_1	CNR_2	σ_2	fc_2
101	20.000	.100	.250	-20.000	.100	.000
102	20.000	.100	.250	-20.000	.100	.200
103	20.000	.100	.250	-20.000	.100	.400
104	20.000	.100	.250	-20.000	.100	.600
105	20.000	.100	.250	-20.000	.100	.800
106	20.000	.100	.250	10.000	.100	.000
107	20.000	.100	.250	10.000	.100	.200
108	20.000	.100	.250	10.000	.100	.400
109	20.000	.100	.250	10.000	.100	.600
110	20.000	.100	.250	10.000	.100	.800
111	20.000	.100	.250	10.000	.200	.000
112	20.000	.100	.250	10.000	.200	.200
113	20.000	.100	.250	10.000	.200	.400
114	20.000	.100	.250	10.000	.200	.600
115	20.000	.100	.250	10.000	.200	.800
116	20.000	.100	.250	30.000	.100	.000
117	20.000	.100	.250	30.000	.100	.200
118	20.000	.100	.250	30.000	.100	.400
119	20.000	.100	.250	30.000	.100	.600
120	20.000	.100	.250	30.000	.100	.800
121	20.000	.100	.250	30.000	.200	.000
122	20.000	.100	.250	30.000	.200	.200
123	20.000	.100	.250	30.000	.200	.400
124	20.000	.100	.250	30.000	.200	.600
125	20.000	.100	.250	30.000	.200	.800
126	20.000	.100	.500	-20.000	.100	.000
127	20.000	.100	.500	-20.000	.100	.200
128	20.000	.100	.500	-20.000	.100	.400
129	20.000	.100	.500	-20.000	.100	.600
130	20.000	.100	.500	-20.000	.100	.800
131	20.000	.100	.500	10.000	.100	.000
132	20.000	.100	.500	10.000	.100	.200
133	20.000	.100	.500	10.000	.100	.400
134	20.000	.100	.500	10.000	.100	.600
135	20.000	.100	.500	10.000	.100	.800
136	20.000	.100	.500	10.000	.200	.000
137	20.000	.100	.500	10.000	.200	.200
138	20.000	.100	.500	10.000	.200	.400
139	20.000	.100	.500	10.000	.200	.600
140	20.000	.100	.500	10.000	.200	.800
141	20.000	.100	.500	30.000	.100	.000
142	20.000	.100	.500	30.000	.100	.200
143	20.000	.100	.500	30.000	.100	.400
144	20.000	.100	.500	30.000	.100	.600
145	20.000	.100	.500	30.000	.100	.800
146	20.000	.100	.500	30.000	.200	.000
147	20.000	.100	.500	30.000	.200	.200
148	20.000	.100	.500	30.000	.200	.400
149	20.000	.100	.500	30.000	.200	.600
150	20.000	.100	.500	30.000	.200	.800

Index	CNR_1	σ_1	fc_1	CNR_2	σ_2	fc_2
151	40.000	.010	.000	-20.000	.010	.000
152	40.000	.010	.000	-20.000	.010	.200
153	40.000	.010	.000	-20.000	.010	.400
154	40.000	.010	.000	-20.000	.010	.600
155	40.000	.010	.000	-20.000	.010	.800
156	40.000	.010	.000	10.000	.010	.000
157	40.000	.010	.000	10.000	.010	.200
158	40.000	.010	.000	10.000	.010	.400
159	40.000	.010	.000	10.000	.010	.600
160	40.000	.010	.000	10.000	.010	.800
161	40.000	.010	.000	10.000	.020	.000
162	40.000	.010	.000	10.000	.020	.200
163	40.000	.010	.000	10.000	.020	.400
164	40.000	.010	.000	10.000	.020	.600
165	40.000	.010	.000	10.000	.020	.800
166	40.000	.010	.000	30.000	.010	.000
167	40.000	.010	.000	30.000	.010	.200
168	40.000	.010	.000	30.000	.010	.400
169	40.000	.010	.000	30.000	.010	.600
170	40.000	.010	.000	30.000	.010	.800
171	40.000	.010	.000	30.000	.020	.000
172	40.000	.010	.000	30.000	.020	.200
173	40.000	.010	.000	30.000	.020	.400
174	40.000	.010	.000	30.000	.020	.600
175	40.000	.010	.000	30.000	.020	.800
176	40.000	.010	.250	-20.000	.010	.000
177	40.000	.010	.250	-20.000	.010	.200
178	40.000	.010	.250	-20.000	.010	.400
179	40.000	.010	.250	-20.000	.010	.600
180	40.000	.010	.250	-20.000	.010	.800
181	40.000	.010	.250	10.000	.010	.000
182	40.000	.010	.250	10.000	.010	.200
183	40.000	.010	.250	10.000	.010	.400
184	40.000	.010	.250	10.000	.010	.600
185	40.000	.010	.250	10.000	.010	.800
186	40.000	.010	.250	10.000	.020	.000
187	40.000	.010	.250	10.000	.020	.200
188	40.000	.010	.250	10.000	.020	.400
189	40.000	.010	.250	10.000	.020	.600
190	40.000	.010	.250	10.000	.020	.800
191	40.000	.010	.250	30.000	.010	.000
192	40.000	.010	.250	30.000	.010	.200
193	40.000	.010	.250	30.000	.010	.400
194	40.000	.010	.250	30.000	.010	.600
195	40.000	.010	.250	30.000	.010	.800
196	40.000	.010	.250	30.000	.020	.000
197	40.000	.010	.250	30.000	.020	.200
198	40.000	.010	.250	30.000	.020	.400
199	40.000	.010	.250	30.000	.020	.600
200	40.000	.010	.250	30.000	.020	.800

Index	CNR_1	σ_1	fc_1	CNR_2	σ_2	fc_2
Z01	40.000	.010	.500	-20.000	.010	.000
Z02	40.000	.010	.500	-20.000	.010	.200
Z03	40.000	.010	.500	-20.000	.010	.400
Z04	40.000	.010	.500	-20.000	.010	.600
Z05	40.000	.010	.500	-20.000	.010	.800
Z06	40.000	.010	.500	10.000	.010	.000
Z07	40.000	.010	.500	10.000	.010	.200
Z08	40.000	.010	.500	10.000	.010	.400
Z09	40.000	.010	.500	10.000	.010	.600
Z10	40.000	.010	.500	10.000	.010	.800
Z11	40.000	.010	.500	10.000	.020	.000
Z12	40.000	.010	.500	10.000	.020	.200
Z13	40.000	.010	.500	10.000	.020	.400
Z14	40.000	.010	.500	10.000	.020	.600
Z15	40.000	.010	.500	10.000	.020	.800
Z16	40.000	.010	.500	30.000	.010	.000
Z17	40.000	.010	.500	30.000	.010	.200
Z18	40.000	.010	.500	30.000	.010	.400
Z19	40.000	.010	.500	30.000	.010	.600
Z20	40.000	.010	.500	30.000	.010	.800
Z21	40.000	.010	.500	30.000	.020	.000
Z22	40.000	.010	.500	30.000	.020	.200
Z23	40.000	.010	.500	30.000	.020	.400
Z24	40.000	.010	.500	30.000	.020	.600
Z25	40.000	.010	.500	30.000	.020	.800
Z26	40.000	.100	.000	-20.000	.100	.000
Z27	40.000	.100	.000	-20.000	.100	.200
Z28	40.000	.100	.000	-20.000	.100	.400
Z29	40.000	.100	.000	-20.000	.100	.600
Z30	40.000	.100	.000	-20.000	.100	.800
Z31	40.000	.100	.000	10.000	.100	.000
Z32	40.000	.100	.000	10.000	.100	.200
Z33	40.000	.100	.000	10.000	.100	.400
Z34	40.000	.100	.000	10.000	.100	.600
Z35	40.000	.100	.000	10.000	.100	.800
Z36	40.000	.100	.000	10.000	.200	.000
Z37	40.000	.100	.000	10.000	.200	.200
Z38	40.000	.100	.000	10.000	.200	.400
Z39	40.000	.100	.000	10.000	.200	.600
Z40	40.000	.100	.000	10.000	.200	.800
Z41	40.000	.100	.000	30.000	.100	.000
Z42	40.000	.100	.000	30.000	.100	.200
Z43	40.000	.100	.000	30.000	.100	.400
Z44	40.000	.100	.000	30.000	.100	.600
Z45	40.000	.100	.000	30.000	.100	.800
Z46	40.000	.100	.000	30.000	.200	.000
Z47	40.000	.100	.000	30.000	.200	.200
Z48	40.000	.100	.000	30.000	.200	.400
Z49	40.000	.100	.000	30.000	.200	.600
Z50	40.000	.100	.000	30.000	.200	.800

Index	CNR_1	σ_1	fc_1	CNR_2	σ_2	fc_2
251	40.000	.100	.250	-20.000	.100	.000
252	40.000	.100	.250	-20.000	.100	.200
253	40.000	.100	.250	-20.000	.100	.400
254	40.000	.100	.250	-20.000	.100	.600
255	40.000	.100	.250	-20.000	.100	.800
256	40.000	.100	.250	10.000	.100	.000
257	40.000	.100	.250	10.000	.100	.200
258	40.000	.100	.250	10.000	.100	.400
259	40.000	.100	.250	10.000	.100	.600
260	40.000	.100	.250	10.000	.100	.800
261	40.000	.100	.250	10.000	.200	.000
262	40.000	.100	.250	10.000	.200	.200
263	40.000	.100	.250	10.000	.200	.400
264	40.000	.100	.250	10.000	.200	.600
265	40.000	.100	.250	10.000	.200	.800
266	40.000	.100	.250	30.000	.100	.000
267	40.000	.100	.250	30.000	.100	.200
268	40.000	.100	.250	30.000	.100	.400
269	40.000	.100	.250	30.000	.100	.600
270	40.000	.100	.250	30.000	.100	.800
271	40.000	.100	.250	30.000	.200	.000
272	40.000	.100	.250	30.000	.200	.200
273	40.000	.100	.250	30.000	.200	.400
274	40.000	.100	.250	30.000	.200	.600
275	40.000	.100	.250	30.000	.200	.800
276	40.000	.100	.500	-20.000	.100	.000
277	40.000	.100	.500	-20.000	.100	.200
278	40.000	.100	.500	-20.000	.100	.400
279	40.000	.100	.500	-20.000	.100	.600
280	40.000	.100	.500	-20.000	.100	.800
281	40.000	.100	.500	10.000	.100	.000
282	40.000	.100	.500	10.000	.100	.200
283	40.000	.100	.500	10.000	.100	.400
284	40.000	.100	.500	10.000	.100	.600
285	40.000	.100	.500	10.000	.100	.800
286	40.000	.100	.500	10.000	.200	.000
287	40.000	.100	.500	10.000	.200	.200
288	40.000	.100	.500	10.000	.200	.400
289	40.000	.100	.500	10.000	.200	.600
290	40.000	.100	.500	10.000	.200	.800
291	40.000	.100	.500	30.000	.100	.000
292	40.000	.100	.500	30.000	.100	.200
293	40.000	.100	.500	30.000	.100	.400
294	40.000	.100	.500	30.000	.100	.600
295	40.000	.100	.500	30.000	.100	.800
296	40.000	.100	.500	30.000	.200	.000
297	40.000	.100	.500	30.000	.200	.200
298	40.000	.100	.500	30.000	.200	.400
299	40.000	.100	.500	30.000	.200	.600
300	40.000	.100	.500	30.000	.200	.800

APPENDIX 3.4

IMPROVEMENT FACTOR ANALYSIS

1. Calculation of False Alarm Rate

Let the desired false alarm rate at the output of the M_b/N_b integrator be P_{fa0}, the false alarm probability at the input to the M_b/N_b integrator be P_{fa1}; and the false alarm probability at the output of each CFAR detector in each doppler bin be P_{fa2}. Assume that P_{fa2} is identical and independent in each doppler bin. Then

$$P_{fa1} = 1 - [1- P_{fa2}]^N \qquad \ldots (A3.4.1)$$

Therefore:

$$P_{fa2} = 1 - [1- P_{fa1}]^{1/N} \approx P_{fa1}/N \qquad \ldots (A3.4.2)$$

Assuming also that P_{fa1} is identical and independent on each of the N_b bursts, the output false alarm probability P_{fa0} is given by

$$P_{fa0} = \sum_{i=M}^{N} \binom{N}{M} P_{fa1}^i [1- P_{fa1}]^{N-i} \qquad \ldots (A3.4.3)$$

The detection threshold in each detector is therefore obtained from inversion of eqn. (A3.4.2) to obtain P_{fa1}, substitution of the answer into eqn. (A3.4.2), and calculation of the threshold from :

$$\begin{aligned} T &= -P_c \ln(P_{fa2}) && \text{for ideal detection} \\ T &= P_c.N_r[P_{fa2}^{-1/N_r} -1] && \text{for a CA CFAR detector} \end{aligned} \qquad \ldots (A3.4.4)$$

where P_c is the clutter residue power.

2. Calculation of Detection Probabilities

Given clutter with covariance matrix **M**, the clutter residue and signal powers out of each filter are given by $P_c = \mathbf{W}^H\mathbf{M}\mathbf{W}$ and $P_s = [\mathbf{W}\mathbf{S}]^2$ respectively, where **W** is the complex filter weight vector and **S** is the complex signal vector, of magnitude S_0 and frequency f_t. Using the threshold and SCR values obtained above the detection probability Pd_i on each

filter channel i is obtained as usual from Marcum's Q function for non-fluctuating targets in Rayleigh backgrounds. On an individual burst k this detection probability is a function of the wavelength λ_k and PRF on that burst, and the target doppler (and is hence periodic with target velocity v with period equal to $\lambda_k.PRF_k/2$).The probability of detection over all filters is obtained from:

$$Pd(v,k) = 1 - \prod_{i=1}^{N} (1 - Pd_i) \approx \max_i(Pd_i) \qquad \ldots (A3.4.5)$$

Then for a given target velocity v the overall detection probability after 1/3 binary integration is given by $\overline{Pd_{1/3}}(v) = 1 - (1 - Pd(v,1))(1 - Pd(v,2))(1 - Pd(v,3))$. The final result is obtained by averaging this over all likely target velocities, ie:

$$\overline{Pd_{1/3}} = \int_{-v_{max}}^{v_{max}} p_v(v).\ \overline{Pd_{1/3}}(v)\ dv \qquad \ldots (A3.4.6)$$

In this study $p_v(v)$ was taken as being uniform between -10 PRF and +10 PRF; the stagger pattern ratio was taken as 12:13:15. Eqn. (A3.4.6) was evaluated for each type of filter in each clutter scenario for signal powers of -10 dB to 50 dB (relative to thermal noise in 2 dB increments). The signal powers S_{dp} (with doppler processing) and S_0 (without doppler processing but assuming non-coherent integration of the same number of pulses in each burst) required to achieve Pd = 50% were found. The true IF was then calculated as IF = S_0/S_{dp}.

APPENDIX 3.5

RESULTS OF IMPROVEMENT FACTOR ANALYSIS

Table 3.5.1

IF for Different Doppler Processors, Land Clutter Scenarios

Scenario Index	MTD						PD&MTI							
	1	2	3	4	5	6	Ham. b=6	Kais. b=6	OF	OF& MTI	LP& MTI	LP	AMTI &MTI	AMTI
1	28.6	28.7	28.9	28.0	29.4	28.8	28.5	27.8	30.0	30.0	21.6	20.9	24.5	23.7
2	29.0	29.1	29.3	28.4	29.7	29.2	28.9	28.2	30.4	30.4	21.9	21.4	24.9	24.1
3	29.0	28.8	28.9	28.4	29.4	29.2	28.8	28.0	30.3	30.2	19.5	21.0	24.9	24.0
4	27.7	27.7	27.8	27.7	28.4	28.3	27.7	27.0	29.8	29.7	18.1	20.4	24.4	22.1
5	31.5	31.4	31.6	30.9	31.6	31.7	31.5	30.8	32.9	32.9	23.6	23.4	27.5	25.6
6	31.4	31.0	31.4	30.9	29.9	31.3	31.0	30.4	32.7	32.7	21.9	23.4	27.5	26.4
7	29.1	29.1	29.3	29.1	28.2	29.8	28.9	27.9	31.1	30.9	19.4	22.5	24.0	18.4
8	38.9	38.6	38.9	38.3	35.4	38.1	38.8	38.0	40.2	40.2	30.0	31.6	34.8	34.0
9	38.4	38.3	38.5	38.3	30.4	35.7	38.3	37.5	40.0	39.9	30.1	30.8	34.8	32.0
10	33.6	33.6	33.6	33.6	28.1	33.3	33.4	31.4	35.6	35.3	25.4	28.3	23.6	16.4
11	28.6	28.4	28.6	28.0	28.8	28.8	28.5	27.8	29.9	29.9	20.6	20.5	24.5	23.7
12	29.0	28.8	29.0	28.4	29.1	29.2	28.9	28.2	30.3	30.3	20.9	20.9	24.9	24.1
13	29.0	28.6	28.9	28.4	28.9	29.1	28.8	28.0	30.3	30.2	19.4	20.7	24.9	24.0
14	27.7	27.7	27.8	27.7	27.9	28.3	27.7	27.0	29.8	29.6	18.0	20.4	24.4	22.1
15	31.5	31.3	31.6	30.9	31.1	31.6	31.5	30.7	32.9	32.9	22.9	23.3	27.5	25.6
16	31.4	31.0	31.4	30.9	29.6	31.3	31.0	30.4	32.7	32.7	21.9	23.5	27.5	26.4
17	29.1	29.1	29.3	29.1	27.9	29.8	28.9	27.9	31.1	30.9	19.4	22.5	24.0	18.4
18	38.9	38.6	38.9	38.3	35.1	38.1	38.7	37.9	40.2	40.2	30.0	31.6	34.8	34.0
19	38.4	38.3	38.5	38.3	30.3	35.7	38.3	37.5	40.0	39.9	30.1	30.9	34.8	32.0
20	33.6	33.6	33.6	33.6	28.0	33.2	33.4	31.4	35.6	35.3	25.4	28.3	23.6	16.4
21	28.4	28.0	28.4	27.9	27.0	28.4	28.0	27.4	29.8	29.7	19.0	20.4	24.5	23.4
22	28.8	28.4	28.8	28.4	27.3	28.8	28.5	27.8	30.2	30.1	19.4	20.8	24.9	23.8
23	28.8	28.4	28.8	28.4	27.2	28.8	28.5	27.8	30.2	30.1	19.4	20.9	24.9	23.8
24	27.7	27.7	27.8	27.7	26.4	28.1	27.7	27.0	29.7	29.6	17.7	20.4	24.4	21.9
25	31.4	31.0	31.4	30.9	29.6	31.3	31.0	30.4	32.7	32.7	21.9	23.5	27.5	26.4
26	31.3	30.9	31.3	30.9	28.4	31.1	31.0	30.3	32.7	32.6	22.4	23.7	27.5	26.1
27	29.1	29.1	29.3	29.1	26.9	29.6	28.9	27.9	31.1	30.8	19.3	22.5	24.0	18.4
28	38.8	38.4	38.8	38.3	34.3	37.9	38.4	37.8	40.1	40.0	29.2	31.1	34.8	33.7
29	38.4	38.3	38.5	38.3	30.1	35.6	38.3	37.5	40.0	39.9	30.0	30.8	34.8	31.8
30	33.6	33.6	33.6	33.6	27.8	33.1	33.4	31.4	35.6	35.3	25.4	28.3	23.6	16.4
31	48.5	48.3	48.5	47.9	44.8	46.8	48.4	47.7	49.9	49.9	40.6	40.7	44.4	43.6
32	48.5	48.3	48.5	47.9	44.8	46.8	48.4	47.7	49.9	49.9	40.6	40.6	44.4	43.6
33	48.5	48.2	48.5	47.9	44.7	46.8	48.3	47.5	49.8	49.8	39.0	40.1	44.4	43.6
34	47.3	47.3	47.4	47.3	44.3	46.7	47.2	46.5	49.3	49.2	37.6	40.0	43.9	41.7
35	48.5	48.3	48.6	47.9	44.6	46.8	48.5	47.8	49.9	49.9	40.0	40.3	44.5	43.6
36	48.4	48.0	48.4	47.9	43.8	46.6	48.0	47.4	49.7	49.7	38.9	40.8	44.5	43.4
37	46.1	46.1	46.3	46.1	42.8	46.0	45.9	44.9	48.1	47.9	36.4	39.5	41.0	35.4
38	48.9	48.6	48.9	48.3	43.2	46.7	48.7	47.9	50.2	50.2	40.1	41.7	44.8	44.0
39	48.4	48.2	48.5	48.2	39.4	45.4	48.3	47.5	49.9	49.9	40.1	40.8	44.8	41.9
40	43.6	43.6	43.6	43.6	37.5	42.9	43.4	41.4	45.5	45.3	35.4	38.3	33.6	26.4
41	48.5	48.1	48.5	47.9	36.7	43.8	48.0	47.4	49.7	49.7	40.1	41.1	44.4	43.3
42	48.5	48.1	48.5	47.9	36.7	43.8	48.0	47.4	49.8	49.7	40.1	41.1	44.4	43.3
43	48.5	48.1	48.5	47.9	36.7	43.7	48.0	47.4	49.7	49.7	39.8	40.7	44.4	43.3
44	47.2	47.2	47.4	47.2	36.7	43.7	47.2	46.5	49.2	49.1	37.4	40.0	43.9	41.5
45	48.5	48.1	48.5	47.9	36.7	43.8	48.1	47.4	49.8	49.7	40.2	41.2	44.5	43.3
46	48.4	47.9	48.4	47.9	36.6	43.7	48.0	47.4	49.7	49.6	38.7	40.6	44.5	43.1
47	46.1	46.1	46.3	46.1	36.1	43.3	45.9	44.9	48.0	47.8	36.3	39.5	41.0	35.4
48	48.9	48.5	48.9	48.3	36.8	43.9	48.4	47.8	50.2	50.1	40.5	41.5	44.8	43.7
49	48.4	48.2	48.5	48.2	35.6	43.2	48.3	47.5	49.9	49.9	39.8	40.8	44.8	41.7
50	43.6	43.6	43.6	43.6	34.4	41.3	43.4	41.4	45.5	45.3	35.4	38.2	33.6	26.4

Table 3.5.1 (Cont)

Index	MTD						PD&MTI							
	1	2	3	4	5	6	Ham. b=6	Kais. b=6	OF	OF& MTI	LP& MTI	LP	AMTI &MTI	AMTI
51	47.8	47.4	47.9	47.4	30.5	39.7	47.5	46.9	49.4	49.2	38.4	41.0	44.3	35.1
52	47.8	47.4	47.9	47.4	30.5	39.7	47.5	46.9	49.4	49.2	38.5	41.1	44.3	35.1
53	47.8	47.4	47.9	47.4	30.5	39.7	47.5	46.9	49.4	49.2	38.5	41.1	44.3	35.1
54	47.2	47.2	47.3	47.2	30.4	39.5	47.2	46.5	49.0	48.8	37.2	39.9	43.8	34.8
55	47.9	47.5	48.0	47.5	30.5	39.7	47.6	47.0	49.4	49.3	38.5	41.1	44.4	35.1
56	47.9	47.5	48.0	47.5	30.5	39.7	47.6	47.0	49.4	49.3	38.5	41.1	44.4	35.1
57	46.0	46.0	46.2	46.0	30.2	39.0	45.9	44.9	47.9	47.6	36.4	39.5	40.9	32.6
58	48.2	47.8	48.4	47.8	30.8	39.9	47.9	47.3	49.8	49.7	38.9	41.5	44.8	35.5
59	48.2	47.8	48.3	47.8	30.5	39.7	47.9	47.3	49.8	49.6	38.9	41.5	44.7	35.1
60	43.5	43.5	43.5	43.5	29.6	38.1	43.4	41.4	45.4	45.1	35.3	38.3	33.6	26.0
61	67.6	67.6	68.1	66.9	46.8	54.0	68.0	67.3	69.9	69.8	61.4	61.9	64.5	63.3
62	67.7	67.7	68.2	67.0	46.8	54.0	68.1	67.4	69.9	69.9	61.4	61.8	64.6	63.4
63	67.5	67.4	68.1	66.7	46.8	54.0	67.9	67.3	69.7	69.7	60.8	61.2	64.4	63.3
64	66.0	65.9	67.1	65.9	46.8	54.0	67.1	66.4	69.0	68.9	57.5	59.8	63.8	61.4
65	67.7	67.6	68.3	66.8	46.8	53.9	68.1	67.5	70.0	70.0	61.5	62.0	64.4	63.4
66	67.6	67.1	68.1	67.0	46.8	54.0	68.0	67.4	69.8	69.7	58.6	60.6	64.6	63.2
67	65.0	65.0	65.8	65.0	46.7	53.9	65.6	64.6	67.7	67.6	56.3	59.2	60.8	55.3
68	67.5	67.5	68.0	66.7	46.7	53.9	67.8	67.2	69.7	69.7	61.3	61.8	64.3	63.2
69	67.6	66.6	68.0	66.6	46.6	53.8	67.9	67.0	69.5	69.4	59.3	60.4	64.2	61.3
70	63.0	63.0	63.0	63.0	46.3	53.6	63.0	61.0	65.1	64.8	54.9	57.8	53.2	46.0
71	67.5	65.5	68.0	65.5	37.0	45.8	68.1	67.1	69.8	69.8	61.4	61.7	64.7	54.2
72	67.5	65.4	67.7	65.4	37.0	45.8	67.9	66.8	69.5	69.5	61.4	61.8	64.3	54.2
73	67.4	65.5	67.9	65.5	37.0	45.8	68.0	67.1	69.7	69.7	61.2	61.6	64.6	54.2
74	65.1	64.7	67.1	64.7	37.0	45.8	67.2	66.5	69.1	68.9	57.9	60.1	63.9	53.9
75	67.6	65.4	67.8	65.4	37.0	45.8	67.9	66.7	69.4	69.4	61.3	61.7	64.2	54.2
76	67.5	65.4	67.8	65.4	37.0	45.8	67.8	66.7	69.3	69.3	60.9	61.3	64.2	54.1
77	64.0	64.0	65.1	64.0	37.0	45.8	65.8	64.8	67.8	67.6	56.3	59.3	60.9	52.0
78	67.6	65.4	67.9	65.4	37.0	45.8	68.0	66.8	69.5	69.5	61.4	61.8	64.3	54.2
79	67.4	65.4	67.9	65.4	37.0	45.8	67.9	66.9	69.4	69.3	58.9	60.7	64.4	53.9
80	61.8	61.8	61.9	61.8	36.9	45.7	63.2	61.1	65.1	64.8	54.8	58.2	53.2	45.4
81	63.3	63.3	65.8	63.3	30.5	40.2	67.3	66.7	69.0	68.9	59.9	61.1	59.5	35.7
82	63.2	63.2	65.7	63.2	30.5	40.2	67.2	66.6	68.8	68.7	59.8	61.0	59.4	35.7
83	63.2	63.2	65.7	63.2	30.5	40.2	67.2	66.6	68.9	68.8	59.9	61.2	59.5	35.7
84	63.1	63.1	65.6	63.1	30.5	40.2	67.0	66.4	68.6	68.5	58.3	60.2	59.3	35.7
85	63.2	63.2	65.5	63.2	30.5	40.2	67.1	66.4	68.7	68.6	59.8	60.9	59.4	35.7
86	63.2	63.2	65.6	63.2	30.5	40.2	67.1	66.4	68.7	68.6	59.8	61.0	59.4	35.7
87	62.1	62.1	63.9	62.1	30.5	40.2	65.7	64.8	67.5	67.2	56.4	59.7	58.0	35.7
88	63.2	63.2	65.6	63.2	30.5	40.2	67.1	66.5	68.8	68.7	59.9	61.2	59.4	35.7
89	63.3	63.3	65.7	63.3	30.5	40.2	67.3	66.7	69.0	68.9	59.9	61.1	59.5	35.7
90	59.4	59.4	59.8	59.4	30.5	40.0	62.7	60.9	64.4	64.1	54.7	57.7	52.5	35.4
91	28.6	28.7	28.9	28.0	29.4	28.8	28.5	27.8	30.0	30.0	21.6	20.9	24.5	23.7
92	28.3	28.6	28.8	28.2	29.4	29.2	28.6	27.9	30.3	30.2	23.5	24.8	24.9	22.5
93	28.2	28.6	28.8	28.2	29.3	29.0	28.6	27.9	30.2	30.1	22.5	24.6	24.9	22.1
94	27.8	27.9	28.1	27.7	28.4	28.3	27.9	27.3	29.8	29.7	19.1	20.9	24.1	19.3
95	30.8	30.9	31.1	30.7	29.5	31.4	31.2	30.2	32.8	32.7	26.1	27.4	27.5	23.7
96	30.7	30.9	30.9	30.7	29.3	31.2	31.1	30.1	32.7	32.5	26.2	27.3	27.5	22.5
97	29.3	29.2	29.4	29.2	28.1	29.8	29.2	28.4	31.2	30.9	21.8	23.6	25.2	15.8
98	37.9	38.1	37.8	38.1	29.7	36.5	38.5	37.5	40.1	40.0	34.2	34.8	34.9	27.4
99	37.7	37.9	37.8	37.9	29.5	36.5	38.1	37.5	39.9	39.7	33.3	34.5	34.9	26.7
100	33.4	33.2	33.8	33.2	28.1	33.3	33.4	31.2	35.6	35.3	27.7	29.2	25.6	16.0

Table 3.5.1 (Cont)

Index	MTD						PD&MTI							
	1	2	3	4	5	6	Ham. b=6	Kais.	OF	OF& MTI	LP& MTI	LP	AMTI &MTI	AMTI
101	28.5	28.4	28.6	28.0	28.8	28.8	28.5	27.8	29.9	29.9	20.6	20.5	24.5	23.7
102	28.3	28.6	28.8	28.2	28.8	29.2	28.6	27.9	30.2	30.2	23.1	24.5	24.9	22.6
103	28.2	28.5	28.8	28.2	28.8	28.9	28.6	27.9	30.1	30.1	22.3	24.5	24.9	22.2
104	27.8	27.9	28.1	27.7	27.9	28.3	27.9	27.3	29.8	29.7	19.0	21.6	24.1	19.4
105	30.8	30.9	31.1	30.7	29.2	31.4	31.1	30.2	32.7	32.7	26.0	26.9	27.5	23.9
106	30.7	30.9	30.9	30.7	29.0	31.2	31.1	30.1	32.6	32.5	26.1	26.8	27.5	22.9
107	29.3	29.2	29.4	29.2	27.8	29.8	29.2	28.4	31.2	30.9	21.7	23.7	25.2	16.2
108	37.9	38.1	37.8	38.1	29.6	36.5	38.5	37.5	40.0	40.0	34.1	34.2	34.9	27.0
109	37.7	37.9	37.8	37.9	29.5	36.4	38.1	37.5	39.8	39.7	33.3	34.1	34.9	26.4
110	33.4	33.2	33.8	33.2	28.0	33.3	33.4	31.2	35.6	35.3	27.7	29.2	25.6	16.1
111	28.4	28.0	28.4	27.9	27.0	28.4	28.0	27.4	29.8	29.7	19.0	20.4	24.5	23.4
112	28.3	28.2	28.7	28.2	27.2	28.8	28.2	27.6	30.1	30.0	17.0	22.9	24.9	22.3
113	28.2	28.2	28.6	28.1	27.1	28.5	28.2	27.6	30.0	29.9	17.3	23.5	24.9	22.0
114	27.8	27.7	28.0	27.7	26.3	28.1	27.8	27.1	29.7	29.5	17.0	22.6	24.1	19.3
115	30.8	30.7	31.0	30.7	28.1	31.0	30.8	30.2	32.6	32.5	22.5	25.2	27.5	22.9
116	30.7	30.7	30.9	30.7	27.9	30.8	30.8	30.1	32.5	32.3	23.2	25.6	27.5	22.1
117	29.3	29.2	29.4	29.2	26.8	29.6	29.2	28.3	31.1	30.9	21.6	24.0	25.1	16.0
118	37.9	38.1	37.8	38.1	29.4	36.1	38.2	37.4	39.9	39.8	30.5	32.5	34.9	26.0
119	37.7	37.9	37.8	37.9	29.2	36.1	38.0	37.4	39.7	39.5	31.6	32.8	34.8	25.5
120	33.4	33.2	33.8	33.2	27.8	33.2	33.4	31.2	35.6	35.3	27.7	29.2	25.6	16.0
121	48.5	48.3	48.5	47.9	44.8	46.8	48.4	47.7	49.9	49.9	40.6	40.7	44.4	43.6
122	47.8	48.1	48.4	47.7	44.6	46.8	48.1	47.4	49.8	49.7	42.7	44.2	44.5	41.6
123	47.8	48.1	48.3	47.7	44.6	46.8	48.1	47.4	49.7	49.6	41.9	44.2	44.4	41.2
124	47.3	47.4	47.7	47.2	44.1	46.1	47.4	46.8	49.3	49.2	38.6	41.8	43.7	38.5
125	47.8	47.8	48.1	47.7	43.5	46.5	48.2	47.2	49.7	49.7	43.0	44.2	44.5	35.4
126	47.7	47.9	47.9	47.7	43.4	46.6	48.1	47.1	49.6	49.5	43.1	44.0	44.5	34.5
127	46.3	46.2	46.5	46.2	42.5	44.7	46.2	45.4	48.1	47.9	38.8	41.3	42.2	30.0
128	47.9	48.1	47.8	48.1	38.8	44.7	48.5	47.5	50.0	50.0	44.2	44.5	44.9	27.4
129	47.7	47.9	47.8	47.9	38.6	45.1	48.1	47.4	49.8	49.7	43.3	44.2	44.9	26.3
130	43.4	43.2	43.8	43.2	37.5	42.1	43.4	41.2	45.6	45.3	37.7	39.5	35.6	21.0
131	48.5	48.1	48.5	47.9	36.7	43.8	48.0	47.4	49.7	49.7	40.1	41.1	44.4	43.3
132	47.8	48.0	48.3	47.7	36.7	43.7	47.8	47.2	49.6	49.6	38.1	43.6	44.5	41.4
133	47.8	48.0	48.3	47.7	36.7	43.7	47.8	47.2	49.6	49.5	38.2	43.8	44.4	41.0
134	47.3	47.3	47.6	47.2	36.4	43.3	47.3	46.7	49.2	49.0	37.1	42.7	43.6	38.4
135	47.7	47.8	48.1	47.7	36.6	43.6	47.8	47.2	49.6	49.5	40.8	43.1	44.5	35.4
136	47.7	47.8	47.9	47.7	36.5	43.7	47.8	47.1	49.5	49.4	41.0	43.3	44.5	34.5
137	46.3	46.1	46.5	46.1	35.8	42.6	46.2	45.4	48.0	47.8	38.5	41.9	42.1	30.0
138	47.9	48.1	47.7	48.1	35.3	42.8	48.2	47.5	49.9	49.8	41.3	43.1	44.9	27.8
139	47.7	47.9	47.8	47.9	35.2	43.0	48.0	47.4	49.7	49.6	42.2	43.7	44.9	26.6
140	43.4	43.2	43.8	43.2	34.2	40.7	43.4	41.2	45.5	45.3	37.7	39.9	35.6	21.1
141	47.8	47.4	47.9	47.4	30.5	39.7	47.5	46.9	49.4	49.2	38.4	41.0	44.3	35.1
142	47.6	47.4	47.8	47.4	30.5	39.6	47.5	46.9	49.3	49.2	39.0	39.6	44.3	34.7
143	47.6	47.4	47.8	47.4	30.5	39.6	47.5	46.9	49.2	49.1	38.6	40.1	44.2	34.7
144	47.2	46.9	47.3	46.9	30.4	39.3	46.9	45.9	48.8	48.6	35.6	42.1	42.3	33.9
145	47.6	47.5	47.7	47.5	30.5	39.6	47.6	46.9	49.3	49.2	38.9	39.4	44.1	32.6
146	47.6	47.4	47.7	47.4	30.5	39.4	47.5	46.7	49.2	49.0	39.7	40.5	43.7	32.1
147	46.2	45.8	46.3	45.8	30.1	38.9	45.8	44.6	47.7	47.5	37.8	43.0	38.7	29.0
148	47.8	47.8	47.7	47.8	30.4	39.5	47.9	46.9	49.6	49.5	38.5	40.4	43.5	27.0
149	47.6	47.6	47.7	47.6	30.3	39.4	47.6	46.8	49.4	49.3	39.3	41.0	42.8	26.1
150	43.3	43.1	43.8	43.1	29.4	38.0	43.3	41.0	45.3	45.0	37.4	40.5	33.8	21.0

Table 3.5.1 (Cont)

Index	MTD						PD&MTI							
	1	2	3	4	5	6	Ham. b=6	Kais. b=6	OF	OF& MTI	LP& MTI	LP	AMTI &MTI	AMTI
151	67.6	67.6	68.1	66.9	46.8	54.0	68.0	67.3	69.9	69.8	61.4	61.9	64.5	63.3
152	67.3	67.2	68.0	66.7	46.8	54.0	67.8	67.2	69.7	69.7	58.3	63.4	64.5	61.4
153	67.1	67.1	67.9	66.6	46.8	54.0	67.8	67.1	69.5	69.5	58.6	63.8	64.4	61.0
154	66.8	66.4	67.4	66.2	46.7	53.9	67.4	66.7	69.2	69.1	57.3	62.7	63.7	58.4
155	67.1	66.9	67.7	66.6	46.8	53.9	67.8	67.1	69.5	69.4	61.2	63.1	64.4	55.2
156	67.0	66.8	67.6	66.5	46.8	53.9	67.6	66.9	69.3	69.2	61.3	63.2	64.3	54.3
157	65.2	64.6	66.5	64.6	46.6	53.6	66.3	65.4	68.1	67.9	58.5	61.9	62.1	49.9
158	66.3	66.5	67.1	66.5	46.6	53.7	67.7	66.9	69.4	69.3	61.4	62.8	64.4	45.8
159	66.8	66.8	67.5	66.8	46.5	53.8	67.8	67.2	69.5	69.4	62.2	63.5	64.7	44.9
160	61.6	61.3	63.4	61.3	45.9	51.7	62.9	60.8	65.0	64.8	57.2	59.6	55.2	40.1
161	67.5	65.5	68.0	65.5	37.0	45.8	68.1	67.1	69.8	69.8	61.4	61.7	64.7	54.2
162	66.8	65.3	67.8	65.3	37.0	45.8	68.0	67.2	69.7	69.6	59.5	61.8	64.6	53.9
163	66.4	65.3	67.7	65.3	37.0	45.8	67.9	67.0	69.6	69.5	58.2	62.9	64.5	53.8
164	66.3	65.0	67.3	65.0	37.0	45.8	67.5	66.5	69.1	69.0	55.9	62.9	62.6	53.2
165	66.3	65.3	67.7	65.3	37.0	45.8	67.9	67.0	69.6	69.5	59.4	61.7	64.5	52.0
166	66.3	65.2	67.5	65.2	37.0	45.8	67.7	66.7	69.3	69.1	60.1	62.4	64.1	51.5
167	64.9	63.8	66.2	63.8	37.0	45.7	66.1	64.9	67.7	67.5	57.8	62.6	59.0	48.6
168	65.5	65.2	67.0	65.2	37.0	45.7	67.8	66.8	69.3	69.2	59.9	62.4	63.8	45.3
169	65.7	65.1	67.0	65.1	37.0	45.8	67.5	66.7	69.1	69.0	60.7	62.4	63.0	44.5
170	61.6	61.2	63.4	61.2	36.7	45.2	63.0	60.8	64.9	64.6	57.0	60.4	53.3	39.9
171	63.3	63.3	65.8	63.3	30.5	40.2	67.3	66.7	69.0	68.9	59.9	61.1	59.5	35.7
172	63.2	63.2	65.5	63.2	30.5	40.2	67.0	66.3	68.6	68.5	59.7	60.9	59.3	35.7
173	63.3	63.3	65.7	63.3	30.5	40.2	67.2	66.5	68.9	68.7	59.4	60.7	59.4	35.7
174	62.4	62.4	64.2	62.4	30.5	40.2	66.0	65.3	67.9	67.8	57.2	60.8	58.2	35.7
175	63.3	63.3	65.8	63.3	30.5	40.2	67.3	66.5	68.9	68.8	58.9	59.7	59.2	35.7
176	63.2	63.2	65.6	63.2	30.5	40.2	67.0	66.3	68.7	68.5	59.1	59.0	58.8	35.7
177	61.6	61.6	63.5	61.6	30.5	40.1	65.0	63.9	66.8	66.5	56.7	62.0	53.5	35.6
178	63.2	63.2	65.2	63.2	30.5	40.2	67.1	66.1	68.7	68.5	53.8	57.8	57.6	35.3
179	63.0	63.0	65.1	63.0	30.5	40.2	66.7	66.0	68.5	68.3	58.1	58.1	56.0	35.2
180	60.1	60.0	61.9	60.0	30.4	39.8	62.6	60.1	64.3	64.0	57.5	61.0	45.5	34.4
181	28.6	28.7	28.9	28.0	29.4	28.8	28.5	27.8	30.0	30.0	21.6	20.9	24.5	23.7
182	28.1	28.7	28.8	27.9	28.9	28.7	28.4	27.9	30.3	30.2	24.9	25.2	24.9	16.1
183	28.0	28.5	28.6	27.9	28.7	28.6	28.4	27.8	30.2	30.1	24.6	25.0	24.8	15.9
184	27.1	27.9	28.0	26.9	28.1	28.0	27.9	27.2	29.7	29.5	22.0	20.3	23.2	14.9
185	30.6	30.9	31.0	30.5	28.5	30.8	31.0	30.4	32.8	32.7	27.8	27.9	27.7	15.2
186	30.4	30.8	30.5	30.3	28.7	30.9	30.7	30.4	32.6	32.5	27.7	27.8	27.5	14.7
187	27.8	29.3	28.5	28.1	27.9	29.5	29.4	28.7	31.0	30.7	24.9	24.3	21.0	11.5
188	37.7	37.8	37.8	37.8	28.5	35.5	38.2	37.5	40.1	40.1	35.1	35.3	35.1	17.5
189	37.1	37.5	37.1	37.4	28.7	35.0	37.5	37.3	39.8	39.6	35.0	35.2	33.6	17.3
190	31.5	33.3	31.8	32.0	27.9	33.1	33.1	31.4	35.5	35.1	30.3	30.4	19.2	13.6
191	28.6	28.4	28.5	28.0	29.8	28.8	28.5	27.8	29.9	29.9	20.6	20.5	24.5	23.7
192	28.1	28.5	28.7	27.9	28.4	28.7	28.4	27.9	30.2	30.1	24.8	25.2	24.9	16.3
193	28.0	28.4	28.5	27.9	28.1	28.6	28.4	27.8	30.1	30.0	24.5	25.0	24.8	16.2
194	27.1	27.8	28.0	26.9	27.5	28.0	27.9	27.2	29.6	29.4	21.9	20.2	23.2	15.1
195	30.6	30.9	31.0	30.5	28.2	30.8	31.0	30.4	32.7	32.7	27.7	27.9	27.7	15.6
196	30.4	30.8	30.5	30.3	28.4	30.9	30.7	30.4	32.5	32.4	27.7	27.8	27.5	15.1
197	27.8	29.3	28.5	28.0	27.6	29.5	29.4	28.7	30.9	30.7	24.9	24.2	21.0	12.0
198	37.7	37.8	37.8	37.8	28.5	35.5	38.2	37.5	40.0	40.0	35.1	35.3	35.1	17.1
199	37.1	37.6	37.1	37.3	28.6	36.0	37.5	37.3	39.7	39.6	35.0	35.3	33.6	17.0
200	31.6	33.3	31.8	31.9	27.9	33.2	33.1	31.4	35.5	35.1	30.3	30.4	19.2	13.6

Table 3.5.1 (Cont)

Scenario Index	MTD						PD&MTI							
	1	2	3	4	5	6	Ham. b=6	Kais. b=6	OF	OF& MTI	LP& MTI	LP	AMTI &MTI	AMTI
201	28.4	28.0	28.4	27.9	27.0	28.4	28.0	27.4	29.8	29.7	19.0	20.4	24.5	23.4
202	28.1	28.0	28.5	27.9	26.8	28.2	28.0	27.4	30.0	29.8	24.6	25.2	24.9	16.3
203	28.0	28.0	28.4	27.9	26.6	28.2	28.0	27.3	29.9	29.7	24.0	24.9	24.7	16.1
204	27.1	27.3	27.8	26.7	25.9	27.4	27.2	25.4	29.1	28.8	20.2	18.9	23.0	15.0
205	30.6	30.5	30.9	30.5	27.3	30.4	30.6	29.7	32.5	32.3	27.6	28.0	27.5	15.1
206	30.4	30.4	30.5	30.3	27.3	30.5	30.3	29.7	32.3	32.1	27.5	27.8	27.3	14.7
207	27.8	28.7	28.5	27.6	26.6	28.9	28.6	27.7	30.4	29.9	24.0	23.7	20.9	11.8
208	37.7	37.8	37.8	37.8	28.3	35.2	37.9	37.0	39.8	39.6	35.1	35.4	34.9	16.9
209	37.1	37.5	37.1	37.2	28.4	35.6	37.2	36.9	39.4	39.2	34.8	35.1	33.4	16.8
210	31.6	32.9	31.8	31.3	27.6	32.7	32.7	30.9	35.2	34.7	30.0	30.5	19.2	13.5
211	48.5	48.3	48.5	47.9	44.8	46.8	48.4	47.7	49.9	49.9	40.6	40.7	44.4	43.6
212	47.7	48.1	48.3	47.5	44.4	46.6	48.0	47.4	49.8	49.7	44.4	44.7	44.5	34.8
213	47.5	48.0	48.1	47.4	44.2	46.3	47.9	47.4	49.6	49.6	44.1	44.5	44.4	34.7
214	46.7	47.4	47.5	46.3	43.2	44.0	47.4	46.8	49.1	49.0	41.4	39.9	42.7	33.9
215	47.6	47.9	48.0	47.5	42.9	46.0	48.0	47.4	49.7	49.7	44.8	44.9	44.7	25.4
216	47.4	47.7	47.5	47.3	42.7	46.1	47.7	47.4	49.5	49.4	44.7	44.9	44.5	25.3
217	44.8	46.3	45.5	44.6	41.2	41.3	46.4	45.7	47.9	47.7	41.9	41.4	38.0	24.4
218	47.7	47.8	47.8	47.8	37.8	44.3	48.2	47.5	50.0	50.0	45.1	45.3	45.1	16.8
219	47.0	47.6	47.1	47.2	37.7	44.6	47.5	47.3	49.7	49.6	45.0	45.3	43.6	16.6
220	41.6	43.3	41.8	41.0	36.5	38.9	43.1	41.4	45.3	45.1	40.3	40.5	29.2	15.4
221	48.5	48.1	48.5	47.9	36.7	43.8	48.0	47.4	49.7	49.7	40.1	41.1	44.4	43.3
222	47.7	47.9	48.2	47.5	36.5	43.6	47.6	46.9	49.6	49.5	44.3	44.9	44.4	34.7
223	47.5	47.8	48.1	47.4	36.5	43.4	47.5	46.8	49.5	49.3	43.9	44.6	44.3	34.6
224	46.7	47.2	47.5	46.3	35.9	42.1	46.8	46.0	48.7	48.5	40.2	38.7	42.5	33.8
225	47.6	47.8	48.0	47.5	36.2	43.3	47.6	46.7	49.6	49.5	44.9	45.1	44.5	25.5
226	47.4	47.6	47.5	47.3	36.0	43.3	47.4	46.7	49.3	49.2	44.7	44.9	44.3	25.3
227	44.8	46.1	45.5	44.6	35.1	40.3	45.7	44.7	47.4	47.1	41.2	40.8	37.9	24.4
228	47.7	47.8	47.8	47.8	34.6	42.4	47.9	47.0	49.8	49.7	45.3	45.5	44.8	17.1
229	47.0	47.5	47.1	47.2	34.6	42.6	47.3	46.9	49.4	49.2	45.0	45.2	43.4	16.9
230	41.6	43.2	41.8	40.9	33.4	38.5	42.8	40.9	45.1	44.8	40.1	40.6	29.2	15.6
231	47.8	47.4	47.9	47.4	30.6	39.7	47.5	46.9	49.4	49.2	38.4	41.0	44.3	35.1
232	47.4	47.2	47.5	47.2	30.3	39.4	47.2	46.3	49.1	49.0	41.7	44.2	42.1	32.2
233	47.4	47.1	47.4	47.1	30.2	39.3	47.2	46.1	49.0	48.9	41.1	44.1	41.7	32.2
234	46.1	45.4	46.2	45.4	30.1	38.7	45.5	43.7	47.6	47.4	36.0	38.5	38.5	31.7
235	47.4	47.2	47.5	47.2	30.2	39.1	47.2	45.7	49.1	48.9	43.3	44.2	38.3	25.1
236	47.2	45.9	47.3	46.9	30.1	39.1	46.8	45.3	48.7	48.5	43.1	44.1	37.8	25.0
237	44.5	43.6	44.6	43.6	29.5	37.7	43.6	40.8	45.9	45.6	39.5	39.2	32.7	24.1
238	47.6	47.5	47.7	47.5	29.9	39.0	47.5	45.6	49.3	49.2	43.9	44.5	37.4	17.0
239	46.9	46.7	46.9	46.7	29.8	39.1	46.5	45.6	48.8	48.6	43.6	44.5	36.6	16.8
240	41.4	40.4	41.4	40.4	28.9	36.1	41.0	37.5	43.1	42.8	38.9	38.6	27.8	15.5
241	67.5	67.6	68.1	66.9	46.8	54.0	68.0	67.3	69.9	69.8	61.4	61.9	64.5	63.3
242	67.2	67.3	67.7	66.7	46.7	54.0	67.6	66.9	69.8	69.7	64.2	64.8	64.4	54.7
243	67.0	67.2	67.7	66.5	46.7	53.9	67.6	66.8	69.5	69.4	63.9	64.5	64.3	54.6
244	66.0	66.4	67.2	64.9	46.6	53.3	66.9	66.1	68.8	68.7	60.4	59.0	62.5	53.8
245	67.0	67.1	67.6	66.5	46.7	53.9	67.6	66.7	69.6	69.5	64.9	65.1	64.5	45.3
246	66.7	66.8	67.3	66.1	46.6	53.8	67.4	66.7	69.3	69.2	64.8	65.0	64.3	45.2
247	64.6	65.7	65.3	63.7	45.9	50.4	65.9	64.8	67.5	67.3	61.3	60.9	57.9	44.3
248	66.6	66.5	67.3	66.5	46.3	53.6	67.5	66.6	69.5	69.4	65.0	65.1	64.4	35.4
249	66.5	66.7	66.6	66.2	46.1	53.5	66.9	66.5	69.0	68.9	64.7	64.9	63.8	35.2
250	61.2	62.6	61.3	60.2	44.8	46.7	62.5	60.6	64.9	64.6	59.8	60.3	49.9	34.3

Table 3.5.1 (Cont)

Scenario Index	MTD						PD&MTI							
	1	2	3	4	5	6	Ham. b=6	Kais. b=6	OF	OF& MTI	LP& MTI	LP	AMTI &MTI	AMTI
251	57.5	55.5	58.0	55.5	37.0	45.8	68.1	67.1	69.8	69.8	61.4	61.7	54.7	54.2
252	66.8	65.2	67.4	65.2	37.0	45.8	67.7	66.7	69.4	69.4	64.1	64.9	62.5	51.7
253	66.4	65.1	67.4	65.1	37.0	45.8	67.7	66.6	69.4	69.3	62.9	64.2	62.2	51.7
254	66.1	64.2	66.9	64.2	37.0	45.7	66.5	64.9	68.4	68.2	57.9	58.6	58.9	51.3
255	66.5	65.2	67.3	65.2	36.9	45.7	67.7	66.2	69.4	69.3	64.6	65.0	58.5	44.8
256	66.3	65.0	67.3	65.0	36.8	45.7	67.4	66.1	69.1	68.9	64.0	64.6	57.8	44.7
257	64.8	62.9	65.2	62.9	36.8	45.0	65.0	62.9	66.7	66.3	60.0	60.1	52.2	43.9
258	65.9	65.1	67.1	65.1	36.9	45.6	67.5	66.0	69.3	69.2	64.5	64.7	56.7	35.3
259	65.6	64.5	66.7	64.5	36.7	45.3	66.7	65.9	68.8	68.7	63.9	64.6	55.8	35.2
260	61.2	60.0	61.3	59.8	36.1	43.4	61.4	58.0	64.0	63.5	59.6	60.1	47.1	34.3
261	63.3	63.3	65.8	63.3	30.5	40.2	67.3	66.7	69.0	68.9	59.9	61.1	59.5	35.7
262	62.6	62.6	64.4	62.6	30.5	40.2	66.7	66.1	68.8	68.7	60.1	63.7	57.1	35.7
263	62.4	62.4	64.2	62.4	30.5	40.2	66.6	65.8	68.5	68.2	59.0	63.9	56.8	35.7
264	61.2	61.2	62.9	61.2	30.5	40.2	64.2	63.0	66.5	66.2	52.7	60.0	54.7	35.7
265	62.4	62.4	64.2	62.4	30.5	40.0	66.8	65.3	68.6	68.3	60.7	63.3	51.2	35.3
266	62.3	62.3	64.2	62.3	30.5	40.0	66.3	64.9	68.2	67.9	61.4	63.7	50.5	35.3
267	58.1	57.4	59.0	57.4	30.5	39.8	58.9	56.7	63.7	63.3	55.2	58.2	47.0	35.2
268	62.4	62.4	64.2	62.4	30.3	40.0	66.7	64.6	68.4	68.1	61.5	63.4	45.4	32.5
269	61.7	61.7	63.7	61.7	30.3	39.8	65.1	64.5	67.6	67.4	61.1	62.9	44.6	32.5
270	54.5	50.8	54.6	50.8	30.2	39.2	50.9	47.5	59.0	58.5	53.7	53.0	39.4	32.0
271	28.6	28.7	28.9	28.0	29.4	28.8	28.5	27.8	30.0	30.0	21.6	20.9	24.5	23.7
272	27.7	28.5	28.7	27.4	28.6	28.6	28.6	27.5	30.2	30.1	24.9	25.3	25.2	11.6
273	27.4	28.3	28.4	27.2	28.6	28.3	28.1	27.5	30.1	30.0	24.6	25.0	24.8	11.6
274	24.7	27.3	27.4	24.5	26.8	26.6	26.8	25.8	28.9	28.5	20.2	19.9	20.5	11.8
275	29.7	30.6	30.3	29.8	28.9	30.9	30.9	29.8	32.7	32.6	27.9	28.0	27.8	9.1
276	28.8	30.0	29.6	29.0	28.5	30.5	30.0	29.7	32.5	32.4	27.6	27.8	26.7	9.0
277	20.4	26.6	25.4	24.2	25.7	27.0	26.7	25.3	29.6	28.7	20.7	22.7	14.7	7.7
278	36.0	37.1	36.8	36.3	29.2	36.9	37.4	36.7	40.0	39.9	35.1	35.4	35.0	12.3
279	35.1	36.5	35.2	36.2	28.8	35.6	35.3	36.0	39.6	39.5	34.6	35.0	29.1	12.3
280	18.3	27.4	24.6	27.5	25.6	29.4	27.7	25.4	34.0	31.6	25.4	28.9	12.2	10.6
281	28.6	28.4	28.6	28.0	28.8	28.8	28.5	27.8	29.9	29.9	20.6	20.5	24.5	23.7
282	27.7	28.3	28.7	27.3	28.1	28.6	28.5	27.5	30.1	30.0	24.9	25.3	25.2	11.8
283	27.4	28.2	28.3	27.2	28.0	28.3	28.1	27.4	30.0	29.9	24.6	25.0	24.8	11.8
284	24.7	27.1	27.2	24.3	26.3	26.7	26.7	25.8	28.6	28.3	20.2	19.7	20.5	12.0
285	29.7	30.6	30.3	29.7	28.5	30.9	30.9	29.7	32.6	32.5	27.8	28.0	27.8	9.5
286	28.8	30.0	29.6	28.9	28.2	30.5	29.9	29.6	32.3	32.2	27.6	27.8	26.6	9.3
287	20.4	26.6	25.4	23.8	25.5	27.1	26.7	25.3	28.9	28.6	20.7	22.7	14.7	8.0
288	36.0	37.1	36.8	36.2	29.1	36.9	37.4	36.7	39.9	39.8	35.1	35.4	35.0	12.0
289	35.1	36.5	35.2	36.0	28.7	35.6	35.3	36.0	39.5	39.3	34.6	34.9	29.1	12.0
290	18.3	27.4	24.6	27.2	25.6	29.5	27.7	25.4	32.6	31.5	25.3	27.6	12.2	10.5
291	28.4	28.0	28.4	27.9	27.0	28.4	28.0	27.4	29.8	29.7	19.0	20.4	24.5	23.4
292	27.6	27.8	28.4	27.2	26.5	27.8	27.7	26.8	29.9	29.7	24.7	25.2	24.4	11.8
293	27.4	27.6	28.1	27.0	26.4	27.8	27.5	26.5	29.6	29.4	24.3	24.8	24.1	11.8
294	24.6	25.6	26.1	23.5	24.9	25.5	25.2	24.4	27.4	27.0	19.3	17.5	20.1	11.9
295	29.7	30.2	30.3	29.6	27.4	30.3	30.2	28.7	32.3	32.1	27.7	28.0	26.7	9.3
296	28.8	29.4	29.6	28.7	27.1	30.0	29.3	28.6	31.8	31.5	27.5	27.7	25.7	9.1
297	20.4	25.7	24.8	21.0	24.6	25.5	25.0	24.0	27.1	26.6	20.2	21.0	14.6	7.8
298	36.0	36.6	36.8	36.0	28.9	36.6	37.1	35.6	39.5	39.3	35.1	35.4	33.9	12.0
299	35.1	36.3	35.2	35.6	28.5	35.1	35.1	35.2	38.7	38.3	34.3	34.9	28.8	12.0
300	18.3	27.2	24.5	25.2	25.3	28.7	27.1	25.1	30.0	29.5	24.2	25.1	12.2	10.5

Table 3.5.1 (Cont)

Scenario Index	MTD						PD&MTI							
	1	2	3	4	5	6	Ham. b=6	Kais.	OF	OF& MTI	LP& MTI	LP	AMTI &MTI	AMTI
301	48.5	48.3	48.5	47.9	44.8	45.8	48.4	47.7	49.9	49.9	40.6	40.7	44.4	43.6
302	47.2	47.9	48.2	46.8	43.6	44.4	48.1	47.1	49.7	49.6	44.4	44.8	44.7	30.5
303	47.0	47.7	47.9	46.6	43.2	44.1	47.6	47.0	49.5	49.4	44.1	44.5	44.4	30.6
304	44.2	46.7	46.8	43.1	41.2	40.4	46.3	45.3	48.1	47.9	39.7	39.4	40.0	30.9
305	46.7	47.6	47.3	46.6	42.1	44.1	47.9	46.8	49.6	49.6	44.8	45.0	44.8	20.8
306	45.8	47.0	46.6	45.7	42.0	43.8	47.0	46.7	49.4	49.3	44.6	44.8	43.7	20.9
307	37.4	43.6	42.4	36.3	37.8	37.0	43.7	42.3	45.8	45.6	37.7	39.8	31.7	21.2
308	46.0	47.1	46.8	46.0	37.8	43.8	47.4	46.7	49.9	49.8	45.1	45.4	45.0	11.8
309	45.1	46.5	45.2	45.6	37.5	42.1	45.3	46.0	49.5	49.3	44.6	44.9	39.1	11.9
310	28.3	37.4	34.5	27.9	33.2	33.7	37.7	35.4	41.8	41.5	35.4	37.0	22.2	12.1
311	48.5	48.1	48.5	47.9	36.7	43.8	48.0	47.4	49.7	49.7	40.1	41.1	44.4	43.3
312	47.2	47.6	48.2	46.8	36.1	42.2	47.3	46.4	49.5	49.3	44.3	44.9	43.8	30.5
313	47.0	47.4	47.8	46.6	35.9	42.0	47.1	46.0	49.3	49.1	44.0	44.4	43.5	30.5
314	44.2	45.7	45.9	43.1	35.1	39.7	45.0	43.9	47.3	47.0	39.3	38.3	39.5	30.9
315	46.7	47.4	47.3	46.6	35.6	41.9	47.3	45.7	49.4	49.3	44.9	45.1	43.4	20.8
316	45.8	46.8	46.6	45.7	35.4	41.8	46.4	45.7	48.9	48.8	44.6	44.7	42.5	20.9
317	37.4	43.2	41.9	36.3	33.7	37.0	42.3	41.0	44.4	44.0	37.5	38.6	31.6	21.2
318	46.0	47.0	46.8	46.0	34.4	41.9	47.1	45.6	49.6	49.5	45.3	45.4	43.6	12.1
319	45.1	46.4	45.2	45.5	34.2	41.0	45.2	45.2	48.9	48.7	44.6	45.0	38.7	12.1
320	28.3	37.3	34.4	27.6	31.1	34.3	37.2	35.1	39.9	39.5	34.2	35.3	22.2	12.2
321	47.8	47.4	47.9	47.4	30.5	39.7	47.5	46.9	49.4	49.2	38.4	41.0	44.3	35.1
322	46.7	46.2	46.8	46.2	30.2	38.8	46.2	44.5	48.9	48.7	43.5	44.6	35.6	29.4
323	46.4	45.9	46.6	45.9	30.1	38.6	46.0	43.6	48.3	48.1	43.2	44.0	35.3	29.4
324	43.2	42.4	43.2	42.4	29.9	37.4	42.5	39.9	45.0	44.7	36.5	33.9	33.3	29.7
325	46.4	45.9	46.7	45.9	30.0	38.2	46.2	41.8	48.7	48.5	44.4	45.0	30.7	20.7
326	45.4	44.7	45.9	44.7	29.7	38.1	44.8	41.3	47.7	47.4	44.2	44.6	30.4	20.7
327	37.0	36.1	37.5	36.1	28.7	34.4	36.9	34.0	40.7	40.5	36.2	33.1	27.0	21.1
328	45.6	44.9	46.5	44.9	29.6	38.4	46.0	41.3	48.6	48.4	45.0	45.4	30.2	12.0
329	44.7	44.2	44.8	44.2	29.5	38.0	43.4	41.1	47.2	46.9	43.8	44.7	29.6	12.0
330	28.3	30.5	32.2	27.1	27.5	29.2	29.1	27.5	34.7	34.2	30.3	28.9	21.2	12.1
331	67.6	67.6	68.1	66.9	46.8	54.0	68.0	67.3	69.9	69.8	61.4	61.9	64.5	63.3
332	66.1	66.8	67.6	65.1	46.4	53.1	67.4	66.3	69.5	69.4	64.2	64.7	63.9	50.5
333	66.1	66.3	67.4	65.1	46.4	52.6	67.2	66.1	69.3	69.2	64.1	64.5	63.6	50.5
334	63.8	65.2	65.2	62.4	46.4	51.3	65.1	64.0	67.3	67.1	59.4	58.6	59.5	50.9
335	65.8	66.3	67.1	65.0	46.2	50.1	67.3	65.7	69.4	69.4	64.9	65.1	63.6	40.7
336	65.4	66.1	66.5	64.6	45.8	49.1	66.4	65.7	69.0	68.9	64.6	64.8	62.6	40.7
337	57.3	62.9	61.5	56.1	44.8	46.4	62.5	61.2	64.4	64.1	57.5	58.6	51.6	41.1
338	65.2	65.8	66.4	64.5	45.4	48.0	66.8	65.4	69.3	69.2	65.2	65.3	63.4	30.7
339	64.6	65.3	64.7	64.1	44.9	47.9	64.7	64.9	68.6	68.5	64.3	64.6	58.3	30.8
340	47.9	56.9	54.0	46.7	42.3	41.4	56.9	54.7	59.7	59.3	53.9	55.2	41.7	31.1
341	67.5	65.5	68.0	65.5	37.0	45.8	68.1	67.1	69.8	69.8	61.4	61.7	64.7	54.2
342	66.2	64.4	67.3	64.4	37.0	45.5	67.0	65.4	69.3	69.2	64.3	64.8	55.8	49.1
343	65.9	64.1	66.9	64.1	37.0	45.5	66.5	64.6	68.7	68.6	63.6	64.0	55.4	49.1
344	63.9	61.8	64.3	61.8	37.0	45.3	63.6	61.4	66.1	65.9	58.1	57.1	53.4	49.4
345	65.6	64.1	66.8	64.1	36.6	44.9	66.6	63.8	68.9	68.8	64.5	64.7	49.7	40.5
346	65.2	63.5	66.1	63.5	36.6	44.6	65.8	63.6	68.3	68.2	64.3	64.4	49.4	40.6
347	57.3	57.1	60.5	55.9	36.6	43.4	57.2	54.3	62.4	61.9	56.9	55.7	46.3	40.9
348	65.0	63.5	66.2	63.5	36.3	43.7	66.3	63.2	68.7	68.6	64.8	65.0	48.7	30.7
349	64.6	63.0	64.7	63.0	36.1	43.5	64.4	63.0	67.7	67.5	63.3	64.2	48.2	30.8
350	47.9	53.4	53.6	46.7	35.3	40.4	49.1	47.0	56.5	55.7	51.7	51.7	40.6	31.1

Table 3.5.1 (Cont)

Scenario Index	MTD						PD&MTI							
	1	2	3	4	5	6	Ham. b=6	Kais. b=6	OF	OF& MTI	LP& MTI	LP	AMTI &MTI	AMTI
351	63.3	63.3	65.8	63.3	30.5	40.2	67.3	66.7	69.0	68.9	59.9	61.1	59.5	35.7
352	61.4	61.3	63.6	61.3	30.5	40.1	65.0	63.6	67.9	67.7	63.5	64.3	51.1	35.6
353	61.0	61.0	63.2	61.0	30.5	40.1	64.4	62.4	67.0	66.8	61.9	62.4	51.0	35.6
354	57.4	56.6	58.0	56.6	30.5	40.1	57.7	56.5	62.6	62.4	51.8	55.0	51.1	35.6
355	61.0	60.8	63.4	60.8	30.5	39.6	64.7	59.1	67.4	67.2	64.6	64.9	43.2	34.5
356	59.6	59.2	62.0	59.2	30.5	39.6	62.4	56.1	66.0	65.5	63.5	63.7	43.1	34.5
357	53.2	50.0	53.2	50.0	30.5	39.4	49.7	47.2	56.6	56.2	50.7	48.2	42.3	34.6
358	59.4	59.0	62.7	59.0	30.2	39.3	64.0	50.4	66.9	66.7	64.8	64.8	35.1	29.6
359	55.7	53.5	57.4	53.5	30.2	39.1	55.6	47.0	64.7	64.3	62.3	62.9	34.9	29.6
360	46.7	45.0	46.8	45.0	29.9	37.8	45.1	41.2	49.2	48.9	45.2	39.1	32.8	29.8
361	28.6	28.7	28.9	28.0	29.4	28.8	28.5	27.8	30.0	30.0	21.6	20.9	24.5	23.7
362	27.9	28.5	28.4	27.0	28.9	28.5	28.6	27.8	30.2	30.2	21.3	21.5	24.0	9.8
363	25.9	28.4	28.3	25.7	28.6	28.3	28.3	27.7	30.0	29.9	21.1	21.5	23.0	9.8
364	22.7	25.7	25.7	22.2	25.4	25.0	25.4	24.3	28.3	27.8	18.9	20.3	16.5	10.5
365	30.0	30.0	30.0	27.0	30.7	30.8	31.0	30.0	32.6	32.6	24.4	24.1	26.7	5.2
366	25.0	30.2	27.4	26.7	29.0	29.9	30.1	29.7	32.4	32.2	22.9	23.7	23.9	5.1
367	16.4	20.6	20.6	18.6	20.9	20.5	21.5	21.7	27.4	26.2	19.5	20.6	10.5	4.8
368	34.4	34.6	34.4	34.1	34.1	36.4	37.1	35.1	39.9	39.8	31.4	32.0	33.6	10.0
369	23.6	35.6	26.8	34.0	29.4	35.4	33.9	33.9	39.5	39.3	30.5	31.5	24.1	9.9
370	13.9	18.3	18.3	16.6	20.1	18.6	19.4	20.2	29.6	25.5	21.3	24.2	8.0	8.7
371	28.6	28.4	28.6	28.0	28.8	28.8	28.5	27.8	29.9	29.9	20.6	20.5	24.5	23.7
372	27.9	28.5	28.4	27.0	28.3	28.5	28.6	27.6	30.1	30.0	20.4	21.4	24.0	9.8
373	26.9	28.2	28.3	25.7	28.1	28.3	28.3	27.6	29.8	29.7	20.2	21.1	23.0	9.9
374	22.7	25.3	25.3	21.8	25.0	25.0	25.1	24.0	27.7	27.4	18.2	20.3	16.5	10.5
375	30.0	30.0	30.0	26.6	30.2	30.8	31.0	29.9	32.5	32.4	23.6	23.9	26.6	5.4
376	25.0	30.2	27.4	26.1	28.6	30.0	30.0	29.6	32.2	32.0	22.1	23.7	23.9	5.3
377	16.4	20.5	20.5	18.5	20.9	20.5	21.3	21.6	26.2	25.9	19.1	20.8	10.5	4.8
378	34.4	34.6	34.4	33.5	33.9	36.5	37.1	35.0	39.7	39.6	30.5	31.5	33.6	9.9
379	23.6	35.6	26.8	33.4	29.3	35.5	33.9	33.9	39.3	39.1	30.0	31.7	24.1	9.9
380	13.9	18.3	18.3	16.6	19.8	18.6	19.4	20.2	26.6	25.4	21.1	20.7	8.0	8.8
381	28.4	28.0	28.4	27.9	27.0	28.4	28.0	27.4	29.8	29.7	19.0	20.4	24.5	23.4
382	27.8	27.7	28.2	27.0	26.5	27.8	27.8	25.7	29.8	29.5	18.7	21.1	21.6	9.8
383	26.9	27.2	28.1	25.7	26.4	27.5	27.1	25.3	29.4	29.1	18.5	21.1	21.0	9.8
384	22.2	23.2	23.5	18.9	23.9	23.6	23.4	21.7	25.5	25.0	15.8	18.4	16.0	10.4
385	30.0	29.0	30.0	26.1	28.6	30.0	30.1	27.6	32.2	32.0	21.9	23.7	23.9	5.3
386	25.0	29.1	27.3	22.3	27.5	28.5	27.6	27.5	31.5	31.1	20.9	23.3	22.2	5.2
387	16.3	18.7	18.6	17.4	20.6	20.2	19.8	17.6	22.5	22.1	15.0	16.5	10.4	4.8
388	34.4	34.0	34.4	29.3	33.2	35.3	35.8	33.3	39.3	39.0	28.7	31.7	31.1	10.0
389	23.6	34.9	26.7	29.2	29.0	33.9	32.6	32.7	38.2	37.7	27.8	30.8	23.7	9.9
390	13.9	17.9	17.9	16.5	18.9	18.3	18.5	19.2	23.8	23.2	17.4	17.6	8.0	8.9
391	48.5	48.3	48.5	47.9	44.8	46.8	48.4	47.7	49.9	49.9	40.6	40.7	44.4	43.6
392	47.4	48.0	48.0	46.6	42.9	41.8	48.2	47.2	49.6	49.5	40.0	41.1	43.5	29.2
393	46.5	47.8	47.8	45.2	42.8	41.7	47.9	47.1	49.4	49.3	39.8	40.9	42.5	29.3
394	42.3	44.9	44.9	37.8	38.5	37.4	44.6	43.5	47.2	47.0	37.8	40.1	36.0	29.9
395	47.0	47.0	47.0	43.1	42.6	41.8	48.0	46.9	49.5	49.4	40.7	41.2	43.6	19.4
396	42.0	47.2	44.4	38.9	41.9	41.0	47.1	46.6	49.2	49.0	39.2	41.0	40.9	19.5
397	33.4	37.6	37.6	28.3	34.9	33.9	38.3	38.6	43.1	42.9	36.2	38.1	27.5	20.1
398	44.4	44.6	44.4	35.3	40.7	41.2	47.1	45.0	49.7	49.7	40.6	41.9	43.6	9.9
399	33.6	45.6	36.8	29.9	37.7	37.4	43.9	43.9	49.3	49.1	40.0	41.9	34.1	10.0
400	23.9	28.3	28.3	23.6	28.3	27.7	29.4	30.2	35.6	35.4	31.2	31.4	18.0	10.6

Table 3.5.1 (Cont)

Scenario Index	MTD						PD&MTI							
	1	2	3	4	5	6	Ham. b=6	Kais. b=6	OF	OF& MTI	LP& MTI	LP	AMTI &MTI	AMTI
401	48.5	48.1	48.5	47.9	36.7	43.8	48.0	47.4	49.7	49.7	40.1	41.1	44.4	43.3
402	47.4	47.8	48.0	46.6	35.8	40.8	47.4	45.3	49.4	49.2	39.8	41.4	40.5	29.2
403	46.5	47.4	47.8	45.2	35.5	40.7	46.8	44.8	49.1	48.9	38.9	41.4	40.0	29.3
404	41.9	43.1	43.1	37.8	34.6	37.4	43.3	41.2	45.8	45.4	36.9	39.8	35.3	29.9
405	47.0	46.7	47.0	43.1	35.3	40.7	47.2	44.5	49.2	49.1	40.0	41.1	40.2	19.4
406	42.0	46.9	44.4	38.9	35.2	40.1	45.0	44.4	48.7	48.5	39.5	41.7	38.7	19.5
407	33.4	35.4	35.3	28.3	32.3	34.4	36.9	34.0	39.8	39.6	33.8	35.0	27.4	20.1
408	44.4	44.5	44.4	35.3	35.3	40.3	46.0	43.3	49.5	49.3	39.5	42.1	40.4	9.9
409	33.6	45.4	36.8	29.9	34.3	37.6	42.9	42.7	48.4	48.1	39.6	41.7	33.6	10.0
410	23.9	27.6	27.6	23.1	27.6	27.8	28.0	28.6	33.0	32.5	26.6	27.2	18.0	10.6
411	47.8	47.4	47.9	47.4	30.5	39.7	47.5	46.9	49.4	49.2	38.4	41.0	44.3	35.1
412	47.0	45.4	47.0	45.4	30.2	38.5	45.5	41.6	48.6	48.3	38.2	41.4	28.9	28.3
413	46.1	44.3	46.1	44.3	30.1	38.4	45.0	40.6	47.9	47.6	37.5	40.6	28.8	28.4
414	38.3	37.6	38.2	37.6	29.8	35.8	38.1	36.0	41.8	41.6	34.0	35.3	28.8	28.9
415	46.6	42.5	46.6	42.5	29.5	38.5	45.4	36.5	48.4	48.1	39.0	41.3	24.2	19.3
416	41.9	38.7	41.9	38.7	29.4	38.1	41.9	34.0	46.8	46.5	37.2	41.1	24.2	19.4
417	32.0	30.8	33.1	28.2	28.2	29.1	29.1	28.0	34.9	34.7	29.7	29.7	22.6	20.0
418	44.2	35.2	44.2	35.2	29.7	38.3	44.3	29.3	48.3	47.9	38.0	41.3	24.5	9.9
419	33.6	32.8	35.0	29.8	29.4	35.8	34.4	28.9	45.6	45.1	38.0	41.6	24.1	10.0
420	23.3	25.0	25.3	19.4	25.8	25.5	25.2	22.9	27.9	27.2	21.3	21.7	17.1	10.6
421	67.6	67.6	68.1	66.9	46.8	54.0	68.0	67.3	69.9	69.8	61.4	61.9	64.5	63.3
422	67.4	67.3	67.5	65.8	46.3	49.5	67.6	65.6	69.4	69.4	61.1	62.1	61.0	49.2
423	66.4	66.8	67.1	64.6	46.2	49.3	66.9	65.0	69.1	69.0	59.8	61.8	60.3	49.3
424	61.5	63.0	62.8	57.6	46.2	50.0	63.7	61.4	66.2	66.0	57.8	60.6	55.5	49.9
425	66.9	66.4	66.9	62.7	45.3	45.3	67.4	64.9	69.4	69.3	61.2	62.0	60.7	39.3
426	61.9	66.4	64.0	58.7	44.9	44.6	65.4	64.7	68.7	68.6	60.2	62.1	59.0	39.4
427	53.2	55.3	55.2	48.2	43.7	43.5	56.9	54.2	59.9	59.8	54.1	55.1	47.4	40.1
428	63.9	63.8	63.9	54.8	44.5	43.1	65.7	63.1	69.0	68.9	59.8	61.9	60.3	29.4
429	53.2	64.8	56.3	49.4	44.4	43.0	62.8	62.5	68.3	68.1	60.0	61.9	53.3	29.4
430	43.5	47.2	47.2	38.3	38.9	37.8	47.7	48.4	52.9	52.4	46.4	47.2	37.6	30.1
431	67.5	65.5	68.0	65.5	37.0	45.8	68.1	67.1	69.8	69.8	61.4	61.7	64.7	54.2
432	67.3	64.7	67.3	64.7	36.9	44.9	67.3	63.5	69.1	69.0	60.4	61.9	48.6	48.1
433	66.2	63.7	66.2	63.7	36.9	44.8	66.3	61.9	68.3	68.2	60.4	61.8	48.6	48.2
434	61.4	57.9	61.8	57.5	36.9	45.0	58.3	56.5	63.7	63.5	57.4	59.0	48.6	48.7
435	67.1	62.2	67.1	62.2	36.6	43.1	67.2	57.0	69.1	69.0	61.2	62.3	42.9	39.2
436	62.0	58.7	63.2	58.5	36.5	42.7	62.6	54.2	68.2	68.0	59.8	61.5	42.8	39.3
437	52.8	53.3	54.6	48.2	36.5	42.1	49.4	47.9	56.8	56.2	51.0	51.2	41.6	39.9
438	64.0	57.2	64.0	54.7	36.0	41.7	65.1	48.8	68.6	68.4	61.0	62.4	42.8	29.4
439	53.2	57.2	56.1	49.4	35.7	41.6	54.1	48.3	67.4	67.1	59.0	62.5	42.5	29.4
440	43.1	45.1	45.1	38.3	34.7	37.8	45.3	42.5	49.4	48.6	43.2	45.0	36.4	30.1
441	63.3	63.3	65.8	63.3	30.5	40.2	67.3	66.7	69.0	68.9	59.9	61.1	59.5	35.7
442	56.9	54.2	56.9	54.2	30.5	40.1	55.0	52.9	67.3	67.1	58.6	61.0	48.4	35.5
443	56.8	53.7	56.8	53.7	30.5	40.1	54.4	52.7	65.9	65.7	59.0	61.6	48.5	35.6
444	54.7	53.1	54.8	53.1	30.5	40.1	53.4	52.8	58.5	58.3	52.3	52.6	49.6	35.6
445	56.8	51.3	56.8	51.3	30.4	39.5	50.2	44.8	66.7	66.5	59.4	62.1	38.7	34.2
446	56.0	50.9	56.0	50.9	30.4	39.5	50.0	44.5	63.5	63.0	58.8	60.9	38.8	34.2
447	48.0	46.6	48.0	46.6	30.4	39.2	46.5	43.4	50.7	50.4	44.9	45.9	39.6	34.4
448	56.5	50.0	56.5	50.0	30.2	39.0	50.1	43.1	65.7	65.4	59.7	62.0	27.9	28.5
449	51.8	47.4	51.8	47.4	30.1	39.0	48.8	41.7	58.9	58.4	54.8	55.4	27.9	28.5
450	38.8	38.1	38.6	38.1	29.8	36.1	38.6	36.4	42.8	42.6	36.8	36.8	27.9	29.1

Table 3.5.2

IF for Different Doppler Processors, Sea Clutter Scenarios

Scenario Index	MTD						PD&MTI							
	1	2	3	4	5	6	Ham. b=6	Kais. b=6	OF	OF& MTI	LP& MTI	LP	AMTI &MTI	AMTI
1	28.5	28.3	28.5	27.9	28.8	28.8	28.4	28.9	29.9	29.9	20.6	20.5	24.5	23.6
2	29.0	28.8	29.0	28.4	29.1	29.2	28.9	29.4	30.3	30.3	20.9	20.9	24.9	24.1
3	29.0	28.7	29.0	28.4	29.0	29.2	28.9	29.4	30.3	30.3	20.2	20.7	24.9	24.1
4	38.9	38.6	38.9	38.3	35.1	38.1	38.7	39.3	40.2	40.2	30.0	31.6	34.8	34.0
5	38.9	38.4	38.8	38.3	31.9	37.2	38.4	39.3	40.1	40.0	29.4	31.0	34.8	33.5
6	27.8	28.1	28.2	28.1	26.0	28.4	28.0	26.9	29.9	29.7	24.8	24.9	24.7	23.6
7	28.0	28.3	28.4	28.0	26.0	28.3	28.4	27.3	30.2	30.2	25.2	25.3	25.1	16.6
8	28.0	28.3	28.4	28.0	25.9	28.3	28.4	27.3	30.2	30.1	25.2	25.3	25.1	16.5
9	37.9	38.3	38.4	37.9	33.4	37.3	38.3	37.3	40.0	40.0	35.0	35.4	35.1	17.0
10	37.9	37.9	38.3	37.9	30.9	36.4	38.0	37.3	39.8	39.7	35.1	35.4	34.7	17.0
11	27.4	27.7	27.4	27.9	28.7	28.7	28.0	23.4	29.8	29.6	21.3	20.5	23.6	23.6
12	27.4	27.4	27.4	27.0	28.3	28.5	28.5	20.7	30.1	30.0	21.7	21.4	24.1	9.9
13	27.4	27.4	27.4	26.6	28.2	28.5	28.4	20.7	29.9	29.8	20.9	21.2	24.0	9.9
14	37.4	37.4	37.4	33.5	33.9	36.5	38.2	30.7	39.7	39.6	30.3	31.5	33.6	9.9
15	37.4	36.4	37.4	33.5	30.8	35.8	37.5	30.7	39.5	39.3	29.2	31.2	29.5	9.9
16	26.1	26.1	26.3	26.1	25.2	26.8	25.9	26.5	28.1	27.9	16.4	19.5	21.0	15.4
17	26.4	26.4	26.6	26.4	25.4	27.2	26.2	26.7	28.5	28.2	16.7	19.8	21.1	15.5
18	21.8	21.8	22.0	21.8	22.1	22.6	21.7	22.6	23.9	23.8	13.6	14.9	17.6	13.7
19	33.4	33.4	33.4	33.4	27.7	33.0	33.3	30.9	35.4	35.1	25.3	28.2	23.2	16.0
20	13.6	13.6	13.7	13.6	14.7	14.4	13.5	14.5	15.9	15.8	6.6	6.5	9.9	7.8
21	24.8	26.3	25.5	26.1	25.0	26.7	26.4	18.5	28.1	27.7	21.9	21.3	18.0	15.4
22	22.8	22.6	23.1	22.5	23.1	23.7	22.7	18.7	25.2	24.9	19.2	18.1	17.4	12.6
23	18.5	18.6	18.9	18.5	19.5	19.5	18.8	17.1	20.9	20.7	14.7	12.1	15.0	12.0
24	24.6	24.6	25.2	24.6	24.6	26.3	24.3	24.4	27.7	27.5	20.0	20.8	17.2	12.8
25	13.0	13.0	13.1	13.0	14.2	13.8	12.9	13.9	15.4	15.3	6.4	5.9	9.3	7.2
26	24.9	25.0	25.0	26.0	25.1	26.8	19.2	17.1	28.1	23.2	16.5	19.4	7.5	15.4
27	13.3	15.3	15.4	14.6	16.3	15.8	15.5	11.2	17.5	17.2	8.8	8.9	7.5	9.2
28	13.9	15.0	15.0	15.1	16.4	16.0	15.0	12.6	17.4	16.5	8.9	8.0	6.9	10.0
29	15.2	14.7	15.2	14.7	16.5	16.0	14.9	15.8	17.7	17.6	9.3	9.1	10.0	9.3
30	10.5	10.4	10.6	10.4	11.6	11.2	10.4	11.5	12.7	12.6	3.2	3.0	7.1	5.9
31	48.5	48.1	48.5	47.9	36.7	43.7	48.0	48.9	49.7	49.7	40.1	41.1	44.4	43.3
32	48.5	48.1	48.5	47.9	36.7	43.8	48.0	48.9	49.8	49.7	40.1	41.1	44.4	43.3
33	48.5	48.1	48.5	47.9	36.7	43.8	48.0	48.9	49.7	49.7	40.1	41.1	44.4	43.3
34	48.9	48.5	48.9	48.3	36.8	43.9	48.4	49.3	50.2	50.1	40.5	41.5	44.8	43.7
35	48.9	48.3	48.8	48.3	36.1	43.5	48.4	49.2	50.1	50.0	39.4	41.3	44.8	43.2
36	46.5	47.1	46.3	47.6	29.4	38.0	46.8	32.1	49.7	49.5	44.8	44.8	44.4	43.2
37	46.2	47.1	46.0	47.3	29.2	37.6	46.8	32.1	49.6	49.6	44.8	44.9	44.5	34.7
38	46.2	47.1	46.0	47.2	29.1	37.6	46.8	32.1	49.5	49.5	44.8	45.0	44.5	34.7
39	46.6	47.5	46.4	47.5	28.9	37.9	47.2	32.5	49.8	49.7	45.2	45.4	44.9	17.1
40	46.6	47.5	46.4	47.5	28.7	37.8	47.1	32.5	49.6	49.4	45.2	45.4	44.5	17.0
41	45.1	45.1	45.1	47.8	36.7	43.7	41.6	26.0	49.7	49.2	41.5	41.1	40.2	43.2
42	36.2	36.7	36.2	46.6	35.8	40.8	41.6	23.6	49.4	49.2	41.3	41.4	40.2	29.2
43	36.2	36.7	36.2	46.1	35.7	40.8	41.6	23.7	49.2	49.1	40.4	40.9	40.2	29.2
44	36.6	37.1	36.6	35.3	35.3	40.3	41.9	21.4	49.5	49.4	40.0	42.1	40.4	9.9
45	36.6	37.0	36.6	32.8	34.7	40.0	40.7	21.4	49.1	48.8	40.3	42.2	38.0	10.0
46	36.6	36.6	36.6	36.6	28.0	35.0	36.3	31.8	39.0	38.7	31.5	33.6	23.5	16.1
47	36.6	36.6	36.6	36.6	28.0	35.0	36.3	31.8	39.0	38.7	31.6	33.6	23.5	16.1
48	35.5	35.5	35.5	35.5	27.9	34.3	35.3	31.5	37.7	37.4	30.1	31.5	23.4	16.0
49	36.6	36.6	36.7	36.6	28.0	35.0	36.4	31.8	39.1	38.8	31.7	33.7	23.5	16.1
50	23.1	23.1	23.3	23.1	23.2	24.0	23.0	23.8	25.2	25.1	16.4	16.4	18.5	14.1

Table 3.5.2 (Cont)

Index	MTD						PD&MTI							
	1	2	3	4	5	6	Ham. b=6	Kais. b=6	OF	OF& MTI	LP& MTI	LP	AMTI &MTI	AMTI &MTI
51	33.0	34.8	33.1	33.8	27.9	34.6	34.5	19.0	39.0	38.4	35.3	34.8	18.9	16.1
52	32.8	33.9	32.8	33.1	27.8	33.9	33.9	19.0	37.3	36.8	33.5	32.9	18.9	16.0
53	31.6	32.8	31.7	32.2	27.5	32.9	32.8	19.0	35.2	34.8	31.4	30.1	18.8	16.0
54	25.0	24.4	25.1	24.4	24.6	26.0	24.5	19.2	28.1	27.8	24.3	22.1	18.1	12.9
55	19.0	19.1	19.4	19.0	20.0	20.1	19.3	17.4	21.4	21.2	15.8	12.9	15.4	12.3
56	36.6	36.6	36.6	36.6	28.0	34.9	19.9	17.7	39.0	25.3	21.6	33.5	7.6	16.1
57	29.0	29.0	29.0	29.5	26.9	30.1	19.8	17.4	31.7	24.9	20.9	23.6	7.6	15.9
58	31.0	31.0	31.0	31.1	27.3	31.4	19.8	17.5	33.3	24.9	20.9	25.4	7.6	15.9
59	13.3	15.5	15.5	14.7	16.5	16.0	15.7	11.3	17.8	17.4	9.2	9.2	7.6	9.3
60	14.1	15.1	15.2	15.3	16.6	16.2	15.1	12.7	17.6	16.6	9.3	8.2	7.0	10.3
61	28.5	28.3	28.5	27.9	28.8	28.8	28.4	28.9	29.9	29.9	20.6	20.5	24.5	23.6
62	28.1	28.5	28.6	28.0	28.8	28.9	28.4	28.0	30.2	30.2	24.9	25.4	24.9	18.9
63	28.1	28.5	28.6	28.0	28.7	28.9	28.4	28.2	30.2	30.1	24.9	25.3	24.9	18.8
64	37.9	37.9	37.9	37.9	34.9	37.8	38.1	25.0	40.0	40.0	35.4	35.4	35.0	20.3
65	37.9	37.9	37.9	37.9	31.6	36.9	38.1	25.7	39.9	39.8	35.4	35.4	34.9	20.2
66	27.8	28.1	28.2	28.1	26.0	28.4	28.0	26.9	29.9	29.7	24.8	24.9	24.7	23.6
67	28.1	28.4	28.3	28.5	26.0	28.9	28.4	26.6	30.3	30.1	25.1	25.3	25.1	24.0
68	28.0	28.3	28.3	28.4	26.0	28.9	28.4	26.7	30.3	30.1	25.0	25.3	25.1	24.0
69	37.9	37.9	37.9	38.3	33.5	37.7	38.1	25.1	40.1	39.9	35.5	35.3	34.7	33.4
70	37.8	37.9	37.9	38.3	31.0	36.9	38.1	25.6	40.1	39.7	35.4	35.3	34.7	33.0
71	27.4	27.7	27.4	27.9	28.7	28.7	28.0	23.4	29.8	29.6	21.3	20.5	23.6	23.6
72	27.2	27.2	27.2	27.8	28.4	28.6	27.8	23.3	30.2	29.8	25.0	25.2	10.9	14.6
73	27.0	27.0	27.0	27.7	28.3	28.6	27.6	22.5	30.1	29.7	25.0	25.2	10.9	14.5
74	34.8	34.5	34.8	37.3	34.5	37.4	36.8	23.8	40.0	39.2	35.5	35.3	14.0	14.6
75	34.7	34.3	34.7	37.3	31.3	36.6	36.8	23.3	39.8	38.9	35.4	35.3	14.1	14.6
76	26.1	26.1	26.3	26.1	25.2	26.8	25.9	26.5	28.1	27.9	16.4	19.5	21.0	15.4
77	24.0	24.0	24.3	24.0	24.0	25.1	23.8	24.5	26.5	26.2	14.8	18.8	18.3	13.5
78	19.6	19.6	19.8	19.6	20.3	20.4	19.5	20.3	21.8	21.7	11.6	12.1	15.2	12.5
79	26.6	26.4	27.1	26.4	25.8	28.1	26.7	21.8	30.2	30.0	24.9	24.2	20.5	13.8
80	13.7	13.5	13.9	13.3	14.5	14.2	13.6	13.4	15.7	15.5	7.6	1.8	10.1	7.5
81	24.8	26.3	25.5	26.1	25.0	26.7	26.4	18.5	28.1	27.7	21.9	21.3	18.0	15.4
82	25.2	26.7	25.9	26.4	25.2	27.1	26.7	18.7	28.4	28.0	22.2	21.6	18.3	15.3
83	21.1	21.9	21.9	21.7	22.0	22.5	22.1	17.6	23.8	23.5	18.0	16.0	16.3	13.7
84	33.3	33.3	33.3	33.1	27.6	32.9	33.2	21.5	35.2	34.7	29.7	30.1	21.4	15.9
85	13.9	13.9	14.2	13.6	14.7	14.4	13.9	13.3	15.9	15.7	8.5	1.9	10.3	7.8
86	24.9	25.0	25.0	26.0	25.1	26.8	19.2	17.1	28.1	23.2	16.5	19.4	7.5	15.4
87	16.5	17.9	17.9	21.0	21.9	22.3	17.2	14.7	23.6	19.9	16.3	13.3	6.7	11.7
88	15.2	16.5	16.5	17.5	18.5	18.3	16.2	13.6	19.9	18.1	12.0	9.8	7.0	11.5
89	17.5	22.7	21.7	22.3	23.0	23.8	23.5	15.9	25.1	24.6	21.4	18.6	12.7	11.9
90	12.5	13.0	13.4	12.5	13.6	13.3	12.9	12.0	14.9	14.7	7.5	.5	8.7	6.9
91	48.5	48.1	48.5	47.9	36.7	43.7	48.0	48.9	49.7	49.7	40.1	41.1	44.4	43.3
92	47.7	47.9	48.1	47.6	36.6	43.7	47.6	47.6	49.6	49.5	43.7	44.6	44.4	37.3
93	47.6	47.9	48.1	47.5	36.5	43.7	47.6	47.8	49.6	49.5	43.6	44.5	44.4	37.2
94	47.8	47.9	47.9	47.9	36.5	43.5	47.7	35.0	49.8	49.7	44.8	45.1	44.9	20.4
95	47.8	47.9	47.9	47.9	36.8	43.1	47.7	35.7	49.6	49.5	44.2	44.9	44.8	20.2
96	46.5	47.1	46.3	47.6	29.4	38.0	46.8	32.1	49.7	49.5	44.8	44.8	44.4	43.2
97	46.4	47.1	46.2	47.6	29.2	38.0	46.8	32.1	49.7	49.5	44.8	44.9	44.4	43.2
98	46.4	47.1	46.2	47.6	29.1	38.0	46.8	32.1	49.7	49.4	44.8	44.9	44.4	43.2
99	46.6	47.5	46.4	48.0	28.9	38.2	46.9	30.6	50.0	49.6	45.3	45.3	43.1	40.0
100	46.6	47.5	46.4	48.0	28.7	38.1	46.9	30.5	50.0	49.6	45.3	45.3	42.7	38.5

Table 3.5.2 (Cont)

Index	MTD						PD&MTI							
	1	2	3	4	5	6	Ham. b=6	Kais. b=6	OF	OF& MTI	LP& MTI	LP	AMTI &MTI	AMTI
101	45.1	45.1	45.1	47.8	36.7	43.7	41.6	26.0	49.7	49.2	41.5	41.1	40.2	43.2
102	44.6	44.6	44.6	47.3	36.3	43.4	40.0	26.0	49.6	48.5	44.6	44.7	29.9	32.7
103	44.1	44.1	44.1	47.3	36.2	43.4	40.0	26.0	49.5	48.4	44.5	44.7	30.0	32.6
104	36.0	36.2	36.0	47.2	36.1	42.8	40.3	25.4	49.8	48.5	45.2	45.4	10.9	14.6
105	35.1	35.4	35.1	47.2	35.4	42.5	40.3	24.1	49.6	48.2	44.8	45.4	11.0	14.6
106	36.6	36.6	36.6	36.6	28.0	35.0	36.3	31.8	39.0	38.7	31.5	33.6	23.5	16.1
107	35.9	35.9	35.9	35.9	28.0	34.6	35.7	31.6	38.3	38.0	30.9	32.6	23.4	16.0
108	33.8	33.8	33.8	33.8	27.8	33.3	33.6	31.0	35.8	35.7	28.1	28.8	23.2	16.0
109	26.7	26.7	27.3	26.7	26.0	28.6	26.3	26.8	31.0	30.9	23.9	25.8	19.0	13.9
110	20.3	20.3	20.5	20.3	20.9	21.2	20.2	21.0	22.6	22.5	12.6	12.9	15.3	12.8
111	33.0	34.8	33.1	33.8	27.9	34.6	34.5	19.0	39.0	38.4	35.3	34.8	18.9	16.1
112	33.0	34.8	33.1	33.8	27.9	34.6	34.5	19.0	39.0	38.4	35.3	34.8	18.9	16.1
113	32.5	34.1	32.6	33.3	27.8	34.0	33.9	19.0	37.5	37.0	33.9	33.1	18.9	16.0
114	33.3	34.5	33.4	33.5	27.9	34.4	34.5	19.2	38.6	37.9	34.8	34.3	19.1	15.9
115	22.4	23.2	23.1	22.9	23.0	23.8	23.3	17.9	25.1	24.8	20.2	17.6	16.8	14.0
116	36.6	36.6	36.6	36.6	28.0	34.9	19.9	17.7	39.0	25.3	21.6	33.5	7.6	16.1
117	33.4	33.4	33.4	33.5	27.7	33.2	19.8	17.6	35.9	24.9	21.0	29.2	7.6	16.0
118	32.3	32.3	32.3	32.4	27.6	32.4	19.8	17.6	34.5	25.0	21.1	27.0	7.6	16.0
119	16.9	18.3	18.3	22.4	23.1	24.0	17.6	14.9	25.3	20.8	18.9	15.5	6.7	11.9
120	15.5	16.8	16.8	17.9	18.9	18.7	16.4	13.8	20.3	18.5	13.3	10.2	7.0	11.7
121	28.5	28.3	28.5	27.9	28.8	28.8	28.4	28.9	29.9	29.9	20.6	20.5	24.5	23.6
122	27.2	28.6	28.6	27.1	28.3	28.5	28.5	24.1	30.1	30.0	24.8	25.3	25.1	11.2
123	27.1	28.3	28.5	27.0	28.2	28.5	28.4	23.5	30.0	29.9	24.9	25.2	25.0	11.2
124	34.8	36.4	35.1	36.0	34.1	36.8	35.8	16.2	39.8	39.7	35.3	35.3	34.8	11.4
125	34.9	36.4	35.0	36.0	31.0	36.0	35.8	15.2	39.6	39.5	34.4	34.8	32.3	11.4
126	27.8	28.1	28.2	28.1	26.0	28.4	28.0	26.9	29.9	29.7	24.8	24.9	24.7	23.6
127	27.9	28.2	28.2	28.3	26.0	28.6	28.0	23.5	30.2	29.9	25.1	25.3	21.3	21.2
128	27.8	28.1	28.2	28.2	25.9	28.6	28.0	22.9	30.2	29.8	25.1	25.3	21.0	21.1
129	37.3	37.6	37.3	38.1	33.6	37.5	35.3	21.5	40.0	39.7	35.1	35.3	21.5	24.5
130	37.4	37.6	37.4	38.1	31.0	36.7	35.4	19.5	39.9	39.4	33.8	34.8	21.2	24.4
131	27.4	27.7	27.4	27.9	28.7	28.7	28.0	23.4	29.8	29.6	21.3	20.5	23.6	23.6
132	27.5	28.2	27.5	28.3	29.1	29.2	28.2	23.3	30.2	29.8	21.8	24.1	19.1	23.6
133	27.5	28.0	27.5	28.2	29.0	29.2	28.2	23.0	30.2	29.7	22.1	24.0	18.7	23.5
134	37.2	36.7	37.2	38.1	35.1	38.0	35.6	24.9	40.1	39.5	31.5	33.3	22.6	29.5
135	37.2	36.8	37.2	38.1	31.9	37.2	35.5	20.9	40.0	39.3	31.8	33.7	22.4	29.3
136	26.1	26.1	26.3	26.1	25.2	26.8	25.9	26.5	28.1	27.9	16.4	19.5	21.0	15.4
137	17.1	16.9	17.3	16.9	18.3	18.0	17.0	17.9	19.9	19.8	10.4	7.5	12.8	10.1
138	16.0	15.9	16.2	15.9	17.0	16.7	15.9	16.9	18.2	18.1	8.8	8.3	11.8	10.7
139	15.8	18.3	18.5	17.2	18.7	18.4	18.1	12.8	20.4	20.1	15.1	13.0	10.5	10.3
140	10.7	11.8	11.9	11.2	12.3	12.0	11.4	9.9	13.6	12.8	6.4	2.0	5.2	6.3
141	24.8	26.3	25.5	26.1	25.0	26.7	26.4	18.5	28.1	27.7	21.9	21.3	18.0	15.4
142	22.3	25.4	24.2	25.3	24.7	26.2	25.5	17.1	27.5	26.7	20.8	20.5	15.6	14.3
143	17.7	19.8	19.7	20.4	21.1	21.3	20.3	15.9	22.7	21.8	16.3	14.5	13.8	13.0
144	19.7	25.0	23.3	29.0	26.8	30.3	25.8	16.4	32.5	29.2	23.2	25.9	10.5	14.7
145	11.8	13.3	13.3	13.5	14.6	14.3	12.6	11.3	15.8	13.9	8.4	4.6	5.2	7.7
146	24.9	25.0	25.0	26.0	25.1	26.8	19.2	17.1	28.1	23.2	16.5	19.4	7.5	15.4
147	25.0	25.1	25.1	26.0	25.2	26.8	19.2	17.1	28.1	22.5	15.7	19.7	7.2	14.9
148	19.3	19.7	19.7	21.2	21.7	22.1	17.5	15.7	23.4	19.8	13.8	14.2	7.0	13.4
149	25.5	26.0	25.8	31.7	27.4	32.1	23.1	17.3	34.3	27.2	20.1	26.7	9.6	15.4
150	12.0	13.3	13.3	13.6	14.7	14.4	12.7	11.4	15.9	13.8	8.4	4.9	5.0	7.8

Table 3.5.2 (Cont)

Index	MTD						PD&MTI							
	1	2	3	4	5	6	Ham. b=6	Kais. b=6	OF	OF& MTI	LP& MTI	LP	AMTI &MTI	AMTI
151	48.5	48.1	48.5	47.9	36.7	43.7	48.0	48.9	49.7	49.7	40.1	41.1	44.4	43.3
152	46.8	47.9	48.1	46.6	35.9	41.9	47.2	43.7	49.4	49.3	44.3	44.9	43.4	30.0
153	46.7	47.6	48.1	46.4	35.8	41.9	47.1	43.0	49.3	49.2	44.3	44.7	43.3	30.1
154	44.8	46.3	45.1	45.5	35.5	41.3	45.6	26.2	49.6	49.4	45.2	45.3	43.0	11.4
155	44.9	46.3	45.0	45.5	35.0	41.0	45.6	25.2	49.2	49.0	44.5	44.9	41.2	11.4
156	46.5	47.1	46.3	47.6	29.4	38.0	46.8	32.1	49.7	49.5	44.8	44.8	44.4	43.2
157	45.9	46.8	46.0	47.5	28.6	37.6	46.6	31.8	49.6	49.3	44.7	44.9	39.1	40.1
158	45.7	46.7	45.8	47.4	28.6	37.6	46.5	31.7	49.6	49.2	44.7	44.9	38.8	40.0
159	44.4	46.6	44.4	47.8	28.9	37.9	44.4	25.1	49.9	49.4	44.8	45.3	24.2	24.9
160	44.4	46.6	44.4	47.8	28.7	37.8	44.4	24.3	49.7	49.2	44.6	45.3	23.6	24.6
161	45.1	45.1	45.1	47.8	36.7	43.7	41.6	26.0	49.7	49.2	41.5	41.1	40.2	43.2
162	45.2	45.2	45.2	47.8	36.7	43.8	41.6	26.0	49.6	49.1	39.5	42.5	36.3	42.4
163	45.2	45.2	45.2	47.7	36.7	43.7	41.6	26.0	49.6	49.0	39.8	43.0	36.0	42.2
164	45.6	45.6	45.6	48.1	36.7	43.8	40.0	25.8	49.9	49.2	41.7	43.0	20.2	31.2
165	45.6	45.6	45.6	48.1	36.1	43.4	39.8	25.1	49.8	49.1	41.9	42.8	19.6	30.5
166	36.6	36.6	36.6	36.6	28.0	35.0	36.3	31.8	39.0	38.7	31.5	33.6	23.5	16.1
167	30.6	30.6	30.7	30.6	27.2	31.0	30.4	29.7	33.0	32.9	24.9	25.2	22.8	15.9
168	31.5	31.5	31.5	31.5	27.4	31.7	31.4	30.1	33.6	33.5	25.7	25.8	22.9	16.0
169	17.5	17.2	17.6	17.2	18.7	18.5	17.4	18.3	20.5	20.4	12.5	7.8	12.7	10.3
170	16.3	16.2	16.4	16.2	17.2	17.0	16.2	17.1	18.5	18.4	9.3	8.6	11.6	10.9
171	33.0	34.8	33.1	33.8	27.9	34.6	34.5	19.0	39.0	38.4	35.3	34.8	18.9	16.1
172	32.8	34.7	32.8	33.7	27.9	34.5	34.3	19.0	38.8	38.2	35.1	34.6	18.8	16.0
173	31.6	33.7	31.7	32.9	27.7	33.6	33.2	19.0	36.5	36.1	32.9	31.9	18.8	16.0
174	24.6	31.6	27.0	31.0	27.0	32.1	30.8	17.4	34.0	33.5	30.3	29.1	16.0	14.8
175	18.1	20.6	20.3	21.2	21.9	22.2	21.1	16.1	23.6	22.7	18.0	15.8	14.0	13.3
176	36.6	36.6	36.6	36.6	28.0	34.9	19.9	17.7	39.0	25.3	21.6	33.5	7.6	16.1
177	36.5	36.5	36.5	36.5	28.0	34.9	19.9	17.7	39.0	25.3	21.6	33.5	7.6	16.1
178	34.9	34.9	34.9	35.0	27.9	34.0	19.9	17.6	37.1	25.2	21.4	30.7	7.6	16.0
179	33.4	33.4	33.4	33.5	27.7	33.7	19.7	17.6	36.8	24.1	19.0	31.1	7.3	15.5
180	20.3	20.6	20.6	22.3	22.6	23.3	17.9	16.1	24.5	20.4	15.7	15.5	7.1	13.7
181	28.5	28.3	28.5	27.9	28.8	28.8	28.4	28.9	29.9	29.9	20.6	20.5	24.5	23.6
182	27.2	28.6	28.6	27.1	28.3	28.5	28.5	24.1	30.1	30.0	24.8	25.3	23.6	9.8
183	27.1	28.3	28.5	27.0	28.2	28.5	28.4	23.5	30.0	29.9	24.9	25.2	23.2	9.8
184	34.8	36.4	35.1	36.0	34.1	36.8	35.8	16.2	39.8	39.7	35.3	35.3	34.8	9.9
185	34.9	36.4	35.0	36.0	31.0	36.0	35.8	15.2	39.6	39.5	34.4	34.8	32.3	9.9
186	27.8	28.1	28.2	28.1	26.0	28.4	28.0	26.9	29.9	29.7	24.8	24.9	24.7	23.6
187	25.7	27.6	27.4	27.8	26.3	28.0	26.2	21.3	30.1	29.5	24.9	25.2	9.7	12.4
188	25.7	27.4	27.4	27.7	26.2	28.0	26.2	20.7	30.1	29.2	24.4	24.9	9.7	12.4
189	35.5	35.9	35.6	37.2	33.4	36.7	31.0	21.4	39.9	38.7	34.7	34.8	9.2	12.8
190	35.5	35.6	35.6	37.2	30.9	36.0	30.4	19.3	39.7	37.6	33.2	33.5	9.2	12.8
191	27.4	27.7	27.4	27.9	28.7	28.7	28.0	23.4	29.8	29.6	21.3	20.5	23.6	23.6
192	27.5	28.2	27.5	28.3	29.1	29.2	28.2	23.3	30.2	29.8	21.8	24.1	18.3	23.1
193	27.5	28.0	27.5	28.2	29.0	29.2	28.2	23.0	30.2	29.7	22.1	24.0	18.0	22.9
194	37.2	36.7	37.2	38.1	35.1	38.0	35.6	24.9	40.1	39.5	31.5	33.3	22.7	29.7
195	37.2	36.8	37.2	38.1	31.9	37.2	35.5	20.9	40.0	39.3	31.8	33.7	22.5	29.4
196	26.1	26.1	26.3	26.1	25.2	26.8	25.9	26.5	28.1	27.9	16.4	19.5	21.0	15.4
197	17.1	16.9	17.3	16.9	18.3	18.0	17.0	17.9	19.9	19.8	10.4	7.5	8.3	9.1
198	16.0	15.9	16.2	15.9	17.0	16.7	15.9	16.9	18.2	18.1	8.8	8.3	9.9	10.1
199	15.8	18.3	18.5	17.2	18.7	18.4	18.1	12.8	20.4	20.1	15.1	13.0	10.3	9.2
200	10.7	11.8	11.9	11.2	12.3	12.0	11.4	9.9	13.6	12.8	6.4	2.0	5.1	5.8

Table 3.5.2 (Cont)

Scenario Index	MTD						PD&MTI							
	1	2	3	4	5	6	Ham. b=6	Kais. b=6	OF	OF& MTI	LP& MTI	LP &MTI	AMTI &MTI	AMTI
Z01	24.8	26.3	25.5	26.1	25.0	26.7	26.4	18.5	28.1	27.7	21.9	21.3	18.0	15.4
Z02	14.2	17.0	16.9	18.9	20.3	20.3	17.1	13.8	21.8	19.5	14.6	13.8	10.1	10.8
Z03	14.9	16.3	16.4	16.8	17.7	17.6	16.2	14.6	19.0	17.9	12.0	9.6	11.6	11.1
Z04	19.2	19.3	19.3	19.5	20.8	20.9	16.5	15.9	22.7	15.6	7.4	11.8	7.5	11.0
Z05	11.1	11.8	11.8	11.8	12.9	12.6	11.3	10.9	14.2	11.6	5.0	4.3	4.0	6.6
Z06	24.9	25.0	25.0	26.0	25.1	26.8	19.2	17.1	28.1	23.2	16.5	19.4	7.5	15.4
Z07	25.0	25.1	25.1	26.0	25.2	26.8	19.2	17.1	28.1	22.5	15.7	19.7	7.2	14.9
Z08	19.3	19.7	19.7	21.2	21.7	22.1	17.5	15.7	23.4	19.8	13.8	14.2	7.0	13.3
Z09	25.5	26.0	25.8	31.7	27.4	32.1	23.1	17.3	34.3	27.2	20.2	26.7	9.6	15.4
Z10	12.0	13.3	13.3	13.6	14.7	14.4	12.7	11.4	15.9	13.8	8.4	4.9	4.9	7.8
Z11	48.5	48.1	48.5	47.9	36.7	43.7	48.0	48.9	49.7	49.7	40.1	41.1	44.4	43.3
Z12	46.8	47.9	48.1	46.5	35.9	41.9	47.2	43.7	49.4	49.3	44.3	44.9	40.5	30.0
Z13	46.7	47.6	48.1	46.4	35.8	41.9	47.1	43.0	49.3	49.2	44.3	44.7	40.2	30.0
Z14	44.8	46.3	45.1	45.5	35.5	41.3	45.6	26.2	49.6	49.4	45.2	45.3	42.9	9.9
Z15	44.9	46.3	45.0	45.5	35.0	41.0	45.6	25.2	49.2	49.0	44.5	44.9	41.1	9.9
Z16	46.5	47.1	46.3	47.6	29.4	38.0	46.8	32.1	49.7	49.5	44.8	44.8	44.4	43.2
Z17	43.1	43.3	43.2	46.9	29.4	37.4	42.7	30.3	49.5	48.7	44.3	44.8	28.7	31.1
Z18	43.1	43.3	43.2	46.7	29.4	37.3	42.6	30.2	49.4	48.3	43.8	44.5	28.8	31.1
Z19	43.5	43.6	43.5	46.5	29.7	37.6	39.7	22.1	49.7	48.0	43.7	44.6	9.8	12.8
Z20	43.5	43.5	43.5	46.5	29.5	37.5	39.4	21.5	49.5	46.6	43.4	43.6	9.8	12.8
Z21	45.1	45.1	45.1	47.8	36.7	43.7	41.6	26.0	49.7	49.2	41.5	41.1	40.2	43.2
Z22	45.2	45.2	45.2	47.8	36.7	43.8	41.6	26.0	49.6	49.1	39.5	42.5	36.3	42.4
Z23	45.2	45.2	45.2	47.7	36.7	43.7	41.6	26.0	49.6	49.0	39.8	43.0	36.0	42.2
Z24	45.6	45.6	45.6	48.1	36.7	43.8	40.0	25.8	49.9	49.2	41.7	43.0	20.2	31.2
Z25	45.6	45.6	45.6	48.1	36.1	43.4	39.8	25.1	49.8	49.1	41.9	42.8	19.6	30.5
Z26	36.6	36.6	36.6	36.6	28.0	35.0	36.3	31.8	39.0	38.7	31.5	33.6	23.5	16.1
Z27	30.6	30.6	30.7	30.6	27.2	31.0	30.4	29.7	33.0	32.9	24.9	25.2	22.7	15.9
Z28	31.5	31.5	31.5	31.5	27.4	31.7	31.4	30.1	33.6	33.5	25.7	25.8	22.9	16.0
Z29	17.5	17.2	17.6	17.2	18.7	18.5	17.4	18.3	20.5	20.4	12.5	7.8	7.8	9.2
Z30	16.3	16.2	16.4	16.2	17.2	17.0	16.2	17.1	18.5	18.4	9.3	8.6	9.4	10.2
Z31	33.0	34.8	33.1	33.8	27.9	34.6	34.5	19.0	39.0	38.4	35.3	34.8	18.9	16.1
Z32	29.2	32.1	29.6	31.7	27.4	32.4	31.7	18.9	34.3	33.9	30.4	29.1	18.6	15.9
Z33	30.0	32.0	30.3	31.5	27.3	32.1	31.7	18.9	34.0	33.7	30.0	28.6	18.7	16.0
Z34	14.3	17.2	17.2	19.5	21.1	21.1	17.5	13.9	22.8	20.1	15.9	15.2	10.1	11.0
Z35	15.1	16.5	16.6	17.1	18.1	17.9	16.4	14.8	19.3	18.1	12.6	10.1	11.6	11.3
Z36	36.6	36.6	36.6	36.6	28.0	34.9	19.9	17.7	39.0	25.3	21.6	33.5	7.6	16.1
Z37	36.5	36.5	36.5	36.5	28.0	34.9	19.9	17.7	39.0	25.3	21.6	33.5	7.6	16.1
Z38	34.9	34.9	34.9	35.0	27.9	34.0	19.9	17.6	37.1	25.2	21.4	30.7	7.6	16.0
Z39	33.4	33.4	33.4	33.5	27.7	33.7	19.7	17.6	36.8	24.1	19.0	31.1	7.3	15.5
Z40	20.3	20.6	20.6	22.3	22.6	23.3	17.9	16.1	24.5	20.4	15.7	15.5	7.1	13.7
Z41	28.5	28.3	28.5	27.9	28.8	28.8	28.4	28.9	29.9	29.9	20.6	20.5	24.5	23.6
Z42	28.1	28.5	28.6	28.0	28.8	28.9	28.4	28.0	30.2	30.2	24.9	25.4	10.3	14.0
Z43	28.1	28.5	28.6	28.0	28.7	28.9	28.4	28.2	30.2	30.1	24.9	25.3	10.4	13.9
Z44	37.9	37.9	37.9	37.9	34.9	37.8	38.1	25.0	40.0	40.0	35.4	35.4	35.0	14.2
Z45	37.9	37.9	37.9	37.9	31.6	36.9	38.1	25.7	39.9	39.8	35.4	35.4	34.9	14.1
Z46	27.8	28.1	28.2	28.1	26.0	28.4	28.0	26.9	29.9	29.7	24.8	24.9	24.7	23.6
Z47	27.6	27.6	27.8	27.6	26.2	28.1	26.8	26.0	30.0	29.8	20.9	22.2	14.8	9.7
Z48	27.4	27.4	27.6	27.4	26.2	28.1	26.7	26.1	29.9	29.7	17.6	20.9	14.6	9.7
Z49	35.6	35.6	35.7	35.6	33.4	35.9	35.5	24.9	39.8	39.3	26.6	32.6	11.0	9.7
Z50	35.5	35.5	35.6	35.5	30.7	35.2	35.5	25.4	39.5	38.9	24.7	32.7	10.9	9.7

Table 3.5.2 (Cont)

Scenario Index	MTD						PD&MTI							
	1	2	3	4	5	6	Ham. b=6	Kais. b=6	OF	OF& MTI	LP& MTI	LP	AMTI &MTI	AMTI
Z51	27.4	27.7	27.4	27.9	28.7	28.7	28.0	23.4	29.8	29.6	21.3	20.5	23.6	23.6
Z52	27.2	27.2	27.2	27.8	28.4	28.6	27.8	23.3	30.2	29.8	25.0	25.2	10.6	13.8
Z53	27.0	27.0	27.0	27.7	28.3	28.6	27.6	22.5	30.1	29.7	25.0	25.2	10.7	13.8
Z54	34.8	34.5	34.8	37.3	34.5	37.4	36.8	23.8	40.0	39.2	35.5	35.3	14.0	14.7
Z55	34.7	34.3	34.7	37.3	31.3	36.6	36.8	23.3	39.8	38.9	35.4	35.3	14.0	14.6
Z56	26.1	26.1	26.3	26.1	25.2	26.8	25.9	26.5	28.1	27.9	16.4	19.5	21.0	15.4
Z57	24.0	24.0	24.3	24.0	24.0	25.1	23.8	24.5	26.5	26.2	14.8	18.8	11.0	10.8
Z58	19.6	19.6	19.8	19.6	20.3	20.4	19.5	20.3	21.8	21.7	11.6	12.1	11.0	11.1
Z59	26.6	26.4	27.1	26.4	25.8	28.1	26.7	21.8	30.2	30.0	24.9	24.2	20.1	10.5
Z60	13.7	13.5	13.9	13.3	14.5	14.2	13.6	13.4	15.7	15.5	7.6	1.8	9.3	5.3
Z61	24.8	26.3	25.5	26.1	25.0	26.7	26.4	18.5	28.1	27.7	21.9	21.3	18.0	15.4
Z62	15.5	15.5	15.8	15.5	17.0	16.6	15.6	15.4	18.3	18.0	11.4	8.8	11.4	9.2
Z63	15.3	15.6	15.8	15.5	16.6	16.3	15.6	15.1	17.6	17.5	11.0	7.7	12.1	10.3
Z64	15.4	15.5	15.6	15.5	17.2	16.8	15.4	16.2	18.6	18.4	10.0	8.3	10.4	9.1
Z65	10.9	11.0	11.2	10.7	11.8	11.4	10.9	11.4	13.0	12.9	3.9	1.5	6.5	5.3
Z66	24.9	25.0	25.0	26.0	25.1	26.8	19.2	17.1	28.1	23.2	16.5	19.4	7.5	15.4
Z67	16.5	17.9	17.9	21.0	21.9	22.3	17.2	14.7	23.6	19.9	16.3	13.3	6.6	11.6
Z68	15.2	16.5	16.5	17.5	18.5	18.3	16.2	13.6	19.9	18.1	12.0	9.8	7.0	11.5
Z69	17.5	22.7	21.7	22.3	23.0	23.8	23.5	15.9	25.1	24.6	21.4	18.6	12.7	11.9
Z70	12.5	13.0	13.4	12.5	13.6	13.3	12.9	12.0	14.9	14.7	7.5	.5	8.1	6.7
Z71	48.5	48.1	48.5	47.9	36.7	43.7	48.0	48.9	49.7	49.7	40.1	41.1	44.4	43.3
Z72	47.7	47.9	48.1	47.6	36.6	43.7	47.6	47.6	49.6	49.5	43.7	44.6	29.4	37.2
Z73	47.6	47.9	48.1	47.5	36.5	43.7	47.6	47.8	49.6	49.5	43.6	44.5	29.5	37.2
Z74	47.8	47.9	47.9	47.9	36.5	43.5	47.7	35.0	49.8	49.7	44.8	45.1	44.9	14.3
Z75	47.8	47.9	47.9	47.9	35.8	43.1	47.7	35.7	49.6	49.5	44.2	44.9	44.7	14.3
Z76	46.5	47.1	46.3	47.6	29.4	38.0	46.8	32.1	49.7	49.5	44.8	44.8	44.4	43.2
Z77	46.1	46.1	46.2	46.1	29.4	37.9	45.2	31.9	49.4	49.0	40.7	41.8	34.8	29.4
Z78	45.8	45.8	45.9	45.8	29.4	37.9	44.8	31.9	49.2	48.9	37.1	40.2	34.7	29.4
Z79	43.6	43.6	43.9	43.6	29.7	38.0	43.4	29.3	49.5	48.7	39.7	40.7	14.9	9.7
Z80	43.5	43.5	43.6	43.5	29.5	37.9	43.3	29.6	49.1	48.1	34.7	37.7	14.8	9.8
Z81	45.1	45.1	45.1	47.8	36.7	43.7	41.6	26.0	49.7	49.2	41.5	41.1	40.2	43.2
Z82	44.6	44.6	44.6	47.3	36.3	43.4	40.0	26.0	49.6	48.5	44.6	44.7	29.9	32.7
Z83	44.1	44.1	44.1	47.3	36.2	43.4	40.0	26.0	49.5	48.4	44.5	44.7	30.0	32.6
Z84	36.0	36.2	36.0	47.2	36.1	42.8	40.3	25.4	49.8	48.5	45.2	45.4	10.9	14.6
Z85	35.1	35.4	35.1	47.2	35.4	42.5	40.3	24.1	49.6	48.2	44.8	45.4	11.0	14.6
Z86	36.6	36.6	36.6	36.6	28.0	35.0	36.3	31.8	39.0	38.7	31.5	33.6	23.5	16.1
Z87	35.9	35.9	35.9	35.9	28.0	34.6	35.7	31.6	38.3	38.0	30.9	32.6	23.4	16.0
Z88	33.8	33.8	33.8	33.8	27.8	33.3	33.6	31.0	35.8	35.7	28.1	28.8	23.2	16.0
Z89	26.7	26.7	27.3	26.7	26.0	28.6	26.3	26.8	31.0	30.9	23.9	25.8	10.0	10.9
Z90	20.3	20.3	20.5	20.3	20.9	21.2	20.2	21.0	22.6	22.5	12.6	12.9	10.3	11.2
Z91	33.0	34.8	33.1	33.8	27.9	34.6	34.5	19.0	39.0	38.4	35.3	34.8	18.9	16.1
Z92	29.2	30.2	29.5	30.1	26.8	30.6	30.3	19.0	32.1	31.8	27.6	26.0	18.7	15.9
Z93	30.0	31.5	30.2	31.0	27.2	31.6	31.4	19.0	33.4	33.1	29.2	27.7	18.7	15.9
Z94	15.7	15.8	16.1	15.8	17.3	16.9	15.8	15.6	18.6	18.3	12.3	9.3	11.3	9.2
Z95	15.5	15.8	16.0	15.7	16.8	16.5	15.8	15.2	17.8	17.7	11.4	8.0	12.1	10.4
Z96	36.6	36.6	36.6	36.6	28.0	34.9	19.9	17.7	39.0	25.3	21.6	33.5	7.6	16.1
Z97	33.4	33.4	33.4	33.5	27.7	33.2	19.8	17.6	35.9	24.9	21.0	29.2	7.6	16.0
Z98	32.3	32.3	32.3	32.4	27.6	32.4	19.8	17.6	34.5	25.0	21.1	27.0	7.6	16.0
Z99	17.0	18.3	18.3	22.4	23.1	24.0	17.6	14.9	25.3	20.8	18.9	15.5	6.7	11.9
300	15.5	16.8	16.8	17.9	18.9	18.7	16.4	13.8	20.3	18.5	13.3	10.2	7.0	11.7

Table 3.5.3

Average L_{if} for Different Doppler Processors,

Averaged over all Land Clutter Scenarios

Filter Type	Mean(L_{if})$_{dB}$				[Mean(L_{if})]$_{dB}$			
	α=5%	α=30%	α=70%	α=100%	α=5%	α=30%	α=70%	α=100%
MTD 1	2.733	3.507	4.114	4.138	4.584	5.071	5.509	5.497
MTD 2	2.651	3.146	3.630	3.654	3.691	4.068	4.397	4.412
MTD 3	2.037	2.616	3.106	3.134	2.845	3.342	3.754	3.771
MTD 4	3.561	4.208	4.870	4.942	5.909	6.265	6.636	6.662
MTD 6	9.533	10.337	10.825	10.870	19.225	19.594	19.458	19.440
PD&MTI[1]	1.922	2.493	2.948	2.977	2.970	3.334	3.627	3.645
OF	.000	.000	.000	.000	.000	.000	.000	.000
PD&MTI[2]	3.435	3.846	4.406	4.445	6.472	6.518	6.502	6.503
OF&MTI	.145	.188	.252	.265	.154	.198	.261	.274
LP&MTI	6.593	7.968	8.649	8.631	7.720	8.613	9.110	9.076
LP	5.246	6.709	7.486	7.483	6.101	7.121	7.792	7.778
AMTI&MTI	8.486	9.170	10.361	10.463	16.102	16.379	16.561	16.574
AMTI	19.625	19.689	20.083	20.156	28.186	28.198	28.215	28.210
MTD 5	15.002	15.432	15.421	15.408	28.396	28.491	27.579	27.396
AMTD 1	1.815	2.344	2.846	2.875	2.282	2.731	3.172	3.197
AMTD 2	2.651	3.146	3.628	3.652	3.691	4.068	4.396	4.410
AMTD 3	2.502	3.036	3.513	3.539	3.507	3.917	4.249	4.265
AMTD 4	1.814	2.363	2.818	2.844	2.714	3.081	3.404	3.422
AMTD 5	1.986	2.551	3.037	3.065	2.654	3.131	3.542	3.562
AMTD 6	1.843	2.436	2.903	2.933	2.456	2.963	3.334	3.356
AMTD 7	1.640	2.181	2.612	2.640	2.129	2.552	2.907	2.930
AMTD 8	2.996	3.654	4.264	4.333	4.790	5.212	5.609	5.649
AMTD 9	1.903	2.475	2.932	2.961	2.886	3.252	3.564	3.584
AMTD 10	1.814	2.363	2.818	2.844	2.714	3.081	3.404	3.422
AMTD 11	1.815	2.344	2.844	2.873	2.282	2.731	3.170	3.195
AMTD 12	1.841	2.424	2.887	2.917	2.455	2.950	3.317	3.339
AMTD 13	1.638	2.175	2.607	2.635	2.127	2.544	2.897	2.920
AMTD 14	1.829	2.388	2.855	2.889	2.802	3.163	3.483	3.506
AMTD 15	1.726	2.283	2.760	2.790	2.170	2.651	3.059	3.084
AMTD 16	1.580	2.122	2.556	2.585	2.043	2.475	2.836	2.860

Table 3.5.4
Average L_{if} for Different Doppler Processors,
Averaged over all Sea Clutter Scenarios

Filter Type	Mean(L_{if})$_{dB}$				[Mean(L_{if})]$_{dB}$			
	α=5%	α=30%	α=70%	α=100%	α=5%	α=30%	α=70%	α=100%
MTD 1	2.594	3.630	4.498	4.542	3.621	4.651	5.611	5.649
MTD 2	2.455	3.119	3.811	3.860	3.250	4.023	4.927	4.978
MTD 3	2.425	3.271	4.016	4.064	3.331	4.269	5.209	5.254
MTD 4	2.174	2.608	3.220	3.292	2.712	3.099	3.800	3.861
MTD 6	2.976	3.654	4.141	4.200	4.241	5.187	5.859	5.927
PD&MTI[1]	3.579	4.417	4.978	5.021	7.252	7.658	7.296	7.296
OF	.000	.000	.000	.000	.000	.000	.000	.000
PD&MTI[2]	9.208	10.838	11.558	11.574	15.382	17.595	18.741	18.700
OF&MTI	1.213	1.349	1.734	1.794	3.685	3.277	3.369	3.388
LP&MTI	6.039	7.698	8.883	8.961	8.711	9.211	9.997	10.055
LP	5.430	7.042	8.041	8.079	7.077	7.726	8.394	8.426
AMTI&MTI	13.097	13.377	14.402	14.542	24.579	24.684	25.288	25.304
AMTI	15.949	15.640	15.973	16.091	25.945	26.153	26.546	26.543
MTD 5	6.743	7.271	7.529	7.540	10.897	12.002	12.463	12.335
AMTD 1	2.306	3.013	3.723	3.773	3.128	3.947	4.869	4.919
AMTD 2	2.005	2.401	2.939	2.993	2.257	2.636	3.265	3.319
AMTD 3	1.647	2.343	2.962	3.013	1.873	2.647	3.465	3.522
AMTD 4	2.088	2.904	3.584	3.632	2.424	3.252	4.095	4.150
AMTD 5	1.910	2.377	2.933	2.989	2.198	2.663	3.322	3.376
AMTD 6	1.653	2.398	3.033	3.085	1.900	2.726	3.581	3.638
AMTD 7	2.064	2.891	3.587	3.637	2.405	3.264	4.141	4.195
AMTD 8	1.525	2.050	2.629	2.699	1.691	2.199	2.846	2.918
AMTD 9	1.819	2.381	2.922	2.979	1.969	2.483	3.067	3.125
AMTD 10	1.797	2.331	2.862	2.915	1.935	2.427	3.004	3.059
AMTD 11	1.873	2.307	2.861	2.917	2.122	2.547	3.196	3.252
AMTD 12	1.474	1.982	2.513	2.569	1.640	2.131	2.725	2.782
AMTD 13	1.748	2.283	2.814	2.868	1.889	2.390	2.971	3.027
AMTD 14	1.458	2.008	2.521	2.581	1.597	2.130	2.692	2.754
AMTD 15	1.458	1.962	2.486	2.542	1.606	2.103	2.683	2.740
AMTD 16	1.435	1.967	2.472	2.528	1.574	2.090	2.645	2.703

APPENDIX 4.1

LIMITING FILTER PERFORMANCE IN AMPLITUDE HETEROGENEOUS CLUTTER

Table 4.1.1
Limiting Filter Performance in Amplitude Heterogeneous Clutter
$P_c = 30$ dB $\sigma_0 = 0.02$ K→ ∞

		ν=0.5	ν=1.0	ν=2.0	ν=4.0	ν→ ∞
				Mean value of S_{50}		
N=5	Δ=10%	9.671	9.845	9.948	9.985	10.028
	Δ=30%	7.627	7.773	7.850	7.877	7.905
	Δ=50%	6.628	6.722	6.762	6.767	6.770
	Δ=70%	6.401	6.492	6.529	6.532	6.535
	Δ=90%	6.524	6.617	6.656	6.660	6.664
N=10	Δ=10%	4.951	5.100	5.186	5.217	5.251
	Δ=30%	3.216	3.301	3.337	3.340	3.342
	Δ=50%	3.069	3.154	3.189	3.192	3.193
	Δ=70%	3.011	3.097	3.131	3.134	3.136
	Δ=90%	2.989	3.075	3.109	3.112	3.114
N=20	Δ=10%	1.037	1.180	1.256	1.282	1.311
	Δ=30%	-.119	-.035	-.001	.002	.004
	Δ=50%	-.189	-.105	-.072	-.069	-.067
	Δ=70%	-.215	-.131	-.097	-.095	-.093
	Δ=90%	-.225	-.141	-.107	-.104	-.103
				Mean IF		
N=5	Δ=10%	33.699	33.924	34.056	34.130	34.211
	Δ=30%	34.741	34.960	35.088	35.159	35.237
	Δ=50%	35.681	35.848	35.940	35.989	36.042
	Δ=70%	36.072	36.165	36.213	36.238	36.264
	Δ=90%	35.679	35.894	36.010	36.072	36.136
N=10	Δ=10%	38.217	38.348	38.417	38.454	38.493
	Δ=30%	39.218	39.336	39.396	39.427	39.459
	Δ=50%	39.417	39.510	39.556	39.580	39.604
	Δ=70%	39.500	39.582	39.621	39.641	39.662
	Δ=90%	39.533	39.610	39.647	39.665	39.684
N=20	Δ=10%	41.817	41.900	41.947	41.972	42.001
	Δ=30%	42.673	42.724	42.747	42.758	42.770
	Δ=50%	42.766	42.806	42.824	42.833	42.842
	Δ=70%	42.801	42.837	42.853	42.860	42.868
	Δ=90%	42.815	42.849	42.864	42.871	42.878

Table 4.1.2
Limiting Filter Performance in Amplitude Heterogeneous Clutter
$P_c = 60$ dB $\sigma_0 = 0.02$ K → ∞

		ν=0.5	ν=1.0	ν=2.0	ν=4.0	ν → ∞
				Mean value of S_{50}		
N=5	Δ=10%	16.501	16.793	16.951	17.048	17.164
	Δ=30%	13.127	13.328	13.413	13.463	13.522
	Δ=50%	10.162	10.294	10.332	10.352	10.375
	Δ=70%	8.107	8.187	8.192	8.194	8.197
	Δ=90%	7.155	7.224	7.225	7.225	7.225
N=10	Δ=10%	7.122	7.220	7.242	7.253	7.266
	Δ=30%	4.875	4.984	5.008	5.021	5.036
	Δ=50%	3.589	3.657	3.659	3.659	3.659
	Δ=70%	3.437	3.506	3.508	3.508	3.509
	Δ=90%	3.390	3.459	3.461	3.461	3.462
N=20	Δ=10%	2.383	2.453	2.454	2.454	2.454
	Δ=30%	.318	.391	.392	.392	.392
	Δ=50%	.103	.177	.178	.178	.178
	Δ=70%	.040	.114	.115	.115	.115
	Δ=90%	.016	.091	.092	.092	.092
				Mean IF		
N=5	Δ=10%	60.238	60.482	60.622	60.700	60.783
	Δ=30%	61.328	61.572	61.712	61.789	61.873
	Δ=50%	62.718	62.953	63.088	63.162	63.241
	Δ=70%	64.264	64.448	64.548	64.602	64.658
	Δ=90%	65.397	65.484	65.527	65.549	65.571
N=10	Δ=10%	66.817	66.968	67.051	67.097	67.146
	Δ=30%	67.907	68.057	68.140	68.186	68.234
	Δ=50%	68.913	69.020	69.073	69.101	69.129
	Δ=70%	69.021	69.147	69.212	69.245	69.279
	Δ=90%	69.056	69.189	69.257	69.292	69.328
N=20	Δ=10%	71.223	71.279	71.305	71.318	71.332
	Δ=30%	72.309	72.365	72.390	72.403	72.416
	Δ=50%	72.515	72.563	72.585	72.596	72.606
	Δ=70%	72.588	72.629	72.646	72.655	72.664
	Δ=90%	72.616	72.654	72.670	72.678	72.686

Table 4.1.3
Limiting Filter Performance in Amplitude Heterogeneous Clutter
$P_c = 30$ dB $\sigma_0 = 0.05$ K→ ∞

		ν=0.5	ν=1.0	ν=2.0	ν=4.0	ν→ ∞
		Mean value of S_{50}				
N=5	Δ=10%	13.693	14.141	14.449	14.587	14.740
	Δ=30%	10.989	11.318	11.537	11.647	11.774
	Δ=50%	8.725	8.922	9.034	9.078	9.127
	Δ=70%	7.478	7.584	7.633	7.643	7.652
	Δ=90%	6.969	7.056	7.092	7.095	7.097
N=10	Δ=10%	8.182	8.489	8.695	8.788	8.894
	Δ=30%	5.609	5.845	5.998	6.077	6.170
	Δ=50%	3.681	3.772	3.810	3.815	3.819
	Δ=70%	3.439	3.525	3.560	3.563	3.565
	Δ=90%	3.368	3.452	3.487	3.490	3.492
N=20	Δ=10%	4.000	4.306	4.505	4.593	4.693
	Δ=30%	1.620	1.870	2.035	2.122	2.223
	Δ=50%	.117	.209	.246	.249	.251
	Δ=70%	-.011	.081	.118	.121	.123
	Δ=90%	-.044	.044	.082	.085	.086
		Mean IF				
N=5	Δ=10%	30.822	31.202	31.431	31.560	31.700
	Δ=30%	31.907	32.287	32.515	32.644	32.785
	Δ=50%	33.218	33.585	33.805	33.929	34.065
	Δ=70%	34.490	34.786	34.957	35.052	35.154
	Δ=90%	35.432	35.564	35.631	35.666	35.702
N=10	Δ=10%	36.182	36.407	36.533	36.602	36.675
	Δ=30%	37.271	37.495	37.622	37.690	37.763
	Δ=50%	38.541	38.742	38.852	38.911	38.973
	Δ=70%	38.934	39.074	39.146	39.183	39.222
	Δ=90%	39.053	39.172	39.233	39.264	39.296
N=20	Δ=10%	40.055	40.187	40.261	40.301	40.342
	Δ=30%	41.144	41.277	41.350	41.390	41.432
	Δ=50%	42.351	42.444	42.491	42.515	42.539
	Δ=70%	42.529	42.595	42.626	42.641	42.657
	Δ=90%	42.579	42.637	42.664	42.678	42.692

Table 4.1.4

Limiting Filter Performance in Amplitude Heterogeneous Clutter

$P_c = 60$ dB $\sigma_0 = 0.05$ K $\rightarrow \infty$

		$\nu=0.5$	$\nu=1.0$	$\nu=2.0$	$\nu=4.0$	$\nu \rightarrow \infty$
		Mean value of S_{50}				
N=5	Δ=10%	30.839	32.481	33.398	33.888	34.398
	Δ=30%	26.454	27.987	28.812	29.189	29.514
	Δ=50%	22.558	24.202	25.075	25.525	25.990
	Δ=70%	20.030	21.603	22.403	22.804	23.201
	Δ=90%	18.817	20.391	21.177	21.562	21.942
N=10	Δ=10%	18.110	18.600	18.776	18.827	18.859
	Δ=30%	12.354	12.613	12.732	12.797	12.869
	Δ=50%	8.395	8.642	8.763	8.837	8.925
	Δ=70%	5.182	5.275	5.291	5.299	5.308
	Δ=90%	4.846	4.917	4.919	4.919	4.920
N=20	Δ=10%	10.791	10.968	11.001	11.008	11.015
	Δ=30%	5.291	5.405	5.441	5.459	5.478
	Δ=50%	2.034	2.190	2.243	2.273	2.306
	Δ=70%	.723	.795	.796	.797	.797
	Δ=90%	.599	.671	.672	.672	.672
		Mean IF				
N=5	Δ=10%	44.748	45.253	45.450	45.515	45.556
	Δ=30%	45.839	46.344	46.541	46.606	46.647
	Δ=50%	47.265	47.771	47.968	48.033	48.075
	Δ=70%	48.894	49.400	49.598	49.663	49.705
	Δ=90%	50.018	50.526	50.724	50.789	50.832
N=10	Δ=10%	62.357	62.692	62.891	63.001	63.122
	Δ=30%	63.448	63.784	63.982	64.093	64.213
	Δ=50%	64.907	65.243	65.441	65.552	65.672
	Δ=70%	66.803	67.111	67.290	67.390	67.497
	Δ=90%	67.600	67.737	67.807	67.844	67.881
N=20	Δ=10%	67.850	68.065	68.190	68.261	68.338
	Δ=30%	68.942	69.156	69.282	69.352	69.430
	Δ=50%	70.402	70.616	70.742	70.812	70.890
	Δ=70%	71.753	71.876	71.939	71.971	72.004
	Δ=90%	71.928	72.027	72.077	72.102	72.127

APPENDIX 4.2

LIMITING FILTER PERFORMANCE IN SPECTRALLY HETEROGENEOUS CLUTTER

Table 4.2.1

Limiting Filter Performance in Spectrally Heterogeneous Clutter

$P_c = 30$ dB $\sigma_0 = 0.02$ K→ ∞

		b_1=0.1	b_1=0.2	b_1=0.3	b_1=0.4	b_1=0.5	b_1=0.6	b_1=0.7	b_1=0.8
					Mean value of S_{50}				
	Δ=10%	10.151	10.240	10.385	10.575	10.797	11.054	11.376	11.782
	Δ=30%	7.971	8.050	8.177	8.344	8.541	8.774	9.087	9.522
N=5	Δ=50%	6.825	6.875	6.955	7.056	7.180	7.351	7.613	7.986
	Δ=70%	6.570	6.592	6.632	6.687	6.762	6.882	7.089	7.394
	Δ=90%	6.714	6.759	6.819	6.876	6.926	6.991	7.109	7.300
	Δ=10%	5.268	5.332	5.456	5.607	5.788	6.054	6.457	6.915
	Δ=30%	3.370	3.437	3.538	3.680	3.878	4.140	4.456	4.814
N=10	Δ=50%	3.210	3.239	3.275	3.311	3.361	3.455	3.631	3.893
	Δ=70%	3.149	3.169	3.190	3.212	3.249	3.329	3.474	3.683
	Δ=90%	3.126	3.143	3.160	3.178	3.211	3.287	3.424	3.620
	Δ=10%	1.402	1.540	1.659	1.768	1.977	2.217	2.510	2.866
	Δ=30%	.024	.063	.113	.182	.300	.486	.730	1.039
N=20	Δ=50%	-.056	-.043	-.024	.005	.050	.128	.274	.505
	Δ=70%	-.084	-.074	-.061	-.039	-.010	.051	.176	.375
	Δ=90%	-.094	-.086	-.074	-.054	-.028	.026	.145	.337
					Mean IF				
	Δ=10%	34.192	34.143	34.057	33.941	33.807	33.645	33.430	33.147
	Δ=30%	35.218	35.166	35.078	34.962	34.827	34.663	34.441	34.150
N=5	Δ=50%	36.025	35.983	35.918	35.835	35.735	35.599	35.392	35.101
	Δ=70%	36.255	36.235	36.200	36.154	36.094	36.000	35.841	35.609
	Δ=90%	36.118	36.077	36.022	35.967	35.920	35.867	35.787	35.667
	Δ=10%	38.468	38.406	38.313	38.193	38.044	37.860	37.639	37.392
	Δ=30%	39.434	39.376	39.291	39.173	39.017	38.833	38.621	38.379
N=10	Δ=50%	39.588	39.559	39.524	39.489	39.447	39.370	39.230	39.027
	Δ=70%	39.649	39.628	39.607	39.587	39.556	39.490	39.375	39.218
	Δ=90%	39.673	39.655	39.637	39.621	39.593	39.531	39.423	39.277
	Δ=10%	41.972	41.899	41.828	41.757	41.635	41.480	41.301	41.094
	Δ=30%	42.754	42.722	42.681	42.629	42.541	42.406	42.240	42.040
N=20	Δ=50%	42.831	42.816	42.798	42.771	42.735	42.680	42.584	42.438
	Δ=70%	42.859	42.848	42.835	42.813	42.787	42.743	42.663	42.541
	Δ=90%	42.869	42.860	42.848	42.829	42.804	42.764	42.688	42.572

Table 4.2.2

Limiting Filter Performance in Spectrally Heterogeneous Clutter

$P_c = 60$ dB $\sigma_0 = 0.02$ K→ ∞

		b_1=0.1	b_1=0.2	b_1=0.3	b_1=0.4	b_1=0.5	b_1=0.6	b_1=0.7	b_1=0.8
					Mean value of S_{50}				
	Δ=10%	17.298	17.821	18.572	19.502	20.618	21.967	23.586	25.559
	Δ=30%	13.673	14.069	14.609	15.382	16.557	18.041	19.792	21.600
N=5	Δ=50%	10.504	10.808	11.244	11.900	13.003	14.490	16.340	18.268
	Δ=70%	8.282	8.472	8.802	9.429	10.517	12.045	13.967	15.960
	Δ=90%	7.307	7.449	7.744	8.290	9.362	10.977	12.890	14.838
	Δ=10%	7.881	8.102	9.268	10.762	12.040	14.609	16.062	17.531
	Δ=30%	5.566	5.691	6.521	7.587	8.805	10.669	11.806	12.930
N=10	Δ=50%	3.938	3.875	4.174	4.875	5.953	7.400	8.444	9.316
	Δ=70%	3.846	3.743	3.895	4.070	4.432	5.268	6.538	7.357
	Δ=90%	3.811	3.694	3.781	3.872	4.321	4.649	4.881	5.371
	Δ=10%	8.623	2.786	3.781	4.924	6.778	8.732	10.723	12.415
	Δ=30%	4.894	.749	1.569	2.439	3.780	5.094	6.485	7.827
N=20	Δ=50%	6.971	.333	.459	.662	1.253	2.091	3.181	4.211
	Δ=70%	11.564	.228	.302	.424	.617	1.044	1.566	2.148
	Δ=90%	2.932	.186	.248	.363	.509	.705	1.078	1.387
					Mean IF				
	Δ=10%	60.714	60.493	60.169	59.637	58.754	57.555	56.140	54.619
	Δ=30%	61.804	61.583	61.259	60.727	59.843	58.644	57.230	55.709
N=5	Δ=50%	63.172	62.962	62.649	62.124	61.238	60.027	58.591	57.038
	Δ=70%	64.599	64.434	64.159	63.656	62.772	61.542	60.081	58.499
	Δ=90%	65.534	65.411	65.170	64.690	63.808	62.566	61.092	59.505
	Δ=10%	66.763	66.772	66.348	65.677	64.865	63.744	62.781	62.195
	Δ=30%	67.851	67.860	67.437	66.767	65.955	64.834	63.872	63.285
N=10	Δ=50%	68.839	68.918	68.647	68.069	67.272	66.217	65.263	64.677
	Δ=70%	68.932	69.048	68.890	68.724	68.391	67.609	66.573	65.990
	Δ=90%	68.969	69.096	69.002	68.919	68.491	68.188	68.025	67.684
	Δ=10%	68.542	71.059	70.505	70.036	69.323	68.535	67.713	67.060
	Δ=30%	69.623	72.145	71.594	71.126	70.414	69.625	68.804	68.150
N=20	Δ=50%	68.945	72.478	72.367	72.186	71.680	70.980	70.190	69.546
	Δ=70%	65.674	72.571	72.506	72.396	72.220	71.829	71.357	70.871
	Δ=90%	69.842	72.608	72.554	72.450	72.318	72.148	71.820	71.586

Table 4.2.3
Limiting Filter Performance in Spectrally Heterogeneous Clutter
$P_c = 30$ dB $\sigma_0 = 0.05$ K→ ∞

		b_1=0.1	b_1=0.2	b_1=0.3	b_1=0.4	b_1=0.5	b_1=0.6	b_1=0.7	b_1=0.8
					Mean value of S_{50}				
N=5	Δ=10%	14.829	15.097	15.533	15.928	16.238	16.536	16.899	17.357
	Δ=30%	11.855	12.111	12.517	12.876	13.122	13.356	13.654	14.027
	Δ=50%	9.251	9.585	10.049	10.503	10.861	11.146	11.439	11.791
	Δ=70%	7.784	8.016	8.356	8.744	9.171	9.619	10.060	10.516
	Δ=90%	7.177	7.320	7.580	7.924	8.332	8.772	9.270	9.804
N=10	Δ=10%	9.000	9.262	9.655	10.243	10.765	11.167	11.539	11.956
	Δ=30%	6.214	6.432	6.791	7.270	7.647	7.926	8.198	8.524
	Δ=50%	3.933	4.236	4.680	5.126	5.496	5.793	6.070	6.419
	Δ=70%	3.597	3.673	3.832	4.119	4.480	4.780	5.047	5.356
	Δ=90%	3.513	3.562	3.678	3.856	4.042	4.247	4.502	4.827
N=20	Δ=10%	4.816	5.024	5.432	5.864	6.320	6.697	7.017	7.370
	Δ=30%	2.190	2.294	2.608	2.958	3.316	3.587	3.826	4.103
	Δ=50%	.316	.498	.813	1.161	1.488	1.761	2.010	2.289
	Δ=70%	.151	.207	.318	.504	.747	.981	1.212	1.483
	Δ=90%	.109	.151	.220	.328	.477	.643	.838	1.090
					Mean IF				
N=5	Δ=10%	31.636	31.436	31.134	30.841	30.615	30.441	30.277	30.103
	Δ=30%	32.720	32.519	32.214	31.919	31.690	31.510	31.340	31.159
	Δ=50%	33.993	33.776	33.455	33.130	32.861	32.650	32.465	32.274
	Δ=70%	35.083	34.894	34.624	34.323	34.020	33.735	33.464	33.200
	Δ=90%	35.664	35.546	35.353	35.096	34.785	34.455	34.129	33.819
N=10	Δ=10%	36.598	36.400	36.103	35.765	35.496	35.321	35.194	35.050
	Δ=30%	37.686	37.487	37.189	36.848	36.576	36.397	36.266	36.118
	Δ=50%	38.883	38.665	38.340	38.001	37.719	37.521	37.369	37.198
	Δ=70%	39.190	39.120	38.987	38.752	38.476	38.268	38.107	37.924
	Δ=90%	39.277	39.230	39.127	38.968	38.825	38.700	38.544	38.340
N=20	Δ=10%	40.337	40.228	39.995	39.747	39.536	39.391	39.281	39.161
	Δ=30%	41.426	41.316	41.081	40.830	40.614	40.464	40.348	40.220
	Δ=50%	42.497	42.366	42.141	41.893	41.665	41.490	41.344	41.185
	Δ=70%	42.639	42.591	42.506	42.371	42.199	42.046	41.906	41.745
	Δ=90%	42.677	42.640	42.584	42.502	42.396	42.289	42.171	42.018

Table 4.2.4

Limiting Filter Performance in Spectrally Heterogeneous Clutter

$P_c = 60$ dB $\sigma_0 = 0.05$ K→ ∞

		b_1=0.1	b_1=0.2	b_1=0.3	b_1=0.4	b_1=0.5	b_1=0.6	b_1=0.7	b_1=0.8
					Mean value of S_{50}				
	Δ=10%	34.713	35.761	37.389	39.367	41.352	42.901	44.126	45.161
	Δ=30%	30.080	31.408	33.095	35.096	37.024	38.592	39.898	40.975
N=5	Δ=50%	26.336	27.529	29.429	31.524	33.378	34.992	36.339	37.558
	Δ=70%	23.626	24.912	26.946	29.291	31.402	33.071	34.529	35.691
	Δ=90%	22.438	23.683	25.853	28.259	30.406	32.193	33.627	34.813
	Δ=10%	20.339	23.779	27.031	30.990	33.692	35.653	37.175	38.439
	Δ=30%	13.846	16.526	19.180	23.917	27.552	30.123	31.964	33.373
N=10	Δ=50%	9.577	11.918	14.112	18.454	22.256	25.181	27.369	29.078
	Δ=70%	5.825	7.825	10.079	13.783	17.931	21.374	23.975	26.022
	Δ=90%	4.992	5.474	7.679	11.896	16.193	19.665	22.374	24.540
	Δ=10%	13.359	17.421	21.437	24.906	27.615	29.556	31.074	32.305
	Δ=30%	7.082	9.546	12.872	16.946	20.711	23.461	25.392	26.808
N=20	Δ=50%	3.424	5.195	7.597	11.032	14.955	18.055	20.386	22.204
	Δ=70%	1.135	1.889	3.285	5.922	10.073	13.709	16.548	18.768
	Δ=90%	.890	1.154	1.695	3.506	7.237	11.063	14.227	16.778
					Mean IF				
	Δ=10%	38.468	38.406	38.313	38.193	38.044	37.860	37.639	37.393
	Δ=30%	39.434	39.376	39.291	39.174	39.017	38.833	38.621	38.380
N=5	Δ=50%	39.588	39.559	39.524	39.489	39.447	39.369	39.230	39.027
	Δ=70%	39.649	39.628	39.607	39.587	39.556	39.490	39.375	39.219
	Δ=90%	39.673	39.655	39.637	39.621	39.593	39.531	39.423	39.278
	Δ=10%	62.731	61.029	59.178	55.790	52.084	49.145	47.138	46.006
	Δ=30%	63.822	62.120	60.269	56.881	53.175	50.236	48.228	47.095
N=10	Δ=50%	65.279	63.577	61.725	58.334	54.620	51.670	49.649	48.507
	Δ=70%	67.129	65.504	63.627	60.308	56.548	53.529	51.453	50.299
	Δ=90%	67.815	67.440	65.603	61.903	58.077	55.194	53.379	52.654
	Δ=10%	67.722	66.719	65.413	63.340	59.938	56.724	54.291	52.656
	Δ=30%	68.813	67.810	66.505	64.431	61.029	57.815	55.381	53.746
N=20	Δ=50%	70.272	69.268	67.962	65.887	62.480	59.258	56.812	55.163
	Δ=70%	71.724	71.035	69.904	67.909	64.485	61.201	58.679	56.962
	Δ=90%	-100.000	-100.000	-100.000	-100.000	-100.000	-100.000	-100.000	-100.000

APPENDIX 4.3

IF LOSS IN AMPLITUDE AND SPECTRALLY HETEROGENEOUS CLUTTER

Table 4.3.1

IF Loss in Amplitude and Spectrally Heterogeneous Clutter, K<∞

		b_1=0.0	b_1=0.15	b_1=0.3	b_1=0.45	b_1=0.6
	K=5	14.28	15.36	15.15	15.24	15.12
	K=10	7.19	7.67	7.67	7.20	7.67
ν→∞	K=20	2.49	2.53	2.46	2.67	2.96
	K=40	1.11	1.01	1.16	1.40	1.91
	K=80	.54	.43	.69	.96	1.59
	K=5	14.74	15.41	15.34	15.75	15.53
	K=10	8.29	8.40	7.99	8.60	8.96
ν=2.0	K=20	3.34	3.20	3.30	3.29	3.64
	K=40	1.43	1.46	1.77	1.79	2.37
	K=80	.87	.67	1.05	1.14	1.96
	K=5	16.19	16.10	16.69	16.76	16.35
	K=10	10.11	8.99	9.81	10.48	9.63
ν=0.5	K=20	5.30	5.33	5.46	5.42	5.59
	K=40	3.41	3.20	3.77	3.74	3.72
	K=80	2.13	2.18	2.54	2.57	2.57
	K=5	33.92	35.12	32.26	29.88	27.22
	K=10	7.81	7.70	7.75	8.17	8.43
ν→∞	K=20	2.53	2.33	3.55	4.06	5.65
	K=40	1.04	1.23	2.68	4.34	7.17
	K=80	.59	1.10	2.78	5.11	9.58
	K=5	34.56	34.68	30.65	28.48	28.25
	K=10	8.95	8.65	8.25	8.94	8.95
ν=2.0	K=20	3.47	3.76	3.66	5.30	6.09
	K=40	1.84	1.81	2.68	5.72	7.28
	K=80	.67	1.04	2.27	6.28	9.24
	K=5	34.88	34.44	33.96	32.54	28.65
	K=10	11.38	11.40	11.86	11.07	11.62
ν=0.5	K=20	5.47	5.66	6.08	6.63	7.42
	K=40	3.10	3.49	4.42	6.14	8.28
	K=80	2.00	2.15	4.72	5.47	9.09

P_c = 30 dB

σ_0 = 0.05

P_c = 60 dB

σ_0 = 0.05

Table 4.3.1 (cont.)

		b_1=0.0	b_1=0.15	b_1=0.3	b_1=0.45	b_1=0.6
	K=5	13.59	13.90	14.15	13.79	13.82
	K=10	8.11	8.29	8.25	7.71	8.09
$\nu \to \infty$	K=20	2.56	2.63	2.89	2.75	2.82
	K=40	1.20	1.29	1.47	1.43	1.46
	K=80	.66	.67	.97	.85	.86
	K=5	14.36	15.18	14.61	14.61	14.83
	K=10	9.64	9.28	9.51	9.25	9.18
ν=2.0	K=20	3.40	3.47	3.19	3.45	3.47
	K=40	1.71	1.91	1.70	1.86	1.75
	K=80	.88	1.17	.91	1.19	1.18
	K=5	15.59	15.46	15.86	16.55	16.82
	K=10	10.71	10.64	11.51	11.35	11.33
ν=0.5	K=20	5.58	5.78	5.43	5.41	5.64
	K=40	3.16	3.44	2.95	3.36	3.09
	K=80	1.77	1.86	1.33	2.25	1.58

P_c = 60 dB

σ_0 = 0.02

Table 4.3.2

Standard Deviation of Simulation Results for Loss in Amplitude and Spectrally Heterogeneous Clutter, K<∞

		b_1=0.0	b_1=0.15	b_1=0.3	b_1=0.45	b_1=0.6
	K=5	2.33	2.19	2.25	2.39	2.67
	K=10	.44	.49	.49	.51	.43
ν→∞	K=20	.10	.08	.14	.16	.25
	K=40	.03	.05	.11	.15	.21
	K=80	.02	.03	.07	.11	.18
	K=5	2.16	1.97	2.80	2.78	2.80
	K=10	.70	.50	.62	.60	.53
ν=2.0	K=20	.11	.14	.15	.28	.39
	K=40	.06	.08	.09	.26	.35
	K=80	.04	.05	.09	.21	.18
	K=5	1.83	2.04	2.40	2.32	3.19
	K=10	.97	1.19	.81	.73	.95
ν=0.5	K=20	.22	.21	.21	.31	.45
	K=40	.13	.12	.10	.27	.36
	K=80	.09	.07	.09	.21	.30

P_c = 30 dB

σ_0 = 0.05

	K=5	1.92	1.40	1.62	2.10	1.16
	K=10	.46	.53	.53	.50	.45
ν→∞	K=20	.10	.08	.10	.12	.09
	K=40	.03	.03	.04	.04	.08
	K=80	.01	.01	.02	.03	.04
	K=5	1.66	1.67	1.77	1.76	1.84
	K=10	.51	.51	.46	.44	.60
ν=2.0	K=20	.12	.12	.14	.12	.17
	K=40	.07	.08	.10	.06	.08
	K=80	.04	.04	.05	.02	.05
	K=5	1.57	1.79	1.59	1.28	1.88
	K=10	.69	.47	.53	.64	.71
ν=0.5	K=20	.22	.23	.27	.23	.27
	K=40	.10	.14	.15	.13	.15
	K=80	.08	.08	.15	.12	.12

P_c = 60 dB

σ_0 = 0.05

Table 4.3.2 (cont.)

		b_1=0.0	b_1=0.15	b_1=0.3	b_1=0.45	b_1=0.6
	K=5	1.72	1.72	1.95	1.50	1.71
	K=10	.92	.85	.72	.64	.53
$\nu \to \infty$	K=20	.09	.10	.09	.08	.09
	K=40	.03	.03	.03	.05	.04
	K=80	.02	.02	.01	.02	.02
	K=5	1.57	2.88	1.80	1.92	1.68
	K=10	1.22	1.80	.79	.83	.88
ν=2.0	K=20	.15	.19	.15	.17	.17
	K=40	.08	.11	.07	.09	.08
	K=80	.07	.07	.07	.05	.06
	K=5	1.81	1.45	1.76	1.70	1.82
	K=10	1.05	.93	1.20	.82	.98
ν=0.5	K=20	.21	.28	.26	.25	.28
	K=40	.11	.15	.17	.10	.13
	K=80	.07	.10	.15	.09	.09

P_c = 60 dB

σ_0 = 0.02

APPENDIX 4.4

CLUTTER SCENARIO INDEX

Table 4.4.1

Scenario Index	P_{pc}	fc_{bg}	σ_{bg}	P_{bg}
1	30	0.0	0.05	30
2	30	0.0	0.05	50
3	30	0.0	0.1	30
4	30	0.0	0.1	50
5	30	0.25	0.05	30
6	30	0.25	0.05	50
7	30	0.25	0.1	30
8	30	0.25	0.1	50
9	30	0.5	0.05	30
10	30	0.5	0.05	50
11	30	0.5	0.1	30
12	30	0.5	0.1	50
13	45	0.0	0.05	30
14	45	0.0	0.05	50
15	45	0.0	0.1	30
16	45	0.0	0.1	50
17	45	0.25	0.05	30
18	45	0.25	0.05	50
19	45	0.25	0.1	30
20	45	0.25	0.1	50
21	45	0.5	0.05	30
22	45	0.5	0.05	50
23	45	0.5	0.1	30
24	45	0.5	0.1	50
25	60	0.0	0.05	30
26	60	0.0	0.05	50
27	60	0.0	0.1	30
28	60	0.0	0.1	50
29	60	0.25	0.05	30
30	60	0.25	0.05	50
31	60	0.25	0.1	30
32	60	0.25	0.1	50
33	60	0.5	0.05	30
34	60	0.5	0.05	50
35	60	0.5	0.1	30
36	60	0.5	0.1	50

fc_{bg} relavite to the PRF

σ_{bg} relative to the PRF

P_{bg} dB relative to thermal noise thermal noise

P_{pc} dB relative to thermal noise thermal noise

APPENDIX 5.1
CFAR LOSS TABLES

All data in this appendix is applicable for Swerling case 1 and 2 targets, with $P_d = 50\%$. The CFAR loss is given in dB relative to ideal fixed threshold detection in clutter of shape parameter ν, as discussed in Chapter 4 of this report.

The CFAR loss associated with the three types of CFAR processors is as follows:

Table 5.1.1
CFAR loss for the CA Processor

	$\nu = 0.1$	$\nu = 0.25$	$\nu = 0.5$	$\nu = 1.5$	$\nu = 2.5$	$\nu = 4.5$	$\nu = 9.5$	$\nu = \infty$
				a) $P_{fa} = 10^{-4}$				
N = 8	26.444	9.781	5.553	3.275	2.951	2.832	2.848	2.835
N = 16	10.615	4.517	2.690	1.643	1.464	1.397	1.400	1.393
N = 24	6.535	2.946	1.781	1.103	.975	.929	.927	.922
N = 32	4.777	2.217	1.324	.816	.734	.699	.695	.691
				b) $P_{fa} = 10^{-6}$				
N = 8	31.043	16.811	8.902	5.040	4.534	4.363	4.411	4.384
N = 16	19.489	7.430	4.237	2.497	2.226	2.123	2.131	2.116
N = 24	11.542	4.810	2.777	1.666	1.484	1.404	1.408	1.397
N = 32	8.202	3.519	2.066	1.244	1.105	1.050	1.050	1.042
				c) $P_{fa} = 10^{-8}$				
N = 8	34.500	24.759	12.505	6.897	6.195	5.974	6.062	6.020
N = 16	29.822	10.570	5.875	3.410	3.020	2.871	2.888	2.864
N = 24	17.462	6.813	3.836	2.281	2.001	1.897	1.895	1.878
N = 32	12.095	4.967	2.848	1.706	1.500	1.414	1.417	1.404

Table 5.1.2
CFAR loss for the CAGO Processor

	$\nu = 0.1$	$\nu = 0.25$	$\nu = 0.5$	$\nu = 1.5$	$\nu = 2.5$	$\nu = 4.5$	$\nu = 9.5$	$\nu = \infty$
				a) $P_{fa} = 10^{-4}$				
N = 8	26.614	10.092	5.979	3.611	3.252	3.090	3.079	3.067
N = 16	10.895	4.796	3.079	1.876	1.691	1.599	1.589	1.582
N = 24	6.794	3.240	2.166	1.281	1.150	1.085	1.079	1.074
N = 32	5.060	2.449	1.681	.967	.872	.821	.814	.810
				b) $P_{fa} = 10^{-6}$				
N = 8	45.746	18.824	9.393	5.440	4.903	4.668	4.690	4.664
N = 16	19.727	7.730	4.672	2.801	2.511	2.369	2.365	2.351
N = 24	11.929	5.171	3.174	1.905	1.713	1.608	1.596	1.586
N = 32	10.000	3.869	2.377	1.445	1.291	1.212	1.207	1.199
				c) $P_{fa} = 10^{-8}$				
N = 8	53.096	26.691	12.910	7.342	6.595	6.312	6.370	6.330
N = 16	30.029	11.019	6.366	3.767	3.345	3.164	3.155	3.131
N = 24	17.796	7.166	4.245	2.547	2.246	2.117	2.104	2.088
N = 32	12.519	5.354	3.221	1.943	1.715	1.603	1.596	1.584

Table 5.1.3
CFAR loss for the OS Processor

	$\nu = 0.1$	$\nu = 0.25$	$\nu = 0.5$	$\nu = 1.5$	$\nu = 2.5$	$\nu = 4.5$	$\nu = 9.5$	$\nu = \infty$
				a) $P_{fa} = 10^{-4}$				
N = 8	36.092	15.352	7.917	4.519	4.075	3.900	3.914	3.897
N = 16	22.366	7.077	3.879	2.299	2.049	1.942	1.927	1.920
N = 24	14.061	4.587	2.584	1.543	1.379	1.288	1.279	1.275
N = 32	10.466	3.366	1.921	1.150	1.026	.956	.945	.944
				b) $P_{fa} = 10^{-6}$				
N = 8	39.554	25.675	12.643	6.907	6.221	5.979	6.078	6.043
N = 16	34.785	11.682	6.104	3.502	3.122	2.944	2.946	2.927
N = 24	23.682	7.470	4.038	2.351	2.089	1.959	1.942	1.930
N = 32	17.328	5.479	3.018	1.767	1.572	1.461	1.447	1.439
				c) $P_{fa} = 10^{-8}$				
N = 8	37.212	35.987	17.722	9.409	8.495	8.232	8.421	8.368
N = 16	39.161	16.629	8.406	4.727	4.184	3.948	3.969	3.940
N = 24	33.140	10.560	5.533	3.187	2.803	2.622	2.615	2.595
N = 32	24.558	7.711	4.143	2.422	2.119	1.975	1.951	1.936

APPENDIX 5.2
PLOTS OF P_{fa} vs. T FOR N = 16 AND N = 8

This appendix presents the contours of constant P_{fa} in the ν-T plane for the CA, CAGO and OS processors for N = 16 and N = 8.

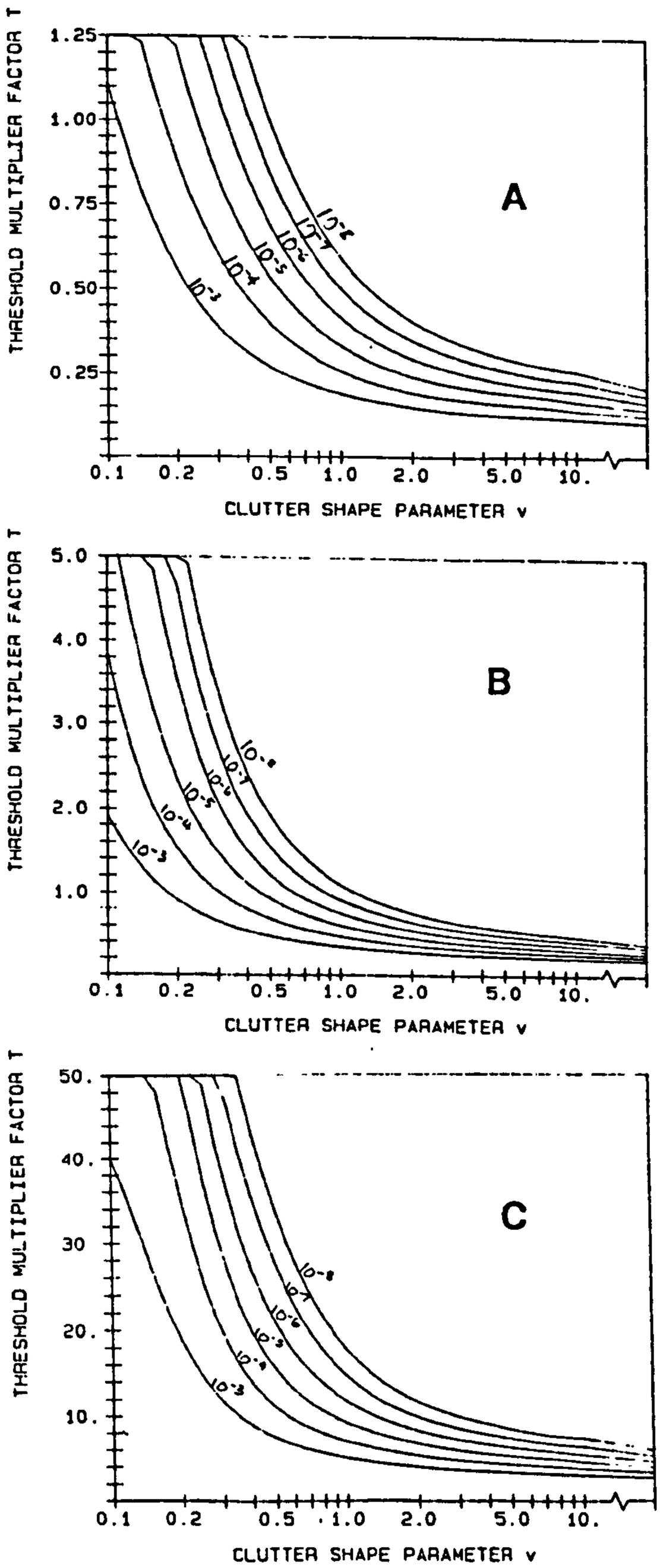

FIg 5.2.2: *Contours of Constant P_{fa} in the ν-T Plane for N = 16*
a) CA b) CAGO c) OS

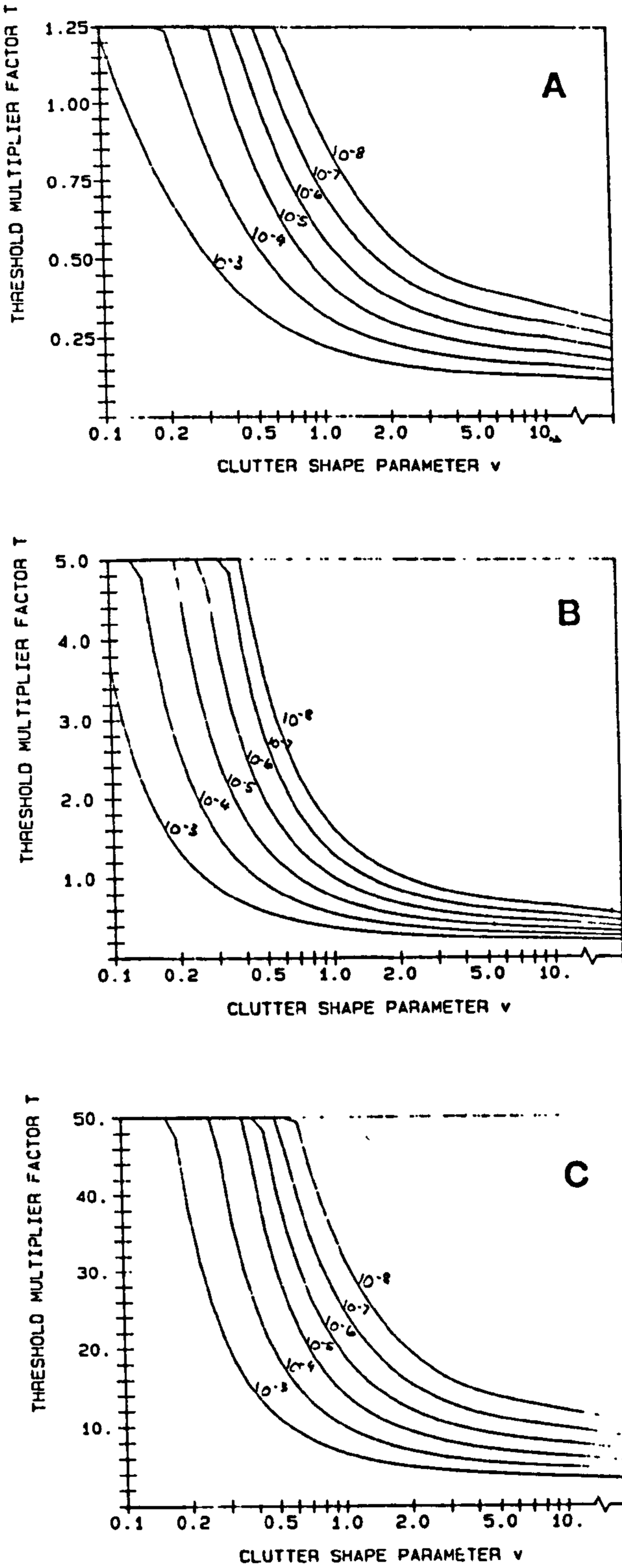

Fig. 5.2.1: *Contours of Constant P_{fa} in the v-T Plane for N = 8*
a) CA b) CAGO c) OS

APPENDIX 5.3
TABLES OF DIFFERENCE IN LOSS FOR $P_d = 50\%$ AND $P_d = 90\%$

All data in this appendix is applicable for Swerling case 1 and 2 targets. The difference in loss is given in dB. The difference in loss for each of the three types of CFAR processors is as follows:

Table 5.3.1
Difference in loss for the CA Processor

	$\nu = 0.1$	$\nu = 0.25$	$\nu = 0.5$	$\nu = 1.5$	$\nu = 2.5$	$\nu = 4.5$	$\nu = 9.5$	$\nu = \infty$
				a) $P_{fa} = 10^{-4}$				
N = 8	2.364	.900	.391	.121	.072	.049	.053	.052
N = 16	1.147	.364	.120	-.007	.004	.015	.025	.023
N = 24	.681	.177	.013	-.026	-.022	-.004	.025	.023
N = 32	.473	.096	-.017	-.058	-.057	-.033	.004	.002
				b) $P_{fa} = 10^{-6}$				
N = 8	2.444	.990	.493	.174	.132	.079	.075	.074
N = 16	1.230	.453	.187	.049	.035	.019	.035	.033
N = 24	.796	.272	.112	.006	.023	.029	.030	.027
N = 32	.589	.187	.055	.001	-.003	-.009	.018	.015
				c) $P_{fa} = 10^{-8}$				
N = 8	2.493	1.047	.931	.201	.150	.124	.091	.090
N = 16	1.280	.484	.232	.085	.048	.061	.041	.039
N = 24	.826	.303	.125	.036	.004	.028	.031	.029
N = 32	.620	.217	.071	.006	.010	.005	.014	.013

Table 5.3.2
Difference in loss for the CAGO Processor

	$\nu = 0.1$	$\nu = 0.25$	$\nu = 0.5$	$\nu = 1.5$	$\nu = 2.5$	$\nu = 4.5$	$\nu = 9.5$	$\nu = \infty$
				a) $P_{fa} = 10^{-4}$				
N = 8	2.071	.701	.531	.172	.132	.102	.089	.086
N = 16	1.018	.200	.169	.015	-.021	-.024	-.005	.019
N = 24	.611	.049	.051	-.040	-.037	-.026	-.008	-.237
N = 32	.417	-.036	-.020	-.057	-.062	-.048	-.016	-.371
				b) $P_{fa} = 10^{-6}$				
N = 8	2.171	.785	.608	.253	.171	.143	.111	.085
N = 16	1.118	.306	.243	.057	.045	.026	.012	.051
N = 24	.712	.112	.109	.011	-.011	-.001	.011	-.348
N = 32	.497	.040	.031	-.024	-.019	-.029	-.028	-.558
				c) $P_{fa} = 10^{-8}$				
N = 8	2.219	.847	1.182	.296	.217	.169	.141	.105
N = 16	1.167	.355	.285	.088	.071	.046	.052	.055
N = 24	.749	.179	.153	.021	.027	.005	.023	-.485
N = 32	.559	.082	.088	.020	-.010	.002	-.017	-.745

Table 5.3.3
Difference in loss for the OS Processor

	$\nu = 0.1$	$\nu = 0.25$	$\nu = 0.5$	$\nu = 1.5$	$\nu = 2.5$	$\nu = 4.5$	$\nu = 9.5$	$\nu = \infty$
				a) $P_{fa} = 10^{-4}$				
N = 8	5.160	1.583	.722	.235	.172	.113	.091	.090
N = 16	2.697	.731	.293	.078	.055	.039	.043	.040
N = 24	1.834	.449	.165	.023	.025	.029	.034	.029
N = 32	1.360	.304	.085	.009	.008	.016	.031	.026
				b) $P_{fa} = 10^{-6}$				
N = 8	5.223	1.650	.777	.270	.178	.150	.114	.115
N = 16	2.751	.768	.335	.095	.047	.037	.034	.034
N = 24	1.876	.496	.200	.047	.018	.009	.019	.018
N = 32	1.434	.373	.151	.033	.028	.034	.032	.029
				c) $P_{fa} = 10^{-8}$				
N = 8	5.270	1.683	24.080	.379	.218	.173	.121	.122
N = 16	2.825	.859	.407	.142	.098	.099	.063	.062
N = 24	1.914	.523	.237	.074	.038	.031	.015	.014
N = 32	1.461	.390	.159	.044	.032	.029	.036	.034

APPENDIX 5.4
TABLES OF ERROR IN LOSS DUE TO WATTS' APPROXIMATION

This appendix tabulates the results of numerical analyses of the error in the Signal to Clutter-plus-Noise Ratio required for detection introduced through the use of Watts' approximation. All data in this appendix is applicable for Swerling case 1 and 2 targets, and represents the unweighted average of the error at Pd = 25%, 50%, 70 % and 90%. The absolute error in loss in dB is given. The error in loss for each of the CA and OS processors is as given in the following tables.

Note: ***** denotes that ν_{eff} is out of the range of the analysis (ie. ν_{eff} >10)

Table 5.4.1

Error for the CA Processor, $P_{fa} = 10^{-4}$

	ν = 0.1	ν = 0.25	ν = 0.5	ν = 1.5	ν = 2.5	ν = 4.5	ν = 9.5	
CNR = -9 dB	-.727	******	******	******	******	******	******	
CNR = -6 dB	-.732	-.532	******	******	******	******	******	
CNR = -3 dB	.361	-.327	-.268	******	******	******	******	
CNR = 0 dB	3.272	.470	-.024	-.119	-.016	******	******	
CNR = 3 dB	7.429	1.806	.430	-.011	-.017	.032	******	
CNR = 6 dB	11.172	3.092	.865	.068	.057	-.004	******	N = 8
CNR = 9 dB	13.517	3.802	1.080	.091	.085	.016	******	
CNR = 12 dB	14.396	3.870	1.013	.097	.097	.035	******	
CNR = 15 dB	14.210	3.530	.830	.080	.093	.046	.054	
CNR = 18 dB	13.308	2.924	.607	.056	.094	.052	.040	
CNR = 21 dB	12.017	2.298	.439	.036	.090	.054	.040	
CNR = -9 dB	-1.139	******	******	******	******	******	******	
CNR = -6 dB	-1.341	-.848	******	******	******	******	******	
CNR = -3 dB	-.698	-.809	-.544	******	******	******	******	
CNR = 0 dB	.797	-.284	-.393	-.218	-.075	******	******	
CNR = 3 dB	2.704	.404	-.084	-.143	-.078	-.003	******	
CNR = 6 dB	4.250	1.019	.189	-.050	-.021	-.019	******	N = 16
CNR = 9 dB	5.070	1.308	.331	.005	.032	.007	******	
CNR = 12 dB	5.159	1.325	.321	.016	.063	.022	******	
CNR = 15 dB	4.767	1.110	.265	.022	.075	.031	.050	
CNR = 18 dB	4.094	.869	.206	.020	.082	.035	.042	
CNR = 21 dB	3.310	.630	.151	.020	.084	.038	.037	
CNR = -9 dB	-1.295	******	******	******	******	******	******	
CNR = -6 dB	-1.548	-.964	******	******	******	******	******	
CNR = -3 dB	-1.038	-.968	-.647	******	******	******	******	
CNR = 0 dB	.074	-.544	-.510	-.262	-.110	******	******	
CNR = 3 dB	1.409	.019	-.237	-.199	-.110	-.018	******	
CNR = 6 dB	2.443	.482	.004	-.096	-.051	-.034	******	N = 24
CNR = 9 dB	2.931	.696	.126	-.031	.000	-.011	******	
CNR = 12 dB	2.944	.711	.169	-.002	.029	.012	******	
CNR = 15 dB	2.645	.627	.144	.013	.047	.021	.045	
CNR = 18 dB	2.191	.483	.106	.020	.057	.028	.036	
CNR = 21 dB	1.694	.347	.077	.022	.062	.032	.032	
CNR = -9 dB	-1.369	******	******	******	******	******	******	
CNR = -6 dB	-1.648	-1.015	******	******	******	******	******	
CNR = -3 dB	-1.216	-1.051	-.687	******	******	******	******	
CNR = 0 dB	-.263	-.683	-.573	-.275	-.119	******	******	
CNR = 3 dB	.856	-.180	-.326	-.217	-.119	-.022	******	
CNR = 6 dB	1.716	.233	-.086	-.118	-.058	-.035	******	N = 32
CNR = 9 dB	2.121	.443	.032	-.053	-.017	-.013	******	
CNR = 12 dB	2.164	.484	.079	-.019	.009	.008	******	
CNR = 15 dB	1.938	.436	.081	-.004	.031	.020	.049	
CNR = 18 dB	1.623	.360	.071	.004	.041	.026	.038	
CNR = 21 dB	1.266	.279	.053	.007	.046	.030	.040	

Table 5.4.2
Error for the CA Processor, $P_{fa} = 10^{-6}$

	ν = 0.1	ν = 0.25	ν = 0.5	ν = 1.5	ν = 2.5	ν = 4.5	ν = 9.5	
CNR = -9 dB	-1.597	******	******	******	******	******	******	
CNR = -6 dB	-1.413	-1.056	******	******	******	******	******	
CNR = -3 dB	.454	-.626	-.584	******	******	******	******	
CNR = 0 dB	5.640	.717	-.077	-.274	-.035	******	******	
CNR = 3 dB	13.576	3.096	.666	-.040	-.108	.045	******	
CNR = 6 dB	21.232	5.630	1.473	.112	.035	-.079	******	N = 8
CNR = 9 dB	26.455	7.287	1.929	.163	.109	-.036	******	
CNR = 12 dB	29.038	7.833	1.963	.135	.123	-.009	******	
CNR = 15 dB	29.659	7.550	1.707	.085	.124	.008	.095	
CNR = 18 dB	29.036	6.767	1.345	.049	.122	.017	.088	
CNR = 21 dB	28.359	5.768	.988	.023	.120	.021	.068	
CNR = -9 dB	-2.285	******	******	******	******	******	******	
CNR = -6 dB	-2.279	-1.555	******	******	******	******	******	
CNR = -3 dB	-1.107	-1.336	-.997	******	******	******	******	
CNR = 0 dB	1.431	-.472	-.650	-.423	-.194	******	******	
CNR = 3 dB	4.776	.773	-.123	-.256	-.181	-.048	******	
CNR = 6 dB	7.657	1.850	.331	-.112	-.057	-.068	******	N = 16
CNR = 9 dB	9.347	2.429	.567	-.022	.021	-.025	******	
CNR = 12 dB	9.853	2.476	.591	.020	.049	.006	******	
CNR = 15 dB	9.485	2.210	.482	.020	.070	.023	.058	
CNR = 18 dB	8.607	1.784	.362	.016	.081	.032	.043	
CNR = 21 dB	7.425	1.368	.250	.009	.085	.037	.041	
CNR = -9 dB	-2.509	******	******	******	******	******	******	
CNR = -6 dB	-2.561	-1.744	******	******	******	******	******	
CNR = -3 dB	-1.610	-1.554	-1.143	******	******	******	******	
CNR = 0 dB	.247	-.843	-.839	-.491	-.235	******	******	
CNR = 3 dB	2.552	.106	-.374	-.333	-.228	-.073	******	
CNR = 6 dB	4.438	.878	.014	-.179	-.113	-.084	******	N = 24
CNR = 9 dB	5.474	1.281	.216	-.066	-.025	-.042	******	
CNR = 12 dB	5.691	1.340	.285	-.024	.042	-.007	******	
CNR = 15 dB	5.317	1.172	.232	-.001	.070	.015	.057	
CNR = 18 dB	4.626	.943	.176	.008	.080	.024	.045	
CNR = 21 dB	3.789	.721	.128	.013	.086	.032	.045	
CNR = -9 dB	-2.639	******	******	******	******	******	******	
CNR = -6 dB	-2.702	-1.830	******	******	******	******	******	
CNR = -3 dB	-1.854	-1.667	-1.217	******	******	******	******	
CNR = 0 dB	-.306	-1.021	-.932	-.519	-.270	******	******	
CNR = 3 dB	1.485	-.190	-.491	-.376	-.244	-.092	******	
CNR = 6 dB	2.871	.461	-.124	-.198	-.127	-.076	******	N = 32
CNR = 9 dB	3.578	.790	.086	-.101	-.047	-.038	******	
CNR = 12 dB	3.666	.850	.149	-.038	.005	-.005	******	
CNR = 15 dB	3.344	.748	.163	-.012	.040	.013	.044	
CNR = 18 dB	2.807	.593	.118	.001	.060	.024	.035	
CNR = 21 dB	2.190	.441	.086	.005	.069	.031	.036	

Table 5.4.3
Error for the CA Processor, $P_{fa} = 10^{-8}$

	ν = 0.1	ν = 0.25	ν = 0.5	ν = 1.5	ν = 2.5	ν = 4.5	ν = 9.5	
CNR = -9 dB	-2.159	******	******	******	******	******	******	
CNR = -6 dB	-1.687	-1.431	******	******	******	******	******	
CNR = -3 dB	.892	-.704	-.780	******	******	******	******	
CNR = 0 dB	8.579	1.137	-.041	-.401	-.093	******	******	
CNR = 3 dB	20.969	4.672	1.007	-.047	-.190	.010	******	
CNR = 6 dB	33.309	8.679	2.214	.178	.038	-.139	******	N = 8
CNR = 9 dB	42.094	11.505	3.015	.245	.134	-.100	******	
CNR = 12 dB	46.867	12.763	3.210	.203	.172	-.052	******	
CNR = 15 dB	48.847	12.755	4.083	.136	.191	-.023	.072	
CNR = 18 dB	51.321	11.972	4.618	.068	.160	-.008	.040	
CNR = 21 dB	52.740	10.760	4.908	.018	.146	-.001	.024	
CNR = -9 dB	-3.043	******	******	******	******	******	******	
CNR = -6 dB	-2.739	-2.076	******	******	******	******	******	
CNR = -3 dB	-1.122	-1.595	-1.311	******	******	******	******	
CNR = 0 dB	2.436	-.411	-.769	-.574	-.287	******	******	
CNR = 3 dB	7.300	1.316	-.064	-.336	-.263	-.091	******	
CNR = 6 dB	11.687	2.888	.573	-.126	-.106	-.119	******	N = 16
CNR = 9 dB	14.426	3.791	.909	-.018	.006	-.060	******	
CNR = 12 dB	15.498	3.966	.935	.030	.053	-.010	******	
CNR = 15 dB	15.339	3.637	.796	.031	.080	.019	.066	
CNR = 18 dB	14.412	3.058	.591	.020	.097	.035	.045	
CNR = 21 dB	14.394	2.404	.419	.012	.105	.043	.041	
CNR = -9 dB	-3.347	******	******	******	******	******	******	
CNR = -6 dB	-3.102	-2.306	******	******	******	******	******	
CNR = -3 dB	-1.792	-1.881	-1.493	******	******	******	******	
CNR = 0 dB	.751	-.911	-1.015	-.671	-.358	******	******	
CNR = 3 dB	4.018	.350	-.396	-.429	-.313	-.128	******	
CNR = 6 dB	6.836	1.444	.112	-.212	-.153	-.121	******	N = 24
CNR = 9 dB	8.483	2.043	.379	-.074	-.030	-.064	******	
CNR = 12 dB	8.978	2.129	.438	-.019	.024	-.012	******	
CNR = 15 dB	8.641	1.914	.377	.002	.053	.014	.046	
CNR = 18 dB	7.802	1.573	.289	.006	.069	.026	.034	
CNR = 21 dB	6.705	1.203	.202	.008	.076	.033	.033	
CNR = -9 dB	-3.485	******	******	******	******	******	******	
CNR = -6 dB	-3.285	-2.417	******	******	******	******	******	
CNR = -3 dB	-2.113	-2.035	-1.581	******	******	******	******	
CNR = 0 dB	-.039	-1.149	-1.131	-.705	-.411	******	******	
CNR = 3 dB	2.444	-.072	-.561	-.472	-.342	-.158	******	
CNR = 6 dB	4.482	.810	-.091	-.264	-.186	-.123	******	N = 32
CNR = 9 dB	5.599	1.269	.172	-.125	-.065	-.054	******	
CNR = 12 dB	5.842	1.344	.242	-.041	.009	-.019	******	
CNR = 15 dB	5.476	1.198	.226	-.020	.041	.007	.045	
CNR = 18 dB	4.767	.970	.174	-.006	.054	.023	.036	
CNR = 21 dB	3.903	.737	.132	.00[illegible]	.063	.031	.032	

Table 5.4.4
Error for the OS Processor, $P_{fa} = 10^{-4}$

	ν = 0.1	ν = 0.25	ν = 0.5	ν = 1.5	ν = 2.5	ν = 4.5	ν = 9.5	
CNR = -9 dB	-.684	******	******	******	******	******	******	
CNR = -6 dB	-.438	-.551	******	******	******	******	******	
CNR = -3 dB	1.048	-.099	-.276	******	******	******	******	
CNR = 0 dB	5.720	.978	.175	-.298	-.182	******	******	
CNR = 3 dB	13.317	3.082	.756	-.082	-.280	-.165	******	
CNR = 6 dB	20.935	5.390	1.325	.002	-.170	-.286	******	N = 8
CNR = 9 dB	26.360	6.876	1.563	-.025	-.113	-.294	******	
CNR = 12 dB	29.260	7.234	1.402	-.123	-.147	-.270	******	
CNR = 15 dB	30.190	6.726	1.006	-.200	-.168	-.263	-.166	
CNR = 18 dB	29.768	5.711	.553	-.254	-.179	-.257	-.189	
CNR = 21 dB	28.428	4.475	.188	-.272	-.189	-.253	-.195	
CNR = -9 dB	-1.149	******	******	******	******	******	******	
CNR = -6 dB	-1.242	-.894	******	******	******	******	******	
CNR = -3 dB	-.385	-.740	-.595	******	******	******	******	
CNR = 0 dB	1.928	-.115	-.356	-.365	-.268	******	******	
CNR = 3 dB	5.325	.925	-.027	-.274	-.300	-.222	******	
CNR = 6 dB	8.520	1.858	.220	-.201	-.250	-.238	******	N = 16
CNR = 9 dB	10.562	2.235	.243	-.209	-.222	-.244	******	
CNR = 12 dB	11.336	2.016	.098	-.229	-.205	-.242	******	
CNR = 15 dB	11.072	1.452	-.056	-.245	-.196	-.226	-.189	
CNR = 18 dB	10.039	.815	-.165	-.247	-.191	-.226	-.197	
CNR = 21 dB	8.503	.279	-.214	-.246	-.189	-.225	-.201	
CNR = -9 dB	-1.339	******	******	******	******	******	******	
CNR = -6 dB	-1.518	-1.016	******	******	******	******	******	
CNR = -3 dB	-.863	-.974	-.706	******	******	******	******	
CNR = 0 dB	.769	-.477	-.536	-.415	-.303	******	******	
CNR = 3 dB	3.028	.274	-.260	-.341	-.322	-.242	******	
CNR = 6 dB	5.025	.870	-.073	-.278	-.261	-.264	******	N = 24
CNR = 9 dB	6.197	1.017	-.059	-.232	-.240	-.252	******	
CNR = 12 dB	6.449	.762	-.132	-.233	-.224	-.227	******	
CNR = 15 dB	5.916	.353	-.183	-.241	-.215	-.212	-.207	
CNR = 18 dB	4.814	.006	-.218	-.236	-.209	-.201	-.192	
CNR = 21 dB	3.371	-.224	-.237	-.236	-.211	-.202	-.203	
CNR = -9 dB	-1.457	******	******	******	******	******	******	
CNR = -6 dB	-1.671	-1.118	******	******	******	******	******	
CNR = -3 dB	-1.126	-1.102	-.781	******	******	******	******	
CNR = 0 dB	.187	-.670	-.640	-.450	-.333	******	******	
CNR = 3 dB	1.909	-.059	-.393	-.371	-.339	-.258	******	N = 32
CNR = 6 dB	3.373	.393	-.225	-.307	-.274	-.276	******	
CNR = 9 dB	4.166	.471	-.195	-.271	-.245	-.252	******	
CNR = 12 dB	4.201	.246	-.207	-.242	-.232	-.234	******	
CNR = 15 dB	3.586	-.040	-.241	-.218	-.223	-.227	-.201	
CNR = 18 dB	2.510	-.237	-.253	-.219	-.221	-.224	-.210	
CNR = 21 dB	1.204	-.349	-.253	-.224	-.209	-.224	-.205	

Table 5.4.5
Error for the OS Processor, $P_{fa} = 10^{-6}$

	ν = 0.1	ν = 0.25	ν = 0.5	ν = 1.5	ν = 2.5	ν = 4.5	ν = 9.5	
CNR = -9 dB	-1.430	******	******	******	******	******	******	
CNR = -6 dB	-.993	-1.051	******	******	******	******	******	
CNR = -3 dB	1.488	-.286	-.540	******	******	******	******	
CNR = 0 dB	9.490	1.495	.215	-.464	-.218	******	******	
CNR = 3 dB	22.889	5.167	1.222	-.102	-.400	-.172	******	
CNR = 6 dB	36.558	9.454	2.385	.098	-.202	-.438	******	N = 8
CNR = 9 dB	46.564	12.521	3.106	.085	-.091	-.396	******	
CNR = 12 dB	52.277	13.822	3.145	-.028	-.129	-.348	******	
CNR = 15 dB	54.863	13.686	2.683	-.152	-.155	-.312	-.164	
CNR = 18 dB	57.888	12.630	2.000	-.245	-.167	-.287	-.206	
CNR = 21 dB	59.633	11.042	1.291	-.280	-.169	-.299	-.223	
CNR = -9 dB	-2.268	******	******	******	******	******	******	
CNR = -6 dB	-2.079	-1.616	******	******	******	******	******	
CNR = -3 dB	-.578	-1.170	-1.000	******	******	******	******	
CNR = 0 dB	3.295	-.087	-.520	-.573	-.369	******	******	
CNR = 3 dB	9.252	1.679	.065	-.348	-.415	-.264	******	
CNR = 6 dB	15.061	3.452	.560	-.219	-.293	-.356	******	N = 16
CNR = 9 dB	19.058	4.425	.715	-.200	-.217	-.288	******	
CNR = 12 dB	20.986	4.449	.556	-.215	-.212	-.285	******	
CNR = 15 dB	21.259	3.815	.274	-.241	-.204	-.273	-.189	
CNR = 18 dB	20.372	2.867	.030	-.269	-.203	-.263	-.206	
CNR = 21 dB	21.172	1.860	-.129	-.275	-.201	-.255	-.214	
CNR = -9 dB	-2.585	******	******	******	******	******	******	
CNR = -6 dB	-2.482	-1.836	******	******	******	******	******	
CNR = -3 dB	-1.293	-1.504	-1.196	******	******	******	******	
CNR = 0 dB	1.418	-.639	-.801	-.644	-.421	******	******	
CNR = 3 dB	5.259	.628	-.316	-.471	-.454	-.297	******	
CNR = 6 dB	8.834	1.736	.041	-.311	-.317	-.338	******	N = 24
CNR = 9 dB	11.134	2.192	.126	-.276	-.276	-.303	******	
CNR = 12 dB	12.009	1.987	.021	-.266	-.247	-.274	******	
CNR = 15 dB	11.700	1.407	-.099	-.258	-.222	-.257	-.199	
CNR = 18 dB	10.550	.751	-.185	-.257	-.217	-.248	-.205	
CNR = 21 dB	9.816	.207	-.231	-.260	-.212	-.242	-.206	
CNR = -9 dB	-2.740	******	******	******	******	******	******	
CNR = -6 dB	-2.686	-1.969	******	******	******	******	******	
CNR = -3 dB	-1.653	-1.688	-1.300	******	******	******	******	
CNR = 0 dB	.524	-.909	-.945	-.693	-.483	******	******	
CNR = 3 dB	3.419	.122	-.495	-.519	-.474	-.332	******	
CNR = 6 dB	6.015	.955	-.191	-.384	-.368	-.335	******	N = 32
CNR = 9 dB	7.598	1.227	-.104	-.311	-.282	-.288	******	
CNR = 12 dB	8.042	.983	-.155	-.286	-.250	-.271	******	
CNR = 15 dB	7.528	.521	-.208	-.266	-.239	-.256	-.205	
CNR = 18 dB	6.309	.092	-.240	-.256	-.229	-.248	-.207	
CNR = 21 dB	4.670	-.190	-.255	-.250	-.226	-.245	-.213	

Table 5.4.6
Error for the OS Processor, $P_{fa} = 10^{-8}$

	ν = 0.1	ν = 0.25	ν = 0.5	ν = 1.5	ν = 2.5	ν = 4.5	ν = 9.5	
CNR = -9 dB	-1.859	******	******	******	******	******	******	
CNR = -6 dB	-1.226	-1.309	******	******	******	******	******	
CNR = -3 dB	2.324	-.348	-.674	******	******	******	******	
CNR = 0 dB	13.660	2.215	.297	-.552	-.276	******	******	
CNR = 3 dB	32.289	7.554	1.804	-.115	-.460	-.192	******	
CNR = 6 dB	51.170	13.768	3.660	.135	-.226	-.499	******	N = 8
CNR = 9 dB	65.003	18.351	4.945	.180	-.130	-.452	******	
CNR = 12 dB	75.024	20.542	5.295	.066	-.135	-.403	******	
CNR = 15 dB	81.549	20.780	5.121	-.089	-.158	-.361	-.169	
CNR = 18 dB	85.326	21.553	5.722	-.218	-.193	-.336	-.233	
CNR = 21 dB	87.458	22.273	6.045	-.293	-.218	-.344	-.264	
CNR = -9 dB	-3.003	******	******	******	******	******	******	
CNR = -6 dB	-2.494	-2.108	******	******	******	******	******	
CNR = -3 dB	-.429	-1.367	-1.281	******	******	******	******	
CNR = 0 dB	5.044	.109	-.552	-.740	-.439	******	******	
CNR = 3 dB	13.756	2.628	.262	-.404	-.522	-.284	******	
CNR = 6 dB	22.464	5.299	1.009	-.185	-.326	-.434	******	N = 16
CNR = 9 dB	28.646	6.983	1.345	-.153	-.232	-.383	******	
CNR = 12 dB	31.903	7.382	1.205	-.204	-.198	-.332	******	
CNR = 15 dB	34.051	6.827	.827	-.241	-.197	-.309	-.179	
CNR = 18 dB	36.123	5.730	.404	-.279	-.195	-.297	-.208	
CNR = 21 dB	37.259	4.379	.058	-.294	-.197	-.291	-.221	
CNR = -9 dB	-3.375	******	******	******	******	******	******	
CNR = -6 dB	-2.981	-2.384	******	******	******	******	******	
CNR = -3 dB	-1.340	-1.782	-1.523	******	******	******	******	
CNR = 0 dB	2.393	-.602	-.911	-.824	-.542	******	******	
CNR = 3 dB	7.938	1.150	-.253	-.538	-.556	-.349	******	
CNR = 6 dB	13.261	2.795	.265	-.347	-.377	-.417	******	N = 24
CNR = 9 dB	16.870	3.641	.420	-.287	-.291	-.345	******	
CNR = 12 dB	18.516	3.579	.294	-.270	-.248	-.310	******	
CNR = 15 dB	18.576	2.927	.076	-.270	-.222	-.282	-.200	
CNR = 18 dB	19.925	2.036	-.090	-.282	-.209	-.271	-.213	
CNR = 21 dB	20.701	1.135	-.196	-.282	-.208	-.264	-.220	
CNR = -9 dB	-3.567	******	******	******	******	******	******	
CNR = -6 dB	-3.230	-2.522	******	******	******	******	******	
CNR = -3 dB	-1.801	-2.000	-1.637	******	******	******	******	
CNR = 0 dB	1.144	-.949	-1.101	-.872	-.603	******	******	
CNR = 3 dB	5.243	.446	-.498	-.614	-.586	-.386	******	
CNR = 6 dB	9.054	1.661	-.070	-.423	-.422	-.414	******	N = 32
CNR = 9 dB	11.519	2.169	.050	-.331	-.320	-.350	******	
CNR = 12 dB	12.458	1.964	-.024	-.292	-.263	-.307	******	
CNR = 15 dB	12.133	1.376	-.137	-.284	-.241	-.273	-.216	
CNR = 18 dB	12.453	.711	-.208	-.281	-.230	-.255	-.222	
CNR = 21 dB	13.057	.157	-.242	-.273	-.226	-.247	-.221	

APPENDIX 5.5
TABLES OF ERROR DUE TO EMPIRICAL FORMULAE FOR CFAR LOSS

This appendix gives the error between the numerically calculated CFAR loss and the approximate loss given by the empirivcal formula, as discussed in chapter 4.4.2. The data in this appendix is applicable for Swerling case 1 and 2 targets for $P_d = 50\%$. The error in CFAR loss is given in dB. The error due to the empirical formal for each of the three types of CFAR processors is as follows:

Table 5.5.1
Approximation Error for the CA Processor

	$\nu = 0.1$	$\nu = 0.25$	$\nu = 0.5$	$\nu = 1.5$	$\nu = 2.5$	$\nu = 4.5$	$\nu = 9.5$
				a) $P_{fa} = 10^{-4}$			
N = 8	-4.264	-.306	.038	.062	.050	.037	-.011
N = 16	.184	.096	.033	-.018	-.003	-.001	-.019
N = 24	.553	.083	.006	-.036	-.016	-.013	-.021
N = 32	.481	.029	.002	-.024	-.022	-.019	-.023
				b) $P_{fa} = 10^{-6}$			
N = 8	3.810	-1.922	-.116	.205	.182	.145	.047
N = 16	-2.519	-.180	.041	.056	.070	.072	.039
N = 24	-.403	-.052	.030	.011	.023	.037	.017
N = 32	.061	.010	.017	-.001	.013	.018	.007
				c) $P_{fa} = 10^{-8}$			
N = 8	13.027	-4.455	-.524	.255	.236	.173	.017
N = 16	-6.681	-.684	-.042	.072	.111	.122	.072
N = 24	-2.272	-.324	-.007	.005	.054	.067	.048
N = 32	-.827	-.154	-.008	-.010	.025	.043	.024

Table 5.5.2
Approximation Error for the CAGO Processor

	$\nu = 0.1$	$\nu = 0.25$	$\nu = 0.5$	$\nu = 1.5$	$\nu = 2.5$	$\nu = 4.5$	$\nu = 9.5$
				a) $P_{fa} = 10^{-4}$			
N = 8	-1.416	-.295	.004	.063	-.014	-.085	-.036
N = 16	1.808	.143	-.063	-.023	-.059	-.084	-.055
N = 24	1.716	.069	-.145	-.041	-.057	-.070	-.051
N = 32	1.344	.041	-.161	-.033	-.049	-.058	-.041
				b) $P_{fa} = 10^{-6}$			
N = 8	-6.149	-3.427	.008	.333	.186	.054	.092
N = 16	.235	.032	.068	.109	.054	.011	.046
N = 24	1.443	.029	.001	.044	.006	-.013	.019
N = 32	.064	.044	.013	.022	.003	-.012	.009
				c) $P_{fa} = 10^{-8}$			
N = 8	.899	-5.695	-.090	.530	.345	.126	.151
N = 16	-2.807	-.434	.097	.201	.154	.082	.133
N = 24	.439	-.075	.084	.112	.098	.058	.099
N = 32	1.204	-.018	.038	.058	.048	.034	.061

Table 5.5.3

Approximation Error for the OS Processor

	$\nu = 0.1$	$\nu = 0.25$	$\nu = 0.5$	$\nu = 1.5$	$\nu = 2.5$	$\nu = 4.5$	$\nu = 9.5$
				a) $P_{fa} = 10^{-4}$			
N = 8	10.034	-.774	.118	.182	.112	.036	-.063
N = 16	.210	.058	.053	.002	.000	-.016	-.043
N = 24	.803	.111	.005	-.029	-.030	-.020	-.038
N = 32	.584	.126	.003	-.024	-.023	-.013	-.023
				b) $P_{fa} = 10^{-6}$			
N = 8	32.930	-2.766	-.017	.480	.359	.204	-.027
N = 16	.692	-.469	.075	.114	.099	.083	.016
N = 24	-.325	-.088	.031	.029	.031	.034	.008
N = 32	.035	.009	.006	.002	.004	.021	.003
				c) $P_{fa} = 10^{-8}$			
N = 8	61.630	-4.748	-.506	.664	.478	.201	-.169
N = 16	9.216	-1.339	.021	.203	.208	.180	.070
N = 24	-1.289	-.493	.015	.059	.089	.096	.044
N = 32	-.881	-.228	-.019	-.009	.031	.045	.026

APPENDIX 7.1

INCREASE IN P_{fa} IN RDT-CFAR PROCESSOR IN CLUTTER WITH FINITE CNR

a) K = 16; M/N = 1/3; $\sigma_0 = 0.03$

b) K = 8; M/N = 3/8; $\sigma_0 = 0.03$

c) K = 16; M/N = 1/3; $\sigma_0 = 0.25$

d) K = 8; M/N = 3/8; $\sigma_0 = 0.25$

(Note: ****** denotes no false alarms occurred in simulation)

a) K = 16; M/N = 1/3; σ_0 = 0.03

	CNR (dB)						
	0	10	20	30	40	50	60
r_0 = 2/3 NK:							
α	-27.45	-23.01	-20.46	-19.75	-21.31	-19.59	-18.42
$\alpha' = 1.5\,\alpha$	******	-30.00	-26.20	-26.58	-30.00	-29.21	-25.23
$\alpha' = 2\,\alpha$	******	-36.99	-36.99	-33.98	-36.99	******	-29.21
$\alpha' = 4\,\alpha$	******	******	******	******	******	******	******
r_0 = NK-2N:							
α	-28.54	-24.20	-23.77	-21.94	-26.20	-26.20	-25.85
$\alpha' = 1.5\,\alpha$	-36.99	-33.98	-30.00	-30.97	-32.22	******	******
$\alpha' = 2\,\alpha$	******	-36.99	******	-33.98	******	******	******
$\alpha' = 4\,\alpha$	******	******	******	******	******	******	******
r_0 = NK-N:							
α	-28.54	-29.21	-26.99	-25.85	-26.99	-29.21	-26.99
$\alpha' = 1.5\,\alpha$	-33.98	-36.99	-36.99	-36.99	-36.99	******	******
$\alpha' = 2\,\alpha$	******	-36.99	******	-36.99	-36.99	******	******
$\alpha' = 4\,\alpha$	******	******	******	******	******	******	******

b) K = 8; M/N = 3/8; σ_0 = 0.03

	CNR (dB)						
	0	10	20	30	40	50	60
r_0 = 2/3 NK:							
α	-28.54	-20.18	-19.83	-21.19	-20.27	-15.20	-15.78
$\alpha' = 1.5\,\alpha$	-36.99	-27.45	-30.00	-30.97	-29.21	-25.23	-29.21
$\alpha' = 2\,\alpha$	******	-33.98	-33.98	******	******	-32.22	******
$\alpha' = 4\,\alpha$	******	******	******	******	******	******	******
r_0 = NK-2N:							
α	-27.96	-20.46	-19.83	-21.94	-22.84	-18.07	-19.00
$\alpha' = 1.5\,\alpha$	-36.99	-27.45	-26.99	-30.00	-36.99	-30.00	-36.99
$\alpha' = 2\,\alpha$	******	-36.99	-36.99	-36.99	******	******	******
$\alpha' = 4\,\alpha$	******	******	******	******	******	******	******
r_0 = NK-N:							
α	-28.54	-22.37	-20.86	-22.37	-28.54	-25.85	-26.58
$\alpha' = 1.5\,\alpha$	-36.99	-30.00	-30.97	-30.97	******	******	******
$\alpha' = 2\,\alpha$	******	******	******	******	******	******	******
$\alpha' = 4\,\alpha$	******	******	******	******	******	******	******

c) K = 16; M/N = 1/3; σ_0 = 0.25

	CNR (dB)						
	0	10	20	30	40	50	60
r_0 = 2/3 NK:							
α	-32.22	******	-32.22	-30.97	-32.22	-36.99	******
$\alpha' = 1.5\,\alpha$	******	******	******	******	******	******	******
$\alpha' = 2\,\alpha$	******	******	******	******	******	******	******
$\alpha' = 4\,\alpha$	******	******	******	******	******	******	******
r_0 = NK-2N:							
α	-32.22	******	-33.98	-33.98	******	-33.98	-33.99
$\alpha' = 1.5\,\alpha$	******	******	******	******	******	******	******
$\alpha' = 2\,\alpha$	******	******	******	******	******	******	******
$\alpha' = 4\,\alpha$	******	******	******	******	******	******	******
r_0 = NK-N:							
α	-33.98	******	-33.98	-32.22	******	******	-36.99
$\alpha' = 1.5\,\alpha$	******	******	******	******	******	******	******
$\alpha' = 2\,\alpha$	******	******	******	******	******	******	******
$\alpha' = 4\,\alpha$	******	******	******	******	******	******	******

d) K = 8; M/N = 3/8; σ_0 = 0.25

	CNR (dB)						
	0	10	20	30	40	50	60
r_0 = 2/3 NK:							
α	******	-36.99	-30.97	-36.99	-36.99	******	******
$\alpha' = 1.5\,\alpha$	******	******	******	******	******	******	******
$\alpha' = 2\,\alpha$	******	******	******	******	******	******	******
$\alpha' = 4\,\alpha$	******	******	******	******	******	******	******
r_0 = NK-2N:							
α	******	-33.98	-32.22	-36.99	******	******	******
$\alpha' = 1.5\,\alpha$	******	******	******	******	******	******	******
$\alpha' = 2\,\alpha$	******	******	******	******	******	******	******
$\alpha' = 4\,\alpha$	******	******	******	******	******	******	******
r_0 = NK-N:							
α	-33.98	-33.98	-33.98	-36.99	-36.99	******	******
$\alpha' = 1.5\,\alpha$	******	******	******	******	******	******	******
$\alpha' = 2\,\alpha$	******	******	******	******	******	******	******
$\alpha' = 4\,\alpha$	******	******	******	******	******	******	******

ERRATA

1. Page 26, paragraph 2, line 5: the words "theoretical and" should be removed; the models for predicting clutter eflectivity do not as yet have generally accepted physical justification.

2. Page 27, paragraph 3, line 6: note that the decorrelation of the fast fluctuations assumes the use of radar frequency agility.

3. Page 28, paragraph 3, line 3: The word "completely" only applies if the clutter has Rayleigh amplitude PDF. Deviations from this case require higher order moments to completely describe the clutter.

4. Page 29, paragraph 1, line18: Guinard and Daley (1970) presented, but did not originate, the composite surface model, which was originally due to Wright (1968[1])

5. Page 30, paragraph 3, line 12: should read "Jakeman and Pusey (**1976**), Oliver (1984) and Lewinski (**1983**)). ...".

6. Page 33, paragraph 1, line 5: in practical radars the speckle is not *entirely* decorrelated from one range bin to the next due to the non-ideal impulse response of the radar matched filter.

7. Page 35, eqn. (2.1b): should be:

$$p_v(v) = \frac{2b^{2v}}{\Gamma(v)} v^{2v-1} e^{-b^2v^2}$$

8. Page 48, paragraph 3: all targets, not only Rayleigh fluctuating targets, will exhibit the behaviour described here if post detection integration is employed.

9. Page 50, paragraph 3, line 8: should read "$(a+1)^{st}$ to $(n-b-1)^{st}$ samples ...".

10. Page 51, eqn. (2.7): the upper limit of the summation should be *n-b-1*.

11. Page 51, footnote, line 3: should read : "... a CA processor using **n-b** reference cells."

12. Page 52: section number should be section **2.3.3** ... .

---

[1]Wright, J. W., "A New Model for Sea Clutter", *IEEE Trans. on Antennas and Propagation*, vol. AP-16, March 1968, pp. 217 - 223.

13. Page 61, last paragraph: the term "zero Doppler component" refers to the spectral component with zero mean doppler.

14. Page 97, 6th last line: "relavite" should be "relative".

15. Page 129, paragraph 3: It should be noted the the following analysis closely follows that presented by Watts (1985).

16. Page 129, paragraph 4, line 3: the term $P_d(S|C)$ should be written $P_d(S(C))$, since S is a function of C rather than being a random variable conditioned on C.

17. Page 130, eqn. (6.1): should be:

$$p(C)=\frac{1}{\lambda^{\nu}\Gamma(\nu)}C^{\nu-1}\exp(-C/\lambda)$$

18. Page 130, eqns. (6.2) and (6.3): the terms (S|C) should be replaced by (S).

19. Page 131, paragraph 1: similar work by Oliver (1986[2], 1988) and Conte et al (1991[3]) is also relevant.

20. Page 133, paragraph 2, line2: should read "... the g_{i1} can be represented as $g_{i1} = \rho g_{i2} + z_i\sqrt{1-\rho^2}\sqrt{1-\rho^2}$ "

21. Page 141, eqn. (6.24b): element (N/2; N/2) of matrix $\mathbf{R_{uu}}$ should be $R_{uu}(0)$, not $R_{uu}(N/2\text{-}1)$.

---

[2]Oliver, C. J., and Tough, R. J. A., "On the simulation of correlated K-distributed random clutter", *Optica Acta* 33, (3), 1986, pp. 223-250.

[3]Conte, E., Longo, M., and Lops, M., "Modelling and simulation of K-distributed clutter", *IEE-Proceedings-F*, Vol. 138 No. 2, April 1991, pp. 121 - 130.